British Journal of Pharmacology

June 1995

Volume 115 Number 3 pages 381–548

British Journal of Pharmacology (1995) 115, 381-382

SPECIAL REPORT

Mexiletine-induced shortening of the action potential duration of ventricular muscles by activation of ATP-sensitive K^+ channels

[1]Toshiaki Sato, Sakuji Shigematsu & Makoto Arita

Department of Physiology, Oita Medical University School of Medicine, 1-1 Idaigaoka, Hasama-machi, Oita 879-55, Japan

A class Ib antiarrhythmic drug, mexiletine (100 μM) significantly shortened the action potential duration (APD) of guinea-pig ventricular muscles and this effect was completely abolished in the presence of glibenclamide (50 μM), a blocker of the ATP-sensitive K^+ channel (K_{ATP}). Mexiletine significantly increased the open probability of uridine diphosphate-primed K_{ATP} channels, recorded in inside-out patches of the ventricular cells. The results suggest that mexiletine shortens the APD of ventricular muscles, at least in part, via activation of K_{ATP}.

Keywords: Mexiletine; ATP-sensitive K^+ channel; action potential duration; glibenclamide; guinea-pig ventricular myocyte

Introduction Activation of ATP-sensitive K^+ channels (K_{ATP}) is responsible for the shortening of action potential duration (APD) in the ischaemic myocardium. In addition, potassium channel opening drugs such as cromakalim and pinacidil reduce the APD of cardiac myocytes by activating K_{ATP} (Nichols & Lederer, 1991). Mexiletine, a class Ib antiarrhythmic drug, decreases the maximum rate of rise of the action potential ($\dot{V}_{max}$) and shortens the APD, characteristics shared by other members of this class and which are currently considered to be due to the blockade of sodium channels. The aim of the present paper was to determine whether the opening of K_{ATP} could contribute to the shortening of the APD by mexiletine.

Methods Papillary muscles and single ventricular cells were prepared from guinea-pigs (250-300 g). A conventional glass microelectrode technique was used to record the action potential in papillary muscles superfused with Tyrode solution (35-36°C). The inside-out patch clamp technique (Hamill *et al.*, 1981) was used to record single K_{ATP} currents from ventricular cells, isolated by enzymatic dissociation (Wu *et al.*, 1992). Experiments were done at room temperature (20-22°C). The composition of the pipette solution was (in mM): KCl 140, $CaCl_2$ 1.8, $MgCl_2$ 0.5, glucose 5.5, HEPES 5 (pH = 7.4), while the bath solution contained (in mM): KCl 140, $MgCl_2$ 2, HEPES 5, EGTA 5, glucose 5.5 (pH = 7.3). Uridine diphosphate (UDP) and mexiletine were added to the bath solution. The channel activity was measured as $N \times P_o$, where N is the number of channels in the patch and P_o is the open probability of each channel.

Results We first examined the effects of mexiletine on action potentials of guinea-pig papillary muscles stimulated at a rate of 2 Hz. As shown in Figure 1, mexiletine (100 μM) decreased the action potential duration measured at 90% repolarization level (APD_{90}) from 174.8 ms to 156.0 ms and the maximum rate of rise of action potential ($\dot{V}_{max}$) from 190.1 Vs^{-1} to 125.0 Vs^{-1}, respectively [(i)→(ii)]. Subsequent application of glibenclamide (50 μM) fully restored the APD_{90} (up to 175.2 ms) while exerting no effect on the $\dot{V}_{max}$ [(ii)→(iii)]. The drug (100 μM) significantly shortened the APD_{90} from 192.9 ± 9.4 ms (mean ± s.e.mean) to 169.3 ± 7.8 ms, i.e., by 12%, within 20 min ($n = 7$, $P < 0.05$), and the APD was completely restored to 192.7 ± 9.2 ms ($n = 7$, $P < 0.05$) within 30 min after application of glibenclamide. Glibenclamide (50 μM) *per se* produced no change in either APD_{90} or $\dot{V}_{max}$ even after 20 min of exposure (not illustrated). Subsequent application of mexiletine (100 μM) failed to shorten the APD_{90}, even though the drug decreased the $\dot{V}_{max}$ from 172 Vs^{-1} to 98.2 Vs^{-1}. In the presence of glibenclamide, mexiletine caused little alteration in the APD_{90} (from 216.2 ± 13.1 ms to 215.2 ± 12.6 ms ($n = 5$, NS) within 20 min).

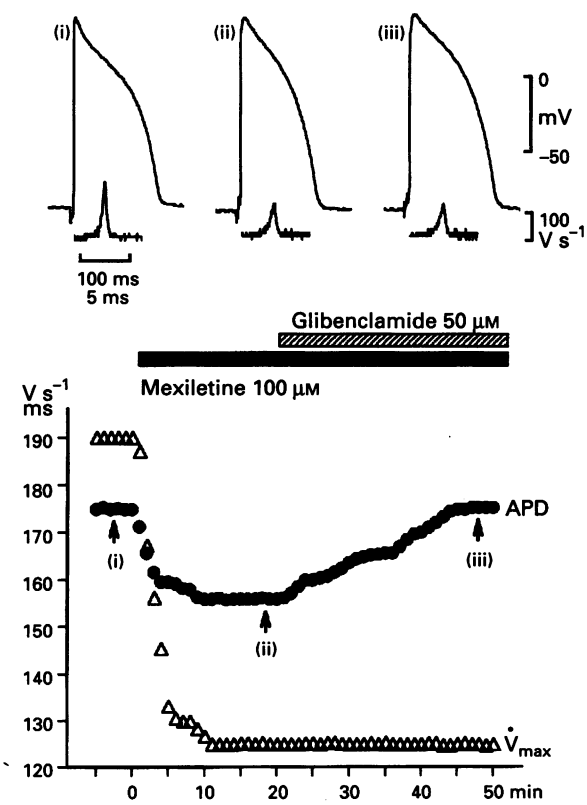

Figure 1 Reversal of mexiletine-induced shortening of action potential duration (APD) by glibenclamide in ventricular papillary muscles (stimulated at 2 Hz). The points designated by arrows (i), (ii) and (iii) in lower figures correspond respectively to the action potential and $\dot{V}_{max}$ shown above. Bars indicate the periods of drug application.

[1]Author for correspondence.

We then examined the effect of mexiletine on K_{ATP} channels using inside-out patch clamp techniques and guinea-pig isolated ventricular cells. Figure 2 shows typical effects of mexiletine on the activity of K_{ATP} channels occurring in the presence of uridine diphosphate (UDP). After the channel 'run-down' (Figure 2a), the application of UDP (3 mM) led to reactivation of K_{ATP} (Figure 2b). Subsequent application of mexiletine (100 μM) further increased the UDP-induced K_{ATP} activity without affecting the current unit amplitude (Figure 2b). This effect was reversed by washout of the drug (Figure 2c). Mexiletine significantly increased NP_o of the UDP-primed K_{ATP} channels from 1.21 ± 0.27 to 1.72 ± 0.31 ($n=5$, $P<0.05$). In the absence of UDP, mexiletine failed to increase the NP_o, measured in the presence of the relatively low ATP concentrations of 10 μM ($n=4$) and 100 μM ($n=8$).

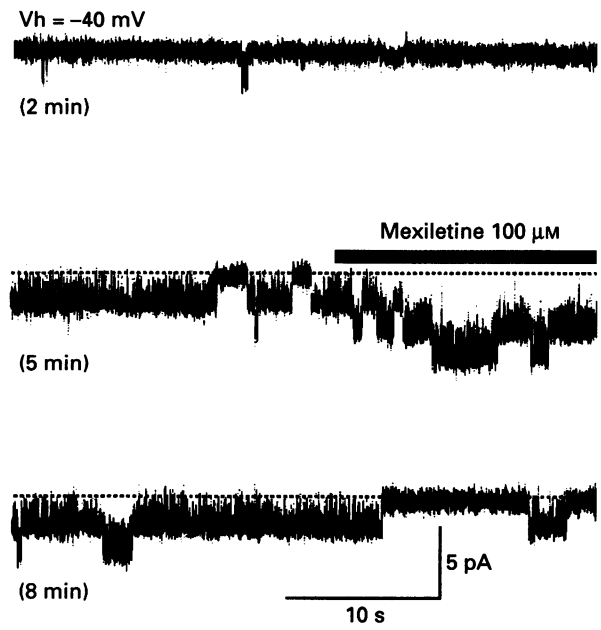

Figure 2 Effects of mexiletine on UDP-induced activation of K_{ATP} recorded from an inside-out patch. Membrane potential (Vh) was held at −40 mV. Each current trace was recorded from the same patch, starting at 2 min (**a**), 5 min (**b**), and 8 min (**c**) after successful formation of the inside-out patch. UDP (3 mM) was introduced between traces (a) and (b) and present until the end of trace (**c**). The horizontal bar above trace (**b**) indicates the period of mexiletine (100 μM) exposure. Dotted lines indicate the zero current level.

Discussion Unexpectedly, we found that mexiletine activated K_{ATP} in guinea-pig ventricular myocytes. We suggested earlier that the mexiletine-induced shortening of APD is partly due to a reduction in the Na^+ window current and partly due to inhibition of calcium currents (Kiyosue & Arita, 1989). Our present data suggest that this drug mainly shortened the APD through the activation of K_{ATP}, since glibenclamide completely antagonized the mexiletine-induced shortening of APD, without affecting the V_{max} (Figure 1). Arita *et al.* (1979) proposed that mexiletine increased the membrane K^+ conductance in depressed canine Purkinje fibres but they did not specify the channels involved. This finding may be readily explained by the finding that the drug activates K_{ATP}. Mexiletine may activate K_{ATP} predominantly in the presence of a nucleoside diphosphate because such an effect was not seen in the absence of the nucleotide, a characteristic shared by nicorandil (Shen *et al.*, 1991). The intracellular concentration of nucleoside diphosphate required for mexiletine to open K_{ATP} is purported to be very low in well-perfused ventricular muscles. We used a relatively high concentration of mexiletine (100 μM) to observe a definite shortening of APD, a concentration higher than that prescribed clinically ($\sim$10 μM). However, it is very likely that much lower concentrations of mexiletine can activate K_{ATP} in the presence of ischaemia, since intracellular ADP concentrations rise dramatically during ischaemia (Nichols & Lederer, 1991). Wu *et al.* (1992) showed that even 30 μM mexiletine shortened the APD of guinea-pig ventricular myocytes (stimulated at 0.2 Hz) by as much as 20%, while at most only $\sim$5% of the APD shortening could be attributed to the blockade of a (window) Na^+ current, when examined using single channel measurements in the presence and absence of 60 μM tetrodotoxin (Kiyosue & Arita, 1989).

K_{ATP} channel openers allegedly protect the myocardium from ischaemia-reperfusion injury (Nichols & Lederer, 1991). The APD-shortening effect of mexiletine, mediated by the activation of K_{ATP} may alter a tolerance of the heart muscle to ischaemic injury, because such changes in APD decrease Ca^{2+} influx carried, e.g., by reversed Na^+-Ca^{2+} exchange. Thus, the properties of Ib antiarrhythmics should be further studied and re-evaluated with regard to the mode of action of these drugs on the K_{ATP}, particularly in the presence of ischaemia.

References

ARITA, M., GOTO, M., NAGAMOTO, Y. & SAIKAWA, T. (1979). Electrophysiological actions of mexiletine (Kö1173) on canine Purkinje fibres and ventricular muscle. *Br. J. Pharmacol.*, **67**, 143–152.

HAMILL, O.P., MARTY, A., NEHER, E., SAKMANN. B. & SIGWORTH, F.J. (1981). Improved patch-clamp techniques for high-resolution current recording from cells and cell-free membrane patches. *Pflügers Arch.*, **391**, 86–100.

KIYOSUE, T. & ARITA, M. (1989). Late sodium current and its contribution to action potential configuration in guinea pig ventricular myocytes. *Circ. Res.*, **64**, 389–397.

NICHOLS, C.G. & LEDERER, W.J. (1991). Adenosine triphosphate-sensitive potassium channels in the cardiovascular system. *Am. J. Physiol.*, **261**, H1675–H1686.

SHEN, W.K., TUNG, R.T., MACHULDA, M.M. & KURACHI, M. (1991). Essential role of nucleotide diphosphates in nicorandil-mediated activation of cardiac ATP-sensitive K^+ channel: A comparison with pinacidil and lemakalim. *Circ. Res.*, **69**, 1152–1158.

WU, B., SATO, T., KIYOSUE, T. & ARITA, M. (1992). Blockade of 2,4-dinitrophenol induced ATP sensitive potassium current in guinea pig ventricular myocytes by class I antiarrhythmic drugs. *Cardiovasc. Res.*, **26**, 1095–1101.

(Received February 9, 1995
Accepted March 6, 1995)

British Journal of Pharmacology (1995) 115, 383-384

SPECIAL REPORT

Promotion by SR 48692 of gastric emptying and defaecation in rats suggesting a role of endogenous neurotensin

[1]Tiziano Croci, Antonina Giudice, Luciano Manara, *Danielle Gully & †Gérard Le Fur

SANOFI-Midy S.p.A. Research Center, Via G.B. Piranesi 38, 20137 Milan, Italy; *SANOFI Recherche, 195 Route d'Espagne, 31036 Toulouse, France and †SANOFI Recherche, 32/34 rue Marbeuf, 75008 Paris, France

We investigated the influence of the nonpeptide neurotensin receptor antagonist, SR 48692, administered orally, on gastric emptying and on acute defaecation. SR 48692 dose-dependently (ED_{50} ~0.7 $\mu g\ kg^{-1}$) increased gastric emptying of a food suspension, but it had no effect on that of a non-caloric meal. SR 48692 also dose-dependently promoted defaecation and increased faecal water content. We suggest that antagonism of endogenous neurotensin accounts for the gastric emptying and defaecation promoting action of SR 48692.

Keywords: Neurotensin; SR 48692; rat gut; gastric emptying; defaecation

Introduction Although it has been suggested that neurotensin is involved in a variety of physiological processes, evidence has been largely contingent on the availability of potent, selective and biologically stable receptor antagonists. Recently we described the biochemical and pharmacological properties of the first non-peptide neurotensin receptor antagonist, SR 48692, 2-{[1-(7-chloroquinolin-4-yl)-5-(2,6-dimethoxyphenyl)-1H-pyrazole-3-carbonyl]amino}-adamantane-2-carboxylic acid (Gully *et al.*, 1993; Vita *et al.*, 1993) that was also shown to inhibit neurotensin binding *in vitro* to specific sites in guinea-pig intestinal tissues (Labbé-Jullié *et al.*, 1994).

The present study was designed to investigate the effects of SR 48692 on rat gastric emptying and acute defaecation, with a view to clarifying the presumed underlying role of endogenous neurotensin.

Methods Crl:CD BR, male rats (220-250 g) handled according to internationally accepted principles for care of laboratory animals, were used. The rats were kept under standard conditions and had free access to water and food (4RF21, Mucedola, Italia).

For assessment of gastric emptying rats were deprived of food 24 h before the test and were placed in cages with a wire mesh bottom with water freely available. A 3 ml bolus of a standard meal at 25°C was given by gavage. The non-caloric meal contained 2 ml of $BaSO_4$ (113% w/v, Prontobario Esofago, Bracco S.p.A., Italia) plus 1 ml 0.5% carboxymethylcellulose (CMC) and 0.05% phenol-red. The caloric meal was a 0.5% CMC suspension of standard chow (2 g of 4RF21 in 3 ml of CMC). Both meals had the same viscosity of about 1900 mPa s^{-1} at 25°C.

Rats were killed by cervical dislocation immediately ($t=0$), 15 and 30 min after the non-caloric meal, or 0, 30 and 60 min after the caloric meal. The pylorus and the oesophageal junction were clamped before excision of the stomach.

After the caloric meal, the gastric content was assessed by weighing the stomachs before and after removing their contents and then cutting, rinsing and blotting on dry tissues. After the non-caloric meal, the stomachs were minced and vigorously stirred for 15 min in 20 ml 0.1 N NaOH. After centrifugation (3,000 r.p.m. for 15 min), 1 ml of supernatant was diluted with 9 ml of 0.1 N NaOH and the samples were read for absorbance at 560 nm.

At each time, the remaining content of the stomach after drug treatment was compared to that of control drug-free rats, killed at $t=0$. The percentage gastric emptying was calculated for each rat: % GE = 1 - (content of treated rats/mean content of control rats) × 100.

The dose of SR 48692 producing 50% of its assumed maximal effect, obtained at 0.1 mg kg^{-1}, (ED_{50}) was calculated graphically from the log-dose response-curve.

Faecal excretion was assessed according to the method previously described (Croci & Bianchetti, 1992).

Drugs were given either s.c. or p.o. (gavage) in 2 ml kg^{-1} vehicles, i.e. CMC (SR 48692) or saline (ICS 205,930); control drug-free rats received only the vehicle.

SR 48692 was synthesized at SANOFI Recherche (Montpellier, France). ICS 205,930 HCl (endo-8-methyl-8-azabicyclo[3.2.1]oct-3-ol-indol-3-yl carboxylate.HCl) was purchased from RBI (Natick, MA, U.S.A.).

Results Gastric emptying was faster in control drug-free rats receiving a non-caloric standard meal (% GE ± s.e.mean, 52 ± 5 and 73 ± 3 respectively, at 15 and 30 min, $n=12$, $P<0.05$) than in those fed the caloric meal (at 30 and 60 min respectively 13 ± 2 and 50 ± 2, $n=7$, $P<0.01$).

SR 48692 had no significant effect on gastric emptying of the non-caloric meal (% GE ± s.e.mean, $n=10-15$, at 15 and 30 min: SR 48692 0.1 mg kg^{-1} 49 ± 5 and 64 ± 3; 1 mg kg^{-1} 42 ± 6 and 68 ± 4) but dose-dependently increased that of the caloric meal (ED_{50} 0.7 and 0.8 $\mu g\ kg^{-1}$ at 30 and 60 min) (Figure 1).

The stimulation of gastric emptying by 1 mg kg^{-1} SR 48692 was also tested in a separate experiment: after 30 min it was 38% more than control. This was slightly less than that achieved by 0.1 mg kg^{-1} SR 48692 (55%), indicating that the neurotensin receptor antagonist had already attained its maximal effect at 0.1 mg kg^{-1}.

The 5-HT_3 receptor antagonist, ICS 205,930 (ICS) (0.1 mg kg^{-1}, s.c. injected 30 min before the meal) significantly increased ($P<0.01$) gastric emptying in rats fed either of the standard meals (% GE ± s.e.mean, $n=7$, at 30 and 60 min after the caloric meal, control 5 ± 5 and 34 ± 3; ICS 38 ± 2 and 73 ± 5, $P<0.01$; 15 min after the non-caloric meal, control 53 ± 5; ICS 79 ± 3, $P<0.01$).

SR 48692 promoted defaecation dose-dependently (AD_1 = 1.9 $\mu g\ kg^{-1}$ p.o.) and the faecal water content was increased concurrently as indicated by the higher ratios of wet to dry weight (Table 1).

[1] Author for correspondence.

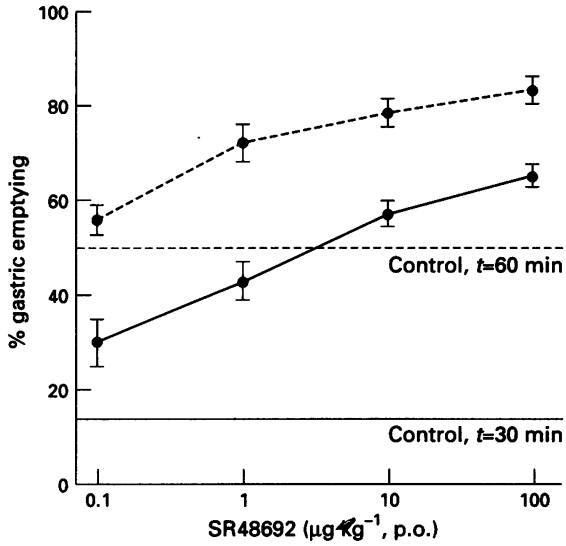

Figure 1 Stimulation of gastric emptying by SR 48692 in rats fed a caloric meal. SR 48692 was given 60 min before the meal, and the gastric content was assessed after 30 (solid line) and 60 min (dotted line). The results are mean ± s.e.mean of seven rats. Values are significantly different from their respective controls ($P < 0.01$, Duncan's test) with the exception of that at 0.1 $\mu g\,kg^{-1}$ SR 48692 (60 min).

Discussion The present study shows that the highly selective, non-peptide, neurotensin receptor antagonist, SR 48692, potently affects rat gut functions such as gastric emptying, faecal output and faecal water content. SR 48692, that is orally effective, has no intrinsic agonist activity, either *in vitro* or *in vivo*, on neurotensin receptors (Gully *et al.*, 1993). It potently and dose-dependently accelerated gastric emptying in rats fed a caloric meal, but not in those receiving a non-caloric meal. The two meals were otherwise identical as to viscosity and volume.

Although drug-free control rats receiving the non-caloric rather than the caloric meal presented substantially faster gastric emptying, the positive control provided by ICS 205,930 confirmed that the test system adequately discloses the ability of any suitable agent to shorten further the time required for stomach emptying. Our results thus suggest that neurotensin released by food, but not by gastric distension, is responsible for the lower rate of gastric emptying in drug-free control animals, and strongly support the involvement of this hormonal factor in the action of SR 48692 on the stomach.

Since SR 48692 stimulated faecal output and increased faecal water content at remarkably low doses, comparable to those effective on gastric emptying, the same neurotensin-mediated mechanism is likely to be involved. This supports an additional role already proposed for neurotensin, in influencing peristalsis as well as fluid secretion and absorption in the intestine (Hellström *et al.*, 1982; Ferris, 1989).

Table 1 Effect of SR 48692 on rat faecal excretion

SR 48692 dose (μg kg^{-1}, p.o.)	*Faecal dry weight* (g)	*AD_1*[a] (μg kg^{-1}, p.o.)	*Wet/dry weight of faeces*
–	0.10 ± 0.07		1.88 ± 0.04[b]
0.1	0.63 ± 0.04**		2.87 ± 0.09**
1	0.90 ± 0.07**	1.9	3.10 ± 0.32**
10	1.19 ± 0.08**	(1–3.6)	3.11 ± 0.11**
100	1.54 ± 0.13**		3.30 ± 0.11**

[a]AD_1 = dose-inducing excretion of 1 g (dry weight) of faeces during 210 min after administration of SR 48692
[b]Faeces collected 2–3 h before treatment
Data are means ± s.e.mean of eight rats with 95% confidence limits in parentheses.
**$P < 0.01$ vs control drug-free rats (Duncan's test)

References

CROCI, T. & BIANCHETTI, A. (1992). Stimulation of faecal excretion in rats by α2-adrenergic antagonists. *J. Pharm. Pharmacol.*, **44**, 358–360.

FERRIS, C.F. (1989). Neurotensin. In *Handbook of Physiology: The Gastrointestinal System*, Vol. 2, ed. Makhlouf, G.M. pp. 559–586. New York: Oxford University Press.

GULLY, D., CANTON, M., BOIGEGRAIN, R., JEANJEAN, F., MOLIMARD, J.C., PONCELET, M., GUEUDET, C., HEAULME, M. *et al.* (1993). Biochemical and pharmacological profile of a potent and selective nonpeptide antagonist of the neurotensin receptor. *Proc. Natl. Acad. Sci. U.S.A.*, **90**, 65–69.

HELLSTRÖM, P.M., NYLANDER, G. & ROSELL, S. (1982). Effects of neurotensin on the transit of gastrointestinal contents in the rat. *Acta Physiol. Scand.*, **115**, 239–243.

LABBÉ-JULLIÉ, C., DESCHAINTRES, S., GULLY, D., LE FUR, G. & KITABGI, P. (1994). Effect of the nonpeptide neurotensin antagonist SR 48692, and two enantiomeric analogs, SR 48527 and SR 49711, on neurotensin binding and contractile responses in guinea-pig ileum and colon. *J. Pharmacol. Exp. Ther.*, **271**, 267–276.

VITA, N., LAURENT, P., LEPORT, S., CHALON, P., DUMONT, X., KAGHAD, M., GULLY, D., LE FUR, G., FERRARA, P. & CAPUT, D. (1993). Cloning and expression of a complementary DNA encoding a high affinity human neurotensin receptor. *FEBS Lett.*, **317**, 139–142.

(Received November 18, 1994
Accepted March 9, 1995)

British Journal of Pharmacology (1995) 115, 385-388

SPECIAL REPORT

Direct demonstration of sulphonylurea-sensitive K_{ATP} channels on nerve terminals of the rat motor cortex

[1]Kevin Lee, Alistair K. Dixon, Iain C.M. Rowe, [2]Michael L.J. Ashford & Peter J. Richardson

Department of Pharmacology, University of Cambridge, Tennis Court Road, Cambridge CB2 1QJ

We examined whether ATP-sensitive potassium (K_{ATP}) channels are present on presynaptic terminals of the rat motor cortex, an area of the CNS exhibiting a high density of sulphonylurea binding. A novel fused nerve terminal preparation was developed which produced structures amenable to patch clamp methods. In inside-out recordings a K^+channel was observed which possessed all the major features of the Type 1 K_{ATP} channel, including sensitivity to ATP and the antidiabetic sulphonylureas.

Keywords: K_{ATP}-channel; motor cortex; sulphonylureas; nerve terminals; potassium

Introduction ATP sensitive $K^+(K_{ATP})$ channels are widely distributed in mammalian tissues and act to provide a link between the metabolic status and electrical excitability of cells (Ashcroft & Ashcroft, 1990). Intracellular ATP concentrations fall during anoxia and ischaemia, and it has been speculated that the consequent activation of these K^+channels mediates cytoprotection through an increased outward current and hyperpolarization. Thus, in regions of the CNS such as the hippocampus, it has been proposed that these channels serve a neuroprotective role under conditions of metabolic stress. Evidence in favour of this hypothesis has been obtained from indirect studies (e.g. by monitoring the release, or the subsequent action, of transmitters) using the antidiabetic sulphonylureas which are considered to be specific ligands for the K_{ATP} channel (Ashcroft & Ashcroft, 1992).

Although K_{ATP} channels have been reported to be present in the somata of rat cultured neonatal cortical neurones (Ashford *et al.*, 1988; Ohno-Shosaku & Yamamoto, 1992) their incidence is extremely low in contrast to the high density of sulphonylurea binding in the cortex (Ashcroft & Ashcroft, 1992). Furthermore, from studies of regulation of transmitter release in the CNS it has been suggested that K_{ATP} channels are present on presynaptic terminals (Miller, 1990). Using a combination of subcellular fractionation and patch clamp recording, we show directly the presence of K_{ATP} channels in nerve terminals of the rat motor cortex and demonstrate that they are coupled functionally to sulphonylurea receptors.

Methods Cerebral cortices from male Sprague Dawley rats (150-250 g) were homogenized in 10 volumes of 50 mM Tris-HCl, (pH 7.4) containing 0.32 M sucrose and nerve terminals prepared by standard methods. Lactate dehydrogenase (LDH), choline acetyltransferase (ChAT), acetylcholinesterase (AChE), and protein content were measured as described by Richardson *et al.* (1984). Citrate synthase was determined by the method of Srere (1969), ATP by the luciferase assay and glutamate by the fluorescent method of Nicholls *et al.* (1987).

Nerve terminals were washed in 5 volumes of HEPES buffer which contained (in mM): NaCl 135.0, KCl 5.0, $CaCl_2$ 1.0, $MgCl_2$ 1.0, HEPES 10.0, glucose 10, pH adjusted to 7.2 with NaOH. The washed nerve terminals were centrifuged at 2,500 g for 5 min, the resultant pellet resuspended in approximately 200 μl and incubated at 37°C for 5 min. Membrane fusion was initiated by the addition of 0.5 ml polyethylene glycol (0.8 g ml^{-1} in HEPES buffer) over 1 min period. After a further minute, the suspension was diluted with 20 ml of HEPES buffer at a rate of 1 ml min^{-1}, and then dialysed against HEPES buffer at 4°C for 2 h. The resulting aggregates of fused nerve terminals were between 5-10 μm in diameter. All experiments were performed at room temperature (20-23°C) using the inside-out configuration of the patch clamp technique. Detection and analysis of single channel currents were as described previously (Lee *et al.*, 1994). The pipette solution contained (in mM): KCl 140.0, EGTA 1.0, $CaCl_2$ 1.0, $MgCl_2$ 1.0, HEPES 10.0 whilst the bath solution composition was (in mM): KCl 140.0, $CaCl_2$ 2.0, $MgCl_2$ 1.0, EGTA 10.0, HEPES 10.0, adjusted to pH 7.2 with KOH.

The following reagents were used: polyethylene glycol (PEG 1300-1600), tolbutamide, glibenclamide, ATP and trypsin (Sigma).

Results The enzyme and ATP content of the fused nerve terminals (fusasomes) are shown in Table 1, where it can be seen that the fused nerve terminals contain the cytoplasmic enzyme lactate dehydrogenase, the plasma membrane marker acetylcholinesterase and the mitochondrial enzyme citrate synthase. In addition small molecules such as ATP and glutamate were retained within the fusasomes.

Using the inside out configuration of the patch clamp technique a total of 15 recordings were obtained from the fusasomes. In 8 recordings, channel activity was observed which displayed no clear dependence of open probability (P_{open}) on membrane potential (-70 mV to +60 mV), and was insensitive to the intracellular Ca^{2+} concentration (60 nM to 1 mM). The channel current-voltage relationship was linear at negative membrane potentials but showed slight inward rectification at positive voltages (Figure 1a). Over the voltage

Table 1 The fused nerve terminal preparation

Marker	*Content*
Protein (mg)	4.8±0.5
AChE (nmol min^{-1})	75.3±19.0
LDH (nmol min^{-1})	37.5±7.7
Citrate synthase (nmol min^{-1})	175.1±32.0
ATP (nmol)	10.2±0.14
Glutamate (nmol)	5.52±0.05

The nerve terminals derived from the motor cortex of two rats were fused and the activities of the markers measured as described. AChE: acetylcholinesterase; LDH, lactate dehydrogenase. The results are means±s.e.mean from three responsive experiments.

[1]Preset address: Vollum Institute, Oregan Health Sciences University, 3181 S.W. Sam Jackson Park Road, Portland, OR 97201, U.S.A.
[2]Author for correspondence.

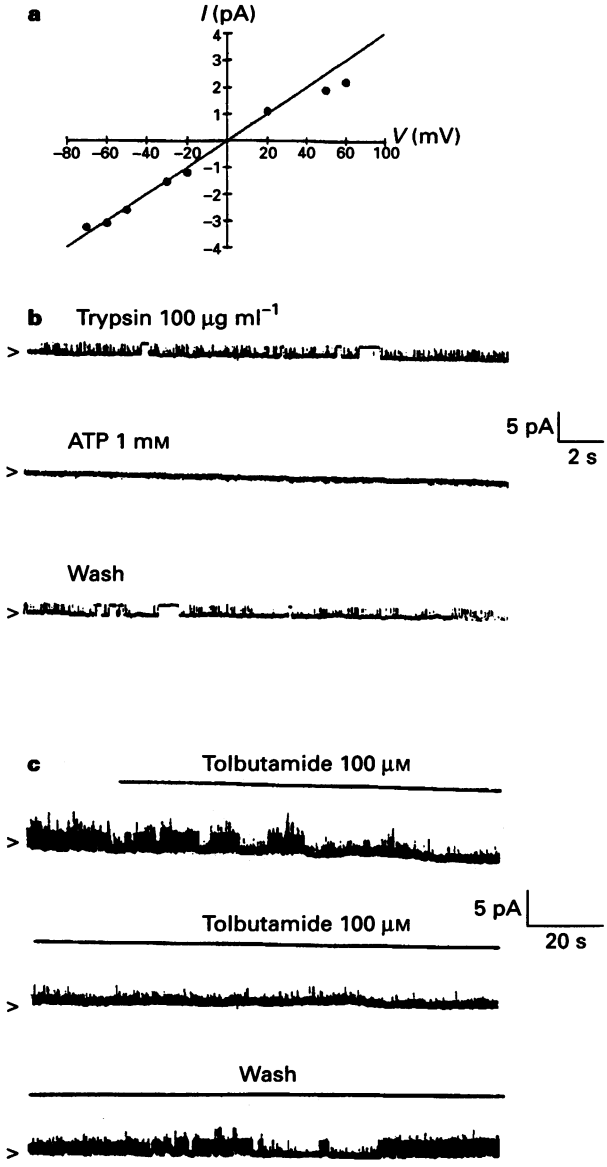

Figure 1 (a) Current voltage relationship of channels recorded in symmetrical 140 mM KCl. The line drawn through the points is the line of best fit for the linear portion of the curve (−70 to +20 mV) determined by linear regression and represents a slope conductance of 52 pS. (b) The effect of 1 mM ATP upon the activity of a trypsinized channel recorded from fusasome membranes. Following patch formation, there was a loss of channel activity within 30 s. Application of 100 μg ml^{-1} trypsin to the intracellular surface of the excised patch activated a 50 pS channel (P_{open} of 0.67). The subsequent application of 1 mM ATP inhibited channel activity (P_{open} of 0.0) in a reversible manner (P_{open} of 0.62 after wash). The holding potential was −50 mV. (c) The effect of tolbutamide upon the activity of the 52 pS channel in an inside-out patch obtained from a fusasome. Prior to the application of tolbutamide the 52 pS channel present in the recording exhibited a P_{open} of 0.46. Following the application of 100 μM tolbutamide, there was a block of channel activity (P_{open} of 0.0). The effects of tolbutamide were reversible following its removal from the bath solution (P_{open} of 0.48). The holding potential was +50 mV.

range −70 to +20 mV, the channel had a mean single channel conductance of 52.5±3.3 pS (n=3). In 50% of recordings there was a rapid loss (within 10 min) of channel activity (rundown) following patch excision. Following rundown, application of 100 μg ml^{-1} trypsin to the intracellular surface of the excised patch resulted in a rapid reactivation of channel activity. Furthermore in 3 patches where no channel activity was observed on patch excision, application of 100 μg ml^{-1} trypsin resulted in the appearance of the channel described above. Application of 1 mM ATP caused a rapid and reversible complete inhibition (n=4) of channel activity (Figure 1b). Channel activity in excised patches was also sensitive to inhibition by the sulphonylureas. Figure 1c shows the reversible inhibition of K_{ATP} channel activity by application of 100 μM tolbutamide (n=3). Complete inhibition of channel activity was also observed on the one occasion when 1 μM glibenclamide was applied to an excised patch. The remaining patches exhibited either large-conductance Ca^{2+}-activated K^+ channels (n=2) or no channel activity even upon trypsinisation (n=2).

Discussion We fused mammalian isolated nerve terminals into larger aggregates using polyethylene glycol, a procedure commonly used to promote membrane fusion. This has the advantage of minimally disrupting the membrane architecture, in contrast to procedures involving solubilization followed by incorporation of membrane components into lipid bilayers.

Using inside-out membrane patches excised from fusasomes, we observed the presence of a particular type of K^+channel in 73% of recordings. This channel had a unitary conductance of 52 pS, exhibited inward rectification at depolarized membrane voltages, had a P_{open} insensitive to membrane voltage or intracellular Ca^{2+}, but underwent a rapid loss of activity with time following patch excision (rundown). The rundown of this channel was variable, in some patches activity was lost prior to excision. This may simply reflect permeabilisation of the membranes to small ions (e.g. Mg^{2+}), during the fusion process resulting in K_{ATP} channel rundown (Lee *et al.*, 1994). Exposure of the intracellular surface of patches containing rundown K_{ATP} channels to trypsin in pancreatic β-cells produces a dramatic reactivation of channel activity (Proks & Ashcroft, 1993). The 52 pS channel present in the fusasomes was also reactivated by the application of trypsin to the intracellular surface of excised patches. The fundamental feature of K_{ATP} channels is the inhibition of channel activity by ATP. The channel described above was also inhibited by the application of millimolar concentrations of ATP to the intracellular aspect of the excised patch. Furthermore channel activity was reversibly inhibited by the sulphonylureas glibenclamide and tolbutamide. Therefore the channel described reproduces the essential properties of the Type I K_{ATP} channel (Ashcroft & Ashcroft, 1990). This is the first direct demonstration of functional sulphonylurea-sensitive K_{ATP} channels in mammalian nerve terminals.

K.L. was a Wellcome Prize student and A.K.D is supported by BBSRC. This work was supported in part by grants from the Wellcome Trust (M.L.J.A.).

References

ASHCROFT, S.J.H. & ASHCROFT, F.M. (1990). Properties and functions of ATP sensitive K^+ channels. *Cell Signal.*, **2**, 197–214.

ASHCROFT, F.M. & ASHCROFT, S.J.H. (1992). The sulphonylurea receptor. *Biochem. Biophys. Acta*, **1175**, 45–59.

ASHFORD, M.L.J., STURGESS, N.C., TROUT, N.J., GARDNER, N.J. & HALES, C.N. (1988). Adenosine-5'-trisphosphate-sensitive ion channels in neonatal cultured central neurones. *Pflügers Arch.*, **412**, 297–304.

LEE, K., OZANNE, S.E., HALES, C.N. & ASHFORD, M.L.J. (1994). Mg^{2+}-dependent inhibition of K_{ATP} channels by sulphonylureas in CRI-G1 insulin secreting cells. *Br. J. Pharmacol.*, **111**, 632–640.

MILLER, R.J. (1990). Glucose-regulated potassium channels are sweet news for neurobiologists. *Trends Neurosci.*, **13**, 197–199.

NICHOLLS, D.G., SIHRA, T.S. & SANCHEZ-PRIETO, J. (1987). Calcium dependent and independent release of glutamate from synaptosomes monitored by continuous fluorometry. *J. Neurochem.*, **49**, 50–57.

OHNO-SHOSAKU, T. & YAMAMOTO, C. (1992). Identification of an ATP-sensitive K+ channel in rat cultured cortical neurons. *Pflügers Arch.*, **422**, 260–266.

PROKS, P. & ASHCROFT, F.M. (1993). Modification of KATP channels in pancreatic β cells by trypsin. *Pflügers Arch.*, **424**, 63–72.

RICHARDSON, P.J., SIDDLE, K. & LUZIO, J.P. (1984). Immunoaffinity purification of intact, metabolically active, cholinergic nerve terminals from mammalian brain. *Biochem. J.*, **219**, 647–654.

SRERE, P.A. (1969). Citrate synthase. In *Methods in Enzymol.* Vol. XIII, pp. 3–8. New York: Academic press.

(Received February 28, 1995
Accepted March 9, 1995)

British Journal of Pharmacology (1995) 115, 389-394

GABA-mediated inhibition of the anaphylactic response in the guinea-pig trachea

[1]Grazia Gentilini, Sergio Franchi-Micheli, Sabrina Mugnai, Daniela Bindi & Lucilla Zilletti

Department of Preclinical and Clinical Pharmacology 'Mario Aiazzi Mancini', University of Florence, Viale G.B.Morgagni, 65, 50134 Florence, Italy

1 In sensitized guinea-pigs, the effects of γ-aminobutyric acid (GABA) and GABAmimetic drugs have been investigated on tracheal segments contracted by cumulative application of an allergen (ovoalbumin, OA) and on serosal mast cells. The same drugs have also been tested on activation of alveolar macrophages isolated from unsensitized guinea-pigs.

2 Superfusion with GABA (1-1000 μM) reduced the contraction intensity of tracheal strips. The effect of GABA (100 μM) was not affected by the carrier blockers, nipecotic acid and β-alanine (300 μM each). It was mimicked by the $GABA_B$ agonist (-)-baclofen (100 μM) but not 3-aminopropanephosphinic acid (100 μM, 3-APA). The $GABA_A$ agonist, isoguvacine (100 μM) did not exert any effect. GABA (10 μM)-induced inhibition of tracheal contractions was reduced by the $GABA_B$ antagonist, 2-hydroxysaclofen (100 μM, 2-HS), but not by the $GABA_A$ antagonist, bicuculline (30 μM).

3 The reduction in contraction intensity induced by GABA (100 μM) was prevented by a 40 min preincubation of tracheal strips with capsaicin (10 μM), but not tetrodotoxin (TTX, 0.3 μM). The effect of GABA (1000 μM) was absent after preincubation with indomethacin (2.8 μM) but unmodified when nordihydroguaiaretic acid (NDGA, 3.3 μM) was used. Finally, removal of the epithelium prevented the GABA effect.

4 Anaphylactic histamine release from serosal mast cells isolated from sensitized animals was not affected either by GABA (10-1000 μM) or the selective receptor agonists (-)-baclofen (0.1-1000 μM) and isoguvacine (10-1000 μM). The release of platelet-activating factor (PAF) from alveolar macrophages stimulated by formyl-Met-Leu-Phe (FMLP; 1 μM) was modified neither by GABA (100 μM) nor by (-)-baclofen (100 μM).

5 In conclusion, these data show that GABA can inhibit allergic phenomena in the guinea-pig airways through activation of $GABA_B$ receptors. An involvement of neuropeptidergic sensory structures is suggested but a role for epithelial cells and arachidonate metabolites is not definitely proved.

Keywords: GABA; baclofen; $GABA_B$ receptors; allergy; guinea-pig trachea; airways; capsaicin; indomethacin; mast cells; alveolar macrophages

Introduction

Sudden occurrence of bronchospasms in allergic asthma depends on both flogistic and autonomic phenomena, and several interactions occur between nerve structures and inflammatory cells. The sensitized cell exocytotic process which follows challenge with the antigen in the anaphylactic reaction can be modulated by various neurotransmitters.

γ-Aminobutyric acid (GABA), acting through $GABA_A$ and $GABA_B$ receptors, appears to have a peculiar role as a neuromodulator in the neurovegetative system, since it can influence the release of neurotransmitters such as acetylcholine, noradrenaline or peptides (for comprehensive reviews see Erdö & Bowery, 1986; Giotti *et al.*, 1990). Following our observation that GABAmimetic agents protect from allergic bronchospasm in guinea-pigs (Luzzi *et al.*, 1986), the existence of both $GABA_A$ and $GABA_B$ receptors has been pharmacologically demonstrated in the mammalian respiratory tract (Tamaoki *et al.*, 1987; Shirakawa *et al.*, 1987; Belvisi *et al.*, 1989; Ray *et al.*, 1991; Chapman *et al.*, 1991; 1993). These receptors for GABA are responsible for the inhibition of tracheal bronchial smooth muscle contraction *in vivo* and *in vitro*, and for the reduced release of transmitters which stimulate the airway smooth muscles.

We have also observed that GABA agonists inhibited the anaphylactic release of histamine from guinea-pig isolated ileum during the Schultz-Dale reaction (Zilletti *et al.*, 1992) and reduced the release of spasmogens in both pulmonary (Luzzi *et al.*, 1987) and tracheal (Gentilini *et al.*, 1990b) guinea-pig tissues. In the present study the effect of several GABAmimetic drugs on allergen-induced contraction of tracheal strips isolated from actively sensitized guinea-pigs has been further examined. The effect of these drugs on histamine release from mast cells and platelet-activating factor (PAF) formation in macrophages has also been assessed.

A preliminary account of this study has been published (Zilletti *et al.*, 1992).

Methods

Tracheal preparations

Male guinea-pigs (250-350 g) were actively sensitized by subcutaneous (s.c.) injection of ovoalbumin (OA, 500 μg) plus Freund's adjuvant. Four to seven weeks later, animals were killed by head trauma and exsanguination. Tracheae were removed, carefully trimmed of fatty and connective tissue, and cut into spiral strips, which were divided into two parts, randomly chosen as control and drug-treated preparations. Some strips had the epithelium removed by gentle rubbing. Each tissue was mounted into a 10 ml organ bath under 2 g of passive tension, continuously superfused with a modified Krebs-Henseleit solution at 37°C, bubbled with 95% O_2 + 5% CO_2 and connected to a recorder via an isometric trans-

[1] Author for correspondence.

ducer (MARB; Italy). Preparations were equilibrated for about 60 min. OA was cumulatively added to the organ bath ($0.001-100\ \mu g\ ml^{-1}$ in $100\ \mu l$ total volume) after transient contraction of tracheal strips with histamine at the maximally active concentration of $28\ \mu M$.

GABA receptor agonists were superfused for 20 min before challenge with the allergen. Receptor antagonists or uptake inhibitors were present 30 min prior to GABA, whilst indomethacin and nordihydroguaiaretic acid (NDGA), capsaicin and tetrodotoxin (TTX) were superfused for 40 min before GABA.

Neither GABA nor all drugs acting at GABA receptors that were tested affected the tracheal smooth muscle tone or the contraction evoked by histamine ($28\ \mu M$).

Responses to OA were calculated as intensity at peak and expressed as % of maximal histamine-evoked contractions. Data are mean ± s.e.mean. Statistical analysis was performed on data referring to two tracheal strips from the same animal by using Student's paired t test with a significant level achieved at $P<0.05$.

Mast cell preparation

Serosal mast cells were isolated from sensitized guinea-pigs as already described (Gentilini *et al.*, 1994). Cell viability was checked by a dye exclusion test (0.4% trypan blue) and the cell count determined by staining with 0.1% toluidine blue. Cells ($130-150 \times 10^3$, 80–85% mast cells) were incubated at 37°C in the presence or absence of drugs acting at GABA receptors for 3 min and challenged with $5\ mg\ ml^{-1}$ OA for a further 3 min. Histamine content in the cell supernatant and pellet (extracted with 0.1 M HCl) was evaluated by fluorimetric determination (Shore *et al.*, 1959; Kremzer & Wilson, 1961). Histamine release was expressed as % of the total content (approximately $1.5-5.0\ \mu g$ per 10^6 cells). Spontaneous release of histamine was less than 8% and subtracted from each sample.

Alveolar macrophages preparation

Monolayers of alveolar macrophages taken from unsensitized guinea-pigs were prepared as described by Brunelleschi *et al.* (1990). Adherent cells (>95% macrophages) were incubated with drugs acting at GABA receptors for 2 min prior to 5 min challenge with formyl-Met-Leu-Phe (FMLP, $1\ \mu M$). Platelet-activating factor (PAF) was determined according to Parente & Flower (1985).

Materials

The following drugs were purchased from Sigma Chemical Co. (Milan, Italy): ovoalbumin, GABA, 5-aminovaleric acid, β-alanine, nipecotic acid, tetrodotoxin, indomethacin, nordihydroguaiaretic acid, FMLP, collagenase type I, o-phthaldialdehyde, Tris(hydroxymethyl)aminomethane, [4-(2-hydroxyethyl)-1-piperazineethane-sulphonic acid] (HEPES), apyrase, gelatin type B. Other drugs and sources were as follows: (−)-baclofen (Giba-Geigy, Basel, Switzerland), isoguvacine hydrochloride (Research Biochemicals Inc., Milan, Italy), 3-aminopropylphosphinic acid (Smith Kline Beecham), bicuculline methiodide (Pierce), 2-hydroxysaclofen (Tocris Neuramin), capsaicin (Serva), histamine hydrochloride (Carlo Erba, Milan), PAF C16 (Bachem Feinchemikalien), fatty acid-free bovine serum albumin, fraction V (Boerhinger Mannheim), Minimum Essential Medium with Earle's salts (Gibco), foetal calf serum (Gibco), streptomycin sulphate (Bristol-Myers Squibb), sodium penicillin G (Farmitalia, Milan). All reagents used were of highest grade (Merck).

Results

In tracheal strips isolated from sensitized guinea-pigs, superfusion with GABA ($100\ \mu M$) induced a significant reduction of OA-elicited contraction intensity (Figure 1). The effect of GABA was concentration-dependent ($1-1000\ \mu M$) (Figure 2). The $GABA_A$ agonist isoguvacine ($100\ \mu M$) did not modify the contractile response to the allergen (Figure 3), nor did 5-aminovaleric acid (5-AVA, 1 mM; not shown). The inhibitory effect of GABA was mimicked by the $GABA_B$ agonist, (−)-baclofen ($100\ \mu M$) but not by the more recently described agonist, 3-aminopropane-phosphinic acid (3-APA, $100\ \mu M$) (Figure 3).

Neither $GABA_A$ nor $GABA_B$ antagonists, bicuculline ($30\ \mu M$) and 2-hydroxysaclofen (2-HS, $100\ \mu M$) respectively, modified the contractile response to OA. The GABA ($10\ \mu M$) inhibitory effect was prevented by 2-HS (Figure 4a) whereas bicuculline was inactive (Figure 4b).

The presence of the GABA uptake inhibitors, β-alanine ($300\ \mu M$) and nipecotic acid ($300\ \mu M$) affected neither the tracheal response to OA nor the effect of GABA ($100\ \mu M$) (not shown).

Perfusion of tracheal strips with TTX ($0.3\ \mu M$) induced a slight but significant increase in OA-induced contraction (Figure 5a). In this experimental condition GABA ($100\ \mu M$) could still exert an inhibitory effect (Figure 5b). Superfusion with capsaicin ($10\ \mu M$) caused a reduction in the contractile

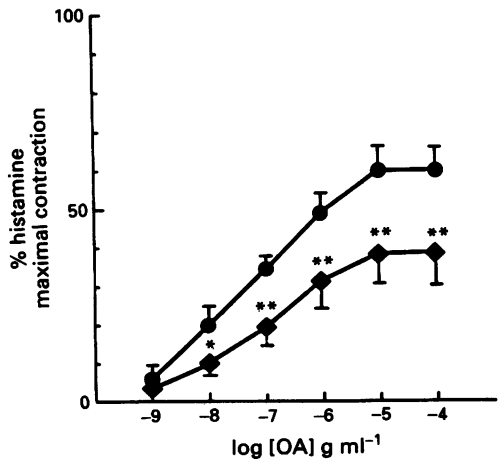

Figure 1 GABA-induced inhibition of tracheal contractile response to ovalbumin (OA) cumulatively administered to strips isolated from sensitized guinea-pigs: (●) controls; (◆) $100\ \mu M$ GABA. $^*P<0.05$; $^{**}P<0.005$; $n=10$.

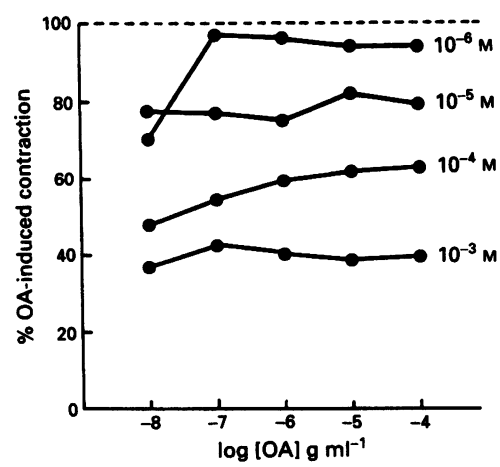

Figure 2 Concentration-dependency of GABA effect. Data are calculated as % of control values for each OA concentration ($n \geq 5$).

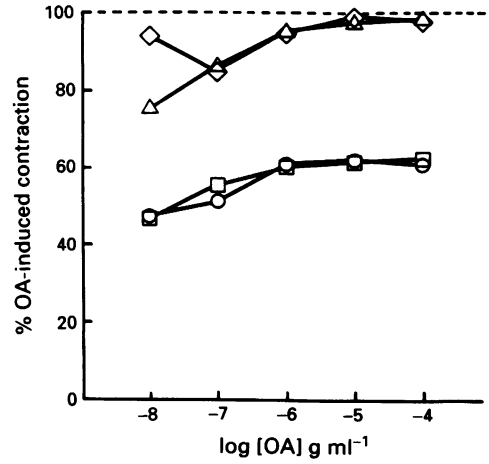

Figure 3 Effect of $GABA_A$ and $GABA_B$ receptor agonists on tracheal contractile response to ovalbumin (OA). Data are calculated as % of control values for each OA concentration. (□) 100 μM GABA; (○) 100 μM (−)-baclofen; (◇) 100 μM 3-aminopropanephosphinic acid (3-APA); (△) 100 μM isoguvacine. GABA and (−)-baclofen effects were statistically significant (compared to respective controls) at every OA concentration whereas the effect of neither 3-APA nor isoguvacine reached statistical significance ($n \geq 5$).

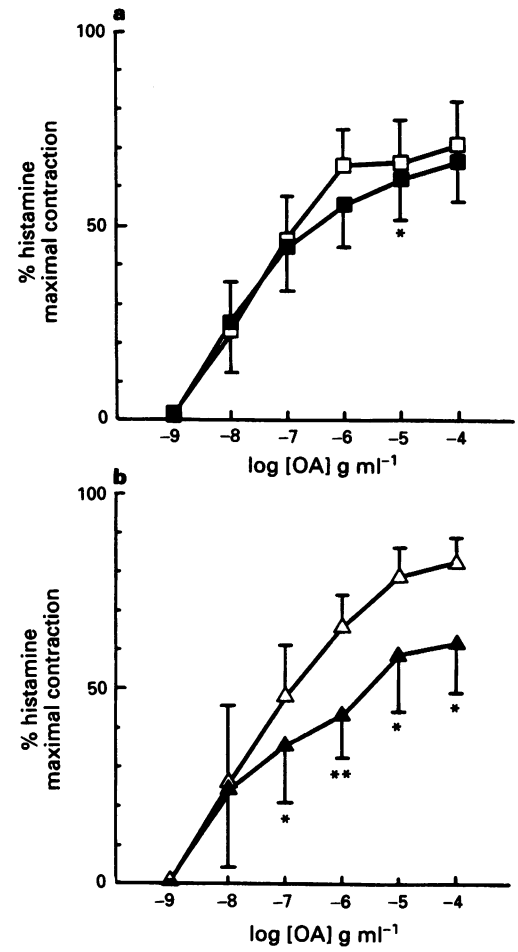

Figure 4 Effect of $GABA_A$ and $GABA_B$ receptor antagonists on GABA-induced inhibition of tracheal contractile response to ovalbumin (OA). (a) GABA (10 μM) + 2-hydroxysaclofen (2-HS, 100 μM) (■); (□) 2-HS alone. (b) GABA (10 μM) + bicuculline (30 μM) (▲); (△) bicuculline alone. $^*P<0.05$; $^{**}P<0.01$; $n \geq 5$.

response evoked by the allergen (Figure 5c) and prevented the effect of GABA (100 μM) (Figure 5d).

Removal of the epithelium significantly reduced the reactivity of the smooth muscle to antigen challenge and no further inhibition was observed upon addition of GABA (100 μM) (Table 1). Superfusion with the cyclo-oxygenase inhibitor, indomethacin (2.8 μM) caused a decrease in the basal tone of tracheal preparations but an increase in the response to histamine and OA challenge was observed. In the presence of indomethacin, GABA did not affect tracheal contractions (Table 1). The lipoxygenase inhibitor, NDGA (3.3 μM) had a slight effect on smooth muscle responsiveness or GABA (100 μM) inhibition (Table 1).

Challenge of serosal mast cells with OA caused a significant release of histamine with an average value of 53% of the total content. GABA (10–1000 μM) and (−)-baclofen (0.1–1000 μM) were inactive and inhibited the histamine release by only 10% and 19% respectively at the highest concentration. Isoguvacine (10–1000 μM) was ineffective. None of the drugs had any effect on the unstimulated release of histamine. Alveolar macrophages stimulated with FMLP (1 μM) released PAF in the supernatant, with an average value of 54% of total content. Neither GABA nor (−)-baclofen (1000 μM) influenced basal or stimulated release of PAF.

Discussion

OA-induced contraction of tracheal strips isolated from sensitized guinea-pigs appears to be a suitable model for immuno-mediated bronchoconstriction in man (Muccitelli *et al.*, 1987). GABA and agonists for the $GABA_B$ receptor can protect from the microshock evoked by allergen in sensitized guinea-pigs (Luzzi *et al.*, 1986) and GABA can inhibit the release of some mediators of anaphylaxis (Gentilini *et al.*, 1990b). In this study, GABA dose-dependently reduced the tracheal contraction induced by OA in sensitized guinea-pigs. However, it did not modify histamine-evoked contractions. The effect of GABA was not prevented by inhibitors of its uptake and appeared to be mediated by the $GABA_B$ receptor. In fact, the effect of GABA was mimicked by the $GABA_B$ agonist, baclofen and antagonized by the $GABA_B$ antagonist, 2-HS. The $GABA_A$ receptor did not appear to be involved in this effect of GABA, since it was not mimicked by isoguvacine or 5-AVA and was not modified by bicuculline. The $GABA_B$ receptor mediating the effect of GABA was not sensitive to the receptor agonist, 3-APA. Since it has been previously reported that contraction of tracheal strips by electrical stimulation was sensitive to both baclofen and 3-APA (Chapman *et al.*, 1991), this discrepancy may suggest $GABA_B$ receptor heterogeneity, although further investigation is required.

Superfusion of tracheal strips with TTX significantly increased OA-induced contractions, suggesting that a neurogenic inhibitory mechanism could be activated in response to challenge with the allergen. For instance, an adrenergic pathway has been reported to modulate negatively both histamine- and allergen-induced contraction of guinea-pig trachea (Undem *et al.*, 1989). However, GABA was equally active after TTX application, thus suggesting that non-neurogenic mechanisms or TTX-insensitive nerve terminals (Maggi & Meli, 1988), are involved in this effect.

In mammalian airways, the existence of capsaicin-sensitive, TTX-sensitive, nerve terminals containing several neuropeptides has been reported (Maggi & Meli, 1988). Though not in every experimental condition (Ingenito *et al.*, 1991), the involvement of capsaicin-sensitive fibres in models of allergy is well established (Saria *et al.*, 1983; Manzini *et al.*, 1987; Alving *et al.*, 1987; 1990; Gentilini *et al.*, 1990c; Kohrogi *et al.*, 1991). This was also confirmed under our experimental conditions, where depletion of neuropeptide-containing terminals by superfusion with capsaicin reduced the tracheal strip response to OA. Thus, neuropeptide release may occur

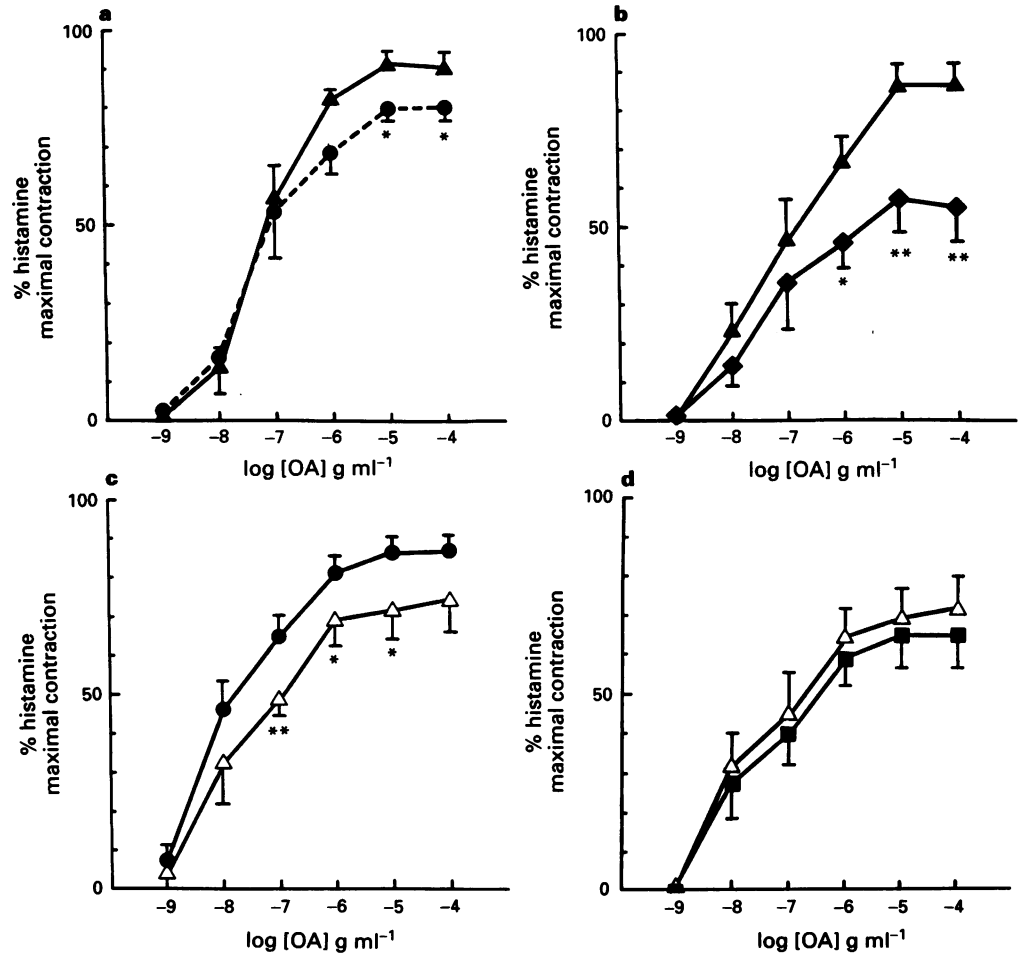

Figure 5 (a) Effect of tetrodotoxin (TTX) on tracheal contractile response to ovalbumin (OA), cumulatively administered, and (b) effect of GABA in the presence of TTX: (▲) 0.3 μM TTX; (●) controls; (◆) 0.3 μM TTX + 100 μM GABA. $*P<0.05$; $**P<0.02$; ($n \geqslant 5$). (c) Effect of capsaicin on tracheal contractile response to OA, and (d) lack of effect of GABA in the presence of capsaicin: (△) 10 μM capsaicin; (●) controls; (■) 10 μM capsaicin + 100 μM GABA. $*P<0.05$; $**P<0.005$; $n \geqslant 5$.

Table 1 Effect of removal of the epithelium and enzyme inhibitors on GABA inhibition of guinea-pig tracheal strip contraction

	Ovalbumin (g ml^{-1})					
Treatment	10^{-9}	10^{-8}	10^{-7}	10^{-6}	10^{-5}	10^{-4}
Control	6 ± 3.7	25.3 ± 8.9	52 ± 10.9 (**)	64.5 ± 9.4 (*)	81 ± 9.6 (**)	82.1 ± 9.1 (*)
No epithelium	4.1 ± 2.5	22.5 ± 7.3	44 ± 10	57 ± 10.4	67.4 ± 10.5	68 ± 10.1
No epithelium	7.7 ± 5.7	49.5 ± 9.5	67.8 ± 8	90.4 ± 3.3	96 ± 3.4	97 ± 3.3
No epithelium + GABA 100 μM	0.75 ± 0.7	37.5 ± 12	64 ± 6	79 ± 4	86.4 ± 4	88.7 ± 4
Control	7.5 ± 7.5	22.5 ± 9.8	35.7 ± 10.6 (**)	46 ± 9 (**)	54.5 ± 10 (***)	58.7 ± 8 (**)
Indomethacin 2.8 μM	0	44 ± 13.9	65.7 ± 9.6	82 ± 9.1	92.2 ± 8.8	95.4 ± 7.6
Indomethacin 2.8 μM	0	30 ± 10	57.6 ± 7	75.8 ± 6.4	84 ± 7.3	85 ± 8
Indomethacin 2.8 μM + GABA 100 μM	0	13.4 ± 3	55.6 ± 6.5	77.2 ± 8	89 ± 7.3	88.6 ± 7.3
Control	0	74.7 ± 4.2 (*)	75.7 ± 10.5 (*)	83.7 ± 7	83 ± 6.7	84.7 ± 6.7
NDGA 3.3 μM	0	55.5 ± 6.8	59 ± 6	78.8 ± 5	81.8 ± 6	84.5 ± 5.1
NDGA 3.3 μM	2.3 ± 2.3	34.2 ± 5.2 (***)	50.3 ± 5 (***)	74.8 ± 5.5 (**)	85.8 ± 4.6 (*)	86.2 ± 4.8 (*)
NDGA 3.3 μM + GABA 100 μM	0	14.6 ± 1.7	31.5 ± 5.5	60.5 ± 8.8	71.7 ± 8.3	74.7 ± 8.4

$*P<0.05$; $**P<0.02$; $***P<0.01$.
Ovalbumin (OA) was cumulatively administered. Contractile response to OA is calculated as percentage of maximal histamine-evoked contraction.

after challenge with the allergen and contribute to the contractile response. The effect of GABA was absent in capsaicin-perfused tracheal strips suggesting that in normal strips, GABA inhibited the OA-induced contraction via release of neuropeptides from TTX-insensitive terminals. These data are supported by previous studies where $GABA_B$ agonists could inhibit guinea-pig bronchospasm mediated by the peptidergic system (Chapman *et al.*, 1993) and reduce K^+-stimulated substance P release from rat trachea (Ray *et al.*, 1991). GABA modulation of peptidergic sensory components in the periphery has also been reported (Giotti *et al.*, 1990). Such a mechanism may well explain the protective effect of baclofen on histamine- and prostaglandin $F_{2\alpha}$-induced bronchospasm in guinea-pig (Luzzi *et al.*, 1987). Indeed, the bronchial smooth muscle contraction elicited by these agents can be achieved either directly or indirectly through a reflex conducted by C-fibres (Coleridge & Coleridge, 1984).

Integrity of the tracheal epithelium was necessary to observe GABA inhibition of OA-induced tracheal strip contractions. Mechanical removal of the epithelium alters tracheal smooth muscle reactivity to spasmogens and to immunological stimuli (Hay *et al.*, 1986; Holroyde, 1986; Frossard & Muller, 1986; Tschirhart *et al.*, 1987; Undem *et al.*, 1988; Goldie *et al.*, 1990), the latter depending on the method used for sensitization (Bertrand *et al.*, 1989). Our data would suggest that some epithelial product is involved in the effect of GABA. This pathway should be *in sequence* and not *alternative* to the effect on neuropeptide terminals, since capsaicin alone dramatically affected GABA action. It is possible that removal of the epithelium alters the functions of the peptidergic terminals intraepithelially located (Lundberg & Saria, 1987) and this would explain the lack of effect of GABA.

After addition of indomethacin to inhibit cyclo-oxygenase activity, the tracheal tone was reduced and OA-induced contraction potentiated, as already reported (Brink *et al.*, 1981; Jones *et al.*, 1988; Braunstein *et al.*, 1988). In these conditions, GABA was not effective. However, GABA maintained its inhibitory action following block of lipoxygenase activity by addition of NDGA, which slightly modified the response to the allergen (Burka, 1983; Franchi-Micheli *et al.*, 1986). From these data the involvement of an endogenous prostanoid in the action of GABA could be proposed. Other explanations cannot be ruled out in view of the fact that indomethacin profoundly affected tracheal responsiveness (Brink *et al.*, 1981; Jones *et al.*, 1988; Braunstein *et al.*, 1988).

Amongst the cells involved in allergic inflammation, mast cells and alveolar macrophages have a pivotal role. Mast cells have high-affinity receptor for IgE and are likely to be primarily involved in the response to allergens (Holgate & Kay, 1985). Macrophages may have a principal role in perpetuating airway flogosis during allergy by releasing several multipotent mediators, like cytokines and PAF (Fuller, 1992). GABA and baclofen were found to be inactive in altering specific mast cell or macrophage activation. Therefore, it is confirmed that, with the exception of platelets (Oset-Gasque *et al.*, 1986; Gentilini *et al.*, 1990a), bone marrow-derived cells probably do not possess receptors for GABA.

In conclusion, these data show that GABA, through an activation of $GABA_B$ receptors, inhibits OA-induced contractions of tracheal strips isolated from sensitized guinea-pigs. This effect of GABA, requiring an intact epithelium, may be mediated by inhibition of the neuropeptidergic terminals activated by the antigen, with a possible involvement of a cyclo-oxygenase product.

This work was supported by National Research Council (CNR) target project 'Prevention and Control of Disease Factors', subproject 2 (n. 93.00763.PF41) and the Ministry of University and Scientific and Technologic Research (MURST, 60%). (−)-Baclofen was kindly supplied by Ciba-Geigy, Basel, Switzerland and 3-APA by Smith, Kline & French Lab Ltd., Herts, U.K.

References

ALVING, K., MATRAN, R., LACROIX, J.S. & LUNDBERG, J.M. (1990). Capsaicin and histamine antagonist-sensitive mechanisms in the immediate allergic reaction of pig airways. *Acta Physiol. Scand.*, **138**, 49–60.

ALVING, K., ULFGREN, A.K., LUNDBERG, J.M. & AHLSTEDT, S. (1987). Effect of capsaicin on bronchial reactivity and inflammation in sensitized adult rats. *Int. Arch. Allergy Appl. Immunol.*, **82**, 377–379.

BELVISI, M.G., ICHINOSE, M. & BARNES, P.J. (1989). Modulation of non-adrenergic non-cholinergic neural bronchoconstriction in guinea-pig airways via $GABA_B$ receptors. *Br. J. Pharmacol.*, **97**, 1225–1231.

BERTRAND, C., TSCHIRHART, E. & LANDRY, Y. (1989). Nedocromil sodium inhibits IgE- and IgG-related antigen-induced contraction in guinea-pig trachea. *Int. Arch. Allergy Appl. Immunol.*, **88**, 439–446.

BRAUNSTEIN, G., LABAT, C., BRUNELLESCHI, S., BENVENISTE, J., MARSAC, J. & BRINK, C. (1988). Evidence that the histamine sensitivity and responsiveness of guinea-pig isolated trachea are modulated by epithelial prostaglandin E_2 production. *Br. J. Pharmacol.*, **95**, 300–308.

BRINK, C., DUNCAN, P.G. & DOUGLAS, J.S. (1981). The response and sensitivity to histamine of respiratory tissues from normal and ovalbumin-sensitized guinea-pigs: effects of cyclooxygenase-oxygenase and lipoxygenase inhibition. *J. Pharmacol. Exp. Ther.*, **217**, 592–601.

BRUNELLESCHI, S., VANNI, L., LEDDA, F., GIOTTI, A., MAGGI, C.A. & FANTOZZI, F. (1990). Tachykinins activate guinea-pig alveolar macrophages: involvement of NK_2 and NK_1 receptors. *Br. J. Pharmacol.*, **100**, 417–420.

BURKA, J.F. (1983). Studies on the role of arachidonic acid metabolites in airways contraction induced *in vitro* by antigen and calcium ionophore A23187. *Agents Actions*, **13**, 318–326.

CHAPMAN, R.W., DANKO, G., RIZZO, C.A., EGAN, R.W., MAUSER, P.J. & KREUTNER, W. (1991). Prejunctional GABA-B inhibition of cholinergic, neurally-mediated airway contractions in guinea-pigs. *Pulm. Pharmacol.*, **4**, 218–224.

CHAPMAN, R.W., HEY, J.A., RIZZO, C.A. & BOLSER, D.C. (1993). $GABA_B$ receptors in the lung. *Trends Pharmacol. Sci.*, **14**, 26–29.

COLERIDGE, J.C.M. & COLERIDGE, H.M. (1984). Afferent vagal C fibers of the lung and airways and its functional significance. *Rev. Physiol. Biochem. Pharmacol.*, **99**, 1–110.

ERDÖ, S.L. & BOWERY, N.G. (1986). *GABAergic Mechanisms in the Mammalian Periphery*. New York: Raven Press.

FRANCHI-MICHELI, S., LUZZI, S., CIUFFI, M. & ZILLETTI, L. (1986). The effect of lypoxygenase inhibitors and leukotriene antagonists on anaphylaxis. *Agents Actions*, **18**, 242–244.

FROSSARD, N. & MULLER, F. (1986). Epithelial modulation of tracheal smooth muscle responses to antigenic stimulation. *J. Appl. Physiol.*, **61**, 1449–1456.

FULLER, R.W. (1992). Macrophages. In *Asthma: Basic Mechanisms and Clinical Management*. ed. Barnes, P.J., Rodger, I.W. & Thomson, N.C. pp. 99–109. London: Academic Press Ltd.

GENTILINI, G., DI BELLO, M.G., RASPANTI, S., BINDI, D., MUGNAI, S. & ZILLETTI, L. (1994). Salmeterol inhibits anaphylactic histamine release from guinea-pig isolated mast cells. *J. Pharm. Pharmacol.*, **46**, 76–77.

GENTILINI, G., FAILLI, P., GIOTTI, A., NARDI-DEI, V. & ZILLETTI, L. (1990a). Does GABA play a role in platelet function? *Eur. J. Pharmacol.*, **183**, 335–336.

GENTILINI, G., FRANCHI-MICHELI, S., CIUFFI, M., BINDI, D. & ZILLETTI, L. (1990b). GABA and neuropeptides affect anaphylaxis in guinea-pig airways. *Pharmacol. Res.*, **22** (Suppl. 1), 23–24.

GENTILINI, G., FRANCHI-MICHELI, S., CIUFFI, M., BINDI, D. & ZILLETTI, L. (1990c). Capsaicin and anaphylactic reactions in the guinea-pig airways. *Agents Actions*, **30**, 92–94.

GIOTTI, A., BARTOLINI, A., FAILLI, P., GENTILINI, G., MALCANGIO, M. & ZILLETTI, L. (1990). Review of peripheral $GABA_B$ effects. In *$GABA_B$ Receptors in Mammalian Function*. ed. Bowery, N.G., Bittiger, H. & Olpe, H.R. pp. 101–123. Chichester: John Wiley and Sons Ltd.

GOLDIE, R.G., FERNANDES, L.B., FARMER, S.G. & HAY, D.W. (1990). Airway epithelium-derived inhibitory factor. *Trends Pharmacol. Sci.*, **11**, 67–69.

HAY, D.W.P., RACBURN, D., FARMER, S.G., FLEMING, W.W. & FEDAN, J.S. (1986). Epithelium modulates the reactivity of ovalbumin-sensitized guinea-pig airway smooth muscle. *Life Sci.*, **38**, 2461–2468.

HOLGATE, S.T. & KAY, A.B. (1985). Mast cells, mediators and asthma. *Clin. Allergy*, **15**, 221–234.

HOLROYDE, M.C. (1986). The influence of epithelium on the responsiveness of guinea-pig isolated trachea. *Br. J. Pharmacol.*, **87**, 501–507.

INGENITO, E.P., PLISS, L.B., MARTINS, M.A. & INGRAM, R.H.Jr. (1991). Effect of capsaicin on mechanical, cellular, and mediator responses to antigen in sensitized guinea-pigs. *Am. Rev. Respir. Dis.*, **143**, 572–577.

JONES, T.R., CHARETTE, L. & DENIS, D. (1988). Antigen-induced contraction of guinea-pig isolated trachea: studies with novel inhibitors and antagonists of arachidonic acid metabolites. *Br. J. Pharmacol.*, **95**, 309–321.

KOHROGI, H., YAMAGUCHI, T., KAWANO, O., HONDA, I., ANDO, M. & ARAKI, S. (1991). Inhibition of neutral endopeptidase potentiates bronchial contraction induced by immune response in guinea-pigs *in vitro*. *Am. Rev. Respir. Dis.*, **144**, 636–641.

KREMZER, L.T. & WILSON, I.B. (1961). A procedure for determination of histamine. *Biochem. Biophys. Acta*, **50**, 364.

LUNDBERG, J.M. & SARIA, A. (1987). Polypeptide-containing neurons in airway smooth muscle. *Ann. Rev. Physiol.*, **49**, 557–572.

LUZZI, S., FRANCHI-MICHELI, S., CIUFFI, M. & ZILLETTI, L. (1986). Effects of GABA agonists on Herxheimer microshock in guinea-pigs. *Agents Actions*, **18**, 245–247.

LUZZI, S., FRANCHI-MICHELI, S., FOLCO, G., ROSSONI, G., CIUFFI, M. & ZILLETTI, L. (1987). Effect of baclofen on different models of bronchial hyperreactivity in the guinea-pig. *Agents Actions*, **20**, 307–309.

MAGGI, C.A. & MELI, A. (1988). The sensory-efferent function of capsaicin-sensitive sensory neurones. *Gen. Pharmacol.*, **19**, 1–43.

MANZINI, S., MAGGI, C.A., GEPPETTI, P. & BACCIARELLI, C. (1987). Capsaicin desensitization protects from antigen-induced bronchospasm in conscious guinea-pigs. *Eur. J. Pharmacol.*, **138**, 307–308.

MUCCITELLI, R.M., TUCKER, S.S., HAY, D.W.P., TORPHY, T.J. & WASSERMAN, M.A. (1987). Is the guinea pig trachea a good *in vitro* model of human large and central airways? Comparison on leukotriene-, methacoline-, histamine- and antigen-induced contractions. *J. Pharmacol. Exp. Ther.*, **243**, 467–473.

OSET-GASQUE, M.H., LAUNAY, J.M. & GONZALEZ, M.P. (1986). GABAergic mechanisms in blood cells: their possible role. In *GABAergic Mechanisms in the Mammalian Periphery*. ed. Erdö, S.L. pp. 305–324. New York: Raven Press.

PARENTE, L. & FLOWER, R.J. (1985). Hydrocortisone and 'macrocortin' inhibit the zymosan-induced release of lyso-PAF from rat peritoneal leucocytes. *Life Sci.*, **36**, 1225–1231.

RAY, N.J., JONES, A.J. & KEEN, P. (1991). $GABA_B$ receptor modulation of the release of substance P from capsaicin-sensitive neurones in the rat trachea *in vitro*. *Br. J. Pharmacol.*, **102**, 801–804.

SARIA, A., LUNDBERG, J.M., SKOFITSCH, G. & LEMBECK, F. (1983). Vascular leakage in various tissues induced by substance P, capsaicin, bradykinin, serotonin, histamine and by antigen challenge. *Naunyn-Schmied. Arch. Pharmacol.*, **324**, 212–218.

SHIRAKAWA, J., TANIYAMA, K. & TANAKA, C. (1987). γ-aminobutyric acid-induced modulation of acetylcholine release from the guinea-pig lung. *J. Pharmacol. Exp. Ther.*, **243**, 364–369.

SHORE, P.A., BURKHALTER, A. & COHN, V.R. (1959). A method for the fluorimetric assay of histamine in tissues. *J. Pharmacol. Exp. Ther.*, **127**, 182–186.

TAMAOKI, J., GRAF, P.D. & NADEL, J.A. (1987). Effect of γ-aminobutyric acid on neurally mediated contraction of guinea-pig trachealis smooth muscle. *J. Pharmacol. Exp. Ther.*, **243**, 86–90.

TSCHIRHART, E., FROSSARD, N., BERTRAND, C. & LANDRY, Y. (1987). Arachidonic acid metabolites and airway epithelium-dependent relaxant factor. *J. Pharmacol. Exp. Ther.*, **243**, 310–316.

UNDEM, B.J., ADAMS, G.K. & BUCKNER, C.K. (1989). Influence of electrical field stimulation on antigen-induced contraction and mediator release in the guinea pig isolated superfused trachea and bronchus. *J. Pharmacol. Exp. Ther.*, **249**, 23–30.

UNDEM, B.J., RAIBLE, D.G., ADKINSON, N.F.Jr. & ADAMS, G.K.W. (1988). Effect of removal of epithelium on antigen-induced smooth muscle contraction and mediator release from guinea-pig isolated trachea. *J. Pharmacol. Exp. Ther.*, **244**, 659–665.

ZILLETTI, L., CIUFFI, M., FRANCHI-MICHELI, S. & GENTILINI, G. (1992). GABAergic mechanisms and modulation of anaphylactic response. In *GABA outside the CNS*. ed. Erdö, S.L. pp. 277–293. Berlin: Springer-Verlag.

(Received January 26, 1994
Revised December 16, 1994
Accepted February 9, 1995)

British Journal of Pharmacology (1995) 115, 395–400

Improved survival and reversal of endothelial dysfunction by the 21-aminosteroid, U-74389G in splanchnic ischaemia-reperfusion injury in the rat

[1]Franceso Squadrito, Domenica Altavilla, Letteria Ammendolia, #Giovanni Squadrito, Giuseppe M. Campo, *Agostino Sperandeo, Patrizia Canale, Mariapatrizia Ioculano, #Antonino Saitta & Achille P. Caputi

Institute of Pharmacology and #Department of Internal Medicine, School of Medicine, University of Messina, and *Upjohn S.p.A., Caponago (MI), Italy

1 Anaesthetized rats subjected to total occlusion of the superior mesenteric artery and the coeliac trunk for 45 min developed a severe shock state (splanchnic artery occlusion, SAO shock) resulting in death within 70–90 min after release of the occlusion. Sham-operated animals were used as controls.

2 Survival rate, survival time, serum tumour necrosis factor (TNF-α), white blood cell (WBC) count, mean arterial blood pressure (MAP), plasma malonylaldehyde (MAL), myeloperoxidase activity (MPO) and the responsiveness to acetylcholine (ACh 10 nM–10 μM) of aortic rings were investigated.

3 SAO shocked rats had a decreased survival rate and survival time (74 ± 10 min, while sham-shocked rats survived more than 4 h), reduced mean arterial blood pressure, increased serum levels of TNF-α (267 ± 13 u ml^{-1}) and plasma levels of MAL (57 ± 7 nmol ml^{-1}), enhanced MPO activity in the ileum (0.23 ± 0.04 u × 10^{-3} g^{-1} tissue) and in the lung (2.2 ± 0.8 u × 10^{-3} g^{-1} tissue), leukopenia and reduced responsiveness to ACh of aortic rings.

4 The 21-aminosteroid U-74389G (30 mg kg^{-1}, i.v.) increased survival (survival time = 232 ± 15 min), lowered the serum levels of TNF-α and the plasma levels of MAL, reduced leukopenia and MPO activity both in the ileum (0.021 ± 0.004 u × 10^{-3} g^{-1} tissue) and in the lung (0.23 ± 0.03 u × 10^{-3} g^{-1} tissue), improved MAP and restored the responsiveness to ACh of aortic rings.

5 Our data suggest that U-74389G is a potent lipid peroxidation inhibitor and that it has antishock and endothelial protective actions.

Keywords: Splanchnic artery occlusion (SAO) shock; endothelial dysfunction; 21-aminosteroid; lipid peroxidation; tumour necrosis factor-α (TNF-α)

Introduction

Circulatory shock is characterized by inadequate perfusion of tissue, altered cell membrane permeability and subsequent cellular dysfunction. A large body of experimental evidence has suggested that oxygen-derived free radicals may have a role in this cascade of pathological events (Horton & Borman, 1987). Highly reactive free radicals, including the superoxide ion (O_2), hydrogen peroxide (H_2O_2) and the hydroxyl radical (OH), contain unpaired electrons in the outer orbit and are reduction products of molecular oxygen (Fridovich, 1983). Because of their extreme reactivity, they react with nearby molecules initiating and propagating several oxygen-derived free radical chain reactions leading finally to lipid peroxidation damage of cells by both direct and indirect actions (McCord, 1985). Indeed lipid peroxidation has been proposed as a major mechanism of oxygen free radical toxicity. Unsaturated fatty acids are particularly susceptible to oxygen free radical attack, owing to the presence of double bonds which can undergo peroxidation through a chain of oxidative reactions (Slater, 1984). Studies performed *in vitro* suggest that exposure to oxygen free radicals results in peroxidation of membrane lipids, and that this is accompanied by damage to cellular organelles and to membrane-bound enzymes (Guarnieri *et al.*, 1983; Tong Mak *et al.*, 1983). If this is the case then inhibition of lipid peroxidation should be of benefit in low-flow states such as circulatory shock. However the phenomenon of lipid peroxidation has not been fully investigated in experimental shock and more specifically in splanchnic artery occlusion shock.

The 21-aminosteroids are a family of compounds that potently inhibit membrane lipid peroxidation (McCall *et al.*, 1987). They achieve this by vitamin E-like scavenging of lipid peroxyl radicals (Braughler *et al.*, 1987) and a scavenging of hydroxyl radicals (Braughler & Pregenzer, 1989). In addition, the 21-aminosteroids blunt the release of arachidonic acid from membranes of cultured cells in response to iron-induced lipid peroxidation (Braughler *et al.*, 1988). They also decrease membrane fluidity (i.e. membrane stabilization) (Bryan *et al.*, 1990), an action that could limit the propagation of lipid peroxidation reactions.

Splanchnic artery occlusion (SAO) shock is an experimental type of shock produced by prolonged ischaemia of the splanchnic region followed by reperfusion (Squadrito *et al.*, 1989). It has been suggested that oxygen free radicals are involved in the pathogenesis of SAO shock (Novelli *et al.*, 1989). Thus we have now studied the effects of U-74389G [21-<4-(2,6-di-1-pyrrolidinyl-4-pyrimidinyl)-1-piperazinyl. -pregna-1,4,9(11)-triene-3,20-dione (z)-2-butenenedionate], a new 21-aminosteroid, on the pathological sequelae associated with SAO shock. This compound seems to be more effective than other family compounds because it possesses a piperazinic group which yields to a greater stabilization of the cell membrane. Besides, the presence of a carboxylic group may cause the compound to scavenge more efficaciously a large amount of detrimental hydroxyl radicals. The drug was found to increase survival, to inhibit lipid peroxidation and leukocyte accumulation and to reverse the impairment in endothelium-dependent relaxation.

[1] Author for correspondence at: Institute of Pharmacology, School of Medicine, Piazza XX Settembre, 4 98121 Messina, Italy.

Methods

Surgical procedures

Male Sprague-Dawley rats weighing 250–300 g were permitted access to food and water *ad libitum*. The rats were anaesthetized with urethane (1.3 g kg^{-1}, i.p.). After anaesthesia, catheters were placed in the carotid artery and jugular vein. After midline laparotomy, the coeliac and superior mesenteric arteries were isolated near their aortic origins. During this procedure, the intestinal tract was maintained at 37°C by placing it between gauze pads soaked with warmed 0.9% NaCl solution.

Rats were given heparin (1,000 u kg^{-1}, i.v.) and were observed for a 30 min stabilization period prior to either splanchnic ischaemia or sham ischaemia. SAO shock was induced by clamping both the superior mesenteric artery and the coeliac trunk so as to produce total occlusion of these arteries for 45 min. The clamps were then removed. Following reperfusion the rats were observed for 4 h. Sham-shocked rats were subjected to the same surgical procedures as SAO shocked rats except that the arteries were not occluded.

Survival evaluation and arterial blood pressure monitoring

A first group of animals was used to study survival ($n = 60$) and arterial blood pressure ($n = 28$). Five minutes after initiating reperfusion, treated rats received intravenously U-74389G as bolus injection over 10 min (7.5, 15 and 30 mg kg^{-1}) dissolved in a citrate buffer (3.8 mg ml^{-1} citric acid, 0.94 mg ml^{-1} sodium citrate dihydrate, 4.7 mg ml^{-1} NaCl) and control rats received the carrier vehicle. Survival was evaluated for 4 h and expressed either as survival time or survival rate. A group of animals ($n = 28$) was also implanted with cannulae (PE 50) inserted into the left common carotid artery and the right jugular vein as described elsewhere (Caputi *et al.*, 1980). The arterial catheter was connected to a pressure transducer. The pressure pulse triggered a cardiotachometer, and arterial blood pressure was displayed on a polygraph. Arterial blood pressure is reported as mean arterial pressure (MAP) in mmHg. Rats were subjected to the same experimental protocol as described above.

Biological assay for tumour necrosis factor-α activity

A third group of animals ($n = 112$) was used to measure tumour necrosis factor-α (TNF-α), myeloperoxidase activity, leukocyte count, plasma malonylaldehyde and vascular reactivity. Blood samples were drawn at 0 and 45 min before initiating reperfusion (by release of the arterial clamp) and at 80 min after reperfusion. The total volume removed was 1.5 ml. It was replaced with the same amount of 0.9% NaCl. Killing of L929 mouse tumour cells was used to measure TNF-α levels in serum on the basis of a standard assay (Rugg & Gifford, 1980). L929 cells in RPMI 1640 medium containing 5% foetal calf serum were seeded at 3×10^4 cells per well in 96-well microdilution plates and incubated overnight at 37°C in an atmosphere of 5% CO_2 in air. Serial dilutions of serum (0.3 ml, drawn at different time intervals) were made in a medium containing actinomycin D (1 μg ml^{-1}) and 100 μl of each dilution was added to the wells. On the next day, cell survival was assessed by fixing and staining the cells with crystal violet (0.2% methanol) and 0.1 ml of 1% sodium dodecyl sulphate was added to each well to solubilize the stained cells. The absorbance of each well was read at 490 nm with a model BT-100 Microelisa Autoreader. The percentage of cytotoxicity was calculated as [1-(A490 of sample/A490 of control)] × 100. One unit of TNF-α was defined as the amount giving 50% cell cytotoxicity. The TNF-α content in the sample was calculated by comparison with a calibration curve obtained with recombinant murine TNF-α (Nuclear Laser Medicine, Italy). To test whether the cytotoxicity tested was due to the presence of TNF-α or to other factors, we preincubated our samples for 2 h at 37°C with an excess of rabbit antirecombinant murine TNF-α polyclonal antibodies (Nuclear Laser Medicine, Milan, Italy) or with control rabbit serum. Our results showed that cytotoxicity against L929 cells was completely neutralized by rabbit anti-recombinant TNF-α polyclonal antibodies, but not by control rabbit serum.

Myeloperoxidase activity

Leukocyte accumulation was investigated using the activity of myeloperoxidase (MPO). MPO activity was determined in intestinal mucosa and in the left lung, as previously reported (Mullane *et al.*, 1985). The samples of intestinal mucosa and left lung were obtained at 0 and 45 min before initiating reperfusion (by release of the arterial clamp) and at 80 min after reperfusion. The samples were first homogenized in a solution containing 20 mM of potassium phosphate buffer (pH 7.4), 0.01 M EDTA, 50 u ml^{-1} of a protease inhibitor (aprotinin) in proportions of 1:10 (W:v) and then centrifuged for 30 min at 20,000 *g* at 4°C. The supernatant of each sample was then discarded and the pellet was immediately frozen on dry ice. The samples were kept at a temperature of 0°C for 14 h before sonication. After thawing, the resulting pellet was added to a buffer solution consisting of 0.5% hexacyltrimethylammonium bromide (Sigma Chemical Co., St. Louis, MO, U.S.A.) dissolved in 50 nM potassium phosphate buffer (pH 6) containing 30 u ml^{-1} of protease inhibitor. Each sample was then sonicated for 1 min at intensity 2 and at a temperature of 4°C. After sonication the samples were allowed to chill on ice for approximately 30 min, and then they were centrifuged for 30 min at 40,000 *g* at 4°C. An aliquot of the supernatant was then allowed to react with 0.167 mg ml^{-1} *o*-dianisidine dihydrochloride (Sigma Chemical Co.) and 0.0010% H_2O_2, and the rate of change in absorbance was measured at 405 nm in a microtitre plate reader. MPO activity was defined as the quantity of enzyme degrading 1 μmol of peroxide min^{-1} at 25°C and was expressed in milliunits g^{-1} weight ($u \times 10^{-3}$) of tissue.

Leukocyte count

Tail vein blood samples for the leukocyte count (Brechner & Cronkite, 1950) were taken at 0 and 45 min before initiating reperfusion, and at 80 min after reperfusion. The number of leukocytes (WBC × 10^3 mm^{-3}) is reported as mean ± s.d.

Assessment of the MAL levels was carried out in plasma samples to give an indication of lipid peroxidation in cellular membranes. Samples of arterial blood were drawn from the carotid catheter at 0 and 45 min before starting reperfusion (release of the arterial clamp) and 80 min after reperfusion. The blood was collected in polyethylene tubes to which had been added 10 μl of heparin solution (1,000 iu). The plasma samples, obtained after centrifugation at 3,000 *g* for 10 min at 4°C, were frozen at −70°C until the analysis. The assay was carried out using a high performance liquid chromatography (h.p.l.c.) technique, as previously described (Ceconi *et al.*, 1991). Briefly, each sample of plasma was diluted with an equal volume of acetonitrile to precipitate proteins. The resulting suspension was vortex-mixed for 30 s and centrifuged at 3,000 *g* for 5 min; the clear supernatant was injected into the h.p.l.c. For separation of MAL a reverse-phase, ion-pair chromatography technique was used. H.p.l.c. analysis was performed on an Altex C_{18} 5 μm reversed-phase column (0.46 × 15 cm) (Beckman Instruments Inc., Berkeley, CA, U.S.A.) with a mobile phase of 10 mM Na_2HPO_4, 2.5 mM myristyltrimethylammonium bromide (Jansessen Chemical Beerse, Belgium), 25% acetonitrile, and corrected with orthophosphoric acid until the pH was 6.7. The flow rate was 1.5 ml min^{-1} at ambient temperature, the injected volume was 50 μl, and the variable wave length detector (mod 165,

Beckman Instruments Inc., San Ramon, U.S.A.) was fixed at 267 nm. The h.p.l.c. instrument was the Beckman Solvent Delivery System (Beckman Instruments Inc., San Ramon, U.S.A.). A calibration chromatogram of an accurately prepared standard MAL solution was also run every time for peak identification and quantitation. Standard MAL was prepared by acid hydrolysis of malonylaldehyde-bisdimethylacetal (Janssen Chemical Beerse, Belgium). In these conditions the detection limit of MAL in the plasma samples was 100 pmol ml^{-1}.

Isolated aortic rings

Animals were killed 80 min after the start of reperfusion. Thoracic aortae were removed (80 min after the start of reperfusion) and placed in cold Krebs solution of the following composition (mM): NaCl 118.4, KCl 4.7, $MgSO_4$ 1.2, $CaCl_2$ 2.5, KH_2PO_4 1.2, $NaHCO_3$ 25.0 and glucose 11.7. Then the aortae were cleaned of adherent connective and fat tissue and cut into rings of approximately 2 mm in length. Cold Krebs solution was only used to prepare aortae before mounting them in the organ bath. The rings were then placed under 1 g of tension in an organ bath containing 10 ml of Krebs solution at 37°C and bubbled with 95% O_2 and 5% CO_2 (pH 7.4). All experiments were carried out in the presence of indomethacin (10 μM) in order to exclude the involvement of eicosanoids and their metabolites. Developed tension was measured with an isometric force transducer and recorded on a polygraph (Ugo Basile, Torino, Italy). After an equilibration period of 60 min during which time the rings were washed with fresh Krebs solution at 15–20 min intervals and basal tension was readjusted to 1 g, the tissue was exposed to phenylephrine (PE, 100 nM). When the contraction was stable, the function integrity of endothelium was assessed by a relaxant response to acetylcholine (ACh, 100 nM). The tissues were then washed three times over 30 min. Endothelium-dependent relaxation was evaluated with cumulative concentrations of ACh (10 nM–1 μM) in aortic rings precontracted with PE (100 nM). Endothelium-independent relaxation was investigated with cumulative concentrations of sodium nitroprusside (SN, 15 nM–30 nM) precontracted with PE (100 nM). Relaxation of the rings was calculated as percentage decrease of contractile force.

Drug

Acetylcholine chloride, sodium nitroprusside, phenylephrine hydrochloride and indomethacin were obtained from Sigma. U-74389G was obtained from Upjohn S.p.A. Italy and was dissolved in a citrate buffer (3.8 mg ml^{-1} citric acid, 0.94 mg ml^{-1} sodium citrate dihydrate, 4.7 mg ml^{-1} NaCl).

Statistical analysis

The difference between the means of two groups was evaluated with ANOVA followed by Bonferroni's test. P values of less than 0.05 were considered to be significant. For survival data, statistical analysis was done with Fisher's exact probability test.

Results

Survival

Sham-shocked rats, treated either with carrier vehicle or with U-74389G, survived the entire 4 h observation period (Table 1). In contrast, in rats treated with vehicle, SAO shock produced a profound shock state characterized by a high lethality and no rats survived at 2 h (survival time = 74 ± 10 min: survival rate = 0%). The administration of U-74389G significantly protected in a dose-dependent manner the rats from death induced by SAO shock. The most effective dose was 30 mg kg^{-1}: in animals that received this dose survival time was 232 ± 15 min and survival rate was 80% (Table 1). Therefore we used this dose in all other studies described below.

Arterial blood pressure

Occlusion of the splanchnic arteries produced a marked increase in mean arterial blood pressure. Upon release of the occlusion pressure decreased substantially and progressively until death (Figure 1). Administration of U-74389G significantly blunted the SAO-induced reduction in mean arterial blood pressure (Figure 1).

Serum TNF-α

Serum levels of TNF-α were undetectable in sham-shocked rats treated either with U-74389G or vehicle. TNF-α was also undetectable during the occlusion period. In contrast, serum TNF-α was significantly enhanced at the end of the reperfusion period in SAO shocked rats (267 ± 13). Treatment with the 21-aminosteroid substantially decreased TNF-α levels during reperfusion (19 ± 2; $P<0.001$).

Plasma malonylaldehyde concentrations

Analysis of plasma malonylaldehyde (MAL) was carried out to evaluate damage by free radicals on biological membranes at 0 and 45 min before initiating reperfusion, and at 80 min of reperfusion. In plasma obtained at time 0 min, prior to occlusion, low levels of MAL were observed in each group

Table 1 Effect of U-74389G on survival time in splanchnic artery occlusion (SAO) shocked rats

Treatment	*Survival time* (min)	*Surviving animals*	*Survival rate (%)*
Sham + vehicle	>240	10/10	100
Sham + U-74389G (30 mg kg^{-1})	>240	10/10	100
SAO + vehicle	74 ± 10*	0/10*	0
SAO + U-74389G (7.5 mg kg^{-1})	123 ± 15	0/10	0
SAO + U-74389G (15 mg kg^{-1})	200 ± 19#	5/10#	50
SAO + U-74389G (30 mg kg^{-1})	232 ± 15†	8/10†	80

Each point represents the mean ± s.d. from 10 rats. *$P<0.001$ vs Sham. #$P<0.05$ vs SAO + vehicle. †$P<0.001$ vs SAO + vehicle.

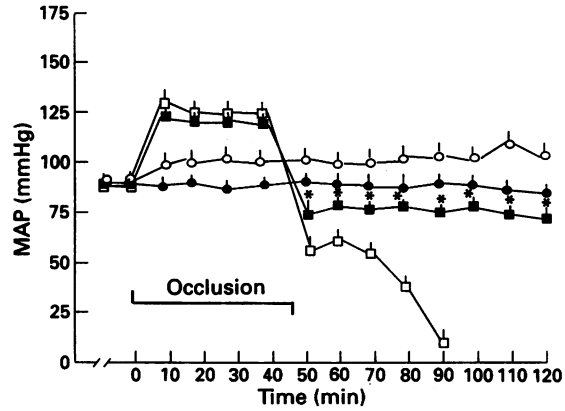

Figure 1 Effects of U-74389G or vehicle on mean arterial blood pressure (MAP) in rats subjected to splanchnic artery occlusion (SAO) shock. Each point represents the mean ± s.d. of seven experiments. *$P<0.05$ vs SAO + vehicle. (●) Sham + vehicle; (○) Sham + U-74389G (30 mg kg^{-1}, i.v.); (□) SAO + vehicle; (■) SAO + U-74389G (30 mg kg^{-1}, i.v.).

studied (<5 nmol ml^{-1}). Moreover, a small increase in the MAL levels was found during reperfusion in the sham-operated groups (Figure 2a). Nevertheless, this change was not statistically significant. In contrast, a large increase in MAL was detected at 80 min after beginning reperfusion in SAO-shocked rats (Figure 2a). The administration of U-74389G significantly reduced this increase in plasma MAL (Figure 2a).

Myeloperoxidase activity

The kinetics of ileal and pulmonary leukocyte infiltration in SAO-shocked rats was determined by measuring the myeloperoxidase (MPO) activity in the ileum and the lung at 0 and 45 min before initiating reperfusion, and at 80 min of reperfusion. MPO levels were significantly increased in the ileum (0.23 ± 0.04 u $\times 10^{-3}$ g^{-1} tissue) and in the lung (2.2 ± 0.8 u $\times 10^{-3}$ g^{-1} tissue) at 80 min after reperfusion (Figure 2b and c) in shocked rats pretreated with the vehicle.

The administration of the 21-aminosteroid significantly reduced the increase in MPO in both tissue in the ileum to 0.021 ± 0.004 u $\times 10^{-3}$ g^{-1} tissue (Figure 2b) and in the lung to 0.23 ± 0.003 u $\times 10^{-3}$ g^{-1} tissue (Figure 2c).

Leukocyte count

The leukocyte count did not change in sham-operated rats during the course of the experiment either when the vehicle or U-74389G was administered (Figure 2d). In contrast, SAO shock produced a marked leukopenia: the leukocyte count was markedly decreased at 80 min of reperfusion (Figure 2d). Administration of U-74389G significantly ameliorated this leukopenia (Figure 2d).

Relaxant response to acetylcholine and sodium nitroprusside

Addition of PE (100 nM) to the organ bath contracted intact aortic rings (80–90% of the maximum response). These rings were relaxed in a concentration-dependent manner by ACh (10 nM–1 μM). The relaxant effect following the 1 μM ACh in aortic rings from shocked rats was significantly lower (Figure 3; $38 \pm 3.2\%$) in SAO-shocked rats than in Sham-shocked rats (Figure 3; $79 \pm 4\%$). The administration of the 21-aminosteroid significantly improved responsiveness to ACh (Figure 3; $81 \pm 5\%$ after 1 μM ACh).

Endothelium-independent relaxation studied by evaluating the effect of sodium nitroprusside (15 nM–30 nM) in aortic

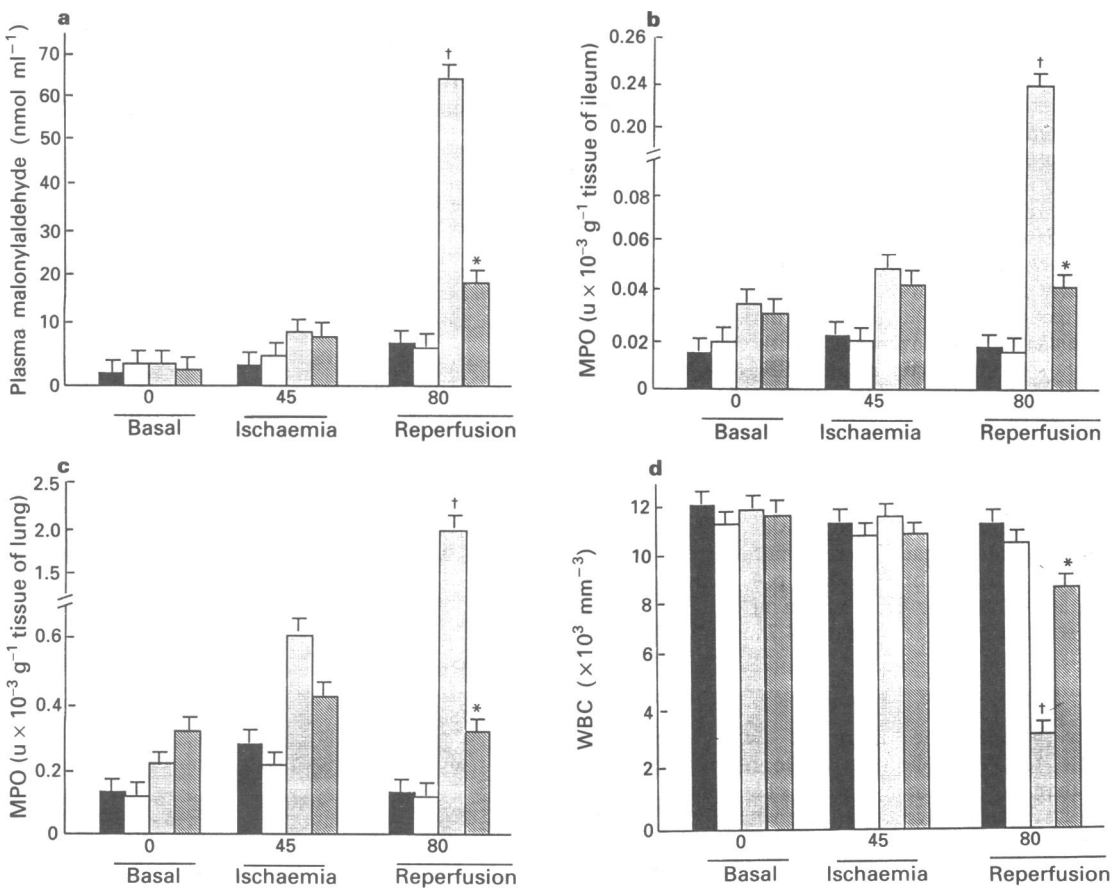

Figure 2 (a) Effects of U-74389G or vehicle on plasma malonylaldehyde (MAL) in rats subjected to splanchnic artery occlusion (SAO) shock. Each column represents the mean ± s.d. of seven experiments. †$P<0.001$ vs Sham; *$P<0.005$ vs SAO + vehicle. Solid columns, Sham + vehicle; open columns, Sham + U-74389G (30 mg kg^{-1}–; stippled columns, SAO + vehicle; hatched columns SAO + U-74389G (30 mg kg^{-1}). (b) Effects of U-74389G or vehicle on ileal myeloperoxidase (MPO) activity of rats subjected to splanchnic artery occlusion (SAO) shock. Each column represents the mean ± s.d. of seven experiments. †$P<0.001$ vs Sham; *$P<0.005$ vs SAO + vehicle. Solid columns, Sham + vehicle; open columns Sham + U-74389G (30 mg kg^{-1}); stippled columns, SAO + vehicle; hatched columns, SAO + U-74389G (30 mg kg^{-1}). (c) Effects of U-74389G or vehicle on pulmonary myeloperoxidase (MPO) activity of rats subjected to splanchnic artery occlusion (SAO) shock. Each column represents the mean ± s.d. of seven experiments. †$P<0.001$ vs Sham; *$P<0.005$ vs SAO + vehicle. Solid columns, Sham + vehicle; open columns, Sham + U-74389G (30 mg kg^{-1}); stippled columns SAO + vehicle; hatched columns SAO + U-74389G (30 mg kg^{-1}). (d) White blood cell count (WBC) in splanchnic artery occlusion (SAO) shocked rats given either U-74389G or vehicle. Column heights represent the mean ± s.d. from seven experiments. †$P<0.001$ vs Sham; *$P<0.001$ vs SAO + vehicle. Solid columns, Sham + vehicle; open columns, Sham + U-74389G (30 mg kg^{-1}); stippled columns, SAO + vehicle; hatched columns, SAO + U-74389G (30 mg kg^{-1}).

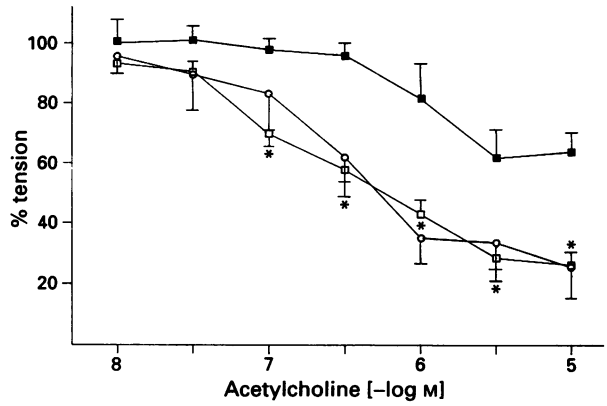

Figure 3 Relaxant effect of acetylcholine in aortic rings (contracted with phenylephrine, 100 nM) of splanchnic artery occlusion (SAO) shocked rats given either U-74389G or vehicle. Each point represents the mean ± s.d. from seven experiments. $*P < 0.005$ vs SAO + vehicle. (○) Sham + vehicle; (■) SAO + vehicle; (□) SAO + U-74389G.

rings precontracted with PE (100 nM) did not show any difference between sham-shocked animals and SAO-shocked rats. The relaxant effect following 30 nM sodium nitroprusside in aortic rings was 83 ± 3% in sham rats and 81 ± 2% in SAO-shocked rats.

Discussion

Splanchnic artery occlusion (SAO) shock is an experimental model of circulatory shock which is the consequence of a prolonged ischaemia of the splanchnic region (Sturniolo *et al.*, 1988).

The pathological sequelae of SAO shock include impaired activity of the reticuloendothelial system (Sturniolo *et al.*, 1989), elevated macrophage and plasma levels of thromboxane B_2 (Squadrito *et al.*, 1992b), increased plasma levels of platelet activating factor (Zingarelli *et al.*, 1992b) and enhanced macrophage and serum levels of TNF-α (Squadrito *et al.*, 1992a). The data so far accumulated on SAO shock suggest that reperfusion is the principle mechanism for the high death rate in this type of experimental shock: in fact death of the animals invariably occurs within 75–90 min after the release of the occlusion (Squadrito *et al.*, 1991).

Free radicals, particularly oxygen-derived and active intermediates such as superoxyl radical, hydrogen peroxide, and hydroxyl radicals are implicated in the cellular damage that follows ischaemia and reperfusion: their toxicity is mainly due to their ability to induce lipid peroxidation (Wills, 1987; McCord, 1985).

Our data are in agreement with this hypothesis: we investigated the phenomenon of lipid peroxidation by measuring the plasma levels of malonylaldehyde (MAL) and found that plasma MAL was significantly increased in our shocked rats at the end of reperfusion.

This result would indicate that lipid peroxidation plays an important role in the pathogenesis of SAO shock. To confirm such a hypothesis, we performed experiments with U-74389G, a pharmacological agent which belongs to the 21-aminosteroids, a family of compounds that potently inhibit lipid peroxidation (McCall *et al.*, 1987). The administration of U-74389G reduced the rise in plasma MAL and significantly increased the survival of rats subjected to the lethal procedures of SAO shock, thus suggesting that lipid peroxidation plays an important role in the pathogenesis of this type of experimental shock. Indeed these findings clearly suggest that U-74389G is a potent inhibitor of lipid peroxidation. In fact the compound, that lacks glucocorticoid and mineralcorticoid activities, possesses the ability to scavenge lipid peroxyl radicals and to inhibit iron-dependent lipid peroxidation, although other mechanisms have been suggested.

Circulatory shock is a low-flow state where leukocyte-endothelium interaction might play a key role. In fact we have previously suggested that leukocytes are deeply involved in the pathogenesis of SAO shock (Canale *et al.*, 1993): leukopenia, induced by administering vinblastine, dramatically increased the resistance of experimental animals to SAO shock.

We therefore investigated whether the phenomenon of lipid peroxidation might be involved *in vivo* in mediating leukocyte accumulation in SAO shock.

Our results show that SAO-shocked rats had a marked systemic leukopenia and increased leukocyte accumulation in the ileum and in the lung at the end of reperfusion. Furthermore, the administration of U-74389G, an inhibitor of lipid peroxidation, reduced leukopenia and leukocyte accumulation in the ileum and in the lung. These data, taken together, strongly suggest that the phenomenon of lipid peroxidation significantly contributes, *in vivo*, to the mechanisms underlying leukocyte accumulation.

It has been suggested that TNF-α might also promote the adherence of leukocytes to the endothelium (Gamble *et al.*, 1985). Our shocked rats had increased serum levels of TNF-α and the administration of U-74389G reduced the increased concentration of this inflammatory cytokine, an effect already reported for 21-aminosteroids (Semrad *et al.*, 1993). Therefore the inhibition of TNF-α serum levels might also contribute to the reduction in leukocyte accumulation. Since our treatment succeeded in reducing the circulating levels of the inflammatory cytokine, it can be also hypothesized that the beneficial effects of U-74389G in intestinal ischaemia-reperfusion injury are, at least in part, due to the inhibition of TNFα.

The mechanisms underlying the irreversible circulatory failure observed in shock are not yet well known. The involvement of the L-arginine/nitric oxide (NO) pathway in the vascular dysfunction that occurs in experimental shock has been proposed (Zingarelli *et al.*, 1992a).

Vane *et al.* (1990) proposed that the L-arginine/nitric oxide pathway may play a key role in the regulation of vascular tone. In all cell types so far studied NO is generated following oxidation and cleavage of the terminal nitrogen atom(s) of L-arginine by an enzyme, NO synthase. At least two types of NO synthase have been identified (Moncada *et al.*, 1991). The enzyme found in the endothelial cells and in the brain is constitutive, Ca^{2+}-dependent and releases picomolar amounts of NO for a short period following receptor stimulation. In contrast the enzyme found in the macrophages is induced following stimulation with cytokines or endotoxin, is Ca^{2+}-independent and releases nanomolar amounts of NO for a long period (Moncada *et al.*, 1991).

So far as SAO shock is concerned, experimental evidence has shown that NO donors exert beneficial effects in feline SAO shock (Aoki *et al.*, 1990), thus suggesting that a dysfunction in the L-arginine/nitric oxide (i.e. a decrease in NO production derived by the constitutive and endothelial NO synthase) pathway might also be present in this type of experimental shock. In accordance with this hypothesis, our present data show that aortic rings from SAO-shocked rats had a marked reduced responsiveness to vasorelaxant effects of ACh. In contrast no difference between SAO-shocked rats and sham-shocked animals was found in the endothelium-independent relaxant effects of sodium nitroprusside. Indeed this result indicates that NO generated by the endothelial and constitutive NO synthase is reduced in SAO shocked rats.

Adherence of leukocytes to the endothelium, by releasing oxygen-derived free radicals, may impair the release of NO from endothelial cells (Aoki *et al.*, 1989).

Therefore therapeutic approaches that reduce oxygen-derived free radical-induced endothelial toxicity are expected to restore the impairment in NO dysfunction.

The administration of U-74389G improved the responsiveness to ACh of aortic rings from SAO-shocked rats.

In conclusion, our study suggests that the 21 aminosteroid U-74389G possesses antishock and endothelial protective properties.

This work was supported by MURST (Fondi 40% and 60%) and by CNR (grant no. 9304295CT04). The authors would like to thank Carole Campbell for correcting and typing the manuscript.

References

AOKI, N., JOHNSON, III, G. & LEFER, A.M. (1990). Beneficial effects of two forms of NO administration in feline splanchnic artery occlusion shock. *Am. Physiol. Soc.*, **321**, G275–G281.

AOKI, N., SIEGFRIED, M. & LEFER, A.M. (1989). Anti-EDRF effect of tumor necrosis factor in isolated perfused cat carotid arteries. *Am. J. Physiol.*, **256**, H1509–H1512.

BRAUGHLER, J.M., CHASE, R.L., NEFF, G.L., YONKERS, P.A., DAY, J.S., HALL, E.D., SETHY, V.H. & LAHTI, R.A. (1988). A new 21-aminosteroid antioxidant lacking glucocorticoid activity stimulates ACTH secretion and blocks arachidonic acid release from mouse pituitary tumor (AtT-20) cells. *J. Pharmacol. Exp. Ther.*, **244**, 423–427.

BRAUGHLER, J.M. & PREGENZER, J.F. (1989). The 21-aminosteroid inhibitors of lipid peroxidation: reactions with peroxyl and phenoxyl radicals. *Free Rad. Biol. Med.*, **7**, 125–130.

BRAUGHLER, J.M., PREGENZER, J.F., CHASE, R.L., DUNCAN, L.A., JACOBSEN, E.J. & MCCALL, J.M. (1987). Novel 21-aminosteroids as potent inhibitors of iron-dependent lipid peroxidation. *J. Biol. Chem.*, **262**, 10438–10440.

BRECHNER, G. & CRONKITE, E.P. (1950). Morphology and enumeration of human blood platelets. *J. Appl. Physiol.*, **3**, 365–368.

BRYAN, C.L., LAWRENCE, R.A., HALL, E.D. & JENKINSON, S.G. (1990). 21-Aminosteroids inhibit microsomal lipid peroxidation independent of iron. *FASEB. J.*, **4**, A630.

CANALE, P., SQUADRITO, F., ZINGARELLI, B., ALTAVILLA, D., IOCULANO, M., CAMPO., G.M. & CAPUTI, A.P. (1993). Splanchnic artery occlusion shock: vinblastine induced leukopenia reduces tumor necrosis factor and thromboxane A_2 formation and increases survival rate. *Pharmacol. Res.*, **27**, 61–71.

CAPUTI, A.P., ROSSI, F., CARNEY, K., BREZENOFF, H.E. (1980). Modulatory effect of brain acetylcholine on reflex-induced bradycardia and tachycardia in conscious rats. *J. Pharmacol. Exp. Ther.*, **215**, 309–316.

CECONI, C., CARGNONI, A., PASINI, E., CONDORELLI, E., CURELLO, S. & FERRARI, R. (1991). Evaluation of phospholipid peroxidation as malonylaldehyde during myocardial ischemia and reperfusion injury. *Am. J. Physiol.*, **260**, H1057–H1061.

FRIDOVICH, I. (1983). Superoxide radical: an endogenous toxicant. *Annu. Rev. Pharmacol. Toxicol.*, **23**, 239–257.

GAMBLE, J.R., HARLAN, J.M., KLEBANOFF, S.G. & VADAS, M.A. (1985). Stimulation of the adherence of neutrophils to umbilical vein endothelium by human necrosis factor. *Proc. Natl. Acad. Sci. U.S.A.*, **82**, 8667–8971.

GUARNIERI, C., MUSCARI, C., CECONI, C., FLAMIGNI, F. & CALDARERA, C.M. (1983). Effect of superoxide generation on rat heart mitochondrial pyruvate utilization. *J. Mol. Cell. Cardiol.*, **15**, 859–862.

HORTON, J.W. & BORMAN, K.R. (1987). Possible role of oxygen-derived, free radicals in cardiocirculatory shock. *Surgery, Gynecol. Obstet.*, **165**, 293–300.

MCCALL, J.M., BRAUGHLER, J.M. & HALL, E.D. (1987). A new class of compounds for stroke and trauma: effects of 21-aminosteroids on lipid peroxidation. *Acta Anaesth. Belg.*, **38**, 417–420.

MCCORD, J.M. (1985). Oxygen-derived free radicals in postischemic tissue injury. *N. Engl. J. Med.*, **312**, 159–163.

MONCADA, S., PALMER, R.M.J. & HIGGS, E.A. (1991). Nitric oxide: physiology, pathophysiology and pharmacology. *Pharmacol. Rev.*, **43**, 109–142.

MULLANE, K.M., KRAEMER, R. & SMITH, B. (1985). Myeloperoxidase activity as a quantitative assessment of neutrophil infiltration into ischaemic myocardium. *J. Pharmacol. Methods.*, **14**, 157–167.

NOVELLI, G.P., ANGIOLINI, P., LIVI, P. & PATERNOSTRO, E. (1989). Oxygen-derived free radicals in the pathogenesis of experimental shock. *Resuscitation*, **18**, 195–205.

RUFF, M.R. & GIFFORD, G.E. (1980). Purification and physicochemical characterization of rabbit tumor necrosis factor. *J. Immunol.*, **125**, 1671–1675.

SEMRAD, S.D., ROSE, M.L. & ADAMS, J.L. (1993). Effect of tirilazad mesylate (U74006F) on eicosanoid and tumor necrosis factor generation in healthy and endotoxemic neonatal calves. *Circ. Shock*, **40**, 235–242.

SLATER, T.F. (1984). Free radical mechanisms in tissue injury. *Biochem. J.*, **222**, 1–15.

SQUADRITO, F., ALTAVILLA, D., IOCULANO, M., CALAPAI, G., ZINGARELLI, B., SAITTA, A., CAMPO, G.M., RIZZO, A. & CAPUTI, A.P. (1992a). Passive immunization with antibodies against tumor necrosis factor (TNF-α) protects from the lethality of splanchnic artery occlusion shock. *Circ. Shock*, **37**, 236–244.

SQUADRITO, F., ALTAVILLA, D., ZINGARELLI, B., IOCULANO, M., CAMPO, G.M., SAITTA, A., URNA, G., SPIGNOLI, G. & CAPUTI, A.P. (1992b). Protective effects of G 619, a dual thromboxane synthase inhibitor and thromboxane A_2 receptor antagonist, in splanchnic artery occlusion shock. *J. Cardiovasc. Pharmacol.*, **19**, 115–119.

SQUADRITO, F., STURNIOLO, R., ALTAVILLA, D., CAMPO, G.M., TRIMARCHI, G.R., SCURI, R. & CAPUTI, A.P. (1989). Effects of fructose 1,6 diphosphate on splanchnic artery occlusion shock in the rat. *Resuscitation*, **18**, 299–307.

SQUADRITO, F., STURNIOLO, R., ALTAVILLA, D., SANTORO, G., CAMPO, G.M., ARENA, A. & CAPUTI, A.P. (1991). Platelet activating factor involvement in splanchnic artery occlusion shock in rats. *Eur. J. Pharmacol.*, **192**, 47–53.

STURNIOLO, R., ALTAVILLA, D., BERLINGHIERI, M.C., SQUADRITO, F. & CAPUTI, A.P. (1988). Splanchnic artery occlusion shock in the rat: effects of calcium entry blockers nimodipine and verapamil. *Circ. Shock*, **24**, 43–53.

STURNIOLO, R., SQUADRITO, F., ALTAVILLA, D., TRIMARCHI, G.R., PROSDOCIMI, M. & CAPUTI, A.P. (1989). Cloricromene improves survival rate and macrophage function in splanchnic artery occlusion shock in rats. *Circ. Shock*, **28**, 267–277.

TONG MAK, I., MISRA, H.P. & WEGLICKI, W.B. (1983). Temporal relationship of free radical induced lipid peroxidation and loss of latent enzyme activity in highly enriched hepatic lysosomes. *J. Biol. Chem.*, **258**, 13733–13737.

WILLIS, E.D. (1987). Evaluation of lipid peroxidation in lipid and biological membranes. In *Biochemical Toxicology: a Practical Approach*. pp. 127–152. ed. Snell, K. & Mullock, B. Oxford: Irl. Press.

VANE, J.R., ANGGARD, E.E. & BOTTING, R.M. (1990). Regulatory functions of the vascular endothelium. *N. Engl. J. Med.*, **323**, 27–36.

ZINGARELLI, B., SQUADRITO, F., ALTAVILLA, D., CALAPAI, G., CAMPO, G.M., SAITTA, A. & CAPUTI, A.P. (1992a). Evidence for a role of nitric oxide in hypovolemic hemorrhagic shock. *J. Cardiovasc. Pharmacol.*, **19**, 982–986.

ZINGARELLI, B., SQUADRITO, F., IOCULANO, M., ALTAVILLA, D., BUSSOLINO, F., CAMPO, G.M. & CAPUTI, A.P. (1992b). Platelet activating factor interaction with tumor necrosis factor and myocardial depressant factor in splanchnic artery occlusion shock. *Eur. J. Pharmacol.*, **222**, 13–19.

(Received November 2, 1994
Revised January 28, 1995
Accepted February 13, 1995)

British Journal of Pharmacology (1995) 115, 401-408

Cytokine-mediated induction of cyclo-oxygenase-2 by activation of tyrosine kinase in bovine endothelial cells stimulated by bacterial lipopolysaccharide

P. Akarasereenont, Y.S. Bakhle, [1]C. Thiemermann & J.R. Vane

The William Harvey Research Institute, St. Bartholomew's Hospital Medical College, Charterhouse Square, London EC1M 6BQ

1 The induction of cyclo-oxygenase-2 (COX-2) afforded by bacterial lipopolysaccharide (LPS, endotoxin) in bovine aortic endothelial cells (BAEC) is mediated by tyrosine kinase. LPS also causes the generation of several cytokines including interleukin-1β (IL-1β), tumour necrosis factor-α (TNF-α), epidermal growth factor (EGF) and platelet-derived growth factor (PDGF). This study investigates whether endogenous IL-1β, TNF-α, EGF or PDGF contribute to the induction of COX-2 elicited by LPS in BAEC and if their action is due to activation of tyrosine kinase. Furthermore, we have studied the induction of COX-2 by exogenous cytokines.

2 Accumulation of 6-oxo-prostaglandin (PG) $F_{1\alpha}$ in cultures of BAEC was measured by radioimmunoassay at 24 h after addition of either LPS (1 μg ml^{-1}) alone or LPS together with a polyclonal antibody to one of the various cytokines. In experiments designed to measure 'COX activity', 6-oxo-$PGF_{1\alpha}$ generated by BAEC activated with recombinant human IL-1β, TNF-α, EGF or PDGF for 12 h was measured after incubation of washed cells with exogenous arachidonic acid (30 μM for 15 min). Western blot analysis determined the expression of COX-2 protein in BAEC.

3 The accumulation of 6-oxo-$PGF_{1\alpha}$ caused by LPS in BAEC was attenuated by co-incubation with one of the polyclonal antibodies, anti-IL-1β, anti-TNF-α, anti-EGF, anti-PDGF or with the IL-1 receptor antagonist, in a dose-dependent manner. Exogenous IL-1β, TNF-α or EGF also caused an increase in COX activity, while PDGF was ineffective. The increase in COX activity elicited by IL-1β (10 ng ml^{-1}), TNF-α (100 ng ml^{-1}) or EGF (1000 ng ml^{-1}) in BAEC was attenuated by erbstatin (0.005 to 5 μg ml^{-1}), as was the expression of COX-2 protein measured by Western blot analysis.

4 PDGF (10 ng ml^{-1}) significantly augmented the rise in COX activity and COX-2 protein caused by shorter incubation of BAEC with LPS (1 μg ml^{-1} for 3 h). Combination of PDGF (10 ng ml^{-1}) with a low concentration of IL-1β (1 ng ml^{-1}) for 12 h, also increased 'COX activity', but combination of PDGF and TNF-α (10 ng ml^{-1}) did not show any increased activity.

5 These results suggest that (*i*) the induction of COX activity and COX-2 protein elicited by LPS in BAEC is mediated by TNF-α with lesser contributions from PDGF, EGF or IL-1β; (*ii*) exogenous IL-1β, TNF-α or EGF alone induce COX-2 activity and protein in BAEC; (*iii*) PDGF synergizes with IL-1β, but not TNF-α, to cause expression of COX-2; and (*iv*) the induction of COX-2 protein and activity caused by these cytokines involves the activation of tyrosine kinase.

Keywords: Endotoxin; tumour necrosis factor; interleukin-1; platelet-derived growth factor; epidermal growth factor; erbstatin; cyclo-oxygenase

Introduction

Bacterial lipopolysaccharide (LPS) is a potent activator of the immune system which induces local or systemic inflammation and septic shock (Morrison & Ryan, 1979; Martich *et al.*, 1993). LPS stimulates the synthesis of arachidonic acid metabolites in a number of cell types including endothelial cells by causing the *de novo* synthesis of an 'inducible' isoform of cyclo-oxygenase (COX-2; Lee *et al.*, 1992; Mitchell *et al.*, 1993; Akarasereenont *et al.*, 1995b). The cellular mechanisms by which LPS causes the induction of COX-2 are largely unknown. Recently, we have shown that tyrosine phosphorylation is part of the signal transduction mechanism that mediates the induction of COX-2 elicited by LPS in endothelial cells (Akarasereenont *et al.*, 1994). LPS stimulates the release of a variety of inflammatory mediators including cytokines and growth factors *in vitro* and *in vivo* (Mantovani *et al.*, 1992; Hewett & Roth, 1993; see Henderson & Blake, 1992; Thiemermann, 1994). We chose four cytokines, interleukin-1β (IL-1β), tumour necrosis factor-α (TNF-α), platelet-derived growth factor (PDGF) and epidermal growth factor (EGF), known to involve tyrosine kinase in their actions (Donato *et al.*, 1989; Ullrich & Schlessinger, 1990; Corbett *et al.*, 1993) and assessed their role in the response of BAEC to LPS. This study was designed to investigate whether or not (*i*) the release of IL-1β, TNF-α, EGF or PDGF by BAEC contributes to the induction of COX-2 caused by LPS in these cells (*ii*) exogenous IL-1β, TNF-α, EGF or PDGF cause the induction of COX-2 in BAEC and (*iii*) this effect is due to activation of tyrosine kinase. Some of these results have been communicated to the British Pharmacological Society (Akarasereenont *et al.*, 1995a).

Methods

Cell culture

Bovine aortic endothelial cells (BAEC) were obtained from fresh bovine aortae as previously described (de Nucci *et al.*, 1988) and cultured in 96-well plates (10^5 cells per well) with Dulbecco's Modified Eagle's Medium (DMEM; 200 μl/well) containing 10% foetal calf serum (Gibco) and 4 mM L-glutamine. The cells were characterized morphologically and by positive staining for von Willebrand Factor (98 ± 2%). These cells were used only between the 6th and 20th passage. To

[1]Author for correspondence.

eliminate any possibility of contamination with other types of cells, a single BAEC was cloned by the spot technique (Doyle *et al.*, 1994) and used after the 6th passage; these cells were also positive for von Willebrand Factor (97 ± 3%). The agents, which were dissolved in distilled water or dimethylsulphoxide (DMSO final concentration less than 0.1%; v/v), were sterilized by filtration through a filter (pore size: 0.22 μm) before being added to the cells under sterile conditions. Cells were incubated at 37°C in a humidified incubator.

Measurement of the activity of cyclo-oxygenase

6-Oxo-prostaglandin $F_{1\alpha}$ (6-oxo-$PGF_{1\alpha}$) is the main COX metabolite released after activation of BAEC with LPS (1 μg ml^{-1}; Akarasereenont *et al.*, 1994b) and its accumulation was measured by radioimmunoassay (Salmon, 1978). In experiments involving cytokine antibodies, BAEC were treated with LPS together with a polyclonal antibody to either IL-1β (anti-IL-1β; 0.1, 1 or 10 μg ml^{-1}), TNF-α (anti-TNF-α; 0.1, 1 or 10 μg ml^{-1}), EGF (anti-EGF; 0.1, 1 or 10 μg ml^{-1}) or PDGF (anti-PDGF; 0.5, 5 or 10 μg ml^{-1}) for 24 h and the medium was subsequently assayed for 6-oxo-$PGF_{1\alpha}$. Identical conditions were used for assessing the effects of the recombinant human IL-1 receptor antagonist (IL-1ra; 1, 10 or 100 ng ml^{-1}).

Separate experiments were designed to measure the effects of exogenous cytokines on COX activity (in order to eliminate any effects of other enzymes involved in the arachidonic acid cascade induced or activated by cytokines). In these experiments, cells were treated with IL-1β (0.1, 1 or 10 ng ml^{-1}), TNF-α (1, 10 or 100 ng ml^{-1}), EGF (1, 10, 100 or 1000 ng ml^{-1}) or PDGF (1, 3 or 10 ng ml^{-1}) for 12 h after which time the cells were washed and fresh medium containing arachidonic acid (30 μM) was added for 15 min at 37°C. Subsequently, the supernatant was removed to measure 6-oxo-$PGF_{1\alpha}$.

To assess the involvement of protein tyrosine kinase, cells were treated with IL-1β (10 ng ml^{-1}), TNF-α (100 ng ml^{-1}) or EGF (1000 ng ml^{-1}) together with the tyrosine kinase inhibitor erbstatin (0.005, 0.05, 0.5 or 5 μg ml^{-1}; Imoto *et al.*, 1987; see also Akarasereenont *et al.*, 1994) for 12 h, after which time the cells were washed and fresh medium containing arachidonic acid (30 μM) was added for 15 min at 37°C and then assayed for 6-oxo-$PGF_{1\alpha}$. The same conditions, but with LPS stimulation only, were used to assess the effects of calphostin C (0.001, 0.01, 0.1 or 1 μg ml^{-1}; Kobayashi *et al.*, 1989) or staurosporine (0.0001, 0.001, 0.01 or 0.1 μg ml^{-1}; Tamaoki *et al.*, 1986) on COX activity.

To study the interactions of PDGF with other cytokines or LPS, BAEC were incubated with LPS (1 μg ml^{-1}) alone for 3 h. The medium was then replaced with fresh medium containing either no further addition or PDGF (10 ng ml^{-1}) alone or PDGF plus erbstatin (5 μg ml^{-1}) and incubation continued for a further 9 h, after which time COX activity was measured. BAEC were also incubated with IL-1β (1 ng ml^{-1}) alone or IL-1β with PDGF (10 ng ml^{-1}) and with TNF-α (10 ng ml^{-1}) alone or TNF-α with PDGF (10 ng ml^{-1}) for 12 h and COX activity measured.

Immunoblot (Western blot) analysis

BAEC were cultured in 6-well plates (37°C) and treated for 24 h with fresh medium alone (control) or containing LPS or LPS plus erbstatin (5 μg ml^{-1}). Similar experiments were done with IL-1β alone (10 ng ml^{-1}), TNF-α alone (100 ng ml^{-1}), EGF alone (1000 ng ml^{-1}) or with the cytokine plus erbstatin (5 μg ml^{-1}). Cells were also cultured with PDGF alone (10 ng ml^{-1}). In addition, cells were activated with LPS (1 μg ml^{-1}) for 3 h and subsequently the medium was removed and replaced with fresh medium containing PDGF (10 ng ml^{-1}) alone or PDGF (10 ng ml^{-1}) plus erbstatin (5 μg ml^{-1}) for a further 21 h. After 24 h, cells were washed with phosphate buffered saline (PBS; pH 7.4) and incubated (5 min) with 1 ml of extraction buffer (composition, mM: Tris 50, EDTA 10, Triton X-100 1% v/v, phenylmethylsulphonyl fluoride 1, pepstatin A 0.05 and leupeptin 0.2) with gentle shaking. The cell extract was then boiled (10 min) in a ratio of 1 : 1 with gel loading buffer (Tris 50 mM, SDS 10% w/v, glycerol 10% v/v, 2-mercaptoethanol 10% v/v and bromphenol blue 2 mg ml^{-1}). Samples were centrifuged at 10,000 *g* for 2 min before being loaded onto gradient gels (4–10% Tris-glycine) and subjected to electrophoresis (1 h at 125 V). The separated proteins were transferred to nitrocellulose (BIOR-AD; 1 h at 200 V). After transfer to nitrocellulose, the blot was incubated in blocking solution (dried minimal-fat milk 5% w/v and Tween-20 0.25% v/v in PBS solution) for 1 h and then primed (1 h) with a rabbit antibody raised to murine COX-2 (primary antibody, dilution 1 : 1000, Cayman Chemical Company, MI, U.S.A.; no detectable cross-reactivity with COX-1) which reacts with bovine COX-2 (Mitchell *et al.*, 1993). The blot was then incubated (1 h) with an anti-rabbit IgG developed in sheep (secondary antibody, dilution 1 : 1000, linked to alkaline phosphatase conjugate). Finally, the blot was developed (for approximately 5 min) with premixed solution containing (mM): 5-bromo-4-chloro-3-indolylphosphate (BCIP), 0.56 nitro blue tetrazolium (NBT) 0.48, Tris 10 and $MgCl_2$ 59.3 (pH 9.2). The detection limit of protein in cell extract was 1–10 ng of protein.

Measurement of the release of TNF-α from endothelial cells

BAEC or the cloned cells were cultured to confluence in 96-well plates as above and the medium replaced with fresh medium before use. Cells were incubated alone, treated with LPS (1 μg ml^{-1}) or treated with LPS plus erbstatin (5 μg ml^{-1}) for 24 h after which time the medium was removed and assayed for its content of TNF-α with ELISA Quantikine kits. The lower detection limit for TNF-α is 4.4 pg ml^{-1}.

Measurement of cell viability

Cell respiration, an indicator of cell viability, was assessed by the mitochondrial dependent reduction of 3-(4,5-dimethylthiazol-2-yl)-2,5-diphenyltetrazolium bromide (MTT) to formazan (Mosmann, 1983). At the end of each experiment, cells in 96-well plates were incubated (37°C; 1 h) with MTT (0.2 mg ml^{-1}) dissolved in culture medium, after which time, the medium was removed by aspiration and cells were solubilized in DMSO (200 μl). The extent of reduction of MTT to formazan within cells was quantitated by measurement of optical density at 650 nm (OD 650) using a Molecular Devices microplate reader (Anthos, Salzburg, Austria).

Positive controls for loss of cell viability were provided by experiments designed to determine limiting concentrations of DMSO. Cell viability was 80 ± 1% with 0.1%, 67 ± 4% with 1% and 40 ± 5% with 10% DMSO (v/v), relative to the control untreated cells over a 24 h incubation period.

Statistical analysis

Results are shown as mean ± s.e.mean from triplicate determinations (wells) from 3 separate experimental days ($n = 9$). ANOVA analysis was used to determine the significance of differences between means and P values of less than 0.05 were taken as statistically significant.

Materials

Escherichia coli lipopolysaccharide (serotype: 0111:B4), DMSO, phosphate buffered saline (PBS; pH 7.4), Trizma base, EDTA, Triton X-100, phenylmethylsulphonyl fluoride (PMSF), pepstatin A, leupeptin, glycerol, 2-mercaptoethanol, bromphenol blue, sulphanilamide, naphthylethylenediamide, phosphoric acid, sodium nitrite, sodium dodecyl sulphate (SDS), calphostin C, staurosporine, anti-rabbit IgG antibody,

goat IgG, premixed BCIP/NBT solution, 3-(4,5-dimethylthiazol-2-yl)-2,5-diphenyltetrazolium bromide (MTT), 6-oxo-$PGF_{1\alpha}$ and its respective antibody were supplied by Sigma Chemical Company (Poole, Dorset). [^{3}H]-6-oxo-$PGF_{1\alpha}$ was purchased from Amersham International (Little Chalfont, Bucks). Dulbecco's modified Eagle's medium (DMEM) was obtained from Flow Laboratories. L-Glutamine was obtained from B.D.H. (Dagenham, Essex) and foetal calf serum was obtained from Gibco BRL (Paisley, Renfrewshire). Recombinant human TNF-α and recombinant human EGF were purchased from Genzyme (West Malling, Kent) and recombinant human IL-1β, recombinant human PDGF and recombinant human IL-1 receptor antagonist were purchased from R&D systems (Abingdon, Berks). The cytokine antibodies, all goat IgG, anti-hTNF-α (no cross-reactivity with TNF-β and other cytokines), anti-IL-1β (no cross-reactivity with IL-1α and other cytokines), anti-hEGF (no cross-reactivity with TGF-α and other cytokines), anti-hPDGF (>10% cross-reactivity with PDGF-AA subtype, nearly 100% cross-reactivity with PDGF-AB as well as PDGF-BB subtype and no cross-reactivity with other cytokines) and the TNF-α ELISA Quantikine kits were purchased from R&D systems. Pure nitrocellulose membrane (0.45 μm) and filter paper were purchased from BIO-RAD (Hemel Hempstead, Hertfordshire). Erbstatin (erbstatin analogue) was obtained from Calbiochem Novabiochem (Nottingham, UK).

Results

Effects of antibodies to cytokines on the induction of COX activity in BAEC activated by LPS

Untreated BAEC released only small amounts of 6-oxo-$PGF_{1\alpha}$ (1–2 ng ml^{-1}) over 24 h. After exposure to LPS (1 μg ml^{-1}) for 24 h, significantly higher amounts of 6-oxo-$PGF_{1\alpha}$ were accumulated (50–60 ng ml^{-1}; Akarasereenont *et al.*, 1995b). When BAEC were treated with LPS given together with anti-IL-1β (0.1, 1 or 10 μg ml^{-1}), anti-TNF-α (0.1, 1 or10 μg ml^{-1}), anti-EGF (0.1, 1 or 10 μg ml^{-1}) or anti-PDGF (0.5, 5 or 10 μg ml^{-1}), the accumulation of 6-oxo-$PGF_{1\alpha}$ was inhibited in a dose-dependent manner with a maximum inhibition of 70±3% for anti-TNF-α, 50±5% for anti-PDGF, 35±3% for EGF and 25±5% for anti-IL-1β (all at 10 μg ml^{-1}; Figure 1).

Cloned BAEC released over 24 h only small amounts of 6-oxo-$PGF_{1\alpha}$ (0.05±0.02 ng ml^{-1}; n=9). After exposure of these cloned BAEC to LPS (1 μg ml^{-1} for 24 h), significantly higher amounts of 6-oxo-$PGF_{1\alpha}$ accumulated (52±5 ng ml^{-1}; n=9; P<0.05). The anti-TNF-α antibody (0.1, 1 or 10 μg ml^{-1}), inhibited the LPS-induced accumulation of 6-oxo-$PGF_{1\alpha}$ in a dose-dependent manner with a maximum inhibition of 75±3% for anti-TNF-α (at 10 μg ml^{-1}).

Incubation with goat IgG (10 μg ml^{-1}), the relevant control for the cytokine-antibodies used, did not affect the accumulation of 6-oxo-$PGF_{1\alpha}$ following LPS (93±3% of LPS, n=9).

The IL-1ra was also assessed as an inhibitor of LPS-induced accumulation of 6-oxo-$PGF_{1\alpha}$. Over the range of concentrations used, (1, 10 or 100 ng ml^{-1}), IL-1ra caused weak, but dose-dependent, inhibitions of 8±3%, 14±3% and 20±4%, respectively (n=9 for each dose).

Incubation of BAEC or cloned BAEC with LPS for 24 h did not affect cell viability as measured by the MTT assay (viability: 86±2% of control). In addition, anti-IL-1β, anti-TNF-α, anti-EGF or anti-PDGF (up to 10 μg ml^{-1}) did not reduce cell viability, when given either alone or in combination with LPS (viability: 83±5% of control).

Effects of exogenous IL-1β, TNF-α, EGF or PDGF on COX activity

Incubation of BAEC with IL-1β (0.1, 1 or 10 ng ml^{-1}), TNF-α (1, 10 or 100 ng ml^{-1}) or EGF (1, 10, 100 or 1000 ng ml^{-1}) for 12 h resulted in a dose-related increase in COX activity (Figure 2). By contrast, incubation of BAEC with PDGF (1, 3 or 10 ng ml^{-1}) did not result in a significant increase in COX activity (Figure 2).

Effects of the tyrosine kinase inhibitor, erbstatin, on the induction of COX activity caused by exogenous IL-1β, TNF-α or EGF

In BAEC activated with TNF-α, the increase in COX activity elicited by TNF-α was inhibited by erbstatin in a dose-depen-

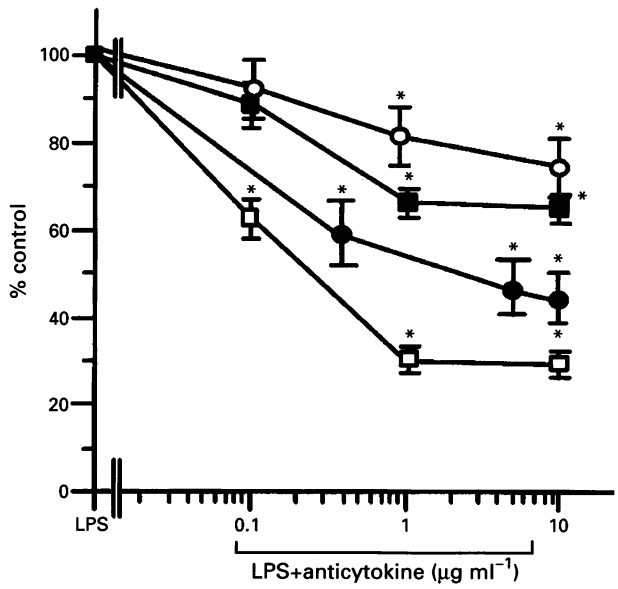

Figure 1 The effects of anti-IL-1β (○), anti-TNF-α (□), anti-EGF (■) or anti-PDGF (●) on the induction of COX in BAEC activated with LPS (1 μg ml^{-1}) measured at 24 h by the accumulation of 6-oxo-$PGF_{1\alpha}$ in the culture medium. For ease of comparison, the values for each antibody have been calculated as a percentage of the corresponding value for LPS alone. Typical values for the accumulation in control cultures were 1±0.03 ng ml^{-1} and after LPS treatment 56±7 ng ml^{-1}, n=9. Data are expressed as mean±s.e.mean from triplicate determinations (wells) from 3 separate experimental days (n=9). *P<0.05 when compared to LPS-treated cells at 24 h (LPS). For abbreviations in this and subsequent figures, see text.

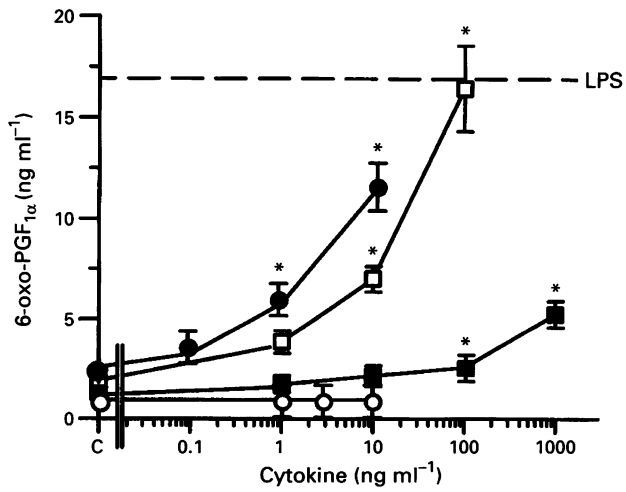

Figure 2 Dose-dependent increase of COX activity in BAEC activated with IL-1β (●), TNF-α (□), EGF (■) or PDGF (○) for 12 h measured by the formation of 6-oxo-$PGF_{1\alpha}$ in the presence of exogenous arachidonic acid (30 μM; 15 min). Data are expressed as mean±s.e. mean from triplicate determinations (wells) from 3 separate experimental days (n=9). *P<0.05 when compared to untreated cells at 12 h (C). Dashed line shows the level of COX activity in BAEC activated with LPS (1 μg ml^{-1}) for 12 h.

dent manner (Figure 3). The inhibition was first significant at a concentration of erbstatin of 0.5 μg ml^{-1}. Similarly, erbstatin caused a dose-dependent inhibition of the increase in COX activity elicited by IL-1β or EGF in BAEC (Figure 3). This inhibition was also first significant with erbstatin at 0.5 μg ml^{-1}. Calphostin C (0.001, 0.01, 0.1 or 1 μg ml^{-1}) or staurosporin (0.0001, 0.001, 0.01 or 0.1 μg ml^{-1}) did not affect increased COX activity induced by LPS ($n=9$).

Incubation of BAEC with erbstatin did not affect cell viability, when given either alone or in combination with LPS (viability: 81 ± 5% of control).

Characterization of COX isoforms present in BAEC treated with LPS, IL-1β, TNF-α, EGF or PDGF

Figure 4 shows that extracts of untreated BAEC contained no detectable COX-2 protein, as determined by Western blot analysis. In contrast, after incubation for 24 h with LPS (1 μg ml^{-1}), TNF-α (100 ng ml^{-1}), EGF (1000 ng ml^{-1}), or IL-1β (10 ng ml^{-1}), the respective cell extracts contained a protein of approximately 70 kDa, which was recognised by a specific antibody to COX-2. Incubation of BAEC with PDGF (10 ng ml^{-1}) did not increase the expression of COX-2 protein (data not shown). Moreover, the induction of COX-2 protein afforded by LPS, TNF-α, EGF or IL-1β in BAEC was prevented by erbstatin (5 μg ml^{-1}).

Effects of the combination of cytokines on COX activity and COX-2 protein expression

Experiments were designed to elucidate whether PDGF, which by itself was inactive (see above), could act synergistically with LPS, IL-1β or TNF-α to increase COX activity and protein. Treatment of BAEC with LPS (1 μg ml^{-1}) for 3 h followed by incubation with medium alone for the next 9 h did not result in a significant increase in COX activity at 12 h (Figure 5). When BAEC were activated with LPS for 3 h and the medium was replaced with fresh medium containing PDGF (10 ng ml^{-1}) for a further 9 h, a significant increase in COX activity (almost three-fold) was observed at 12 h (Figure 5). This increase in COX activity caused by PDGF after LPS was abolished by pretreatment of BAEC with erbstatin (5 μg ml^{-1}). In addition, treatment of BAEC with PDGF after LPS caused a substantial expression of COX-2 protein (Figure 4) which was greater than the one caused by LPS alone (Figure 4b; lane 5). The increase in COX-2 protein caused by PDGF after LPS was also inhibited by erbstatin (5 μg ml^{-1}; Figure 4).

In separate experiments we looked for synergism between exogenous cytokines, using PDGF with sub-maximal concentrations of other cytokines (Figure 5). Here, PDGF (10 ng ml^{-1}) given together with IL-1β for 12 h significantly enhanced the level of COX activity induced by IL-1β (1 ng ml^{-1} for 12 h) alone. In contrast, PDGF (10 ng ml^{-1}; given together with TNF-α for 12 h) did not augment the rise in COX activity afforded by TNF-α (10 ng ml^{-1}) alone.

The release of TNF-α from BAEC in culture

Untreated BAEC released only small amounts of TNF-α, as measured by ELISA (Table 1). Treatment of BAEC with LPS (1 μg ml^{-1} for 24 h) resulted in a 4 fold rise in TNF-α levels in the supernatant. This release of TNF-α caused by LPS was not inhibited by erbstatin (5 μg ml^{-1}; Table 1). Table 1 additionally shows that the cloned BAEC also released TNF-α following exposure to LPS.

Discussion

We have demonstrated the expression of COX-2 activity in three ways: (*i*) by accumulation over 24 h of 6-oxo-PGF$_{1\alpha}$, (*ii*) by the ability of the cells to convert exogenous arachidonic

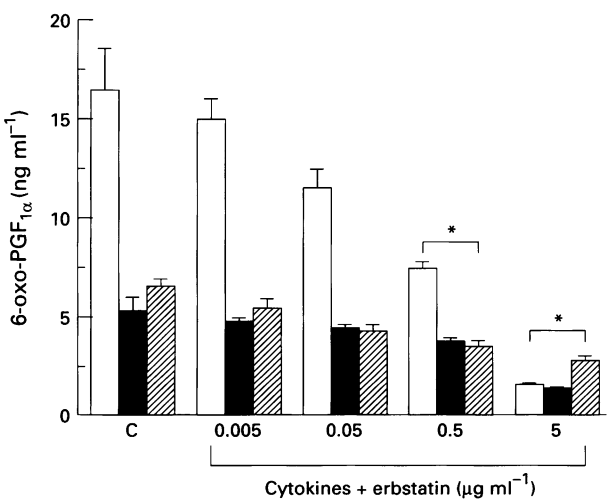

Figure 3 Dose-dependent inhibition of COX activity by erbstatin in BAEC treated with TNF-α (100 ng ml^{-1}; open columns), EGF (1000 ng ml^{-1}; solid columns) or IL-1β (10 ng ml^{-1}; hatched columns), measured at 12 h by the formation of 6-oxo-PGF$_{1\alpha}$. Values are shown for the effects of cytokines alone (C) and for cytokines with increasing concentrations of erbstatin; note that for all three cytokines, erbstatin inhibition was significant at concentrations of 0.5 μg ml^{-1} or higher. Data are expressed as mean ± s.e. mean from triplicate determinations (wells) from 3 separate experimental days ($n=9$). *$P<0.05$ when compared to cytokine alone (C).

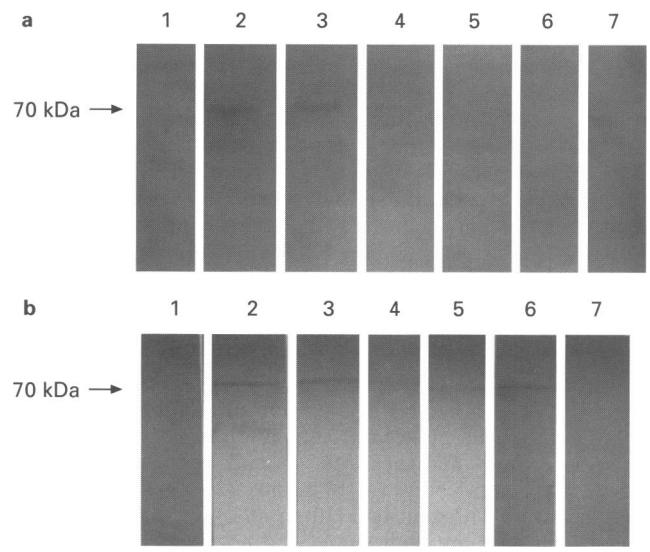

Figure 4 The figure shows Western blots using polyclonal antibodies to COX-2 of cell extracts from mitogen-treated and untreated BAEC. (a) Equal amounts of protein were loaded in all lanes (30 μg/lane). Control untreated BAEC (lane 1) contained no detectable COX-2 protein. In contrast, BAEC activated with LPS (1 μg ml^{-1} for 24 h; lane 2), TNF-α (100 ng ml^{-1} for 24 h; lane 3) or EGF (1000 ng ml^{-1} for 24 h; lane 4) contained COX-2 protein. The induction of COX-2 protein by LPS, TNF-α or EGF in BAEC was prevented by erbstatin (5 μg ml^{-1}; lane 5, 6 and 7, respectively). (b) Equal amounts of protein were loaded in all lanes (10 μg/lane). Control, untreated BAEC (lane 1) contained no detectable COX-2 protein. In contrast, BAEC activated with LPS (lane 2), IL-1β (10 ng ml^{-1} for 24 h; lane 3) contained COX-2 protein. The induction of COX-2 protein by IL-1β in BAEC was prevented by erbstatin (5 μg ml^{-1}; lane 4). Lower levels of COX-2 protein were also detected in BAEC treated with LPS for 3 h (lane 5) and these were increased after subsequent treatment with PDGF (10 ng ml^{-1} for 21 h; lane 6). This increase in COX activity by PDGF was also inhibited by erbstatin (5 μg ml^{-1}; lane 7). Similar results were obtained using cell extracts from 3 separate batches of cells.

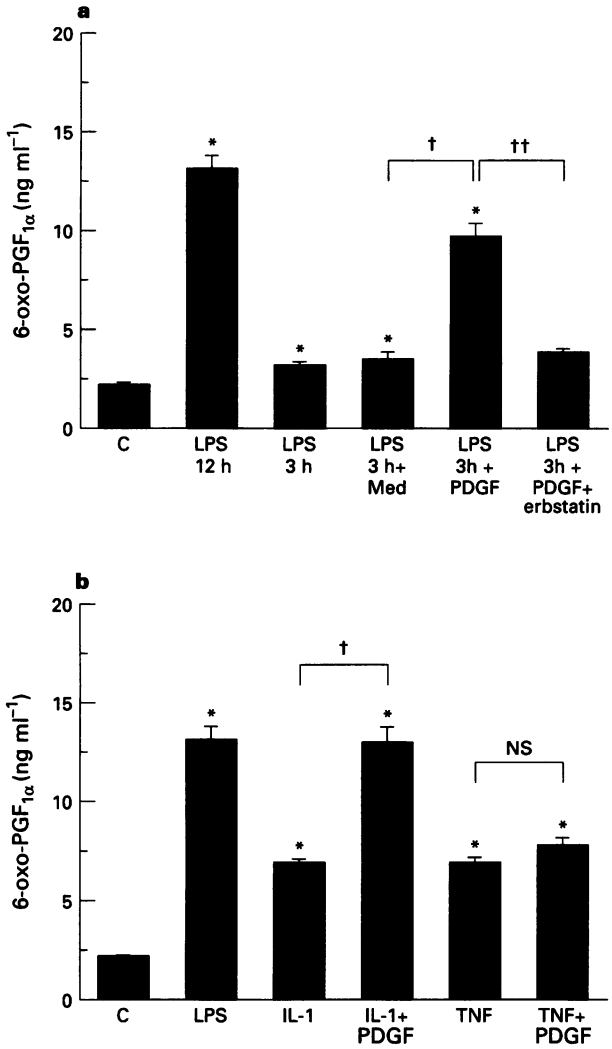

Figure 5 (a) Increase in COX activity (measured by the formation of 6-oxo-$PGF_{1\alpha}$) in BAEC treated with PDGF ($10\,ng\,ml^{-1}$ for 9 h) after prior LPS incubation ($1\,\mu g\,ml^{-1}$ for 3 h); this increase was inhibited by erbstatin ($5\,\mu g\,ml^{-1}$; together with PDGF). *$P<0.05$ when compared to untreated cells at 12 h (C); †$P<0.05$ when compared to LPS-treated cells at 3 h and containing medium alone for a further 9 h incubation; ††$P<0.05$ when compared to LPS treated cells at 3 h and containing PDGF alone for further 9 h. (b) Synergistic increase in COX activity (measured by the formation of 6-oxo-$PGF_{1\alpha}$ in BAEC treated with IL-1β ($1\,ng\,ml^{-1}$; 12 h) plus PDGF ($10\,ng\,ml^{-1}$; together with IL-1β) when compared to BAEC treated with IL-1β alone. In contrast, BAEC treated with TNF-α ($10\,ng\,ml^{-1}$; 12 h) plus PDGF ($10\,ng\,ml^{-1}$; together with TNF-α) did not increase COX activity when compared to BAEC treated with TNF-α alone. *$P<0.05$ when compared to untreated cells at 12 h (C); †$P<0.05$ when compared to IL-1β treated cells at 12 h. Data are expressed as mean ± s.e. mean from triplicate determinations (wells) from 3 separate experimental days ($n=9$).

acid and (*iii*) by Western blot analysis of the COX-2 protein. We shall refer to all these concordant results as an increase in COX-2 activity. Pretreatment of BAEC with polyclonal antibodies to TNF-α, IL-1β, EGF or PDGF attenuated the increase of COX-2 activity caused by LPS in BAEC. In addition, exogenous TNF-α, IL-1β or EGF, but not PDGF, enhanced COX-2 activity. These effects were largely attenuated by the tyrosine kinase inhibitor, erbstatin. Although incubation with PDGF alone did not increase COX-2 activity, PDGF acted synergistically with IL-1β or LPS, but not with TNF-α, in enhancing COX-2 activity. Thus, the induction of COX-2 afforded by LPS in BAEC is mediated by endogenous TNF-α and to a lesser extent by PDGF, EGF and IL-1β and is due to activation of tyrosine kinase by these cytokines.

We undertook these experiments as a result of our earlier work (Akarasereenont *et al.*, 1994) demonstrating that tyrosine kinase was involved in the increased output of prostaglandins from BAEC following exposure to LPS. We inferred from those results that cytokines acting through a tyrosine kinase were the mediators of the expression of COX-2 caused by LPS in endothelial cells. A variety of cells secrete a number of cytokines in response to any given stimulus (Mantovani *et al.*, 1992; Henderson & Blake, 1992) and the complexity of the cytokine system is compounded by the possibilities of interactions between cytokines (Pober & Cotran, 1990; Floege *et al.*, 1990). We chose to study four cytokines which either are secreted by endothelial cells or are known to activate tyrosine kinase, namely TNF-α, EGF, IL-1β and PDGF (Libby *et al.*, 1986; Ullrich & Schlessinger, 1990; Pober & Cotran, 1990; Kohno *et al.*, 1990).

Our experiments with selective antibodies to these cytokines showed clearly that TNF-α played the most important role in mediating the induction of COX-2 afforded by LPS, anti-TNF-α producing about 70% inhibition. Although polyclonal antibodies to PDGF, EGF or IL-1β also attenuated the rise in COX-2 activity caused by LPS, their effects were less pronounced. Exogenous cytokines incubated with the cells in the absence of LPS were also active in inducing COX-2 with TNF-α almost 100 fold more potent than EGF. These results were not unexpected, for TNF-α mediates most of the consequences of LPS in animals and man, including induction of COX-2 (Wheeler *et al.*, 1992; Fletcher, 1993; Hewett & Roth, 1993; Tracey & Cerami, 1993). Furthermore, EGF increases COX activity in human endothelial cells (Kawakami *et al.*, 1986; Ristimäki *et al.*, 1988; Zavoico *et al.*, 1989).

We found that exogenous IL-1β was very effective in inducing COX-2 activity in BAEC, as it is in human cells (Endo *et al.*, 1988; Maier *et al.*, 1990a). However, the comparatively weak inhibition by IL-1β antibody of the increase of COX activity caused by LPS in BAEC suggests that this cytokine was not secreted in adequate amounts following LPS. There are at least two other explanations for the discrepancy. Firstly, it is possible that the antibody we used, to human IL-1β, did not cross-react fully with bovine IL-1. However, this is less likely, for the receptors on the BAEC appeared to recognize the exogenous human IL-1β adequately. Secondly, it is conceivable that LPS stimulates the formation of IL-1β, but this

Table 1 The release of immunoreactive tumour necrosis factor-α (TNF-α) in the medium of cultured endothelial cells treated with lipopolysaccharide (LPS, 1 $\mu g\ ml^{-1}$) alone or LPS plus erbstatin (5 $\mu g\ ml^{-1}$) at 24 h incubation

Bovine aortic endothelial cells (BAEC)	*TNF-α (pg ml^{-1})*
Untreated	10.4 ± 0.4
With LPS (1 $\mu g\ ml^{-1}$)	37.4 ± 0.8
With LPS (1 $\mu g\ ml^{-1}$) plus erbstatin (5 $\mu g\ ml^{-1}$)	39.1 ± 0.7
Cloned	< 4.4
Cloned with LPS (1 $\mu g\ ml^{-1}$)	122.0 ± 1.2
Cloned with LPS (1 $\mu g\ ml^{-1}$) plus erbstatin (5 $\mu g\ ml^{-1}$)	124.4 ± 1.4

Data are expressed as mean ± s.e.mean from triplicate determinations (wells) from 3 separate experimental days ($n=9$).

cytokine could be functioning either intracellularly (Maier *et al.*, 1990b) or bound tightly to its membrane receptors (Kurt-Jones *et al.*, 1987). In either of these locations the IL-1β may be less accessible to the antibody.

Surprisingly, exogenous PDGF was completely inactive in inducing COX-2 in contrast to the clear inhibitory effects of anti-PDGF on the expression of COX-2 by LPS. Others have also found that PDGF increased COX activity and COX-2 protein in several cell types (Lin *et al.*, 1989; Floege *et al.*, 1990; Pomerantz *et al.*, 1993). One explanation of the lack of activity of exogenous PDGF in our model is that this cytokine needs another factor to be present in order to induce COX-2. This additional factor is neither normally present in our BAEC cultures, nor is it induced in BAEC by PDGF, but it is released by LPS. Synergy or co-operation between cytokines has been frequently reported (Pober & Cotran, 1990). For instance, IL-1β potentiates many fold the stimulation of PGI_2 induced by PDGF in human mesangial cells (Floege *et al.*, 1990). In our BAEC cultures such synergism was clearly possible between PDGF and IL-1β. It is less likely with LPS as a stimulus, for the IL-1β antibody should have reduced markedly the overall effect if PDGF were a major mediator only through synergism with IL-1β. The lack of synergism between TNF-α and PDGF demonstrates some divergence between IL-1β and TNF-α, cytokines which frequently exert common effects (Pober & Cotran, 1990), and that TNF-α and PDGF act independently in changing COX levels in BAEC although both pathways involve tyrosine kinase.

For both EGF and PDGF, tyrosine kinase activity is linked to the receptors (Ullrich & Schlessinger, 1990) and although TNF-α can in tumour cells activate the tyrosine kinase of the EGF receptor (Donato *et al.*, 1989), it is clear from the relative activities of EGF and PDGF that activation of the receptor-linked tyrosine kinase *per se* is not crucial for the induction of COX-2. In monocytes, LPS directly activates a tyrosine kinase linked to its membrane-bound CD14 receptor (Wright *et al.*, 1990). However, a direct activation of this tyrosine kinase by LPS cannot explain our results in endothelial cells, for these cells lack the membrane-bound CD14 receptor (Pugin *et al.*, 1993; Goldblum *et al.*, 1994). From the assay of immuno-reactive TNF-α in cell supernatants after treatment with LPS it is clear that although the tyrosine kinase inhibitor, erbstatin, totally prevented the increase in COX-2 activity (Akarasereenont *et al.*, 1994), it did not prevent TNF-α secretion. This finding together with the efficacy of erbstatin against all exogenous cytokines tested (TNF-α, EGF, IL-1β and PDGF after LPS), would imply that the protein tyrosine phosphorylation was common to all effective stimuli, subsequent to secretion of the cytokines. This scheme might be more likely to involve a common group of tyrosine kinases rather than those more specifically associated with each cytokine or its receptor. One possible candidate is the src family of tyrosine kinases as the viral enzyme, pp60-v-src, is known to induce COX-2 protein (Xie *et al.*, 1991). The crucial substrate for tyrosine kinase is also unknown, although in human endothelial cells, the LPS-induced activation of the nuclear transcription factor, NF-κB, is decreased by inhibitors of tyrosine kinase (Read *et al.*, 1993), as is the IL-1 induced activation of NF-κB in lymphoid cells (Iwasaki *et al.*, 1992). For both these stimuli, activation of NF-κB actually represents phosphorylation of the corresponding inhibitor protein, I-κB (Cordle *et al.*, 1993). The promoter region of the gene for COX-2 contains elements responsive to NF-κB (Kosaka *et al.*, 1994).

Which of the four cytokines we have used are the most likely mediators of the effects of LPS in our model? Three of them, IL-1β, PDGF and EGF, are either known to be present in, or secreted from, endothelial cells following LPS or IL-1β (Libby *et al.*, 1986; Hajjar *et al.*, 1987; Suzuki *et al.*, 1989; Albelda *et al.*, 1989; Pusztai *et al.*, 1993; Hewett & Roth, 1993; Tracey & Cerami, 1993; Wilson *et al.*, 1994). However, Pober & Cotran (1990) in their review state that there is no convincing demonstration of TNF release from endothelial cells and neither Libby *et al.* (1986) nor Palkama *et al.* (1993) were able to show TNF release from endothelial cells. Clearly, this cytokine was produced by our monoculture of endothelial cells on stimulation by LPS. Although the BAEC were derived from a primary culture which could be contaminated by macrophages or monocytes (the normal source of TNF-α), the endothelial cells used in these experiments were passaged at least six times before use. This we would argue, as did Libby *et al.* (1986), decreases considerably the possibility of such contamination. Furthermore, LPS under identical conditions strongly induces NO synthase activity in macrophages (Salvemini *et al.*, 1993; Akarasereenont *et al.*, 1994; 1995b), while the release of nitrite from our BAEC cultures activated with LPS was less than 5% of that observed in LPS-activated macrophages (Akarasereenont *et al.*, 1995b). Finally in a clone of endothelial cells, the antibody to TNF-α was as effective as it was in the standard BAEC cultures, in inhibiting the increase in COX-2 activity elicited by LPS. This clone also released immunoreactive TNF-α following LPS.

Thus, the increase in COX-2 activity caused by LPS in BAEC is mediated by cytokines released by LPS from the same cells. The major mediator is TNF-α, with PDGF, EGF and IL-1β making successively lesser contributions. As already noted for LPS, the effects of these individual cytokines involve a tyrosine kinase, sensitive to inhibition with erbstatin. The induction of NO synthase caused by LPS in aortic smooth muscle cells or in J774.2 macrophages is also susceptible to inhibitors of tyrosine kinase (Marczin *et al.*, 1993; Akarasereenont *et al.*, 1994). The essential part played by tyrosine kinase in the induction of both these enzymes, critical components of the response to LPS *in vivo* (see Thiemermann, 1994), suggest that the new generation of tyrosine kinase inhibitors (Levitzki *et al.*, 1992) may have real therapeutic potential in septic shock (Novogrodsky *et al.*, 1994) and other pathological conditions which are associated with the induction of COX-2 and/or NO synthase.

The authors are indebted to Ms Elizabeth Wood for supplying the cultured cells and Ms Ivana Vojnovic for technical assistance.

References

AKARASEREENONT, P., BAKHLE, Y.S., THIEMERMANN, C. & VANE, J.R. (1995a). The role of cytokines in the effects of bacterial lipopolysaccharide (LPS) on cyclo-oxygenase activity in cultured bovine aortic endothelial cells (BAEC). *Br. J. Pharmacol.*, (in press).

AKARASEREENONT, P., MITCHELL, J.A., APPLETON, I., THIEMERMANN, C. & VANE, J.R. (1994). Involvement of tyrosine kinase in the induction of cyclo-oxygenase and nitric oxide synthase by endotoxin in cultured cells. *Br. J. Pharmacol.*, **113**, 1522–1528.

AKARASEREENONT, P., MITCHELL, J.A., BAKHLE, Y.S., THIEMERMANN, C. & VANE, J.R. (1995b). Comparison of the induction of cyclo-oxygenase and nitric oxide synthase by endotoxin in endothelial cells and macrophages. *Eur. J. Pharmacol.*, **273**, 121–128.

ALBEDLDA, S.M., ELIAS, J.A., LEVINE, E.M. & KERN, J.A. (1989). Endotoxin stimulates platelet-derived growth factor production from cultured human pulmonary endothelial cells. *Am. J. Physiol.*, **257**, L65–L70.

CORBETT, J.A., SWEETLAND, M.A., LANCASTER, J.R. & MCDANIEL, M.L. (1993). A 1-hour pulse with IL-1β induces formation of nitric oxide and inhibits insulin secretion by rat islets of Langerhans: evidence for a tyrosine kinase signaling mechanism. *FASEB. J.*, **7**, 369–374.

CORDLE, S.R., DONALD, R., READ, M.A. & HAWIGER, J. (1993). Lipopolysaccharide induces phosphorylation of MAD3 and activation of c-Rel and related NF-κB proteins in human monocytic THP-1 cells. *J. Biol. Chem.*, **268**, 11803–11810.

DE NUCCI, G., GRYGLEWSKI, R.J., WARNER, T.D. & VANE, J.R. (1988). Receptor mediated release of endothelium-derived relaxing factor and prostacyclin from bovine aortic endothelial cells is coupled. *Proc. Natl. Acad. Sci. U.S.A.*, **85**, 2334–2338.

DONATO, N.J., GALLICK, G.E., STECK, P.A. & ROSENBLUM, M.G. (1989). Tumor necrosis factor modulates epidermal growth factor receptor phosphorylation and kinase activity in human tumor cells: correlation with cytotoxicity. *J. Biol. Chem.*, **264**, 20474–20481.

DOYLE, A., GRIFFITHS, J.B. & NEWELL, D.G. (1994). In *Cell and Tissue Culture: Laboratory Procedures: Cloning Procedure* p. 4D:1.3. Chichester, UK: Wiley and Sons.

ENDO, H., AKAHOSHI, T. & KASHIWAZAKI, S. (1988). Additive effects of IL-1 and TNF on induction of prostacyclin synthesis in human vascular endothelial cells. *Biochem. Biophys. Res. Commun.*, **156**, 1007–1014.

FLETCHER, J.R. (1993). Eicosanoids. Critical agents in the physiological process and cellular injury. *Arch. Surg.*, **128**, 1192–1196.

FLOEGE, J., TOPLEY, N., WESSEL, K., KAEVER, V., RADEKE, H., HOPPE, J., KISHIMOTO, T. & RESCH, K. (1990). Monokines and platelet-derived growth factor modulate prostanoid production in growth arrested, human mesangial cells. *Kidney Int.*, **37**, 859–869.

GOLDBLUM, S.E., BRANN, T.W., DING, X., PUGIN, J. & TOBIAS, P.S. (1994). Lipopolysaccharide (LPS)-binding protein and soluble CD14 function as accessory molecules for LPS-induced changes in endothelial barrier function, *in vitro*. *J. Clin. Invest.*, **93**, 692–702.

HAJJAR, K.A., HAJJAR, D.P., SILVERSTEIN, R.L. & NACHMAN, R.L. (1987). Tumor necrosis factor-mediated release of platelet-derived growth factor from cultured endothelial cells. *J. Exp. Med.*, **166**, 235–245.

HENDERSON, B. & BLAKE, S. (1992). Therapeutic potential of cytokine manipulation. *Trends Pharmacol. Sci.*, **13**, 145–152.

HEWETT, J.A. & ROTH, R.A. (1993). Hepatic and extrahepatic pathobiology of bacterial lipopolysaccharides. *Pharmacol. Rev.*, **45**, 381–411.

IMOTO, M., UMEZAWA, K., ISSHIKI, K., KUNIMOTO, S., SAWA, T., TAKEUCHI, T. & UMEZAWA, H. (1987). Kinetic studies of tyrosine inhibition by erbstatin. *J. Antibio. Tokyo.*, **40**, 1471–1473.

IWASAKI, T., UEHARA, Y., GRAVES, L., RACHIE, N. & BOMSZTYK, K. (1992). Herbimycin A blocks IL-1-induced NF-κB DNA-binding activity in lymphoid cell lines. *FEBS. Lett.*, **298**, 240–244.

KAWAKAMI, M., ISHIBASHI, S., OGAWA, H., MURASE, T., TAKAHU, F. & SHIBATA, S. (1986). Cachectin/TNF as well as interleukin-1 induces prostacyclin synthesis in cultured vascular endothelial cells. *Biochem. Biophys. Res. Commun.*, **141**, 482–487.

KOBAYASHI, E., NAKANO, H., MORIMOTO, M. & TAMAOKI, T. (1989). Calphostin C (UCN-1028C), a novel microbial compound, is a highly potent and specific inhibitor of protein kinase C. *Biochem. Biophys. Res. Commun.*, **159**, 548–553.

KOHNO, M., NISHIZAWA, N., TSUJIMOTO, M. & NOMOTO, H. (1990). Mitogenic signalling pathway of tumour necrosis factor involves the rapid tyrosine phosphorylation of 41,000-Mr and 43,000-Mr cytosol proteins. *Biochem. J.*, **267**, 91–98.

KOSAKA, T., MIYATA, A., IHARA, H., HARA, S., SUGIMOTO, T., TAKEDA, O., TAKAHASHI, E. & TANABE, T. (1994). Characterization of the human gene (PTGS2) encoding prostaglandin-endoperoxide synthase 2. *Eur. J. Biochem.*, **221**, 889–897.

KURT-JONES, E.A., FIERS, W. & PBER, J.S. (1987). Membrane interleukin 1 induction on human endothelial cells and dermal fibroblasts. *J. Immunol.*, **139**, 2317–2324.

LEE, S.H., SOYOOLA, E., CHANMUGAM, P., HART, S., SUN, W., ZHONG, H., LIOU, S., SIMMONS, D. & HWANG, D. (1992). Selective expression of mitogen inducible cyclo-oxygenase in macrophages stimulated with lipopolysaccharide. *J. Biol. Chem.*, **267**, 25934–25938.

LEVITZKI, A. (1992). Tyrphostins: tyrosine kinase blockers as novel antiproliferative agents and dissectors of signal transduction. *FASEB. J.*, **6**, 3275–3282.

LIBBY, P., ORDOVAS, J.M., AUGER, K.R., ROBBINS, A.H., BIRINYI, L.K. & DINARELLO, C.A. (1986). Endotoxin and tumor necrosis factor induce interleukin-1 gene expression in adult human vascular endothelial cells. *Am. J. Pathol.*, **124**, 179–185.

LIN, A.H., BIENKOWSKI, M.J. & GORMAN, R.R. (1989). Regulation of prostaglandin H synthase mRNA levels and prostaglandin biosynthesis by platelet-derived growth factor. *J. Biol. Chem.*, **264**, 17379–17383.

MAIER, J.A.M., HLA, T. & MACIAG, T. (1990a). Cyclo-oxygenase is an immediate early gene induced by interleukin-1 in human endothelial cells. *J. Biol. Chem.*, **265**, 10805–10808.

MAIER, J.A.M., VOULALAS, P., ROEDER, D. & MACIAG, T. (1990b). Extension of the life-span of human endothelial cells by an interleukin-1α antisense oligomer. *Science*, **249**, 1570–1574.

MANTOVANI, A., BUSSOLINO, F. & DEJANA, E. (1992). Cytokine regulation of endothelial cell function. *FASEB. J.*, **6**, 2591–2599.

MARCZIN, N., PAPAPETROPOULOS, A. & CATRAVAS, J.D. (1993). Tyrosine kinase inhibitors suppress endotoxin- and IL-1beta-induced NO synthesis in aortic smooth muscle cells. *Am. J. Physiol.*, **265**, H1014–H1018.

MARTICH, G.D., BOUJOUKOS, A.J. & SUFFREDINI, A.F. (1993). Response of man to endotoxin. *Immunobiol.*, **187**, 403–416.

MITCHELL, J.A., AKARASEREENONT, P., THIEMERMANN, C., FLOWER, R.J. & VANE, J.R. (1993). Selectivity of nonsteroidal anti-inflammatory drugs as inhibitors of constitutive and inducible cyclo-oxygenase. *Proc. Natl. Acad. Sci. U.S.A.*, **90**, 11693–11697.

MORRISON, D.C. & RYAN, J.L. (1979). Bacterial endotoxins and host immune responses. *Adv. Immunol.*, **28**, 293–450.

MOSMANN, T. (1983). Rapid colorimetric assay for cellular growth and survival: application to proliferation and cytotoxicity assays. *J. Immunol. Methods.*, **65**, 55–63.

NOVOGRODSKY, A., VANICHKIN, A., PATYA, M., GAZIT, A., OSHEROV, N. & LEVITZKI, A. (1994). Prevention of lipopolysaccharide-induced lethal toxicity by tyrosine kinase inhibitors. *Science*, **264**, 1319–1322.

PALKAMA, T., MAJURI, M.L., MATTILA, P., HURME, M. & RENKONEN, R. (1993). Regulation of endothelial adhesion molecules by ligands binding to the scavenger receptor. *Clin. Exp. Immunol.*, **92**, 353–360.

POBER, J.S. & COTRAN, R.S. (1990). Cytokines and endothelial cell biology. *Physiol. Rev.*, **70**, 427–451.

POMERANTZ, K.B., SUMMERS, B. & HAJJAR, D.P. (1993). Eicosanoid metabolism in cholesterol-enriched arterial smooth muscle cells: evidence for reduced posttranscriptional processing of cyclo-oxygenase I and reduced cyclo-oxygenase II gene expression. *Biochemistry*, **32**, 13624–13635.

PUGIN, J., SCHURER-MALY, C.C., LETURCQ, D., MORIARTY, A., ULEVITCH, R.J. & TOBIAS, P.S. (1993). Lipopolysaccharide activation of human endothelial and epithelial cells is mediated by lipopolysaccharide-binding protein and soluble CD14. *Proc. Natl. Acad. Sci. U.S.A.*, **90**, 2744–2748.

PUSZTAI, L., LEWIS, C.E., LORENZEN, J. & MCGEE, J.O'D. (1993). Growth factors: regulation of normal and neoplastic growth. *J. Pathol.*, **169**, 191–201.

READ, M.A., CORDLE, S.R., VEACH, R.A., CARLISLE, C.D. & HAWIGER, J. (1993). Cell-free pool of CD14 mediates activation of transcription factor NF-κB by lipopolysaccharide in human endothelial cells. *Proc. Natl. Acad. Sci. U.S.A.*, **90**, 9887–9891.

RISTIMÄKI, A., YLIKORKALA, O., PERHEENTUPA, J., & VIINIKKA, L. (1988). Epidermal growth factor stimulates prostacyclin production by cultured human vascular endothelial cells. *Thromb. Haemost.*, **59**, 248–250.

SALMON, J.A. (1978). A radioimmunoassay for 6-keto-prostaglandin $F_{1\alpha}$. *Prostaglandins*, **15**, 383–397.

SALVEMINI, D., MISKO, T.P., MASFERRER, J.L., SEIBERT, K., CURRIE, M.G. & NEEDLEMAN, P. (1993). Nitric oxide activates cyclo-oxygenase enzymes. *Proc. Natl. Acad. Sci. U.S.A.*, **90**, 7240–7244.

SUZUKI, H., SHIBONO, K., OKANE, M., KONO, I., MATSUI, Y., YAMANE, K. & KASHIWAGI, H. (1989). Interferon-γ modulates messenger RNA levels of c-sis (PDGF-B chain), PDGF-A chain and IL-1 γ genes in human vascular endothelial cells. *Am. J. Pathol.*, **134**, 35–43.

TAMAOKI, T., NOMOTO, H., TAKAHASHI, I., KATO, Y., MORIMOTO, M. & TOMITA, F. (1986). Staurosporine, a potent inhibitor of phospholipid/Ca^{++}dependent protein kinase. *Biochem. Biophys. Res. Commun.*, **135**, 397–402.

THIEMERMANN, C. (1994). The role of arginine: nitric oxide pathway in circulatory shock. *Adv. Pharmacol.*, **28**, 45–79.

TRACEY, K.J. & CERAMI, A. (1993). Tumor necrosis factor, other cytokines and disease. *Annu. Rev. Cell. Biol.*, **9**, 317–343.

ULLRICH, A. & SCHLESSINGER, J. (1990). Signal transduction by receptors with tyrosine kinase activity. *Cell*, **61**, 203–212.

WHEELER, A.P., HARDIE, W.D. & BERNARD, G.R. (1992). The role of cyclo-oxygenase products in lung injury induced by tumor necrosis factor in sheep. *Am. Rev. Resp. Dis.*, **145**, 632–639.

WILSON, S.E., SCHULTZ, G.S., CHEGINI, N., WENG, J. & HE, Y.G. (1994). Epidermal growth factor, transforming growth factor alpha, transforming growth factor beta, acidic fibroblast growth factor, basic fibroblast growth factor, and interleukin-1 proteins in the cornea. *Exp. Eye Res.*, **59**, 63–72.

WRIGHT, S.D., RAMOS, R.A., TOBIAS, P.S., ULEVITCH, R.J. & MATHISON, J.C. (1990). CD14, a receptor for complexes of lipopolysaccharide (LPS) and LPS binding protein. *Science*, **249**, 1431–1433.

XIE, W.L., CHIPMAN, J.G., ROBERTSON, D.L., ERIKSON, R.L. & SIMMONS, D.L. (1991). Expression of a mitogen-responsive gene encoding prostaglandin synthase is regulated by mRNA splicing. *Proc. Natl. Acad.. Sci. U.S.A.*, **88**, 2692–2696.

ZAVOICO, G.B., EWENSTEIN, B.M., SCHAFER, A.I. & POBER, J.S. (1989). Interleukin-1 and related cytokines enhance thrombin-stimulated PGI_2 production in cultured endothelial cells without affecting thrombin-stimulated von Willebrand factor secretion or platelet-activating factor biosynthesis. *J. Immunol.*, **142**, 3993–3999.

(Received November 3, 1994
Revised February 1, 1995
Accepted February 17, 1995)

British Journal of Pharmacology (1995) 115, 409-414

Effect of diabetes and elevated glucose on nitric oxide-mediated neurotransmission in rat anococcygeus muscle

[1]Kerrie J. Way & [1,2]Julianne J. Reid

Department of Pharmacology, University of Melbourne, Parkville, Victoria 3052, Australia

1 Nitric oxide (NO)-mediated neurotransmission is impaired in anococcygeus muscle from 8-week streptozotocin-induced diabetic rats. This study investigated the effects of insulin treatment, and the duration of diabetes on this impairment. In addition, the effect of *in vitro* exposure to elevated glucose has been investigated on NO-mediated relaxations, in muscles from untreated rats.

2 Relaxant responses to field stimulation (0.5–5 Hz, 10 s train), sodium nitroprusside (SNP; 5 and 10 nM) and NO (1 and 3 μM) were significantly impaired in anococcygeus muscles from 8-week diabetic rats, compared to responses from control rats. Insulin treatment (5 u Lente day^{-1}, s.c.) of diabetic rats prevented the development of this impairment.

3 Consistent with findings in 8-week diabetic rats, relaxations induced by field stimulation, SNP and NO were attenuated in tissues from 2-week and 4-week diabetic rats compared to corresponding control responses, whereas relaxations to papaverine (3 and 10 μM) were not reduced. In contrast, diabetes of 3-days duration did not affect relaxations to field stimulation, SNP or NO.

4 Incubation of anococcygeus muscles from untreated rats in medium containing elevated glucose (44.1 mM) for 6 h, significantly impaired relaxations to field stimulation compared to responses obtained after normal glucose (11.1 mM) incubation. Relaxations to SNP and to NO were not affected by 6 h exposure to elevated glucose. Similarly, incubation in hyperosmolar solutions containing mannose or sucrose for 6 h, impaired relaxations to field stimulation, but not to SNP or NO.

5 The results indicate that the diabetes-induced impairment of NO-mediated neurotransmission in the rat anococcygeus muscle develops between 3 days and 2 weeks after the induction of diabetes with streptozotocin. Prevention of the impairment by insulin treatment suggests that it is specific for the diabetic state. In addition, the impairment may be related to hyperglycaemia and the consequent rise in osmolarity, since *in vitro* exposure to high glucose as well as to other hyperosmolar media impaired NO-mediated relaxations to field stimulation.

Keywords: Anococcygeus muscle (rat); diabetes; elevated glucose medium; insulin; nitrergic transmission; nitric oxide (NO); nonvascular smooth muscle; sodium nitroprusside; streptozotocin

Introduction

Dysfunction of the autonomic nervous system is an important complication of diabetes mellitus contributing to alterations in cardiovascular, gastrointestinal and genitourinary function (Hosking *et al.*, 1978; Clarke *et al.*, 1979). Morphological, histological and functional alterations in autonomic neurotransmission have been reported for noradrenergic, cholinergic, 5-hydroxytryptaminergic, peptidergic and purinergic nerves (Lincoln *et al.*, 1984; MacLeod & McNeill, 1985; Longhurst & Belis, 1986; Nowak *et al.*, 1986; Belai *et al.*, 1985; 1988; Mathison & Davison, 1988), using experimental animal models of diabetes mellitus, in particular the streptozotocin (STZ) diabetic rat. However, few studies have examined the effects of the diabetic state on nonadrenergic noncholinergic (NANC) inhibitory neurotransmission mediated by nitric oxide (NO), or nitrergic neurotransmission. We have recently shown that nitrergic neurotransmission is attenuated in the anococcygeus muscle from diabetic rats 8 weeks after treatment with STZ (Way & Reid, 1994a,b). Relaxant responses to nitrergic nerve stimulation, sodium nitroprusside (SNP) and NO were impaired, whereas responses to papaverine, which does not act through NO, were not (Way & Reid, 1994a). In addition, relaxations to the cell permeable analogue of guanosine 3':5'-cyclic monophosphate (cyclic GMP), 8-bromo-cyclic GMP, were attenuated in tissues from diabetic rats (Way & Reid, 1994b). Together these results suggest that diabetes impairs reactivity to NO in anococcygeus smooth muscle, at least partly through alterations in the cyclic GMP-relaxation pathway.

In the present study we investigate further the specificity and the development of this impaired nitrergic neurotransmission in diabetes. Firstly, the effects of insulin treatment on NO-mediated relaxations have been examined in muscles from 8-week STZ-treated rats, to assess whether the impairment of responses is specific for the production of a diabetic state and not due to any non-specific effect of STZ. Secondly, the effects of diabetes durations shorter than 8 weeks on smooth muscle responsiveness have been determined to assess the development of changes in nitrergic neurotransmission; relaxant responses were examined in muscles from rats at 3 days, 2 weeks and 4 weeks after treatment. Finally, in a separate series of experiments, anococcygeus muscles isolated from untreated rats were exposed to medium containing elevated glucose, to determine the direct effects of an elevated-glucose environment *per se* on NO-mediated relaxations in rat anococcygeus muscle.

Methods

Induction of diabetes

Diabetes was induced in male Sprague-Dawley rats (200–250 g) by a single injection of STZ (65 mg kg^{-1}, i.v.).

[1] Authors present address: Pharmacology Research Laboratories, Department of Medical Laboratory Science, Royal Melbourne Institute of Technology, GPO Box 2476V, Melbourne, Victoria 3001, Australia.
[2]Author for correspondence (at present address).

Age-matched control rats were treated with citrate-buffer vehicle alone (20 mM, pH 4.5, i.v.). All rats were placed under light anaesthesia before injection (pentobarbitone 40 mg kg^{-1}, i.p.). Food and water were available *ad libitum*, however for 48 h after treatment the drinking water for STZ-treated rats contained 2% sucrose to help reduce the severity of the hypoglycaemia following STZ administration. Thereafter, rats were monitored for glucosuria (Tes-Tape urine sugar-analysis paper; Eli Lilly, Australia) and for changes in body weight. Blood samples were collected from all animals after decapitation for measurement of blood glucose levels (Ames Glucometer II; Miles Laboratories Inc., Australia).

Insulin treatment

Insulin (5 u day^{-1} Lente MC, s.c.) was administered to a separate group of STZ-treated rats, between 09 h 00 min-12 h 00 min for 8 weeks, except on the day of the experiment. Treatment commenced 48 h after STZ injection when animals displayed glucosuria and hyperglycaemia. Blood samples were obtained from the tail vein every 2–4 days for measurement of blood glucose levels; samples were collected approximately 8 h after insulin injection.

Tissue preparation

At specific time periods after treatment, rats were killed by stunning with a blow to the head followed by decapitation. Anococcygeus muscles were then isolated according to the method described by Gillespie (1972). After exposure, the colon was cut at the pelvic brim and the pelvic portion pulled forward to reveal two underlying muscles surrounded by connective tissue. A maximal length of muscle was obtained and mounted under 1 g tension in a 5 ml organ bath for isometric recording, using a Grass FT03 C force displacement transducer and a Rikadenki potentiometric recorder. Muscles were bathed in physiological salt solution (PSS) of the following composition (mM; pH 7.4): NaCl 118, KCl 4.7, $CaCl_2$ 2.5, $NaHCO_3$ 25, KH_2PO_4 1.03, $MgSO_4$ 0.45, D-(+)-glucose 11.1, disodium edetate 0.067, and ascorbic acid 0.14. The PSS was maintained at 37°C and gassed continuously with 95% O_2/5% CO_2. Field stimulation was delivered from a Grass S88 stimulator through two platinum wire electrodes, one on either side of the tissue with square wave pulses of 0.8 ms duration and supramaximal voltage (17 V cm^{-1}).

Relaxant responses

After a 20 min equilibration period, guanethidine (10–30 μM) and clonidine (0.01–0.05 μM) were used to block noradrenergically-mediated contractions and to raise tissue tone. Relaxant responses were obtained to increasing frequencies of field stimulation (0.5–5 Hz, 10 s train) at 3 min intervals, or to SNP (5 and 10 nM) and NO (1 and 3 μM), or to papaverine (3 and 10 μM). In some experiments relaxant responses were obtained in PSS containing 30 mM D-(+)-glucose.

Elevated glucose incubation of tissues from untreated rats

In a separate series of experiments, anococcygeus muscles isolated from untreated rats (450–500 g) were mounted under 1 g tension for isometric recording, and incubated for 6 h in PSS containing normal (11.1 mM) or elevated glucose (44.1 mM); mannose or sucrose (33 mM plus 11.1 mM glucose) were used as hyperosmolar controls. After incubation, relaxations to field stimulation (0.5-5 Hz, 10 s train), SNP (5 and 10 nM) and NO (1 and 3 μM) were obtained in the continued presence of normal or elevated glucose.

Drugs and drug solutions

Guanethidine sulphate, papaverine hydrochloride, sodium nitroprusside and streptozotocin were all purchased from Sigma Chemical Co. Ltd. (U.S.A.). Clonidine hydrochloride and pentobarbitone sodium were obtained from Boehringer Ingelheim (Australia), and insulin zinc suspension (Lente MC) from Commonwealth Serum Laboratories-Novo (Australia). A saturated solution of NO (2 mM) was prepared daily by a modification of the method described by Feelisch (1991). In brief, distilled water initially deoxygenated by gassing with argon (1 h), was bubbled with NO gas (Commonwealth Industrial Gases, Australia) for 30 min.

Statistical analysis

Results are expressed as mean ± s.e. mean and *n* indicates the number of animals tested. Differences between means were assessed with Student's *t* test or by one- or two-way analysis of variance (ANOVA). Analyses were performed using the computer package, Complete Statistical System (Statsoft, U.S.A.). Probability levels less than 0.05 were considered significant.

Results

Assessment of diabetes

At 3 days and 2, 4 and 8 weeks after injection, blood glucose levels of all STZ-treated rats were significantly greater than levels for the corresponding vehicle-treated groups (Table 1; $P<0.05$, Student's unpaired *t* test or one-way ANOVA). Furthermore, increases in body weight of all STZ-treated rats were significantly less than those of vehicle-treated rats of the same duration (Table 1; $P<0.05$, Student's unpaired *t* test or one-way ANOVA). Successful induction of diabetes was also confirmed in the STZ-treated groups by the presence of glucosuria, polyuria and polydipsia.

Insulin treatment of 8-week diabetic rats prevented the reduction in growth rate, and the increase in body weight was not different from that for vehicle-treated rats of the same duration, but was significantly greater than that for the corresponding STZ-treated group (Table 1; $P<0.05$, one-way ANOVA). Blood glucose levels of insulin-treated rats were significantly less than those of STZ-treated animals (Table 1; $P<0.05$, one-way ANOVA); however, as rats were not administered insulin on the morning of the experiment and as final blood samples were therefore obtained approximately 24 h after insulin injection, blood glucose levels of

Table 1 Blood glucose levels and body weights of vehicle- and streptozotocin (STZ)-treated rats at different time periods after injection

Duration and treatment	*Blood glucose* (mM)		*Body weight* (% initial weight)	
3 day – Vehicle	8.2 ± 0.2	(6)	106.9 ± 1.1	(6)
– STZ	22.1 ± 0.9	(6)*	99.2 ± 1.4	(6)*
2 week – Vehicle	7.8 ± 0.1	(33)	138.3 ± 1.8	(40)
– STZ	29.4 ± 0.7	(31)*	115.5 ± 1.9	(33)*
4 week – Vehicle	6.7 ± 0.2	(19)	166.3 ± 4.1	(21)
– STZ	29.2 ± 0.7	(20)*	124.7 ± 4.3	(21)*
8 week – Vehicle	7.8 ± 0.1	(8)	249.7 ± 8.7	(8)
– STZ	26.3 ± 1.7	(8)*	129.9 ± 5.1	(8)*
– STZ plus insulin	14.5 ± 0.6	(6)*	240.2 ± 9.8	(6)

Values are mean ± s.e.mean for the number of animals tested indicated in parentheses. *Significant difference from the corresponding vehicle-treated group ($P<0.05$, Student's unpaired *t* test, and one-way ANOVA for 8-week treatment group).

insulin-treated rats remained significantly greater than control values (Table 1; $P<0.05$, one-way ANOVA). Regular blood glucose measurements of insulin-treated rats demonstrated that levels remained consistently below 10 mM approximately 8 h after insulin injection (e.g. 8.2 ± 0.9 mM, $n = 6$, taken 42 days after induction of diabetes).

Effect of insulin treatment on relaxant responses

Consistent with our previous findings (Way & Reid, 1994a,b), relaxations to field stimulation (0.5–5 Hz, 10 s train), SNP (5 and 10 nM) and NO (1 and 3 μM) in muscles from diabetic rats were significantly reduced, compared to responses obtained from control tissues (Figures 1–3; $P<0.05$, two-way ANOVA). These reductions were completely prevented by insulin treatment; relaxant responses in tissues from diabetic rats which received insulin, were not significantly different from the corresponding control values (Figures 1–3; $P>0.05$, two-way ANOVA).

In a separate series of experiments, relaxant responses from both control and diabetic tissues were obtained in the presence of PSS containing high glucose (30 mM) in order to confirm that the alteration in functioning of diabetic tissue was not due to the acute change in glucose concentration from that present *in vivo* (25–30 mM) to that in PSS *in vitro* (11.1 mM). Relaxant responses to field stimulation (0.5–5 Hz, 10 s train), SNP (5 and 10 nM) and NO (1 and 3 μM) in muscles from 8-week diabetic rats were still significantly smaller than responses from 8-week control tissues, in PSS containing 30 mM glucose (Table 2; $P<0.05$, two-way ANOVA). Furthermore, relaxant responses from 8-week control and diabetic tissues obtained in PSS containing 30 mM glucose (Table 2) were not significantly different ($P>0.05$, two-way ANOVA) from those obtained in PSS containing 11.1 mM glucose ($n = 4–7$; data not shown).

Effect of duration of diabetes on relaxant responses

Relaxant responses to field stimulation (0.5–5 Hz, 10 s train) were significantly smaller in tissues from 2- and 4-week diabetic rats than in tissues from corresponding control rats (Figure 4; $P<0.05$, two-way ANOVA). Relaxations to SNP (5 and 10 nM) and NO (1 and 3 μM) were also reduced in muscles from 2- and 4-week diabetic rats compared to control responses (Figure 5). However, at 3-days duration, responses to field stimulation, SNP and NO were not

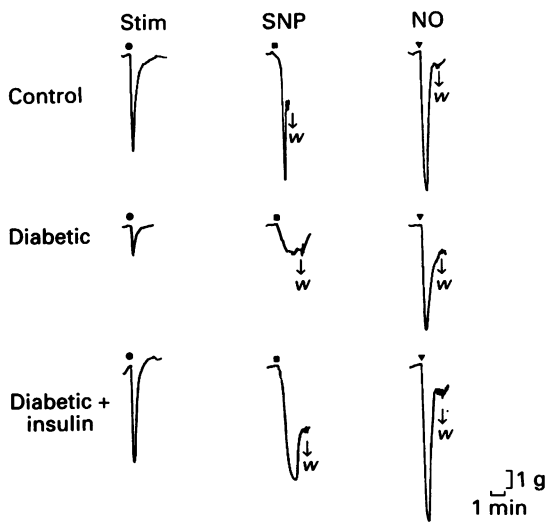

Figure 1 Representative traces showing relaxant responses to field stimulation (Stim; 1 Hz, 10 s train), to sodium nitroprusside (SNP; 5 nM) and to nitric oxide (NO; 1 μM) in anococcygeus muscles from 8-week control, diabetic and insulin-treated diabetic rats. Tissues were precontracted with guanethidine (10–30 μM) and clonidine (0.01–0.05 μM) and *w* indicates tissue washes.

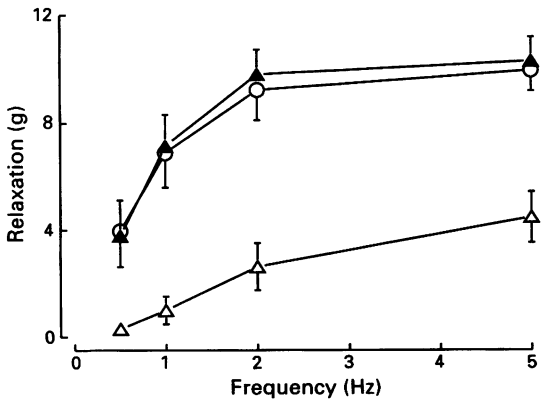

Figure 2 Relaxant responses to field stimulation (0.5–5 Hz, 10 s train) in anococcygeus muscles from 8-week control (○), diabetic (△) and insulin-treated diabetic (▲) rats. Results are mean ± s.e. mean from 6–8 experiments, expressed as reductions in tension produced in tissues precontracted with guanethidine (10–30 μM) and clonidine (0.01–0.05 μM).

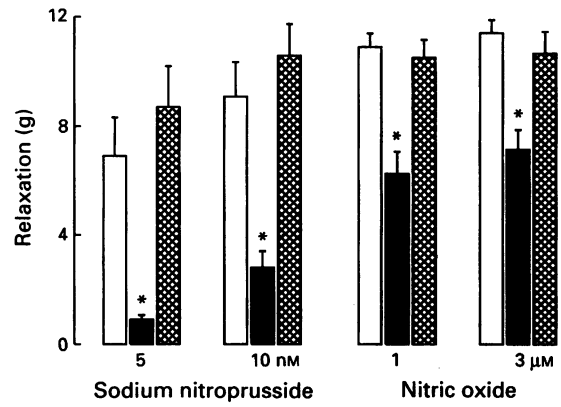

Figure 3 Relaxant responses to sodium nitroprusside and nitric oxide in anococcygeus muscles from 8-week control (open columns), diabetic (solid columns), and insulin-treated diabetic (cross-hatched columns) rats. Results are mean ± s.e. mean from 6–8 experiments expressed as reductions in tension produced in tissues precontracted with guanethidine (10–30 μM) and clonidine (0.01–0.05 μM). *Significant difference from the corresponding control value ($P<0.05$, two-way ANOVA).

Table 2 Relaxant responses to field stimulation (0.5–5 Hz, 10 s train), sodium nitroprusside (5 and 10 nM) and nitric oxide (1 and 3 μM) in anococcygeus muscles from 8-week control and diabetic rats, incubated in physiological salt solution containing 30 mM glucose

		Relaxant response (g) *Control*	*Diabetic*
Field stimulation (Hz)	0.5	6.24 ± 1.29 (5)	0.14 ± 0.11 (4)*
	1	7.98 ± 0.75 (5)	0.79 ± 0.44 (4)*
	2	9.13 ± 0.78 (5)	2.49 ± 0.91 (4)*
	5	9.69 ± 0.65 (5)	4.28 ± 1.05 (4)*
Sodium nitroprusside	5	7.05 ± 0.90 (5)	0.40 ± 0.12 (4)*
(nM)	10	9.42 ± 0.79 (5)	1.08 ± 0.22 (4)*
Nitric oxide (μM)	1	9.07 ± 1.03 (5)	3.28 ± 0.83 (4)*
	3	9.56 ± 0.65 (5)	4.53 ± 0.91 (4)*

Values are mean ± s.e.mean for the number of animals tested indicated in parentheses. *Significant difference from the corresponding control value ($P<0.05$, two-way ANOVA).

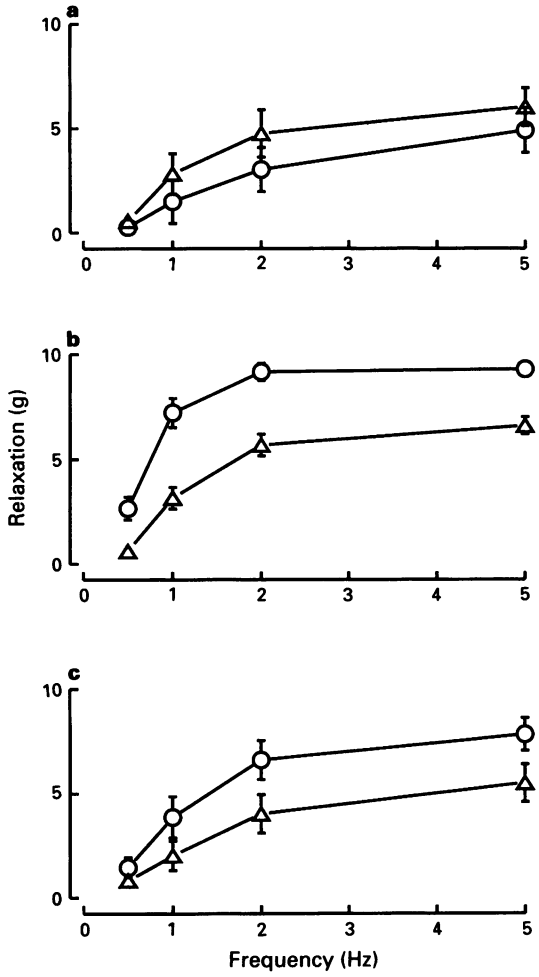

Figure 4 Relaxant responses to field stimulation (0.5–5 Hz, 10 s train) in anococcygeus muscles from rats at 3 days (a), 2 weeks (b) and 4 weeks (c) after induction of diabetes. Responses from control (○) and diabetic (△) rats are shown as reductions in tension produced in tissues precontracted with guanethidine (10–30 μM) and clonidine (0.01–0.05 μM). Values are mean ± s.e. mean from 6–13 experiments.

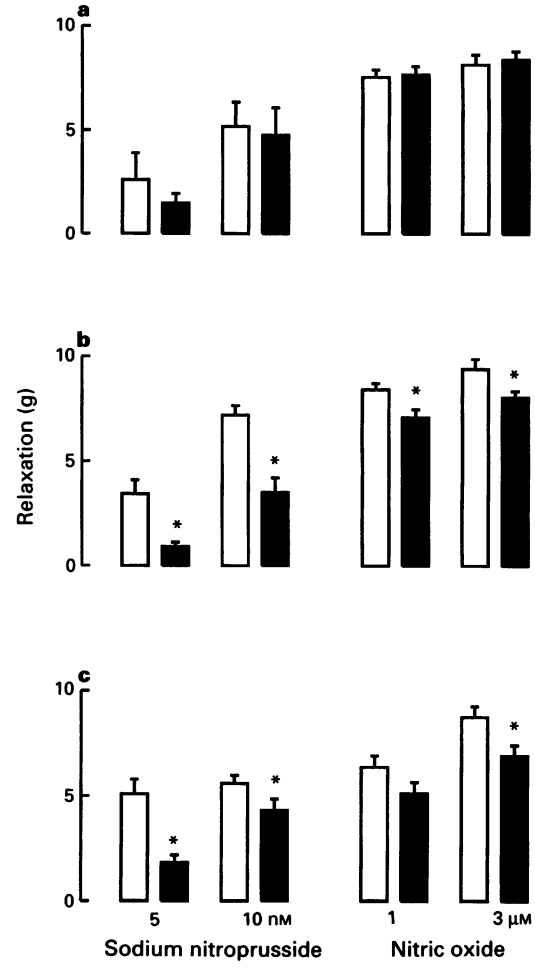

Figure 5 Relaxant responses to sodium nitroprusside and nitric oxide in anococcygeus muscles obtained at 3 days (a), 2 weeks (b) and 4 weeks (c) after induction of diabetes. Responses from control (open columns) and diabetic (solid columns) rats are shown as reductions in tension produced in tissues precontracted with guanethidine (10–30 μM) and clonidine (0.01–0.05 μM). Values are mean ± s.e. mean from 6–15 experiments. *Significant difference from the corresponding control value ($P<0.05$, Student's t test).

significantly different between control and diabetic animals (Figures 4 and 5; $P>0.05$, two-way ANOVA and Student's unpaired t test).

Relaxant responses to papaverine (3 and 10 μM) in tissues from diabetic rats of both 2-weeks and 4-weeks duration were not reduced compared to the corresponding control values (Table 3); the response to 3 μM papaverine in muscles from 4-week diabetic rats was in fact slightly but significantly greater than the response from 4-week control rats (Table 3; $P<0.05$, Student's unpaired t test).

Table 3 Relaxant responses obtained to papaverine (3 and 10 μM) in anococcygeus muscles from control and diabetic rats at 2 and 4 weeks after the induction of diabetes

Duration and group	*Relaxant response* (g) *Papaverine* (μM) *3*		*10*	
2 week – Control	1.08 ± 0.11	(12)	6.71 ± 0.33	(11)
– Diabetic	0.82 ± 0.12	(9)	6.38 ± 0.27	(9)
4 week – Control	0.55 ± 0.12	(8)	4.10 ± 0.41	(11)
– Diabetic	0.88 ± 0.09	(8)*	4.94 ± 0.37	(8)

Values are mean ± s.e.mean for the number of animals tested indicated in parentheses. *Significant difference from the corresponding control value ($P<0.05$, Student's unpaired t test).

Effect of exposure to elevated glucose on relaxant responses in tissues from untreated rats

Incubation of anococcygeus muscles from untreated rats in PSS containing high glucose (44.1 mM) for 6 h, significantly impaired relaxant responses to field stimulation (0.5–5 Hz, 10 s train), compared to relaxations obtained in tissues exposed to normal glucose (11.1 mM) for 6 h (Figure 6; $P<0.05$, two-way ANOVA). Responses to SNP (5 and 10 nM) or to NO (1 and 3 μM) in the presence of elevated glucose were not significantly different from responses obtained after normal glucose incubation (Figure 7; $P>0.05$, one-way ANOVA). Similarly, incubation of muscles in hyperosmolar solutions containing mannose or sucrose (33 mM plus 11.1 mM glucose) for 6 h significantly reduced relaxations to field stimulation compared to relaxations in muscles incubated in normal glucose (Figure 6; $P<0.05$, two-way ANOVA), but did not alter responses to SNP or NO (Figure 7; $P>0.05$, one-way ANOVA).

Discussion

The present study confirms our previous findings (Way & Reid, 1994a,b) that smooth muscle reactivity to NO is

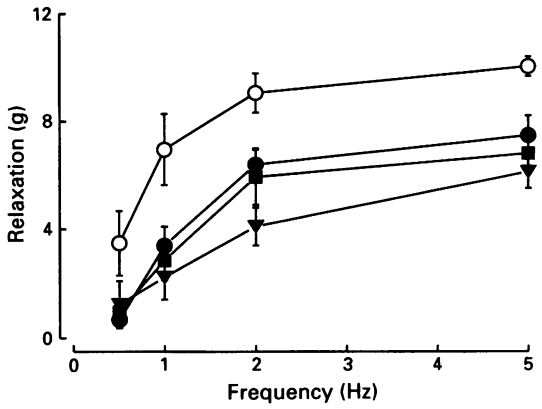

Figure 6 Relaxant responses to field stimulation (0.5–5 Hz, 10 s train) in anococcygeus muscles after 6 h incubation in medium containing normal glucose (11.1 mM; ○), or elevated glucose (44.1 mM; ●) or an equiosmolar medium containing mannose (▼) or sucrose (■; 33 mM plus 11.1 mM glucose). Values are mean ± s.e. mean from 5–8 experiments, expressed as reductions in tension produced in tissues precontracted with guanethidine (10–30 μM) and clonidine (0.01–0.05 μM).

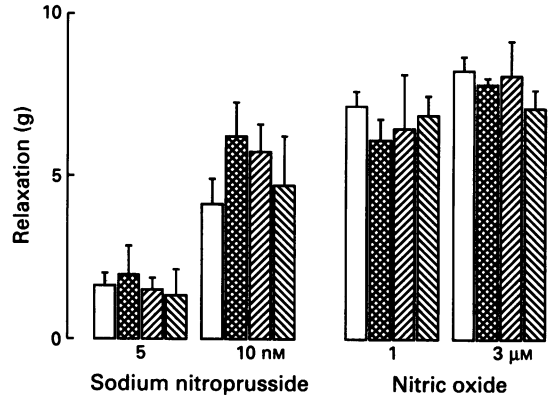

Figure 7 Relaxant responses to sodium nitroprusside and nitric oxide in anococcygeus muscles after 6 h incubation in medium containing normal glucose (11.1 mM; open columns), or elevated glucose (44.1 mM; cross-hatched columns) or an equiosmolar medium containing mannose (right-hatched columns) or sucrose (left-hatched columns; 33 mM plus 11.1 mM glucose). Values are mean ± s.e. mean from 4–8 experiments, expressed as reductions in tension produced in tissues precontracted with guanethidine (10–30 μM) and clonidine (0.01–0.05 μM).

attenuated in anococcygeus muscle from 8-week diabetic rats. We now report that treatment of 8-week diabetic rats with 5 u Lente insulin day^{-1} prevents the development of impaired responses to field stimulation, to the NO donor SNP and to NO, in anococcygeus muscle. These results suggest that the observed alteration in nitrergic neurotransmission is due to the production of a diabetic state by STZ and is not due to any non-specific effect of STZ itself. This is in agreement with numerous studies using other smooth muscle preparations where the effects of STZ-induced diabetes have been reversed or prevented by insulin treatment (Nowak *et al.*, 1986; Longhurst *et al.*, 1991; Hodgson & King, 1992; Stevens *et al.*, 1993).

Exposure of tissues from 8-week diabetic rats to a high glucose medium (30 mM), containing a similar concentration of glucose to blood levels in diabetic rats, did not affect the impairment in smooth muscle reactivity to NO. Other studies have also reported no change in functioning of diabetic tissue after incubation in high glucose medium (Cameron & Cotter, 1992; Booth & Hodgson, 1993). However, prevention of diabetes-induced changes in tissue responsiveness has been reported in aortae from 2-week but not 6-week STZ-treated rats after incubation in PSS containing 30 mM glucose (Hodgson & King, 1992). Nevertheless, in the present study, we have demonstrated that the impairment of nitrergic transmission in the anococcygeus muscle from 8-week diabetic rats is not related to the acute change in glucose concentration from that present *in vivo* (approximately 25–30 mM), to the comparatively reduced concentration *in vitro* (11 mM).

Other studies have also shown changes to NANC-inhibitory innervation induced by the diabetic state. These include alterations to both the purinergic (Belai *et al.*, 1991) and peptidergic (Belai *et al.*, 1987; D'Amato & Curró, 1990) components of rat gastrointestinal tissue, and impaired NANC neurotransmission in human corporal smooth muscle from impotent diabetic men (Saenz de Tejada *et al.*, 1989). Furthermore, previous studies have demonstrated that the development of diabetes-induced changes may depend on the duration of the diabetic state (MacLeod & McNeill, 1985; Belai *et al.*, 1988; Morff, 1990; Nowak *et al.*, 1990). For example, in the myenteric plexus of STZ-diabetic rats, biochemical results showed a trend at 8 weeks for an increase in noradrenaline content, followed by a decrease in both tissue content and nerve fibre density at 16 and 24 weeks after diabetes induction (Belai *et al.*, 1988). Another study described defective cholinergic neuromuscular transmission in diabetic rat small intestine after 4 weeks, but this defect was less evident at 8 weeks, and after 12 weeks the changes had spontaneously resolved (Nowak *et al.*, 1990). Therefore, diabetes-induced changes do not necessarily follow a consistent pattern with an increase in the duration of the diabetic state.

To address the question of changes in the development of diabetes-induced alterations over time, we have examined the relationship between altered NO-mediated relaxations and the time course after the onset of diabetes, up to an 8-week period. At 3 days after the induction of diabetes with STZ, there were no apparent changes in relaxant responses to field stimulation, SNP or NO, when compared with appropriate controls. However, consistent with our findings at the 8-week period, relaxations to field stimulation, SNP and NO were attenuated at 2 weeks and 4 weeks after the induction of diabetes, whereas relaxant responses to papaverine, which does not act through NO, were not impaired at either duration. Our results therefore indicate that the specific impairment of NO-mediated relaxations in rat anococcygeus muscle develops within the first 2 weeks of diabetes and persists for a further 6-week period; the influence of chronic experimental diabetes on the progression of the changes seen at 8 weeks remains to be determined.

The direct effects of an elevated glucose environment *per se* on tissue responsiveness has been previously examined by exposing preparations to elevated glucose media for a sufficient period (Williamson *et al.*, 1990; Tesfamariam *et al.*, 1990; 1991; Bohlen & Lash, 1993; Taylor & Poston, 1994). Tesfamariam and colleagues (1990) demonstrated that the incubation of rabbit aortic rings in high glucose for 6 h impaired cholinergic endothelium-dependent relaxations, similar to the impairment demonstrated in aortae from alloxan-diabetic rabbits. In the present study a similar experimental protocol to that used by Tesfamariam *et al.* (1990, 1991) was employed to investigate whether impaired NO-mediated neurotransmission in diabetic rat anococcygeus muscle could be mimicked by exposure of muscles from untreated rats to acute hyperglycaemic conditions. With a glucose concentration of 44 mM and an incubation period of 6 h (see Tesfamariam *et al.*, 1990; 1991), exposure of muscles *in vitro* to elevated glucose specifically attenuated relaxant responses to field stimulation, but not to SNP or to NO. However, the effects of 44 mM glucose were also produced after a 6 h incubation in equiosmolar solutions containing mannose or sucrose, suggesting that hyperosmolarity *per se* was responsible for the impairment.

The differences in the effects on NO-mediated neurotrans-

mission produced by incubation in high glucose media and by the diabetic state, may reflect acute *versus* chronic exposure to elevated glucose. Acute 6 h exposure to a hyperosmolar environment specifically impaired the response to nitrergic nerve stimulation, possibly affecting NO synthesis, release, or breakdown, without altering the smooth muscle responsiveness to NO. In contrast, diabetes of 2-, 4- and 8-weeks duration, with consequent chronic exposure of muscles to high glucose, impaired the smooth muscle reactivity to NO; this may follow an initial impairment in the release of NO from nitrergic nerves, or a concurrent impairment could exist. The mechanism by which *in vitro* exposure to elevated glucose impairs the response to nitrergic nerve stimulation in anococcygeus muscle is as yet unknown. Free radical generation has been implicated in the impairment of endothelium-dependent relaxations in rabbit aortae exposed to elevated glucose (Tesfamariam & Cohen, 1992), whereas the increased metabolism of glucose via the polyol pathway is thought to contribute to functional changes in rat microvessels subjected to high glucose media (Williamson *et al.*, 1990). Such mechanisms could similarly contribute to alterations in NO-mediated neurotransmission produced in anococcygeus muscle by elevated glucose both *in vitro* and by the diabetic state *in vivo*.

In conclusion, impaired NO-mediated neurotransmission in anococcygeus muscle from 8-week diabetic rats, is prevented by insulin treatment and is thus specific for the production of a diabetic state by STZ. Relaxations to nitrergic nerve stimulation and to exogenously added NO were similarly impaired at diabetes durations of 2 and 4 weeks but not 3 days, suggesting the observed alterations develop during the first 2 weeks of diabetes. *In vitro* incubation of anococcygeus muscles in high osmolar media specifically impaired NO-mediated relaxation to nerve stimulation. Therefore elevated glucose levels *in vivo* may contribute towards the development of impaired NO-mediated neurotransmission in anococcygeus muscles from diabetic rats.

This work was supported by a Programme Grant from the National Health and Medical Research Council of Australia.

References

BELAI, A., LEFEBVRE, R.A. & BURNSTOCK, G. (1991). Motor activity and neurotransmitter release in the gastric fundus of streptozotocin-diabetic rats. *Eur. J. Pharmacol.*, **194**, 225–234.

BELAI, A., LINCOLN, J. & BURNSTOCK, G. (1987). Lack of release of vasoactive intestinal polypeptide and calcitonin gene-related peptide during electrical stimulation of enteric nerves in streptozotocin-diabetic rats. *Gastroenterology*, **93**, 1034–1040.

BELAI, A., LINCOLN, J., MILNER, P. & BURNSTOCK, G. (1988). Progressive changes in adrenergic, serotonergic, and peptidergic nerves in proximal colon of streptozotocin-diabetic rats. *Gastroenterology*, **95**, 1234–1241.

BELAI, A., LINCOLN, J., MILNER, P., CROWE, R., LOESCH, A. & BURNSTOCK, G. (1985). Enteric nerves in diabetic rats: increase in vasoactive intestinal polypeptide but not substance P. *Gastroenterology*, **89**, 967–976.

BOHLEN, H.G. & LASH, J.M. (1993). Topical hyperglycaemia rapidly suppresses EDRF-mediated vasodilation of normal rat arterioles. *Am. J. Physiol.*, **265**, H219–H225.

BOOTH, R.J. & HODGSON, W.C. (1993). Effects of aldose reductase inhibition with epalrestat on diabetes-induced changes in rat isolated atria. *Clin. Exp. Pharmacol. Physiol.*, **20**, 207–213.

CAMERON, N.E. & COTTER, M.A. (1992). Dissociation between biochemical and functional effects of the aldose reductase inhibitor, ponalrestat, on peripheral nerve in diabetic rats. *Br. J. Pharmacol.*, **107**, 939–944.

CLARKE, B.F., EWING, D.J. & CAMPBELL, I.W. (1979). Diabetic autonomic neuropathy. *Diabetologia*, **17**, 195–212.

D'AMATO, M. & CURRO, D. (1990). Non-adrenergic non-cholinergic inhibitory innervation of the gastric fundus in streptozotocin-diabetic rats. *Acta Physiol. Hung.*, **75**, (Suppl.), 77–78.

FEELISH, M. (1991). The biochemical pathways of nitric oxide formation from nitrovasodilators: appropriate choice of exogenous NO donors and aspects of preparation and handling of aqueous NO solutions. *J. Cardiovasc. Pharmacol.*, **17** (Suppl. 3), S25–S33.

GILLESPIE, J.S. (1972). The rat anococcygeus muscle and its response to nerve stimulation and to some drugs. *Br. J. Pharmacol.*, **45**, 404–416.

HODGSON, W.C. & KING, R.G. (1992). Effects of glucose, insulin or aldose reductase inhibition on responses to endothelin-1 of aortic rings from streptozotocin-induced diabetic rats. *Br. J. Pharmacol.*, **106**, 644–649.

HOSKING, D.J., BENNETT, T. & HAMPTON, J.R. (1978). Diabetic autonomic neuropathy. *Diabetes*, **27**, 1043–1054.

LINCOLN, J., BOKOR, J.T., CROWE, R., GRIFFITH, S.G., HAVEN, A.J. & BURNSTOCK, G. (1984). Myenteric plexus in streptozotocin-treated rats. Neurochemical and histochemical evidence for diabetic neuropathy in the gut. *Gastroenterology*, **86**, 654–661.

LONGHURST, P.A. & BELIS, J.A. (1986). Abnormalities of rat bladder contractility in streptozotocin-induced diabetes mellitus. *J. Pharmacol. Exp. Ther.*, **238**, 773–777.

LONGHURST, P.A., KAUER, J. & LEVIN, R.M. (1991). The ability of insulin treatment to reverse or prevent the changes in urinary bladder function caused by streptozotocin-induced diabetes mellitus. *Gen. Pharmacol.*, **22**, 305–311.

MACLEOD, K.M. & MCNEILL, J.H. (1985). The influence of chronic experimental diabetes on contractile responses of rat isolated blood vessels. *Can. J. Physiol. Pharmacol.*, **63**, 52–57.

MATHISON, R. & DAVISON, J.S. (1988). Modified smooth muscle responses of jejunum in streptozotocin-diabetic rats. *J. Pharmacol. Exp. Ther.*, **244**, 1045–1050.

MORFF, R.J. (1990). Microvascular reactivity to norepinephrine at different arteriolar levels and durations of streptozotocin-induced diabetes. *Diabetes*, **39**, 354–360.

NOWAK, T.V., HARRINGTON, B. & KALBFLEISCH, J.H. (1990). Adaptation of cholinergic enteric neuromuscular transmission in diabetic rat small intestine. *Diabetes*, **39**, 891–897.

NOWAK, T.V., HARRINGTON, B., KALBFLEISCH, J.H. & AMATRUDA, J.M. (1986). Evidence for abnormal cholinergic neuromuscular transmission in diabetic rat small intestine. *Gastroenterology*, **91**, 124–132.

SAENZ DE TEJADA, I., GOLDSTEIN, I., AZADZOI, K., KRANE, R.J. & COHEN, R.A. (1989). Impaired neurogenic and endothelium-mediated relaxation of penile smooth muscle from diabetic men with impotence. *N. Engl. J. Med.*, **320**, 1025–1030.

STEVENS, E.J., WILLARS, G.B., LIDBURY, P., HOUSE, F. & TOMLINSON, D.R. (1993). Vasoreactivity and prostacyclin release in streptozotocin-diabetic rats: effects of insulin or aldose reductase inhibition. *Br. J. Pharmacol.*, **109**, 980–986.

TAYLOR, P.D. & POSTON, L. (1994). The effect of hyperglycaemia on function of rat isolated mesenteric resistance artery. *Br. J. Pharmacol.*, **113**, 801–808.

TESFAMARIAM, B., BROWN, M.L. & COHEN, R.A. (1991). Elevated glucose impairs endothelium-dependent relaxation by activating protein kinase C. *J. Clin. Invest.*, **87**, 1643–1648.

TESFAMARIAM, B., BROWN, M.L., DEYKIN, D. & COHEN, R.A. (1990). Elevated glucose promotes generation of endothelium-derived vasoconstrictor prostanoids in rabbit aorta. *J. Clin. Invest.*, **85**, 929–932.

TESFAMARIAM, B. & COHEN, R.A. (1992). Free radicals mediate endothelial cell dysfunction caused by elevated glucose. *Am. J. Physiol.*, **263**, H321–H326.

WAY, K.J. & REID, J.J. (1994a). Nitric oxide mediated neurotransmission is attenuated in the anococcygeus muscle from diabetic rats. *Diabetologia*, **37**, 232–237.

WAY, K.J. & REID, J.J. (1994b). Effect of aminoguanidine on the impaired nitric oxide-mediated neurotransmission in anococcygeus muscle from diabetic rats. *Neuropharmacology*, **33**, 1315–1322.

WILLIAMSON, J.R., OSTROW, E., EADES, D., CHANG, K., ALLISON, W., KILO, C. & SHERMAN, W.R. (1990). Glucose-induced microvascular functional changes in nondiabetic rats are stereospecific and are prevented by an aldose reductase inhibitor. *J. Clin. Invest.*, **85**, 1167–1172.

(Received January 23, 1995
Accepted February 13, 1995)

British Journal of Pharmacology (1995) 115, 415-420

Effects of vitamin E deficiency on vasomotor activity and ultrastructural organisation of rat thoracic aorta

[1]Annalisa Rubino, Andrzej Loesch, *Mark A. Goss-Sampson, *Peter Milla & Geoffrey Burnstock

Department of Anatomy and Developmental Biology, University College London, Gower Street, London WC1E 6BT and *Division of Biochemistry, Institute of Child Health, Guilford Street, London WC1 N1IH

1 The effects of vitamin E deficiency were evaluated in aortic rings isolated from rats maintained on a diet deficient in vitamin E.

2 Endothelium-dependent vasodilator responses to acetylcholine (ACh) and calcium ionophore, A23187, were reduced in preparations from treated animals, compared to the age-matched controls. The maximal vasodilatation to ACh was 66.4 ± 9 (n = 4) and 38.8 ± 7 (n = 4) % in control and 10 month-treated preparations, respectively.

3 The endothelium-independent vasodilator responses to sodium nitroprusside as well as the concentration-dependent contractile responses to noradrenaline, did not differ between treated and control preparations.

4 Electron microscopic examination of vascular segments and revealed that, following vitamin E deficiency, normal tissue organisation was disrupted, the endothelial monolayer either not being in contact with the underlying tissue or being absent in most of the areas analysed.

5 It is concluded that during vitamin E deficiency both morphological disruption and functional impairment of endothelium occur without observable modification of muscle cell function and morphology.

Keywords: Vitamin E deficiency; rat aorta; endothelium-mediated vasodilatation; ultrastructural vascular morphology

Introduction

For several years since its discovery, the role of vitamin E in human nutrition has been the subject of much debate and controversy. However, it is now clear that vitamin E is necessary for the maintenance of some biological structures and that it has pathophysiological roles. The mechanisms involved in these actions are still not established. The biological activity of vitamin E results principally from its antioxidant properties and subsequently the protection of molecules and biological systems from oxidative damage by oxygen-derived free radicals. Vitamin E can in fact halt the chain oxidative reactions generated by oxygen-derived free radicals by trapping these highly reactive chemical species (Burton *et al.*, 1983; Muller & Goss-Sampson, 1990). In addition to its role as an antioxidant, vitamin E may have membrane stabilizing effects, its incorporation into the bilayer of biological membranes resulting in decreased membrane fluidity (Lucy, 1972; Patel *et al.*, 1991).

In vitamin E-deprived rats and monkeys, no changes in resting heart rate and blood pressure were observed (Filer *et al.*, 1949; Hubel *et al.*, 1989). However, pharmacological studies on rats kept on a diet deficient in vitamin E have indicated reduced vasodilator responses to acetylcholine (ACh), associated with an enhanced vascular responsiveness to angiotensin II (Hubel *et al.*, 1989). Moreover, in aorta isolated from an animal model of vitamin E deficiency, an increase of the expression of prostaglandin endoperoxide synthase and a decrease of thromboxan A synthase has been demonstrated (Davidge *et al.*, 1993). This evidence suggests that vitamin E may play a role in the control of vascular function.

The present study was designed to extend preliminary observations on the effects of vitamin E deficiency on vasomotor activity and to examine the ultrastructual organization in the vessel wall during vitamin E deficiency.

Some of these data were presented as an abstract at the Meeting of the British Pharmacological Society, Cambridge, January 1993 (see Rubino *et al.*, 1993).

[1] Author for correspondence.

Methods

Animal treatment

The animal model of vitamin E deficiency has been described in detail (Goss-Sampson *et al.*, 1990). Briefly, post-weaning (21-23 days old) male Wistar rats (Charles Rivers Ltd., U.K.) were maintained on a vitamin E deficient diet (Machlin/Draper-HLR no. 814, supplied by Dyets, Pennsylvania, U.S.A.) which comprised tocopherol-stripped corn oil (10%), glucose (65%), salt mix (4%), vitamin-free casein (20%) and full vitamin supplementation (excluding vitamin E). The diet was sterilized by irradiation (1.5 Mrads). Control animals were fed the same diet with the addition of α-tocopherol acetate (40 mg kg^{-1} diet). The two groups of animals were kept on their respective diets for 6 or 10 months, being allowed free access to food and water. Each group of animals (treated and age-matched controls) included 6-8 rats. A group of three animals and their age-matched controls were kept on their respective diets for 12 months and were used for morphological investigations. Following this treatment, plasma and tissue stores of α-tocopherol were depleted in rats receiving the vitamin E deficient diet, as assayed in previous investigations (Goss-Sampson *et al.*, 1990).

Pharmacological investigation

Animals were heparinised (1000 units i.p.) 15 min before they were killed by an overdose of sodium pentobarbitone (Sagatal, RMB Animal Health, Dagenham, England) and exsanguinated. The abdomen was opened and the descending thoracic aorta was removed and cleaned of all loosely adherent connective tissue. Rings (4-5 mm wide) were prepared and mounted between two hooks in 10 ml organ baths containing Krebs solution of the following composition (mM): NaCl 133, KCl 4.7, NaH_2PO_4 1.35, $NaHCO_3$ 16.3, $MgSO_4$ 0.61, $CaCl_2$ 2.52 and glucose 7.8, gassed with 95% O_2, 5% CO_2 and maintained at 37°C. Preparations were allowed to equilibrate for at least 60 min, under a resting tension of 1.5 g. Isometric responses were recorded by use of a Grass FTO3C transducer and displayed on a Grass ink-writing polygraph (model 79).

After 30 min, the tension on the rings was readjusted to 1.5 g and the experiments started after a further 30 min equilibration period. Cumulative concentrations of noradrenaline (NA) were added to the bath to detect contractile responses. In order to evaluate vasodilatation, rings were preconstricted to their EC_{75} value with NA to obtain a stable plateau and challenged with increasing concentrations of the vasodilator tested. The next concentration of the agonist was added to the bath when the previous response had reached a plateua. Cumulative concentration-response curves were obtained in each preparation at intervals of 20 min. No more than 3 reproducible responses to the EC_{75} concentration of NA could be obtained in each preparation. Therefore endothelium-dependent and -independent responses to ACh and sodium nitroprusside (SNP) were evaluated in both age groups while vasodilator responses to ATP and A23187 were alternatively tested in 6 and 10 month-old rats, respectively.

Morphological studies

For ultrastructural purposes aortic segments isolated from 12 months vitamin E-deprived rats ($n=3$) and age-matched controls ($n=3$), were fixed for 3 h at 4°C with fixture containing 2% paraformaldehyde and 2% glutaraldehyde in 0.1 M phosphate buffer, pH 7.4. Vessels were then washed in phosphate buffer, post-fixed in 1% osmium tetroxide dehydrated through an ethanol series and embedded in araldite. Ultrathin circumferential sections (at least 5 sections were taken from 3 different levels of each specimen) were stained with uranyl acetate and lead citrate and subsequently examined using a JEM-1010 electron microscope.

Calculations and statistics

Vascular responses were evaluated as changes in tension (mg) and vasodilatration was calculated as percentage of the NA-sustained tome. EC_{50} values were calculated from the concentration of drug which produced 50% of its maximal response in each concentration-response curve. Results are expressed as means ± s.e.mean. Analysis of variance was used for comparing dose-response curves of treated animals with their age-matched controls. Student's t test for unpaired data was applied in order to compare 2 groups of data (i.e. EC_{50} values of vitamin E-deficient rats versus age-matched controls; EC_{50} values of 6 versus 10 month-old rats). Results were considered significantly different when $P>0.05$. n refers to the number of animals from which vessels were used.

Drugs

The following drugs were used: noradrenaline HCl, sodium nitroprusside, calcium ionophore A23187, adenosine 5'-triphoshpate (ATP), acetylcholine chloride (Sigma). A23187 was dissolved in 100% dimethylsulphoxide (DMSO) in order to obtain a stock solution of 0.01 M. Further dilutions were prepared in Krebs solution. NA was made up in 0.1% ascorbic acid.

Results

Animal model

The following mean weights were found at each age for control and vitamin E deficient rats, respectively. 6 months: 518.8 ± 7.6 ($n=9$) and 524.1 ± 28.7 ($n=8$) g; 10 months: 593.8 ± 23.1 ($n=8$) and 554.9 ± 25.9 ($n=8$) g. No significant differences were observed in the body weight between control and treated animals.

Effect of acetylcholine (ACh)

In aortic rings preconstricted with NA, ACh (0.01 – 10 μM) induced concentration-dependent vasodilation. The maximal effect achieved with 1 μM ACh in rings from 6 month-old control animals was 79.6 ± 1.8 ($n=9$; $EC_{50}=97.2\pm20.5$ nM) % relaxation. In contrast, in rings from 6 month-treated animals, the vasodilator responses to ACh were significantly reduced at all the concentrations tested and the maximal relaxation obtained was 40 ± 12 ($n=9$; $EC_{50}=210\pm50$ nM) % of the NA sustained tone (Figure 1a). Similar results were obtained in rings from rats treated for 10 months and age-matched controls. The maximal effect achieved with 1 μM ACh induced a vasodilatation of 66.4 ± 9 ($n=4$; $EC_{50}=36\pm6$ nM) % in control rings and only 38.8 ± 7 ($n=4$; $EC_{50}=112\pm23$ nM) & relaxation in preparations from treated animals (Figure 1b).

Effect of A23187 and ATP

In order to verify whether the reduced vasodilator responses of treated preparations were selective for ACh, the vasodilatation of the calcium ionophore, A23187 and ATP was also tested in animals treated for 10 and 6 months, respectively. A23187 (1 – 300 nM) induced concentration-dependent vasodilatation up to 76.6 ± 4.4 ($n=5$; $EC_{50}=23.5\pm4$ nM) % in control preparations and only up to 25 ± 8.3 ($n=5$; $EC_{50}=66\pm7.2$ nM) % in rings isolated from rats treated for 10 months (Figure 2a). There was no significant difference between the control and

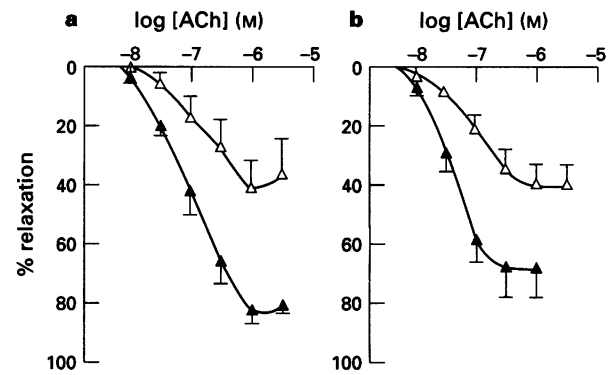

Figure 1 Vasodilator responses to increasing concentrations of acetylcholine (ACh) in 6 (a) and 10 months (b) vitamin E-deficient rats (△) and age-matched control (▲) vessel groups. Statistically significant differences (P at least >0.05) were observed between control and treated preparations at all the concentrations of ACh tested.

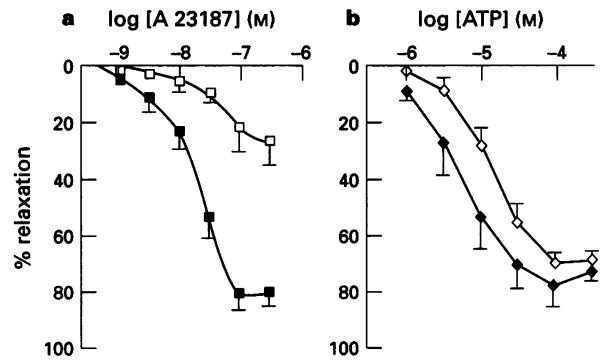

Figure 2 Vasodilator responses to increasing concentrations of calcium ionophore A23187 (a) and ATP (b). (a) Control (■) and 10 months vitamin E-deficient (□) vessel groups. Statistically significant differences (P at least <0.05) were observed between control and treated preparations at all the concentrations of A23187 tested. (b) Control (◆) and 6 months vitamin E-deficient (◇) vessel groups. No statistically significant difference was detected between treated and control preparations at any of the concentrations of ATP tested.

treated preparations when the vasodilator responses to ATP (1–300 μM) were evaluated (Figure 2b). The maximal responses to 300 μM ATP were similar in control and 6 month-treated preparations, being a vasodilatation of 69.0±3.1 and 66.2±2.3% of the NA sustained tone, respectively. EC_{50} values differed significantly, being 3.8±1.2 μM ($n=4$) in rings from control animals and 12.4±3.1 μM ($n=4$) in rings from treated rats.

Effect of sodium nitroprusside (SNP)

When the vasodilator responses to SNP were evaluated, no significant difference was detected between vitamin E-deficient and age-matched control animals. SNP (1–300 nM) induced concentration-dependent vasodilatation up to 100% relaxation of the NA sustained tone in control and treated rings of both age groups studied (Figure 3a, b). EC_{50} values were 13.3±2.3 ($n=9$) and 6.2±0.6 ($n=9$) nM in 6 month-control and treated rings, respectively (Figure 3a). Similarly, EC_{50} values were 9.3±3.5 ($n=5$) and 7.3±1.9 ($n=5$) nM in 10 month-control and vitamin E-deficient preparations, respectively (Figure 3b).

Effect of noradrenaline (NA)

Aortic rings isolated from control and vitamin E-deficient animals showed contractile responses of the same magnitude to increasing concentrations of NA (0.3–1 μM). In rings from 6 month-treated and age-matched control rats, the maximal responses achieved were 986±120 ($n=9$; $EC_{50}=51.9\pm4.6$ nM) and 912±67 ($n=11$; $EC_{50}=45.6\pm9.9$ nM) mg of tension, respectively (Figure 4a). Similarly, the effect of 1 μM NA was a contraction of 787±30 ($n=5$; $EC_{50}=38.7\pm9$ nM) mg in preparations from 10 month-treated rats, and 712±159 ($n=5$; $EC_{50}=39.4\pm12.1$ nM) mg in age-matched control rats (Figure 4b).

Vascular morphology

Aortic segments of the control preparations displayed well-preserved ultrastructural organisation including intima, media and adventitia. Endothelial cells were in close contact with the underlying vessel wall (Figure 5A) and were characterized by the presence of moderate-density intracellular organelles, such as endoplasmic reticulum, mitochondria and cytoplasmic vesicles. The cell nuclei were rich in heterochromatin (Figure 5b). In contrast to segments from control animals, aortae isolated from 12 month-vitamin E-deficient rats displayed marked ultrastructural alterations in the endothelium. It was estimated that on at least 30% of the luminal site of the vascular wall,

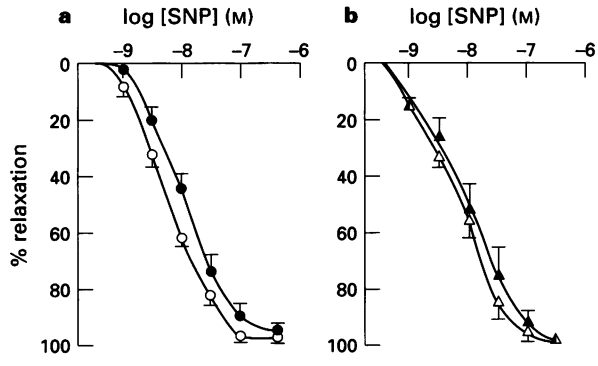

Figure 3 Vasodilator responses to increasing concentrations of sodium nitroprusside (SNP) in 6 (a) and 10 months (b) vitamin E-deficient rats (○ ◇) and age-matched control (● ◆) vessel groups. No statistically significant difference was observed between treated and control preparations at any of the concentrations of SNP tested.

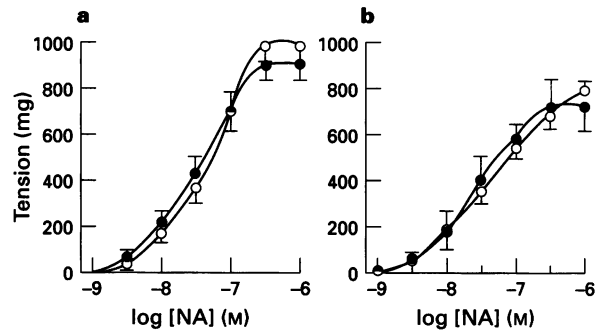

Figure 4 Contractile responses to increasing concentrations of noradrenaline (NA) in 6 (a) and 10 months (b) vitamin E-deficient rats (○) and age-matched control (●) vessel groups. No statistically significant difference was detected between treated and control preparations at any of the concentrations of NA tested.

endothelial cells were either separated from the vessel wall (Figure 5c) or absent (Figure 5d). The cell nuclei were swollen, less electron-dense than those of controls and displayed relatively less marginal heterochromatin. In those regions of the vessels free of endothelium some subendothelial changes were also evident, in particular the appearance of unusual structures protruding into the lumen, which displayed membrane-free granulated dense material (Figure 5e). In contrast to altered endothelium, smooth muscle cells and extracellular matrix showed an organisation similar to that observed in control sections.

Discussion

The present study demonstrates that dietary vitamin E deficiency is associated with impairment of vasomotor activity and drastic changes in the ultrastructural organisation of the vascular wall.

It is well established that vasodilatation results from complex biochemical and pharmacological interactions among different constituents of the vascular wall (for review see Ralevic & Burnstock, 1993). However, pharmacological tools are available to discriminate between endothelium-dependent and -independent mechanisms of vasodilatation. In general the former mechanism of vasodilatation is related to production of endothelium-derived relaxing factor (EDRF) from endothelial cells, which in turn acts on smooth muscle cells (Furchgott, 1983; 1984). To date the general consensus is that EDRF is nitric oxide (NO) or a labile nitroso compound (Ignarro *et al.*, 1987; Palmer *et al.*, 1988). Endothelium-independent relaxation can be achieved by using donors of NO, such as SNP, which induce vascular smooth muscle relaxation, or via direct pharmacological activation of receptors located on smooth muscle cells, such as adenosine receptors (see Olsson & Pearson, 1990). The finding that the endothelium-dependent vasodilatation to ACh and calcium ionophore A23187 was drastically reduced in treated preparations compared to controls, whilst the endothelium-independent relaxation to SNP was similar in treated and control aortic rings, indicated that vitamin E deficiency selectively impaired endothelial function, without affecting the ability of smooth muscle cells to respond to vasoactive agents.

In the present study, contractile responses to NA did not differ between control and vitamin E-deficient animals, thus further supporting the hypothesis that endothelial rather than smooth muscle function is affected by vitamin E deficiency. The presence of α_2-adrenoceptors which induce release of EDRF has been shown in the endothelium of the rat aorta (Bullock *et al.*, 1986). Impaired endothelial function in vitamin E deficiency could therefore result in enhanced contractile responses to NA. However, our results are not in favour of this

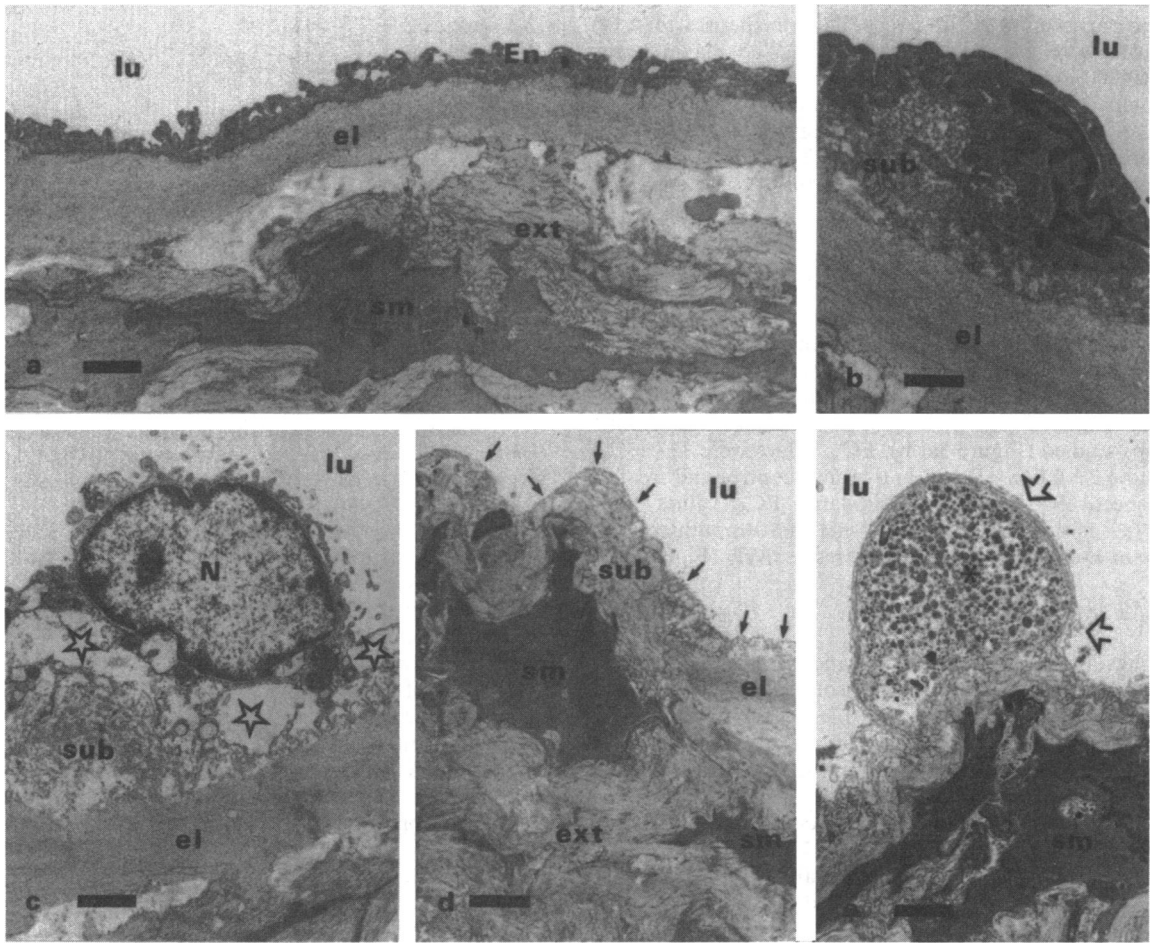

Figure 5 Electron microscopy of rat thoracic aorta in control (a and b) and in 12 months vitamin E-deficient preparations (c, d and e). (a) Note the endothelium (En) in contact with the vessel wall; el, elastic lamina; ext, extracellular matrix; sm, smooth muscle; lu, arterial lumen. (b) Note the endothelial cell contacting subendothelial matrix (sub); N, nucleus. (c) Note altered endothelial cell partially separated (☆) from subendothelial matrix. (d) Arrows indicate luminal side of the vessel segment free from endothelium. (e) A fragment of vessel free of endothelium shows sub-endothelium-associated protrusion-like structure (*) and the patchy distribution of the residue-like material. Arrows indicate basement membrane and/or collagenous fibres. Calibration bar = 2 μm (a, d and e) and 1 μm (b and c).

possibility and rather suggest that a dominant population of α_1-adrenoceptors located on smooth muscle cells accounts for vascular responses to NA in this tissue.

The pharmacological data of the present study confirm and extend our previous observations (Rubino *et al.*, 1993; Rubino & Burnstock, 1994) and are consistent with findings showing that in mesenteric arteries isolated from rats kept on a vitamin E-deficient diet for 8 months, ACh-induced vasodilatation was reduced, while contractile responses to calcium were unaffected (Hubel *et al.*, 1989). In contrast, in mesenteric arteries isolated from rats deprived of dietary vitamin E for only 2 months there was no impairment of the vasodilator response to methacholine (Davidge *et al.*, 1993). These contrasting observations could suggest a correlation between duration of treatment and vascular effects of vitamin E deficiency. The present study indicates a similar impairment of vasodilator responses to ACh in both age groups studied, the maximal vasodilatation achieved being reduced by about 49% in 6 month-treated animals compared to the age-matched controls and by about 42% following 10 months treatment. Further, parallel investigations indicated that endothelium-dependent vascular responses to ACh were similarly affected in aortic rings isolated from 4 and 12 month-vitamin E-deficient rats (Rubino & Burnstock, 1994). A detailed study carried out in the rat described the loss of α-tocopherol, which is the most abundant and active natural form of vitamin E, in several tissues during the course of dietary vitamin E deficiency from weaning to one year of age, indicating that all tissues showed two phases of depletion during the dietary treatment, an initial rapid loss during the first 1–2 months, followed by a slow prolonged depletion which led in 6 months to the total depletion of α-tocopherol in some tissues and in 10 months to the maximal reduction of the content of α-tocopherol in all tissues analysed (Goss-Sampson *et al.*, 1988). Further investigations suggested that the latter phase of depletion relates to the loss of the functional and more critical component of tissue vitamin E (Goss-Sampson *et al.*, 1988; Muller & Goss-Sampson, 1990). These observations could explain the fact that after only 2 months of dietary vitamin E deprivation, Davidge and coworkers could detect a reduction of vitamin E tissue contents but no changes in the endothelium-dependent vasodilatation of isolated mesenteric arteries (Davidge *et al.*, 1993). In contrast, impairment of vascular responsiveness occurs during prolonged treatments (Hubel *et al.*, 1989; the present study).

A comparative evaluation of vascular reactivity in the two groups of rats (6 and 10 months old) used in the present study demonstrated no significant differences in the maximal responses and EC_{50} values for NA between 6 and 10 month-old control rats. Moreover, maximal vasodilator responses to ACh did not differ between 6 and 10 month-old control rats, while EC_{50} values were significantly reduced in the 10 month-old rats. These findings are consistent with previous reports indicating that adrenergic responsiveness of vascular smooth muscle is well maintained in aging (Duckles, 1987; Docherty,

1990), while in rat aorta the potency of ACh in producing endothelium-dependent vasodilatation is increased by aging (reduced EC_{50} value) without change in the maximum relaxation (Hynes & Duckles, 1987; Docherty, 1990).

Possible reasons for the reduced endothelial-mediated responses observed in the present study may include (1) receptor down grading, (2) reduced synthesis and/or release of EDRF and (3) endothelial cell damage. Abnormal receptor turnover and function of receptor structures appeared to account for the impaired responses to muscarinic receptor activation observed in an experimental model of balloon-induced endothelial damage (De Meyer *et al.*, 1991). However, the present study showed that vitamin E deficiency reduced not only vasodilator responses mediated by activation of muscarinic receptors but also vasodilatation induced by a receptor-independent stimulus, such as the calcium ionophore A23187, thus indicating that vitamin E deficiency impaired the general ability of endothelium to respond to vasodilators.

In rabbit aortic rings, it has been shown that the vasodilator responses to ATP are mediated by both endothelial and muscular P_{2y}-purinoceptors (Chinellato *et al.*, 1992). The fact that in treated rings the maximal vasodilator responses to ATP were not significantly reduced, may reflect the dual localization on endothelial and smooth muscle cells of P_{2y}-purinoceptors in aortic rings. Furthermore, the rapid dephosphorylation of ATP by ectonucleotidases makes it difficult to divorce the pharmacological actions of ATP from those of its metabolite adenosine, which is a well established vasodilator. Therefore, the possibility cannot be excluded that the vasodilator responses to ATP were partially due to adenosine acting on specific P_1-purinoceptors mainly located on smooth muscle cells (Olsson & Pearson, 1990). These observations give further support to the hypothesis that endothelial, but not muscle function, is impaired by vitamin E deficiency. Since a defect of endothelium-dependent vasodilatation existed without a decreased responsiveness to the NO donor SNP, it is possible that during vitamin E deficiency the ability of the endothelium to produce and release EDRF is reduced. Further, increased levels of free radical species, due to lack of vitamin E antioxidative actions could inhibit the action of EDRF. However, this hypothesis is in conflict with recent data, suggesting an increased release of EDRF in a model of mild vitamin E deficiency (Davidge *et al.*, 1993). Moreover, conflicting results in the literature describe the effects of oxidative environment on EDRF release and actions. Whilst superoxide anions inhibited the action of EDRF (Rubanyi & Vanhouttem 1986a; Todoki *et al.*, 1992), it was suggested that H_2O_2 might potentiate production and release of EDRF (Rubanyo & Vanhoutte, 1986b).

In addition to a defect in the release of EDRF, an enhanced release of endothelium-derived vasoconstrictors, such as prostaglandin H_2 (Kato *et al.*, 1990), might occur during vitamin E deficiency in response to ACh, which could account for the reduced vasodilatation observed. An increase in the expression of prostaglandin endoperoxide synthase has been reported following 2 months of dietary vitamin E deprivation by Davidge e al. (1993). However, the same authors failed to demonstrate any changes in the vasodilator responses to ACh in this model of mild vitamin E deficiency (Davidge *et al.*, 1993), as discussed above.

The ultrastructural examination carried out in this study shows that in aortic preparations from 12 month-vitamin E-deficient rats, normal tissue organisation is disrupted. Although functional evidence in the present study was obtained after 6 and 10 months of vitamin E deficiency, it could be suggested that the ultrastructural changes following 12 months of deprivation of dietary vitamin E provide an explanation for the functional impairment observed. Based on the observation that the duration of vitamin E deficiency (6 or 10 months) did not modify the impairment of endothelial function, a relation cause-effect can be suggested between the morphological and functional changes observed in the present study after 12 and 6 or 10 months of vitamin E deficiency, respectively. This hypothesis is further supported by our previous data showing an impairment of endothelial function comparable to that observed in the present study following 12 months of vitamin E deficiency (Rubino & Burnstock, 1994). Although impairment of endothelial NO-synthase or changes in substrate dependency cannot be excluded by the results of this study, the disruption of the endothelium and the loss of endothelial cells observed in several regions of aortic segment could account for the reduction in endothelium-dependent vasodilatation. In contrast, a regular organisation of smooth muscles was associated with a lack of functional defect on smooth muscle cells. To our knowledge, this is the first study demonstrating, by transmission electron microscopy, ultrastructural changes of the vascular wall during vitamin E deficiency. Our findings are consistent with results obtained in femoral arteries of vitamin E-deficient rats, where a scanning electron micrograph of the endothelial surface showed an irregular endothelial layer. Numerous 'balloon-like projections' into the vascular lumen were also observed (Hubel *et al.*, 1989), which could be compared to the unusual protrusions observed in this study.

Endothelial damage is associated with several vascular diseases, such as atherosclerosis and hypertension (Luscher & Vanhoutte, 1986; Vanhoutte, 1992). Structural changes of the endothelial cells have been described during hypertension (Luscher, 1988; Todd, 1992). Although no changes on heart rate and blood pressure have been detected during dietary vitamin E-deprivation (Filer *et al.*, 1949; Hubel *et al.*, 1989), in the light of the observations made so far it appears that vitamin E deficiency can contribute to the development of vascular pathological conditions comparable to those observed in cardiovascular diseases, such as atherosclerosis and hypertension. In summary, the present study indicates that both ultrastructural disruption of endothelial cells and impairment of endothelial function occur during dietary vitamin E deficiency, while the morphology and general ability of smooth muscles to contract or relax is unaffected. Since endothelial cells have been shown to have a profound influence on vascular function, it appears that the effects of vitamin E deficiency have pathophysiological significance for the control of vasomotor activity.

This work was supported by the British Heart Foundation.

References

BULLOCK, G.R., TAYLOR, S.G. & WESTON, A.H. (1986). Influence of the vascular endothelium on agonist induced contractions and relaxations in rat aorta. *Br. J. Pharmacol.*, **89**, 819–830.

BURTON, G.W., JOYCE, A. & INGOLD, K.U. (1983). Is vitamin E the only lipid soluble, chain breaking antioxidant in human blood plasma and erythrocyte membranes? *Arch. Biochem. Biophys.*, **221**, 281–289.

CHINELLATO, A., RAGAZZI, E., PANDOLFO, L., FROLDI, G., CAPARROTTA, L. & FASSINA, G. (1992). Pharmacological characterization of ATP receptors mediating vasodilatation on isolated rabbit aorta. *Gen. Pharmacol.*, **23**, 861–865.

DAVIDGE, S.T., HUBEL, C.A. & MCLAUGHLIN, M.K. (1993). Cyclooxygenase-dependent vasoconstrictor alters vascular function in the vitamin E-deprived rat. *Circ. Res.*, **73**, 79–88.

DE MEYER, G.R.Y., BULT, H., VAN HOYDONCK, A.E., JORDAENS, F.H., BUYSSENS, N. & HERMAN, A.G. (1991). Neointima formation impairs endothelial muscarinic receptors while enhancing prostacyclin-mediated responses in the rabbit carotid artery. *Circ. Res.*, **68,** 1669–1680.

DOCHERTY, J.R. (1990). Cardiovascular responses in ageing: a review. *Pharmacol. Rev.*, **42,** 103–125.

DUCKLES, S.P. (1987). Influence of age on vascular adrenergic responsiveness. *Blood Vessels*, **24,** 113–116.

FILER, L.J., RUMERY, R.E., YU, P.N.G. & MASON, K.E. (1949). Studies on vitamin E deficiency in the monkey. *Ann. N.Y. Acad. Sci.*, **52,** 284–291.

FURCHGOTT, R.F. (1983). Role of endothelium in responses of vascular smooth muscles. *Circ. Res.*, **53,** 557–573.

FURCHGOTT, R.F. (1984). The role of the endothelium in the responses of vascular smooth muscle to drugs. *Am. Rev. Pharmacol. Toxicol.*, **24,** 175–197.

GOSS-SAMPSON, M.A., MACEVILLY, C.J. & MULLER, D.P.R. (1988). Longitudinal studies of the neurobiology of vitamin E and other antioxidant systems, and neurological function in the vitamin E deficient rat. *J. Neurol. Sci.*, **87,** 25–35.

GOSS-SAMPSON, M.A., KRISS, A. & MULLER, D.P.R. (1990). a longitudinal study of somatosensory, brainstem auditory and peripheral sensory-motor conduction during vitamin E deficiency in the rat. *J. Neurol. Sci.*, **100,** 79–84.

HUBEL, C.A., GRIGGS, K.C. & MCLAUGHLIN, M.K. (1989). Lipid peroxidation and altered vascular function in vitamin E-deficient rats. *Am. J. Physiol.*, **256,** H1539–H1545.

HYNES, M.R. & DUCKLES, S.P. (1987). Effect of increasing age on the endothelium-mediated relaxation of rat blood vessels *in vitro*. *J. Pharmacol. Exp. Ther.*, **241,** 387–392.

IGNARRO, L.J., BYRNS, R.E., BUGA, G.M. & WOOD, K.S. (1987). Endothelium-derived relaxing factor from pulmonary artery and vein possess pharmacological and chemical properties identical to those of nitric oxide radical. *Circ. Res.*, **61,** 866–879.

KATO, T., IWAMA, Y., OKAMURA, K., HASHIMOTO, H., ITO, T. & SATAKE, T. (1990). Prostaglandin H_2 may be the endothelium-derived contracting factor released by acetylcholine in the aorta of the rat. *Hypertension*, **15,** 475–481.

LUCY, J.A. (1972). Functional and structural aspects of biomembranes: a suggested structural role of vitamin E in the control of membrane permeability and stability. *Ann. N.Y. Acad. Sci.*, **230,** 4–16.

LUSCHER, T.F. (1988). *Endothelial Vasoactive Substances and Cardiovascular Disease*. London: Karger.

LUCSHER, T.F. & VANHOUTTE, P.M. (1986). Endothelium-dependent contractions to acetylcholine in the rat aorta of the spontaneously hypertensive rat. *Hypertension*, **8,** 344–348.

MULLER, D.P.R. & GOSS-SAMPSON, M.A. (1990). Neurochemical, neurophysiological, and neuropathological studies in vitamin E deficiency. *Crit. Rev. Neurobiol.*, **5,** 239–263.

OLSSON, R.A. & PEARSON, J.D. (1990). Cardiovascular purinoceptors. *Physiol. Rev.*, **70,** 761–845.

PALMER, R.M.J., ASHTON, D.S. & MONCADA, S. (1988). Vascular endothelial cells synthesize nitric oxide from L-arginine. *Nature*, **333,** 664–666.

PATEL, J.M., SEKHARAM, M. & BLOCK, E.R. (1991). Vitamin E distribution and modulation of the physical state and function of pulmonary endothelial cell membranes. *Exp. Lung Res.*, **17,** 707–723

RALEVIC, V. & BURNSTOCK, G. (1993). Monograph. *Neuronal-endothelial Interactions in the Control of Local Vascular Tone*. Medical Intelligence Unit. Austin, Texas: R.G. Landes Company, Medical Publishers.

RUBANYI, G.M. & VANHOUTTE, P.M. (1986a). Oxygen derived free radicals, endothelium and responsiveness of vascular smooth muscles. *Am. J. Physiol.*, **250,** H815–H821.

RUBANYI, G.M. & VANHOUTTE, P.M. (1986b). Superoxide anions and hyperoxia inactivate endothelium-derived relaxing factor. *Am. J. Physiol.*, **250,** H822–H827.

RUBINO, A. & BURNSTOCK, G. (1994). Recovery after dietary vitamin E supplementation of impaired endothelial function in vitamin E deficient rats. *Br. J. Pharmacol.*, **112,** 515–518.

RUBINO, A., GOSS-SAMPSON, M.A., HOYLE, C.H.V. & BURNSTOCK, G. (1993). Impaired endothelium-mediated vasodilatation in aorta of rats with vitamin E deficiency. *Br. J. Pharmacol.*, **108,** 6P.

TODD. M.E. (1992). Hypertensive structural changes in blood vessels: Do endothelial cells hold the key? *Can. J. Physiol. Pharmacol.*, **70,** 536–551.

TODOKI, K., OKABE, E., KIYOSE, T., SEKISHITA, T. & ITO, H. (1992). Oxygen free radical-mediated selective endothelial disfunction in isolated coronary artery. *Am. J. Physiol.*, **262,** H806–H812.

VANHOUTTE, P.M. (1992). Role of calcium and endothelium in hypertension, cardiovascular diseases, and subsequent vascular events. *J. Cardiovasc. Pharmacol.*, **19,** S6–S10.

(Received September 26, 1994
Revised January 26, 1995
Accepted February 13, 1995)

British Journal of Pharmacology (1995) 115, 421-426

Biphasic inhibition of stimulated endogenous dopamine release by 7-OH-DPAT in slices of rat nucleus accumbens

[1]Jyoti Patel, Stephen J. Trout, *Peter Palij, Robin Whelpton & Zygmunt L. Kruk

Department of Pharmacology, Queen Mary & Westfield College, Mile End Road, London E1 4NS and *Anaesthetics Unit, London Hospital Medical College, The Royal London Hospital, Whitechapel, London E1 1BB.

1 Fast cyclic voltammetry was used to investigate the effect of 7-OH-DPAT (7-hydroxy-*N*,*N*-di-n-propyl-2-aminotetralin), a putative D_3 receptor agonist, on electrically stimulated endogenous dopamine release in slices of rat nucleus accumbens.

2 7-OH-DPAT inhibited single pulse stimulated dopamine release in a concentration-dependent manner with a maximum inhibition of 95.5%. Analysis of concentration-response curves to 7-OH-DPAT showed that they were biphasic, with the high affinity component contributing 18.0% to the total inhibition and the low affinity component 77.5%. 7-OH-DPAT exhibited a 560 fold selectivity between the high and low affinity components (0.015 nM compared to 8.4 nM).

3 Concentration-response curves to the non-selective D_2/D_3 agonist, apomorphine, were monophasic. The maximum inhibition was 93.1% and the EC_{50} value 82 nM.

4 The selective D_2 antagonist, haloperidol (30 nM), antagonized the low affinity component of the concentration-response cuve to 7-OH-DPAT whilst the high affinity component was essentially unaffected. The pK_B values calculated for the high and low affinity components were 7.89 and 9.45 respectively.

5 In conclusion, these results demonstrate that 7-OH-DPAT inhibits stimulated dopamine release by acting at two different sites. Furthermore, the results are consistent with the hypothesis that the high and low affinity components of the concentration-response curve to 7-OH-DPAT may reflect activation of functional D_3 and D_2 release-regulating autoreceptors respectively. However, the possibility that the biphasic nature of the curve may reflect different subtypes of the D_2 receptor cannot be excluded.

Keywords: Dopamine release; dopamine D_3 receptor; dopamine D_2 receptor; 7-hydroxy-*N*,*N*-di-n-propyl-2-aminotetralin (7-OH-DPAT); apomorphine; fast cyclic voltammetry; rat nucleus accumbens

Introduction

Dopamine D_2 receptors have been shown to be located on the axon terminals of A9 and A10 dopaminergic neurones where they are involved in modulating dopamine release and synthesis (for review see Starke *et al.*, 1989). The recent molecular cloning of the gene for a novel D_2-like dopamine receptor, designated the D_3 receptor (Sokoloff *et al.*, 1990), has instigated research into potential functional roles of the D_3 receptor. Messenger RNA (mRNA) distribution studies have shown that the localizations of D_2 and D_3 receptors are anatomically distinct. In contrast to D_2 receptors, D_3 receptors are preferentially distributed in the limbic system with highest densities in the Islands of Calleja, olfactory tubercles and nucleus accumbens (NAc) (Sokoloff *et al.*, 1990). In addition, low concentrations of D_3 receptor mRNA are also detected in the dopamine cell bodies of the rat substantia nigra and ventral tegmental area raising the possibility that the D_3 receptor may act as a dopamine autoreceptor (Bouthenet *et al.*, 1991).

Stable expression of rat and human D_2 and D_3 receptors in Chinese hamster ovary (CHO) recombinant cell lines has established further pharmacological differences between the D_2 and D_3 receptors. For instance, dopamine and other D_2 receptor agonists (e.g. quinpirole), generally display higher affinities at the D_3 receptor. In contrast, many dopamine receptor antagonists tend to exhibit a preference for D_2 receptors. In fact, the only available D_2 antagonists showing limited selectivity (3 to 4 fold) at D_3 receptors are (+)-UH232 (*cis*-(+)-(1S,2R)-5-methoxy-1-methyl-2-(n-dipropylamino)tetralin) and (+)-AJ76 (*cis*-(+)-(1S,2R)-5-methoxy-1-methyl-2-(n-propylamino)tetralin) (Sokoloff *et al.*, 1990). The lack of selective antagonists for this receptor has therefore limited research into its functional significance. 7-OH-DPAT (7-hydroxy-*N*,*N*-di-n-propyl-2-aminotetralin) is a selective dopamine receptor agonist (El Mestikawy *et al.*, 1986), which in CHO cell line binding studies has about an 80 fold greater affinity for the D_3 receptor (0.78 nM) than the D_2 receptor (61 nM) (Lévesque *et al.*, 1992). Its affinity at D_4 and D_1 receptors is relatively lower (650 nM and 5300 nM respectively). Binding studies with [^{3}H]-7-OH-DPAT in rat brain have confirmed D_3 receptor distribution indicated by *in situ* D_3 mRNA hybridisation (Bouthenet *et al.*, 1991) and also shown low concentrations of D_3 receptor binding sites in the caudate putamen (CPu) (Lévesque *et al.*, 1992).

Sokoloff *et al.* (1990) found that in contrast to the D_2 receptor, stimulation of the rat D_3 receptor transfected into CHO cells did not inhibit adenylate cyclase activity. Subsequent studies on the human D_3 receptor transfected into various other cell lines have confirmed this finding and that it fails to couple to other second messenger systems including release of arachidonic acid, phosphoinositide hydrolysis, whole cell potassium currents and calcium mobilization (Freedman *et al.*, 1994; MacKenzie *et al.*, 1994; Tang *et al.*, 1994a). However, a few studies have shown coupling of human D_3 receptors to a functional response. Potenza *et al.* (1994) showed that activation of human D_3 receptors transfected into cultured *Xenopus laevis* melanophores causes pigment granule aggregation. This action is thought to be mediated via inhibition of cyclic AMP accumulation. In the NG108-15 cell line, stimulation of transfected human D_3 receptors depresses calcium currents (Seabrook *et al.*, 1994) and stimulates c-fos expression and mitogenesis (Pilon *et al.*, 1994). These effects are sensitive to the action of pertussis toxin, suggesting the involvement of G_i and/or G_o G-proteins.

Evidence for a functional role for D_3 receptors, using 7-OH-DPAT or other D_3-selective ligands, comes mainly from be-

[1] Author for correspondence.

havioural studies. Caine & Koob (1993) have proposed that the D_3 receptor may be involved in the reinforcing effect of cocaine. Other behavioural studies have suggested that activation of D_3 receptors is associated with hypolocomotor activity (Daly & Waddington, 1993; Waters *et al.*, 1993; Svensson *et al.*, 1994), induction of yawning (Damsma *et al.*, 1993) and hypothermia in rats (Millan *et al.*, 1994). However, the assignment of *in vivo* behavioural responses to mediation by any receptor sub-type remains highly speculative (Large & Stubbs, 1994).

Biochemical studies have suggested that striatal dopamine synthesis-inhibiting autoreceptors and release-regulating autoreceptors may be of the D_3 rather than the D_2 type (Meller *et al.*, 1993; Damsma *et al.*, 1993). Furthermore, Tang *et al.* (1994b) have shown that stimulation of rat D_2 and human D_3 receptors transfected into the MN9D mesencephalic cell line causes inhibition of dopamine release whilst activation of transfected rat D_4 receptors is without effect. This cell line has the ability to synthesize and release dopamine and possesses many of the characteristics of CNS dopaminergic neurones. This observation suggests that the D_3 receptor may have the capacity to act as a release-regulating autoreceptor within the CNS.

In this study, the possible role of a functional dopamine D_3 receptor acting as a release-regulating autoreceptor in the rat NAc was investigated. Fast cyclic voltammetry (FCV) was used to examine the inhibition of dopamine release in brain slices by the selective D_3 agonist, 7-OH-DPAT, and the non-selective D_2/D_3 agonist, apomorphine. FCV is an electrochemical technique which has been used to detect endogenous dopamine release (Bull *et al.*, 1990; Palij *et al.*, 1990; Bull & Sheehan, 1991; Trout & Kruk, 1992; Patel *et al.*, 1992a). Release may be measured following single pulse electrical stimulation in the absence of a reuptake inhibitor. This avoids endogenously released transmitter activating the release-inhibiting autoreceptors and interfering with the action of the exogenous agonist (Starke *et al.*, 1989; Limberger *et al.*, 1991). This method can therefore be used for quantitative determination of the potency of agonists and affinity constants for competitive antagonists (Palij *et al.*, 1990; Bull & Sheehan, 1991). In addition, the temporal resolution of FCV can be exploited to measure the kinetics of reuptake of the released transmitter (Trout & Kruk, 1992; Patel *et al.*, 1992b; Hafizi *et al.*, 1992; Davidson & Stamford, 1993).

Methods

Preparation of brain slices

Slices were prepared as previously described (Bull *et al.*, 1990; Trout & Kruk, 1992; Patel *et al.*, 1992a). Briefly, coronal brain slices (350 μm thick) containing the nucleus accumbens were prepared from male Wistar rats (230 to 300 g). Slices were placed in a Perspex brain slice chamber and superfused (1.2 ml min^{-1}) with artificial cerebrospinal fluid (ACSF: composition in mM; NaCl 124.0, KCl 2.0, KH_2PO_4 1.25, $MgSO_4$ 2.0, $NaHCO_3$ 25.0, $CaCl_2$ 2.0, (+)-glucose 11.0). This solution was saturated with 5% CO_2 in O_2 and maintained at 32°C. Slices were illuminated from below and, with the aid of a binocular dissection microscope, recording and stimulating electrodes were positioned in the slice 80 μm below the surface in the core region of the NAc.

Fast cyclic voltammetry

Fast cyclic voltammetry was used to monitor electrically evoked dopamine efflux by measuring the current generated at a carbon fibre microelectrode (exposed tip 8 μm in diameter, 20 to 50 μm in length) when dopamine is oxidised. Using a Millar voltammeter (PD Systems Ltd., UK), 1½ cycles of a 100 Hz triangular waveform (−1.0 to +1.4 V peak to peak, 15 ms duration) were applied to the carbon fibre microelectrode twice a second. Changes at the peak oxidation potential for dopamine (+595 mV relative to a Ag/AgCl reference electrode) were monitored by a 'sample and hold' circuit: this signal was output to a chart recorder and to a Cambridge Electronic Design (CED) 1401 computer interface. The 'sample and hold' circuit recorded changes at the oxidation current with time. Data were captured and digitally stored as files using CED software (Signal Averager and Chart). In addition, the applied voltage waveform and the waveform showing the current flowing in the recording electrode were monitored on a digital storage oscilloscope (Nicolet 310).

Electrical stimulation

Bipolar tungsten wire stimulating electrodes (tip separation 200 μm) were placed about 200 to 300 μm away from the carbon fibre recording electrode. The stimulating electrodes were connected to a Digitimer DS2 constant voltage stimulator controlled by a Neurolog (Digitimer) modular timing system. Dopamine efflux was evoked by single electrical pulses (0.1 ms duration, 20 V amplitude) applied every 2 min.

Protocol

Responses to single pulse stimulation were allowed to stabilize under control conditions for at least 60 min after which a dopamine autoreceptor agonist (7-OH-DPAT or apomorphine) was added to the superfusion fluid at increasing concentrations. Each drug concentration was superfused until its effect on responses achieved a plateau or for a minimum of 20 min if no effect was observed. Concentration-response curves to 7-OH-DPAT were constructed either in the absence or presence of a dopamine autoreceptor antagonist (haloperidol or (+)-AJ76) added at least 60 min prior to the first concentration of agonist. Dopamine release was studied by agreement with calibration curves obtained when the carbon fibre microelectrode was exposed to known concentrations of dopamine post-experimentally.

Analysis of data

Concentration-response data (% inhibition of peak dopamine efflux) were fitted to the following equation:

$$E = \sum_{i=1}^{n} \frac{E_{max_i} 10^{\log_{10}[D]}}{10^{\log_{10}EC_{50_i}} + 10^{\log_{10}[D]}}$$

where E = response (% inhibition of stimulated dopamine efflux), E_{max} = maximum response, EC_{50} = concentration required to produce half-maximum response, [D] = agonist concentration, n = 1 (monophasic model) or 2 (biphasic model) and i refers to the appropriate component of the curve. Curves were fitted by a least-squares iterative method using the Solver function in Microsoft Excel. Each set of data was fitted to both a one component (n = 1 in the above equation) and a two component model (n = 2). Slopes were constrained to unity. The goodness of fit to a biphasic over a monophasic model was evaluated by the *F* statistic from the residual sums of squares (Kenakin, 1993). Pharmacological parameters such as the EC_{50} and E_{max} values were calculated from individual fitted curves. The pK_B values were calculated from concentration-ratios at the EC_{50} level in the absence and presence of antagonist using the following equation:

$$pK_B = \log_{10}(\text{concentration-ratio} - 1) - \log_{10}(\text{antagonist concentration})$$

Data are expressed as the arithmetic mean ± s.e.mean, except EC_{50} values, which are expressed as the geometric mean with

95% confidence limits (CL). Student's t test (two-tailed, unpaired) was used to compare $\log_{10}$ EC_{50} and E_{max} values obtained for 7-OH-DPAT in the absence and presence of antagonists. The number of experiments conducted is referred to by n, each of which was performed in a brain slice prepared from a different animal.

Drugs

Salts for the ACSF (see above for composition) were of Analar grade and obtained from BDH Ltd. Drugs were obtained from the following sources: dopamine HCl, apomorphine and haloperidol were obtained from Sigma Chemical Company Ltd., (±)-7-OH-DPAT (7-hydroxy-*N*,*N*-di-n-propyl-2-aminotetralin) was obtained from Research Biochemicals Incorporated (RBI, distributed under the NIMH special synthesis programme) and (+)-AJ76 (*cis*-(+)-(1S,2R)-5-methoxy-1-methyl-2-(n-propylamino)tetralin) was donated by Dr K. Svensson, University of Göteborg, Sweden. All drugs were dissolved initially in deionised water and then diluted further in ACSF, except haloperidol, which was initially dissolved in tartaric acid (0.01 M).

Results

Using FCV it was possible to detect endogenous dopamine efflux in response to a single electrical pulse from rat brain slices containing the NAc. The rapid transient responses following stimulation reached a maximum within 1 s and returned to pre-stimulation levels within 5 s. The amount of dopamine evoked by a single pulse in the NAc was 118 ± 8 nM (n = 21), determined by post-experimental calibration of the recording electrode, and was stable for up to 10 h (data not shown).

7-OH-DPAT (0.01 nM to 3 μM) inhibited single pulse stimulated dopamine efflux in a concentration-dependent manner, the maximum inhibition being 95.5 ± 0.6%. Figure 1 shows 'sample and hold' traces of evoked dopamine efflux obtained in the absence and presence of increasing concentrations of 7-OH-DPAT. Analysis of the concentration-response data by curve fitting revealed that the inhibition of dopamine efflux by 7-OH-DPAT could be fitted significantly better to a biphasic concentration-response curve than a monophasic curve (F = 142.9, d.f. = 2.8; P < 0.005) (Figure 2). The relative EC_{50} and E_{max} values calculated by curve fitting for the high and low affinity components of the curve are shown in Table 1.

The non-selective D_2/D_3 receptor agonist, apomorphine (0.1 nM to 10 μM) also inhibited evoked dopamine efflux in a concentration-dependent manner. However, in contrast to 7-OH-DPAT, analysis of the data by curve fitting showed that a biphasic curve was not a significant improvement over a monophasic one (F = 0.62, d.f. = 2.7; P > 0.05) (see Figure 3 and Table 1 for calculated EC_{50} and E_{max} values).

In the presence of 30 nM haloperidol, a selective D_2 receptor antagonist (Sokoloff *et al.*, 1990), the two components of the concentration-response curve to 7-OH-DPAT were differentially affected without any significant reduction in the total inhibition achieved (95.5 ± 0.6% in the absence of haloperidol (n = 7) compared to 93.7 ± 1.3% in the presence of haloperidol

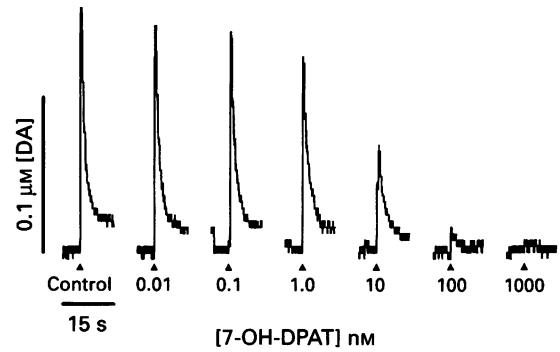

Figure 1 Sample and hold traces showing the concentration-dependent effect of the selective D_3 agonist 7-OH-DPAT on stimulated dopamine efflux in the rat nucleus accumbens. Dopamine (DA) efflux was evoked by single electrical pulses (0.1 ms duration, 20 V amplitude). Data were captured from a single experiment using a Cambridge Electronic Design (CED) 1401 analogue to digital interface with CED Chart and Signal Averager software.

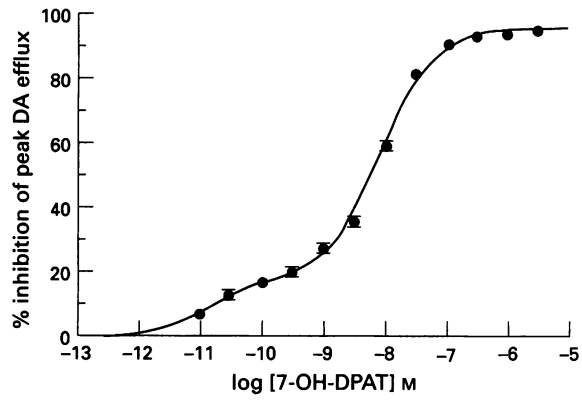

Figure 2 Concentration-response curve for the inhibition of stimulated dopamine (DA) efflux in rat brain slices containing the nucleus accumbens by 7-OH-DPAT. Values are expressed as percentage inhibition of peak dopamine efflux (mean ± s.e.mean), against log concentration of agonist (n = 7). The mean data were best fitted to a two component model (solid line).

(n = 5); P > 0.05), (Figure 4). The EC_{50} value for the high affinity component of the curve was not significantly altered (0.015 nM (CL 0.007–0.032) in the absence of haloperidol (n = 7) compared to 0.050 nM (CL 0.012–0.204) in the presence of haloperidol (n = 5, P > 0.05)) although there was a significant increase in the E_{max} value of this phase (18.0 ± 2.1% to 30.2 ± 3.2%; P < 0.05, n = 7 and 5 respectively). In contrast, there was a significant right-ward displacement of the low affinity component (EC_{50}:724 nM (CL 493–1062) in the presence of haloperidol (n = 5) compared to 8.4 nM (CL 6.3–11.1) in the absence of haloperidol (n = 7, P < 0.001)), accompanied by a significant reduction in the E_{max} value of this component (77.5 ± 2.7% (n = 7) to 63.4 ± 3.0% (n = 5); P < 0.01). The pK_B values calculated for haloperidol at the high and low affinity sites were 7.89 and 9.45 (n = 5) respectively.

The putative D_3 receptor antagonist, (+)-AJ76 (1 μM), also

Table 1 EC_{50} (nM) and E_{max} values obtained for 7-hydroxy-*N*,*N*-di-n-propyl-2-aminotetralin (7-OH-DPAT) and apomorphine on dopamine efflux evoked by single pulse stimulation in rat nucleus accumbens (NAc)

Drug	*EC_{50} (nM) (geometric mean)*	*E_{max} (%) (mean ± s.e.mean)*	n
7-OH-DPAT (High)	0.015 (0.007–0.032)	18.0 ± 2.1	7
7-OH-DPAT (Low)	8.4 (6.3–11.1)	77.5 ± 2.7	7
Apomorphine	82 (50–136)	93.1 ± 1.3	5

Individual values were calculated by curve fitting; EC_{50} values are expressed as geometric means with 95% confidence intervals whereas E_{max} values are expressed as arithmetic means ± s.e.mean.

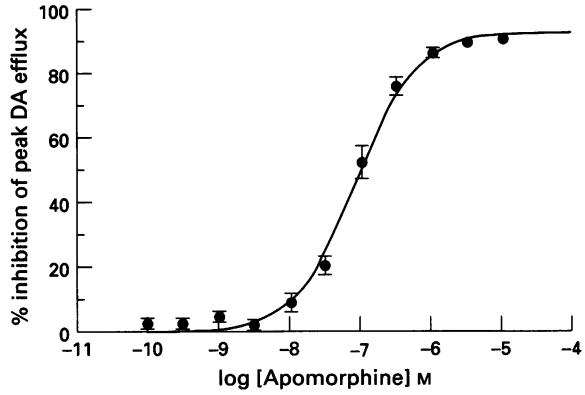

Figure 3 Concentration-response curve for the inhibition of stimulated dopamine (DA) efflux in rat brain slices containing the nucleus accumbens by apomorphine. Values are expressed as percentage inhibition of peak dopamine efflux (mean ± s.e.mean), against log concentration of agonist ($n = 5$). The mean data were best fitted to a one component model (solid line).

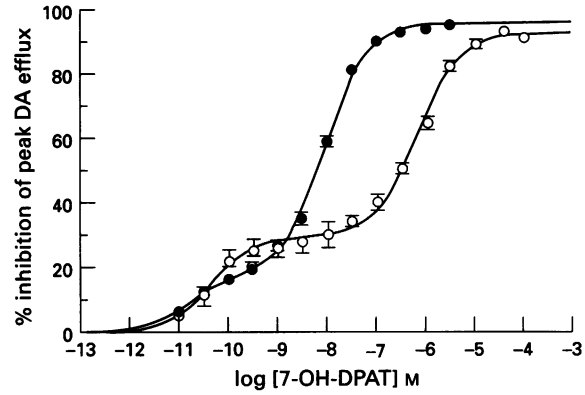

Figure 4 Concentration-response curves for the inhibition of stimulated dopamine (DA) efflux in rat brain slices containing the nucleus accumbens by 7-OH-DPAT in the absence (●, $n = 7$) and presence (○, $n = 5$) of haloperidol (30 nM). Values are expressed as percentage inhibition of peak dopamine efflux (mean ± s.e.mean), against log concentration of agonist. Each curve was individually fitted to mean data using a two component model (solid lines).

displaced the low affinity component of the 7-OH-DPAT concentration-response curve (EC_{50}: 8.4 nM (CL 6.3–11.1) in the absence of (+)-AJ76 ($n = 7$) compared to 105 nM (CL 23–49) in the presence of (+)-AJ76 ($n = 4$), $P < 0.05$) and had a small non-significant effect at the high affinity site (EC_{50}: 0.015 nM (CL 0.007–0.032) in the absence of (+)-AJ76 ($n = 7$) compared to 0.017 nM (CL 0.008–0.038) in the presence of (+)-AJ76 ($n = 4$), $P > 0.05$). In addition, there was no significant change in the E_{max} values at the high (18.0 ± 2.6%) and low (77.8 ± 3.5%) affinity components, or in the total inhibition (95.8 ± 1.4%), $P > 0.05$ and $n = 4$ in all cases (Figure 5). The pK_B values calculated at the high and low affinity sites were 5.05 ($n = 3$) and 7.06 ($n = 4$) respectively.

In order to establish the effect of 7-OH-DPAT on dopamine reuptake, the half decay times, i.e. the time taken for the observed peak dopamine efflux to decline to half its value were measured. In the presence of 10 nM 7-OH-DPAT (a concentration which inhibits dopamine efflux by more than 50%), the mean half decay time did not significantly increase (1167 ± 167 ms in the presence of 7-OH-DPAT compared to 1250 ± 281 ms under control conditions, $P > 0.05$; $n = 6$).

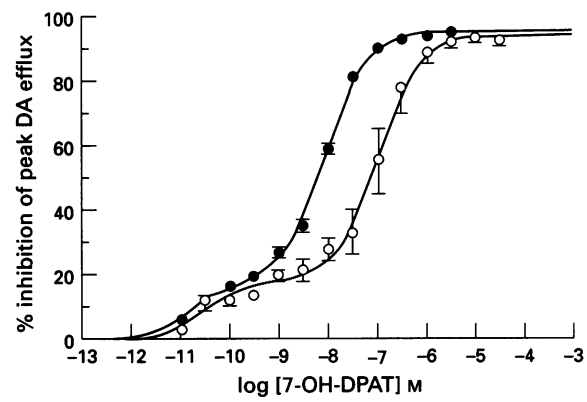

Figure 5 Concentration-response curves for the inhibition of stimulated dopamine (DA) efflux in rat brain slices containing the nucleus accumbens by 7-OH-DPAT in the absence (●, $n = 7$) and presence (○, $n = 4$) of (+)-AJ76 (1 μM). Values are expressed as percentage inhibition of peak dopamine efflux (mean ± s.e.mean), against log concentration of agonist. Each curve was individually fitted to mean data using a two component model (solid lines).

Discussion

The possibility of a functional dopamine D_3 receptor acting as an axon terminal release-regulating autoreceptor was investigated using the selective D_3 receptor agonist 7-OH-DPAT (Lévesque *et al.*, 1992). Although it is difficult to establish positively a role for the D_3 receptor in the absence of selective antagonists for this receptor, 7-OH-DPAT can be used to provide evidence consistent with this possibility. Effects were examined on stimulated dopamine release evoked by single electrical pulses in the absence of a reuptake inhibitor. In this way, the possibility of released dopamine activating autoreceptors and thus interfering with the action of the exogenous agonist was avoided. Agonist concentration-response curves were therefore constructed in the absence of competition from the endogenous ligand.

Statistical analysis of data from concentration-response curves obtained in the NAc showed that 7-OH-DPAT inhibited evoked dopamine release in a biphasic manner and that the two components resolved contributed different amounts to the total inhibition. This initial finding indicates that there may be a mixed population of dopamine autoreceptors in the NAc: the high affinity component of the curve may be due to activation of D_3 receptors whereas the low affinity component may be due to D_2 receptors. In contrast, monophasic concentration-response curves were obtained for the non-selective D_2/D_3 agonist, apomorphine (Sokoloff *et al.*, 1990). This observation is also consistent with a mixed D_2/D_3 receptor population and furthermore, eliminates the possibility that the biphasic curve to 7-OH-DPAT might be an artifact of the experimental technique used. Interestingly, visual examination of the experimental data from a recent study demonstrating the inhibitory effect of 7-OH-DPAT on stimulated dopamine release in the NAc suggests that the concentration-response curve to 7-OH-DPAT may be biphasic (Yamada *et al.*, 1994). This would be in agreement with our own data. However, it is unclear why an analysis to show this was not made.

In the presence of haloperidol, a D_2 antagonist displaying about 20 fold selectivity for D_2 over D_3 receptors (Sokoloff *et al.*, 1990), the biphasic nature of the concentration-response curve to 7-OH-DPAT became more pronounced. In this functional assay, haloperidol antagonized the high and low affinity components of the concentration-response curve to 7-OH-DPAT with similar affinities (K_B 12.9 nM and 0.35 nM respectively) to those reported at rat D_3 and D_2 receptors (K_i 9.8 nM and 0.45 nM respectively) in CHO cell lines (Sokoloff *et al.*, 1990).

In the present study it was found that the E_{max} values for the two components were changed in the presence of haloperidol without any change in the total inhibition achieved. The E_{max} for the high affinity component was increased and that for the low affinity component reduced. This effect was surprising as

haloperidol is considered to be a competitive antagonist and as such would be expected to affect the EC_{50} value without altering the E_{max}. However, it is unclear whether the changes in the E_{max} values for the high and low affinity components are both direct effects of the antagonist. It may be that the antagonist causes a decrease in the E_{max} for the low affinity component and the E_{max} for the high affinity component increases as a consequence of the unchanged total inhibition, or *vice versa*.

(+)-AJ76, a putative D_3 antagonist with 3 fold selectivity over D_2 receptors (Sokoloff *et al.*, 1990) was also unable to shift significantly the high affinity component of the concentration-response curve to 7-OH-DPAT. This appears to be inconsistent with the suggestion that the high affinity component is due to activation of the D_3 receptor. However, it should be noted that this compound is not a highly selective D_3 antagonist, its weak selectivity being demonstrated only in binding and not in functional studies. A recent study by Rivet *et al.* (1994) showed that basal dopamine flux into dialysate was markedly reduced in both the striatum and the NAc by systemic administration of 7-OH-DPAT. This effect was partially blocked by pretreatment with S 14297 (+)-[7-(*N*,*N*-dipropylamino)-5,6,7,8-tetrahydro-naphto(2,3b)dihydro,2,3-furane] a D_3 antagonist displaying about 23 fold selectivity for human D_3 receptors over D_2 in transfected CHO cells (Gobert *et al.*, 1994; Millan *et al.*, 1994). This compound could not be made available to us for the present study.

The **R**-(+)-isomer has been shown to be the active isomer of 7-OH-DPAT (Baldessarini *et al.*, 1993; Damsma *et al.*, 1993). In this study the EC_{50} values obtained for racemic 7-OH-DPAT at the two sites were much lower (0.015 nM and 8.4 nM) than K_i values obtained for D_3 (0.78 nM) and D_2 (61 nM) receptors in transfected CHO cell lines (Lévesque *et al.*, 1992). In addition, there was a greater selectivity of the drug between the two sites (560 fold) than those reported (about 80 fold) between D_3 and D_2 receptors. The reasons why such discrepancies exist may be because the affinities determined in recombinant cell lines measure receptor occupancy whereas in the present study a functional response was measured. This response depends not only on receptor occupancy but also on other factors such as efficacy and receptor reserve. It has been shown that there is a 50–60% receptor reserve for terminal release-regulating autoreceptors in the NAc and CPu (Yokoo *et al.*, 1988), which may account for the lower EC_{50} values observed in this study. A greater receptor reserve for the D_3 receptor would also contribute to the greater selectivity of 7-OH-DPAT between the two components.

The possibility that the biphasic concentration-response curve for 7-OH-DPAT may be due to factors other than a mixed D_2/D_3 autoreceptor population cannot be ruled out. One possibility is that the effect of 7-OH-DPAT may not be specific for the dopaminergic system. The affinity of 7-OH-DPAT at receptor subtypes other than dopamine receptors is generally relatively lower (K_i in nM: α_1 10 000; α_2 1 610; 5-HT_{2A} > 10 000; 5-HT_{2C} > 10 000; M_1 5 400; and M_2 880) (personal communication from Mark J. Millan, Institut de Recherches Servier, France). In addition, it has been shown, using FCV, that phenylephephrine, clonidine, isoprenaline, 5-HT, acetylcholine, muscimol, CCK-8 and neurotensin do not significantly alter evoked dopamine release in slices of rat NAc (Bull & Sheehan, 1991). However, 7-OH-DPAT does have high affinity for 5-HT_{1A} receptors expressed in CHO cells (K_i 81 nM personal communication from Mark J. Millan) and 72.7 nM in rat hippocampal membrane homogenates (Zhuang *et al.*, 1993). The 5-HT_{1A} receptor is a 5-HT somatodendritic autoreceptor in the dorsal raphe nucleus (O'Connor & Kruk, 1992). The selective 5-HT_{1A} agonist 8-OH-DPAT (8-hydroxy-*N*,*N*-di-n-propyl-2-aminotetralin) does not affect stimulated endogenous dopamine release in the striatum (at concentrations up to 1 μM), when examined using FCV (O'Connor & Kruk, unpublished observations). It is therefore unlikely that the biphasic nature of the 7-OH-DPAT curve is due to actions of 7-OH-DPAT at other non dopaminergic receptors.

At present we have no knowledge of the affinity of 7-OH-DPAT for the dopamine transporter. However, when using FCV, if a drug inhibits dopamine reuptake the observed peak dopamine detected is potentiated (by as much as 4 to 5 fold) and the rate of its decline prolonged (2 to 3 fold) (Trout & Kruk, 1992; Patel *et al.*, 1992b; Hafizi *et al.*, 1992; Davidson & Stamford, 1993). In these experiments 7-OH-DPAT did not increase the peak dopamine detected, or have any significant effect on the time for half decay.

The D_2 receptor agonist, *N*,*N*-dipropylamino-5,6-dihydroxytetralin (dpADTN), inhibits stimulated dopamine release in both the CPu and NAc: this inhibition is resistant to the atypical antipsychotic clozapine and is poorly antagonized by haloperidol, sulpiride and metoclopramide (Sheehan *et al.*, 1993). In addition, the inhibitory effect of dpADTN is resistant to pertussis toxin (Bull *et al.*, 1993). It was suggested by Sheehan *et al.* (1993), that dpADTN may inhibit stimulated dopamine release by acting at a novel D_2-like receptor other than D_3 or D_4 receptors. The possibility therefore exists that the high affinity component of the 7-OH-DPAT concentration-response curve may be due to activation of this novel D_2-like receptor.

Another possibility is that the two components reflect the two affinity states of the same receptor. In the nucleus accumbens the D_2 receptor exists primarily in the high affinity state (66%) under normal conditions (Richfield *et al.*, 1989). The possibility therefore exists that the high affinity component of the concentration-response curve to 7-OH-DPAT is due to an action mediated by the high affinity state of the receptor and the low affinity component is due to an action mediated via the low affinity state. However, the relative contributions of the high (18.0%) and low (77.5%) affinity components do not correspond to the distribution of D_2 receptors between high and low affinity states. In addition, the action of haloperidol observed in the present study is inconsistent with this possibility, as antagonists are not thought to be able to distinguish between different receptor affinity states (Richfield *et al.*, 1989).

In conclusion, the results of this study are consistent with the existence of at least two receptors, acting as autoreceptors, regulating evoked dopamine efflux in the NAc. These experiments with selective D_2/D_3 ligands suggest that the high affinity component of the concentration-response curve to 7-OH-DPAT, in the NAc, may reflect a functional D_3 autoreceptor, whereas the low affinity component reflects D_2 receptor function. Highly selective D_3 receptor antagonists are required to confirm this. The possibility that there may be an as yet unidentified dopamine autoreceptor cannot be excluded.

References

BALDESSARINI, R.J., KULA, N.S., MCGRATH, C.R., BAKTHAVACHALAM, V., KEBABIAN, J.W. & NEUMEYER, J.L. (1993). Isomeric selectivity at dopamine D_3 receptors. *Eur. J. Pharmacol.*, **239**, 269–270.

BOUTHENET, M.-L., SOUIL, E., MATRES, M.P., SOKOLOFF, P., GIROS, B. & SCHWARTZ, J.-C. (1991). Localization of dopamine D_3 receptor mRNA in the rat brain using in situ hybridization histochemistry: comparison with dopamine D_2 receptor mRNA. *Brain Res.*, **564**, 203–219.

BULL, D.R., HAYES, A.G. & SHEEHAN, M.J. (1993). A clozapine-insensitive response to the dopamine agonist, N,N-dipropylamino-5,6-dihydroxytetralin (dpADTN): Regional localisation and effect of pertussis toxin. *Br. J. Pharmacol.*, **110**, 6P.

BULL, D.R., PALIJ, P., SHEEHAN, M.J., MILLAR, J., STAMFORD, J.A., KRUK, Z.L. & HUMPHREY, P.P.A. (1990). Application of fast cyclic voltammetry to measurement of electrically evoked dopamine overflow from brain slices in vitro. *J. Neurosci. Methods*, **32**, 37–44.

BULL, D.R. & SHEEHAN, M.J. (1991). Presynaptic regulation of electrically evoked dopamine overflow in nucleus accumbens: a pharmacological study using fast cyclic voltammetry *in vitro*. *Naunyn-Schmied Arch. Pharmacol.*, **343,** 260–265.

CAINE, S.B. & KOOB, G.F. (1993). Modulation of cocaine self-administration in the rat through D-3 dopamine receptors. *Science*, **260,** 1814–1816.

DALY, S.A. & WADDINGTON, J.L. (1993). Behavioural effects of the putative D-3 dopamine receptor agonist 7-OH-DPAT in relation to other 'D-2-like' agonists. *Neuropharmacology*, **32,** 509–510.

DAMSMA, G., BOTTEMA, T., WESTERINK, B.H.C., TEPPER, P.G., DIJKSTRA, D., PUGSLEY, T.A., MACKENZIE, R.G., HEFFNER, T.G. & WIKSTRÖM, H. (1993). Pharmacological aspects of R-(+)-7-OH-DPAT, a putative dopamine D_3 receptor ligand. *Eur. J. Pharmacol.*, **249,** R9–R10.

DAVIDSON, C. & STAMFORD, J.A. (1993). Effects of GBR 12935 on dopamine efflux and uptake in three striatal subregions. *Br. J. Pharmacol.*, **109,** 88P.

EL MESTIKAWY, S., GLOWINSKI, J. & HAMON, M. (1986). Presynaptic dopamine autoreceptors control tyrosine hydroxylase activation in depolarized striatal dopaminergic terminals. *J. Neurochem.*, **46,** 12–22.

FREEDMAN, S.B., PATEL, S., MARWOOD, R., EMMS, F., SEABROOK, G.R., KNOWLES, M.R. & MCALLISTER, G. (1994). Expression and pharmacological characterization of the human D_3 dopamine receptor. *J. Pharmacol. Exp. Ther.*, **268,** 417–426.

GOBERT, A., RIVET, J.-M., AUDINOT, V., GIRARDON, S., CHAPUT, C., JACQUES, V., PEGLION, J.-L. & MILLAN, M.J. (1994). Modulation of mesolimbic and nigrostriatal dopamine synthesis by dopamine D_3 autoreceptors: influence of the novel, selective D_3 antagonist, S 14297. In *Monitoring Molecules in Neuroscience*, Proceedings of the 6th International Conference on *in vivo* Methods. pp. 93–94.

HAFIZI, S., PALIJ, P. & STAMFORD, J.A. (1992). Activity of two primary human metabolites of nomifensine on stimulated efflux and uptake of dopamine in the striatum: *In vitro* voltammetric data in slices of rat brain. *Neuropharmacology*, **31,** 817–824.

KENAKIN, T. (1993). Analysis of dose-response data. In *The Pharmacological Analysis of Drug-Receptor Interaction*. Second Edition. pp. 176–220. New York: Raven Press.

LARGE, C.H. & STUBBS, C.M. (1994). The dopamine D_3 receptor: Chinese hamsters or Chinese whispers? *Trends Pharmacol. Sci.*, **15,** 46–47.

LÉVESQUE, D., DIAZ, J., PILON, C., MARTRES, M.-P., GIROS, B., SOUIL, E., SCHOTT, D., MORGAT, J.-L., SCHWARTZ, J.-C. & SOKOLOFF, P. (1992). Identification, characterization, and localization of the dopamine D_3 receptor in rat brain using 7-[^{3}H]hydroxy-*N,N*-di-*n*-propyl-2-aminotetralin. *Proc. Natl. Acad. Sci. USA*, **89,** 8155–8159.

LIMBERGER, N., TROUT, S.J., KRUK, Z.L. & STARKE, K. (1991). 'Real time' measurement of endogenous dopamine release during short trains of pulses in slices of rat neostriatum and nucleus accumbens: role of autoinhibition. *Naunyn Schmied Arch Pharmacol.*, **344,** 623–629.

MACKENZIE, R.G., VANLEEUWEN, D., PUGSLEY, T.A., SHIH, Y.-H., DEMATTOS, S., TANG, L., TODD, R.D. & O'MALLEY, K.L. (1994). Characterization of the human dopamine D_3 receptor expressed in transfected cell lines. *Eur. J. Pharmacol.*, **266,** 79–85.

MELLER, E., BOHMAKER, K., GOLDSTEIN, M. & BASHAM, D.A. (1993). Evidence that striatal synthesis-inhibiting autoreceptors are dopamine D_3 receptors. *Eur. J. Pharmacol.*, **249,** R5–R6.

MILLAN, M.J., AUDINOT, V., RIVET, J.-M., GOBERT, A., VIAN, J., PROST, J.-F., SPEDDING, M. & PEGLION, J.-L. (1994). S 14297, a novel selective ligand at cloned human dopamine D3 receptors, blocks 7-OH-DPAT-induced hypothermia in rats. *Eur. J. Pharmacol.*, **260,** R3–R5.

O'CONNOR, J.J. & KRUK, Z.L. (1992). Pharmacological characteristics of 5-hydroxytryptamine autoreceptors in rat brain slices incorporating the dorsal raphe or the suprachiasmatic nucleus. *Br. J. Pharmacol.*, **106,** 524–532.

PALIJ, P., BULL, D.R., SHEEHAN, M.J., MILLAR, J., STAMFORD, J., KRUK, Z.L. & HUMPHREY, P.P.A. (1990). Presynaptic regulation of dopamine release in corpus striatum monitored *in vitro* in real time by fast cyclic voltammetry. *Brain Res.*, **509,** 172–174.

PATEL, J., TROUT, S.J. & KRUK, Z.L. (1992a). Regional differences in evoked dopamine efflux in brain slices of rat anterior and posterior caudate putamen. *Naunyn Schmied Arch. Pharmacol.*, **346,** 267–276.

PATEL, J., TROUT, S.J. & KRUK, Z.L. (1992b). Differences in dopamine reuptake inhibition by GBR 12909 in rat anterior and posterior caudate putamen brain slices. *Br. J. Pharmacol.*, **107,** 413P.

PILON, C., LÉVESQUE, D., DIMITRIADOU, V., GRIFFON, N., MARTRES, M.-P., SCHWARTZ, J.-C. & SOKOLOFF, P. (1994). Functional coupling to the human dopamine D_3 receptor in a transfected NG 108-15 neuroblastoma-glioma hybrid cell line. *Eur. J. Pharmacol. [Mol. Pharmacol. Sect.]*, **268,** 129–139.

POTENZA, M.N., GRAMINSKI, G.F., SCHMAUSS, C. & LERNER, M.R. (1994). Functional expression and characterization of human D_2 and D_3 dopamine receptors. *J. Neurosci.*, **14,** 1463–1476.

RICHFIELD, E.K., PENNEY, J.B. & YOUNG, A.B. (1989). Anatomical and affinity state comparisons between dopamine D_1 and D_2 receptors in the rat central nervous system. *Neuroscience*, **30,** 767–777.

RIVET, J.-M., GOBERT, A., CISTARELLI, L., AUDINOT, V., PEGLION, J.-L. & MILLAN, M.J. (1994). Modulation by dopamine D_3 autoreceptors of mesolimbic and nigrostriatal dopamine release: influence of the novel, selective D_3 antagonist, S 14297. In *Monitoring Molecules in Neuroscience*, Proceedings of the 6th International Conference on *in vivo* Methods. pp. 95–96.

SEABROOK, G.R., KEMP, J.A., FREEDMAN, S.B., PATEL, S., SINCLAIR, H.A. & MCALLISTER, G. (1994). Functional expression of human D_3 dopamine receptors in differentiated neuroblastoma x glioma NG108-15 cells. *Br. J. Pharmacol.*, **111,** 391–393.

SHEEHAN, M.J., HAYES, A.G. & BULL, D.R. (1993). Evidence for a clozapine-insensitive response to the dopamine agonist, N,N-dipropylamino-5,6-dihydroxytetralin (dpADTN), on dopaminergic nerve terminals. *Br. J. Pharmacol.*, **108,** 56P.

SOKOLOFF, P., GIROS, B., MARTRES, M.-P., BOUTHENET, M.-L. & SCHWARTZ, J.-C. (1990). Molecular cloning and characterization of a novel dopamine receptor (D_3) as a target for neuroleptics. *Nature*, **347,** 146–151.

STARKE, K., GÖTHERT, M. & KILBINGER, H. (1989). Modulation of neurotransmitter release by presynaptic autoreceptors. *Physiol. Rev.*, **69,** 864–989.

SVENSSON, K., CARLSSON, A. & WATERS, N. (1994). Locomotor inhibition by the D_3 ligand R-(+)-7-OH-DPAT is independent of changes in dopamine release. *J. Neural. Transm. [Gen. Sect.]*, **95,** 71–74.

TANG, L., TODD, R.D., HELLER, A. & O'MALLEY, K.L. (1994a). Pharmacological and functional characterization of D_2, D_3 and D_4 dopamine receptors in fibroblast and dopaminergic cell lines. *J. Pharmacol. Exp. Ther.*, **268,** 495–502.

TANG, L., TODD, R.D. & O'MALLEY, K.L. (1994b). Dopamine D_2 and D_3 receptors inhibit dopamine release. *J. Pharmacol. Exp. Ther.*, **270,** 475–479.

TROUT, S.J. & KRUK, Z.L. (1992). Differences in evoked dopamine efflux in rat caudate putamen, nucleus accumbens and tuberculum olfactorium in the absence of uptake inhibition: influence of autoreceptors. *Br. J. Pharmacol.*, **106,** 452–458.

WATERS, N., SVENSSON, K., HAADSMA-SVENSSON, S.R., SMITH, M.W. & CARLSSON, A. (1993). The dopamine D3-receptor: a postsynaptic receptor inhibitory on rat locomotor activity. *J. Neural Transm. [Gen. Sect.]*, **94,** 11–19.

YAMADA, S., YOKOO, H. & NISHI, S. (1994). Differential effects of dopamine agonists on evoked dopamine release from slices of striatum and nucleus accumbens in rats. *Brain Res.*, **648,** 176–179.

YOKOO, H., GOLDSTEIN, M. & MELLER, E. (1988). Receptor reserve at striatal dopamine receptors modulating the release of [^{3}H]dopamine. *Eur. J. Pharmacol.*, **155,** 323–327.

ZHUANG, Z.P., KUNG, M.-P. & KUNG, H.F. (1993). Synthesis of (R,S)-*trans*-8-Hydroxy-2-[N-*n*-propyl-N-(3'-iodo-2'-propenyl)amino]tetraline (*trans*-8-OH-PIPAT): A new 5-HT_{1A} receptor ligand. *J. Med. Chem.*, **36,** 3161–3165.

(Received January 11, 1995
Accepted February 14, 1995)

British Journal of Pharmacology (1995) 115, 427-432

Discrimination between UTP- and P_2-purinoceptor-mediated depolarization of rat superior cervical ganglia by 4,4'-diisothiocyanatostilbene-2,2'-disulphonate (DIDS) and uniblue A

[1]G.P. Connolly & P.J. Harrison

Department of Physiology, University College London, Gower Street, London WC1E 6BT

1 Using a grease-gap recording technique we have investigated the effects of some antagonists of P_2-purinoceptors on the depolarization of the rat isolated superior cervical ganglion evoked by 100 μM α,β-methylene-adenosine 5'-triphosphate (α,β-MeATP) or uridine 5'-triphosphate (UTP). The effects of the putative P_{2Z}-purinoceptor antagonist, coomassie brilliant blue G, putative P_{2X}-purinoceptor antagonist, 4,4'-diisothiocyanatostilbene-2,2'-disulphonate (DIDS) and uniblue A (an analogue of the P_{2Y}- and P_{2X}-purinoceptor antagonist reactive blue 2) were investigated.

2 At the highest concentration examined uniblue A (300 μM) depressed α,β-MeATP-induced depolarization and at 100 and 300 μM enhanced UTP-evoked depolarizations. Coomassie brilliant blue G (1 and 10 μM) did not affect depolarizations evoked by α,β-MeATP or UTP. Depolarizations evoked by potassium (5 mM) or muscarine (100 nM) were unaltered by either coomassie brilliant blue G or uniblue A. Uniblue A (100 and 300 μM) produced a concentration-dependent depression of hyperpolarizations evoked by adenosine (100 μM) whereas coomassie brilliant blue G at up to 10 μM, did not alter adenosine-induced hyperpolarizations.

3 DIDS (30 and 100 μM) did not alter adenosine-evoked hyperpolarizations, or depolarizations evoked by potassium or UTP. DIDS at 100 μM did not alter depolarizations evoked by muscarine. In contrast DIDS produced a concentration-dependent depression of α,β-MeATP-evoked depolarizations.

4 These results are consistent with the proposal that uniblue A and DIDS but not coomassie brilliant blue G are antagonists of P_2-purinoceptors and that uniblue A is also an antagonist at P_1-purinoceptors present on the rat superior cervical ganglion.

5 The ability of uniblue A and DIDS to distinguish between depolarizations evoked by UTP and α,β-MeATP provides further justification for the proposal that these nucleotides activate separate receptors present on the rat superior cervical ganglion, i.e. pyrimidinoceptors and P_2-purinoceptors respectively.

Keywords: Superior cervical ganglion; P_2-purinoceptors; uridine 5'-triphosphate (UTP); uniblue A; coomassie brilliant blue G; DIDS

Introduction

Purinoceptors as defined by Burnstock (1978) belong to two major subtypes, i.e. P_1-purinceptors which show greater selectivity for adenosine than adenosine 5'-triphosphate (ATP), and P_2-purinoceptors which show the opposite selectivity. Since this original classification, the extracellular effects of ATP on many more tissues have been described and attributed to the activation of various P_2-purinoceptor subtypes (Burnstock & Kennedy, 1985; Gordon, 1986). The present classification of P_2-purinoceptors includes P_{2X}-, P_{2Y}-, and P_{2Z}-purinoceptor subtypes. P_{2X}-purinoceptor-mediated responses are characterized by the following order of potency: α,β-methylene ATP (α,β-MeATP) > β,γ-methylene ATP (β,γ-MeATP) > > ATP = 2-methylthio-ATP (2-MeSATP), whereas P_{2Y}-purinoceptors exhibit a rank order of potency of 2-MeSATP > ATP > α,β-MeATP = β,γ-MeATP (Burnstock & Kennedy, 1985). In contrast P_{2Z}-purinoceptors show greater selectivity for ATP^{4-} (Gordon, 1986) with a potency order of ATP^{4-} > 2-MeSATP > α,β-MeATP > ATP.

Recently the classification of P_2-purinoceptor subtypes has been challenged and extended by the inclusion of data obtained with pyridimine nucleotides. Consequently the classification of extracellular receptors for purine nucleotides may now be too restricted and needs to be reclassified to include the effects of pyrimidine nucleotides (O'Connor *et al.*, 1991). On tissues believed to contain receptors for nucleotides, i.e. P_{2U}-purinoceptors, uridine 5'-triphosphate (UTP) and ATP activate this receptor with equipotency and α,β-MeATP has little or no activity (O'Connor *et al.*, 1991). In addition it has also been proposed that UTP activates distinct receptors, i.e. 'pyrimidinoceptors' (von Kügelgen *et al.*, 1987; Haüssinger *et al.*, 1987) as reviewed by Seifert & Schultz (1989).

We have reported preliminary evidence to show that UTP, α,β-MeATP and ATP depolarize (in that order of potency) rat superior cervical ganglia (SCG) and suggested that the effects of ATP and α,β-MeATP are mediated via the activation of P_2-purinoceptors whereas depolarizations by UTP are mediated by a suramin-resistant mechanism (Connolly *et al.*, 1993b; Connolly, 1994b; Connolly & Harrison, 1994a), and may be mediated by a pyrimidinoceptor (Connolly, 1994a). Other compounds apart from suramin have been suggested to antagonize P_2-purinceptors, e.g. 4,4'-diisothiocyanatostilbene-2,2'-disulphonate (DIDS) (Figure 1a) (Fedan & Lamport, 1990; Soltoff *et al.*, 1993; Bültmann & Starke, 1994), coomassie brilliant blue G (Figure 1b) (Soltolf *et al.*, 1989; Inoue *et al.*, 1991) and reactive blue 2 (Figure 1c) (Burnstock, 1978; Burnstock & Kennedy, 1985) and thus we sought to examine the effect of some of these P_2-purinoceptor antagonists on depolarizations of rat SCG elicited by α,β-MeATP and UTP. Our studies were designed to verify if α,β-MeATP-mediated depolarizations were due to activation of P_2-purinceptors and

[1]Author for correspondence at: Physiology Group, Biomedical Sciences Division, King's College, Strand, London WC2R 2LS.

also to investigate whether depolarizations evoked by UTP were mediated by P_2-purinoceptors or distinct pyrimidinoceptors. As well as studying the effects of coomassie brilliant blue G and DIDS, the effects of an analogue of reactive blue 2, i.e. uniblue A (UBA) on the response of rat SCG evoked by α,β-MeATP, UTP, adenosine, potassium and muscarine were determined. The rationale for the use of uniblue A in this study was based upon the hypothesis that being an analogue of reactive blue 2 (cf. Figure 1c and 1d) it might share some properties exhibited by reactive blue 2 (as reported in a previous study, see Connolly & Harrison, 1994a) and therefore elucidate how reactive blue 2 alters depolarizations of the rat SCG evoked by α,β-MeATP and UTP. A preliminary report of some of this work has been published recently (Connolly & Harrison, 1994b).

Methods

Male Wistar rats (200 to 400 g) were killed by a lethal dose of urethane. Ganglia were removed and desheathed in physiological salt solution (PSS) at room temperature (19 to 23°C) and prepared for recording of d.c. potentials via the internal carotid nerve and the body of the ganglion as described before (Connolly *et al.*, 1993b). In brief, desheathed ganglia were mounted in a tissue bath with three compartments, with the ganglion in the central chamber (bath volume ca. 0.5 ml) and the pre- and postganglionic trunks protruding through lightly greased slots into the outer chambers. All chambers were filled with PSS containing (mM): NaCl 125, $NaHCO_3$ 25, KCl 2, KH_2PO_4 1, $MgSO_4$, 1, glucose 10 and $CaCl_2$ 0.1. The central chamber was perfused with PSS at 25 ± 1°C, pH 7.4, equilibrated with 5% CO_2/95%O_2. The potential differences between the earthed central chamber and the internal carotid nerve were recorded with Ag/AgCl electrodes. Signals were filtered through a low pass filter, amplified via d.c. pre-amplifiers and recorded on a pen recorder.

Drugs were dissolved in PSS at 10 or 100 mM stock solutions and frozen (−20°C) as aliquots. New aliquots of drugs were used for each experiment and stock and dilutions of drugs in PSS were kept on ice during experiments. Agonists were applied at submaximal concentrations for times that were sufficient for potential changes to reach a plateau and allow repeated applications without desensitization. Ganglia were equilibrated for 2 to 3 h before use. Muscarine (100 nM) or potassium (K^+) (5 mM) were applied for 1 min and α,β-MeATP, adenosine or UTP (all at 100 μM) were applied for 2 min, at about 20 min intervals. Concentrations refer to those in contact with the ganglion. Peak responses to drugs were measured from a baseline drawn between the potentials at the start of the application of a drug and the finish of the response. Responses are expressed as a mean ± s.e. mean (n), where n is the number of ganglia studied. Antagonists were dissolved immediately before use to the required concentration. Ganglia were incubated with only one antagonist for a minimum of 20 to 40 min before retesting responses elicited by agonists. The effect of DIDS on agonist-evoked responses was determined in near darkness to avoid degradation of DIDS. Responses in the absence and presence of an antagonist were compared for statistically significant difference by Student's paired t test and P values were considered statistically significant if less than 0.05.

Adenosine hemisulphate, α,β-MeATP, coomassie brilliant blue G (60% pure), DIDS, uniblue A (98% pure) and UTP were obtained from Sigma Chemical Co., U.K. (±)-Muscarine was bought from Semat Technical (U.K.) Ltd., Hertfordshire, England. Salts for the perfusate were of Analar grade.

Results

An example of the effects of uniblue A and DIDS on agonist-induced responses produced by a single rat superior cervical ganglion is illustrated in Figure 2 and the result obtained from a number of ganglia summarized in Figure 3.

Depolarizations evoked by potassium (K^+, 5 mM) or 100 nM muscarine were unaltered by coomassie brilliant blue G (Figure 3a), 100 or 300 μM uniblue A (Figure 2a and 3b) and

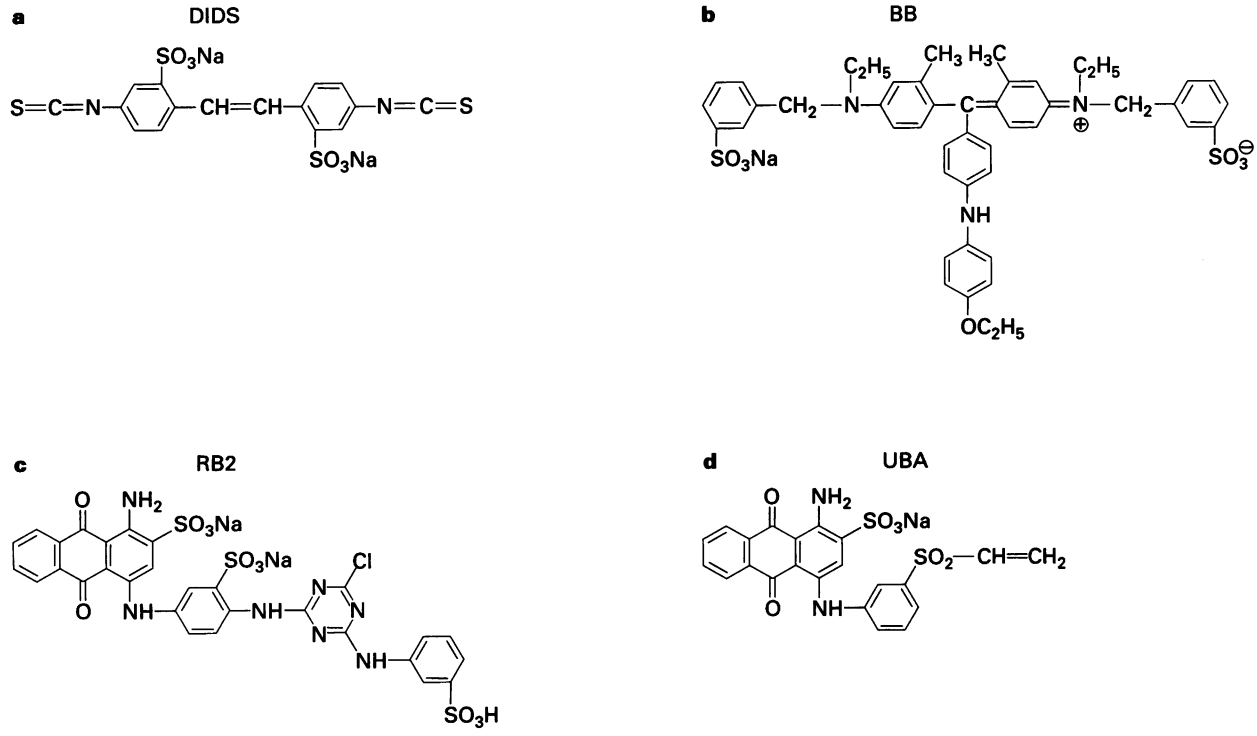

Figure 1 Chemical structures of (a) 4,4′-diisothiocyanatostilbene-2,2′-disulphonate (DIDS), (b) coomassie brilliant blue G (BB), (c) reactive blue 2 (RB2) and (d) uniblue A (UBA).

unaltered by DIDS (Figures 2b and 3c). Depolarizations evoked by potassium (5 mM) were unaltered by uniblue A 30 μM (control = 152 ± 24 μV, + uniblue A = 127 ± 26 μV, $n=6$). Hyperpolerizations evoked by 100 μM adenosine were unaltered by coomassie brilliant blue G (Figure 3a), DIDS (Figures 2b and 3c), uniblue A at 30 μM (control = 174 ± 28 μV, + uniblue A = 156 ± 20 μV, $n=6$) and depressed in a concentration-dependant manner by 100 and 300 μM uniblue A (Figure 3b, e.g. Figure 2a).

Depolarizations evoked by 100 μM α, β-MeATP were unaltered by coomassie brilliant G (Figure 3a), depressed in a concentration-dependent manner by DIDS (Figure 3c) and depressed by a high (300 μM) but not lower concentrations of uniblue A (control = 130 ± 10 μV, + uniblue A (30 μM) = 124 ± 15 μV, $n=5$) (for 100 μM uniblue A, see Figure 3b).

Depolarizations evoked by 100 μM UTP were unaltered by coomassie brilliant blue G (Figure 3a), DIDS (Figures 2b and 3c) and uniblue A at 30 μM (control = 312 ± 89 μV, + uniblue A = 294 ± 50 μV, $n=6$) but enhanced by uniblue A at 100 and 300 μM (Figures 2a and 3b).

Discussion

Antagonism of P_2-purinceptors

Depolarizations evoked by potassium, muscarine and UTP were unaltered by DIDS, whereas depolarizations evoked by α,β-MeATP (a selective P_{2X}-purinoceptor agonist) were depressed in a conentration-dependent manner suggesting that DIDS is an antagonist of P_{2X}-purinoceptors. This conclusion is consistent with the observations that DIDS antagonized ATP-evoked contraction of the guinea-pig vas deferens (Fedan & Lamport, 1990) and more recently was shown to antagonize contractions of the rat vas deferens elicted by α,β-MeATP (Bültmann & Starke, 1994) indicating that it is a P_{2X}-purinoceptor antagonist.

The inability of coomassie brilliant blue G (at up to 25 times the IC_{50} for the inhibition of the activation by ATP of P_{2Z}-purinoceptors on rat parotid acinar cells, Soltoff *et al.*, 1989) to alter hyperpolarizations evoked by adenosine or depolarizations elicted by potassium, α,β-MeATP, UTP or muscarine suggests that this dye is not an antagonist of A_1-adenosine, M_1-muscarinic or P_{2X}-purinceptors. A similar lack of antagonism by coomassie brilliant blue G of the activation of P_2-purinoceptors on rat PC12 phaeochromocytoma cells was also reported by Inoue *et al.* (1991). Here it should be noted that the effects of coomassie brilliant blue G were not examined at a concentration above 10 μM and thus it is possible that at higher concentrations coomassie brilliant blue G may have other effects, e.g. depression of α,β-MeATP-evoked depolarization. The lack of antagonism of α,β-MeATP-evoked depolarizations by coomassie brilliant blue G, but their depression by DIDS supports the idea that α,β-MeATP depolarizes the superior cervical ganglion by activating P_{2X}-purincoeptors. Uniblue A (a structural analogue of the P_2-purinoceptor or antagonist, reactive blue 2, see Figure 1) at 300 μM depressed depolarizations evoked by α,β-MeATP indicating it is (albeit a weak)/antagonist of P_{2X}-purinoceptors. This finding is consistent with recently published observations showing that reactive blue 2 depresses depolarizations of the rat superior cervical ganglion evoked by α,β-MeATP (Connolly & Harrison, 1994a). Another property of uniblue A, reported here, was its ability to depress in a concentration-dependent manner hyperpolarizations evoked by adenosine, suggesting that this dye is also an antagonist at P_1-purinoceptors. Because the rat superior cervical ganglion is thought to contain only A_1-adenosine receptors (and few if any A_2-adenosine receptors; Connolly *et al.*, 1993a) the antagonistic effects of uniblue A are presumably due to antagonism of A_1-adenosine receptors.

Potentiation of UTP-evoked depolarizations

Besides depression of depolarizations elicited by α,β-MeATP, uniblue A also potentiated UTP-evoked depolarizations of the rat SCG. The mechanism(s) responsible for the potentiation of UTP-evoked depolarization by uniblue-A is unknown. Various mechanisms could account for the potentiation of UTP-

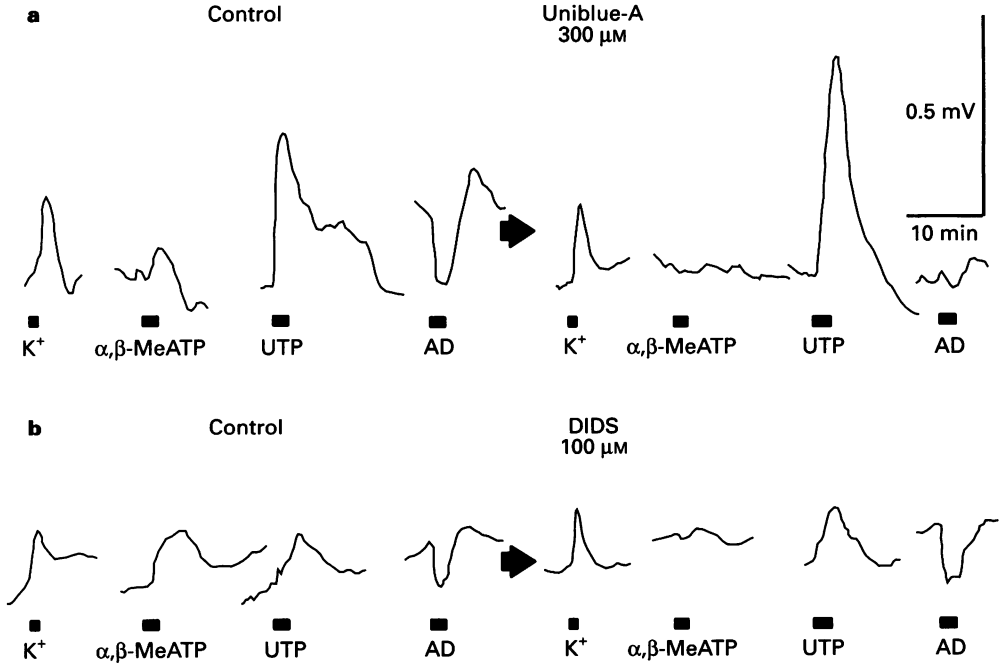

Figure 2 Sample responses of a rat single superior cervical ganglion evoked by potassium (K^+), α,β-methylene-adenosine 5′-triphosphate (α,β-MeATP), uridine 5′-triphosphate (UTP) and adenosine (AD). Responses evoked by K^+ (5 mM), α,β-MeATP (100 μM), UTP (100 μM) and AD (100 μM) in (a) the absence (Control) and in the presence of uniblue A (300 μM), and (b) responses of another ganglion in the absence (Control) and the presence of 4,4′-diisothiocyanatostilbene-2,2′-disulphonate (DIDS) (100 μM). Bars under the traces refer to the application times.

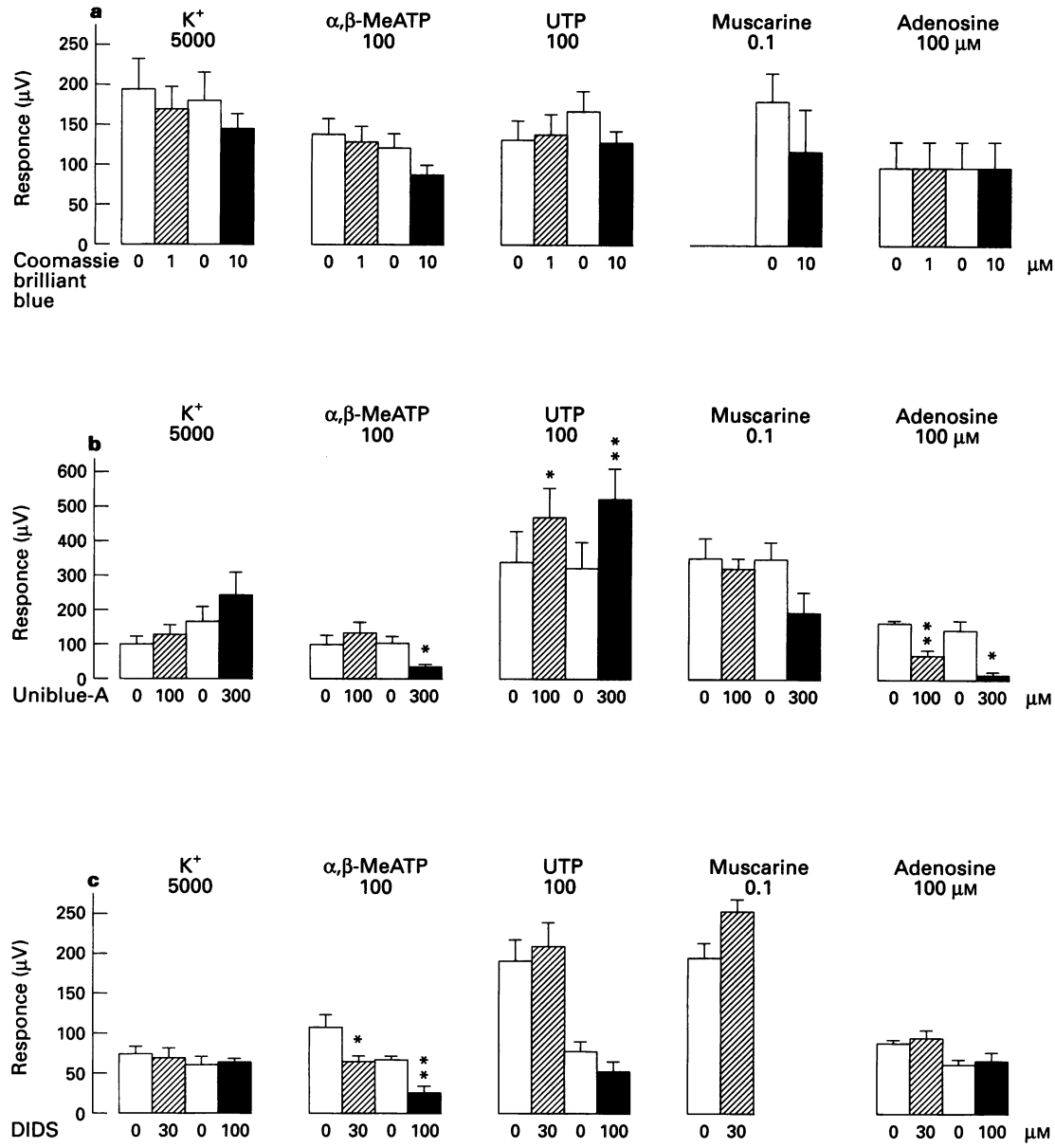

Figure 3 Effect of (a) coomassie brilliant blue G, (b) uniblue A and (c) 4,4'-diisothiocyanatostilbene-2,2'-disulphonate (DIDS) on the response of the rat SCG to potassium (K^+), α,β-methylene-adenosine 5'-triphosphate (α,β-MeATP), uridine 5'-triphosphate (UTP), muscarine and adenosine. The first and third columns (open columns) are the control responses without antagonist. The second and fourth columns (hatched and solid columns) are the responses to an agonist in the presence of different concentrations of antagonists. Numbers under each bar refer to the concentration in μM of antagonist. The column represents the mean response (μV) with s.e.mean from 4 to 10 ganglia. Statistical differences between responses in the absence and those in the presence of an antagonist are denoted by $*P>0.05$ and $**P>0.01$ respectively (paired t test). NB For convenience, hyperpolarizations evoked by adenosine are shown in the same direction as other agonist-evoked responses.

evoked depolarizations, namely an antagonism of an underlying UTP-evoked hyperpolarization, a change in the metabolism of UTP or its metabolites or an allosteric interaction. These effects remain to be investigated, but some evidence in favour of the latter hypotheses is suggested by the observation that on some ganglia, uniblue A potentiated the peak response evoked by UTP and sharpened the time-course of the response. Because unlike UTP, α,β-Me-ATP is relatively resistant to degradation by ectonucleotidases (Welford *et al.*, 1986; 1987), the ability of uniblue A to enhance depolarizations evoked by UTP (but depress α,β-Me-ATP-evoked depolarizations) could have arisen from the net effect of inhibition of ectonucleotidase activity and an antagonism of P_{2X}-purinoceptors, thus raising the possibility that UTP and α,β-Me-ATP activate the same receptor. This hypothesis seems unlikely given that reactive blue 2 does not inhibit ectonucleotidases (Hourani & Chown, 1989) and thus similarly uniblue A (a structural analogue of reactive blue 2) would be expected to lack any inhibitory activity against ectonucleotidases. Nevertheless experiments to examine the effect of specific inhibitors of ectonucleotidases on purine and pyrimidine evoked responses of the rat SCG should provide useful information on the metabolism of these compounds and resolve these issues.

Because other P_2-purinoceptor antagonists including suramin (Connolly *et al.*, 1993b; Connolly, 1994b), pyridoxalphosphate-6-azophenyl-2',4'-disulphonic acid (PPADS) (Connolly, 1994c) and reactive blue 2 (Connolly & Harrison, 1994a) also caused a potentiation of UTP-evoked depolarizations and inhibited α,β-MeATP-evoked depolarizations these two effects may be interdependent possibly via a common intracellular messenger. If it is observed on other tissues that P_2-purinoceptor antagonists depress P_2-purinoceptor- and en-

hance UTP-evoked responses, then this phenomenon may have important implications for the design and development of selective P_2-purinoceptor antagonists. The results of this study, however, also provide some evidence against the effects of UTP and α,β-MeATP being interdependent. It was observed that DIDS produced a significant and concentration-dependent depression of α,β-MeATP-evoked depolarizations with no effect on UTP-evoked depolarizations and conversely uniblue A (at 100 μM) caused a significant potentiation of UTP-evoked depolarizations without depressing α,β-MeATP-evoked depolarizations. Similarly we reported that reactive blue 2 (at 30 μM) antagonized depolarizations evoked by α,β-MeATP without affecting depolarizations evoked by UTP (Connolly & Harrison, 1994a, see Figure 2d). Thus, whether the depolarizing effects of UTP or α,β-MeATP on the rat SCG are mediated via a common intracellular messenger or independent of each other is unresolved.

The lack of antagonism of UTP-evoked depolarizations by DIDS, coomassie brilliant blue G and uniblue A suggests that UTP does not depolarize the rat SCG by activating P_{2X}-, P_{2Z}- or P_{2Y}-purinoceptors; rather it activates a distinct receptor, i.e. a pyrimidinoceptor as has been proposed in earlier studies (Connolly *et al.*, 1993b; Connolly, 1994a). Although the effects of DIDS on P_2-purinoceptor subtypes other than at P_{2Z}- and P_{2X}-purinoceptors (Fedan *et al.*, 1990; Soltoff *et al*, 1993; Bültmann & Starke, 1994), including the P_{2Y}-purinoceptor have yet to be reported, it seems unlikely that the inability of DIDS to potentiate UTP-evoked depolarizations results from a lack of antagonism of an opposing P_{2Y}-purinoceptor-mediated hyperpolarization. This assumption is based upon the observation that suramin and reactive blue 2 (two antagonists of P_{2X}- and P_{2Y}-purinoceptors) and PPADS (a selective P_{2X}-purinoceptor antagonist) all produced an enhancement of UTP- and a corresponding depression of α,β-MeATP or ATP-evoked depolarizations of the rat SCG (Connolly *et al.*, 1993b; Connolly, 1994b; Connolly & Harrison, 1994a; Connolly, 1994c respectively). Further support for this idea comes from the observation that 2-methylthio-ATP, an agonist at P_{2Y}-purinceptors (Burnstock & Kennedy, 1985) was virtually inactive on rat SCG (Connolly *et al.*, 1993b) suggesting P_{2Y}-purinoceptors are absent on this ganglion.

Like reactive blue 2 (Connolly & Harrison, 1994a), uniblue A potentiated UTP-evoked depolarizations of the rat SCG. This potentiation is unlikely to have occurred because of any antagonism of adenosine receptors, because both reactive blue 2 (Connolly & Harrison, 1994a) and suramin (Connolly *et al.*, 1993b; Connolly, 1994b) potentiated UTP-evoked depolarizations but did not alter hyperpolarizations elicited by adenosine. The observation that uniblue A was less potent than reactive blue 2 (cf. Figure 3b this study and Figure 2d in Connolly & Harrison, 1994a) in enhancing UTP-evoked depolarizations, suggests that the presence of a triazine group in reactive blue 2 (but not uniblue A, see Figure 1) enhances, but is not essential for potentiation of UTP-evoked depolarizations. It is tempting to speculate that because reactive blue 2 and uniblue A have an aminobenzyl group with a sulphonic acid substituent (and the same antraquinone moiety, see Figure 1) and suramin contains O-methyl groups linked to aminobenzyl groups with sulphonic acid substituents, that the enhancement of UTP-evoked depolarizations arises from the presence of these common chemical substituents in these three compounds. Further studies using other sulphonic acid substitued dyes including analogues of suramin should help define which specific chemical groups are responsible for this positive modulation of UTP-evoked depolarizations.

In summary the results presented here provide further evidence for the presence on the rat superior cervical ganglion of distinct purinoceptors and pyrimidinoceptors, supporting the proposal that this ganglion is a useful preparation for studying neuronal pyrimidinoceptors (Connolly & Harrison, 1993). The existence of distinct purinoceptors and pyrimidinoceptors on rat superior cervical ganglion neurones and their potential activation by ATP and UTP respectively, at physiologically relevant concentrations suggests that they could have important and specific neuromodulatory functions.

References

BÜLTMANN, R. & STARKE, K. (1994). Blockade by 4,4'-diisothiocyanatostilbene-2,2'-disulphonate (DIDS) of P_{2X}-purinoceptors in rat vas deferens. *Br. J. Pharmacol.*, **112**, 690–694.

BURNSTOCK, G. (1978). A basis for distinguishing two types of purinergic receptor. In *Cell Membrane Receptors for Drugs and Hormones: Multidisciplinary Approach*. ed. Straub, R.W. & Bolis, L. pp. 107–118. New York: Raven Press.

BURNSTOCK, G. & KENNEDY, C. (1985). Is there a basis for distinguishing between two types of P2-purinoceptor? *Gen. Pharmacol.*, **16**, 433–440.

CONNOLLY, G.P. (1994a). Evidence from desensitisation studies for distinct receptors for ATP and UTP on the rat superior cervical ganglion. *Br. J. Pharmacol.*, **112**, 357–359.

CONNOLLY, G.P. (1994b). Effect of suramin on depolarisation of rat superior cervical ganglia (SCG) evoked by purine and pyrimidine 5'-triphosphates. *Br. J. Pharmacol.*, **113**, 56P.

CONNOLLY, G.P. (1994c). Pyridoxalphosphate (PP) and pyridoxalphosphate-6-azophenyl-2',4'-disulphonic acid (PPADS) enhance UTP- and depress α,β-methylene ATP-evoked depolarisation of rat superior cervical ganglia. *Br. J. Pharmacol.*, **113**, 115P.

CONNOLLY, G.P., BROWN, F. & STONE, T.W. (1993a). Characterisation of the adenosine receptors on the rat isolated superior cervical ganglion. *Br. J. Pharmacol.*, **110**, 854–860.

CONNOLLY, G.P. & HARRISON, P.J. (1993). The isolated rat superior cervical ganglion (SCG) as a model tissue for the study of neuronal pyrimidine receptors. *Pharmacol. World Sci.*, **4**, Supp F. p5.

CONNOLLY, G.P. & HARRISON, P.J. (1994a). Reactive blue 2 discriminates between responses medated by UTP and those evoked by ATP or α,β-methylene-ATP on rat sympathetic ganglia. *Eur. J. Pharmacol.*, **259**, 95–99.

CONNOLLY, G.P. & HARRISON, P.J. (1994b). Uniblue A (UBA) but not coomassie brilliant blue G (BB) antagonises α,β-MethyleneATP- but not UTP-evoked depolarisations of rat superior cervical ganglia. *Br. J. Pharmacol.*, C117, In Press. December Meeting.

CONNOLLY, G.P., HARRISON, P.J. & STONE, T.W. (1993b). Action of purine and pyrimidine nucleotides on the rat superior cervical ganglion. *Br. J. Pharmacol.*, **110**, 1297–1304.

FEDAN, J.S. & LAMPORT, S.J. (1990). Effects of reactive blue 2 (RB2), p-chloromercuribenzene sulphonate (PCMBS), 4,4'-diisothiocyano-2,2'-disulphonic acid stilbene (DIDS), phorbol myristate acetate (PMA) and Cs^+ on contractions of guinea-pig isolated vas deferens (VD) to ATP. *FASEB*, **4**, A1118.

GORDON, J.L. (1986). Extracellular ATP: effects, sources and fate. *Biochem. J.*, **233**, 309–319.

HAÜSSINGER, D., STEHLE, T. & GEROK, W. (1987). Actions of extracellular UTP and ATP in perfused rat liver. *Eur. J. Pharmacol.*, **167**, 65–71.

HOURANI, S.M.O. & CHOWN, J.A. (1989). The effects of some possible inhibitors of ectonucleotidases on the breakdown and pharmacological effects of ATP in the guinea-pig urinary bladder. *Gen. Pharmacol.*, **20**, 413–416.

INOUE, K., NAKAZAWA, K., OHARA-IMAIZUMI, M., OBAMA, T., FUJMORI, K. & TAKANAKA. (1991). Antagonism by reactive blue 2 but not by brilliant blue G of extracellular ATP-evoked responses in PC12 phaeochromocytoma cells. *Br. J. Pharmacol.*, **102**, 851–854.

O'CONNOR, S.E., DAINTY, I.A. & LEFF, P. (1991). Further subclassification of ATP receptors based on agonist studies. *Trends Pharmacol. Sci.*, **12**, 137–141.

SEIFERT, R. & SCHULTZ, G. (1989). Involvement of pyrimidinoceptors in the regulation of cell functions by uridine and by uracil nucleotides. *Trends Pharmacol. Sci.*, **10**, 365–369.

SOLTOFF, S.P., MCMILLIAN, M.K. & TALAMO, B.R. (1989). Coomassie brilliant blue G is a more potent antagonist of P_2 purinergic responses than reactive blue 2 (Cibachron blue 3GA) in rat parotid acinar cells. *Biochem. Biophys. Res. Commun.*, **165**, 1279–1285.

SOLTOFF, S.P., MCMILLIAN, M.K., TALAMO, B.R. & CANTLEY, L.C. (1993). Blockade of ATP binding site of P_2 purinoceptors in rat parotid acinar cells by isothiocyanate compounds. *Biochem. Pharmacol.*, **45**, 1936–1940.

VON KÜGELGEN, I., HAÜSSINGER, D. & STARKE, K. (1987). Evidence for a vasoconstriction-mediating receptors for UTP, distinct from the P_{2X}-purinoceptor, in rabbit ear artery. *Naunyn Schmied. Arch. Pharmacol.*, **336**, 556–560.

WELFORD, L.A., CUSACK, N.J. & HOURANI, S.M.O. (1986). ATP analogues and the guinea-pig taenia coli: a comparison of the structure-activity relationships of ectonucleotidases with those of the P2-purinoceptor. *Eur. J. Pharmacol.*, **129**, 217–224.

WELFORD, L.A., CUSACK, N.J. & HOURANI, S.M.O. (1987). The structure-activity relationships of ectonucleotidases and of excitatory P2-purinoceptors: evidence that dephosphorylation of ATP analogues reduces pharmacological potency. *Eur. J. Pharmacol.*, **141**, 123–130.

(Received January 11, 1995
Accepted February 14, 1995)

British Journal of Pharmacology (1995) 115, 433-440

Activation of rabbit platelets by Ca^{2+} influx and thromboxane A_2 release in an external Ca^{2+}-dependent manner by zooxanthellatoxin-A, a novel polyol

Mun-Chual Rho, Norimichi Nakahata, *Hideshi Nakamura, *Akio Murai & [1]Yasushi Ohizumi

Department of Pharmaceutical Molecular Biology, Faculty of Pharmaceutical Sciences, Tohoku University, Aoba, Aramaki, Aoba-ku, Sendai 980, Japan and *Department of Chemistry, Faculty of Sciences, Hokkaido University, Sapporo 060, Japan

1 Zooxanthellatoxin-A (ZT-A), a novel polyhydroxylated long chain compound, isolated from a symbiotic marine alga *Simbiodinium* sp., caused aggregation in rabbit washed platelets in a concentration-dependent manner (1-4 μM), accompanied by an increase in cytosolic Ca^{2+} concentration ($[Ca^{2+}]_i$).

2 ZT-A did not cause platelet aggregation or increase $[Ca^{2+}]_i$ in a Ca^{2+}-free solution, and Cd^{2+} (0.1-1 mM), Co^{2+} (1-10 mM) and Mn^{2+} (1-10 mM) inhibited ZT-A-induced aggregation. SK&F96365 (1-100 μM), a receptor operated Ca^{2+} channel antagonist, and mefenamic acid (0.1-10 μM), a non-specific divalent cation channel antagonist, inhibited platelet aggregation and the increase in $[Ca^{2+}]_i$ induced by ZT-A.

3 Indomethacin (0.1-10 μM), a cyclo-oxygenase inhibitor, and SQ-29548 (0.1-10 μM), a thromboxane A_2 (TXA_2) receptor antagonist, inhibited platelet aggregation and the increase in $[Ca^{2+}]_i$ induced by ZT-A.

4 Methysergide (0.01-1 μM), a 5-HT_2 receptor antagonist, inhibited ZT-A-induced platelet aggregation but did not affect the increase in $[Ca^{2+}]_i$ induced by ZT-A.

5 Tetrodotoxin (1 μM), a Na^+ channel blocker and chlorpheniramine (1 μM), a H_1-histamine receptor antagonist, neither affected ZT-A-induced platelet aggregation nor the increase in $[Ca^{2+}]_i$ induced by ZT-A.

6 Genistein (1-100 μM), a protein tyrosine kinase inhibitor, and staurosporine (0.01-1 μM), a protein kinase C inhibitor, also inhibited ZT-A-induced platelet aggregation.

7 The present results suggest that ZT-A elicits Ca^{2+}-influx from platelet plasma membranes. The resulting increase in $[Ca^{2+}]_i$ subsequently stimulates the secondary release of TXA_2 from platelets. Furthermore, the response to ZT-A may be associated with tyrosine phosphorylation.

Keywords: Aggregation; platelets; Ca^{2+}; zooxanthellatoxin-A; cytosolic free Ca^{2+}; thromboxane A_2

Introduction

Platelets which play a role in thrombus formation, haemostasis and regeneration of vessels respond to a wide variety of stimuli. These small disc-shaped cells recognize even minor damages on the surface of the endothelial cells lining blood vessels and promptly respond to the physical or chemical stimuli by undergoing adhesion, shape change, secretion and aggregation. Such a series of cell responses ends in the formation of a haemostatic plug or thrombus (Nozawa *et al.*, 1991). Platelets have frequently been used as a potentially useful model for studying transmembrane signalling since they are highly responsive to various agents and also influence active biochemical and morphological events.

Recently, a number of natural products have been isolated from marine organisms and have been extensively studied by numerous investigators. Marine products such as palytoxin (Ishida *et al.*, 1985; Hirata *et al.*, 1988) and maitotoxin (MTX) (Kobayashi *et al.*, 1987; Gusovsky & Daly, 1990; Watanabe *et al.*, 1993) have proved to be useful chemical tools for helping to resolve the mechanism of cellular functions.

Zooxanthellatoxin-A (ZT-A) and -B, novel polyhydroxylated long chain compounds, were recently isolated from a symbiotic marine alga *Simbiodinium* sp. as potent vasoconstrictor substances (Nakamura *et al.*, 1993a,b; 1995). They were characterized as relatively large molecules (molecular weight 2,872Da) containing a large number of oxygen atoms and olefinic carbons. These chemical characters are different from those of other marine toxins such as palytoxin and MTX which exhibit potent vasoconstrictor activities and contain a large number of olefins and a small number of ethereal rings, respectively (Asari *et al.*, 1993; Nakamura *et al.*, 1993a).

Although ZT-A is known to contract vascular smooth muscle, it is unknown whether it activates platelets. Thus, we have investigated the effects of ZT-A on aggregation and Ca^{2+} metabolism in rabbit platelets. This is the first report concerning the pharmacological properties of ZT-A in rabbit washed platelets.

Methods

Isolation of ZT-A

ZT-A was isolated as described previously (Nakamura *et al.*, 1993b). The cultured dinoflagellate (*Symbiodinium* sp.) was extracted three times by suspension with 70% ethanol and the ethanol extract (22.9 g) was subsequently dissolved in water and extracted with ethyl acetate, followed by n-butanol. The n-butanol extracts (5.8 g) were fractionated on a polystyrene column (MCl gel CHP-20P, 75-150 μm, Mitsubishi Chemical Industries Ltd., Tokyo, Japan). The 40% ethanol eluate was chromatographed on a diethyl amino ethyl Sepadex A-25 (1/30 M phosphate buffer, pH 6.9). The eluate was applied to a polystyrene column, eluted with 80% ethanol, and then sepa-

[1] Author for correspondence.

rated by a reversed phase high performance liquid chromatography column (YMC Pack D-ODS-5, 2 cm × 20 cm, YMC Ltd., Kyoto, Japan) using 4:1 methanol-water containing 0.2 M NaCl (9 ml min^{-1}), to give two active substances named ZT-A and -B, after desalting with a polystyrene column. The negative fast atom bombardment mass spectrum of ZT-A exhibited a predominant ion peak at m/z 2872. Figure 1 shows the full structure of ZT-A. This compound has characteristic functions such as a diepoxide, two conjugated dienes, macrolactone ring, a sulphate ester and an exomethylene (Nakamura *et al.*, 1995).

Preparation of washed platelets

Fresh blood was obtained from male rabbits (Japanese white rabbits weighing about 2–3 kg), collected into plastic tubes containing acid citrate dextrose solution (1/6 volume of blood) composed of citric acid (65 mM), trisodium citrate (85 mM), and dextrose (2%) at pH 4.5, subsequently centrifuged at 250 *g* for 10 min to obtain platelet-rich plasma (PRP). PRP was centrifuged at 650 *g* for 10 min at room temperature (20–25°C). The pellet was washed twice with Tyrode/4-(2-hydroxyethyl)-1-piperazineethanesulphonic acid (HEPES) solution (pH 6.35). The resultant pellet was resuspended in the second Tyrode/HEPES solution (pH 7.35) with a final density of approximately 5×10^8 cells ml^{-1}. The Tyrode/HEPES solution was composed of (mM): NaCl 138.3, KCl 2.68, $MgCl_2$ $6H_2O$ 1.0, $NaHCO_3$ 4.0, HEPES 10, glucose 0.1% (w/v) and albumin 0.35% (w/v) at pH 6.35 or 7.35.

Determination of platelet aggregation

Platelet aggregation was determined by a standard turbidometric method (Born, 1962) in an aggregometer (PAM-6C, Merbanix, Tokyo, Japan). Platelet aggregation was expressed as an increase in light transmission. The levels of light transmission were calibrated as 0% for a platelet suspension and 100% for the Tyrode/HEPES solution. Platelet suspension (0.3 ml) in the aggregometer cuvette was preincubated for 5 min at 37°C under continuous stirring at 1000 r.p.m. and then $CaCl_2$ or ethylene glycol *bis*(β-aminoethyl ether)-*N,N'*-tetraacetic acid (EGTA) was added at the final concentration of 1 mM. After 5 min, ZT-A was added and platelet aggregation was monitored for 10 min. Divalent cation and various blockers were preincubated for 5 min before the addition of ZT-A.

Measurement of intracellular Ca^{2+} concentration

For loading fura-2 into platelets, the platelet pellets prepared as described above were resuspended in the Tyrode/HEPES solution (pH 7.35) containing 1 μM fura-2/AM and incubated for 15 min at 37°C. Platelets were subsequently washed with the Tyrode/HEPES solution (pH 7.35) to remove extracellular fura-2/AM. After the number of platelets was adjusted to 1×10^8 ml^{-1}, the fura-2-Ca^{2+} signal was measured with a fluorescence spectrophotometer (F-2000, Hitachi). Platelets were exposed at excitation light with wavelengths at 340/380 nm and the light emission was measured at 510 nm. The platelet suspension (1.5 ml) in a quartz cuvette was preincubated for 2 min at 37°C in the spectrophotometer. Two min after the addition of $CaCl_2$ at a final concentration of 1 mM, ZT-A was added and the responses were monitored for a maximum of 10 min. Various blockers were preincubated for 1 min before the addition of ZT-A.

Radioimmunoassay of thromboxane B_2

The release of thromboxane B_2 (TXB_2) from rabbit platelets was determined by radioimmunoassay (Matsuoka *et al.*, 1989). In brief, platelet aggregation was terminated by addition of an equal volume of ice-cold 50 μM indomethacin/50 mM ethylenediaminetetraacetic acid solution and the sample solution was centrifuged at 1700 *g* for 10 min at 4°C. The assay mixture of 0.1 ml sample (1700 *g* supernatant) or standard (0.1–3000 ng ml^{-1}), 0.1 ml antiserum against TXB_2 (20,000 times dilution) and 0.1 ml [^{3}H]-TXB_2 (10 nCi) was incubated overnight at 4°C. [^{3}H]-TXB_2 bound to antiserum was assayed in a liquid scintilation spectrophotometer after the sedimentation of free [^{3}H]-TXB_2 with dextran-coated charcol.

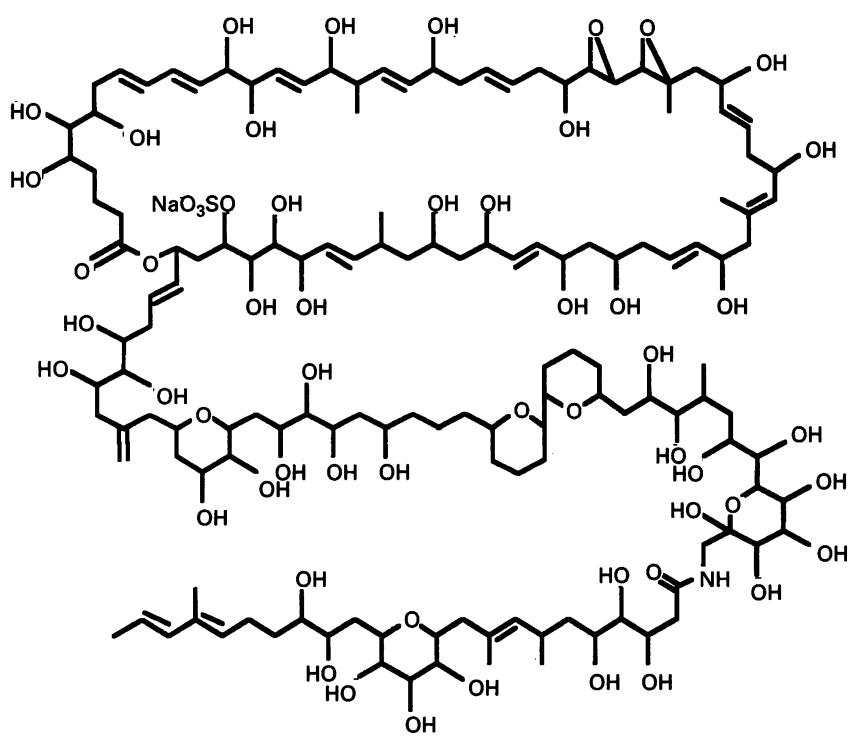

Figure 1 Chemical structure of zooxanthellatoxin-A (ZT-A).

Materials

The following drugs were used; verapamil hydrochloride (Eisai Co. Ltd., Tokyo, Japan), mefenamic acid (Wako Pure Chemical Industries Ltd., Osaka, Japan), tetrodotoxin (Sankyo Co. Ltd., Tokyo, Japan), indomethacin (Merck Company Inc., Rahway, NJ, U.S.A.), [1S-[1α,2β(5Z),3β,4α]]-7-[3-[[2-[(phenylamino)carbonyl]hydrazino]methyl]-7-oxabicyclo[2,2,1]hepta-2-yl]-5-heptenoic acid (SQ-29548, Squibb Japan Inc., Tokyo, Japan), methysergide (Sandoz Pharmaceuticals, Hanover, NJ, U.S.A.), genistein (Wako Pure Chemical Industries Ltd., Osaka, Japan), staurosporine (Wako Pure Chemical Industries Ltd., Osaka, Japan), chlorpheniramine maleate (Sankyo Co. Ltd., Tokyo, Japan), maitotoxin (Wako Pure Chemical Industries Ltd., Osaka, Japan), bovine serum albumin (Sigma Chemical Co., St. Louis, MO, U.S.A.). [^{3}H]-thromboxane B_2 (110.6 Ci mmol^{-1}) was obtained from DuPont/NEN (Boston, MA, U.S.A.). Anti-thromboxane B_2 serum was given to us by ONO Pharmaceutical (Osaka, Japan). 1-{β-[3-4-methoxyphenyl)propoxy]-4-methoxyphenethyl}-1H-imidazole hydrochloride (SK&F96365) was provided by Smith Kline Beecham (London, England). All other chemicals were of analytical grade.

Data analysis

The data are presented as mean ± s.e.mean. Statistical comparisons were made by Student's *t* test.

Results

Effects of ZT-A on platelet aggregation and $[Ca^{2+}]_i$

ZT-A elicited platelet aggregation after a lag time of 10–90 s (Figure 2a). During the lag time, light transmission often decreased transiently, presumably reflecting a platelet shape change (Milton & Frojmovic 1983). The lag time was dependent on the concentration of ZT-A tested (Figure 2a). ZT-A-induced aggregation was concentration-dependent with an EC_{50} value of 1.85 μM (Figure 3). On the other hand, ZT-A (0.5–4 μM) elicited an increase in $[Ca^{2+}]_i$ of the fura-2-loaded platelets (Figure 2b). The increase in $[Ca^{2+}]_i$ was dependent on concentrations of ZT-A with the EC_{50} of 1.7 μM, which was similar to that for platelet aggregation (Figure 3). While ZT-A at a concentration of 1 μM failed to cause platelet aggregation, it significantly increased $[Ca^{2+}]_i$, suggesting that a slight increase in $[Ca^{2+}]_i$ was not enough to cause aggregation.

Effects of external Ca^{2+} concentrations and Ca^{2+} channel blockers on ZT-A-induced aggregation and increase in $[Ca^{2+}]_i$

ZT-A could not induce platelet aggregation nor increase $[Ca^{2+}]_i$ in a Ca^{2+}-free solution (Figure 4). ZT-A caused aggregation to a small extent below 0.3 mM external Ca^{2+} (Figure 4a) and the ZT-A-induced increase in $[Ca^{2+}]_i$ was dependent on external Ca^{2+} concentrations from 0.3 mM to 3 mM (Figure 4b). Figure 5 shows the external Ca^{2+}-dependency of ZT-A (2 μM)-induced platelet aggregation and increase in $[Ca^{2+}]_i$. Since Co^{2+}, Cd^{2+} and Mn^{2+} are known to interfere with Ca^{2+} influx through Ca^{2+} channels at the plasma membrane (Evans, 1988), we investigated the effects of these divalent cations on the platelet aggregation induced by ZT-A (2 μM) in the presence of 1 mM Ca^{2+} (Figure 6). Cd^{2+} (0.1–1 mM), Co^{2+} (1–10 mM) and Mn^{2+} (1–10 mM) inhibited platelet aggregation induced by ZT-A (2 μM) (Figure 6). We further investigated the effects of verapamil, an organic Ca^{2+} antagonist, mefenamic acid, a non selective Ca^{2+} channel blocker, SK&F96365, a receptor-operated Ca^{2+} entry blocker and tetrodotoxin, a Na^+ channel blocker (Figure 7). The platelet aggregation induced by ZT-A was slightly inhibited by verapamil (10 μM). SK&F96365 (100 μM) and mefenamic acid (10 μM) inhibited the aggregation induced by ZT-A by approximately 70–90% of control (Figure 7a), suggesting that platelet aggregation in response to ZT-A requires an increase

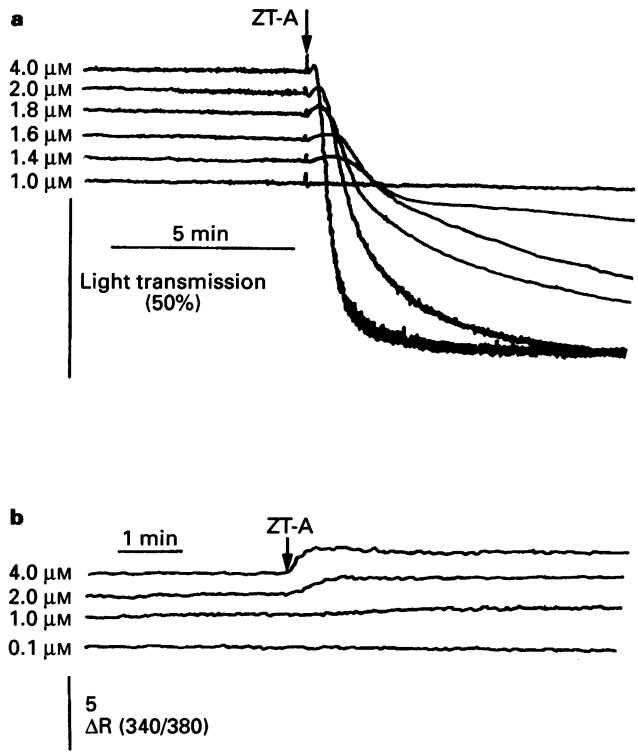

Figure 2 Typical recordings of aggregation (a) and increase in $[Ca^{2+}]_i$ (b) of rabbit washed platelets in response to zooxanthellatoxin-A (ZT-A). ZT-A (0.1–4 μM) was applied 5 (a) or 2 min (b) after addition of 1 mM $CaCl_2$ to the nominally Ca^{2+}-free solution. Aggregation response was measured by a turbidometric method. R340/380 on the ordinate scale of the lower panel represents the ratio of fluorescence intensity at 510 nm excited by 340 nm to 380 nm.

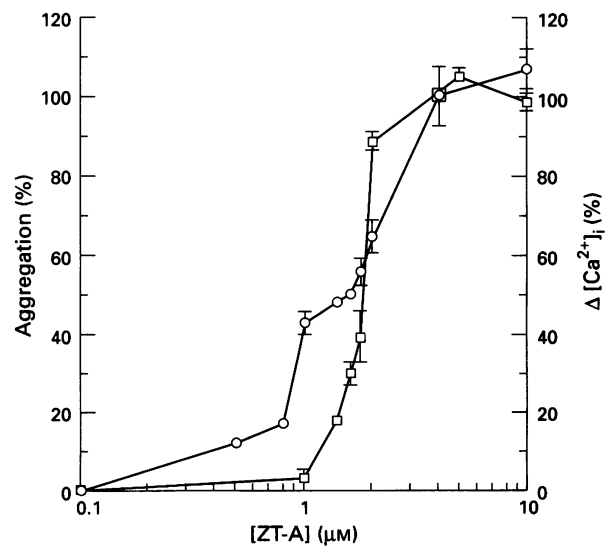

Figure 3 The concentration-response relationships for zooxanthellatoxin-A (ZT-A, 1–10 μM) on aggregation level (□) and increase in $[Ca^{2+}]_i$ (○). Platelet aggregation or $[Ca^{2+}]_i$ change in response to ZT-A (4 μM) in the presence of 1 mM Ca^{2+} was taken as 100%. The level of light transmission induced by 4 μM ZT-A was 75.9% ± 1.55 (n=4). The ratio of $[Ca^{2+}]_i$ change after addition of 4 μM ZT-A was 2.14 ± 0.161 (n=4). Values are given as mean ± s.e.mean (n=4).

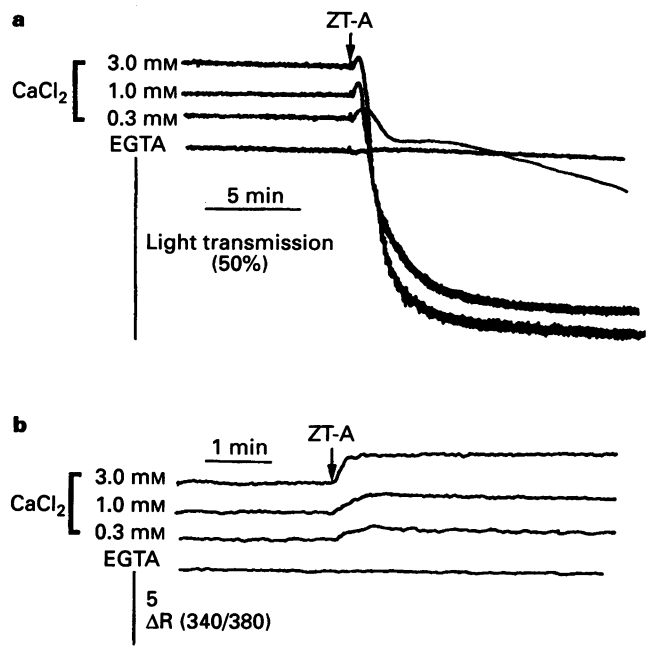

Figure 4 Typical recordings of the concentration-response relationships for external Ca^{2+} on zooxanthellatoxin-A (ZT-A)-induced aggregation (a) and increase in $[Ca^{2+}]_i$ (b). ZT-A (2 μM) was applied to 5 (a) or 2 min (b) after addition of $CaCl_2$ (0.3–3.0 mM) to the nominally Ca^{2+}-free solution. EGTA (1 mM) was added instead of $CaCl_2$. R340/380 on the ordinate scale of (b) represents the ratio of fluorescence intensity at 510 nm excited by 340 nm to 380 nm.

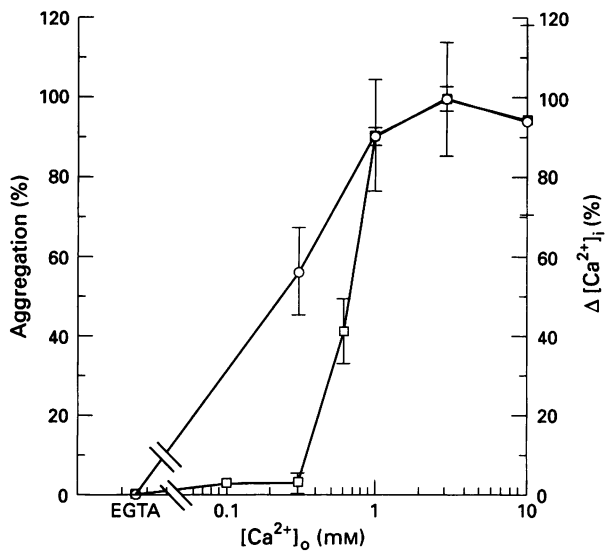

Figure 5 Effects of various external Ca^{2+} concentrations ($[Ca^{2+}]_o$) on platelet aggregation (□) and increase in $[Ca^{2+}]_i$ (○) induced by zooxanthellatoxin-A (ZT-A). ZT-A (2 μM) was applied 5 (□) or 2 (○) min after addition of $CaCl_2$ (0.1–10.0 mM) to the nominally Ca^{2+}-free solution. EGTA (1 mM) was added instead of $CaCl_2$. Platelet aggregation or $[Ca^{2+}]_i$ change induced by ZT-A (2 μM) in the presence of 3 mM Ca^{2+} was taken as 100%. The maximum level of light transmission in the presence of 3 mM $CaCl_2$ was 74.7% ± 2.33 (n=4). Values are given as mean ± s.e.mean (n=4).

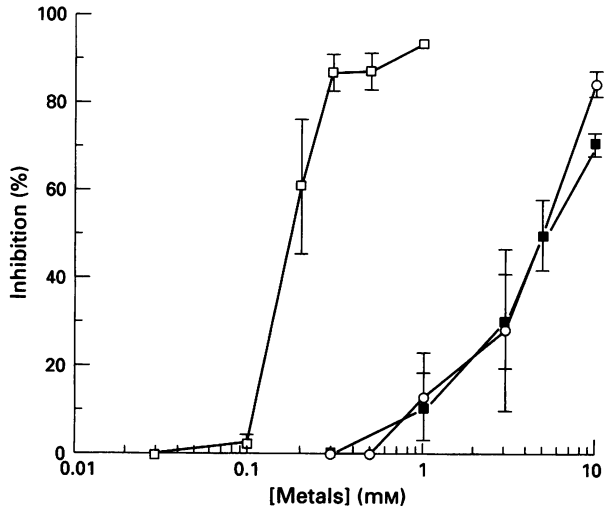

Figure 6 Effects of transition metals on zooxanthellatoxin-A (ZT-A)-induced platelet aggregation. Cd^{2+} (□), Co^{2+} (○) or Mn^{2+} (■) was added 5 min before addition of ZT-A in the presence of 1 mM Ca^{2+}. ZT-A (2 μM)-induced aggregation in the presence of 1 mM Ca^{2+} was taken as 100% (control). Values are given as mean ± s.e.mean (n=4).

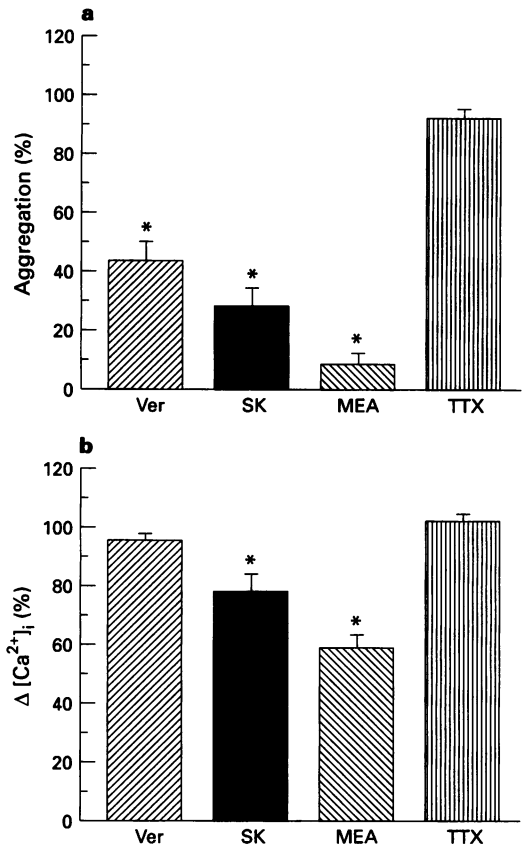

Figure 7 Effects of Ca^{2+} channel blockers on zooxanthellatoxin-A (ZT-A, 2 μM)-induced platelet aggregation (a) and increase in $[Ca^{2+}]_i$ (b). Aggregation or $[Ca^{2+}]_i$ change induced by ZT-A (2 μM) in the presence of 1 mM Ca^{2+} was taken as 100% (control). The following drugs were applied 5 (a) or 2 min (b) before addition of ZT-A in the presence of 1 mM Ca^{2+}: verapamil (Ver, 10 μM), SK&F96365 (SK, 100 μM), mefenamic acid (MEA, 10 μM), tetrodotoxin (TTX, 1 μM). Values are given as mean ± s.e.mean (n=4–6). Significant difference (*P<0.05) by paired t test when compared to control.

in $[Ca^{2+}]_i$ and therefore implying that ZT-A stimulates Ca^{2+} influx. The inhibition of ZT-A-induced platelet aggregation by the above drugs was concentration-dependent, and the IC_{50} values of the drugs are shown in Table 1. ZT-A-induced increase in $[Ca^{2+}]_i$ was also inhibited by SK&F96365 (100 μM) and mefenamic acid (10 μM), but not verapamil (10 μM) (Figure 7b). Tetrodotoxin (1 μM) did not affect either ZT-A-

induced platelet aggregation or increase in $[Ca^{2+}]_i$, suggesting no involvment of Na^+-influx in the action of ZT-A (Figure 7).

Table 1 IC_{50} values of various drugs in zooxanthellatoxin-A (ZT-A)-induced aggregation

Drug	*IC_{50} (μM)*
Verapamil	10.9 ± 3.20
SK&F96365	28.0 ± 11.7
Mefenamic acid	6.60 ± 1.40
Indomethacin	5.12 ± 1.52
SQ-29548	0.57 ± 0.25
Methysergide	0.39 ± 0.14
Genistein	20.1 ± 7.31
Staurosporine	0.20 ± 0.07

Drugs were preincubated with rabbit platelet suspensions 5 min before the addition of ZT-A in the presence of 1 mM Ca^{2+}. ZT-A (2 μM)-induced aggregation in the presence of 1 mM Ca^{2+} was taken as 100% (control). Each IC_{50} was obtained from 3–4 separate concentrations of the drugs. Values are given as mean ± s.e.mean (n = 3–5).

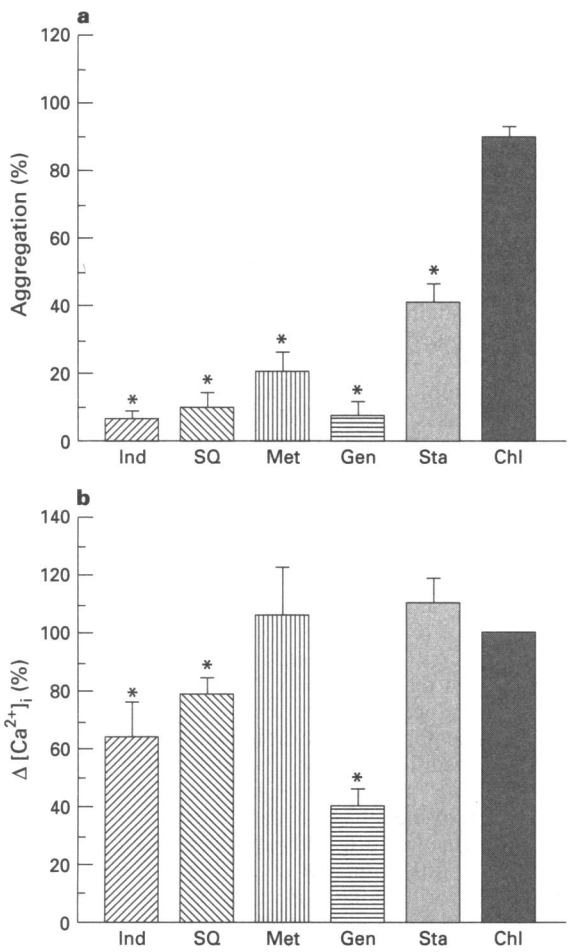

Figure 8 Effects of receptor antagonists and protein kinase inhibitors on zooxanthellatoxin-A (ZT-A, 2 μM)-induced aggregation (a) and increase in $[Ca^{2+}]_i$ (b). Aggregation or $[Ca^{2+}]_i$ change induced by ZT-A (2 μM) in the presence of 1 mM Ca^{2+} was taken as 100% (control). The following drugs were applied 5 (a) or 2 min (b) before addition of ZT-A in the presence of 1 mM Ca^{2+}: indomethacin (Ind, 10 μM), SQ-29548 (SQ, 10 μM), methysergide (Met, 1 μM), genistein (Gen, 100 μM), staurosporine (Sta, 0.1 μM), chlorpheniramine (Chl, 1 μM). Values are given as mean ± s.e.mean (n = 4–6). Significant difference (*P < 0.05) by paired t test when compared to control.

Effects of receptor antagonists, a cyclo-oxygenase inhibitor and protein kinase inhibitors on ZT-A-induced aggregation and increase in $[Ca^{2+}]_i$

We next investigated several receptor antagonists on ZT-A (2 μM)-induced aggregation (Figure 8). ZT-A-induced platelet aggregation was inhibited by SQ-29548 (10 μM), a TXA_2 receptor antagonist, and methysergide (1 μM), a 5-HT_2 receptor antagonist, suggesting the involvement of TXA_2 and 5-HT in ZT-A-induced aggregation (Figure 8a). Indomethacin, a cyclo-oxygenase inhibitor also inhibited ZT-A-induced aggregation, supporting the results obtained with SQ-29548 (Figure 8a). SQ-29548 and indomethacin also significantly reduced ZT-A-induced increase in $[Ca^{2+}]_i$ (Figure 8b). However, methysergide did not affect ZT-A-induced increase in $[Ca^{2+}]_i$ (Figure 8b). Chlorpheniramine (1 μM), a H_1-histamine receptor antagonist, neither affected ZT-A-induced platelet aggregation nor the increase in $[Ca^{2+}]_i$ (Figure 8b).

Furthermore, we investigated the effects of protein kinase inhibitors on ZT-A (2 μM)-induced platelet aggregation (Figure 8a) and increase in $[Ca^{2+}]_i$ (Figure 8b) in the presence of external Ca^{2+}. ZT-A-induced aggregation and increase in $[Ca^{2+}]_i$ were inhibited by genistein (100 μM), suggesting the involvement of tyrosine kinase in ZT-A action. Staurosporine, a protein kinase C (PKC) inhibitor, inhibited ZT-A-induced aggregation (Figure 8a), but not the increase in $[Ca^{2+}]_i$ (Figure 8b). Inhibitory effects of indomethacin, SQ-29548, methysergide, genistein and staurosporine on ZT-A-induced aggregation were concentration-dependent, and the IC_{50} values of these agents are shown in Table 1.

Effects of ZT-A on TXB_2 release from rabbit platelets

Since SQ-29548 and indomethacin inhibited ZT-A-induced platelet aggregation, TXA_2 would be involved in ZT-A action. Thus, the effect of ZT-A (2 μM) on the release of TXB_2, a stable metabolite of TXA_2, was investigated in the presence or absence of external Ca^{2+}. ZT-A stimulated TXB_2 release from platelets in the presence of 1 mM Ca^{2+} (Figure 9). However, ZT-A failed to release TXB_2 in a Ca^{2+}-free solution (Figure 9).

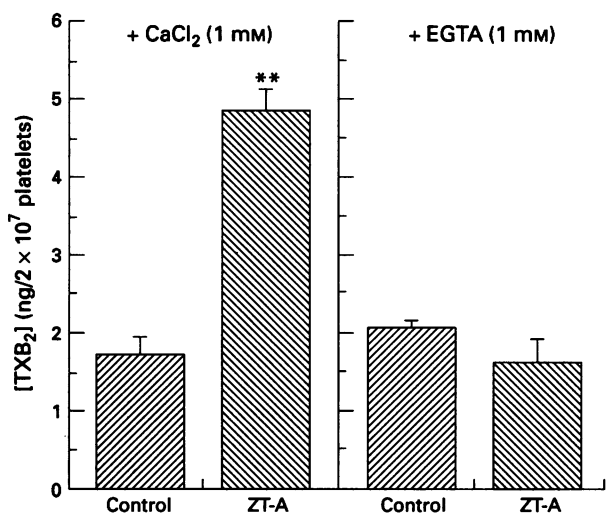

Figure 9 Effect of zooxanthellatoxin-A (ZT-A, 2 μM) on thromboxane B_2 (TXB_2) release from rabbit platelets determined with radioimmunoassay. ZT-A was added 5 min after addition of 1 mM $CaCl_2$ to the nominally Ca^{2+}-free solution. EGTA (1 mM) was added instead of $CaCl_2$. Reaction was terminated 2 min after addition of ZT-A by ice-cold 50 μM indomethacin/50 mM ethylenediaminetetraacetic acid solution. Values are given as mean ± s.e.mean (n = 3). Significant difference (**P < 0.01) by paired t test when compared to control.

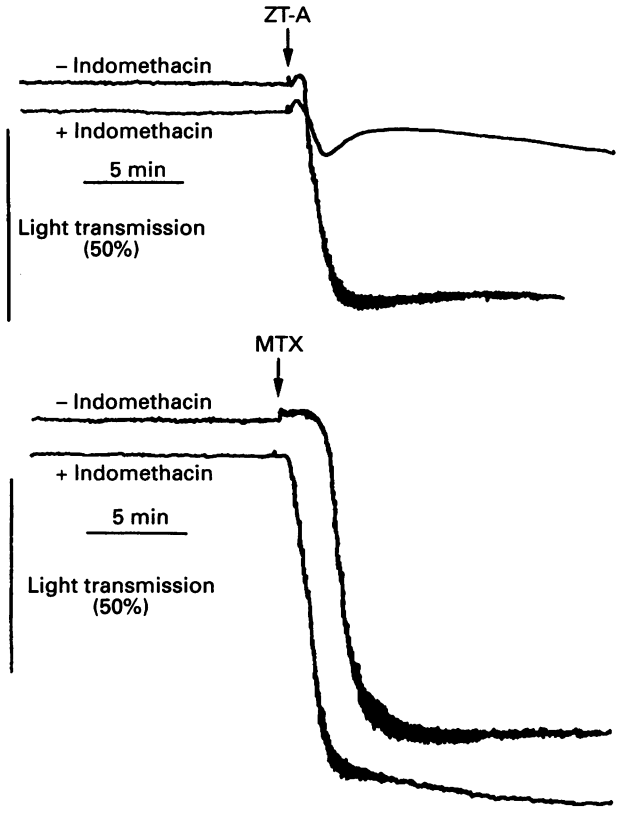

Figure 10 Inhibitory effect of indomethacin on zooxanthellatoxin-A (ZT-A)- or maitotoxin (MTX)-induced platelet aggregation. Aggregation response was measured by turbidometric method. Indomethacin (10 μM) was added 5 min before addition of ZT-A (2 μM) or MTX (30 ng ml^{-1}) in the presence of 1 mM Ca^{2+}. Data are representative of three separate experiments.

Effect of a cyclo-oxygenase inhibitor on ZT-A- or MTX-induced platelet aggregation

ZT-A-induced platelet aggregation is similar to MTX-induced platelet aggregation in the dependency on external Ca^{2+}. We compared the effects of indomethacin (10 μM), a cyclo-oxygenase inhibitor on MTX (30 ng ml^{-1})-induced platelet aggregation and ZT-A (2 μM)-induced platelet aggregation (Figure 10). ZT-A-induced platelet aggregation was significantly inhibited by indomethacin (10 μM) as already shown in Figure 8 and Table 1, but MTX-induced platelet aggregation was scarcely inhibited by indomethacin, showing the different contribution of cyclo-oxygenase metabolites to ZT-A- and MTX-induced platelet aggregation.

Discussion

The present experiments demonstrate that ZT-A is capable of eliciting an initial shape change followed by a prolonged aggregation accompanied by an increase in $[Ca^{2+}]_i$ in rabbit washed platelets. These stimulatory effects of ZT-A are specifically characterized by the very strict dependency on the presence of external Ca^{2+} and by the involvement of TXA_2. The Ca^{2+} influx across the plasma membrane may be solely responsible for ZT-A-induced aggregation of platelets. Thus, ZT-A-induced platelet aggregation was inhibited by inorganic Ca^{2+} channel antagonists such as Cd^{2+}, Co^{2+} and Mn^{2+} (Evans, 1988). Doyle & Rüegg (1985) reported that depolarization of platelets with 50 mM KCl did not induce Ca^{2+} entry into platelets and that a Ca^{2+} channel agonist, Bay K 8644, did not affect the Ca^{2+} influx or $[Ca^{2+}]_i$ in platelets, showing that platelets may lack voltage-gated Ca^{2+} channels (Siess, 1989; Rink & Sage, 1990). Although verapamil inhibited ZT-A-induced aggregation, the inhibition may be due to a non-specific action rather than the inhibition of voltage-gated Ca^{2+} channels, since its concentration exceeds the specific range (Godfraind *et al.*, 1986). In addition, mefenamic acid, a non selective Ca^{2+} channel blocker, and SK&F96365, a receptor-operated Ca^{2+} entry blocker also inhibited aggregation and Ca^{2+} entry induced by ZT-A (Figure 7a). These results suggest that ZT-A-induced aggregation occurs through the operation of voltage-independent Ca^{2+} channels in rabbit platelets. Alternatively, ZT-A may activate a new voltage-independent Ca^{2+} channel.

Platelet stimulating agents such as the Ca^{2+} ionophore A23187, collagen and U46619 induce the liberation of arachidonic acid (AA) from membrane phospholipids (Rittenhouse, 1984; Hanasaki & Arita, 1988). Once released, AA is rapidly converted to biologically active metabolites by the actions of cyclo-oxygenase and lipoxygenase enzymes (Siess *et al.*, 1983). In platelets, AA may be converted to prostaglandin endoperoxides, prostaglandin G_2 (PGG_2) and PGH_2 by cyclo-oxygenase, then to TXA_2 by TXA_2 synthase (Hamberg *et al.*, 1975). TXA_2, a predominant metabolite of AA in platelets, is a very potent inducer of platelet aggregation (Ogletree, 1987). TXA_2 activates phospholipase C via a G protein of $G_{q/11}$ family (Baldassare *et al.*, 1993), resulting in generation of the two second messengers, inositol-1,4,5,trisphosphate, a Ca^{2+} mobilizer, and diacylglycerol, a PKC activator (Wilson *et al.*, 1985; Priess *et al.*, 1986). Our results showing that indomethacin, a cyclo-oxygenase inhibitor and SQ-29548, a TXA_2 receptor antagonist inhibited the platelet aggregation induced by ZT-A indicate that ZT-A also activates TXA_2 generation after Ca^{2+} entry and that the released TXA_2 activates platelets to induce aggregation. In fact, ZT-A released TXA_2 from platelets (Figure 9). Methysergide, a 5-HT_2 receptor antagonist, potently inhibited the aggregation induced by ZT-A, showing a possible involvement of 5-HT in ZT-A-induced platelet aggregation. However, methysergide did not affect ZT-A-induced increase in $[Ca^{2+}]_i$. The reason for this discrepancy remains unknown.

Platelets possess a high level of tyrosine kinase activity, most of which is attributed to pp $60^{c\text{-}src}$ (Golden *et al.*, 1986; Feder & Bishop, 1990). Activation of platelets by several agonists increases the level of tyrosine phosphorylation resulting in the appearance of a new set of tyrosine-phosphorylated proteins (Ferrel & Martin, 1988; Golden & Bruggs, 1989; Nakamura & Yamamura, 1989; Bachelot *et al.*, 1992). Fibrinogen binding to the glycoprotein IIb/IIIa which plays a critical role in platelet aggregation appears to regulate protein tyrosine phosphorylation (Ferrel & Martin, 1989; Golden *et al.*, 1990). Tyrosine phosphorylation may also be induced by the elevation of $[Ca^{2+}]_i$ or by Ca^{2+} depletion in intracellular Ca^{2+} storage sites (Vostal *et al.*, 1991; Paul *et al.*, 1993). These findings suggest the possible involvement of tyrosine kinase in the signal transduction system in platelets, although the precise role of tyrosine phosphorylation in platelet activation remains elusive. Genistein inhibited the increase in $[Ca^{2+}]_i$ in response to ZT-A, as well as platelet aggregation, indicating the importance of tyrosine kinase in Ca^{2+} entry.

Staurosporine was originally considered as a protein kinase C (PKC) inhibitor (Tamaoki *et al.*, 1986). Recent studies indicate staurosporine inhibits a variety of tyrosine kinase (Daniel *et al.*, 1994) as well as other serine-threonine kinases including protein kinase A (PKA) (Spacey *et al.*, 1990; Tamaoki, 1991; Rasouly & Lazarovici, 1994). If staurosporine inhibits PKA activity, ZT-A-induced platelet aggregation may be enhanced. However, staurosporine inhibited ZT-A-induced aggregation, but it did not affect Ca^{2+} mobilization (Figure 9). Therefore, PKA might not be involved in the action of staurosporine in the ZT-A-induced platelet activation and PKC might be involved in secondary activation after Ca^{2+} entry by ZT-A.

Although ZT-A activates platelets in a similar manner to a Ca^{2+} ionophore, ZT-A is not a Ca^{2+} ionophore. Ionomycin, a

Ca^{2+} ionophore elicits an increase in $[Ca^{2+}]_i$ of platelets in the absence of external Ca^{2+} (Rink *et al.*, 1982), but ZT-A could not increase $[Ca^{2+}]_i$ in the absence of external Ca^{2+}. ZT-A-induced platelet aggregation is similar to MTX-induced platelet aggregation, but ZT-A has different characteristics from MTX. MTX-induced platelet aggregation was inhibited by the presence of Co^{2+} (0.3 mM) or Cd^{2+} (0.3 mM) (Watanabe *et al.*, 1993). Although ZT-A-induced platelet aggregation was inhibited by Cd^{2+}, Co^{2+} and Mn^{2+}, effective concentration of Co^{2+} was different from the effective concentration on MTX-induced aggregation (Figure 6). Furthermore, ZT-A-induced platelet aggregation was inhibited by treatment of a cyclooxygenase inhibitor as described above, but MTX-induced platelet aggregation was not affected (Figure 10). Thus, ZT-A activates platelets in a different manner from a Ca^{2+} ionophore or MTX.

In conclusion, ZT-A elicits Ca^{2+}-influx in platelet plasma membranes. The resulting increase in cytosolic Ca^{2+} appears to stimulate the release of TXA_2, which thereafter activates platelets to cause aggregation. The Ca^{2+}-influx may be associated with tyrosine phosphorylation.

We are very grateful to Squibb Japan for providing us with SQ-29548, to Smith Kline Beecham for providing us with SK&F96365 and to ONO Pharmaceutical for providing us with anti-TXB_2 serum. This work was supported by a Grant-in-Aid from Scientific Research (No. 04304048, 05271102 and 05671805 to N.N. and No. 05152011, 05256203, 05454567 and 05557103 to Y.O.) from the Ministry of Education, Science and Culture of Japan, and by a Grant-in-Aid from the Marine Biotechnology Institute and Sapporo Bioscience Foundation.

References

ASARI, T., NAKAMURA, H., MURAI, A. & KAN, Y. (1993). Structures of periodate oxidation products with a conjugated diene or an exomethylene from zooxanthellatoxin-A. *Tetrahedron Lett.*, **34**, 4059–4062.

BACHELOT, C., CANO, E., GRELAC, F., SALEUM, S., DRUKER, B.J., LEVY-TOLEDANO, S., FISCHER, S. & RENDU, F. (1992). Functional implications of tyrosine protein phosphorylation in platelet. *Biochem. J.*, **284**, 923–928.

BALDASSARE, J.J., TARVER, A.P., HANDERSON, P.A., MACKIN, W.M., SAHAGAN, B. & FISHER, G.J. (1993). Reconstitution of thromboxane A_2 receptor-stimulated phosphoinositide hydrolysis in isolated platelet membranes: involvement of phosphoinositide-specific phospholipase C-β and GTP-binding protein G_q. *Biochem. J.*, **291**, 235–240.

BORN, G.V.R. (1962). Aggregation of blood platelets by adenosine diphosphate and its reversal. *Nature*, **194**, 927–929.

DANIEL, J.D., DANGELMAIER, C. & SMITH, J.B. (1994). Evidence for a role for tyrosine phosphorylation of phospholipase Cγ2 in collagen-induced platelet cytosolic calcium mobilization. *Biochem. J.*, **302**, 617–622.

DOYLE, V.M. & RÜEGG, U.T. (1985). Lack of evidence for voltage dependent calcium channels on platelets. *Biochem. Biophys. Res. Commun.*, **127**, 161–167.

EVANS, C.H. (1988). Alkaline earths, transition metals, and lanthanides. In *Calcium in Drug Action*. ed. Backer, P.F. pp. 527–546. Berlin: Springer-Verlag.

FEDER, D. & BISHOP, J.M. (1990). Purification and enzymatic characterization of $pp60^{c\text{-}src}$ from human platelets. *J. Biol. Chem.*, **265**, 8205–8211.

FERREL, J.E. JR & MARTIN, G.S. (1988). Platelet tyrosine-specific protein phosphorylation is regulated by thrombin. *Mol. Cell. Biol.*, **8**, 3603–3610.

FERREL, J.E. JR & MARTIN, G.S. (1989). Tyrosine-specific protein phosphorylation is regulated by glycoprotein IIb–IIIa in platelets. *Proc. Natl. Acad. Sci. U.S.A.*, **86**, 2234–2238.

GODFRAIND, T., MILLER, R. & WIBO, M. (1986). Calcium antagonism and calcium entry blockade. *Pharmacol. Rev.*, **38**, 321–416.

GOLDEN, A. & BRUGGS, J.S. (1989). Thrombin treatment induces rapid changes in tyrosine phosphorylation. *Proc. Natl. Acad. Sci. U.S.A.*, **86**, 901–905.

GOLDEN, A., BRUGGS, J.S. & SHATTIL, S.J. (1990). Role of platelet membrane glycoprotein IIb–IIIa in agonist-induced tyrosine phosphorylation of platelet proteins. *J. Cell. Biol.*, **111**, 3117–3127.

GOLDEN, A., NEMETH, S.P. & BRUGGE, J.S. (1986). Blood platelets express high levels of the $pp60^{c\text{-}src}$ specific tyrosine kinase activity. *Proc. Natl. Acad. Sci. U.S.A.*, **83**, 852–856.

GUSOVSKY, F. & DALY, W. (1990). Maitotoxin: a unique pharmacological tool for research on calcium-dependent mechanisms. *Biochem. Pharmacol.*, **39**, 1633–1639.

HAMBERG, M., SVENSSON, J. & SAMUELSSON, B. (1975). Thromboxanes: a new group of biologically active compounds derived from prostaglandin endoperoxides. *Proc. Natl. Acad. Sci. U.S.A.*, **72**, 2994–2998.

HANASAKI, K. & ARITA, H. (1988). Characterization of a new compound, S-145, as a specific TXA_2 receptor antagonist in platelets. *Thrombosis Res.*, **50**, 365–376.

HIRATA, Y., UEMURA, D. & OHIZUMI, Y. (1988). Chemistry and pharmacology of palytoxin. In *Handbook of Natural Toxins*. ed. Tu, A.T. pp. 241–258. New York: Marcel Dekker, Inc.

ISHIDA, Y., SATAKE, N., HABON, J., KITANO, H. & SHIBATA, S. (1985). Inhibitory effect of ouabain on the palytoxin-induced contraction of human umbilical artery. *J. Pharmacol. Exp. Ther.*, **232**, 557–560.

KOBAYASHI, M., OCHI, R. & OHIZUMI, Y. (1987). Maitotoxin-activated single calcium channels in guinea-pig cardiac cells. *Br. J. Pharmacol.*, **92**, 665–671.

MATSUOKA, I., NAKAHATA, N. & NAKANISHI, H. (1989). Inhibitory effect of 8-bromo cyclic GMP on an extracellular Ca^{2+}-dependent arachidonic acid liberation in collagen-stimulated rabbit platelets. *Biochem. Pharmacol.*, **38**, 1841–1847.

MILTON, J.G. & FROJMOVIC, M.M. (1983). Turbidometric evaluations of platelet aggregation: relative contributions of measured shape change, volume, and early aggregation. *J. Pharmacol. Methods*, **9**, 101–115.

NAKAMURA, H., ASARI, T. & MURAI, A. (1993a). Structure of periodate oxidation products with characteristic partial structures of zooxanthellatoxin-A, a potent vasoconstrictive polyol from a symbiotic dinoflagellate. *J. Org. Chem.*, **58**, 313–314.

NAKAMURA, H., ASARI, T. & MURAI, A. (1995). Zooxanthellatoxin-A, a potent vasoconstrictive 62-membered lactone from a symbiotic dinoflagellate. *J. Am. Chem. Soc.*, **117**, 550–551.

NAKAMURA, H., ASARI, T., OHIZUMI, Y., KOBAYASHI, J., YAMASU, T. & MURAI, A. (1993b). Isolation of zooxanthellatoxins, novel vasoconstrictive substances from the zooxanthella *Symbiodinium* sp. *Toxicon.*, **31**, 371–376.

NAKAMURA, S. & YAMAMURA, H. (1989). Thrombin and collagen induce rapid phosphorylation of a common set of cellular proteins on tyrosine in human platelets. *J. Biol. Chem.*, **264**, 7089–7091.

NOZAWA, Y., NAKASHIMA, S. & NAGATA, K. (1991). Phospholipid-mediated signaling in receptor activation of human platelets. *Biochim. Biophys. Acta*, **1082**, 219–238.

OGLETREE, M.L. (1987). Overview of physiological and pathophysiological effects of thromboxane A_2. *Fed. Proc.*, **46**, 133–138.

PAUL, S., FARNDALE, R.W. & SAGE, S.O. (1993). The tyrosine kinase inhibitors methyl 2,5-dihydroxycinnamate and genistein educe thrombin-evoked tyrosine phosphorylation and Ca^{2+} entry in human platelets. *FEBS Lett.*, **315**, 242–246.

PRIESS, J., LOOMIS, C.R., BISHOP, W.R., STEIN, R., NIEDEL, J.E. & BELL, R.M. (1986). Quantitative measurement of sn-1,2-diacylglycerols present in platelets, hepatocytes, and ras- and sis-transformed normal rat kidney cells. *J. Biol. Chem.*, **261**, 8597–8600.

RASOULY, D. & LAZAROVICI, P. (1994). Staurosporine induces tyrosine phosphorylation of a 145 kDa protein but does not activate $gp140^{trk}$ in PC12 cells. *Eur. J. Pharmacol.*, **269**, 255–264.

RINK, T.J. & SAGE S.O. (1990). Calcium signaling in human platelets. *Annu. Rev. Physiol.*, **52**, 431–449.

RINK, T.J., SMITH, S.W. & TSIEN, R.Y. (1982). Cytoplasmic free Ca^{2+} in human platelets: Ca^{2+} thresholds and Ca^{2+}-independent activation for shape-change and secretion. *FEBS Lett.*, **148,** 21–26.

RITTENHOUSE, S.E. (1984). Activation of human platelet phospholipase C by ionophore A23187 is totally dependent upon cyclooxygenase products and ADP. *Biochem. J.*, **222,** 103–110.

SIESS, W. (1989). Molecular mechanisms of platelet activation. *Physiol. Rev.*, **69,** 58–178.

SIESS, W., SIEGEL, F.L. & LAPETINA, E.G. (1983). Arachidonic acid stimulates the formation of 1,2-diacylglycerol and phosphatidic acid in human platelets. *J. Biol. Chem.*, **258,** 11236–11242.

SPACEY, G.D., BONSER, R.W., RANDALL, R.W. & GARLAND, L.G. (1990). Selectivity of protein kinase inhibitors in human intact platelets. *Cell Signal.*, **2,** 329–338.

TAMAOKI, T. (1991). Use and specificity of staurosporine, UCN-01, and calphostin C as protein kinase inhibitors. *Methods Enzymol.*, **201,** 340–347.

TAMAOKI, T., NOMOTO, H., TAKAHASHI, I., KATO, Y., MORIMOTO, M. & TOMITA, F. (1986). Staurosporine, a potent inhibitor of phospholipid Ca^{2+} dependent protein kinase. *Biochem. Biophys. Res. Commun.*, **135,** 397–402.

VOSTAL, J.G., JACKSON, W.L & RAPHAEL-SHULMAN, N. (1991). Cytosolic and stored calcium antagonistically control tyrosine phosphorylation of specific platelet proteins. *J. Biol. Chem.*, **266,** 16911–16916.

WATANABE, A., ISHIDA, Y., HONDA, H., KOBAYASHI, M. & OHIZUMI, Y. (1993). Ca^{2+}-dependent aggregation of rabbit platelets induced by maitotoxin, a potent marine toxin, isolated from a dinoflagellate. *Br. J. Pharmacol.*, **109,** 29–36.

WILSON, D.B., NEUFELD, E.J. & MAJERUS, P.W. (1985). Phosphoinositide interconversion in thrombin-stimulated human platelets. *J. Biol. Chem.*, **260,** 1046–1051.

(Received December 5, 1994
Revised February 6, 1995
Accepted February 22, 1995)

British Journal of Pharmacology (1995) 115, 441-450

The effect of opiates on the terminal nerve impulse and quantal secretion from visualized amphibian nerve terminals

Nickolas A. Lavidis

The Neurobiology Laboratory, Department of Physiology, The University of Sydney, N.S.W., Australia, 2006

1 Secretion of transmitter from amphibian motor nerve terminal release sites is intermittent, spatially non-uniform and varies considerably throughout the year and during development. The role of opioid receptors in modulating transmitter secretion from amphibian motor nerve terminals is evaluated in this study.

2 Dynorphin-A (24 μM) and morphine (500 μM) did not significantly change the shape of the nerve impulse or the consistency with which it was observed, but decreased evoked quantal secretion by more than 50%. These effects of dynorphin-A and morphine were largely reversed by naloxone (50 μM).

3 Dynorphin-A and morphine did not significantly change either the amplitude or the frequency of spontaneous quantal secretions.

4 There was a uniform decrease in evoked quantal secretion from release sites along terminal branches, irrespective of the quantal content value before drug treatment, indicating no difference in the susceptibility of proximal vs distal release sites to opiates.

5 Increasing the extracellular calcium concentration (0.3 to 0.4 mM) or trains of conditioning-test impulses (25 to 100 Hz) resulted in smaller dynorphin-A or morphine-induced decreases in evoked quantal secretion.

6 The decrease in evoked quantal secretion occurs as a result of a uniform decrease in the probability of quantal secretion from release sites without any affect on the propagation of the nerve terminal impulse. Low probability release sites become effectively silent.

Keywords: Neurotransmission; action potential; opiates; amphibian nerve terminals

Introduction

At the amphibian motor nerve terminal the nerve impulse, evoked and spontaneous quantal secretion can be recorded simultaneously with an extracellular electrode if placed within 10 μm of the release sites (del Castillo & Katz, 1956). Using this method, secretion of quanta from small groups of release sites has been shown to be intermittent and spatially non-uniform (Bennett & Lavidis, 1979; D'Alonzo & Grinnell, 1985). The release sites found closest to the point of first axon contact with the muscle fibre membrane have a higher average probability of quantal secretion than more distal release sites (Bennett & Lavidis, 1982; Bennett *et al.*, 1986). Furthermore within the field of recording of the extracellular electrode it was shown by Bennett & Lavidis (1989) that very low probability release sites exist amongst the relatively high probability sites. The probability of quantal secretion of release sites in amphibian motor nerve terminals is modulated during development (Bennett & Lavidis, 1988) and by seasonal factors (Bennett & Lavidis, 1992). For example, during development, approximately 25% of muscle fibres receive dual innervation from adjacent segmental motor nerves, usually one of these terminals has release sites with relatively much lower probabilities of quantal secretion then the other terminal innervating the same muscle fibre (Bennett & Lavidis, 1988). Furthermore, the average probability of quantal secretion of release sites varies by as much as eight fold between late summer and late autumn in the southern hemisphere (Bennett & Lavidis, 1992). Some endogenous chemicals have been shown to produce an affect on quantal secretion from release sites such as, α-melanocyte stimulating hormone (Oren *et al.*, 1987) and adenosine (Ginsborg & Hirst, 1972; Ribeiro & Walker, 1975; Bennett *et al.*, 1991). Opiates such as dynorphin, which is found in relatively high concentrations in brain and spinal cord of *Bufo marinus* (Cone & Goldstein, 1982), or dermorphine found on the skin of frogs (Montecucchi *et al.*, 1981), may act as modulators of quantal secretion by decreasing the probability of quantal secretion from release sites. The effects of dynorphin-A, morphine and dermorphine on the secretion of quanta from release sites innervating toad (*Bufo marinus*) iliofibularis muscle fibres have been evaluated in the present study.

At the amphibian neuromuscular junction, high concentrations of morphine (500 μM) produced a decrease in the amount of acetylcholine secreted from cholinergic terminals during nerve stimulation (Frederickson & Pinsky, 1971). Methionine enkephalin has also been shown to reduce the number of quanta secreted during sympathetic ganglion transmission (Hirai & Katayama, 1988) and modulate motor neurone activity in the spinal cord of the bullfrog *Rana catesbeiana* (Suzuki *et al.*, 1987). Also high concentrations of methionine-enkephalin (20 μM) decrease quantal secretion from the release sites of *Rana pipiens* (Bixby & Spitzer, 1983). How these opiates decrease quantal secretion from release sites is not fully understood. Two main mechanisms of how opiates decrease quantal secretion have been proposed. First, in most neuronal cell bodies studied, opiates have been shown to increase the activity of potassium channels resulting in either hyperpolarization of the cell or shortening the duration of the action potential (Pepper & Henderson, 1980; Morita & North, 1982; North & Williams, 1983; Werz & MacDonald, 1985). Second, an alternative mechanism has been proposed from studies conducted on nerve terminals such as the sympathetic varicosities of the mouse vas deferens (Bennett & Lavidis, 1980; Illes *et al.*, 1980) and the amphibian motor nerve terminal (Bixby & Spitzer, 1983). In these preparations, indirect evidence such as overcoming the inhibitory affect of morphine by increasing $[Ca^{2+}]_o$ and local depolarization of release sites suggest that opiates inhibit a calcium-dependent process rather than conduction failure of the nerve impulse during nerve stimulation. Opiates have been shown to decrease the opening times of calcium channels in dorsal root ganglion cells (Werz &

MacDonald, 1985; MacDonald & Werz, 1986; Gross & MacDonald, 1987). Since we are able in this preparation to record both the nerve impulse and evoked quantal secretion it is possible to test whether the nerve impulse is affected during the decrease in quantal content which occurs when opiates are applied.

Methods

Housing of animals

Toads (*Bufo marinus*) ranging in length from 55 to 70 mm from tail to nose were maintained in a room which was fitted with 15% ultra violet lights. Lights were turned on for 16 h per day. The temperature of the room was maintained between 25° and 30°C and the animals were fed 2 times per week with a mixture of minced meat and fish brittle. Even under these environmental conditions animals still displayed seasonal changes consisting of a uniform decrease in the probability of quantal secretion from release sites during the period May to November (Southern hemisphere; Bennett & Lavidis, 1992).

Tissue preparation

Animals were anaesthetized with tricaine methanesulphonate (MS222, Rural Chemical Industries Australia) and then killed by a cervical fracture. The right iliofibularis muscle with its nerve supply was dissected from its surrounding connective tissue and cut at its tendinous insertions at the pelvis and knee. The muscle was then pinned to the Sylgard covered base of a 3 ml organ bath with the surface where the nerve enters the muscle facing up. The muscle was stretched to approximately 110% of its resting length in the limb to form a flat parallelogram. The preparation was continuously perfused at a rate of 5 ml min^{-1} with a modified Ringer solution containing (mM): NaCl 99.4, KCl 3.0, $MgCl_2$ 1.2, NaH_2PO_4 1.3, $NaHCO_3$ 16.3, $CaCl_2$ 0.3 to 0.4, glucose, 7.8. The temperature of the bath was maintained between 12° and 16°C. The reservoir supplying the bath was continuously gassed with 95% O_2 and 5% CO_2, and the pH was maintained between 7.2 and 7.5. The extracellular calcium concentration ($[Ca^{2+}]_o$) was changed by altering the amount of $CaCl_2$ dissolved in the Ringer solution supplying the bath. Possible changes in the conduction of the nerve impulse were avoided by maintaining the external magnesium concentration above 0.7 mM (Frankenhauser & Hodgkin, 1957).

Visualization of the nerve terminal

The preparation was left bathing in the low $[Ca^{2+}]_o$ Ringer for about 40 min while contractions due to nerve stimulation diminished. The muscle was then bathed for 30 s in 3.3-diethyloxardicarbocyanine iodide ($DiOC_2(5)$, 0.1 μM, Yoshikami & Okun, 1984) and then washed with Ringer for 10 min to label fluorescently accumulations of mitochondria corresponding to the nerve terminal branches. Excitation at 560 nm of the $DiOC_2(5)$ resulted in a fluorescence which was visible using a Rhodamine filter set (Olympus BH2 microscope). Terminals were chosen by viewing the fluorescent image via an image intensifier camera (National) on a video monitor (National). The effects of exposing the neuromuscular junction to $DiOC_2(5)$ and fluorescence have been previously described (Bennett *et al.*, 1986). Use of $DiOC_2(5)$, 0.1 μM and 1 to 3 min excitation did not affect the nerve terminal impulse or evoked or spontaneous quantal secretion. To avoid long periods of fluorescing the preparation and the need for repeated applications of $DiOC_2(5)$, the image of the fluorescing terminals was traced onto the video monitor screen at the outset and the fluorescence was turned off. The preparation was then illuminated by a tungsten filament lamp and other visible structures such as pigment cells, blood vessels and bundles of axons were drawn on the video monitor screen 'map'. The position of the terminals with respect to such structures was rechecked before hunting with an extracellular electrode for the extracellular signs of the nerve terminal impulse or the endplate potential.

Stimulation

The iliofibularis nerve was gently sucked into a pipette filled with the Ringer solution up to a silver/silver chloride wire and stimulated with square wave stimuli of 0.08 ms duration and 8V amplitude. At least 200 samples of evoked release were recorded at 0.25 Hz for each electrode placement.

Recording

Extracellular recordings of the endplate potential give a good approximation of the time course of the synaptic current (Fatt & Katz, 1952; Del Castillo & Katz, 1956; Brock & Cunnane, 1988) and are therefore referred to as the endplate current (e.p.c.) in this study. E.p.cs were obtained with microelectrodes filled with NaCl (2 M) and having resistances of 10 to 30 MΩ. Focal extracellular recordings were obtained by positioning the electrode about 2 to 3 μm on either side of the terminal branch. The external signs of the endplate potential could then be observed on the oscilloscope screen while stimulating the nerve. In most cases small e.p.cs could be recorded within 20 impulses. The electrode was then lifted off the muscle fibre and moved in either direction along the same axis as the terminal branch until the source of these small e.p.cs was located (this procedure involved searching for the most active release site). The external electrode was then lifted off the muscle fibre and moved transversely to improve the recording of the nerve impulse. Two hundred samples of evoked release at a stimulation frequency of 0.25 Hz were recorded before lifting the electrode off the muscle and looking for another active site about 20 μm along the terminal branch.

Extracellular recordings were abandoned if: e.p.cs were mostly less than 1.0 mV in amplitude; presence of e.p.cs without detecting the nerve terminal impulse; any shift greater than 25% in quantal release rates over the first 100 trials as compared to the last 100 trials (see Bennett *et al.*, 1986); any change in the amplitude of the largest recorded e.p.c. at the end of the recording period compared to the beginning.

Avoidance of damage to the terminal by the recording electrode

To avoid the effects of electrode pressure on nerve terminals (Fatt & Katz, 1952) the microelectrode tip, clearly visible on the video monitor, was carefully positioned about 2 to 3 μm from the terminal branch as drawn on the video monitor following the hunting procedure previously described. The frequency of spontaneous miniature endplate current's (m.e.p.cs) was determined at different times, prior to the start of recording evoked release and after having recorded the 200 evoked trials. The frequency of m.e.p.cs normally varied between 0.02 to 0.3 Hz. If this frequency increased by more than 25% of the initial estimate the recording was abandoned (see Bennett *et al.*, 1986). The order of positioning the extracellular electrode at different groups of release sites was randomized along the nerve terminal branch to ensure that the peripheral parts of the branch did not have relatively lower evoked quantal secretion rates then more proximal sites, perhaps due to terminal damage by the recording electrode.

Data analysis

E.p.cs were recorded on an IBM-AT microcomputer using p-Clamp version 5.0 software (Axon Instruments). The interval between two quanta following an impulse had to be greater than 0.14 ms, otherwise they were measured as single quanta. To reduce the chance of this happening, the preparation was kept between 12° and 16°C and the $[Ca^{2+}]_o$ less than or equal to 0.4 mM. Selected records were measured by eye from time to

time to monitor the accuracy of the computer analysis, the difference was $\leqslant 7\%$. Histograms of the number of quanta released were constructed for the e.p.cs and only those which occurred within 5 ms of the negative peak of the nerve impulse were included. The region of recording was restricted to less than a 7 μm radius by only counting e.p.cs with amplitudes $\geqslant 1.0$ mV (Del Castillo & Katz, 1956; Bennett *et al.*, 1986). Quantal content ($\overline{m}_e$) was determined from the ratio of the total number of quanta released to the number of trials.

Drugs

Drugs were dissolved in different 200 ml capacity reservoirs. Each reservoir was gassed with 95% O_2 and 5% CO_2. Solutions supplying the preparation bath were changed by 3 way taps. Morphine hydrochloride and naloxone hydrochloride (gifts from the Department of Pharmacology, University of Sydney) were dissolved in distilled H_2O and kept refrigerated as stock solutions at a concentration of 10 mM. Dynorphin-A and dermorphine (Sigma) were dissolved in acetic acid (40 μM) and aliquots placed in vials. Each vial contained dynorphin-A or dermorphine (0.1 ml at a concentration of 10 mM) and was stored at -70°C. Tissues were bathed in drug-containing solution for more than 40 min before recording. Following drug treatment tissues were washed for more than 40 min before determining whether the effects were reversible.

Results

Effect of morphine on $\overline{m}_e$ along motor nerve terminal branches

Extracellular recordings of the e.p.cs and m.e.p.cs (Figure 1) were taken from different positions along terminal branches. The visualized profile of terminals, following $DiOC_2(5)$-fluorescence was used to draw the shape of the terminal branches on a video monitor and to determine the distance of the electrode from the point of first axon contact with the muscle. The average number of quanta secreted in the recording field of the electrode per nerve impulse ($\overline{m}_e$) was estimated by taking 200 trials from each position before and after the application of morphine or dynorphin-A to the preparation. Following morphine (320 μM) there was a decrease in the frequency of evoked quantal secretions with an increase in the tails of the e.p.cs (compare in Figure 1, morphine-treated, traces 1 and 3 with control, traces 1 to 5). There was also an increase in the noise level following morphine treatment which lasted only for about 16 ms following the stimulus artefact. This increase in the duration of the e.p.cs and the increase in noise is probably due to the known anti-cholinesterase action of morphine (Haynes & Smith, 1982).

Along each of the four terminal branches studied there was a proximal to distal decline in $\overline{m}_e$ (Figure 2). For example in Figure 2a and b where $\overline{m}_e$ was determined at 8 to 12 μm intervals along the terminal branches, the maximum m_e recorded declined proximal-distally. Intercalated amongst the high probability release sites, low probability release sites were recorded (Figure 2a and b). If however, a different procedure (described in the Methods) is used to record from only the highest probability release sites in any region, a profile of the maximum $\overline{m}_e$ s is obtained along terminal branches (Figure 2c and d). Of the 21 terminal branches studied, in 6 branches the maximum $\overline{m}_e$ did not significantly decrease along the length of the branches. Only one terminal branch showed an increase in the maximum $\overline{m}_e$ as the electrode was moved in the proximal to distal direction from the point of first nerve contact with the muscle. The rest of the terminal branches (14/21) showed a decline in the maximum $\overline{m}_e$ in the proximal-distal direction. The average decline in $\overline{m}_e$ for all the control terminal branches studied are shown in Figure 3a. There was a significant difference ($P < 0.01$) in the maximum $\overline{m}_e$ only for the distal 60% of the terminal branches (Figure 3a).

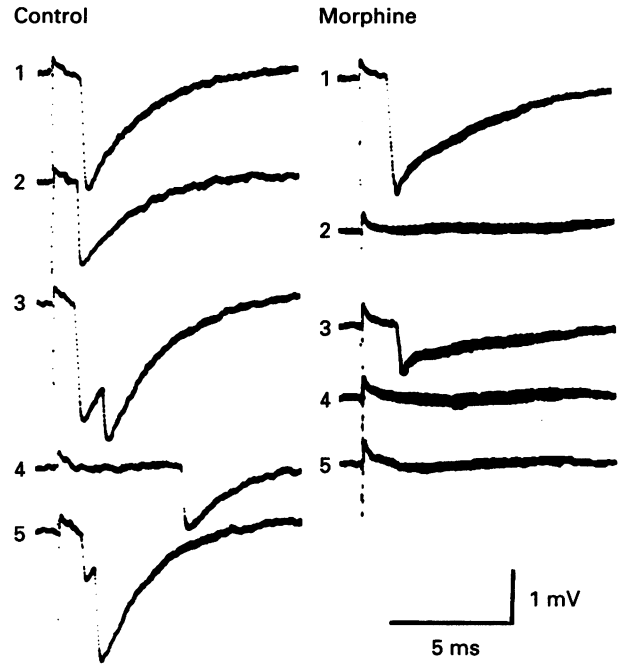

Figure 1 The effect of morphine on e.p.cs. Five consecutive nerve stimulations for control and morphine (500 μM)-treated preparations are shown. The extracellular calcium concentration ($[Ca^{2+}]_o$) was 0.35 mM. Evoked quantal secretions can be seen in traces 1,2,3 and 5 (control) and 1 and 3 (morphine). There is an increase in the duration of the e.p.cs following morphine treatment (compare traces 1 and 3 (morphine) with traces 1,2,3 and 5 (control)). An increase in the noise level is also seen following the administration of morphine (morphine traces 2, 4 and 5), and the duration of this increase in noise is equivalent to the duration of the e.p.cs seen in traces 1 and 3 (morphine). The nerve terminal impulse is also evident, at the left of each recording.

Very high concentrations of morphine (500 μM) but comparable to the concentration used by Frederickson & Pinsky (1971) decreased the frequency of evoked quantal secretions (Figure 1) uniformly along the whole length of the terminal branches (Figures 2a,c and 3a). The 47% decrease in $\overline{m}_e$ induced by morphine (500 μM) was almost reversed by the application of naloxone (50 μM). The ED_{50} for morphine on quantal secretion from amphibian nerve terminals was 510 μM (personal observation). The averaged results of 9 preparations is shown in Figure 3a where the decrease in $\overline{m}_e$ is greater for the proximal site with the remainder of the decrease being uniform for at least 75% of the terminal branches. The relationship between the magnitude of decrease in $\overline{m}_e$ produced by morphine and position from the point of first axon contact with the muscle was determined (Figure 4a). Although there appeared to be a slightly greater percentage decrease in $\overline{m}_e$ for proximal release sites when compared to more distal release sites, the difference was not significant ($P > 0.05$). The relationship between the magnitude of decrease in $\overline{m}_e$ following morphine administration and initial $\overline{m}_e$ (pre morphine administration) was also determined (Figure 4c). Linear regression fit of the data appeared to indicate that the magnitude of the reduction in $\overline{m}_e$ following morphine application appeared to be greatest for high initial $\overline{m}_e$ s however again the difference was not significant ($P > 0.05$). Thus morphine reduces $\overline{m}_e$ along the terminal branches in a uniform manner.

Effect of dynorphin-A on $\overline{m}_e$ along motor nerve terminal branches

Extracellular recordings of the e.p.cs were taken from different positions along terminal branches before and after treatment

with dynorphin-A (Figure 2b and d). The visualized profile of terminals following $DiOC_2(5)$-fluorescence was used to draw the shape of the terminal branches on a video monitor and to determine the distance of the electrode from the point of first axon contact with the muscle. The $\overline{m}_e$ values at each extracellular electrode position were determined by recording 200 trials from each position before and after dynorphin-A administration. The two terminal branches shown in Figure 2b and 2d demonstrated a significant decrease in $\overline{m}_e$ for the distal half of the release sites. Dynorphin-A produced a relatively uniform decrease in $\overline{m}_e$ along the length of the two terminal branches shown in Figure 2b and 2d. Out of the 8 terminal branches studied, 2 showed no significant decline in $\overline{m}_e$ along the terminal branch while 6 showed a decline at least in the distal half of the terminal branches. Overall there was a significant decline in $\overline{m}_e$ ($P<0.05$) level among the more distal halves of the terminal branches (Figure 3b).

While dynorphin-A (24 μM) reduced $\overline{m}_e$ along the length of most terminal branches studied, a significant decrease ($P<0.05$) could be demonstrated only for the proximal region of the terminal branches (Figure 3b). The ED_{50} of dynorphin-A on quantal secretion at amphibian motor nerve terminal release sites was 24 μM (personal observation). The relationship between the magnitude of decrease in $\overline{m}_e$ produced by dynorphin-A and distance of release sites from the point of first axon contact with the muscle was evaluated (Figure 4b). Although there was a slightly greater decrease in $\overline{m}_e$ produced by dynorphin-A in the proximal part of the terminal branches studied, the difference was not significant ($P>0.05$). Regression analysis of the relationship between the magnitude of decrease in $\overline{m}_e$ following dynorphin-A and the initial $\overline{m}_e$ (before dynorphin-A administration) also revealed no significant trend (see Figure 4d and legend). Thus dynorphin-A at a twenty fold lower concentration than morphine reduced $\overline{m}_e$ along the terminal branches in a fairly uniform manner. Naloxone (50 μM) reduced the dynorphin-A induced decrease in $\overline{m}_e$.

The effect of demorphine on $\overline{m}_e$ along nerve terminal branches

The effect of dermorphine (83 μM) on $\overline{m}_e$ along four terminal branches was evaluated using the same procedures as described in the two previous sections. There was no significant differ-

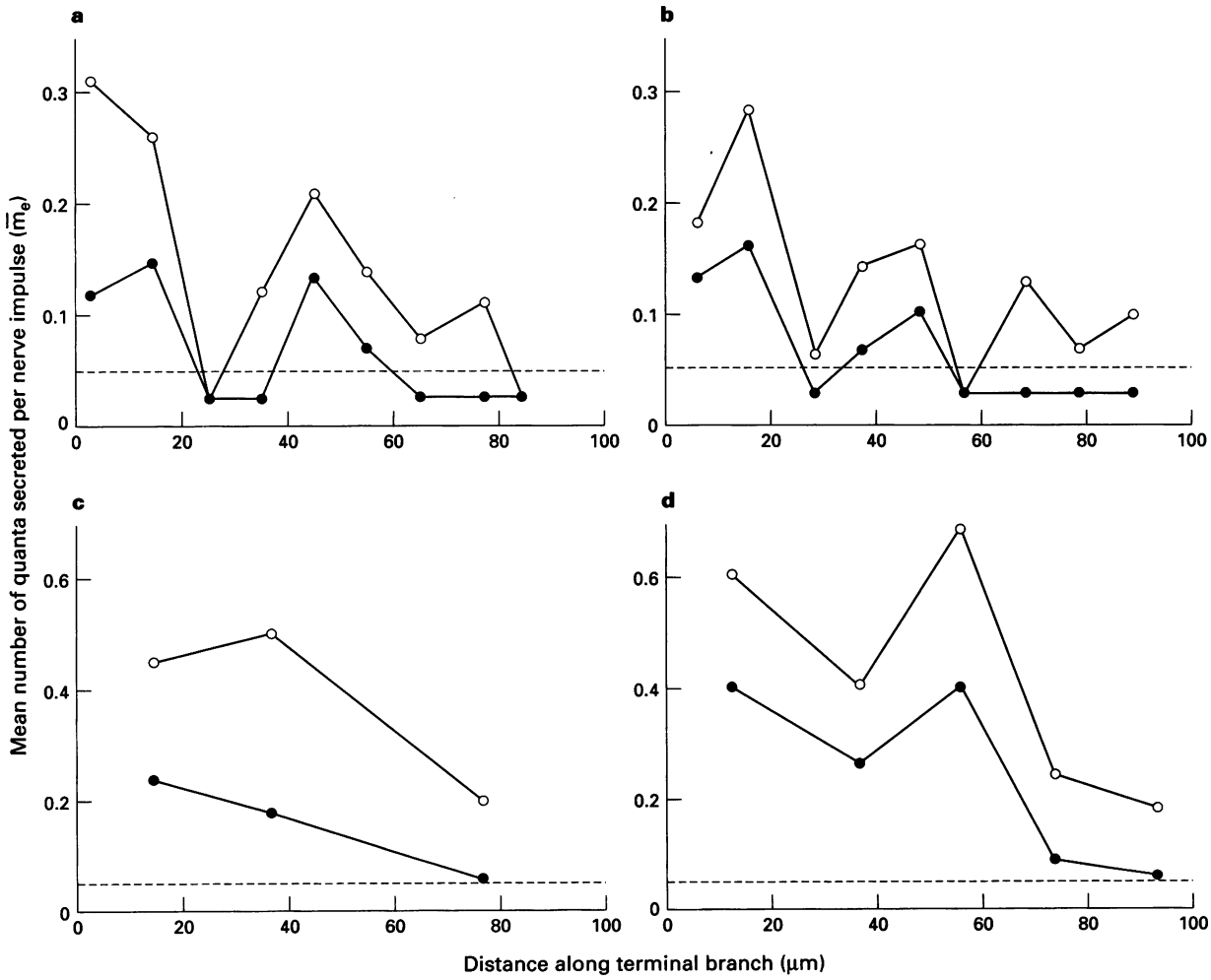

Figure 2 The effect of morphine and dynorphin-A on quantal content ($\overline{m}_e$) along the length of nerve terminal branches. Traces of the $DiOC_2(5)$-fluorescent terminal branches were drawn onto the video monitor and from these measurements of the distance of electrode position from the point of first nerve contact with the muscle estimated. In (a) and (b) the extracellular electrode was placed at about 8 to 12 μm intervals along the length of the terminal branch before and after treatment with morphine (a) and dynorphin-A (b). In (c) and (d) the position of the extracellular electrode was optimized to record the secretion from the most active regions of a terminal branch before and after morphine (c) and dynorphin-A (d) treatment. $\overline{m}_e$ vs distance along the terminal branch measure from the point of first axon contact with the muscle was plotted for each terminal branch. (○) Control data; (●) data after morphine or dynorphin-A administration. The broken lines indicate a release rate less than one quanta per 20 nerve impulses ($\overline{m}_e<0.05$).

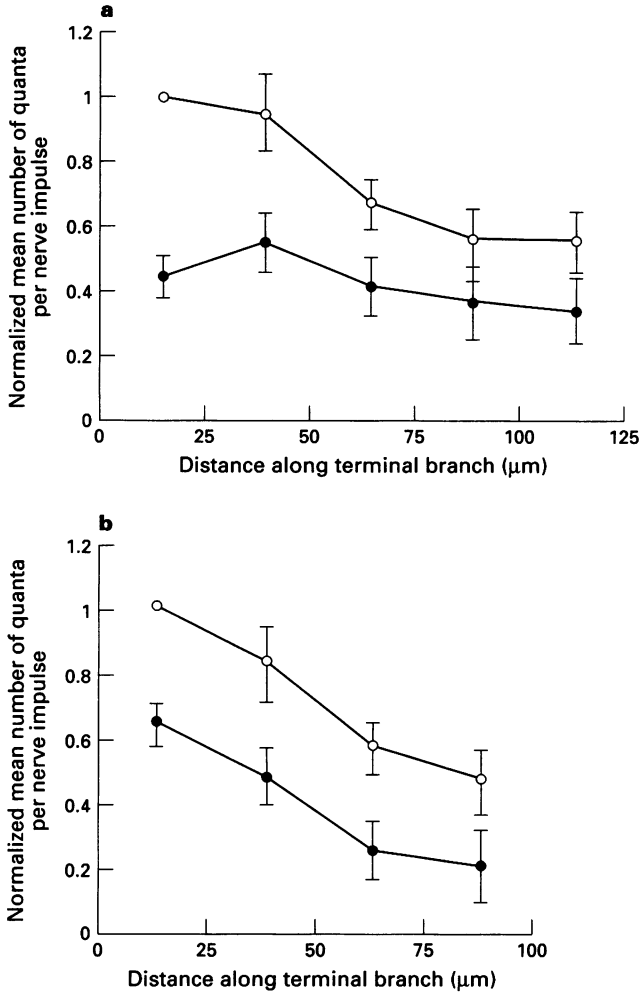

Figure 3 The averaged effect of morphine (a) and dynorphin-A (b) on $\overline{m}_e$ along the lengths of several nerve terminals. The $\overline{m}_e$ determined at various positions along terminal branches, for control, morphine- and dynorphin-A-treated preparations, was normalized with respect to the maximum $\overline{m}_e$ value of the most proximal recorded site in the control preparation. The normalized values were then grouped into 25 μm bins along the length of terminal branches and the mean normalised $\overline{m}_e$ value and its standard deviation calculated. The effects of morphine, 500 μM (a) and dynorphin-A, 24 μM (b) are shown. (○) Means for the control preparations; (●) means for the morphine (a) and dynorphin-A (b)-treated preparations. There was a statistically significant ($P < 0.05$) difference in (a) between control and morphine-treated, and in (b) between control and dynorphin-A-treated for the proximal 75% of the terminals studied.

ence in the $\overline{m}_e$s of untreated release sites vs treated release sites; the average difference was minus 8 ± 9% ($n = 4$).

The effect of changing $[Ca^{2+}]_o$ on $\overline{m}_e$ in control and morphine-treated preparations

The mean quantal content of the e.p.c. was first determined for 0.3 mM, $[Ca^{2+}]_o$ before raising $[Ca^{2+}]_o$ to 0.4 mM and re-determining $\overline{m}_e$. Morphine (500 μM) was then added to the bath containing 0.4 mM $[Ca^{2+}]_o$ and $\overline{m}_e$ estimated. Finally morphine was added to the 0.3 mM, $[Ca^{2+}]_o$ reservoir and $\overline{m}_e$ redetermined. In the six experiments shown in Figure 5, $\overline{m}_e$ increased by about the same amount (fourth power of $[Ca^{2+}]_o$) in the presence or absence of morphine. In control preparations the mean power relationship between $\overline{m}_e$ and $[Ca^{2+}]_o$ was 3.67 ± 0.55 (mean ± s.d.) while for morphine-treated preparations it was 3.64 ± 0.56. the decrease in $\overline{m}_e$ of about 47% induced by morphine (500 μM) treatment was reduced by increasing $[Ca^{2+}]_o$, there was however no significant difference between the gradient of the $\overline{m}_e$ vs $[Ca^{2+}]_o$ before and after morphine treatment ($P > 0.9$) indicating that the dependence of $\overline{m}_e$ on $[Ca^{2+}]_o$ was not changed by morphine.

The effect of dynorphin-A on the ability of the terminal to facilitate during conditioning-test impulses

Following a conditioning nerve impulse there is an increase (facilitation) in the amount of quanta secreted by a test impulse (Figure 6) or subsequent impulses in a train that declines as the interval between conditioning and test impulses increases. The time-constant of decline in facilitation of $\overline{m}_e$ by a test impulse was 30 ms. Dynorphin-A (24 μM) reduced $\overline{m}_e$ of the conditioning impulse by about 49% and this inhibition could be overcome if a test nerve impulse was applied shortly (time interval less than 60 ms) after the conditioning impulse. The time-constant of decay in facilitation was unchanged (34 ms) by dynorphin-A.

The effect of dynorphin-A or morphine on the nerve terminal impulse

Following stimulation of the iliofibularis nerve, nerve impulses are generated which propagate to the last node of Ranvier actively propagate for only about 1/3 the length of the terminal and then passively for the distal 2/3 of the terminal (Brigant & Mallart, 1982). The nerve impulse is clearly visible in the traces shown in Figure 6 even after treatment with dynorphin-A (24 μM) which halved evoked quantal secretion. Morphine and dynorphin-A did not alter the nerve impulse from any position recorded along terminal branches (Figure 7a and b). Each trace in Figure 7a represents the average of 200 trials, the stimulus artefact is shown (sa) followed by the nerve impulse (ni) and the extracellular signs of the endplate current (e.p.c). Neither the shape of the nerve impulse nor the consistency with which it was observed was changed (Figure 7a) following dynorphin-A (24 μM) or morphine (500 μM) treatment or after washing out the drug. There was a decrease in the average size of the e.p.cs following dynorphin-A treatment with a partial recovery after washing or naloxone (50 μM). This decrease in the averaged e.p.c. amplitude was not caused by a postsynaptic effect since there was no reduction in the size of m.e.p.cs (Figure 7c). The average size of m.e.p.cs was: control, 0.91 ± 0.22 mV ($n = 105$, mean ± s.d.); dynorphin-A treated for 40 min, 0.84 ± 0.19 mV ($n = 57$); after washing out the drug for more than 40 min, 0.88 ± 0.18 mV ($n = 85$). Thus the decrease in e.p.c. amplitude was produced by a decrease in the number of quanta being released and an increase in the number of failures to release any quanta (Figure 7d). Thus, although there was no significant change in the size of the nerve impulse, morphine and dynorphin-A were able to produce a large decrease in $\overline{m}_e$.

Discussion

Is dynorphin contributing to the decrease in probability of quantal secretion along terminal branches?

In most terminal branches studied there was a decline in the number of quanta secreted along the proximal to distal axis of the terminal branch from the point of first axon contact with the muscle fibre (see also Bennett & Lavidis, 1982; D'Alonzo & Grinnell, 1985; Bennett *et al.*, 1986). This however was not always the case: six out of the twenty-one terminal branches studied did not show any decline, with $\overline{m}_e$ remaining uniform throughout the length of the branches. Indeed one out of twenty-one branches studied showed an increase. When the results were normalized with respect to the most proximal section of the terminal branch and results for all the terminal branches averaged there was a significant decline in the maximum $\overline{m}_e$ in the distal half of the terminal branches. The rea-

sons for this decline are not known but a number of possibilities have been considered which include: first, the area of the close apposition (< 200 nm) between pre- and postsynaptic membranes decreases in the proximal to distal direction along terminal branches (Bennett *et al.*, 1987; 1989). If the maximum area of the close apposition between nerve terminal and muscle membrane is a measure of the largest active zones it could be argued that the larger active zones have a greater release area available for vesicle release and that this is the determinant of the secretion probability of release sites. Although a reasonable correlation between close apposition length and $\overline{m}_e$ has been shown (Bennett *et al.*, 1989), the variation in close apposition lengths measured is not as great as the variation in $\overline{m}_e$ of release sites measured. Second, secretion of a quantum of acetylcholine and/or another cotransmitter (ATP) may act back on presynaptic membrane receptors to inhibit subsequent quantal secretions. This may restrict large active zones to secrete only one quantum per stimulus but with a higher probability of release. Although the release of ATP has been demonstrated (Silinsky, 1975) and that in its dephosphorylated

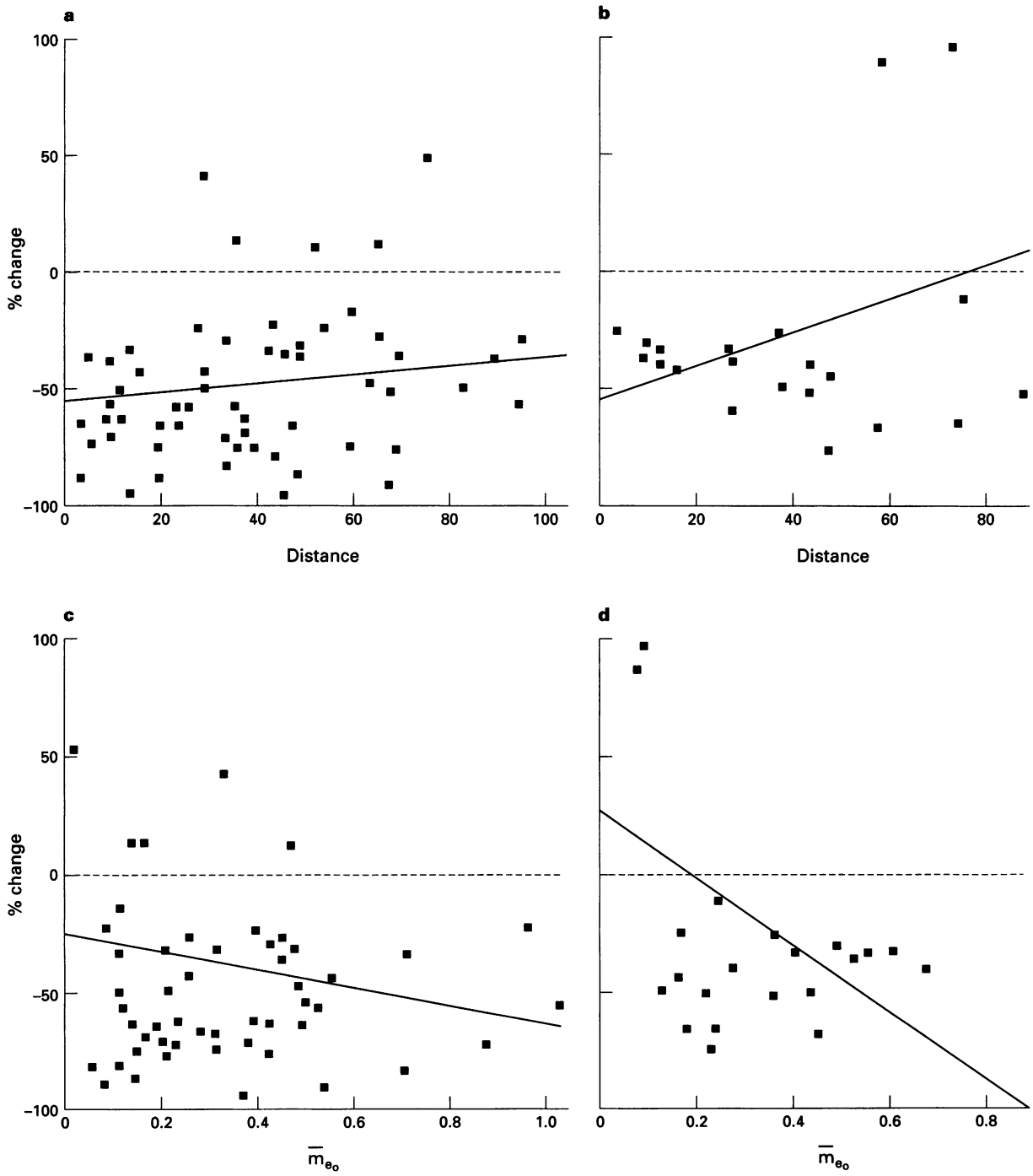

Figure 4 The relationship between percentage change in quantal secretion and either distance of release sites from the point of first axon contact with the muscle fibre or control quantal secretion ($\overline{m}_{e_o}$). (a) Percentage change in $\overline{m}_e$ induced by morphine vs distance along terminal branch. Solid line fitted by linear regression to the data (■) has a slope of 0.28 and a correlation coefficient of 0.20. (b) Percentage change in $\overline{m}_e$ induced by dynorphin-A vs distance along terminal branch. Solid line fitted by linear regression has a slope of 0.39 and c.c. 0.22. (c) Percentage change in $\overline{m}_e$ induced by morphine vs control (pre drug) $\overline{m}_{e_o}$. Slope of −0.16 and c.c. 0.08. (d) Percentage change in $\overline{m}_e$ induced by dynorphin-A vs control $\overline{m}_{e_o}$. Slope of −1.00 and a c.c. 0.39. Dashed lines indicate no change in secretion.

form, adenosine binds to presynaptic purinoceptors to decrease the probability of quantal secretion (Ginsborg & Hirst, 1972; Ribeiro & Walker, 1975; Bennett *et al.*, 1991), addition of purinoceptor antagonists such as theophylline or 8-phenyltheophylline does not lead to any significant increase in quantal content or the variance of quanta secreted under the nerve stimulus frequency used by Bennett *et al.* (1991). Third, opiates such as dynorphin (Cone & Goldstein, 1982) and dermorphine (Montecucchi *et al.*, 1981) have been shown to exist in amphibia. Relatively high concentrations of morphine (Frederickson & Pinsky, 1971; Bixby & Spitzer, 1983) and Met-enkephalin (Bixby & Spitzer, 1983) have been shown to decrease transmitter secretion from amphibian motor nerve terminals. Dynorphin-A and morphine have also been shown to decrease quantal content and the variance in the number of quanta secreted. This has been interpreted as a decrease in the number of release sites secreting during a nerve impulse since the average probability of quantal secretion calculated from intracellular recordings remained constant (personal observation). As demonstrated here, this decrease in quantal content is due to a uniform decrease in $\overline{m}_e$ along the length of terminal branches irrespective of their initial $\overline{m}_e$. Since the probability of secretion of release sites varies greatly within the field of the extracellular recording electrode (about 7 μm radius), release sites which initially have low probabilities of quantal secretion become effectively silent (they do not register any evoked quantal secretion during the 200 nerve stimulations) when morphine or dynorphin-A is applied. These results indicate the presence of a dynorphin-sensitive receptor on the motor nerve terminal which when activated by exogenously applied dynorphin produces a decrease in evoked quantal secretion without affecting the propagation of the nerve impulse.

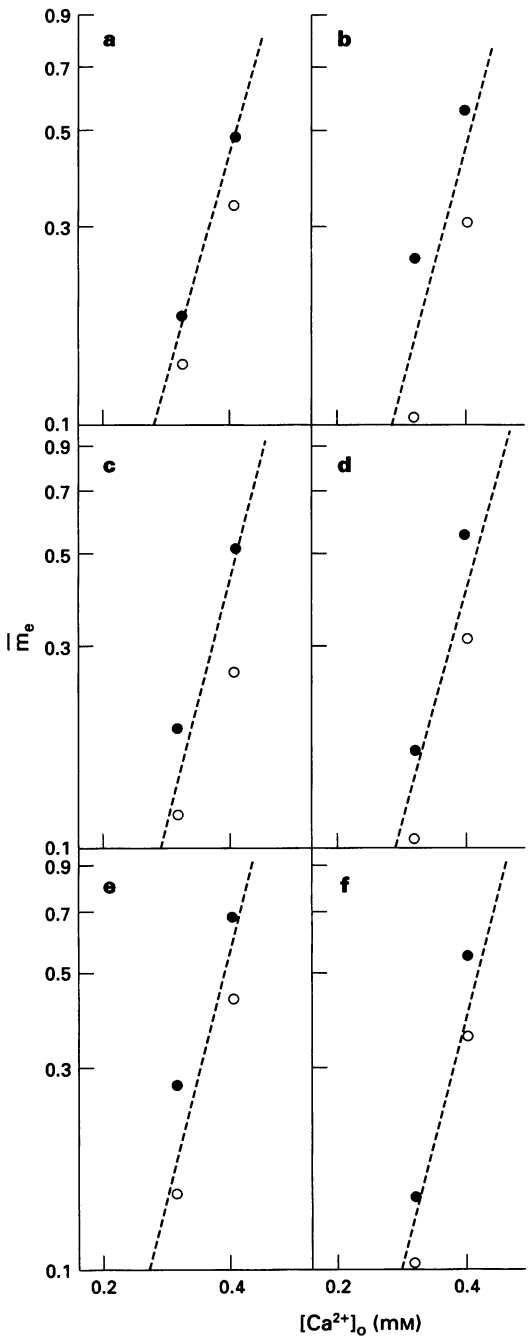

Figure 5 The effect of morphine on the relationship between $\overline{m}_e$ and $[Ca^{2+}]_o$. Six experiments are shown. Log $\overline{m}_e$ is plotted against log $[Ca^{2+}]_o$ and the dashed lines indicate a 4th power relationship. (○) $\overline{m}_e$ values of control branches; (●) results for the morphine-treated preparations.

It is possible that release sites have different numbers of dynorphin-sensitive opioid receptors and therefore are affected differently by dynorphin-A and morphine. The effect of dynorphin-A and morphine on release sites along the length of terminal branches was evaluated. There was no significant difference in the percentage inhibition produced by dynorphin-A or morphine along the length of terminal branches. The effect of dynorphin-A and morphine on release sites with very different secretion probabilities was next evaluated. No significant difference was found between release sites of very different secretion probabilities. These results indicate that the density of dynorphin-sensitive opioid receptors found on the terminal is uniformly distributed and therefore it is unlikely that opiates contribute to the differences in probability of quantal secretion of release sites along terminal branches.

How do opiates decrease the probability of quantal secretion from release sites?

Opiates can produce a decrease in the release of quanta in two ways: in many neuronal cell bodies, opiates acting on μ-opioid

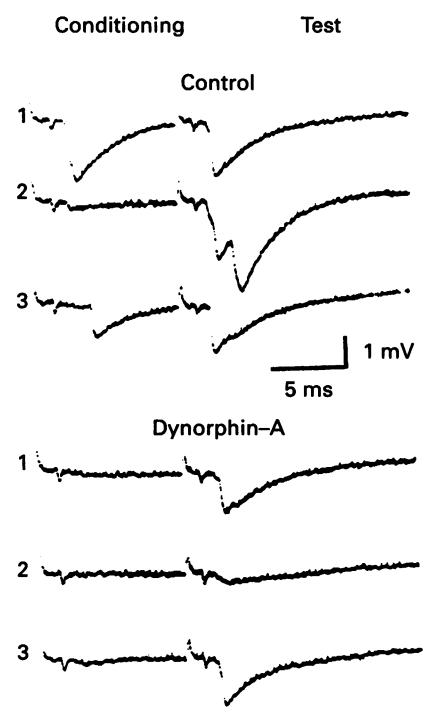

Figure 6 The effect of dynorphin-A on the secretion of quanta during test-conditioning impulses. Three consecutive test-conditioning trials are shown for control (trials 1, 2 and 3) and dynorphin-A (24 μM, trials 1, 2 and 3)-treated preparation. The interval between conditioning and test impulses is 12 ms. The $[Ca^{2+}]_o$ was 0.35 mM.

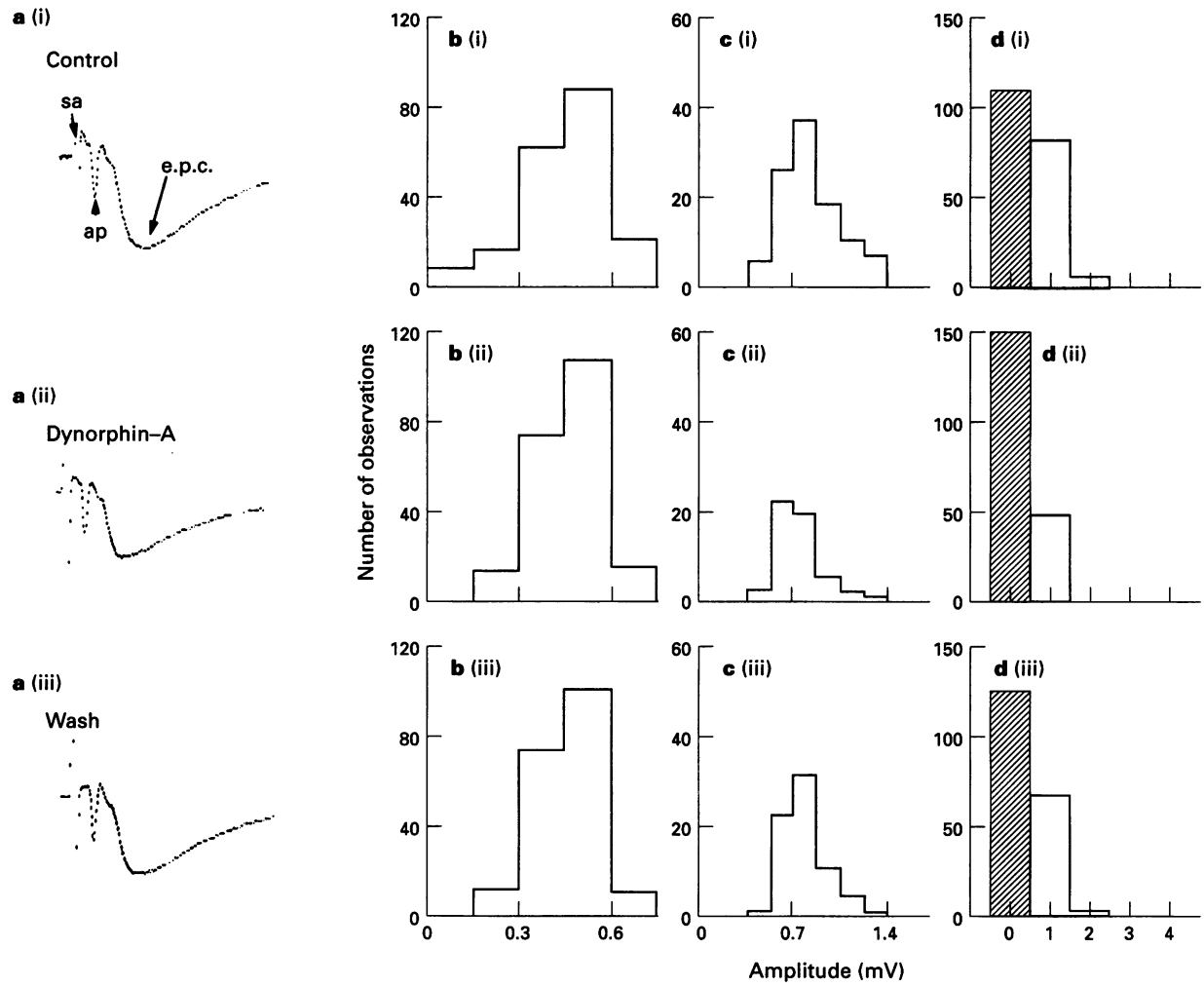

Figure 7 The effect of dynorphin-A on the nerve impulse, quantal size and $\overline{m}_e$. (a) The average signal of 200 trials is displayed for control (ai), dynorphin-A-treated (24 μM, aii) and after washing out the drug (aiii). Amplitude-frequency histograms of the nerve impulse (b) are shown for control (bi), dynorphin-A-treated (bii) and after washing (biii). Amplitude-frequency histograms of the m.e.p.cs (c) are shown for control (ci), dynorphin-A-treated (cii) and after washing (ciii). Number of quanta secreted per nerve impulse during 200 nerve stimulations are shown (d) for controls (di), dynorphin-A-treated (dii) and after washing (diii). The nerve impulse (ni) amplitude was not significantly changed by dynorphin-A (control, 0.39 ± 0.12 (mean $\pm$ s.d.); dynorphin-A-treated, 0.39 ± 0.10; after washing, 0.38 ± 0.10). The amplitude of the m.e.p.cs also did not change (control, 0.91 ± 0.22 mV (mean $\pm$ s.d.); dynorphin-treated, 0.84 ± 0.19 mV; after washing, 0.88 ± 0.18 mV). The number of quanta secreted per nerve impulse decreased from 0.52 (control) to 0.26 (dynorphin-A-treated) and then to 0.38 (after washing). The stimulus artefact (sa) and averaged e.p.c. of 200 consecutive stimulations are shown in (a).

receptors affect a G-protein which is directly linked to K^+ channels causing the conductance of K^+ ions to increase and the cells to hyperpolarize making them less excitable or shortening the duration of the nerve action potential (Cherubini & North, 1985; North, 1986; North *et al.*, 1987). Nerve impulse conduction failure has been suggested (Illes *et al.*, 1982; Milner *et al.*, 1982) as a possible mechanism responsible for the opiate-induced decrease in excitatory junctional potential amplitude from the mouse vas deferens (Bennett & Lavidis, 1980). At the release sites of the amphibian motor nerve terminal, morphine and dynorphin-A acting on dynorphin-A-sensitive opioid receptors, decrease the amount of quanta secreted during nerve stimulation without detectably affecting the configuration or the non intermittent nature of the nerve terminal impulse even at these very high concentrations of dynorphin-A or morphine. Thus it is likely that dynorphin-A acting on κ-like opioid receptors produces a decrease in the secretion of quanta possibly by interfering with the influx of calcium ions following nerve stimulation and not by blocking the propagation of the nerve impulse along terminal branches.

Conditions which reduce the effects of opiates on quantal secretion

Effect of changing $[Ca^{2+}]_o$ on $\overline{m}_e$ In the absence of morphine, increasing the external calcium concentration from 0.3 to 0.4 mM increases the amount of transmitter secreted by about a 4th power (Dodge & Rahamimoff, 1967). It is likely that more than four calcium ions are required to interact in a co-operative manner on the secretory mechanism before a quantum of transmitter is secreted (Bennett & Lavidis, 1979). The sites of action of these calcium ions involved in the secretory process are not known. Morphine shifted the calcium versus quantal secretion relationship to the right without any change to the 4th power relationship indicating that the dependence was not changed but that the probability of secretion had decreased. This morphine- and dynorphin-A-induced competitive inhibition of the action of calcium ions in the secretory process is similar to that produced by magnesium ions (Jenkinson, 1957; Bennett & Florin, 1974). This conjecture has been challenged by two studies involving the inhibitory effect of normorphine on transmitter secretion from the varicosities

of the mouse vas deferens (Illes *et al.*, 1982; Milner *et al.*, 1982). In both studies relatively high concentrations of normorphine induced a change in the gradient of the relationship between log e.j.p. amplitude and log $[Ca^{2+}]_o$. It is possible that high concentrations of normorphine induce failure in conduction of the nerve impulse along the sympathetic axons of the mouse vas deferens. It has been suggested that morphine directly affects the voltage-dependent calcium channels to inhibit the influx of calcium during nerve stimulation (Werz & MacDonald, 1983; 1985) or that it inhibits the vesicle secretory process. An action on the vesicle secretory process is unlikely since the secretion of spontaneous quanta continues even after evoked quantal secretion has been abolished (personal observation). It is more likely that opiates affect either the entry of calcium ions during nerve stimulation or the action of these calcium ions activating the secretion of vesicles.

Short high frequency nerve stimulation If a test impulse follows a conditioning impulse within 60 ms, there is an increase in the probability of quantal secretion of release sites. This facilitated secretion declines as a single exponential with a time course of about 30 ms (Balnave & Gage, 1977; Bennett & Lavidis, 1989). An inverse relationship exists between $[Ca^{2+}]_o$ and facilitation in $\overline{m}_e$ (Bennett & Lavidis, 1982). The facilitated increase in $\overline{m}_e$ during conditioning-test impulses is probably due to intra-terminal accumulation of calcium ions (residual calcium hypothesis, Katz & Miledi, 1979; Zucker & Fogelson, 1986). In the sympathetic varicosities of the mouse vas deferens, morphine decreases evoked transmitter secretion and increases the level of facilitation during trains of nerve impulses (Einstein & Lavidis, 1984a,b). Similarly in this study dynorphin-A decreased $\overline{m}_e$ and enhanced the ability of release sites to facilitate during conditioning-test impulses without changing the time course of decay in facilitation, suggesting that the sequestration of calcium ions within the nerve terminal is not affected by dynorphin-A.

In summary this study has demonstrated that dynorphin-A and to a lesser extent morphine, decrease the evoked secretion of quanta from release sites uniformly along the length of visualized terminal branches. Procedures which are thought to increase the intraterminal stores of free calcium ions during nerve stimulation, such as increasing the extracellular calcium ion concentration or use of a conditioning-test set of impulses, decrease the ability of opiates to inhibit quantal secretion. Inhibition of quantal secretion by dynorphin-A and morphine occurs without any noticeable change in the configuration of the nerve terminal impulse. It is likely that dynorphin-A and morphine affect the potential-dependent calcium channels in such a way as to decrease the influx of calcium ions following the successful invasion of the terminal by the nerve impulse. This results in a uniform reduction of the probability of quantal secretion of release sites. The changes in probability of quantal secretion from release sites during different seasons are not produced by regulation of opioid receptors since the release sites were equally responsive to exogenously applied opiates throughout the year. It is possible that the levels of circulating dynorphin or dynorphin-like substances increase during May to November resulting in a general decrease in the probability of quantal secretion.

This work was supported by a National Health and Medical Research Council project grant and a Clive and Vera Ramaciotti equipment grant. N.A.L is in receipt of a R. Douglas Wright Fellowship, N.H. & M.R.C.

References

BALNAVE, R. & GAGE, P.W. (1977). Facilitation of transmitter secretion from toad motor nerve terminals during brief trains of action potentials. *J. Physiol.*, **266**, 435–451.

BENNETT, M.R. & FLORIN, T. (1974). A statistical analysis of the release of acetylcholine at newly formed synapses in striated muscle. *J. Physiol.*, **238**, 93–107.

BENNETT, M.R., JONES, P. & LAVIDIS, N.A. (1986). The probability of quantal secretion along visualised terminal branches at amphibian (*Bufo marinus*) neuromuscular synapses. *J. Physiol.*, **379**, 257–274.

BENNETT, M.R., KARUNANITHI, S. & LAVIDIS, N.A. (1991). Probabilistic secretion of quanta from nerve terminals in toad (*Bufo marinus*) muscle modulated by adenosine. *J. Physiol.*, **433**, 421–434.

BENNETT, M.R. & LAVIDIS, N.A. (1979). The effect of calcium ions on the secretion of quanta evoked by an impulse at nerve terminal release sites. *J. Gen. Physiol.*, **74**, 429–456.

BENNETT, M.R. & LAVIDIS, N.A. (1980). An electrophysiological analysis of the effects of morphine on the calcium dependence of neuromuscular transmission in the mouse vas deferens. *Br. J. Pharmacol.*, 69, 185–191.

BENNETT, M.R. & LAVIDIS, N.A. (1982). Variation in quantal secretion at different release sites along developing and mature motor terminal branches. *Dev. Brain Res.*, **5**, 1–9.

BENNETT, M.R. & LAVIDIS, N.A. (1988). Quantal secretion at release sites of nerve terminal in toad (*Bufo marinus*) muscle during formation of topographical maps. *J. Physiol.*, **401**, 567–579.

BENNETT, M.R. & LAVIDIS, N.A. (1989). The probability of quantal secretion at release sites in different calcium concentrations in toad (*Bufo marinus*) muscle. *J. Physiol.*, **418**, 291–233.

BENNETT, M.R. & LAVIDIS, N.A. (1992). Probabilistic secretion of quanta from the release sites of nerve terminals in amphibian muscle modulated by seasonal changes. *Neurosci. Lett.*, **134**, 79–82.

BENNETT, M.R., LAVIDIS, N.A. & ARMSON, F.M. (1987). Changes in the dimensions of release sites along terminal branches at amphibian (*Bufo marinus*) neuromuscular synapses. *J. Neurocytol.*, **16**, 221–247.

BENNETT, M.R., LAVIDIS, N.A. & LAVIDIS-ARMSON, F.M. (1989). The probability of quantal secretion at release sites of different length in toad (*Bufo marinus*) muscle. *J. Physiol.*, **418**, 235–249.

BIXBY, J.L. & SPITZER, N.C. (1983). Enkephalin reduces quantal content at the frog neuromuscular junction. *Nature*, **301**, 431–432.

BORNSTEIN, J.C. & FIELDS H.L. (1979). Morphine presynaptically inhibits a glanglionic cholinergic synapses. *Neurosci. Lett.*, **15**, 77–82.

BRIGANT, J.L. & MALLART, A. (1982). Presynaptic currents in mouse motor endings. *J. Physiol.*, **333**, 619–636.

BROCK, J.A. & CUNNANE, T.C. (1988). Electrical activity at the sympathetic neuroeffector junction in the guinea-pig vas deferens. *J. Physiol.*, **399**, 607–632.

CHERUBINI, E. & NORTH, R.A. (1985). m and k opioids inhibit transmitter release by different mechanisms. *Proc. Natl. Acad. Sci. U.S.A.*, **82**, 1860–1863.

CONE, R.I. & GOLDSTEIN, A. (1982). A dynorphin-like opioid in the central nervous system of an amphibian. *Proc. Natl. Acad. Sci. U.S.A.*, **79**, 3345–3349.

D'ALONZO, A.J. & GRINNELL, A.D. (1985). Profiles of evoked release along the length of frog motor nerve terminals. *J. Physiol.*, **359**, 233–258.

DEL CASTILLO J & KATZ, B. (1956). Localisation of active spots within the neuromuscular junction of the frog. *J. Physiol.*, **132**, 630–649.

DODGE, F.A. & RAHAMIMOFF, R. (1967). Co-operative action of calcium ions in transmitter release at the neuromuscular junction. *J. Physiol.*, **193**, 419–432.

EINSTEIN, R. & LAVIDIS, N.A. (1984a). The dependence of excitatory junction potential amplitude on the external calcium concentration in narcotic tolerant mouse vas deferens. *Br. J. Pharmacol.*, **83**, 853–861.

EINSTEIN, R. & LAVIDIS, N.A. (1984b). The dependence of excitatory junction potential amplitude on the external calcium concentration in mouse vas deferens during narcotic withdrawal. *Br. J. Pharmacol.*, **83**, 863–870.

FATT, P. & KATZ, B. (1952). Spontaneous subthreshold activity at motor nerve endings. *J. Physiol.*, **117**, 109–118.

FRANKENHAURER, B. & HODGKIN, A.L. (1957). The action of calcium on the electrical properties of squid axons. *J. Physiol.*, **137**, 218–244.

FREDERICKSON, R.C.A. & PINSKY, C. (1971). Morphine impairs acetylcholine release but facilitates acetylcholine action at a skeletal neuromuscular junction. *Nature*, **231**, 93–94.

GINSBORG, B.L. & HIRST, G.D.S. (1972). The effect of adenosine on the release of the transmitter from the phrenic nerve of the rat. *J. Physiol.*, **224**, 629–645.

GROSS, R.A. & MACDONALD, R.L. (1987). Dynorphin-A selectively reduces a large transient (N-type) calcium current of mouse dorsal root ganglion neurones in cell culture. *Proc. Natl. Acad. Sci. U.S.A.*, **84**, 5469–5473.

HAYNES, L.W. & SMITH, M.E. (1982). Selective inhibition of motor endplate-specific acetylcholinesterase by beta-endorphin and related peptides. *Neuroscience*, **7**, 1007–1013.

HIRAI, K. & KATAYAMA, Y. (1988). Methionine enkephalin presynaptically facilitates and inhibits bullfrog sympathetic ganglionic transmission. *Brain Res.*, **448**, 299–307.

ILLES, P., MEIER, C. & STARKE, K. (1982). Non-competitive interaction between normorphine and calcium on the release of noradrenaline. *Brain Res.*, **251**, 192–1195.

ILLES, P., ZIEGLAGANSBERGER, W. & HERZ, A. (1980). Calcium reverses the inhibitory action of morphine on neuroeffector transmission in the mouse vas deferens. *Brain Res.*, **191**, 511–522.

JENKINSON, D.H. (1957). The nature of the antagonism between calcium and magnesium ions at the neuromuscular junction. *J. Physiol.*, **138**, 434–444.

KATZ, B. & MILEDI, R. (1979). Estimates of quantal content during 'chemical potentiation' of transmitter release. *Proc. R. Soc. B.*, **205**, 369–378.

MACDONALD, R.L. & WERZ, M.A. (1986). Dynorphin A decreased voltage-dependent calcium conductance of mouse dorsal root ganglion neurones. *J. Physiol.*, **377**, 237–249.

MILNER, J.D., NORTH, R.A. & VITEK, L.V. (1982). Interactions among the effects of normorphine, calcium and magnesium on transmitter release in the mouse vas deferens. *Br. J. Pharmacol.*, **76**, 45–49.

MONTECUCCHI, P.C., DE CASTIGLIONE, R., PIANI, S., GOZZINI, L. & ERSPAMER, V. (1981). Amino acid composition and sequence of dermorphine, a novel opiate-like peptide from the skin of Phylomedusa saragei. *Int. J. Pept. Prot. Res.*, **17**, 275–277.

MORITA, K. & NORTH, R.A. (1982). Opiate activation of potassium conductances in myenteric neurones: inhibition by calcium ion. *Brain Res.*, **242**, 145–150.

NORTH, R.A. (1986). Opioid receptor types and membrane ion channels. *Trends Neurosci.*, **9**, 114–117.

NORTH, R.A. & WILLIAMS, J.T. (1983). Opiate activation of potassium conductance inhibits calcium action potentials in rat locus coeruleus neurones. *Br. J. Pharmacol.*, **80**, 225–228.

NORTH, R.A., WILLIAMS, J.T., SURPRENANT, A. & CHRISTIE, M.J. (1987). Mu and delta receptors belong to a family of receptors that are coupled to potassium channels. *Proc. Natl. Acad. Sci. U.S.A.*, **84**, 5487–5491.

OREN, N., MICEVYCH, P.E. & LETINSKY, M.S. (1987). The possible role of alpha-melanocyte stimulating hormone in the regulation of synapse elimination in the frog. *Soc. Neurosci. Abstr.*, **13**, 1421.

PEPPER, C.M. & HENDERSON, G. (1980). Opiates and opioid peptides hyperpolarize locus coeruleus neurones *in vitro*. *Science*, **209**, 394–396.

RIBEIRO, J.A. & WALKER, J. (1975). The effects of adenosine triphosphate and adenosine diphosphate on transmission at the rat and frog neuromuscular junctions. *Br. J. Pharmacol.*, **71**, 191–194.

SILINSKY, E.M. (1975). On the association between transmitter secretion and the release of adenine nucleotides from mammalian motor nerve terminals. *J. Physiol.*, **247**, 145.

SUZUKI, T., OKA, J. & FUKUDA, H. (1987). *In vitro* studies of the effects of naloxone on the root potentials in the frog spinal cord: enkephalin-like effects on the recurrent presynaptic inhibition. *Comp. Biochem. Physiol.*, **87**, 221–225.

WERZ, M.A. & MACDONALD, R.L. (1983). Opioid peptides with differential affinity for mu- and delta-receptors decrease sensory neurone calcium-dependent action potentials. *J. Pharmacol. Exp. Ther.*, **227**, 394–402.

WERZ, M.A. & MACDONALD, R.L. (1985). Dynorphin and neoendorphin peptides decrease dorsal root ganglion neuron calcium-dependent action potential duration. *J Pharmacol. Exp. Ther.*, **234**, 49–56.

YOSHIKAMI, D. & OKUN, L.M. (1984). Staining of living presynaptic nerve terminals with selective fluorescent dyes. *Nature*, **310**, 53–56.

ZUCKER, R.S. & FOGELSON, A.L. (1986). Relationship between transmitter release and presynaptic calcium influx when calcium enters through discrete channels. *Proc. Natl. Acad. Sci. U.S.A.*, **83**, 3032–3036.

(Received June 27, 1994
Revised February 10, 1995
Accepted February 22, 1995)

British Journal of Pharmacology (1995) 115, 451-458

Dose-response comparisons of five lung surfactant factor (LSF) preparations in an animal model of adult respiratory distress syndrome (ARDS)

[1]Dietrich Häfner, Rolf Beume, Ulrich Kilian, Georg Krasznai & *Burkhard Lachmann

Byk Gulden, Department of Respiratory Pharmacology, Konstanz, Germany and *Department of Anaesthesiology, Erasmus University, Rotterdam, The Netherlands

1 We have examined the effects of five different lung surfactant factor (LSF) preparations in the rat lung lavage model. In this model repetitive lung lavage leads to lung injury with some similarities to adult respiratory distress syndrome with poor gas exchange and protein leakage into the alveolar spaces. These pathological sequelae can be reversed by LSF instillation soon after lavage.

2 The tested LSF preparations were: two bovine: Survanta and Alveofact: two synthetic: Exosurf and a protein-free phospholipid based LSF (PL-LSF) and one Recombinant LSF at doses of 25, 50 and 100 mg kg^{-1} body weight and an untreated control group.

3 Tracheotomized rats (10-12 per dose) were pressure-controlled ventilated (Siemens Servo Ventilator 900C) with 100% oxygen at a respiratory rate of 30 breaths min^{-1}, inspiration expiration ratio of 1 : 2, peak inspiratory pressure (PIP) of 28 cmH_2O at positive end-expiratory pressure (PEEP) of 8 cmH_2O. Two hours after LSF administration, PEEP and in parallel PIP was reduced from 8 to 6 (1st reduction), from 6 to 3 (2nd reduction) and from 3 to 0 cmH_2O (3rd reduction).

4 Partial arterial oxygen pressure (Pa_{O_2}, mmHg) at 5 min and 120 min after LSF administration and during the 2nd PEEP reduction (Pa_{O_2}(PEEP23/3)) were used for statistical comparison. All LSF preparations caused a dose-dependent increase for the Pa_{O_2}(120'), whereas during the 2nd PEEP reduction only bovine and recombinant LSF exhibited dose-dependency. Exosurf did not increase Pa_{O_2} after administration of the highest dose. At the highest dose Exosurf exerted no further improvement but rather a tendency to relapse. The bovine and the Recombinant LSF are superior to both synthetic LSF preparations.

5 In this animal model and under the described specific ventilatory settings, even between bovine LSF preparations there are detectable differences that are pronounced when compared to synthetic LSF without any surfactant proteins. We conclude that the difference between bovine and synthetic LSF preparations can be overcome by addition of the surfactant protein C.

Keywords: Adult respiratory distress syndrome (ARDS)-model; dose-response comparisons; synthetic lung surfactant factor; bovine lung surfactant factor; recombinant lung surfactant factor; gas exchange; surfactant protein C (SP-C)

Introduction

Since its first description by Ashbaugh *et al.* (1967) mortality due to the adult respiratory distress syndrome (ARDS), currently about 50-65% (Shale, 1987), has not changed (Shale, 1987; Villar & Slutsky 1989), suggesting little advance in therapy. Despite pharmacological approaches such as therapy with prostaglandin E_1 (PGE_1) (Russel *et al.*, 1990) corticosteroids (Bernard *et al.*, 1987), conventional ventilatory interventions (Marini & Kelsen, 1992; Swami & Keogh, 1992) or even extracorporeal membrane oxygenation (ECMO) (Evans & Keogh, 1991) no therapy has so far demonstrated improved survival of patients in clinical testing, whereas optimal ventilator settings have shown some beneficial effects related to outcome (Hickling *et al.*, 1990; East *et al.*, 1992). A recently published report concerning the use of ECMO also shows controversial beneficial effects of ECMO (Lewandowski *et al.*, 1992), but the techniques used are very complex, labour intensive and limited to a few clinical centres (Swami & Keogh, 1992).

For the development of alternate therapeutic interventions a major focus of current research is the role of the lung surfactant factor (LSF) system. Alterations in the surfactant system are proposed to contribute significantly to the pathophysiology of human ARDS (Lachmann & Danzmann, 1984). Changes in LSF composition (Lachmann & Danzmann, 1984) and function (Lachmann & Danzmann, 1984; Gregory *et al.*, 1991) are detectable in the lavage fluid of ARDS patients. Moreover, there are a few case reports on surfactant treatment in adult subjects (Lachmann, 1987; Richman *et al.*, 1989; Nosaka *et al.*, 1990) which reported some beneficial effects in ARDS patients (for review see Gommers & Lachmann, 1993).

As several animal models of ARDS are now available, it is reasonable to test the efficacy of LSF preparations in suitable and well-defined animal models, before testing such preparations in man. Furthermore, it is thus possible to compare the efficacy of different LSF preparations under systematic and standardized conditions in dose-response experiments. In various animal species, including rats, surfactant depletion by repetitive total lung lavage leads to lung injury with some similarities to that seen in ARDS (Lachmann *et al.*, 1980; van Daal *et al.*, 1991). The pathological changes observed are atelectasis, protein leakage leading to formation of hyaline membranes and oedema (Lachmann *et al.*, 1980; Berggren *et al.*, 1986). These changes lead to severe deterioration of gas exchange (Berggren *et al.*, 1986). Several reports consistently showed alleviation of these pathological sequelae after administration of LSF (Lachmann *et al.*, 1980; Berggren *et al.*, 1986; Lachmann *et al.*, 1994). We have employed a modification of the lung lavage model originally described by Lachmann *et al.* (1980). The aim of our study was to assess dose-response curves of five different LSF preparations in the rat lung lavage model under conditions standardized with respect

[1]Author for correspondence: Department of Respiratory Pharmacology, Byk Gulden, Postbox 100310, D-78403 Konstanz, Germany.

to the ventilatory settings as well as the mode and volume of LSF administration. The examined LSF preparations were: (1) a bovine LSF preparation, Alveofact (Dr Karl Thomae GmbH, Biberach, Germany), (2) Survanta (Abbott GmbH, Wiesbaden, Germany), another bovine LSF preparation, (3) a synthetic LSF, Exosurf (Burroughs Wellcome Co., Research Triangle Park, U.S.A.) that contains only one phospholipid and no surfactant proteins, (4) another synthetic LSF, (PL-LSF, Byk Gulden, Konstanz, Germany) that contains two phospholipids and no surfactant proteins and (5) a Recombinant LSF (Byk Gulden, Konstanz, Germany). We selected these LSF preparations in order to compare the efficacy of the two natural, bovine LSF preparations and the two protein-free synthetic LSF preparations with a Recombinant LSF preparation that contains human identical s,s-dipalmitoylated surfactant protein C as potential treatments of ARDS patients.

Preliminary results were presented at the ALA/ATS meeting in Miami (Häfner *et al.*, 1993).

Methods

Preparation of the rats

This study protocol was reviewed and approved by the Laboratory Animal Care Committee at the district presidency of Freiburg, Germany. The study was performed with a total of 186 male Sprague Dawley rats (Harlan CBP, Zeist, The Netherlands), weighing 230–290 g.

After induction of anaesthesia with a halothane nitrous oxide (N_2O), oxygen (O_2) mixture (1–2% halothane, 70% N_2O and 28–29% O_2) a catheter was placed in one carotid artery. These catheters contained heparinized, isotonic saline solution (from the stock solution [5000 iu heparin-Na ml^{-1}], 0.5 ml was given in 250 ml 0.9% NaCl solution). Before tracheotomy the animals received an intraperitoneal (i.p.) injection of pentobarbitone (stock solution: 60 mg ml^{-1}; 1 ml kg^{-1} body weight). The trachea of each animal was cannulated with a tracheal tube (internal diameter: 1.8 mm; external diameter: 2.4 mm). The tube was secured by ligature. Before artificial ventilation was started, the animals were given an i.m. injection of pancuronium bromide as muscle-relaxant (2 mg kg^{-1}). During the experiment additional pentobarbitone (0.25 ml kg^{-1} of the stock solution) was given i.p. at hourly intervals. Pancuronium bromide was additionally injected i.m. if spontaneous breathing was observed. Six animals were connected to a distributor unit that in turn was connected to a Servo Ventilator. The animals were ventilated simultaneously at a respiratory rate of 30 breaths min^{-1}, a fraction of inspired oxygen (FiO_2) of 1.0, an inspiration expiration ratio of 1:2 and a peak inspiratory pressure (PIP) of 15 cmH_2O which included a positive end-expiratory pressure (PEEP) of 2 cmH_2O.

Protocols for the animal experiments

The reported parameters are arterial PaO_2 and $PaCO_2$. At the start of the experiment, blood was taken from the arterial catheter to determine pretreatment values of the animals under the described ventilatory settings. Only animals with PaO_2 values of more than 480 mmHg were included in the experiments. Before lavage the peak inspiration pressure (PIP) was raised to 28 cmH_2O and PEEP to 8 cmH_2O. The animals were then subjected to multiple lavage (6–8 times) with 1 ml 30 g^{-1} body wt. of isotonic saline solution warmed to body temperature. To avoid metabolic acidosis, 4 ml kg^{-1} of a glucose/$NaHCO_3$-solution (5 g glucose-monohydrate and 8.4 g $NaHCO_3$ dissolved in 100 ml 0.9% NaCl-solution) were given by i.p. injection to each animal after lavage. Additionally, the same amount of glucose/$NaHCO_3$ was given if the HCO_3-value in the arterial blood gas analysis fell below 20 mmol l^{-1} during the experiment. Five minutes after the PaO_2 fell to between 50 and 110 mmHg, LSF was instilled intratracheally as described below. Blood gases were subsequently determined at 5, 30, 60, 90 and 120 min after LSF instillation. After this, PIP was lowered from 28 cmH_2O to 26 cmH_2O and PEEP from 8 to 6 cmH_2O (= 1st PEEP reduction). This was followed by a 2nd PEEP reduction from 6 to 3 cmH_2O and a 3rd PEEP reduction to 0 cmH_2O PEEP. Five minutes after each PEEP reduction, blood gases were measured (for the experimental scheme see Figure 1). Immediately after the measurement of the blood gases of the last animal, PEEP was lowered as described.

Instruments

Blood gas analysis was performed with a blood gas analyzer (Radiometer Copenhagen ABL 500, Radiometer Deutschland GmbH, Willich, Germany). Ventilation of the animals was performed with a Servo Ventilator (900C, SIEMENS-ELEMA, Solna, Sweden). For induction of anaesthesia a halothane vaporizer (Draegerwerk GmbH, Lübeck, Germany) was used.

Surfactants

The following were used: Alveofact (Batch No. 102108, Dr Karl Thomae GmbH, Biberach, Germany) is a natural surfactant purified from bovine lung lavage containing varying amounts of surfactant proteins B and C. It is available as a ready-to-use suspension. Each vial contains 1.2 ml solution containing 50 mg phospholipids (PL). Survanta (Batch No. 56-763 AN-21, Abbott GmbH, Wiesbaden, Germany) is also a natural, bovine surfactant. It is obtained from minced cow lungs containing varying amounts of surfactant proteins B and C and is enriched with dipalmitolphosphatidylcholine, palmitic acid and tripalmitin. It is also available as a ready-to-use suspension. Each vial contains 8 ml solution at a concentration of 25 mg PL per ml. Exosurf (Batch No. PN17191, Burroughs Wellcome Co., Research Triangle Park, U.S.A.) is a protein-free synthetic surfactant made of dipalmitoylphosphatidylcholine (DPPC), tyloxapol and cetyl alcohol. It is a lyophilisate that needs to be resuspended with a supplied solvent to achieve a volume of 8 ml/vial. For the purpose of this study each vial was resuspended with 4.3 ml to achieve a concentration of 25 mg DPPC per ml. Another protein-free phospholipid-based surfactant (PL-LSF) made of diplamitoylphophatidylcholine (DPPC) and palmitoyloleoylphosphatidylglycerol (POPG) at a ratio of 70 : 30 plus 2.5% (w/w) palmitic acid as related to phospholipids. The PL-LSF was prepared as a lyophilisate that had to be resuspended before use. Therefore, each vial of PL-LSF was resuspended with 6 ml 0.9% NaCl solution giving a concentration of 25 mg PL per ml. A Recombinant LSF (Byk Gulden, Konstanz, Germany) made of phospholipids (dipalmitoylphosphatidylcholine and palmitoyloleoylphosphatidylglycerol at a ratio of 70 : 30) plus 2.5% (w/w) palmitic acid and 2% human identical s,s-dipalmitoylated surfactant protein C as related to phospholipids. The Recombinant LSF was also prepared as a lyophilisate that had to be resuspended before use. Therefore, each vial of recombinant LSF was resuspended with 6 ml 0.9% NaCl solution giving a concentration of 25 mg PL per ml.

Dosage

The different LSF preparations were instilled intratracheally (i.t.) at doses of 25, 50 and 100 mg total phospholipids per kg body weight in a volume of 1.2 ml per animal. To achieve the required concentrations of 6.25, 12.5 and 25 mg total phospholipids per 1.2 ml the LSF preparations were diluted with 0.9% saline solution.

Mode of LSF administration: Administration was performed using 5 ml syringes which contained 1.2 ml LSF solution and 3.8 ml air. The syringes were connected to the tracheal tubes of the animals and LSF was administered first, followed directly by the administration of air. The syringe was disconnected and then a further 3 ml of air was administered into the tracheal

tube of each animal to empty both, the syringe and the tube.

In the control group the animals underwent multiple lavage only, without any administration of surfactant.

Statistics

For each LSF preparation and each dose level and also for the control group 10–12 rats were used. The influence of LSF instillation on the test parameters (Pa_{O_2} and Pa_{CO_2}) was described in absolute values showing mean and standard deviation (s.d.). Values for the Pa_{O_2} at 5 and 120 min after LSF administration as well as for the different PEEP reductions are presented. From the values of Pa_{O_2} during the 2nd PEEP reduction (Pa_{O_2}(PEEP23/3)) dose-response curves were plotted. These values were also used to test for statistically significant differences between the LSF preparations at each dose level. Additionally, each dose was compared to the control group.

Before testing for inter-group differences we performed the Dixon test to eliminate outliers. Homogeneity of variances was tested with Bartlett's test and as the variances differed significantly we used the paired Student-Welch test with α-adjustment for multiple comparison (Sachs, 1986). The comparison between the different LSF preparations and each dose level was performed using the Pa_{O_2}(PEEP23/3).

Results

Feasibility of the comparison

The experimental procedures were validated in pilot experiments prior to the study. The whole study was performed within three months without any dropouts. After lavage none of the animals in the control group showed a spontaneous improvement of the Pa_{O_2} values or the Pa_{CO_2} values (Figure 1).

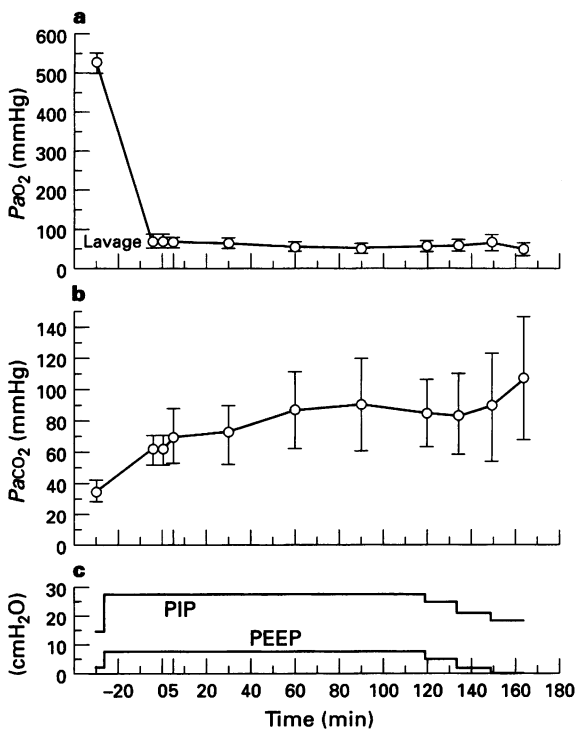

Figure 1 Mean (○) and individual values of Pa_{O_2} (mmHg) (a) and Pa_{CO_2} (mmHg) (b) after ventilation only of lung lavaged rats ($n = 12$). Lavage marks the period where the repetitive lavage was performed. (c) Shows the corresponding time course of the peak inspiratory pressure (PIP, cmH_2O) and the positive end-expiratory pressure (PEEP, cmH_2O) during the experiment.

Time course of the registered parameters

Two hours after administration of the two lowest doses (25 and 50 mg kg^{-1} body wt). of Alveofact Pa_{O_2} decreased compared to the 5 min values of Pa_{O_2}. In contrast, the Pa_{O_2} values of those animals treated with Survanta or Recombinant LSF showed stable values during this period after administration of either doses (Figures 2 and 3). In contrast, animals receiving Exosurf displayed stable values during this period but on a lower level as shown by comparison of the mean curves, but this LSF preparation led to a larger standard deviation during this period. The second synthetic LSF preparation (PL-LSF) showed a decrease of Pa_{O_2} after all three doses during the ventilation period with constant PEEP. The Pa_{O_2} values increased with higher doses but remained below the values of Recombinant LSF and the two bovine LSF preparations. Blood gases after administration of Survanta and Recombinant LSF improved within 5 min after administration and remained stable until 2 h after LSF administration. During this period PEEP remained unchanged. Comparing the different doses it is obvious that with increasing dose the response becomes more homogeneous and the variability between the animals becomes smaller. This dose-dependent effect is less pronounced after administration of Exosurf. Response to this LSF preparation showed a great variability, even at a dose of 100 mg kg^{-1} (Figure 4).

During the PEEP reduction manoeuvre, significant dose-dependent impairments of Pa_{O_2} were observed after administration of the two bovine LSF preparations, Recombinant LSF and the protein-free PL-LSF. The synthetic LSF Exosurf behaved differently: the lowest dose exerted moderate activity whereas after the highest dose a decrease in activity with respect to Pa_{O_2} values were observed. However, in the control group none of the animals showed any improvements in the low Pa_{O_2} level at any time after lavage (Figure 1).

Pa_{CO_2} values showed an almost inverse pattern of response to the Pa_{O_2} values after administration of the different LSF preparations at all three doses (Table 1–3). During lavage Pa_{CO_2} increased and after administration of LSF it decreased. During the PEEP reduction manoeuvre the Pa_{CO_2} increased towards the third PEEP reduction. After administration of Alveofact the changes in Pa_{CO_2} showed a dose-dependency. This was particularly marked when comparing the values during the third PEEP reduction (Tables 1–3). Only the Recombinant LSF behaved in a similar way to Alveofact. Survanta, Exosurf and PL-LSF showed only weak dose-dependency for this parameter. The PL-LSF behaved similarly to Exosurf. The Pa_{CO_2} value at 120 min after LSF administration was only slightly lower than the 5 min value after administration of both protein-free LSF's at all three doses tested. However, in the control group none of the animals reached the Pa_{CO_2} level seen before the start of experiment.

Dose-response curve calculations and statistical inter-group comparison

Dose-response curves (Figure 5) were constructed based on the values of Pa_{O_2} during the 2nd PEEP reduction (Pa_{O_2} (PEEP23/3)).

The results of the comparison of the different LSF preparations at a dose of 25 mg kg^{-1} and in comparison to controls showed that only Recombinant LSF and Survanta were significantly better than controls, whereas Alveofact, Exosurf and PL-LSF did not differ significantly from the control group. In addition, the dose of 25 mg kg^{-1} Alveofact or PL-LSF differed significantly to Survanta ($P \leqslant 0.05$) and to Recombinant LSF ($P \leqslant 0.01$), showing that a dose of 25 mg kg^{-1} Survanta or Recombinant LSF is more effective than a dose of 25 mg kg^{-1} Alveofact or PL-LSF, respectively. There was no significant difference between Exosurf and the other LSF preparations.

Evaluation of the different LSF preparations after administration of 50 mg kg^{-1} LSF showed no significant difference

between the different commercially available LSF preparations and the Recombinant LSF but all surfactants differed to PL-LSF at different levels of significance (Alveofact and Exosurf vs. PL-LSF with $P \leqslant 0.05$ and Recombinant LSF and Survanta vs. PL-LSF with $P \leqslant 0.01$). However, all commercially available LSF preparations and Recombinant LSF were significantly better than controls, but the preparations differed with respect to the significance level (Recombinant LSF and

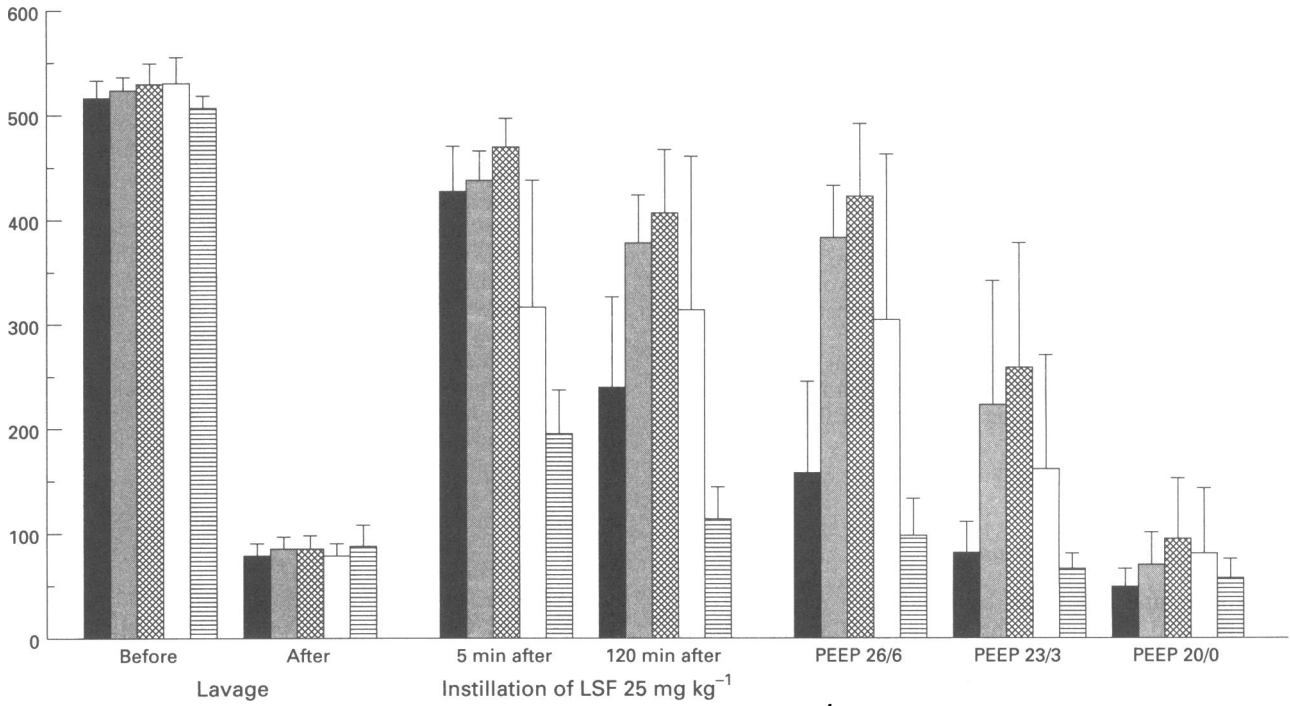

Figure 2 Comparison of Pa_{O_2} (mmHg) values after administration of 25 mg kg^{-1} body weight of Alveofact (solid columns); Survanta (stippled columns); Exosurf (open columns); protein-free, phospholipid-based LSF (hatched columns) and Recombinant LSF (cross-hatched columns). All values are given as mean plus s.d., $n = 10-12$ for each dose. The figure shows the values before and after lavage as well as 5 and 120 min after instillation of 25 mg kg^{-1} body weight of the different LSF preparations. The last three groups of columns show the values during the stepwise decrease of positive end-expiratory pressure (PEEP) to zero.

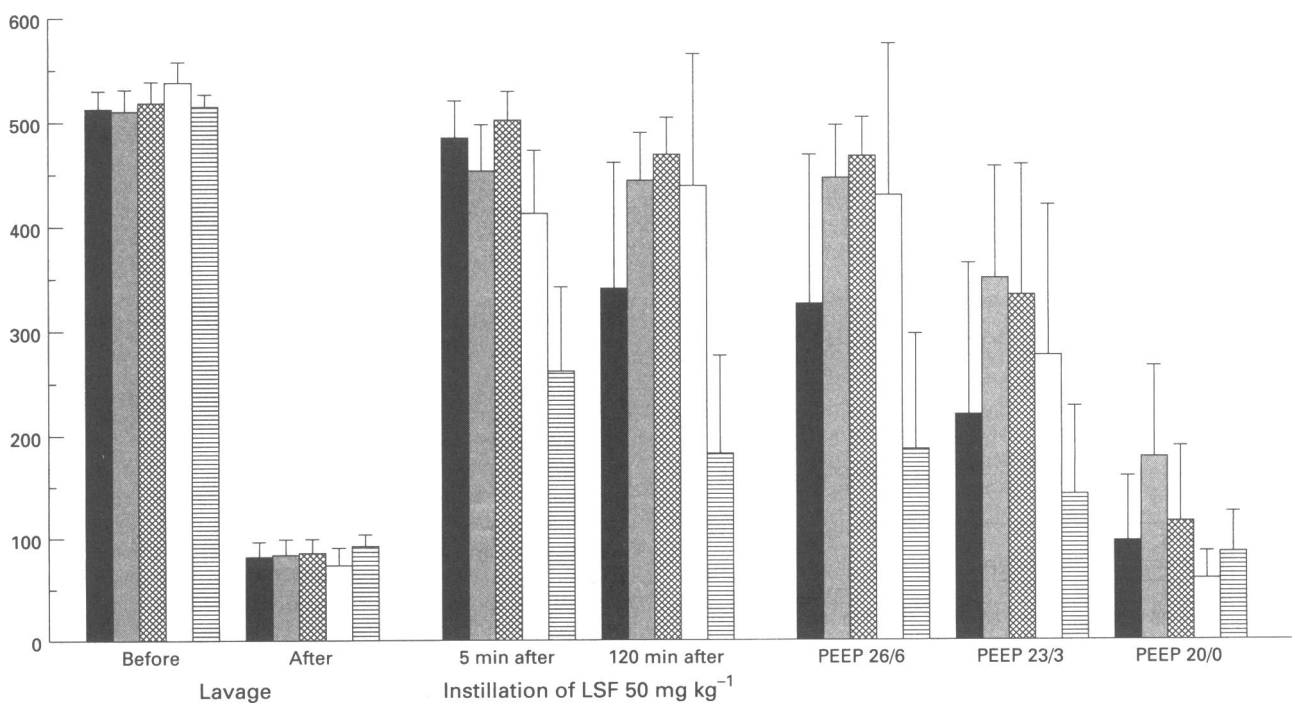

Figure 3 Comparison of Pa_{O_2} (mmHg) values after administration of 50 mg kg^{-1} body weight of Alveofact (solid columns); Survanta (stippled columns); Exosurf (open columns); protein-free, phospholipid-based LSF (hatched columns) and Recombinant LSF (cross-hatched columns). All values are given as mean plus s.d., $n = 10-12$ for each dose. The figure shows the values before and after lavage as well as 5 and 120 min after instillation of 50 mg kg^{-1} body weight of the different LSF preparations. The last three groups of columns show the values during the stepwise decrease of positive end-expiratory pressure (PEEP) to zero.

Survanta $P \leqslant 0.001$, Alveofact and Exosurf $P \leqslant 0.01$). At this dose level there was no statistically significant difference between PL-LSF and controls.

Comparisons based on a dose of 100 mg kg^{-1} of the different LSF preparations showed that Recombinant LSF, Alveofact and Survanta exerted significantly better effects than controls with $P \leqslant 0.001$, whereas this comparison for Exosurf resulted in significance only at the $P \leqslant 0.05$ level and for PL-LSF at the $P \leqslant 0.01$ level. Furthermore, Recombinant LSF, Alveofact and Survanta showed no significant difference when compared with each other, but they differed significantly from Exosurf and PL-LSF. Recombinant LSF and Alveofact dif-

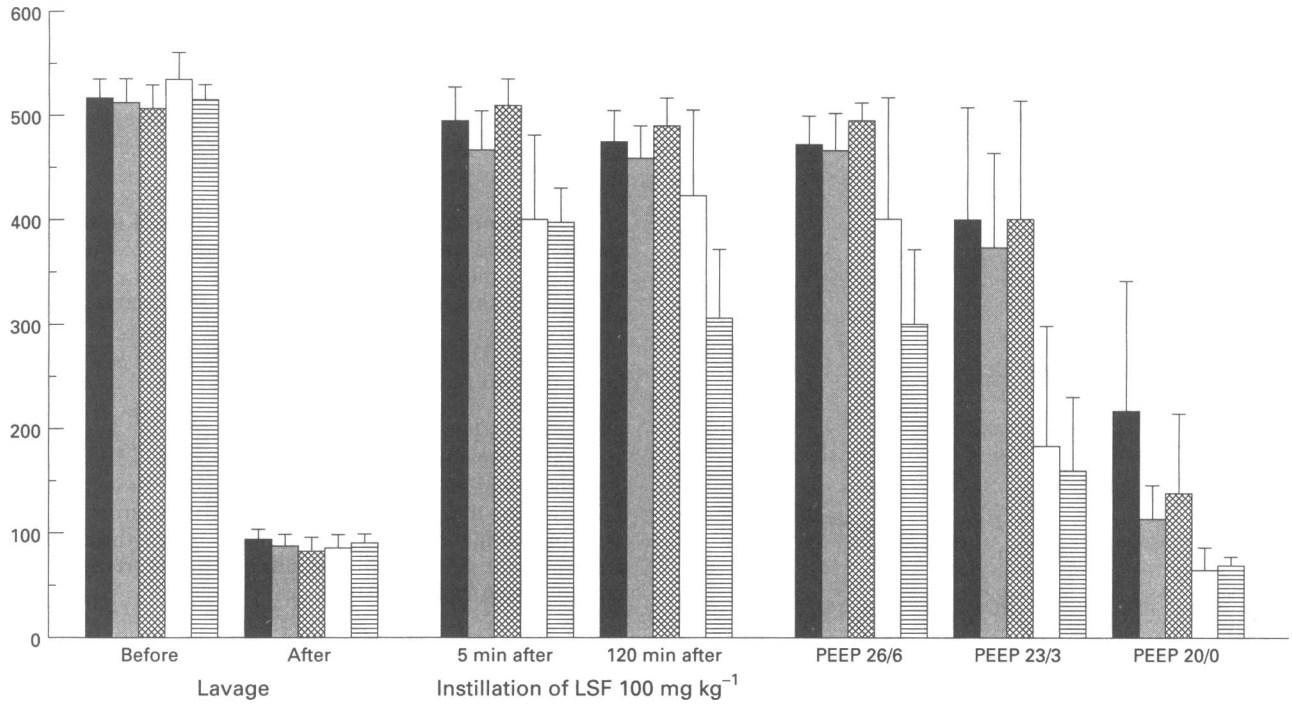

Figure 4 Comparison of Pa_{O_2} (mmHg) values after administration of 100 mg kg^{-1} body weight of Alveofact (solid columns); Survanta (stippled columns); Exosurf (open columns); protein-free, phospholipid-based LSF (hatched columns) and Recombinant LSF (cross-hatched columns). All values are given as mean plus s.d., $n = 10-12$ for each dose. The figure shows the values before and after lavage as well as 5 and 120 min after instillation of 100 mg kg^{-1} body weight of the different LSF preparations. The last three groups of columns show the values during the stepwise decrease of positive end-expiratory pressure (PEEP) to zero.

Table 1 Comparison of $Paco_2$ (mmHg) values after administration of 25 mg kg^{-1} body weight of Alveofact, Survanta, Recombinant LSF, protein-free, phospholipid-based LSF and Exosurf

	Before	*After*	*5 min after*	*120 min after*	*PEEP reductions*		
	Lavage		*instillation of 25 mg kg^{-1} LSF*		*26/6*	*23/3*	*20/0*
Alveofact	39 ± 5	72 ± 13	61 ± 7	62 ± 11	62 ± 14	75 ± 26	109 ± 39
Survanta	39 ± 10	66 ± 13	60 ± 8	47 ± 7	44 ± 5	52 ± 8	86 ± 19
Recombinant LSF	34 ± 7	60 ± 6	49 ± 4	48 ± 5	44 ± 4	48 ± 12	73 ± 27
Protein-free LSF	33 ± 5	65 ± 17	64 ± 17	67 ± 19	69 ± 24	89 ± 20	73 ± 27
Exosurf	35 ± 9	60 ± 12	59 ± 13	51 ± 14	48 ± 14	59 ± 26	89 ± 30

All values are given as mean ± standard deviation, $n = 10$-12 for each dose. The table shows the values before and after lavage as well as 5 and 120 min after instillation of 25 mg kg^{-1} body weight of the different LSF preparations. The last three columns show the values during the stepwise decrease of positive end-expiratory pressure (PEEP) to zero.

Table 2 Comparison of $Paco_2$ (mmHg) values after administration of 50 mg kg^{-1} body weight of Alveofact, Survanta, Recombinant LSF, protein-free, phospholipid-based LSF and Exosurf

	Before	*After*	*5 min after*	*120 min after*	*PEEP reductions*		
	Lavage		*instillation of 50 mg kg^{-1} LSF*		*26/6*	*23/3*	*20/0*
Alveofact	42 ± 7	76 ± 11	60 ± 7	56 ± 11	55 ± 14	57 ± 20	78 ± 33
Survanta	38 ± 6	69 ± 11	58 ± 7	48 ± 6	42 ± 5	42 ± 10	61 ± 15
Recombinant LSF	38 ± 7	60 ± 12	52 ± 9	48 ± 9	39 ± 6	38 ± 8	66 ± 25
Protein-free LSF	35 ± 6	60 ± 10	57 ± 10	56 ± 10	56 ± 10	61 ± 13	70 ± 9
Exosurf	38 ± 7	75 ± 13	64 ± 8	55 ± 6	48 ± 8	54 ± 11	93 ± 28

All values are given as mean ± standard deviation. $n = 10$-12 for each dose. The table shows the values before and after lavage as well as 5 and 120 min after instillation of 50 mg kg^{-1} body weight of the different LSF preparations. The last three columns show the values during the stepwise decrease of positive end-expiratory pressure (PEEP) to zero.

Table 3 Comparison of $Paco_2$ (mmHg) values after administration of 100 mg kg^{-1} body weight of Alveofact, Survanta, Recombinant LSF, protein-free, phospholipid-based LSF and Exosurf

	Before Lavage	*After Lavage*	*5 min after instillation of 100 mg kg^{-1} LSF*	*120 min after instillation of 100 mg kg^{-1} LSF*	*PEEP reductions 26/6*	*23/3*	*20/0*
Alveofact	40±9	70±9	61±6	56±6	46±7	38±6	45±10
Survanta	38±6	67±10	58±9	50±5	46±7	48±11	72±21
Recombinant LSF	44±9	63±10	53±7	46±11	39±8	39±10	48±11
Protein-free LSF	38±3	60±9	52±6	50±6	46±6	59±17	62±18
Exosurf	45±10	67±13	60±9	58±10	53±9	57±10	85±22

All values are given as mean ± standard deviation, $n = 10$-12 for each dose. The table shows the values before and after lavage as well as 5 and 120 min after instillation of 100 mg kg^{-1} body weight of the different LSF preparations. The last three columns show the values during the stepwise decrease of positive end-expiratory pressure (PEEP) to zero.

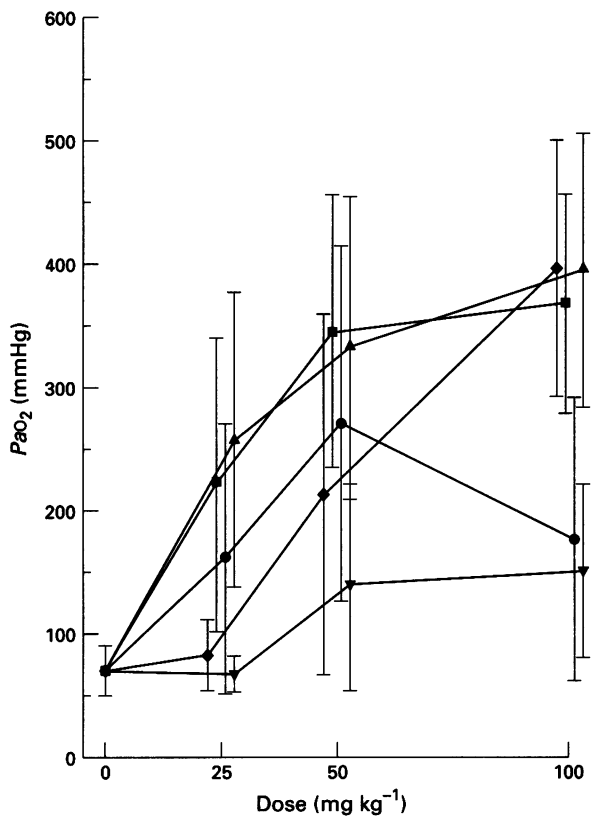

Figure 5 Dose response curves of Alveofact (◆); Survanta (■); Exosurf (●); protein-free, phospholipid-based LSF (▼) and Recombinant LSF (▲). The values represent mean ± s.d. based on the individual Pao_2 values during the 2nd PEEP reduction (PEEP = 3 cmH_2O) after administration of the different doses of the different LSF preparations.

fered significantly from Exosurf with $P \leqslant 0.001$ and Survanta differed significantly from Exosurf with $P \leqslant 0.01$. Recombinant LSF, Alveofact and Survanta differed significantly from PL-LSF with $P \leqslant 0.001$, whereas there was no statistically significant difference between PL-LSF and Exosurf.

This dose-response comparison shows that Recombinant LSF and Survanta behaved similarly after administration of the different doses, whereas Alveofact and Exosurf were different. Alveofact developed a clear dose-dependent efficacy with only little effect after administration of 25 mg kg^{-1} and after 100 mg kg^{-1} the efficacy was similar to Survanta or Recombinant LSF. Exosurf showed dose-dependency only after administration of the 25 and 50 mg kg^{-1} dose, whereas after administration of the 100 mg kg^{-1} dose the effect decreased. PL-LSF showed dose-dependency but was significantly worse than all protein-containing LSF preparations.

Comparison of the different doses of Exosurf to the control group showed that after administration of 25 mg kg^{-1} no significant difference was detectable, with a dose of 50 mg kg^{-1} this comparison resulted in significance ($P \leqslant 0.01$) but after a dose of 100 mg kg^{-1} the significance level decreased to $P \leqslant 0.05$. This was in contrast to the other LSF preparations, the two bovine LSF preparations showed an increasing significance level with increasing doses (Alveofact: 25 mg kg^{-1}, NS; 50 mg kg^{-1}, $P \leqslant 0.01$; and 100 mg kg^{-1}, $P \leqslant 0.001$; Survanta: 25 mg kg^{-1}, $P \leqslant 0.01$; 50 mg kg^{-1}, $P \leqslant 0.001$; and 100 mg kg^{-1}, $P \leqslant 0.001$). The protein-free PL-LSF showed a significant difference from controls only at a dose of 100 mg kg^{-1} ($P \leqslant 0.01$). However, all three doses of Recombinant LSF differed significantly with respect to the control group with $P \leqslant 0.001$.

Discussion

Using the rat lung lavage model, it is possible to characterize new synthetic LSF preparations in a standardized and systematic fashion (Lewis & Jobe, 1993) with commercially available surfactants. This was done by use of comparable doses of LSF with similar concentrations, the same mode of administration and the same volume for administration of the different LSF preparations. The results of this study on an ARDS model of pure surfactant depletion demonstrate that during ventilation with PEEP of 8 cmH_2O the two bovine, the Recombinant and the synthetic LSF preparations were almost equally effective but differed from the protein-free only phospholipid-based surfactant (PL-LSF); however, Exosurf showed highly variable activity (Figures 2, 3 and 4). The differences between the protein-free and the protein-containing LSF preparations were even more pronounced if dose-response comparisons were performed based on the Pao_2 values during the 2nd PEEP reduction. It is well known that PEEP by itself has beneficial effects on oxygenation (Stokke, 1976). Thus, if a moderately active LSF like Exosurf or PL-LSF is combined with ventilation under high PEEP, it is possible to re-establish gas exchange in the lung (Rider *et al.*, 1992). But the stabilization of the lungs due to LSF activity vanishes if the PEEP is reduced. We found that after administration of the different doses of both protein-free synthetic LSF preparations, the decrease by steps of PEEP to zero reduces the Pao_2 values to the level of the control group.

With respect to Exosurf, the results differ somewhat from the results of Cummings *et al.* (1992) and Ikegami *et al.* (1993) obtained with the pre-term lamb. Both groups have consistently shown that Exosurf did not improve oxygenation or lung mechanics in pre-term lambs. But there is at least one important difference between our data and those obtained by these other workers. We have used animals that are able to produce their own LSF i.e. the alveolar type II cells would be expected to have preformed LSF that can be secreted or can be released by the detergents that Exosurf contains. Another possible explanation regarding the slightly greater activity of

Exosurf in our experiments may be derived from the results of Ikegami *et al.* (1993). They have demonstrated that the activity of exogenous LSF can be improved after exposure to the preterm lung. These activation events are competing with inactivation phenomena within the lung to yield a net physiological effect. They assume that the balance probably depends on the surfactant used and the degree of maturation of the lung, which will influence endogenous surfactant availability (Ikegami *et al.*, 1993). Thus, this activation (or improvement) of Exosurf may be due to the association of exogenous surfactant with components of the endogenous surfactant. This may be more prominent in adult animals in which the superficial surfactant is washed out and the alveolar type II cells are intact, as can be concluded from the work of Ikegami *et al.* (1993). Surprisingly, this activation is more pronounced after Exosurf than after PL-LSF. But even this improvement by endogenous surfactant, whether through secretion of preformed LSF or stimulated synthesis of surfactant, vanishes during PEEP reduction. This activity also vanishes at the highest dose of Exosurf used (Figure 5) indicating that despite DPPC being one of the major components of surfactant (Lewis & Jobe, 1993), it is not solely responsible for the formation of an adequate surfactant layer in the lung and even an improved phospholipid matrix (as used with PL-LSF) is not able to achieve the same activity as that seen with the protein-containing LSF preparations. Taking these points together, the PEEP reduction manoeuvre serves as a good criterion when judging the real efficacy of LSF preparations.

Due to the differing behaviour during the 5–120 min period with constant PEEP and the differing dose-response characteristics between Recombinant LSF, Exosurf and the PL-LSF (that differs from Recombinant LSF only with respect to the surfactant protein C) but the lack of difference between Recombinant LSF and Survanta, we conclude that surfactant protein C (SP-C) is an important additive in achieving the same activity as bovine surfactants. Further evidence derives from data of Seeger *et al.* (1993) who have quantified the phospholipid as well as the surfactant protein B (SP-B) content of Alveofact and Survanta. Their data suggest that Alveofact is a SP-B driven LSF, whereas Survanta is principally a SP-C-based LSF. This is in good accordance with unpublished investigations from our department of molecular biology (personal communication Prof. Dr K.-P. Schäfer) showing that the SP-B and SP-C ratio of Alveofact is 2:1 and of Survanta is about 1 : 3. Seeger *et al.* (1993) have quantified the SP-B content of Survanta as $<0.25\%$ and that of Alveofact as $>1.5\%$ related to phospholipids. Concerning this essential role of lung surfactant proteins, our data further confirm that Recombinant LSF, an SP-C based surfactant, is equally as active as bovine LSF (Van Daal *et al.*, 1991). The failure of the synthetic LSF preparations Exosurf and PL-LSF to restore PaO_2 values after the PEEP reduction may be further explained by the observations of other authors who have found that LSF can be inhibited by certain proteins (Hallmann *et al.*, 1991; Kobayashi *et al.*, 1991). However, as Lachmann *et al.* (1994) have shown, normally, the inhibitory effects of plasma proteins can be neutralized by large amounts of an active exogenous surfactant, whereas in this work high concentrations of Exosurf had no additional beneficial effects. Furthermore, it is likely that active LSF preparations are able to influence transcapillary-interstitial-epithelial lung leakage (Lewis & Jobe, 1993) and can interfere with plasma proteins (Lachmann *et al.*, 1994). This is essential to prevent the formation of hyaline membranes (Enhörning, 1989; Nosaka *et al.*, 1990).

However, the present results of Exosurf are in good accordance with the results published so far after administration to ARDS patients (Wiedemann *et al.*, 1992). These authors were also unable to detect dose-dependent activity after administration of Exosurf. This is further evidence that an active LSF preparation should contain at least one surfactant protein. In addition, the recently published data of a large clinical trial with Exosurf (Anzueto *et al.*, 1994) and a pilot study using Survanta (Gregory *et al.*, 1994) provide further support. While Exosurf (Anzueto *et al.*, 1994) failed to show superior effects compared to conventional therapy, Survanta (Gregory *et al.*, 1994) showed statistically significant improvements. Thus, comparison of results from the rat lung lavage model described here with clinical data suggests that it is suitable for investigation of the effects and activity of LSF preparations that may be used for treatment of ARDS patients.

Values of $PaCO_2$ do not have such a great variablility as those of PaO_2 due to the administration of bicarbonate in our experiments, although they can normalize after administration of a very active LSF preparation and remain low during a decrease in PEEP (Tables 1–3). Again we have shown, even for this parameter, that LSF preparations that stabilize the lungs can tolerate a reduction of PEEP to zero. The results obtained in this specific model using the described ventilatory settings and a defined volume and dose of surfactant, suggest that protein-free surfactants based only on one phospholipid or a phospholipid mixture do not achieve the same activity as bovine LSF preparations. The conclusion that protein-containing LSF preparations are better than protein-free surfactants is based on the different dose-response curves (Figure 5) under ventilation with a PEEP of 3 cmH_2O (=2nd PEEP reduction, equivalent to about 150 min after LSF administration). However, the activity of such phospholipid-based LSF preparations can be enhanced by addition of surfactant protein C (SP-C). With s,s-dipalmitoylated SP-C identical to that of man it is possible to achieve the same activity as natural bovine LSF preparations. The advantage of such an LSF preparation is that an SP-C can be manufactured which is similar to human SP-C but in a way that keeps it free of all possible contaminants. Strict standards of quality control and analytical procedures can be applied throughout all steps of production to ensure that the amount of protein does not vary. In addition, the amounts of SP-C as well as all phospholipids will not be a limiting factor (Kendig *et al.*, 1988) in the manufacture of an active LSF preparation. Thus, it would solve one of the most frustrating problems in LSF research and treatment of ARDS patients, that is, the lack of sufficient amounts of LSF material for clinical trials and therapy.

The skilful technical assistance of Ms G. Dillman and Ms S. Kuklinski are gratefully acknowledged. Furthermore, the authors wish to thank L. Visser for revising the manuscript and the group of Professor Schäfer (Department of Molecular Biology), the group of Dr. Eistetter (Pharmaceutical Department) and the group of Dr. Sturm (Analytical Chemistry) for preparation and analytical confirmation of the Recombinant LSF and the PL-LSF.

References

ANZUETO, A., BAUGHAM, R., GUNTUPALLI, K., DEMARIA, E., DAVIS, K., WEG, J., LONG, W., HORTON, J., PATTISHALL, E. & THE EXOSURF ARDS SEPSIS STUDY GROUP (1994). An international, randomized, placebo-controlled trial evaluating the safety and efficacy of aerosolized surfactant in patients with sepsis-induced ARDS. *Am. J. Respir. Crit. Care. Med.*, **149**, A567.

ASHBAUGH, D.G., BIGELOW, D.B., PETTY, T.L. & LEVINE, B.E. (1967). Acute respiratory distress in adults. *Lancet*, **ii**, 319–323.

BERGGREN, P., LACHMANN, B., CURSTEDT, T., GROSSMANN, G. & ROBERTSON, B. (1986). Gas exchange and lung morphology after surfactant replacement in experimental adult respiratory distress syndrome induced by repeated lung lavage. *Acta Anaesthesiol. Scand.*, **30**, 321–328.

BERNARD, G.R., LUCE, J.M., SPRUNG, C.L., RINALDO, J.E., TATE, R.M., SIBBALD, W.J., KARIMAN, K., HIGGINS, S., BRADLEY, R., METZ, C.A., HARRIS, T.R. & BRIGHAM, K.L. (1987). High dose corticosteroids in patients with the adult respiratory distress syndrome. *N. Engl. J. Med.*, **317**, 1565–1570.

CUMMINGS, J.J., HOLM, B.A., HUDAK, M.L., HUDAK, B.B., FERGUSON, W.H. & EGAN, E.A. (1992). A controlled clinical comparison of four different surfactant preparations in surfactant-deficient preterm lambs. *Am. Rev. Respir. Dis.*, **145**, 999–1004.

EAST, T.D., BÖHM, S.H., WALLACE, C.J., CLEMMER, T.P., WEAVER, L.K., ORME, J.F. & MORRIS, A.H. (1992). A successful computerized protocol for clinical management of pressure control inverse ratio ventilation in ARDS patients. *Chest*, **101**, 697–710.

ENHÖRNING, G. (1989). Surfactant replacement in adult respiratory distress syndrome. *Am. Rev. Respir. Dis.*, **140**, 281–283.

EVANS, T.W. & KEOGH, B.F. (1991). Extracorporeal membrane oxygenation: a breath of fresh air or yesterday's treatment? *Thorax*, **46**, 692–694.

GOMMERS, D. & LACHMANN, B. (1993). Surfactant therapy: does it have a role in adults? *Clin. Int. Care*, **4**, 284–95.

GREGORY, T.J., LONGMORE, W.J., MOXLEY, M.A., WHITSETT, J.A., REED, C.R., FOWLER, A.A., HUDSON, L.D., MAUNDER, R.J., CRIM, C. & HYERS, T.M. (1991). Surfactant chemical composition and biophysical activity in acute respiratory distress syndrome. *J. Clin. Invest.*, **88**, 1976–1981.

GREGORY, T.J., GADEK, J.E., WEILAND, J.E., HYERS, T.M., CRIM, C., HUDSON, L.D., STEINBERG, K.P., MAUNDER, R.A., SPRAGG, R.G., SMITH, R.M., TIERNEY, D.F., GIPE, B., LONGMORE, W.J. & MOXLEY, M.A. (1994). Survanta ® supplementation in patients with acute respiratory distress syndrome (ARDS). *Am. J. Respir. Crit. Care Med.*, **149**, A567.

HÄFNER, D., BEUME, R. & KILIAN, U. Comparison of four lung surfactant factor (LSF) preparations in an animal model of adult respiratory distress syndrome (ARDS). (1993). *Am. Rev. Resp. Dis.*, **147**, A719.

HALLMANN, M., MERRITT, T.A., AKINO, T. & BRY, K. (1991). Surfactant protein A, phosphatidylcholine and surfactant inhibitors in epithelial lining fluid. *Am. Rev. Respir. Dis.*, **144**, 1376–1384.

HICKLING, K.G., HENDERSON, S.J. & JACKSON, R. (1990). Low mortality associated with low volume pressure limited ventilation with permissive hypercapnia in severe adult respiratory distress syndrome. *Intensive Care Med.*, **16**, 372–377.

IKEGAMI, M., UEDA, T., ABSOLOM, D., BAXTER, C., RIDER, E. & JOBE, A.H. (1993). Changes in exogenous surfactant in ventilated preterm lamb lungs. *Am. Rev. Respir. Dis.*, **148**, 837–844.

KENDIG, J.W., NOTTER, R.H., DAVIS, J.M., BARTOLETTI, A., DWECK, H.S., RISEMBERG, H.M., COX, C. & SHAPIRO, D.L. (1988). A multicenter randomized trial of surfactant replacement with calf lung surfactant extract: effects of pre- and post-ventilatory instillation and multiple doses. In *Surfactant Replacement Therapy in Neonatal and Adult Respiratory Distress Syndrome*. ed. Lachmann, B. pp. 108–122 Berlin, Heidelberg, New York: Springer Verlag.

KOBAYASHI, T., NITTA, K., GANZUKA, M., INUI, S., GROSSMANN, G. & ROBERTSON, B. (1991). Inactivation of exogenous surfactant by pulmonary edema fluid. *Pediatr. Res.*, **29**, 353–356.

LACHMANN, B. (1987). The role of pulmonary surfactant in the pathogenesis and therapy of ARDS. In *Update in Intensive Care and Emergency Medicine*. ed. Vincent, J.L. pp. 123–134. Berlin, Heidelberg, New York: Springer Verlag.

LACHMANN, B. & DANZMANN, E. (1984). Adult respiratory distress syndrome. In *Pulmonary Surfactant*. ed. Robertson, B., van Golde, L.M.G. & Batenburg, J.J. pp. 505–548. Amsterdam, New York, Oxford: Elsevier Science Publishers B.V.

LACHMANN, B., EIJKING, E.P., SO, K.L. & GOMMERS, D. (1994). In vivo evaluation of the inhibitory capacity of human plasma on exogenous surfactant function. *Intensive Care Med.*, **20**, 6–11.

LACHMANN, B., ROBERTSON, B. & VOGEL, J. (1980). In vivo lung lavage as an experimental model of the respiratory distress syndrome. *Acta Anaesthesiol. Scand.*, **24**, 231–236.

LEWANDOWSKI, K., SLAMA, K. & FALKE, K. (1992). Approaches to improve survival in severe ARDS. In *Yearbook of Intensive Care and Emergency Medicine*. ed. Vincent, J.L. pp. 372–383. Berlin: Springer.

LEWIS, J.F. & JOBE, A.H. (1993). Surfactant and the adult respiratory distress syndrome. *Am. Rev. Respir. Dis.*, **147**, 218–233.

MARINI, J.J. & KELSEN, S.G. (1992). Re-targeting ventilatory objectives in adult respiratory distress syndrome. *Am. Rev. Respir. Dis.*, **146**, 2–3.

NOSAKA, S., SAKAI, T., YONEKURA, M. & YOSHIKAWA, K. (1990). Surfactant for adults with respiratory failure. *Lancet*, **336**, 947–948.

RICHMAN, P.S., SPRAGG, R.G., ROBERTSON, B., MERRITT, T.A. & CURSTEDT, T. (1989). The adult respiratory distress syndrome: first trials with surfactant replacement. *Eur. Respir. J.*, **2**, 109S–111S.

RIDER, E.D., JOBE, A.H., IKEGAMI, M. & SUN, B. (1992). Effects of positive end-expiratory pressure (PEEP) on surfactant treatment responses in ventilated premature rabbits. *Clin. Res.*, **40**, 8A.

RUSSEL, J.A., RONCO, J.J. & DODEK, P.M. (1990). Physiologic effects and side effects of prostaglandin E1 in the adult respiratory distress syndrome. *Chest*, **97**, 684–692.

SACHS, L. (1986). *Angewandte Statistik*, 6th ed. Berlin, Heidelberg, New York: Springer Verlag.

SEEGER, W., GRUBE, C., GÜNTHER, A. & SCHMIDT, R. (1993). Surtactant inhibition by plasma proteins: differential sensitivity of various surfactant preparations. *Eur. Respir. J.*, **6**, 971–977.

SHALE, D.J. (1987). The adult respiratory distress syndrome: 20 years on. *Thorax*, **42**, 641–645.

STOKKE, D.B. (1976). Review: Artificial ventilation with positive end-expiratory pressure (PEEP). *Eur. J. Intens. Care Med.*, **2**, 77–85.

SWAMI, A. & KEOGH, B.F. (1992). The injured lung: conventional and novel respiratory therapy. *Thorax*, **47**, 555–562.

VAN DAAL, G.J., GOMMERS, D., BOS, A.H., VAN GOLDE, P.H.M., VAN DE KAMP, R. & LACHMANN, B. (1991). Human recombinant surfactant is as effective as commercially available natural surfactants. *Eur. Respir. J.*, **4**, Suppl 14, 492S.

VILLAR, J. & SLUTSKY, A.S. (1989). The incidence of the adult respiratory distress syndrome. *Am. Rev. Respir. Dis.*, **140**, 814–816.

WIEDEMANN, H., BAUGHMAN, R., DEBOISBLANC, B., SCHUSTER, D., CALDWELL, E., WEG, J., BALK, R., JENKINSON, S., WIEGELT, J., THARRAT, R., HORTON, J., PATTISHALL, E., LONG, W. & THE EXOSURF-ARDS SEPSIS STUDY GROUP. (1992). A multicenter trial in human sepsis-induced ARDS of an aerosolized synthetic surfactant (EXOSURF®). *Am. Rev. Respir. Dis.*, **145**, A184.

(Received December 5, 1994
Revised February 9, 1995
Accepted February 24, 1995)

British Journal of Pharmacology (1995) 115, 459-466

Phosphorylation- and voltage-dependent inhibition of neuronal calcium currents by activation of human $D_{2(short)}$ dopamine receptors

Nicola A. Brown & Guy R. Seabrook

Department of Pharmacology, Merck Sharp & Dohme Research Laboratories, Neuroscience Research Centre, Terlings Park, Eastwick Road, Harlow, Essex, CM20 2QR

1 Activation of human $D_{2(s)}$ dopamine receptors with quinpirole (10 nM) inhibits ω-conotoxin GVIa-sensitive, high-threshold calcium currents when expressed in differentiated NG108-15 cells (55% inhibition at +10 mV). This inhibition was made irreversible following intracellular dialysis with the non-hydrolysable guanosine triphosphate analogue GTP-γ-S (100 μM), and was prevented by pretreatment with pertussis toxin (1 μg ml^{-1} for 24 h).

2 Stimulation of protein kinase C with the diacylglycerol analogue, 1-oleoyl-2-acetyl-sn-glycerol (100 μM), also attenuated the inhibition of the sustained calcium current but did not affect the receptor-mediated decrease in rate of current activation. Similarly, okadaic acid (100 nM), a protein phosphatase 1/2A inhibitor, selectively occluded the inhibition of the sustained current.

3 The depression of calcium currents by quinpirole (10 nM) was enhanced following intracellular dialysis with 100 μM cyclic adenosine monophosphate (cyclic AMP, 72.8±9.8% depression), but was not mimicked by the membrane permeant cyclic GMP analogue, Sp-8-bromoguanosine-3',5':cyclic monophosphorothioate (100 μM).

4 Inhibition of calcium currents was only partly attenuated by 100 ms depolarizing prepulses to +100 mV immediately preceding the test pulse. However, following occlusion of the sustained depression with okadaic acid (100 nM) the residual kinetic slowing was reversed in a voltage-dependent manner ($P<0.05$).

5 Thus pertussis toxin-sensitive G-proteins liberated upon activation of human $D_{2(short)}$ dopamine receptors inhibited high-threshold calcium currents in two distinct ways. The decrease in rate of calcium current activation involved a voltage-dependent pathway, whereas the sustained inhibition of calcium current involved, in part, the voltage-resistant phosphorylation by cyclic AMP-dependent protein kinases and subsequent dephosphorylation by protein phosphatases 1/2A.

Keywords: Calcium channels; D_2 dopamine receptor; G-proteins; neuronal calcium currents; cyclic nucleotides; protein kinases

Introduction

Dopamine receptors regulate the function of calcium currents in several cell types. One of the best characterized are rat pituitary melanotrophs in which low-threshold, and dihydropyridine sensitive high-threshold calcium currents are inhibited by activation of D_2 dopamine receptors (Lledo *et al.*, 1990; Keja *et al.*, 1992; Nussinovitch & Kleinhaus, 1992; Seabrook *et al.*, 1994a). Since the discovery that the $D_{2\text{-like}}$ dopamine receptor family is composed of multiple structural subtypes, including several isoforms of the D_2, D_3, and D_4 subtypes, much interest has been generated concerning possible differences in the functional properties of these subtypes both within brain tissue and at the cellular level (reviewed in Grandy & Civelli, 1992; Schwartz *et al.*, 1992). However there are few, if any, ligands available that can discriminate between the short and long isoforms of the D_2 receptor subtype (Leysen *et al.*, 1993; however see also Castro & Strange, 1993), and this has made a detailed examination of their functional properties difficult. The separate transfection of receptor cDNA's into heterologous cell lines permits studies that are independent of other receptor isoforms, and furthermore allows the characterization of the functional properties of human receptors. Consequently we have transfected the short isoform of the human D_2 dopamine receptor into neuroblastoma x glioma NG108-15 cells (Seabrook *et al.*, 1994b). The present study was carried out to determine the mechanism(s) by which $D_{2(short)}$ receptors regulate the function of neuronal calcium channels that are not present in pituitary melanotrophs.

In mammalian brain, the release of dopamine is co-operatively dependent upon calcium influx into nerve terminals (Nachshen & Sanchez-Armass, 1987), and this occurs mainly through ω-conotoxin GVIa-sensitive calcium channels (Herdon & Nahorski, 1989). The behavioural effects of stimulation of D_2 receptors are in many cases accentuated by the co-application of D_1 receptor agonists (reviewed in Clark & White, 1987; LaHoste & Marshall, 1993). This synergy is paradoxical considering that D_1 and D_2 receptors have stimulatory and inhibitory effects respectively on adenylate cyclase activity (Kebabian & Calne, 1979). However, Piomelli and colleagues (1991) have recently shown that arachidonic acid release following D_2 receptor activation is also potentiated by D_1 receptor stimulation via an increase in adenosine 3':5'-cyclic monophosphate (cyclic AMP) production. Whether the inhibition of neuronal calcium currents by D_2 receptor activation is similarly modulated by cyclic AMP remains to be determined.

When differentiated into a neuronal phenotype, neuroblastoma x glioma NG108-15 cells express at least three types of calcium current. These can be distinguished by their voltage-dependence of activation into a low-threshold T-type, and at least two high-threshold subtypes (Fishman & Spector, 1981; Hering *et al.*, 1985; Docherty, 1988). The latter include dihydropyridine resistant N-type currents that are blocked by ω-conotoxin GVIa (Caulfield *et al.*, 1992; Kasai & Neher, 1992; Seabrook *et al.*, 1994b). These high-threshold currents are depressed by activation of various endogenous G-protein

[1] Author for correspondence.

linked receptors such as opiate, muscarinic, and somatostatin receptors (Tsunoo *et al.*, 1986; McFadzean & Docherty, 1989; Caulfield *et al.*, 1992). This neurotransmitter regulation of calcium channels typically involves pertussis toxin sensitive G-proteins such as $G\alpha_o$ subunits (reviewed in Scott *et al.*, 1991; Hille 1992; McCleskey, 1994), but also in some cases their $\beta\gamma$ counterparts (Kleuss *et al.*, 1991). Furthermore the second messenger systems involved may act via membrane delimited and/or by cytosolic pathways through protein phosphorylation (Hille, 1992). Consistent with this the pore forming $\alpha 1$ subunit of calcium channels can be phosphorylated by several protein kinases, including protein kinase A and C, the actions of which can be terminated by dephosphorylation with protein phosphatases 1 or 2 (Hell *et al.*, 1994; Zhao *et al.*, 1994). To investigate the role of G-proteins and protein phosphorylation in the function of human $D_{2(short)}$ dopamine receptors, this study examined the involvement of cyclic nucleotides as well as protein kinases in receptor mediated inhibition of N-type calcium currents in transfected neuroblastoma cells.

Methods

Calcium currents were recorded from transfected NG108-15 cells by methods described previously (Seabrook *et al.*, 1994b). Cells were grown in tissue culture in a medium that contained Dulbecco's Modified Eagles Medium (GIBCO), 10% foetal calf serum, 2 mM L-glutamine (Geneticin), and were plated on poly-L-lysine coated coverslips. Cells were differentiated for 3 to 5 days using 10 μM prostaglandin E_1 and 50 μM isobutylmethylxanthine (Docherty, 1988). Whole cell patch clamp recordings were made with borosilicate glass microelectrodes (Clark Electromedical Instruments) which were filled with a solution that contained (in mM): CsCl 110, tetraethylammonium.Cl 25, EGTA 10, HEPES 40 and $MgCl_2$ 3, adjusted to pH 7.3 with CsOH. Cells were perfused at a rate of 1 to 2 ml min^{-1} with an extracellular solution that contained (in mM): NaCl 135, glucose 10, HEPES 10, KCL 5, $CaCl_2$ or $BaCl_2$ 5 and tetrodotoxin 0.5 μM, pH 7.4, at 22°C. Drugs were applied via the superfusion system. Nystatin perforated patch clamp recordings were made using a pipette solution that contained (in mM): CsH_3O_3SCs 100, CsCl 25, $MgCl_2$ 3, HEPES 40, adjusted to pH 7.3 with CsOH. Cells were voltage-clamped and calcium currents were elicited by 100 ms depolarizing pulses from −60 to +10 mV at 0.033 Hz, Currents were amplified with an Axopatch 200 patch clamp amplifier (Axon Instruments), and captured on line via a CED1401 interface (Cambridge Electronic Design) which was connected to a Compaq 486 microcomputer. Linear leak currents were subtracted with the amplifier, and by the CED voltage-clamp

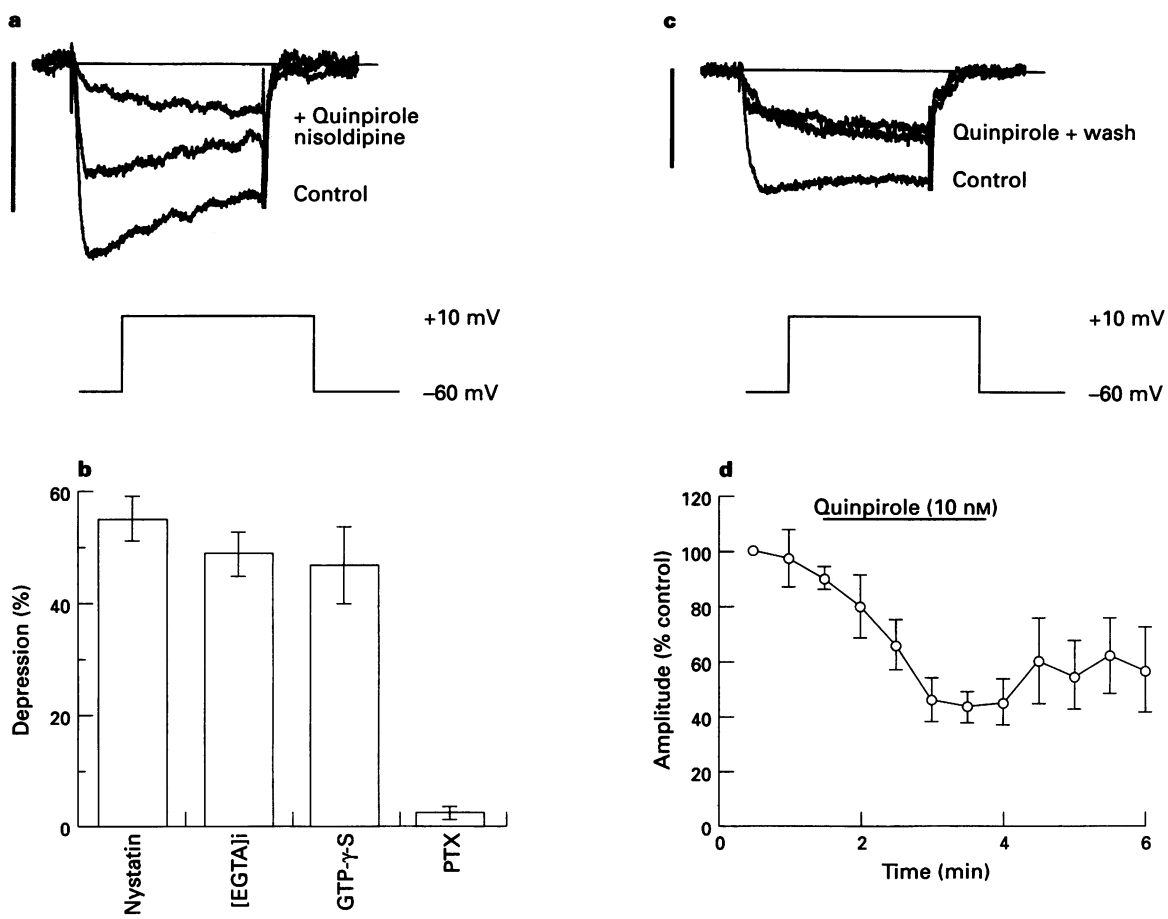

Figure 1 Persistence of D_2 receptor inhibition of calcium currents following inhibition of L-type currents with nisoldipine, chelation of $[Ca^{2+}]_i$ with EGTA, and following intracellular dialysis with the non-hydrolysable GTP analogue, GTP-γ-S. (a) Superimposed calcium currents in control conditions and following equilibration in nisoldipine (10 μM) and quinpirole (10 nM). Lower trace represents the change in membrane holding potential during a 100 ms pulse. Calibration bar = 500 pA. (b) Histogram depicting the maximal inhibition of the high-threshold calcium current obtained at +10 mV using nystatin-perforated patch clamp recording ($n = 21$), whole cell recording with electrodes containing 10 mM EGTA ($n = 5$), and with 100 μM GTP-γ-S ($n = 4$). Following pretreatment with pertussis toxin (PTX, 1 $\mu g\,ml^{-1}$ 24 h) the responses to D_2 receptor activation were abolished ($n = 4$). (c) Superimposed currents following internal dialysis with GTP-γ-S (100 μM, control) demonstrating the slowing in rate of activation of current with quinpirole (10 nM), and its lack of reversal with $[GTP\text{-}\gamma\text{-}S]_i$ following wash off. Calibration bar = 400 pA. (d) Time course of irreversible inhibition with quinpirole (10 nM applied for duration of horizontal line) following treatment with GTP-γ-S (100 μM), data are pooled from 4 cells (cf. Figure 3).

analysis software using a P:N leak subtraction protocol (5:1). The series resistance in nystatin perforated patch clamp recordings (typically 10–20 MOhm cf. whole cell 5–10 MOhm) would introduce a clamp error of up to ±5 mV assuming a maximum inward current of 500 pA, but series resistance compensation was not used in the present study to minimize noise. Currents were filtered at either 2 or 5 kHz high frequency cut off. Data are expressed as the mean ± s.e.mean, and unless stated percentages are the calcium current inhibition obtained with quinpirole (10 nM) normalized to the control current amplitude. Statistical analysis was carried out by analysis of variance in Microsoft Excel (version 5.0).

Drugs were obtained from the following companies: ethylene glycol *bis*(β-aminoethyl ether)-*N,N,N,N'*-tetraacetic acid (EGTA), adenosine 3':5'-cyclic monophosphate (cyclic AMP), guanosine 5'-O-[3-thiotriphosphate] (GTP-γ-S), ω-conotoxin GVIa, and 4-(2-hydroxyethyl)-1-piperazineethanesulphonic acid (HEPES) were purchased from Sigma. Quinpirole was purchased from Research Biochemical Inc. The Sp (Sp-8-Br-cGMPs) and Rp isomers (Rp-8-Br-cGMPs) of 8-bromoguanosine-3',5':cyclic monophosphorothioate sodium salt were purchased from Biolog Life Sciences Institute. Okadaic acid and 1-oleoyl-2-acetyl-sn-glycerol (OAG) were purchased from Calbiochem. Nisoldopine was obtained from Miles Pharmaceuticals. Drugs were dissolved either in distilled water, or as in the case of nisoldipine in dimethylsulphoxide (DMSO) with a final bath concentration of < 0.1% DMSO which alone had no effect upon calcium current amplitudes.

Results

Calcium currents were recorded from 157 cells to which drugs were applied, by either nystatin-perforated or conventional whole cell techniques. Depolarizations from a holding potential of −100 mV to greater than −50 mV elicited a biphasic inward current. This consisted of a low-threshold (at −30 mV) transient current that was completely inactivated within a 200 ms pulse, and a non-inactivating high-threshold current. Cells had a mean capacitance of 78.6 ± 4.3 pF, and a high-threshold current density of 12.2 ± 3.4 pA pF^{-1} at +10 mV ($n = 12$). In nystatin perforated patch recordings this high-threshold current (−60 to +10 mV) was maximally depressed by 55.3 ± 4.0% ($n = 21$) following perfusion with the $D_{2\text{-like}}$ dopamine receptor agonist, quinpirole (10 nM). This effect was restricted to the high-threshold current in that no depression of low-threshold currents was observed (Seabrook *et al.*, 1994b). Furthermore the depression was still observed after inhibition of L-type calcium currents with the dihydropyridine, nisoldipine (10 μM). In the presence of nisoldipine, quinpirole (10 nM) caused a 36.6 ± 7.0% ($n = 5$) depression of the peak calcium current (Figure 1a). Co-application of nisoldipine and ω-conotoxin GVIa (100 nM) inhibited >95% of the inward current under these recording conditions ($n = 4$).

Involvement of pertussis toxin-sensitive G-proteins but not $[Ca^{2+}]_i$

In conventional whole cell recordings, in which EGTA (10 mM) was included in the patch pipette to chelate intracellular calcium, no change in the maximal inhibition obtained following D_2 receptor activation was observed compared to experiments using nystatin-perforated patch recording (Figure 1). However, when extracellular Ba^{2+} ions (5 mM) were substituted as the charge carrier in place of $[Ca^{2+}]_o$, the percentage inhibition of the peak current following D_2 receptor activation was accentuated from 55% to 79.9 ± 7.6% ($P < 0.001$; $n = 9$). Consistent with the involvement of G-proteins, the effects of quinpirole were rendered irreversible when the non-hydrolysable GTP analogue GTP-γ-S (100 μM, $n = 4$) was included in the patch pipette (Figure 1). Furthermore responses were blocked by pretreatment of cells with pertussis toxin (1 μg ml^{-1} for 24 h; Figure 1) which selectively ADP ribosylates G-proteins of the G_i and G_o subtype.

Role of protein phosphorylation

When cells were dialysed, via the patch pipette, with the diacylgylcerol analogue, OAG (100 μM) to activate protein kinase C, the depression of the high-threshold calcium current following the subsequent activation of D_2 receptors was attenuated (Figure 2). This effect was most evident on the sustained current (90 ms into the voltage step) where a 18.0 ± 9.8% depression was observed, compared to control values of 39.3 ± 7.5% ($P < 0.05$, $n = 5$). In contrast, no significant attenuation of the depression of the peak current (10 ms into the voltage step) was observed (27.4 ± 6.3%, $n = 5$).

Inclusion of the cyclic nucleotide, cyclic AMP (100 μM) in the recording electrode potentiated the inhibition observed following D_2 receptor activation (Figure 3). This effect was fully reversible, and was evident on both the peak (72.8 ± 9.8%, $P < 0.01$, $n = 5$) and sustained calcium current (70.4 ± 14.8%, $P < 0.01$, $n = 5$). This increase in depression was not associated with the potentiation of a 'D_2 susceptible current' because the current density in 100 μM cyclic AMP was unaffected (7.06 ± 1.57 pA pF^{-1}, $n = 5$) compared to the control in the same batch of cells (7.20 ± 2.90 pA pF^{-1}, $n = 5$). Furthermore forskolin (10 μM), an irreversible activator of adenylate cyclase, did not alter the amplitude of whole cell

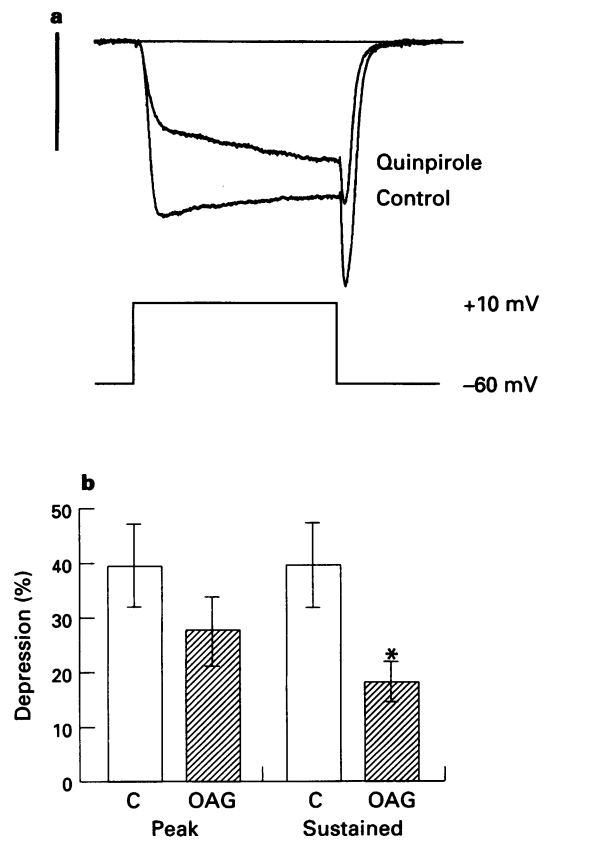

Figure 2 Modulation of D_2 receptor inhibition of calcium currents by diacylglycerol. (a) Superimposed calcium currents measured after intracellular dialysis with 100 μM OAG (control) and following application of quinpirole (10 nM). Calibration bar = 1 nA. (b) Histogram comparing the inhibition of the peak and sustained components of the calcium current (see methods) with quinpirole under control conditions (open columns, $n = 6$), and with 100 μM $[OAG]_i$ (shaded columns, $n = 5$). The depression of the peak current was unaffected, whereas the inhibition of the sustained current was significantly reduced ($P < 0.05$).

calcium currents in these cells (see also Kasai, 1991). In contrast to the effects of cyclic AMP, extracellular application of the membrane permeant cyclic GMP analogue, Sp-8-bromoguanosine-3',5':cyclic monophosphorothioate (100 μM for 2 min, $n=4$) did not mimic the effect of D_2 receptor activation. Consistent with the lack of involvement of cyclic GMP-dependent protein kinases, the inhibition caused by quinpirole was not blocked by the cyclic GMP-dependent protein kinase inhibitor Rp-8-Br-cGMP (100 μM).

To test further for the involvement of channel phosphorylation the effect of okadaic acid, a protein phosphatase inhibitor, was examined. Prevention of channel dephosphorylation by including okadaic acid (100 nM) in the patch pipette significantly ($P<0.01$) occluded the depression of the sustained current but not that of the peak current (Figure 3). Furthermore this treatment selectively unmasked the decrease in rate of calcium current activation that is superimposed on the sustained calcium current inhibition in control conditions.

The voltage-dependence of calcium current regulation by D_2 receptor activation was also examined by voltage-clamping cells at -60 mV, and immediately preceding the test pulse a depolarization to $+100$ mV was applied (Figure 4). Alone this prepulse had no effect on the amplitude of calcium currents elicited by subsequent potential steps to $+10$ mV. Although the sustained inhibition following D_2 receptor activation was partly relieved with these depolarizing prepulses ($P<0.05$, $n=7$), the decrease in rate of current activation was almost entirely voltage-dependent in that the transient inhibition observed when cells had been dialysed with okadaic acid was reversed by these prepulses (Figure 4).

Discussion

In neurones several signal transduction pathways are regulated by the activity of D_2 dopamine receptors. These include the inhibition of adenylate cyclase activity, potentiation of arachidonic acid release, activation of potassium currents, and decrease in calcium channel activity (reviewed in Grandy & Civelli, 1992; Schwartz *et al.*, 1992). However, the relative importance of each pathway in modulating cellular excitability and consequently the function of discrete brain regions, depends not only upon the tissue studied but also the neurotransmitter system that is modified. In this study we investigated the influence of D_2 dopamine receptors on neuronal calcium currents because it is this channel subtype that regulates dopamine release within the mammalian striatum (Herdon & Nahorski, 1989).

Activation of human $D_{2(short)}$ dopamine receptors expressed in NG108-15 cells selectively inhibits the ω-conotoxin GVIa-sensitive high-threshold calcium current, a component of

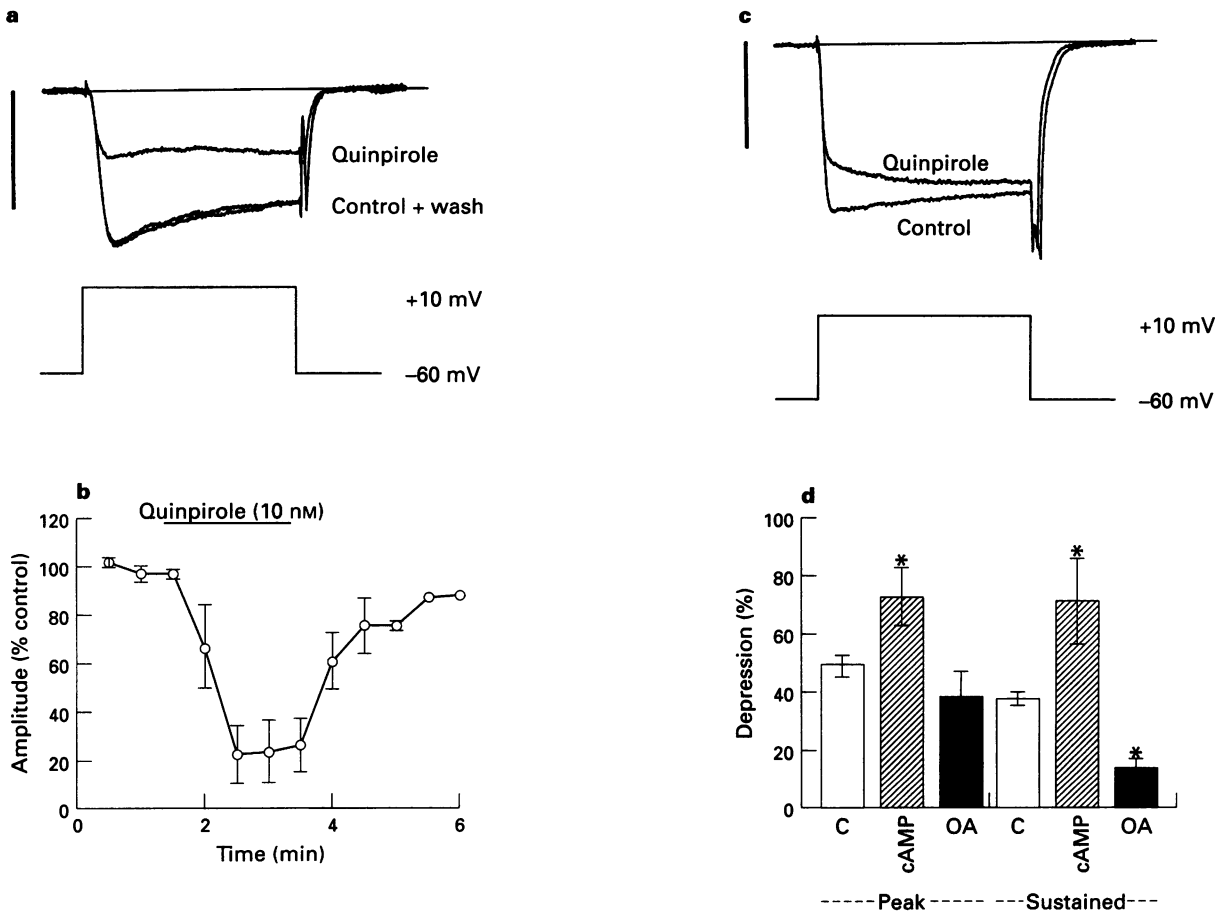

Figure 3 Potentiation of D_2 receptor depression of calcium currents by elevation of intracellular cyclic AMP, and the selective occlusion of the sustained depression by inhibition of protein phosphatase activity with okadaic acid. (a) Superimposed calcium currents recorded after dialysis with 100 μM cyclic AMP (control), following equilibration in quinpirole (10 nM), and after washing for 2 min. Calibration bar = 1 nA. (b) Time course of depression of calcium currents with quinpirole demonstrating that the potentiation of the responses to quinpirole with $[\text{cyclic AMP}]_i$ was readily reversible. Data are pooled from 5 cells. (c) Superimposed whole cell calcium currents elicited after equilibration in 100 nM okadaic acid (control) and following perfusion with quinpirole (10 nM). Calibration bar = 1 nA. (d) Histogram depicting increase in both the peak and sustained inhibition of calcium currents by 100 μM $[\text{cyclic AMP}]_i$ ($n=5$), and the selective attenuation of the depression of the sustained calcium current with 100 nM okadaic acid ($n=4$). Asterisks denote significant difference at $P<0.01$ from control.

which is also attenuated by dihydropyridines (Seabrook *et al.*, 1994b). The proportion of the high-threshold current inhibited by D_2 receptors in differentiated NG108-15 cells was much greater than that observed in D_2 transfected GH_4C_1 pituitary cells (Seabrook *et al.*, 1994a,b). This is most likely due to the low density, if any, of dihydropyridine resistant N-type calcium channels in GH_4C_1 cells. In the present study two components to the inhibition of ω-conotoxin GVIa-sensitive high-threshold calcium current were observed. These involved a decrease in rate of current activation (type 1) and the steady state depression of the sustained current at the end of a 100 ms voltage step (type 2). Both type 1 and type 2 depression were evident on N-type calcium currents that were recorded in the presence of nisoldipine, a dihydropyridine calcium channel antagonist. A decrease in rate of calcium current activation has also been described following activation of other receptor subtypes including $GABA_B$ receptors (Scott *et al.*, 1991) which are known to couple by signal transduction mechanisms similar to $D_{2\text{-like}}$ dopamine receptors on midbrain dopamine neurones (Lacey *et al.*, 1987). In rat dorsal root ganglia neurones, $GABA_B$ receptors inhibit calcium channels via α_o G-protein subunits (Campbell *et al.*, 1993). Similarly, inhibition of L-type calcium channels in pituitary cells by D_2 receptors can be blocked by antibodies and antisense oligonucleotides designed against α_o G-protein subunits (Lledo *et al.*, 1992). Consistent with the direct involvement of G-proteins in D_2 receptor inhibition of N-type calcium channels in NG108-15 cells, responses to quinpirole were rendered irreversible by the non-hydrolysable GTP analogue GTP-γ-S and were inhibited by pertussis toxin.

D_2 dopamine receptors can also activate α_i G-protein subunits which in turn inhibit adenylate cyclase activity (e.g. Kebabian & Calne, 1979). This enzyme catalyses the production of cyclic AMP from ATP, and thus activation of D_2 receptors can decrease intracellular cyclic AMP levels. To exclude the possibility that inhibition of calcium currents was due to a reduction in $[\text{cyclic AMP}]_i$ the effect of raising $[\text{cyclic AMP}]_i$ by including it in the patch pipette was examined. However, instead of masking the effects of D_2 receptor activation, raised $[\text{cyclic AMP}]_i$ increased the proportion of the calcium current that was depressed. Consequently inhibition of adenylate cyclase activity was not the mechanism by which D_2 receptors depress calcium currents in these cells. Stimulation of cyclic AMP-dependent protein kinases has been shown to increase L-type calcium currents (reviewed in Hescheler *et al.*, 1990), suggesting that cyclic AMP may be increasing the proportion

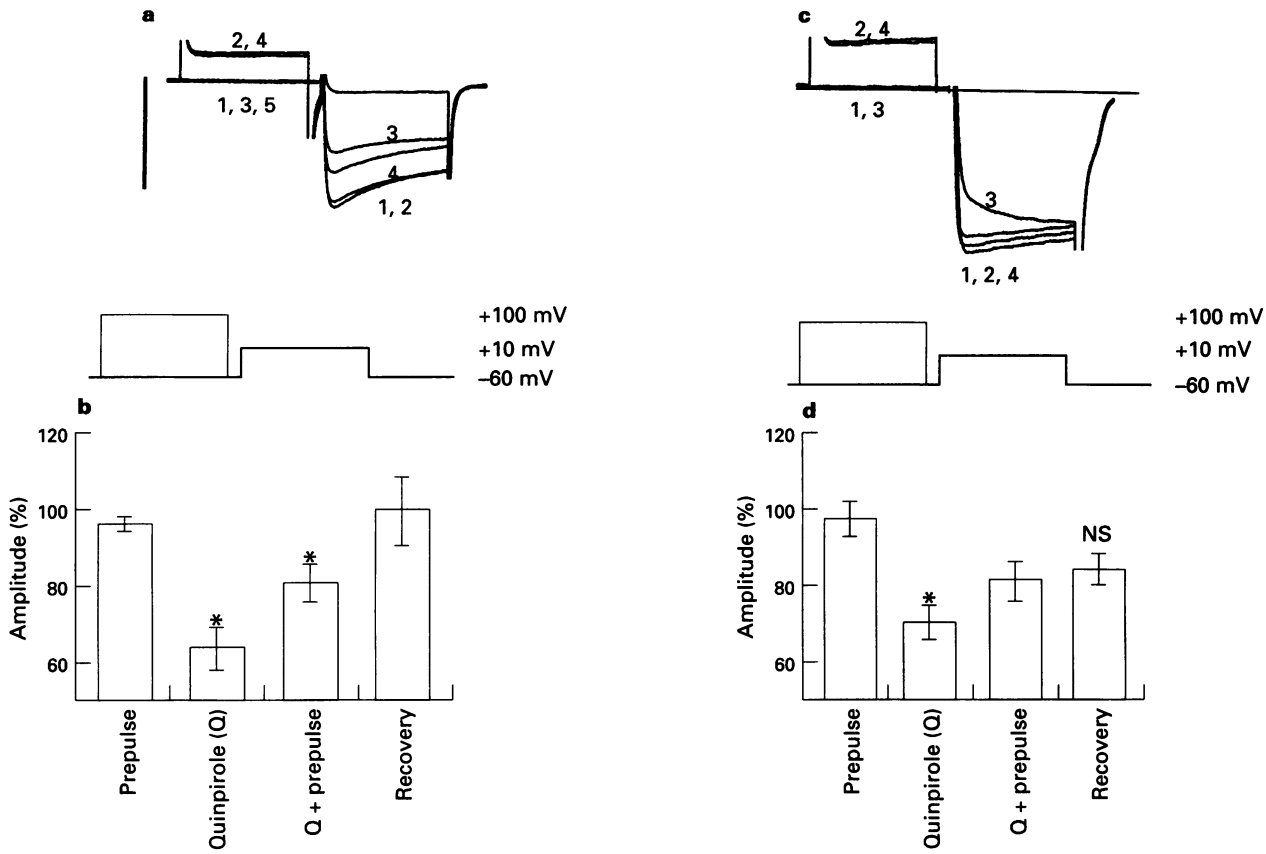

Figure 4 Voltage-dependence of calcium current inhibition under control conditions, and after the selective depression of the sustained inhibition with intracellular perfusion with okadaic acid. (a) Superimposed calcium currents recorded under control conditions (1) and following a 100 ms prepulse to +100 mV, and in the presence of 10 nM quinpirole (3) and following the +100 mV prepulse (4). Note that both the outward current elicited at +100 mV, which is probably due to the outward flux of Cs^+ ions through calcium channels, and the inward calcium currents are completely inhibited by bath application of 100 μM $CdCl_2$. Lower trace represents superimposed holding potentials used to elicit the currents described above, calibration bar = 2 nA. (b) Histogram summarising the voltage-dependence of D_2-receptor mediated inhibition of calcium currents under control conditions. The prepulse alone did not affect the amplitude of the calcium current, but significantly reduced the depression, albeit incompletely, caused by 10 nM quinpirole ($n=7$, $P<0.01$). (c) Reversal of the decrease in rate of calcium current activation, that was unmasked following treatment with 100 nM okadaic acid, with prepulses to +100 mV. Annotations are the same as in (a). Capacitance transients are blanked for clarity. (d) Histogram depicting the mean depression with quinpirole (10 nM) under control conditions and with a prepulse to +100 mV. Note that the rundown of the calcium current was more accentuated after treatment with okadaic acid, and that the slowing in rate of current activation was fully reversed with the depolarizing prepulse compared to the recovery. $^*P<0.05$; NS = non-significant.

of the D_2-sensitive current. However, this cannot explain our data because the principal effect of D_2 receptor activation was on the dihydropyridine-insensitive high-threshold current, and the calcium current density in cyclic AMP dialysed cells was not significantly affected. Furthermore, in whole cell patch clamp studies where adenylate cyclase was directly activated with forskolin the amplitude of N-type calcium current was unaffected (Kasai 1991; this study). This insensitivity to forskolin contrasts with the effect of directly increasing [cyclic AMP]$_i$ levels which potentiated the calcium current inhibition by D_2 receptors. This may be a consequence of either forskolin generating less [cyclic AMP]$_i$ during relatively short incubation periods (< 10 min), the effects of channel phosphorylation being evident only on channels that have been modified by G-protein subunits following D_2 receptor stimulation, or alternatively to a direct action of cyclic AMP on D_2 receptors or its associated signal transduction pathway(s). N-type calcium channel $\alpha 1$ subunits are indeed substrates for phosphorylation by cyclic AMP-dependent protein kinase A (Hell *et al.*, 1994). Thus potentiation of responses to D_2 receptor activation with elevated [cyclic AMP]$_i$ may involve direct phosphorylation of channels by PKA. Irrespective of the precise mechanisms involved, potentiation of D_2 receptor-mediated inhibition of calcium channel function with [cyclic AMP]$_i$ may help explain the paradoxical functional synergism between these receptors and the D_1 dopamine subtype (Clark & White, 1987; Momiyama *et al.*, 1993), which are known to have opposing effects on adenylate cyclase activity (Kebabian & Calne, 1979). To test further the hypothesis that phosphorylation was necessary for D_2 receptor-mediated inhibition of N-type calcium currents, the effects of stimulating protein kinase C and inhibition of protein phosphatase activity were examined.

It was unlikely that $[Ca^{2+}]_i$ mobilisation was a critical determinant of calcium current regulation by D_2 receptor activation in NG108-15 cells because chelation of $[Ca^{2+}]_i$ with EGTA did not block this effect. Likewise, substitution of Ca^{2+} ions with Ba^{2+} as the charge carrier did not prevent the inhibition of calcium currents but actually enhanced it, a phenomenon that was probably due to the removal of calcium-dependent inactivation (Kalman *et al.*, 1991). Further evidence that D_2 receptor inhibition of calcium currents did not involve $[Ca^{2+}]_i$ mobilisation was that quinpirole (10 nM to 10 μM) had no effects upon $[Ca^{2+}]_i$ levels, which was studied using FURA-2 microspectrofluorimetry in the same clonal cell line (unpublished observations; however cf. rat D_2 receptors in Castellano *et al.*, 1993). Calcium-dependent enzymes, such as protein kinase C, have also been implicated in the regulation of calcium channel activity (Rane & Dunlap, 1986; 1990). Thus to test for its involvement the action of the diacylglycerol analogue OAG was examined (Gilmore & Martin, 1983; Nishizuka, 1984). When calcium was used as the charge carrier the sustained depression of calcium currents (type 2 inhibition) was selectively attenuated by pretreatment with OAG, without any effect on the D_2 receptor mediated decrease in rate of calcium current activation (type 1). Thus under certain circumstances calcium influx through channels in NG108-15 cells may contribute to N-type calcium current inhibition via PKC activation.

D_2 dopamine receptors can also potentiate phospholipase A_2 (PLA_2) activity in a cyclic AMP-dependent manner (Kanterman *et al.*, 1991). PLA_2 catalyses the hydrolysis of phospholipids to produce arachidonic acid which can directly modulate ion channel activity. However, PLA_2, like PKC, is a Ca^{2+}-dependent enzyme and alone arachidonic acid does not modulate N-type calcium current activity in these cells (Kasai, 1991). Other kinases including cyclic GMP-dependent protein kinases have also been implicated in neurotransmitter receptor modulation of calcium channel function (Meriney *et al.*, 1994). No evidence for this pathway in regulating N-type calcium currents in NG108-15 cells was found because these currents were unaffected by either the membrane permeant cyclic GMP analogue Sp-8-Br-cGMP, or by the cyclic GMP antagonist Rp-8-Br-cGMP.

Thus D_2 receptors inhibit calcium currents in NG108-15 cells by mechanism(s) that do not involve inhibition of adenylate cyclase activity, calcium mobilisation, or potentiation of arachidonic acid release, but that under certain circumstances is dependent upon channel phosphorylation by PKC, and cyclic AMP-dependent protein kinases. The involvement of channel phosphorylation was confirmed by the ability of okadaic acid to occlude the inhibition of the sustained calcium current following receptor activation. Okadaic acid selectively inhibits protein phosphatases 1/2A and thus can prevent protein dephosphorylation. Under circumstances where there are background levels of phosphorylation, inhibition of phosphatase activity would increase the number of channels that were phosphorylated and hence inactivated. Therefore control calcium currents in okadaic acid would already be partly depressed. Consistent with this no sustained inhibition of the high-threshold calcium current was observed with quinpirole after treatment with intracellular okadaic acid. Furthermore, okadaic acid selectively isolated the kinetic slowing that was associated with receptor activation. Thus type 1 and type 2 inhibition of N-type calcium currents were mediated by two distinct processes. It was possible to distinguish further between these components by their voltage-dependence.

Neurotransmitter receptor modulation of N- and L-type calcium currents in neurones of sympathetic ganglia involves both cytosolic and membrane delimited pathways (Beech *et al.*, 1992; Hille, 1992). These pathways are distinguished into components that are voltage-dependent and voltage-resistant in that depolarizing prepulses applied immediately preceding the test pulse can relieve the inhibition. In differentiated NG108-15 cells the decrease in rate of activation of N-type calcium currents caused by activation of endogenous opiate receptors can also be reversed in a voltage-dependent manner (Kasai, 1992). Likewise in the present study the kinetic slowing of calcium currents caused by D_2 receptors, which was unmasked following pretreatment with okadaic acid, could be reversed by depolarizing prepulses to +100 mV. In contrast, the sustained inhibition of calcium currents was only partly reduced by these prepulses and thus was voltage-resistant. The term voltage-resistant is used here intentionally because it is known that disruption of the direct interaction of G-proteins with calcium channels by positive membrane potentials undergoes a time-dependent relaxation when the membrane is repolarized to negative values. However, unlike noradrenoceptor inhibition of calcium currents in sympathetic neurones (Beech *et al.*, 1992), both the sustained depression and kinetic slowing following D_2 receptor activation in NG108-15 cells involved pertussis toxin-sensitive G-proteins.

The importance of protein phosphorylation for the inhibition of ω-conotoxin GVIa-sensitive calcium currents by D_2 receptors in NG108-15 cells contrasts with the effects of phosphorylation on dihydrophyridine-sensitive calcium channels. Phosphorylation of these calcium channel α subunits, for example by cyclic AMP-dependent PKA, increases single channel activity and can thus potentiate the amplitude of macroscopic L-type calcium currents (reviewed in Dolphin, 1995). In sympathetic neurones, PKC activation also precludes neurotransmitter-mediated inhibition of N-type calcium currents (Rane & Dunlap, 1986; 1990). These latter findings have been considered controversial (reviewed by Scott *et al.*, 1991; Dolphin, 1995). But combined with results from the present study this suggests that the importance of phosphorylation, whether inhibitory by increasing the susceptibility of calcium currents to inhibition by G-proteins, or excitatory, depends upon the calcium channel subtype that is affected.

In conclusion, this study demonstrates that the short isoform of the human D_2 dopamine receptor can selectively inhibit N-type calcium currents in differentiated NG108-15 cells. Modulation of these calcium channel currents was mediated via pertussis toxin-sensitive G-proteins and involved two distinct pathways. The decrease in rate of calcium current activation (type 1) involved a voltage-dependent pathway, whereas the sustained inhibition of the calcium current (type 2) in-

volved, in part, the voltage-resistant phosphorylation by cyclic AMP-dependent protein kinases and dephosphorylation by protein phosphates 1/2A. The accentuation of D_2 receptor-mediated inhibition of neuronal calcium currents by cyclic AMP may help explain how D_1 receptor activation can potentiate the effects of D_2 receptor agonists in brain.

The authors are grateful for technical assistance from Jan Myers.

References

BEECH, D.J., BERNHEIM, L. & HILLE, B. (1992). Pertussis toxin and voltage-dependence distinguish multiple pathways modulating calcium channels of rat sympathetic neurons. *Neuron*, **8**, 97–106.

CAMPBELL, V., BERROW, N. & DOLPHIN, A.C. (1993). $GABA_B$ receptor modulation of Ca^{2+} currents in rat sensory neurones by the G protein G_o: antisense oligonucleotide studies. *J. Physiol.*, **470**, 1–11.

CASTELLANO, M.A., LIU, L.-X., MONSMA, F.J., SIBLEY, D.R., KAPATOS, G. & CHIODO, L.A. (1993). Transfected D_2 short dopamine receptors inhibit voltage-dependent potassium current in neuroblastoma x glioma hybrid (NG108-15) cells. *Mol. Pharmacol.*, **44**, 649–656.

CASTRO, S.W. & STRANGE, P.G. (1993). Differences in the ligand binding properties of the short and long versions of the D_2 dopamine receptor. *J. Neurochem.*, **60**, 373–375.

CAULFIELD, M.P., ROBBINS, J. & BROWN, D.A. (1992). Neurotransmitters inhibit the omega-conotoxin sensitive component of calcium current in neuroblastoma x glioma hybrid (NG-108-15) cells, not the nifedipine-sensitive component. *Pflügers Arch.*, **420**, 486–492.

CLARK, D. & WHITE, F.J. (1987). Review: D_1 dopamine receptor–the search for function: A critical evaluation of the $D_{1/D2}$ dopamine receptor classification. *Synapse*, **1**, 347–388.

DOCHERTY, R.J. (1988). Gadolinium blocks a component of calcium current in rodent neuroblastoma x glioma hybrid (NG108-15) cells. *J. Physiol.*, **398**, 33–47.

DOLPHIN, A.C. (1995). Voltage-dependent calcium channels and their modulation by neurotransmitters and G proteins. *Exp. Physiol.*, (in press).

FISHMAN, M.C. & SPECTOR, I. (1981). Potassium current suppression by quinidine reveals additional calcium currents in neuroblastoma cells. *Proc. Natl. Acad. Sci. U.S.A.*, **78**, 5245–5249.

GILMORE, T. & MARTIN, G.S. (1983). Phorbol ester and diacylglycerol induce protein phosphorylation at tyrosine. *Nature*, **306**, 487–490.

GRANDY, D.K. & CIVELLI, O. (1992). G-protein coupled receptors: the new dopamine receptor subtypes. *Curr. Opin. Neurobiol.*, **2**, 275–281.

HELL, J.W., APPLEYARD, S.M., YOKOYAMA, C.T., WARNER, C. & CATTERALL, W.A. (1994). Differential phosphorylation of two size forms of the N-type calcium channel α1 subunit which have different COOH termini. *J. Biol. Chem.*, **269**, 7390–7396.

HERDON, H. & NAHORSKI, S.R. (1989). Investigations of the roles of dihydropyridine and ω-conotoxin-sensitive calcium channels in mediating depolarisation-evoked endogenous dopamine release from striatal slices. *Naunyn-Schmied. Arch Pharmacol.*, **340**, 36–40.

HERING, S., BODEWEI, R., SCHUBERT, B., ROHDE, K. & WOLLENBERGER, A. (1985). A kinetic analysis of the inward current in 108CC15 neuroblastoma x glioma hybrid cells. *Gen. Physiol. Biophys.*, **4**, 129–141.

HESCHELER, J., ROSENTHAL, W., TRAUTWEIN, W. & SCHULTZ, G. (1990). Receptor-ion channel coupling through G-protein. pp. 383–408. Chapter 16 in *G proteins* ed. Iyengar, R. & Birnbaumer, L. New York: Academic Press.

HILLE, B. (1992). G-protein coupled mechanisms and neurones signalling. *Neuron*, **9**, 187–195.

KALMAN, D., O'LAGUE, P.H., ERXLEBEN, C. & ARMSTRONG, D.L. (1991). Calcium-dependent inactivation of the dihydropyridine-sensitive calcium channel. *J. Gen. Physiol.*, **92**, 531–548.

KANTERMAN, R.Y., MAHAN, L.C., BRILEY, E.M., MONSMA, F.J., SIBLEY, D.R., AXELROD, J. & FELDER, C.C. (1991). Transfected D_2 dopamine receptors mediate the potentiation of arachidonic acid release in chinese hamster ovary cells. *Mol. Pharmacol.*, **39**, 364–369.

KASAI, H. (1991). Tonic inhibition and rebound facilitation of a neuronal calcium channel by a GTP-binding protein. *Proc. Natl. Acad. Sci. U.S.A.*, **88**, 8855–8859.

KASAI, H. (1992). Voltage- and time-dependent inhibition of neuronal calcium channels by a GTP-binding protein in a mammalian cell line. *J. Physiol.*, **448**, 189–209.

KASAI, H. & NEHER, E. (1992). Dihydropyridine-sensitive and ω-conotoxin-sensitive calcium channels in a mammalian neuroblastoma-glioma cell line. *J. Physiol.*, **448**, 161–188.

KEBABIAN, J.W. & CALNE, D.B. (1979). Multiple receptors for dopamine. *Nature*, **277**, 93–96.

KEJA, J.A., STOOF, J.C. & KITS, K.S. (1992). Dopamine D_2 receptor stimulation differentially affects voltage-activated calcium channels in rat pituitary melanotropic cells. *J. Physiol.*, **450**, 409–435.

KLEUSS, C., HESCHELER, J., EWEL, C., ROSENTHAL, W., SCHULTZ, G. & WITTIG, B. (1991). Assignment of G-protein subtypes to specific receptors inducing inhibition of calcium currents. *Nature*, **353**, 43–48.

LACEY, M.G., MERCURI, N.B. & NORTH, R.A. (1987). Dopamine acts on D_2 receptors to increase potassium conductance in neurones of the rat substantia nigra zona compacta. *J. Physiol.*, **392**, 397–416.

LAHOSTE, G.J. & MARSHALL, J.F. (1993). The role of dopamine in the maintenance and breakdown of D1/D2 synergyism. *Brain Res.*, **611**, 108–116.

LEYSEN, J.E., GOMMERGEN, W., MERTENS, J., LUYTEN, W.H.M.L., PAUWELS, P.J., EWERT, M. & SEEBURG, P. (1993). Comparison of *in vitro* binding properties of a series of dopamine antagonists and agonists for cloned human dopamine D_{2S} and D_{2L} receptors and for D_2 receptors in rat striatal and mesolimbic tissues, using [^{125}I] 2′-iodospiperone. *Psychopharmacology*, **110**, 27–36.

LLEDO, P.M., HOMBURGER, V., BOCKAERT, J. & VINCENT, J.-D. (1992). Differential G protein-mediated coupling of D_2 dopamine receptors to K^+ and Ca^{2+} currents in rat anterior pituitary cells. *Neuron*, **8**, 455–463.

LLEDO, P.M., LEGENDRE, P., ISRAEL, J.-M. & VINCENT, J.-D. (1990). Dopamine inhibits two characterised voltage-dependent calcium currents in identified rat lactotroph cells. *Endocrinology*, **127**, 990–1001.

MCCLESKEY, E.W. (1994). Calcium channels: cellular roles and molecular mechanisms. *Curr. Opin. Neurobiol.*, **4**, 304–312.

MCFADZEAN, I. & DOCHERTY, R.J. (1989). Noradrenaline and enkephaline-induced inhibition of voltage-sensitive calcium currents in NG108-15 hybrid cells. *Eur. J. Neurosci.*, **1**, 141–147.

MERINEY, S.D., GRAY, D.B. & PILAR, G.R. (1994). Somatostatin-induced inhibition of neuronal Ca^{2+} current modulated by cGMP-dependent protein kinase. *Nature*, **369**, 336–339.

MOMIYAMA, T., TODO, N. & SASA, M. (1993). A mechanism underlying D_1 and D_2 receptor-mediated inhibition of dopaminergic neurones in the ventral tegmental area *in vitro*. *Br. J. Pharmacol.*, **109**, 933–940.

NACHSHEN, D.A. & SANCHEZ-ARMASS, S. (1987). Co-operative action of calcium ions in dopamine release from rat brain synaptosomes. *J. Physiol.*, **387**, 415–423.

NISHIZUKA, Y. (1984). The role of protein kinase C in cell surface signal transduction and tumor production. *Nature*, **308**, 693–698.

NUSSINOVITCH, I. & KLEINHAUS, A.L. (1992). Dopamine inhibits voltage-activated calcium channel currents in rat pars intermedia pituitary cells. *Brain Res.*, **574**, 49–55.

PIOMELLI, D., PILON, C., GIROS, B., SOKOLOFF, P., MARTRES, M.-P. & SCHWARTZ, J.-C. (1991). Dopamine activation of the arachidonic acid cascade as a basis for D_1/D_2 receptor synergism. *Nature*, **353**, 164–167.

RANE, S.G. & DUNLAP, K. (1986). Kinase C activator 1,2-oleoylacetylglycerol attenuates voltage-dependent calcium currents in sensory neurones. *Proc. Natl. Acad. Sci. U.S.A.*, **83**, 184–188.

RANE, S.G. & DUNLAP, K. (1990). G-protein and protein kinase C-mediated regulation of voltage-dependent calcium channels. pp. 357–381, Chapter 15 in *G-proteins*. ed. Iyengar, R. & Birnbaumer, L. New York: Academic Press.

SCHWARTZ, J.-C., GIROS, B., MARTRES, M.-P. & SOKOLOFF, P. (1992). The dopamine receptor family: molecular biology and pharmacology. *Semin. Neurosci.*, **4**, 99–108.

SCOTT, R.H., PEARSON, H.A. & DOLPHIN, A.C. (1991). Aspects of vetebrate neuronal voltage-activated calcium currents and their regulation. *Prog. Neurobiol.*, **36**, 485–520.

SEABROOK, G.R., MCALLISTER, G., KNOWLES, M.R., MYERS, J., SINCLAIR, H.A., PATEL, S., FREEDMAN, S.B. & KEMP, J.A. (1994b). Depression of high-threshold calcium currents by activation of human $D_{2(short)}$ dopamine receptors expressed in differentiated NG108-15 cells. *Br. J. Pharmacol.*, **111**, 1061–1066.

SEABROOK, G.R., KNOWLES, M.R., BROWN, N., MYERS, J., SINCLAIR, H.A., FREEDMAN, S.B. & MCALLISTER, G. (1994a). Pharmacology of high-threshold calcium currents in GH4C1 pituitary cells and their regulation by activation of human D_2 and D_4 receptors. *Br. J. Pharmacol.*, **112**, 728–734.

TSUNOO, A., YOSHI, M. & NARAHASHI, T. (1986). Block of calcium channels by enkephalin and somatostatin in neuroblastoma-glioma hybrid NG108-15 cells. *Proc. Natl. Acad. Sci. U.S.A.*, **83**, 9832–9836.

ZHAO, X.-I., GUTIERREZ, L.M., CHANG, C.F. & HOSEY, M.M. (1994). The α1-subunit of skeletal muscle L-type calcium channels is the key target for regulation by A-kinase and protein phosphatase 1C. *Biochem. Biophys. Res. Commun.*, **198**, 166–173.

(Received January 16, 1995
Revised February 16, 1995
Accepted March 1, 1995)

British Journal of Pharmacology (1995) 115, 467-475

Evidence for a functional α_{1A}- (α_{1C}-) adrenoceptor mediating contraction of the rat epididymal vas deferens and an α_{1B}-adrenoceptor mediating contraction of the rat spleen

Richard P. Burt, *Christopher R. Chapple & [1]Ian Marshall

Department of Pharmacology, University College London, Gower Street, London WC1E 6BT and *Department of Urology, The Royal Hallamshire Hospital, Glossop Road, Sheffield S10 2JF

1 The α_1-adrenoceptor subtype mediating contraction of the rat epididymal vas deferens and rat spleen has been investigated by use of α_1-adrenoceptor antagonists that have shown selectivity between the different cloned receptor subtypes.

2 In the rat epididymal vas deferens the potency of noradrenaline and phenylephrine was increased in the presence of neuronal and extra-neuronal uptake blockers, cocaine and β-oestradiol, but these did not alter that of methoxamine. The order of potency of the agonists in the presence or absence of uptake blockade was noradrenaline > phenylephrine > methoxamine. In the rat spleen the potency of these agonists was not altered in the presence of cocaine and β-oestradiol, and their order of potency was the same as in the vas deferens.

3 The non subtype selective α_1-adrenoceptor antagonist prazosin (up to 1×10^{-7} M) was found to antagonize contractions to noradrenaline in the vas deferens competitively (pA_2 9.2), but only in a non competitive manner in the spleen. Contractions to phenylephrine in the spleen however were competitively antagonized by prazosin (up to 1×10^{-7} M) with a pA_2 of 9.2. This suggests that there is an α_1- and a non α_1-adrenoceptor response to noradrenaline in the rat spleen.

4 Pretreatment with chlorethylclonidine (10^{-4} M for 30 min) did not alter the noradrenaline contractions in the vas deferens, but contractions to noradrenaline and phenylephrine in the spleen were shifted 30 and 300 fold to the right of the control curve, respectively. This suggests that only the contractions in the spleen were mediated by α_{1B}-adrenoceptors.

5 The noradrenaline contractions in the vas deferens were competitively antagonized by WB 4101 (pA_2 9.6), 5-methyl-urapidil (pA_2 8.7), phentolamine (pA_2 8.3), benoxathian (pA_2 9.4), spiperone (pA_2 7.5), indoramin (pA_2 8.4) and BMY 7378 (pA_2 6.7), consistent with the affinities of these antagonists in binding studies on tissue α_{1A}-adrenoceptors. These values correlated best with their published affinities on the expressed α_{1c}-adrenoceptor clone and poorly with those at either the expressed α_{1b}- or α_{1d}-adrenoceptor clones. Therefore the classical α_{1A}-adrenoceptor appears to be the same as the expressed α_{1c}-adrenoceptor clone.

6 The phenylephrine contractions in the spleen were competitively antagonized by WB 4101 (pA_2 8.1), 5-methyl-urapidil (pA_2 7.1), phentolamine (pA_2 7.3), benoxathian (pA_2 7.4), spiperone (pA_2 7.9), indoramin (pA_2 7.5) and BMY 7378 (pA_2 7.4), consistent with the affinities of these antagonists in binding studies on tissue α_{1B}-adrenoceptors. The pA_2 values correlated best with the published affinities of these compounds on the expressed α_{1b}-adrenoceptor clone and poorly with those at either the expressed α_{1d}- or α_{1c}-adrenoceptor clones. Therefore the α_{1B}-adrenoceptor appears to be the same as the expressed α_{1b}-adrenoceptor clone.

7 The results provide pharmacological evidence that the α_1-adrenoceptor mediating noradrenaline contractions in the epididymal portion of the rat vas deferens is the α_{1A}-(α_{1C}) subtype and that contractions to phenylephrine in the rat spleen are mediated by the α_{1B}-subtype.

Keywords: α_1-Adrenoceptor subtypes; rat vas deferens; rat spleen; WB 4101; 5-methyl-urapidil; spiperone; benoxathian; indoramin; BMY 7378; chlorethylclonidine

Introduction

There has been evidence for the existence of subtypes of the α_1-adrenoceptor for several years. High and low affinity site binding of WB 4101 for α_1-adrenoceptors in rat brain was found by Morrow & Creese (1986). Functional and binding studies showed that chlorethylclonidine alkylated α_1-adrenoceptors in certain tissues to a much greater extent than in others, and these chlorethylclonidine-sensitive receptors had a lower affinity for the competitive α_1-adrenoceptor antagonist, WB 4101 as compared with the chlorethylclonidine-insensitive receptors (Han *et al.*, 1987a,b). Receptors with a higher affinity for WB4101 were termed the α_{1A} subtype while those being more sensitive to alkylation by chlorethylclonidine were termed the α_{1B} subtype. Functionally defined receptors are now denoted by upper case and cloned receptors by lower case letters (Bylund *et al.*, 1994).

Two α_1-adrenoceptors have now been cloned from a rat cerebral cortex cDNA library (using a probe based on a hamster α_{1b}-adrenoceptor, Cotecchia *et al.*, 1988), which appeared to have pharmacological profiles in cell lines where they have been expressed corresponding to the α_{1A} and α_{1B} subtypes (Lomasney *et al.*, 1991). However a near identical clone to the one thought to correspond with the α_{1A} subtype was cloned by Perez *et al.* (1991). When expressed in cell lines this clone had a different pharmacological profile from the α_{1A} subtype as it was found to be partially chlorethylclonidine-sensitive and had a lower affinity for 5-methyl urapidil compared with tissue α_{1A}-

[1] Author for correspondence.

adrenoceptors. It was therefore termed the α_{1d} subtype and the two near identical clones were then sometimes referred to as the $\alpha_{1a/d}$ subtype. Schwinn & Lomasney (1992) subsequently agreed with Perez *et al.* (1991), showing that their clone when expressed in cell lines also had a low affinity for 5-methyl urapidil and benoxathian.

A third α_1-adrenoceptor has also been cloned, initially from a bovine brain cDNA library which when expressed had a similar pharmacology to the α_{1A} subtype except that it was also partially chlorethylclonidine-sensitive (Schwinn *et al.*, 1990) and was not thought to be expressed in the rat as it could not be detected by Northern blot analysis (Schwinn *et al.*, 1991). This receptor was termed α_{1c} (Schwinn *et al.*, 1990). A homologous clone of this subtype has now been found in the rat (Laz *et al.*, 1993; Perez *et al.*, 1994) and it has been suggested by Laz *et al.* (1993) and Forray *et al.* (1994a) that the rat α_{1c} clone is quite insensitive to chlorethylclonidine compared with the bovine clone. Recently using RNAse protection assays the α_{1c} clone has been found to be expressed in several rat tissues (Perez *et al.*, 1994; Rokosh *et al.*, 1994).

The affinities of several different antagonists have now been measured in binding studies using membranes from cells transfected with the cDNA for the three subtypes (Faure *et al.*, 1994; Forray *et al.*, 1994b; Kenny *et al.*, 1994a,b; Saussy *et al.*, 1994; Testa *et al.*, 1994; Goetz *et al.*, 1995). While prazosin was shown to be non selective, WB 4101, 5-methyl urapidil, phentolamine, benoxathian, spiperone, indoramin and BMY 7378 all showed some degree of selectivity. In particular BMY 7378 has recently been shown to be very selective for the α_{1d} subtype (Saussy *et al.*, 1994; Goetz *et al.*, 1995).

Using RNAse protection assays the α_{1b}, α_{1c} and α_{1d} clones have been found to be expressed in the rat vas deferens, while the α_{1b} and α_{1d} clones have been found to be expressed in the rat spleen (Perez *et al.*, 1994; Price *et al.*, 1994; Rokosh *et al.*, 1994). Functional experiments have shown that contractions to noradrenaline in the rat vas deferens were unaffected by chlorethylclonidine and had a relatively high affinity for WB 4101, suggesting that only the α_{1A}-adrenoceptor mediates the contraction here (Han *et al.*, 1987b; Burt *et al.*, 1992; Aboud *et al.*, 1993). Similar experiments showed that contractions to noradrenaline in the rat spleen were sensitive to chlorethylclonidine suggesting that the α_{1B} subtype mediates at least part of this contraction (Han *et al.*, 1987b; Burt *et al.*, 1992; Aboud *et al.*, 1993). The aims of this investigation were to characterize functionally the α_1-adrenoceptor mediating contractions in the rat epididymal vas deferens and rat spleen by use of the antagonists mentioned above and to see how well their affinities correlated with those that had previously been obtained on the three cloned subtypes.

Methods

Male Sprague Dawley rats between 350–450 g were stunned and killed by cervical dislocation. The vasa deferentia were removed, associated blood vessels and mesentery were dissected away and were then bisected so that only the epididymal portion (15–20 mm in length) was used. The spleen was also removed and bisected longitudinally into two strips. All the tissues were suspended in 5 ml tissue baths containing Krebs solution of the following composition (mM): Na^+ 143, K^+ 5.9, Ca^{2+} 2.5, Mg^{2+} 1.2, Cl^- 128, HCO_3^- 25, HPO_4^{2-} 1.2, SO_4^{2-} 1.2 and glucose 11, at 37°C and bubbled with 95% O_2/5% CO_2. The vas was placed under 0.5 g resting tension and equilibrated for 1 h. The spleen was placed under 1.0 g resting tension and equilibrated for 1.5 h. Changes in isometric tension were measured with Grass FT.03 transducers and recorded by Biopac Systems Inc. MP100WS for Windows.

Vas deferens

Non-cumulative additions of noradrenaline were used with a separation of 10 min between doses. The curve was then either repeated, or repeated in the presence of cocaine and β-oestradiol (both 10^{-5} M). In other tissues, cocaine and β-oestradiol were always present and after an initial concentration-effect curve to noradrenaline had been obtained, this was either repeated in the presence of an antagonist (equilibrated for 30 min) or a concentration-effect curve to another agonist was measured. When chlorethylclonidine was the antagonist it was incubated with the tissues for 30 min and then washed out for 30 min before another concentration-effect curve was established. All the responses were calculated as a percentage of the maximum response in the initial concentration-effect curve to noradrenaline.

Spleen

An initial contraction to a concentration of noradrenaline (1×10^{-4} M) which gave a maximum response was first measured in all the tissues followed 1 h later by a cumulative concentration-effect curve to noradrenaline or phenylephrine or methoxamine. These were then repeated either as repeat control curves or in the presence of cocaine and β-oestradiol (both 10^{-5} M) or in the presence of an antagonist (equilibrated for 30 min). When chlorethylclonidine was the antagonist it was incubated with the tissues for 30 min and then washed out for 30 min. In all experiments the repeat noradrenaline and methoxamine curves were carried out 1 h after the first curve. However, the repeat phenylephrine curve was begun 2 h after the first curve because contractions to phenylephrine took much longer to return to baseline during the washout period. The responses were calculated either as a percentage of the initial maximum response to noradrenaline (1×10^{-4} M) or the maximum response in the first concentration-effect curve.

Data analysis

All the results were plotted as the mean of at least 4 separate experiments with vertical bars representing standard error of the mean (s.e.mean). For the competitive antagonists prazosin, WB 4101, 5-methyl-urapidil, phentolamine, benoxathian, spiperone, indoramin and BMY 7378, Schild plots were constructed where the x axis intercept is equal to the pA_2 (Arunlakshana & Schild, 1959). Curve fitting for the calculation of EC_{50} values by non linear regression and linear regression for the calculation of pA_2 values was performed using InPlot (GraphPAD Software, San Diego, Calif., U.S.A.). Dose-ratios were calculated using the second concentration-response curve in the absence and presence of antagonist for both the vas and spleen.

Drugs and solutions

Prazosin hydrochloride, WB 4101 (2(2,6-dimethoxyphenoxyethyl)aminomethyl-1,4-benzodioxane hydrochloride), and chlorethylclonidine were donated by Pfizer Central Research, Kent; noradrenaline bitartrate, phenylephrine hydrochloride, methoxamine hydrochloride, cocaine hydrochloride, β-oestradiol and phentolamine were obtained from Sigma and 5-methyl-urapidil, benoxathian hydrochloride, spiperone hydrochloride and BMY 7378 dihydrochloride (8-(2-(4-(2-methoxyphenyl)-1-piperazinyl)ethyl)-8-azaspiro(4,5)decane-7,9-dione dihydrochloride) were obtained from RBI. All stock solutions were made in distilled water and diluted to working concentrations in Krebs solution except for prazosin, spiperone and β-oestradiol which were dissolved first in dimethylsulphoxide (DMSO) and then diluted in Krebs solution. Stock solutions of antagonists were stored frozen while agonists were prepared fresh each day.

Results

The potency of noradrenaline in the epididymal vas deferens and spleen was compared with that of phenylephrine and

methoxamine. On the vas deferens in the absence of uptake blocking drugs, noradrenaline and phenylephrine were equipotent and 2 times more potent than methoxamine (pD_2 5.6±0.1; 5.6±0.1 and 5.3±0.1 respectively, Figure 1a). In the presence of cocaine and β-eostradiol, both at 10^{-5} M, the noradrenaline and phenylephrine concentration-effect curves were shifted to the left but the methoxamine curve remained the same. Under these conditions noradrenaline was 3 and 50 times more potent than phenylephrine and methoxamine respectively (pD_2 7.0±0.1; 6.5±0.1 and 5.3±0.1 respectively, Figure 1b). All subsequent experiments with noradrenaline were carried out in the presence of the uptake inhibitors. Phenylephrine and methoxamine were both full agonists with respect to the maximum contraction evoked by noradrenaline (2.77±0.18 g). In the rat spleen the same order of potency for the agonists was obtained but they were not all full agonists. Noradrenaline (pD_2 5.2±0.1, maximum tension 0.35 g±0.02) was the most potent, followed by phenylephrine (pD_2 4.8±0.1, maximum response compared with noradrenaline of 95±2%) and methoxamine (pD_2 3.3±0.1 but which had not reached a maximum at the highest concentration used, 73±3% of noradrenaline maximum at 3×10^{-3} M) (Figure 2a). The addition of both cocaine and β-oestradiol (each 10^{-5} M) had no effect on the noradrenaline, phenylephrine or methoxamine curves (Figure 2b).

On the vas deferens, prazosin was a competitive antagonist of the noradrenaline contractions (pA_2 9.2 slope 1.02±0.03, Figure 3a). On the rat spleen prazosin at concentrations of 3×10^{-9} M and 1×10^{-8} M produced relatively small rightward shifts in the noradrenaline curve in an apparently competitive manner but at higher concentrations (3×10^{-8} M and 1×10^{-7} M) prazosin was not a competitive antagonist, with a slope of 0.71±0.08 for the Schild plot using all four concentrations (Figure 3b). Prazosin also produced a rightward shift of the phenylephrine curve and this time it acted as a competitive antagonist up to 1×10^{-7} M, (pA_2 9.2 slope 1.06±0.08, Figure 4).

Chlorethylclonidine at a concentration of 1×10^{-4} M had no effect on contractions to noradrenaline in the vas deferens (Figure 5a) but produced a 30 fold shift to the right in the noradrenaline control curve in the spleen (Figure 5b). However chlorethylclonidine (1×10^{-4} M) produced a 300 fold shift to

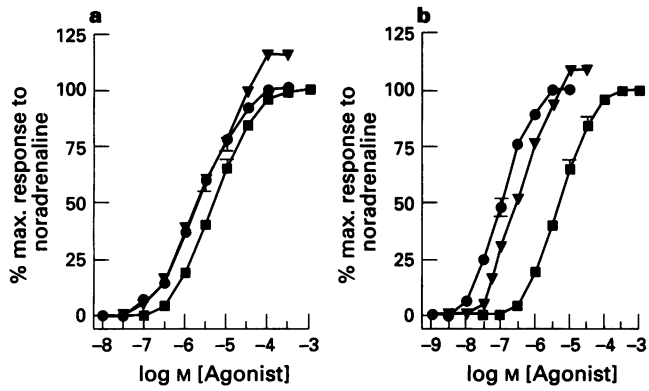

Figure 1 Non-cumulative concentration-effect curves for noradrenaline (●), phenylephrine (▼), and methoxamine (■), in rat epididymal vas deferens (a) without uptake blockade and (b) in the presence of cocaine (10^{-5}M) and β-oestradiol (10^{-5}M). Each plot represents the mean with s.e.mean of at least 4 separate experiments.

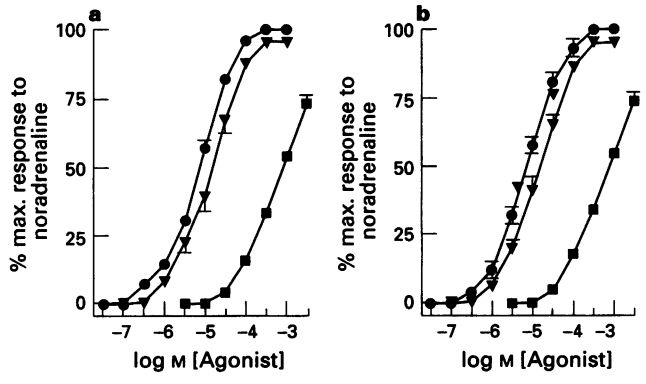

Figure 2 Cumulative concentration-effect curves for noradrenaline (●), phenylephrine (▼), and methoxamine (■), in rat spleen (a) without uptake blockade and (b) in the presence of cocaine (10^{-5}M) and β-oestradiol (10^{-5}M). Each plot represents the mean with s.e.mean of at least 4 separate experiments.

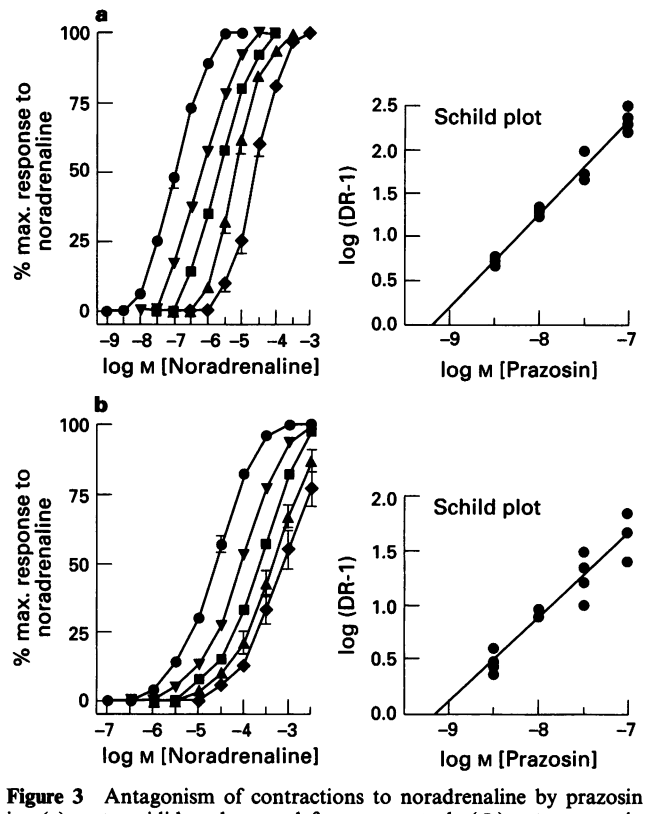

Figure 3 Antagonism of contractions to noradrenaline by prazosin in (a) rat epididymal vas deferens, control (●), + prazosin 3×10^{-9}M (▼), 1×10^{-8}M (■), 3×10^{-8}M (▲), and 1×10^{-7}M (◆) and (b) in rat spleen, control (●), + prazosin 3×10^{-9}M (▼), 1×10^{-8}M (■), 3×10^{-8}M (▲), and 1×10^{-7}M (◆). Each plot represents the mean with s.e.mean of at least 4 separate experiments.

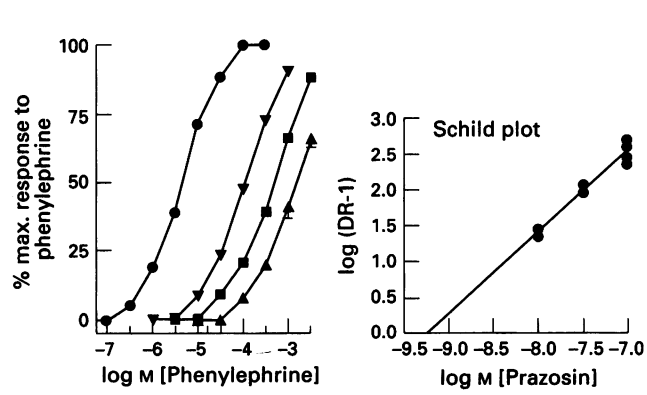

Figure 4 Antagonism of contractions to phenylephrine in rat spleen by prazosin: control (●), + prazosin 1×10^{-8}M (▼), 3×10^{-8}M (■), and 1×10^{-7}M (▲). Each plot represents the mean with s.e.mean of at least 4 separate experiments.

the right in the phenylephrine control curve in the spleen (Figure 5b), ten times greater than that produced against noradrenaline.

WB 4101, 5-methyl-urapidil, phentolamine, benoxathian, spiperone, indoramin and BMY 7378 were all competitive antagonists of the noradrenaline contractions in the vas deferens with pA_2 values of 9.6 (slope 1.00±0.08), 8.7 (slope 1.04±0.07), 8.3 (slope 1.02±0.03), 9.4 (slope 1.05±0.09), 7.5

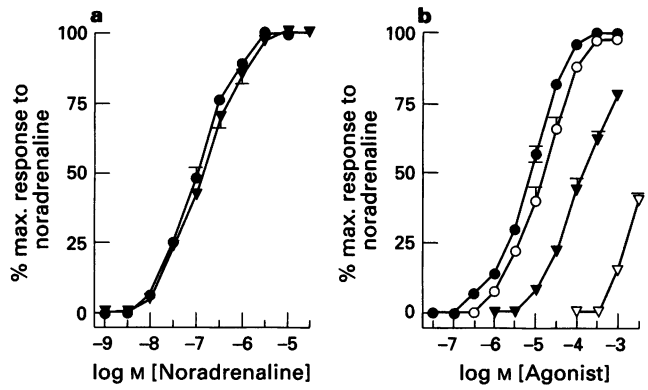

Figure 5 The effect of chlorethylclonidine (30 min incubation followed by 30 min washout) on (a) contractions in the rat epididymal vas deferens to noradrenaline: control (●), + chlorethylclonidine 10^{-4}M (▼) and (b) contractions in the rat spleen to noradrenaline, control (●), + chlorethylclonidine 10^{-4}M (▼) and phenylephrine control (○), + chlorethylclonidine 10^{-4}M (▽). Each plot represents the mean with s.e.mean of at least 4 separate experiments.

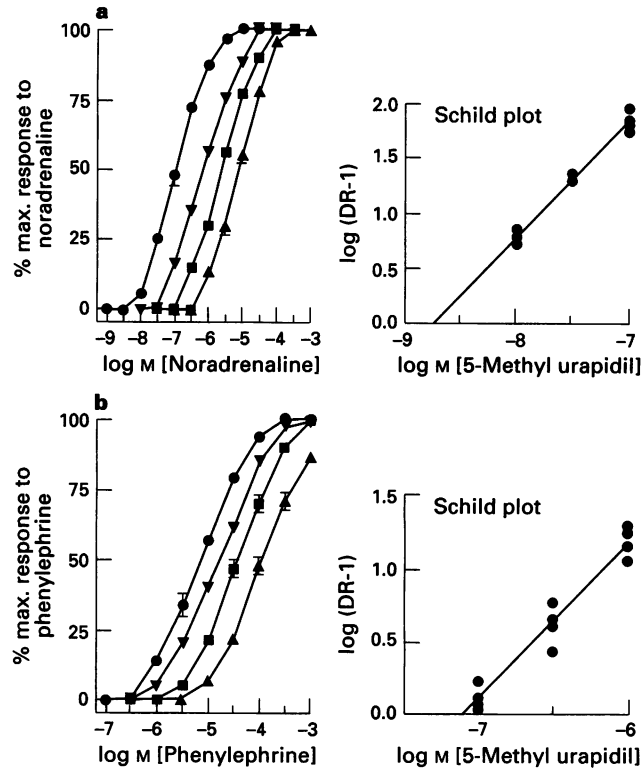

Figure 7 (a) Antagonism of contractions to noradrenaline in rat epididymal vas deferens by 5-methyl urapidil. Control (●), + 5-methyl urapidil 1×10^{-8}M (▼), 3×10^{-8}M (■), and 1×10^{-7}M (▲). (b) Antagonism of contractions to phenylephrine in rat spleen by 5-methyl urapidil. Control (●), + 5-methyl urapidil 1×10^{-7}M (▼), 3×10^{-7}M (■), and 1×10^{-6}M (▲). Each plot represents the mean with s.e.mean of at least 4 separate experiments.

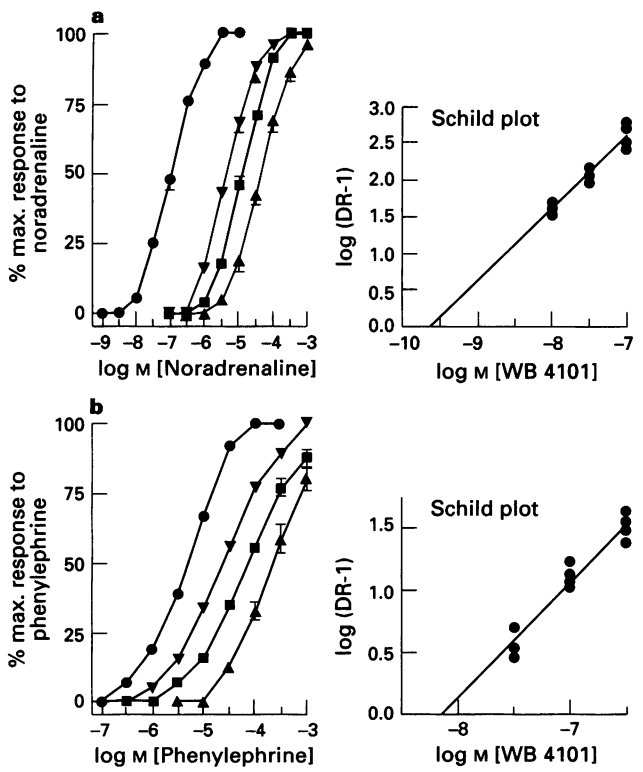

Figure 6 (a) Antagonism of contractions to noradrenaline in rat epididymal vas deferens by WB 4101. Control (●), + WB 4101 1×10^{-8}M (▼), 3×10^{-8}M (■), and 1×10^{-7}M (▲). (b) Antagonism of contractions to phenylephrine in rat spleen by WB 4101. Control (●), + WB 4101 3×10^{-8}M (▼), 1×10^{-7}M (■), and 3×10^{-7}M (▲). Each plot represents the mean with s.e.mean of at least 4 separate experiments.

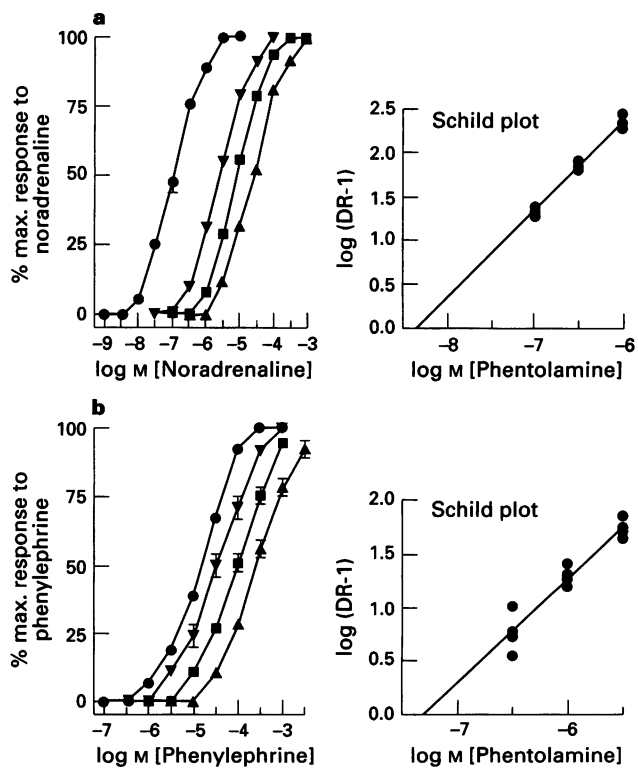

Figure 8 (a) Antagonism of contractions to noradrenaline in rat epididymal vas deferens by phentolamine. Control (●), + phentolamine 1×10^{-7}M (▼), 3×10^{-7}M (■), and 1×10^{-6}M (▲). (b) Antagonism of contractions to phenylephrine in rat spleen by phentolamine. Control (●), + phentolamine 3×10^{-7}M (▼), 1×10^{-6}M (■), and 3×10^{-6}M (▲). Each plot represents the mean with s.e.mean of at least 4 separate experiments.

(slope 1.02±0.03), 8.4 (slope 0.97±0.05) and 6.7 (slope 1.02±0.04) respectively (Figures 6a–12a). They were also competitive antagonists of the phenylephrine contractions in the spleen with the following pA_2 values, WB 4101 8.1 (slope 0.95±0.07), 5 methyl-urapidil 7.1 (slope 1.08±0.08), phentolamine 7.3 (slope 0.98±0.09), benoxathian 7.4 (slope 0.96±0.07), spiperone 7.9 (slope 0.96±0.05), indoramin 7.5 (slope 0.94±0.08) and BMY 7378 7.4 (slope 0.93±0.08) respectively (Figures 6b–12b).

Discussion

The α_1-adrenoceptor mediating contraction of rat epididymal vas deferens and rat spleen has been characterized by use of antagonists that have been found to show some subtype specificity when used in binding experiments on membranes from cells transfected with either the cloned α_{1d}- or the α_{1b}- or the α_{1c}-adrenoceptor.

When uptake mechanisms were blocked in the epididymal vas deferens the order of potency for the agonists was noradrenaline > phenylephrine > methoxamine. The agonists had the same order of potency in contracting the rat spleen but were not affected by uptake mechanisms. The order of affinity of these agonists measured in binding studies on membranes from rat 1 fibroblast cells expressing the three cloned α_1-adrenoceptor subtypes (Lomasney *et al.*, 1991) was the same for all three subtypes and the same as the functional order of potency in the vas deferens and spleen (Table 1). Thus this comparison is not very helpful in distinguishing between subtypes and as potency is a combination of affinity and efficacy it is not directly comparable.

In the vas deferens the competitive antagonism of noradrenaline contractions by prazosin was consistent with that expected for α_1-adrenoceptors. The concentration-response curve to noradrenaline was not altered by the alkylating agent chlorethylclonidine which shows that the contractions are not mediated via an α_{1B}-adrenoceptor subtype. WB 4101, 5-methyl-urapidil and benoxathian were all competitive antagonists with affinities similar to other reported values in this tissue (e.g. Aboud *et al.*, 1993). The high affinities of WB 4101, benoxathian, 5-methyl-urapidil and phentolamine and the low affinity of spiperone are consistent with the affinities of these antagonists measured in binding studies on α_{1A}-adrenoceptors using tissues expressing either just the α_{1A}-adrenoceptor e.g. guinea-pig liver (Garcia-Sainz & Romero-Avila, 1993) or only the α_{1A}-adrenoceptor after chlorethylclonidine treatment e.g. rat hippocampus (Testa *et al.*, 1993) and rat cerebral cortex (Kenny *et al.*, 1994a). Taken together these results show that the contractions to noradrenaline in the epididymal portion of the rat vas deferens are mediated by pharmacologically defined α_{1A}-adrenoceptors. This conclusion is in line with that of a number of other workers (Han *et al.*, 1987b; Hanft & Gross, 1989; Aboud *et al.*, 1993).

The nomenclature used so far to describe the α_1-subtypes is that most commonly employed (see *Trends Pharmacol. Sci.* Receptor Nomenclature Supplement, 1994) although one based on different affinities for prazosin and HV723 in the vasculature has been described (Muramatsu *et al.*, 1990). The latter group has recently reported that contractions to exogenous noradrenaline in the rat epididymal vas deferens are predominantly mediated via an α_{1L}-subtype which is characterized by low affinities for prazosin, WB 4101 and HV723 (Ohmura *et al.*, 1992). However their results differ from the present results and those of other workers who have not found the lower affinity of WB 4101 prazosin and benoxathian (Table 2). In addition the α_{1A} and α_{1B} subtypes have been classified by Muramatsu as part of the α_{1H} rather than α_{1L} group and thus this conclusion (Ohmura *et al.*, 1992) is incompatible with that of the present results and that of other workers.

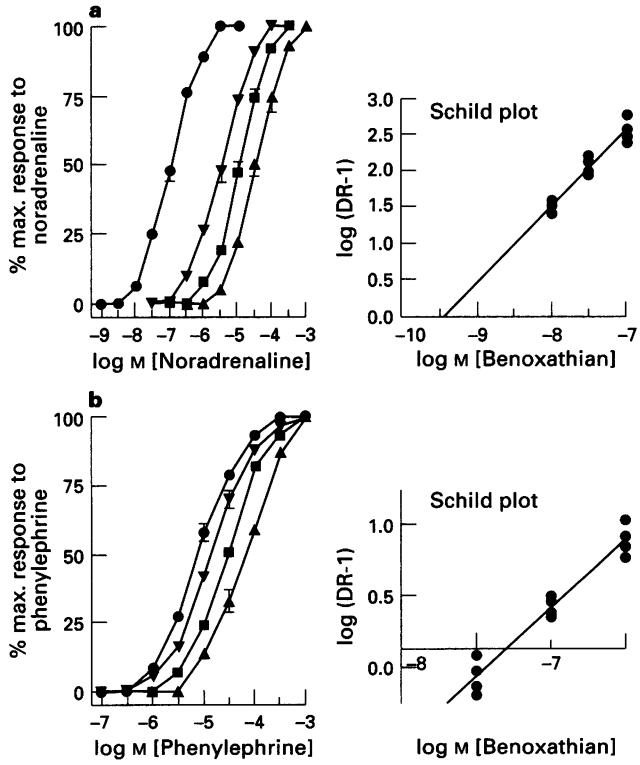

Figure 9 (a) Antagonism of contractions to noradrenaline in rat epididymal vas deferens by benoxathian. Control (●), + benoxathian 1×10^{-8}M (▼), 3×10^{-8}M (■), and 1×10^{-7}M (▲). (b) Antagonism of contractions to phenylephrine in rat spleen by benoxathian. Control (●), + benoxathian 3×10^{-8}M (▼), 1×10^{-7}M (■), and 3×10^{-7}M (▲). Each plot represents the mean with s.e.mean of at least 4 separate experiments.

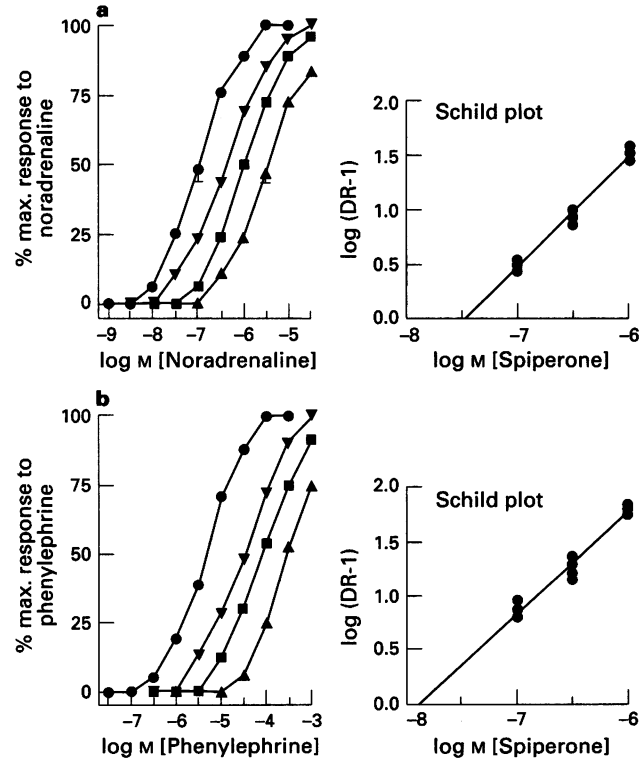

Figure 10 (a) Antagonism of contractions to noradrenaline in rat epididymal vas deferens by spiperone. Control (●), + spiperone 1×10^{-7}M (▼), 3×10^{-7}M (■), and 1×10^{-6}M (▲). (b) Antagonism of contractions to phenylephrine in rat spleen by spiperone. Control (●), + spiperone 1×10^{-7}M (▼), 3×10^{-7}M (■), and 1×10^{-6}M (▲). Each plot represents the mean with s.e.mean of at least 4 separate experiments.

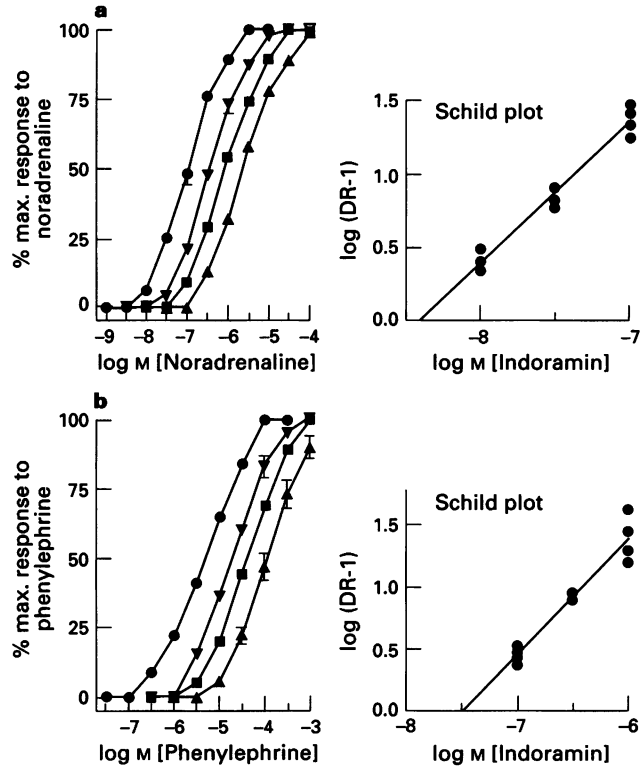

Figure 11 (a) Antagonism of contractions to noradrenaline in rat epididymal vas deferens by indoramin. Control (●), + indoramin 1×10^{-8} M (▼), 3×10^{-8} M (■), and 1×10^{-7} M (▲). (b) Antagonism of contractions to phenylephrine in rat spleen by indoramin. Control (●), + indoramin 1×10^{-7} M (▼), 3×10^{-7} M (■), and 1×10^{-6} M (▲). Each plot represents the mean with s.e.mean of at least 4 separate experiments.

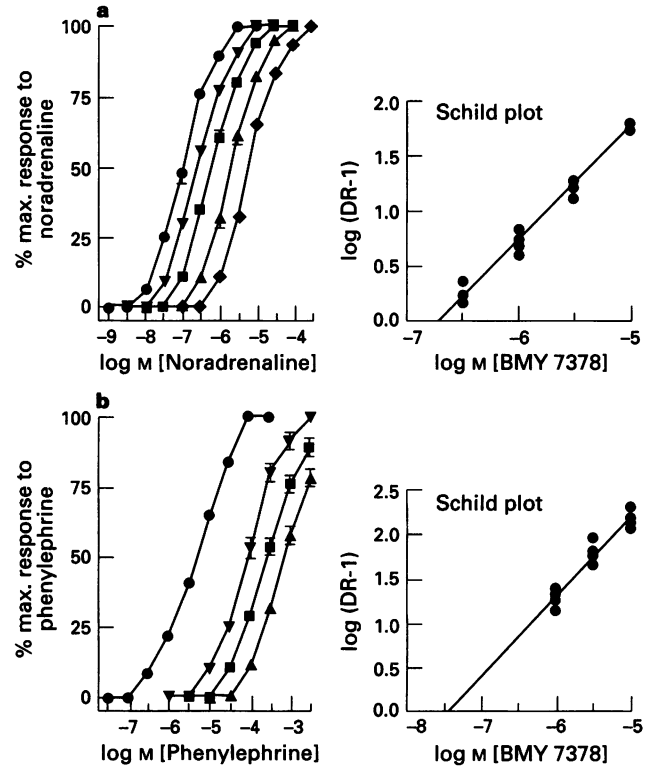

Figure 12 (a) Antagonism of contractions to noradrenaline in rat epididymal vas deferens by BMY 7378. Control (●), + BMY 7378 3×10^{-7} M (▼), 1×10^{-6} M (■), and 3×10^{-6} M (▲), and 1×10^{-5} M (◆). (b) Antagonism of contractions to phenylephrine in rat spleen by BMY 7378. Control (●), + BMY 7378 1×10^{-6} M (▼), 3×10^{-6} M (■), and 1×10^{-5} M (▲). Each plot represents the mean with s.e.mean of at least 4 separate experiments.

Table 1 Comparison of pD_2 values for the agonists with their published pK_i on cloned subtypes

	*pK_i values on cloned receptors expressed in COS-7 cells**			*pD_2 for contractile response*	
Agonist	rat $\alpha_{1a/d}$	rat α_{1b}	bovine α_{1c}	vas deferens	spleen
Noradrenaline	7.0	5.0	5.0	7.0	5.2
Phenylephrine	5.8	4.6	4.3	6.5	4.8
Methoxamine	4.0	2.8	3.7	5.3	3.3

*Data from Lomasney *et al.*, 1991.

Table 2 Comparison of pA_2 values for the antagonists with their published pK_i on cloned subtypes

	*pK_I on cloned α_1-adrenoceptors expressed in cells**			*pA_2 on contractile response*	
Antagonist	α_{1b}	α_{1c}	α_{1d}	vas deferens	spleen
Prazosin	9.6±0.2	9.2±0.2	9.4±0.2	9.2	9.2
WB 4101	8.2±0.1	9.5±0.3	9.2±0.1	9.6	8.1
5-Methyl urapidil	6.8±0.3	8.8±0.1	7.3±0.3	8.7	7.1
Phentolamine	7.3±0.2	8.1±0.3	7.6±0.2	8.3	7.3
Benoxathian	7.8	9.0	8.7	9.4	7.4
Spiperone	8.3±0.2	7.9±0.3	7.9±0.2	7.5	7.9
Indoramin	7.3±0.1	8.2±0.3	6.8±0.2	8.4	7.5
BMY 7378	7.2	6.6	9.4	6.7	7.4

*Data are mean±s.e.mean for values from Faure *et al.*, 1994; Forray *et al.*, 1994b; Kenny *et al.*, 1994a,b; Testa *et al.*, 1994 and Goetz *et al.*, 1995 (no s.e.mean for compounds with only one or two values). In each study the hamster α_{1b}, bovine α_{1c} and rat α_{1d} clones were used except for Forray *et al.*, (1994b) and Goetz *et al.*, (1995) where the three human α_1-subtype clones were used.

Prazosin caused a shift in the noradrenaline curve on the spleen but was a competitive antagonist only at concentrations which produced a relatively small shift to the right. At higher concentrations of prazosin the shift was no longer in a competitive manner. Prazosin is not a subtype selective α_1-antagonist so the response to noradrenaline in the rat spleen must contain a non α_1-adrenoceptor component, possibly mediated by α_2-adrenoceptors (Kenakin & Novak, 1987). To isolate only the α_1-adrenoceptor component of the contraction, phenylephrine was therefore tried as the agonist. In this case the phenylephrine contractions, unlike those to noradrenaline, were competitively antagonized by prazosin (pA_2 9.2), up to 1×10^{-7} M. This confirmed that the phenylephrine contractions were mediated by α_1-adrenoceptors with no non-α_1-adrenoceptor mediated component.

The responses to noradrenaline in the spleen were antagonized by the α_{1B} alkylating agent, chlorethylclonidine (Taddei *et al.*, 1993) at a concentration which had no effect on con-

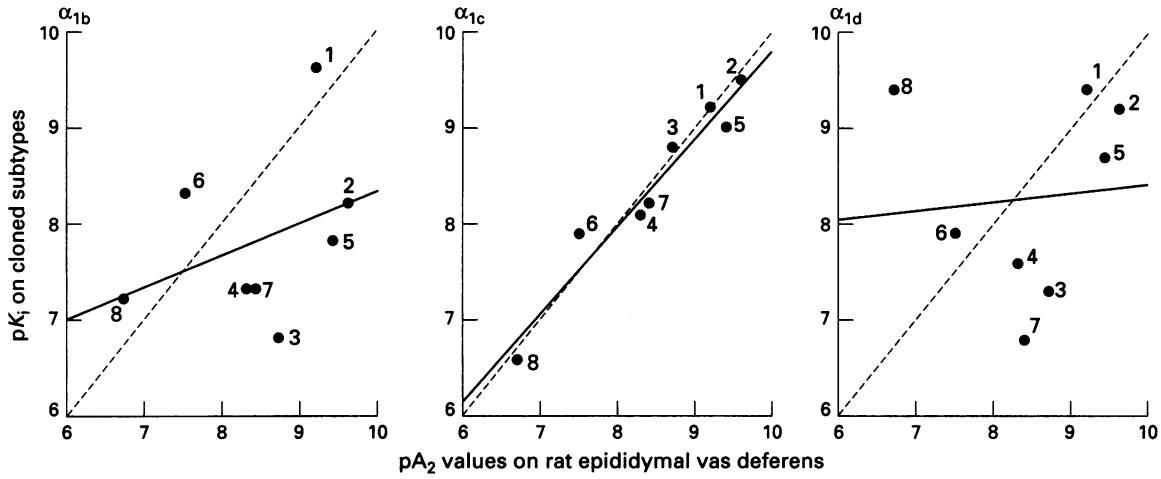

Figure 13 Correlation of average pK_i values for the displacement of [^{3}H]-prazosin on cloned α_1-adrenoceptor subtypes from Faure *et al.*, 1994; Forray *et al.*, 1994b; Kenny *et al.*, 1994a,b; Testa *et al.*, 1994 and Goetz *et al.*, 1995 with pA_2 values for the antagonists prazosin (1), WB 4101 (2), 5-methyl urapidil (3), phentolamine (4), benoxathian (5), spiperone (6), indoramin (7) and BMY 7378 (8) against rat epididymal vas deferens noradrenaline contractions. The solid line is a linear regression fit through all the points and the dashed line has a slope equal to unity, passing through the origin.

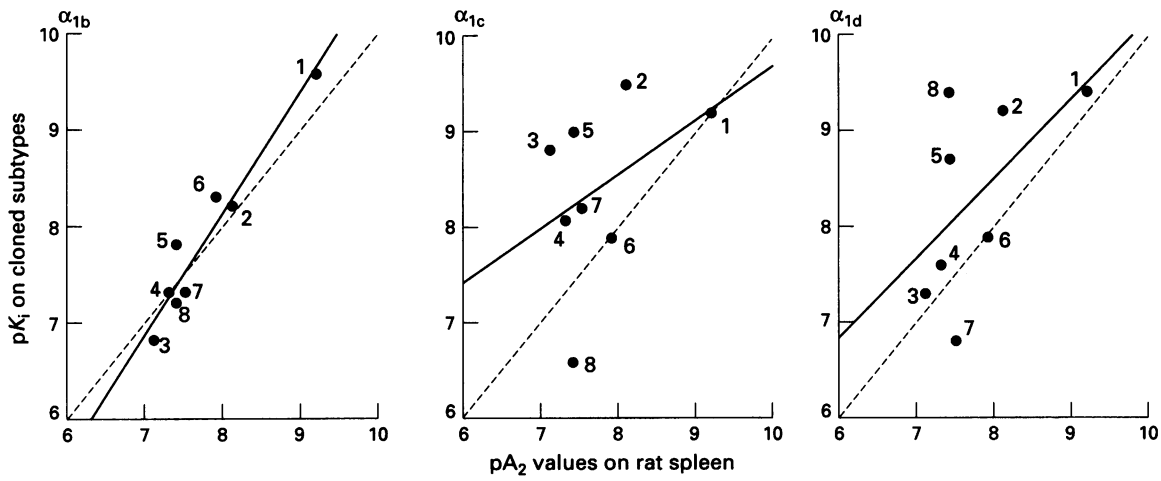

Figure 14 Correlation of average pK_i values for the displacement of [^{3}H]-prazosin on cloned α_1-adrenoceptor subtypes from Faure *et al.*, 1994; Forray *et al.*, 1994b; Kenny *et al.*, 1994a,b; Testa *et al.*, 1994 and Goetz *et al.*, 1995 with pA_2 values for the antagonists prazosin (1), WB 4101 (2), 5-methyl urapidil (3), phentolamine (4), benoxathian (5), spiperone (6), indoramin (7) and BMY 7378 (8) against rat spleen phenylephrine contractions. The solid line is a linear regression fit through all the points and the dashed line has a slope equal to unity, passing through the origin.

Table 3 Correlation values and slopes of the correlations for the pA_2 values with their pK_i values shown in Table 2

	Rat vas deferens		*Rat spleen*	
α_1-subtype	correlation (r)	slope	correlation (r)	slope
α_{1b}	0.36	0.33 ± 0.34	0.96	1.27 ± 0.14
α_{1c}	0.97	0.91 ± 0.09	0.42	0.57 ± 0.51
α_{1d}	0.09	0.09 ± 0.42	0.55	0.84 ± 0.51

tractions to noradrenaline in the rat epididymal vas deferens (see above). This suggests that at least part of the response was mediated by the α_{1B} subtype. However the response was not antagonized as much as might be expected when compared with the ability of chlorethylclonidine to reduce the B_{max} of the α_{1B} subtype in binding experiments, which is over 80% (Taddei *et al.*, 1993). Chlorethylclonidine (1×10^{-4} M) caused a much greater shift to the right of the control curve for phenylephrine than with noradrenaline. With the selective α_1-adrenoceptor agonist the effect of chlorethylclonidine appeared to agree with that expected for the α_{1B} subtype when compared with binding data for reduction in B_{max} in tissues (Han *et al.*, 1987a; Taddei *et al.*, 1993).

The relatively low pA_2 values for WB 4101, 5-methyl urapidil, phentolamine and benoxathian and relatively high pA_2 value for spiperone that were measured against phenylephrine contractions in rat spleen (Table 2) are also consistent with the affinities of these antagonists measured in binding studies using tissues thought to express just α_{1B}-adrenoceptors e.g. rat liver (Taddei *et al.*, 1993; Kenny *et al.*, 1994), rat white fat cells (Torres-Marquez *et al.*, 1992) and rat spleen (Veenstra *et al.*, 1992). Taken together, these results show that the contractions to α_1-adrenoceptor agonists in the rat spleen are mediated by pharmacologically defined α_{1B}-adrenoceptors, in agreement with the conclusions of other workers (Han *et al.*, 1987b; Aboud *et al.*, 1993). It is clear that at least two pharmacologically distinct α_1-adrenoceptors exist in the rat as the spleen results are markedly different from those obtained in the rat epididymal vas deferens

Using cell membranes from cells transfected with the cDNA for either the α_{1b}, α_{1c} or α_{1d} subtype, pK_i values for different antagonists at these α_1-adrenoceptors have been determined in several binding studies (Faure *et al.*, 1994; Forray *et al.*, 1994b; Kenny *et al.*, 1994a,b; Testa *et al.*, 1994; Goetz *et al.*, 1995). While prazosin appears to have equal affinity for the three subtypes, other compounds show some subtype selectivity. In particular, 5-methyl urapidil and indoramin have a higher affinity for the α_{1c} subtype and BMY 7378 has a much higher affinity for the α_{1d} subtype. Table 2 compares the average affinities of antagonists from these binding studies on cell lines expressing either the cloned α_{1b}, α_{1c} or α_{1d} adrenoceptors (Faure *et al.*, 1994; Forray *et al.*, 1994b; Kenny *et al.*, 1994a,b; Testa *et al.*, 1994; Goetz *et al.*, 1995) with their pA_2 values in either the rat epididymal vas deferens or spleen obtained in this study. The pK_i values on each subtype for the antagonists were plotted against their pA_2 values on the vas deferens and spleen. Linear regression was used to see how well the pA_2 and pK_i values correlated for each cloned subtype (vas deferens Figure 13, spleen Figure 14). Correlation values (r), and slopes for each plot are shown in Table 3, a correlation value of one and slope of unity would result from the pK_i and pA_2 values for each antagonist being identical and therefore pharmacologically the same receptor.

It is clear from the correlations that the functional response in the vas deferens is unlikely to be mediated via a receptor similar to either the α_{1b}-clone or α_{1d}-clone. However there is a very good correlation between the pA_2 values and the pK_i values at the α_{1c}-clone (r 0.97, slope 0.91 ± 0.09). This suggests that the functional α_{1A}-adrenoceptor in the vas deferens and the expressed α_{1c}-clone are the same. Due to initial reports showing the bovine α_{1c}-clone to be chlorethylclonidine-sensitive and not expressed in the rat (Schwinn *et al.*, 1991) the α_{1c}-adrenoceptor clone was originally thought not to correspond to the α_{1A}-adrenoceptor found in rat tissues. However now, following recent results, this is a possibility as the α_{1c} subtype is expressed in the rat (Perez *et al.*, 1994; Rokosh *et al.*, 1994) and this subtype may not be eliminated from a rat tissue by chlorethylclonidine treatment (Laz *et al.*, 1993; Forray *et al.*, 1994a). Further, there is evidence consistent with the presence of both α_{1c} and α_{1d} subtypes in rat lung, i.e. chlorethylclonidine treatment removed low affinity (α_{1B}) WB 1401 sites after which this antagonist could only bind to a single population of high affinity sites whereas 5-methyl urapidil could still distinguish two different affinity sites (Hiramatsu *et al.*, 1994). This can be explained by WB4101 being relatively non selective and 5-methyl urapidil having some selectivity between the α_{1d}-clone and the α_{1c}-clone. This is further supported by the RNA for all three subtypes being detected by RNAse protection assay in rat lung (Rokosh *et al.*, 1994).

On the other hand the correlations showed that the subtype mediating contraction in the rat spleen was most similar to the α_{1b}-clone (r 0.96, slope 1.27 ± 0.14) and did not correlate well with the other two subtypes. This confirms that the expressed α_{1b}-clone is the same as the α_{1B}-adrenoceptor found in tissues. Although the slope of the correlation differed significantly from unity this is probably due to the narrow range of affinities for most of these antagonists on the rat spleen. This reflects the narrow range of affinities of these compounds for the expressed α_{1b} clone.

The effect of chlorethylclonidine on B_{max} has also been measured in binding studies on the cloned receptors expressed in cell lines (Schwinn *et al.*, 1990; Lomasney *et al.*, 1991; Perez *et al.*, 1991; Marshall *et al.*, 1992; Forray *et al.*, 1994a,b). It is clear that the cloned α_{1b} subtype is most sensitive to alkylation, in agreement with its effects both on B_{max} in tissues and its effects on the functional response in the spleen. However the other two α_1 clones are also partially sensitive to chlorethylclonidine and it is not yet clear whether the α_{1c} or α_{1d} clone is more so. Therefore chlorethylclonidine may be useful in identifying the α_{1b} subtype but cannot be used to distinguish between the α_{1c} and α_{1d} subtypes. This is particularly true in functional studies when a tissue with a large receptor reserve (perhaps the epididymal vas deferens) may appear to be relatively less sensitive to a receptor alkylating agent compared with a tissue with a smaller receptor reserve. This may explain why contraction of the human prostate to noradrenaline which is mediated by α_{1A}-adrenoceptors (Marshall *et al.*, 1995), appears to be more sensitive to chlorethylclonidine than the rat vas deferens.

In conclusion, contractions of the rat epididymal vas deferens to noradrenaline are mediated by a receptor similar to the classical α_{1A}-adrenoceptor as previously defined in tissues. The α_{1A} functional receptor also correlated very well pharmacologically with the expressed α_{1c} clone and appears to be the same subtype. Contractions to phenylephrine in the rat spleen are mediated by the α_{1B}-adrenoceptor. The good correlation between the affinities of the selective competitive antagonists on the expressed α_{1b} cloned receptor and the α_{1B}-adrenoceptor in the rat spleen show that these receptors are pharmacologically the same. The rat epididymal vas deferens and rat spleen therefore are useful tissues in which to study functional α_{1A}-adrenoceptors (such as those mediating contraction of human prostate, Marshall *et al.*, 1992; 1995) and α_{1B}-adrenoceptors respectively.

We thank Pfizer Central Research, Kent, for supporting this work.

References

ABOUD, R., SHAFI, M. & DOCHERTY, J.R. (1993). Investigations of the subtypes of α_1-adrenoceptor mediating contractions of rat aorta, vas deferens and spleen. *Br. J. Pharmacol.*, **109**, 80–87.

ARUNLAKSHANA, O. & SCHILD, H.O. (1959). Some quantitative uses of drug antagonists. *Br. J. Pharmacol. Chemother.*, **14**, 48–52.

BURT, R.P., CHAPPLE, C.R. & MARSHALL, I. (1992). Functional identification of an α_{1A}-adrenoceptor in rat epididymal vas deferens and an α_{1B}-adrenoceptor in rat spleen. *Br. J. Pharmacol.*, **107**, 325P.

BYLUND, D.B., EIKENBERG, D.C., HIEBLE, J.P., LANGER, S.Z., LEFKOWITZ, R.J., MINNEMAN, K.P., MOLINOFF, P.B., RUFFOLO, R.R. & TRENDELENBURG, U. (1994). IV. International Union of Pharmacology nomenclature of adrenoceptors. *Pharmacol. Rev.*, **46**, 121–136.

COTECCHIA, S., SCHWINN, D.A., RANDALL, R.R., LEFKOWITZ, R.J., CARON, M.G. & KOBILKA, B.K. (1988). Molecular cloning and expression of the cDNA for the hamster α_1-adrenergic receptor. *Proc. Natl. Acad. Sci. U.S.A.*, **85**, 7159–7163.

FAURE, C., PIMOULE, C., ARBILLA, S., LANGER, S. & GRAHAM, D. (1994). Expression of α_1-adrenoceptor subtypes in rat tissues: implications for α_1-adrenoceptor classification. *Eur. J. Pharmacol. (Mol. Pharmacol. Section)*, **268**, 141–149

FORRAY, C., BARD, J.A., LAZ, T.M., SMITH, K.E., VAYSSE, P.J.-J., WEINSHANK, R.L., GLUCHOWSKI, C. & BRANCHEK, T.A. (1994a). Comparison of the pharmacological properties of the cloned bovine, human and rat α_{1c}-adrenergic receptors. *FASEB J.*, **8**, A253.

FORRAY, C., BARD, J.A., WETZEL, J.M., CHIU, G., SHAPIRO, E., TANG, R., LEPOR, H., HARTIG, P.R., WEINSHANK, R.L., BRANCHEK, T.A. & GLUCHOWSKI, C. (1994b). The α_1-adrenergic receptor that mediates smooth muscle contraction in human prostate has the pharmacological properties of the cloned human α_{1c} subtype. *Mol. Pharmacol.*, **45**, 703–708.

GARCIA-SAINZ, J.A. & ROMERO-AVILA, M.T. (1993). Characterization of the α_1-adrenoceptors of guinea pig liver membranes: studies using 5-[^{3}H]methylurapidil. *Mol. Pharmacol.*, **44**, 589–594.

GOETZ, A.S., KING, H.K., WARD, S.D.C., TRUE, T.A., RIMELE, T.J. & SAUSSY, D.L. (1995). BMY 7378 is a selective antagonist of the D subtype of α_1-adrenoceptors. *Eur. J. Pharmacol.*, **272**, R5–R6.

HAN, C., ABEL, P.W. & MINNEMAN, K.P. (1987a). Heterogeneity of α_1-adrenergic receptors revealed by chlorethyclonidine. *Mol. Pharmacol.*, **32**, 505–510.

HAN, C., ABEL, P.W. & MINNEMAN, K.P. (1987b). α_1-Adrenoceptor subtypes linked to different mechanisms for increasing intracellular Ca^{2+} in smooth muscle. *Nature*, **329**, 333–335.

HANFT, G. & GROSS, G. (1989). Subclassification of α_1-adrenoceptor recognition sites by urapidil derivatives and other selective antagonists. *Br. J. Pharmacol.*, **97**, 691–700.

HIRAMATSU, Y., MURAOKA, R., KIGOSHI, S. & MURAMATSU, I. (1994). Identification of α_1-adrenoceptor subtypes in rat lung by binding of [^{3}H]-prazosin and [^{3}H]-WB 4101. *J. Receptor Res.*, **14**, 75–98.

KENAKIN, T.P. & NOVAK, P.J. (1987). Classification of phenoxybenzamine/prazosin-resistant contractions of rat spleen to norepinephrine by Schild analysis: similarities and differences to postsynaptic alpha-2 adrenoceptors. *J. Pharmacol. Exp. Ther.*, **244**, 206–244.

KENNY, B.A., NAYLOR, A.M., GREENGRASS, P.M., RUSSELL, M.J., FRIEND, S.J., READ, A.M. & WYLLIE, M.G. (1994a). Pharmacological properties of the cloned $\alpha_{1A/D}$-adrenoceptor subtype are consistent with the α_{1A}-adrenoceptor characterized in rat cerebral cortex and vas deferens. *Br. J. Pharmacol.*, **111**, 1003–1008.

KENNY, B.A., PHILPOTT, P.C., NAYLOR, A.M. & WYLLIE, M.G. (1994b). Comparative properties of cloned mammalian and human $\alpha_{1A/D}$ and α_{1C} adrenoceptors. *Br. J. Pharmacol.*, **113**, 98P.

LAZ, T.M., FORRAY, C., SMITH, K.E., VACSSE, P.J.J., HARTIG, P.R., GLUCHOWSKI, C., BRANCHEK, T.A. & WEINSHANK, R.L. (1993). Cloned rat homolog of the bovine α_{1c}-adrenergic receptor exhibits an α_{1A}-like receptor pharmacology. *Soc. Neurosci. Abstracts*, **19**, 1788.

LOMASNEY, J.W., COTECCHIA, S., LORENZ, W., LEUNG, W.Y., SCHWINN, D.A., YANG-FENG, T.L., BROWNSTEIN, M., LEFKOWITZ, R.J. & CARON, M.G. (1991). Molecular cloning and expression of the cDNA for the α_{1A}-adrenergic receptor. *J. Biol. Chem.*, **266**, 6365–6369.

MARSHALL, I., BURT, R.P., ANDERSSON, P.O., CHAPPLE, C.R., GREENGRASS, P.M., JOHNSON, G.I. & WYLLIE, M.G. (1992). Human α_{1C}-adrenoceptor: functional characterization in prostate. *Br. J. Pharmacol.*, **107**, 327P.

MARSHALL, I., BURT, RP. & CHAPPLE, C.R. (1995). α_{1A}-adrenoceptor subtype mediates noradrenaline contractions of human prostate. *Br. J. Pharmacol.*, (in press).

MORROW, A.L. & CREESE, I. (1986). Characterization of α_1-adrenergic receptor subtypes in rat brain: a reevaluation of [^{3}H]WB 4101 and [^{3}H]prazosin binding. *Mol. Pharmacol.*, **29**, 321–330.

MURAMATSU, I., OHMURA, T., KIGOSHI, S., HASHIMOTO, S. & OSHITA, M. (1990). Pharmacological subclassification of α_1-adrenoceptors in vascular smooth muscle. *Br. J. Pharmacol.*, **99**, 197–201.

OHMURA, T., OSHITA, M., KIGOSHI, S. & MURAMATSU, I. (1992). Identification of α_1-adrenoceptor subtypes in the rat vas deferens: binding and functional studies. *Br. J. Pharmacol.*, **107**, 697–704.

PEREZ, D.M., CHEN, J.-L., MALIK, N. & GRAHAM, R.M. (1994). Is the α_{1c}-adrenergic receptor the α_{1A} subtype. *FASEB J.*, **8**, A353.

PEREZ, D.M., PIASCIK, M.T. & GRAHAM, R.M. (1991). Solution phase library screening for the identification of rare clones: isolation of an α_{1D} adrenergic receptor cDNA. *Mol. Pharmacol.*, **40**, 876–883.

PRICE, D.T., CHARI, R.S., BERKOWITZ, D.E., MEYERS, W.C. & SCHWINN, D.A. (1994). Expression of α_1-adrenergic receptor subtype mRNA in rat tissues and human neuronal cells: implications for α_1-adrenergic receptor classification. *Mol. Pharmacol.*, **46**, 221–226.

ROKOSH, D.G., BAILEY, B.A., STEWART, A.F.R., KARNS, L.R., LONG, C.S. & SIMPSON, P.C. (1994). Distribution of α_{1c}-adrenergic receptor mRNA in adult rat tissues by RNAse protection assay and comparison with α_{1b} and α_{1d}. *Biochem. Biophys. Res. Commun.*, **200**, 1177–1184.

SAUSSY, D.L., GOETZ, A.S., KING, H.K. & TRUE, T. (1994). BMY 7378 is a selective antagonist of α_{1d}-adrenoceptors (AR): further evidence that vascular α_{1d}-AR are of the α_{1d} subtype. *Can. J. Physiol Pharmacol.*, **72**, (Suppl. 1), P31.1.008.

SCHWINN, D.A. & LOMASNEY, J.W. (1992). Pharmacological characterization of cloned α_1-adrenoceptor subtypes: selective antagonists suggest the existence of a fourth subtype. *Eur. J. Pharmacol.*, **227**, 433–436.

SCHWINN, D.A., LOMASNEY, J.W., LORENZ, W., SZKLUT, P.J., FREMEAU, Jr, R.T., YANG-FENG, T.L., CARON, M.G., LEFKOWITZ, R.J. & COTECCHIA, S. (1990). Molecular cloning and expression of the cDNA for a novel α_1-adrenergic receptor subtype. *J. Biol. Chem.*, **265**, 8183–8189.

SCHWINN, D.A., PAGE, S.O., MIDDLETON, J.P., LORENZ, W., LIGGET, S.B., YAMAMOTO, K., LAPETINA, E.G., CARRON, M.G., LEFKOWITZ, J. & COTECCHIA, S. (1991). The α_{1c}-adrenergic receptor: characterization of signal transduction pathways and mammalian tissue heterogeneity. *Mol. Pharmacol.*, **40**, 619–626.

TADDEI, C., POGGESI, E., LEONARDI, A. & TESTA, R. (1993). Affinity of different α_1-agonists and antagonists for the α_1-adrenoceptors of rabbit and rat liver membranes. *Life Sci.*, **53**, 177–181.

TESTA, R., GUARNERI, L., IBBA, M., STRADA, G., POGGESI, E., TADDEI, C., SIMONAZZI, I. & LEONARDI, A. (1993). Characterization of α_1-adrenoceptor subtypes in prostate and prostatic urethra of rat, rabbit, dog and man. *Eur. J. Pharmacol.*, **249**, 307–315.

TESTA, R., POGGESI, E., TADDEI, C., GUARNERI, L., IBBA, M. & LEONARDI, A. (1994). REC 15/2739, a new α_1-antagonist selective for the lower urinary tract: *in vitro* studies. *Neurourol. Urodynam.*, **13**, 84B.

TORRES-MARQUEZ, M.E., ROMERO-AVILA, M.T., GONZALEZ-ESPINOSA, C. & GARCIA-SAINZ, J.A. (1992). Characterization of rat white fat cell α_{1B}-adrenoceptors. *Mol. Pharmacol.*, **42**, 403–406.

VEENSTRA, D.M.J., VAN BUUREN, K.J.H. & NIJKAMP, F.P. (1992). Determination of α_1-adrenoceptor subtype selectivity by [^{3}H]-prazosin displacement studies in guinea pig cerebral cortex and rat spleen membranes. *Br. J. Pharmacol.*, **107**, 202–206.

(Received November 21, 1994
Revised February 13, 1995
Accepted February 28, 1995)

British Journal of Pharmacology (1995) 115, 476-478

Effect of enalaprilat on bradykinin and des-Arg^9-bradykinin release following reperfusion of the ischaemic rat heart

[1]Daniel Lamontagne, *Réginald Nadeau & Albert Adam

Faculté de pharmacie, and *Département de médecine, Faculté de Médecine, Université de Montréal, C.P. 6128, succursale Centre-ville, Montréal (Québec) Canada, H3C 3J7

1 The release of bradykinin (BK) and its metabolite, des-Arg^9-bradykinin (des-Arg^9-BK), was studied following reperfusion of a globally ischaemic rat heart.

2 BK-like immunoreactivity increased from 13±3 (preischaemic value) to 48±12 fmol min^{-1} g^{-1} ($P<0.05$, $n=14$) 30 s after reperfusion. No difference in BK release was found between control hearts and hearts pretreated with the angiotensin converting enzyme (ACE or kininase II) inhibitor, enalaprilat (50 ng ml^{-1}).

3 No significant change in des-Arg^9-BK-like immunoreactivity during reperfusion was observed in control hearts. In contrast, des-Arg^9-BK-like immunoreactivity rose from 44 ± 15 to 177 ± 61 fmol min^{-1} g^{-1} ($P<0.05$, $n=7$) 30 s after reperfusion in enalaprilat-treated hearts.

4 In conclusion, BK is released upon reperfusion of the globally ischaemic rat heart. ACE inhibitors, through the inhibition of kininase II, increase the formation of the active metabolite, des-Arg^9-BK.

Keywords: Bradykinin; des-Arg^9-bradykinin; ischaemia; reperfusion; angiotensin-converting enzyme inhibitors; rat heart

Introduction

Angiotensin converting enzyme (ACE), also known as kininase II, is responsible for the conversion of angiotensin I to angiotensin II. ACE is also involved in the catabolism of kinins. ACE inhibitors have been shown to reduce infarct size (Hartman *et al.*, 1993) and to improve ventricular function (Linz *et al.*, 1992; Massoudy *et al.*, 1994) following myocardial ischaemia and reperfusion. The reversal by the bradykinin (BK) receptor antagonist, Hoe 140, of the protective effects of ACE inhibitors suggests an important contribution of kinins in the cardioprotection afforded by these drugs.

Studies reporting changes in BK formation during ischaemia and reperfusion are sparse. It has been recently reported that ischaemia is accompanied by an increase in BK-like immunoreactivity in the coronary effluent (Baumgarten *et al.*, 1993). The ischaemia-induced BK release was enhanced in the presence of the ACE inhibitor, ramiprilat (Baumgarten *et al.*, 1993). BK is also a substrate for kininase I, which yields the biologically active metabolite, des-Arg^9-bradykinin (des-Arg^9-BK). However, the effect of ischaemia on des-Arg^9-BK formation has not been documented until now. The aim of this study was therefore to evaluate simultaneously the release of both BK and des-Arg^9-BK following ischaemia and reperfusion, in the presence or absence of an ACE inhibitor.

Methods

Preparation of hearts

The investigation was performed in accordance with the Canadian Council on Animal Care. Male Sprague-Dawley rats (300-350 g) were narcotised by a short exposure (10-20 s) to a 100% CO_2 atmosphere and killed by decapitation. The thorax was rapidly opened and the heart excised and immersed into ice-cold buffer containing heparin (20 iu ml^{-1}). Hearts were then mounted on the experimental setup and perfused at constant flow (10 ml min^{-1}) by means of a digital roller pump (Masterflex Microprocessor Pump Drive, Cole Parmer Instruments Co. Chicago, IL, U.S.A.). A 20-ml compliance chamber along the perfusion line ensured a continuous flow. The perfusion solution consisted of a modified Krebs-Henseleit buffer containing (mmol l^{-1}): NaCl 118, KCl 4, $CaCl_2$ 2.5, KH_2PO_4 1.2, $MgSO_4$ 1, $NaHCO_3$ 24, D-glucose 5, and pyruvate 2. The perfusate was gassed with 95% O_2: 5% CO_2 (pH 7.4) and kept at a constant temperature of 37°C. Enalaprilat or its vehicle (water) were administered through a Y-connector in the aortic cannula with a syringe pump (Harvard Model 11 Microprocessor Syringe Pump, England) at 1/100th of the coronary flow rate. Adequate mixing of the drug was ensured by the turbulent flow created in the reverse-drop shaped aortic cannula. Coronary perfusion pressure was measured with a pressure transducer (Cobe, model CDX3) connected to a sidearm of the aortic perfusion cannula. Isovolumetric left ventricular pressure and its first derivative (dP/dt) was measured by a fluid-filled latex balloon (Size no. 4, Hugo Sachs Elektronik, March-Hugstetten, Germany) inserted into the left ventricle through a pulmonary vein and connected to a second pressure transducer. The volume of the balloon was adjusted to obtain a diastolic pressure between 5 and 10 mmHg. Heart rate was derived from the left ventricular pressure signal. Data were recorded on a Grass Model 79 polygraph system.

Experimental protocol

After a 15-min stabilization period, perfusion of enalaprilat (50 ng ml^{-1}) or its vehicle was started, and the hearts were left to stabilize for a further 15 min. The hearts were then exposed to a 20-min zero-flow ischaemia, followed by a 10 min reperfusion. Ischaemia was induced by turning off perfusion pumps. Conversely, restarting both roller (Krebs-Henseleit buffer) and syringe (enalaprilat or vehicle) pumps to their pre-ischaemic flow rates ensured reperfusion. During the ischaemic period, hearts were immersed into Krebs-Henseleit buffer kept at 37°C. Collection of the coronary effluent for the assay of kinin-like immunoreactivity was performed prior to ischaemia, and during the whole reperfusion period, between the following time-points: 0-1, 1-3, 3-6 and 6-10 min of reperfusion.

Assay of kinin-like immunoreactivity

BK- and des-Arg^9-BK-like immunoreactivity was assayed in the coronary effluent. For this purpose, the perfusate was

[1] Author for correspondence.

collected into tubes containing ice-cold trifluoroacetic acid (0.05 ml of a 10% solution per ml of perfusate) under constant agitation. The perfusate was then cleaned by chromatography on C_8-silica column (Waters, Milford MA, U.S.A.) as described earlier (Décarie *et al.*, 1994; Raymond *et al.*, 1995). The eluate containing kinins was evaporated to dryness in a Speed Vac system (Savant, Farmingdale, NJ, U.S.A.). The residue was dissolved in 400 μl of a Tris-HCl buffer (50 mmol l^{-1}) containing Tween 20 (0.5 ml l^{-1}) and NaCl (100 mmol l^{-1}). BK (Décarie *et al.*, 1994) and des-Arg^9-BK (Raymond *et al.*, 1995) were quantified using a specific chemiluminescence enzyme immunoassay as described earlier. These assays use highly specific polyclonal immunoglobulins induced in rabbit against the carboxyterminal structure of BK and des-Arg^9-BK, respectively. Both assays are characterized by a sensitivity level of 0.1 fmol ml^{-1} (BK) and 27 fmol ml^{-1} (des-Arg^9-BK), respectively.

Statistical analysis

All data are presented as a mean value ± s.e.mean. Single values in control and treated hearts were compared by Student's unpaired *t* test. Bradykinin and des-Arg^9-BK release upon reperfusion was analysed using a 2 by 5 factorial analysis of variance. Probability less than 0.05 was considered to be statistically significant.

Results

The mean weight of control ($n=7$) and enalaprilat-treated ($n=7$) hearts was 1.22 ± 0.03 and 1.26 ± 0.05 g, respectively. At a constant flow rate of 10 ml min^{-1}, coronary perfusion pressure measured prior to ischaemia was 70 ± 9 and 67 ± 7 mmHg for control and enalaprilat-treated hearts, respectively (Table 1). Values of heart rate, left ventricular developed pressure (peak systolic pressure minus diastolic pressure), and *dP/dt* were also comparable between control and enalaprilat-treated hearts (Table 1).

During ischaemia, all hearts stopped beating and left ventricular diastolic pressure rose to 43 ± 9 and 35 ± 8 mmHg in control and enalaprilat-treated hearts, respectively. Following reperfusion, coronary perfusion pressure returned promptly to preischaemic values (65 ± 2 and 64 ± 4 mmHg for control and enalaprilat-treated hearts, respectively). Left ventricular diastolic pressure rose further, reaching values at the end of the reperfusion period of 67 ± 6 and 55 ± 7 mmHg for control and enalaprilat-treated hearts, respectively. Only one control (out of 7) and one enalaprilat-treated (out of 7) heart exhibited a complete and stable recovery upon reperfusion, with left ventricular *dP/dt* above 1200 mmHg s^{-1}: the others showed either no recovery, or transient periods of recovery that were interrupted by events compatible with either rapid ventricular tachycardia or fibrillation. Left ventricular developed pressure and *dP/dt* values at the end of the reperfusion period were 15 ± 3 mmHg and 521 ± 143 mmHg s^{-1} for control, and 26 ± 11 mmHg and 579 ± 222 mmHg s^{-1} for enalaprilat-treated hearts, respectively.

Table 1 Haemodynamic variable values before ischaemia

	Control ($n=7$)	*Enalaprilat* ($n=7$)
Coronary perfusion pressure (mmHg)	70 ± 9	67 ± 7
Heart rate (beats min^{-1})	293 ± 16	288 ± 8
Left ventricular developed pressure (mmHg)	101 ± 9	100 ± 10
Maximum left *dP/dt* (mmHg s^{-1})	2114 ± 105	2257 ± 211

A rapid and transient increase in BK-like immunoreactivity (from 16 ± 5 to 55 ± 19 fmol min^{-1} g^{-1}, $P<0.05$, $n=7$) was observed 30 s after reperfusion in control hearts (Figure 1). A statistically comparable increase was found in enalaprilat-treated hearts (from 11 ± 3 to 41 ± 16 fmol min^{-1} g^{-1},

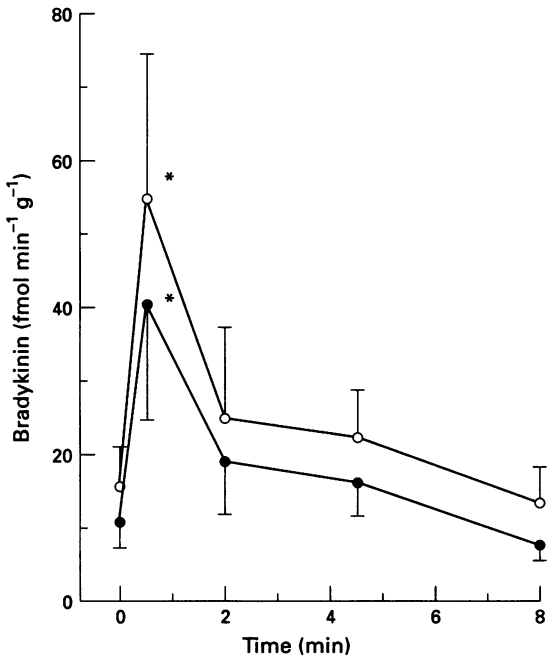

Figure 1 Bradykinin-like immunoreactivity measured in the coronary effluent before ischaemia and following reperfusion of globally ischaemic rat hearts in the absence (○) and presence (●) of 50 ng ml^{-1} enalaprilat. *$P<0.05$, compared to the corresponding preischaemic (0 min) value.

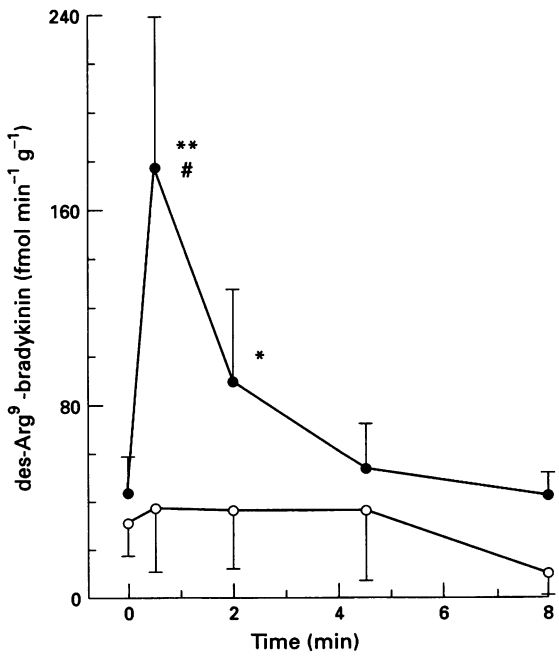

Figure 2 Des-Arg^9-bradykinin-like immunoreactivity measured in the coronary effluent before ischaemia and following reperfusion of globally ischaemic rat hearts in the absence (○) and presence (●) of 50 ng ml^{-1} enalaprilat. *$P<0.05$, **$P<0.01$, compared to the corresponding preischaemic (0 min) value. #$P<0.05$, compared to the corresponding value in control hearts.

$P<0.05$, $n=7$). No increase in des-Arg^9-BK-like immunoreactivity was observed in control hearts (Figure 2). In contrast, a marked increase in des-Arg^9-BK-like immunoreactivity (from 44 ± 15 to 177 ± 61 fmol min^{-1} g^{-1}, $P<0.05$, $n=7$) was observed 30 s after reperfusion in enalaprilat-treated hearts (Figure 2).

Discussion

In the present study, we have observed a marked release of BK upon reperfusion of the globally ischaemic rat heart. In contrast, release of des-Arg^9-BK upon reperfusion was observed only in the presence of enalaprilat.

A recent study has reported an increase in BK outflow during regional ischaemia produced by coronary artery ligation in the rat isolated heart (Baumgarten *et al.*, 1993). In contrast to our study, BK outflow fell upon reperfusion. The increased BK outflow during the ligation period, with no further increase upon reperfusion, suggested that BK originated from normal tissue surrounding the ischaemic myocardium. In our study, the whole heart was made ischaemic. Furthermore, BK peaked in the first fraction collected, and declined thereafter. Therefore, in our experimental conditions, it is most likely that BK originated from, and accumulated in, the ischaemic myocardium, being washed away upon reperfusion. It should be noted that, in the study by Baumgarten *et al.* (1993), BK release was expressed relative to the right ventricle in the ischaemic period and to the whole heart for the reperfusion.

Pretreatment of hearts with the ACE inhibitor, enalaprilat, did not enhance the release of BK upon reperfusion. This is in contrast with the study by Baumgarten *et al.* (1993) in which a more important BK outflow during ischaemia was observed in the presence of ACE inhibition. The absence of enhanced BK release in the presence of enalaprilat suggests that metabolic pathways distinct from kininase II can play an important role in the catabolism of BK in our experimental model. For example, kininase II inhibition with the ACE inhibitor could shunt BK towards other catabolic pathways such as kininase I. This hypothesis is supported by the huge release of des-Arg^9-BK in enalaprilat-treated hearts.

Baumgarten *et al.* (1993) measured a concentration of immunoreactive kinins in the ng ml^{-1} g^{-1} range. This is in contrast with our results, which are in the pg ml^{-1} g^{-1} range. This discrepancy could be explained by analytical differences. The presence of kinin precursors and/or kinin-forming enzymes in the perfusate could interfere with the assay. In the present study, the efficacy of the extraction step and the specificity of the quantification method have been carefully validated (Décarie *et al.*, 1994; Raymond *et al.*, 1995).

Our study is the first report of a major release of des-Arg^9-BK upon reperfusion. Des-Arg^9-BK is a natural agonist for the B_1 kinin receptor (Marceau & Regoli, 1991). This receptor is believed to be expressed in different pathological states (Marceau & Regoli, 1991). However, a constitutive B_1 kinin receptor has been described recently in the dog *in vivo* (Nakhostine *et al.*, 1993). Pretreatment of hearts with des-Arg^9-BK prior to global ischaemia has been found to reduce the incidence of ventricular fibrillation and noradrenaline outflow (Chahine *et al.*, 1993), as well as atrial natriuretic peptide release (Lévesque Rouleau *et al.*, 1994), upon reperfusion of the ischaemic rat heart. In the present study, enalaprilat failed to improve ventricular functional recovery upon reperfusion, despite the increase in endogenous des-Arg^9-BK formation. The experimental conditions in the present study are slightly different from the earlier work. Therefore, direct comparison may be perilous. Furthermore, the mean concentration of endogenous des-Arg^9-BK measured in the coronary effluent was 2.3×10^{-11} mol l^{-1}, which is low compared to the concentration (10^{-7} mol l^{-1}) of exogenous des-Arg^9-BK used to achieve cardioprotection (Chahine *et al.*, 1993). However, the fate of exogenous des-Arg^9-BK administered in such conditions, and thus the concentration reaching the myocytes, is unknown and will be the subject of future studies.

In conclusion, BK is released upon reperfusion of the globally ischaemic rat heart. ACE inhibitors, through the inhibition of kininase II, increase the formation of the active metabolite, des-Arg^9-BK. Further studies are needed to assess the role of des-Arg^9-BK in the cardioprotective effect of ACE inhibitors.

This study was supported by grants from the Medical Research Council of Canada (MRCC, grants MT-12531 and MT-12260) D.L. is a scholar of the Fonds de la recherche en santé du Québec, and R.N. is a career investigator of the MRCC.

References

BAUMGARTEN, C.R., LINZ, W., KUNKEL, G., SCHÖLKENS, B.A. & WIEMER, G. (1993). Ramiprilat increases bradykinin outflow from isolated hearts of rat. *Br. J. Pharmacol*, **108**, 293–295.

CHAHINE, R., ADAM, A., YAMAGUCHI, N., GASPO, R., REGOLI, D. & NADEAU, R. (1993). Protective effects of bradykinin on the ischaemic heart: implication of the B_1 receptor. *Br. J. Pharmacol.*, **108**, 318–322.

DÉCARIE, A., DRAPEAU, G., CLOSSET, J., COUTURE, R. & ADAM, A. (1994). Development of digoxigenin-labelled peptides: application to chemiluminoenzyme immunoassay of bradykinin in inflamed tissues. *Peptides*, **15**, 511–518.

HARTMAN, J.C., WALL, T.M., HULLINGER, T.G. & SHEBUSKI, R.J. (1993). Reduction of myocardial infarct size in rabbits by ramiprilat: Reversal by the bradykinin antagonist HOE 140. *J. Cardiovasc. Pharmacol.*, **21**, 996–1003.

LÉVESQUE ROULEAU, M., RAUT, R., DRAPEAU, G., ONG, H., ADAM, A. & LAMONTAGNE, D. (1994). The role of bradykinin in the release of atrial natriuretic factor (ANF) from the ischemic heart. *Can. J. Physiol. Pharmacol.*, **72** (suppl. 2), 37(Abstract).

LINZ, W., WIEMER, G. & SCHÖLKENS, B.A. (1992). ACE-inhibition induces NO-formation in cultured bovine endothelial cells and protects isolated ischemic rat hearts. *J. Mol. Cell. Cardiol.*, **24**, 909–919.

MARCEAU, F. & REGOLI, D. (1991). Kinins receptors of the B_1 type and their antagonists. In *Bradykinin Antagonists: Basic and Clinical Research*. ed. Burch, R.M. pp. 33–49. New York: Marcel Dekker.

MASSOUDY, P., BECKER, B.F. & GERLACH, E. (1994). Bradykinin accounts for improved postischemic function and decreased glutathione release of guinea pig heart treated with the angiotensin-converting enzyme inhibitor ramiprilat. *J. Cardiovasc. Pharmacol.*, **23**, 632–639.

NAKHOSTINE, N., RIBOUT, C., LAMONTAGNE, D., NADEAU, R. & COUTURE, R. (1993). Mediation by B_1 and B_2 receptors of vasodepressor responses to intravenoulsy administered kinins in anaesthetized dogs. *Br. J. Pharmacol.*, **110**, 71–76.

RAYMOND, P., DRAPEAU, G., RAUT, R., AUDET, R., MARCEAU, F., ONG, H. & ADAM, A. (1995). Quantification of des-Arg^9-bradykinin using a chemiluminescence enzyme immunoassay: application to its kinetic profile during plasma activation. *J. Immunol. Method.*, (in press).

(Received December 14, 1994
Revised February 6, 1995
Accepted February 17, 1995)

British Journal of Pharmacology (1995) 115, 479–485

Long-lasting activation of cation current by low concentration of endothelin-1 in mouse fibroblasts and smooth muscle cells of rabbit aorta

Taijiro Enoki, Soichi Miwa, Aiji Sakamoto, Tetsuya Minowa, Taro Komuro, *Shigeo Kobayashi, Haruaki Ninomiya & [1]Tomoh Masaki

Department of Pharmacology, Kyoto University Faculty of Medicine, Kyoto 606, Japan and *Division of Neuroscience, Graduate School of Human and Environmental Studies, Kyoto University, Kyoto 606, Japan

1 Recombinant human ET_A receptors were expressed in a mouse fibroblast cell line (*Ltk*$^-$cell) and functional coupling of the receptors with Ca^{2+} permeable channels at low concentrations of endothelin-1 (ET-1) was investigated using whole-cell recordings and monitoring the changes in intracellular free Ca^{2+} concentrations ($[Ca^{2+}]_i$) with a Ca^{2+} indicator, fluo-3. A similar type of coupling was investigated in freshly dispersed vascular smooth muscle cells (VSMCs) of rabbit thoracic aorta by use of whole-cell recordings.

2 In *Ltk*$^-$ cells expressing recombinant human ET_A receptors, concentrations of ET-1 (10^{-8} M, 10^{-9} M) evoked an initial transient peak and a subsequent sustained elevation in $[Ca^{2+}]_i$ whereas a lower concentration of ET-1 (10^{-10} M) evoked only a sustained elevation of $[Ca^{2+}]_i$. After removal of extracellular Ca^{2+}, ET-1 evoked only an initial peak without a sustained elevation of $[Ca^{2+}]_i$. The sustained elevation induced by 10^{-10} M ET-1 was blocked by 300 μM mefenamic acid (a cation channel blocker) but not by 10 μM nifedipine (a blocker of voltage-operated Ca^{2+} channel).

3 In whole-cell recordings with *Ltk*$^-$ cells, a brief (3–5 min) application of ET-1 (10^{-10} M) induced a sustained inward current at a holding potential of −60 mV. The current-voltage relationship revealed that the reversal potential of the ET-1-induced current was close to 0 mV (1.9 mV) and was not altered by reducing the concentration of Cl^- in the bath solution, indicating that the current is carried by cations. The current was reversibly blocked by 300 μM mefenamic acid, and it persisted after all cations in the bath solution had been replaced by Ca^{2+} (5 or 30 mM) and nonpermeant cation N-methyl-D-glucamine, indicating that the ET-1-activated channel is permeable to Ca^{2+}. Activation of the current was independent of membrane potential and the current was induced even after addition of a high concentration (10 mM) of a Ca^{2+} chelator, EGTA, to the pipette solution.

4 In whole-cell recordings from rabbit aortic VSMCs, ET-1 (10^{-10} M) induced a sustained inward current at a holding potential of −60 mV. The reversal potential was −12 mV and was not altered when the concentration of Cl^- in the pipette solution was decreased, indicating that the current is carried by cations. Again activation of the current was independent of membrane potential and was observed even after addition of a high concentration (10 mM) of a Ca^{2+} chelator, EGTA to the pipette solution. The current was reversibly blocked by 300 μM mefenamic acid and was permeable to Ca^{2+}, showing marked similarities to ET-1-induced cationic current in *Ltk*$^-$ cells.

5 These results indicate that in *Ltk*$^-$ cells transfected with cDNA for recombinant ET_A receptors and VSMCs, ET_A receptors can functionally couple with a nonselective cation channel permeable to Ca^{2+}. Thus the present data suggest that the cation channel plays an essential role in the sustained elevation of $[Ca^{2+}]_i$ at low concentrations of ET-1 by causing Ca^{2+} entry through the channel.

Keywords: Endothelin-1; nonselective cation channel; mefenamic acid; calcium; vascular smooth muscle; rabbit aorta

Introduction

Endothelin-1 (ET-1) is a potent vasoconstrictive peptide with a long duration of action (Yanagisawa *et al.*, 1988). The EC_{50} of ET-1 for vascular contraction is very low, e.g., 5.2×10^{-10} M in porcine coronary artery, and the contraction lasts for more than 3 h even after removal of the peptide (Kasuya *et al.*, 1989a). ET-1 binds to receptors on vascular smooth muscle cells (VSMCs) and subsequently raises the intracellular free Ca^{2+} concentration ($[Ca^{2+}]_i$), which is a primary event for contraction of the cells. Three mechanisms have been proposed by which ET-1 elevates $[Ca^{2+}]_i$: (1) release of intracellularly stored Ca^{2+} via increased formation of inositol trisphosphates (IP_3) (van Renterghem *et al.*, 1988; Kasuya *et al.*, 1989b), (2) activation of voltage-operated Ca^{2+} channels (VOCs) (Goto *et al.*, 1989; Inoue *et al.*, 1990) and (3) Ca^{2+} entry via other types of channels (Huang *et al.*, 1990; Simpson *et al.*, 1990). Several lines of evidence indicate that mechanisms for ET-1-induced vasoconstriction differ, depending on its concentration. Many investigators consider that at high concentrations of ET-1, increased formation of IP_3 and 1,2-diacylglycerol, an activator of protein kinase C, plays a primary role in vasoconstriction (Kasuya *et al.*, 1989b; Rubanyi & Polokoff, 1994). The mechanisms of vasoconstriction induced by low concentrations of ET-1 (lower than 10^{-10} M) have not been extensively studied, although these concentrations seem to be more physiological (Masaki, 1994). At this concentration-range, it is noted that vasoconstriction is not accompanied by increased formation of IP_3 and 1,2-diacylglycerol but depends on Ca^{2+} entry. Controversy exists regarding the Ca^{2+} entry pathway. Some investigators assume that Ca^{2+} entry is conducted through VOC based on its sensitivity to Ca^{2+} channel antagonists (Yanagisawa *et al.*, 1988; Goto *et al.*, 1989), whereas others report that it is resistant to the antagonists (Chabrier *et al.*, 1989; Huang *et al.*, 1990; Simpson *et al.*, 1990). In this context, other types of ion channels such as a nonselective

[1] Author for correspondence.

cation channel which could be permeable to Ca^{2+} are possible candidates for the Ca^{2+} entry channel (van Renterghem *et al.*, 1988; Chen & Wagoner, 1991).

The main purpose of the present study was to clarify the functional coupling of type A endothelin receptors (ET_A receptors) with a nonselective cation channel at low concentrations of ET-1 and to investigate the permeability of the conductance to Ca^{2+}. For this purpose, we used a simple model system in which recombinant ET_A receptors were expressed in a mouse fibroblast cell line (L*tk*$^-$ cell). This system is advantageous, because the cell line possesses cation channels (Frace & Gargus, 1989) but not VOC (Perez-Reyes *et al.*, 1989) and because larger responses can be obtained owing to overexpression of the receptors. We also examined other properties of the channel such as sensitivity to blockers, duration of activation, and mode of activation (dependence on an increase in $[Ca^{2+}]_i$ and membrane potential). Furthermore, we investigated whether endothelin receptors are functionally coupled with a similar type of nonselective cation channel in VSMCs. From these results, we demonstrated that low concentrations of ET-1 persistently activate a Ca^{2+}-permeable nonselective cation channel.

Methods

Preparation of Ltk$^-$ cells expressing recombinant human ET_A receptors and vascular smooth muscle cells

The full-length human ET_A receptor cDNA was cloned into a mammalian expression vector pME18Sf- as previously described (Sakamoto *et al.*, 1993). The plasmid was co-transfected with pSV2neo containing neomycin resistant gene into L*tk*$^-$ cells by a calcium phosphate method. Stable transfectants were selected in G418 500 $\mu g\ ml^{-1}$ and isolated. The L*tk*$^-$ cells were cultured in monolayer in Dulbecco's modified Eagle's medium supplemented with 10% foetal bovine serum (Hyclone) at 37°C in a humidified 5% CO_2/95% air atmosphere. A subclone which expressed maximal receptor density was used in the present study.

Isolated smooth muscle cells were prepared from rabbit thoracic aortae as described (Inoue & Kuriyama, 1993). Male rabbits (2.4–2.8 kg) were killed by an overdose of i.v. sodium pentobarbitone. The thoracic aorta was removed, cleaned of surrounding tissues, dissected into thin strips and kept in Ca^{2+}-free Krebs-HEPES solution containing (in mM): NaCl 140, KCl 3, $MgCl_2$ 1, glucose 11 and HEPES 10 (pH 7.3, adjusted with NaOH). Strips of the aorta were enzymatically digested in Ca^{2+}-free Krebs-HEPES solution with papain (0.2–0.3 $mg\ ml^{-1}$) for 8–12 min at 35°C and then with collagenase (0.25–0.5 $mg\ ml^{-1}$) for 10 min at 35°C. Smooth muscle cells were dissociated by triturating cut pieces of strips with a blunt-ended pipette.

Measurement of $[Ca^{2+}]_i$ in Ltk$^-$ cells

$[Ca^{2+}]_i$ was measured using a fluorescent probe fluo-3 (Minta *et al.*, 1989) instead of the prevailing fluorescent probe fura-2, because mefenamic acid was found to disturb measurement of $[Ca^{2+}]_i$ by absorbing the light at excitation wavelengths for fura-2. For loading the cells with fluo-3, the L*tk*$^-$ cells were incubated in Krebs-HEPES containing 10 μM fluo-3/AM for 30 min at 37°C. The Krebs-HEPES solution contained (in mM): NaCl 140, KCl 3, $CaCl_2$ 2, $MgCl_2$ 1, glucose 11 and HEPES 10 (pH 7.3, adjusted with NaOH). After washing, the cells were suspended in Krebs-HEPES at a density of approximately 2×10^7 cells ml^{-1}, and 0.5 ml aliquots were used for measurement of fluorescence by a CAF 110 spectrophotometer (JASCO, Toyko, Japan) with an excitation wavelength at 490 nm and an emission wavelength at 540 nm. At the end of the experiment, Triton X-100 and subsequently EGTA were added at final concentrations of 0.1% and 5 mM, respectively, to obtain the fluorescence maximum (F_{max}) and the fluorescence minimum (F_{min}). $[Ca^{2+}]_i$ was determined from the equilibrium equation, $[Ca^{2+}]_i = K_d(F\text{-}F_{min})/(F_{max}\text{-}F)$, where F was the experimental value of fluorescence and K_d was defined as 0.40 μM (Minta *et al.*, 1989). ET-1, mefenamic acid or nifedipine was added to a cuvette in 5 μl solution. For experiments in the absence of Ca^{2+}, the cells were suspended in Ca^{2+}-free Krebs-HEPES in which Ca^{2+} was replaced with 5 mM EGTA.

Whole-cell recordings in Ltk$^-$ cells and VSMCs

L*tk*$^-$ cells and freshly dispersed VSMCs were perfused with Krebs-HEPES, visualized with Nomarski optics (Zeiss) and whole-cell recordings were made with thin-wall borosilicate glass patch pipettes (resistance, 3–5 MΩ) as previously described (Kobayashi & Takahashi, 1993). Pipettes were filled with CsCl solution containing (in mM): CsCl 135, $MgCl_2$ 2, EGTA 0.2, HEPES 5, (pH 7.3, adjusted with NaOH). Tight seal whole-cell currents were acquired using the pClamp software package (Axon Instruments) and an EPC7 patch clamp amplifier (List, Darmstadt, Germany). Perfusion rate was maintained at 2.2–2.5 $ml\ min^{-1}$ and the bath volume was ~1.0 ml. ET-1 and mefenamic acid were bath-applied through the same perfusion line. All experiments were done under voltage-clamp at a holding potential of −60 mV at room temperature (20–24°C). To test the contribution of Cl^- current in L*tk*$^-$ cells, bath solution was switched from Krebs-HEPES to low Cl^- solution containing (in mM): sodium gluconate 140, KCl 3, $CaCl_2$ 2, $MgCl_2$ 1, glucose 11, HEPES 10 (pH 7.3, adjusted with NaOH). For VSMCs, pipette solution was changed to Cs-aspartate solution which contained (in mM): Cs-aspartate 120, CsCl 20, $MgCl_2$ 2, EGTA 0.2, HEPES 5, (pH 7.3, adjusted with Tris). To test the permeability of Ca^{2+} through the channel, the bath solution was switched from Krebs-HEPES to either 5 mM Ca^{2+}/140 mM N-methyl-D-glucamine (NMDG) or 30 mM Ca^{2+}/100 mM NMDG which contained (in mM): $CaCl_2$ 5, NMDG chloride 140, glucose 11, HEPES 10 (pH 7.3, adjusted with Tris) and $CaCl_2$ 30, NMDG chloride 100, glucose 11, HEPES 10 (pH 7.3, adjusted with Tris), respectively. In some experiments, EGTA was added to the pipette solution at a final concentration of 10 mM, which has enough buffering capacity for Ca^{2+} to prevent a transient increase in $[Ca^{2+}]_i$ (Neher, 1988), and the concentration of Ca^{2+} in the solution was maintained at 100 nM by adding the calculated amount of $CaCl_2$ (van Heeswijk *et al.*, 1984).

Drugs

Endothelin-1 was purchased from Peptide Institute (Osaka, Japan). Fluo-3/AM and EGTA were purchased from Dojin Chemicals (Tokyo, Japan). Mefenamic acid, N-methyl-D-glucamine, nifedipine, indomethacin, papain and collagenase were purchased from Sigma. Mefenamic acid, nifedipine and indomethacin were dissolved in dimethyl sulphoxide and the final concentration of dimethyl sulphoxide was 0.1% in whole-cell recordings and 1% in $[Ca^{2+}]_i$ measurements, which alone had little effect on the measurements.

Results

$[Ca^{2+}]_i$ measurement in Ltk$^-$ cells

ET-1 at concentrations of 10^{-8} M and 10^{-9} M evoked biphasic changes in $[Ca^{2+}]_i$ in L*tk*$^-$ cells expressing recombinant human ET_A receptors: an initial transient peak and a subsequent sustained phase (Figure 1a). However, a lower concentration of ET-1 (10^{-10} M and lower) evoked only sustained elevation of $[Ca^{2+}]_i$ (Figure 1a). In the absence of external Ca^{2+}, the sustained phase was abolished while the initial peak persisted (Figure 1b). These data indicate that the initial peak of $[Ca^{2+}]_i$ increase is the result of Ca^{2+} mobiliza-

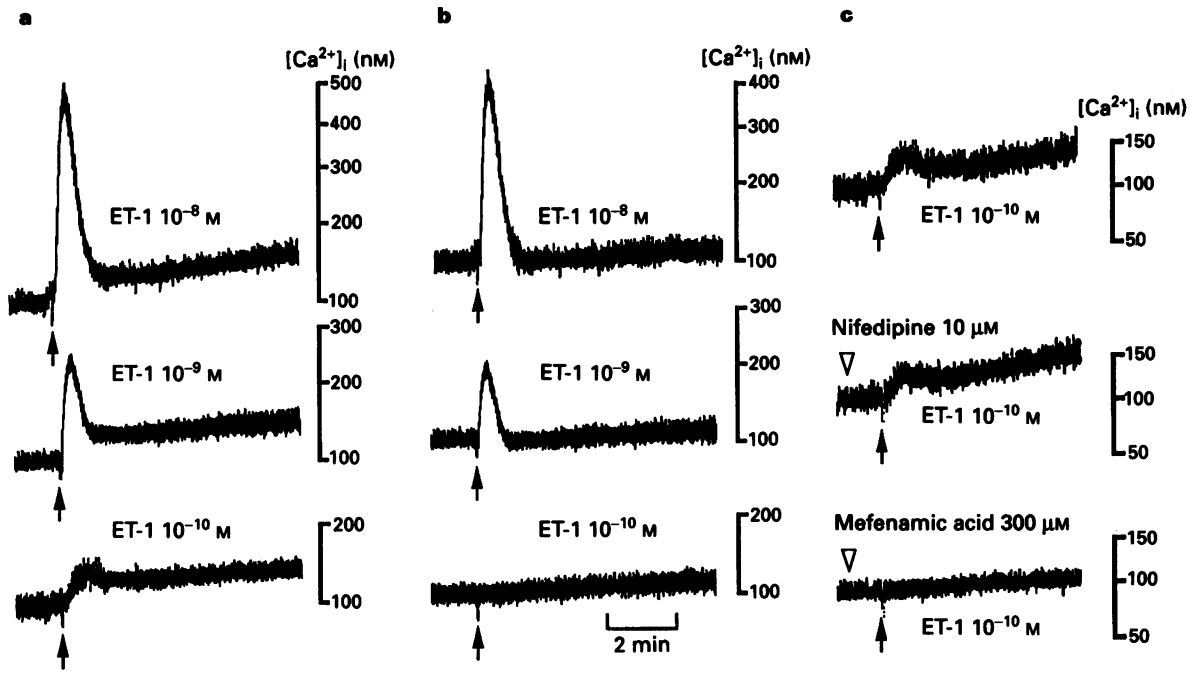

Figure 1 Endothelin-1 (ET-1)-induced elevations in intracellular free Ca^{2+} concentrations ($[Ca^{2+}]_i$) in Ltk^- cells expressing human recombinant ET_A receptors and their modification by removal of extracellular Ca^{2+}, nifedipine and mefenamic acid. (a) Changes in $[Ca^{2+}]_i$ in normal Krebs-HEPES following administration of various concentrations of ET-1. (b) ET-1-induced changes in $[Ca^{2+}]_i$ in media lacking Ca^{2+}. (c) Effects of nifedipine (10 μM) and mefenamic acid (300 μM) on 10^{-10} M ET-1-induced increase in $[Ca^{2+}]_i$. Ltk^- cells, loaded with a Ca^{2+} indicator fluo-3, were stimulated by ET-1 which was added to media at the time indicated by arrows. Nifedipine and mefenamic acid were added at the time indicated by open triangles.

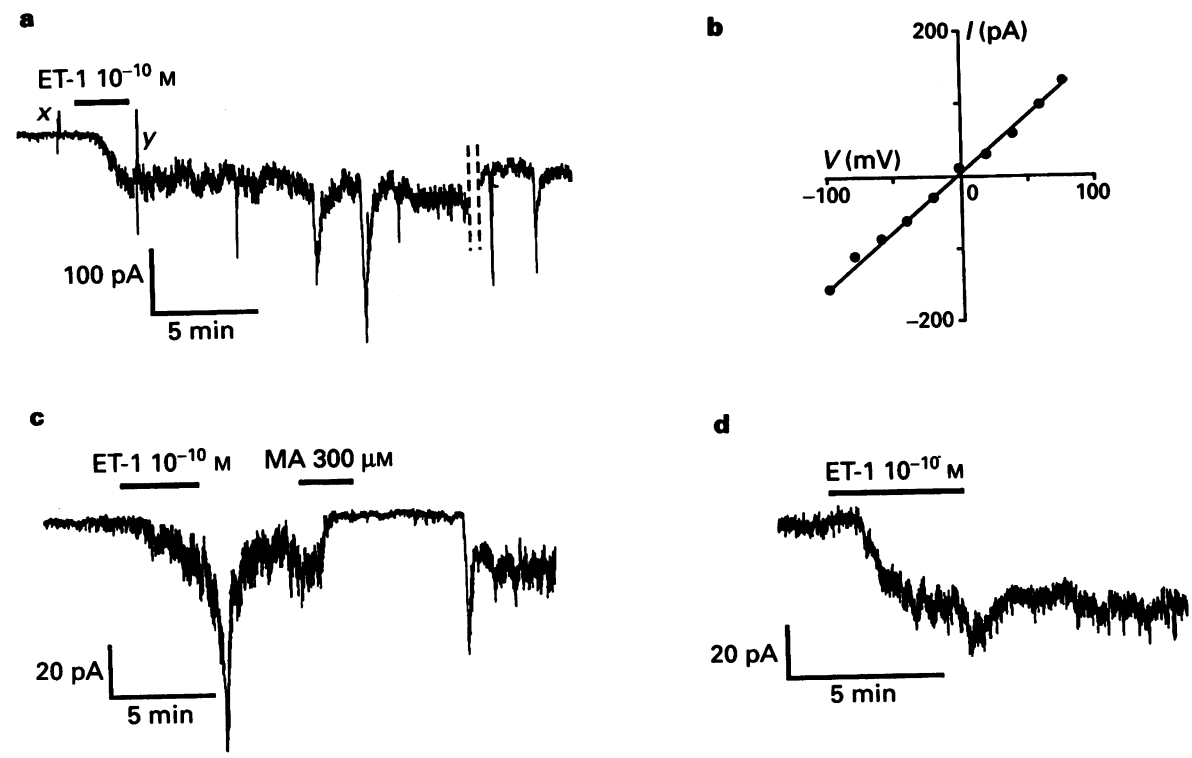

Figure 2 Whole-cell recordings of endothelin-1 (ET-1)-induced current in Ltk^- cells expressing human recombinant ET_A receptors. The holding potential was −60 mV. Krebs-HEPES and CsCl solution were used for the bath solution and the pipette solution, respectively. ET-1 (10^{-10} M) was added to the bath solution during the time interval indicated by a horizontal bar. (a) A trace showing the sustained inward current induced by ET-1. The sustained current was observed 50 min after washout of ET-1 (a trace after a break). The properties of transient large inward currents were not examined in detail. (b) Current-voltage relationships for ET-1-induced current. In the same cell as in (a), voltage steps ranging from −100 to +80 mV in 20-mV increments were applied before and after the application of ET-1 (x and y in a) and the ET-1-induced currents at each membrane potential were determined by subtracting currents before application of ET-1 from currents after its application. (c) Inhibition of ET-1-induced inward current by mefenamic acid (MA). Mefenamic acid (300 μM) was added to the bath solution 5 min after washout of ET-1. (d) ET-1-induced inward current in the presence of 10 mM EGTA in the pipette solution.

tion from intracellular stores, possibly via increased formation of IP_3, whereas the sustained phase is the result of entry of extracellular Ca^{2+}. Thus, the involvement of intracellular Ca^{2+} mobilization appears to be negligible in the response evoked by 10^{-10} M ET-1 as reported previously in VSMCs (Kasuya *et al.*, 1989a; b). Therefore, stimulation by 10^{-10} M ET-1 was used in the following experiments to characterize the properties of the Ca^{2+} entry channel activated by ET-1.

Ca^{2+} entry is considered to be conducted through nonselective cation channels but not through VOCs for the following reasons: (1) L*tk*$^-$ cells apparently lack VOCs as shown by Perez-Reyes *et al.* (1989). We confirmed it in measurement of $[Ca^{2+}]_i$ in which depolarization by high K^+ stimulation does not increase $[Ca^{2+}]_i$ (data not shown). (2) The ET-1-evoked increase in $[Ca^{2+}]_i$ is resistant to nifedipine, a specific blocker of L-type VOC (Figure 1c). (3) The increase is completely blocked by mefenamic acid (Figure 1c), which is considered to be a blocker of nonselective cation channel (Gögelein *et al.*, 1990; Jung *et al.*, 1992).

Since mefenamic acid is also known as an inhibitor of cyclo-oxygenase (Flower & Vane, 1974), we tested its effects after treatment with indomethacin, an inhibitor of cyclo-oxygenase. Indomethacin up to the concentration of 10 μM had little effect on resting $[Ca^{2+}]_i$ and on the ET-1-evoked increase in $[Ca^{2+}]_i$ (data not shown), indicating that inhibition of ET-1-evoked increase in $[Ca^{2+}]_i$ by mefenamic acid is not due to blockade of prostaglandin synthesis.

Whole-cell current in Ltk$^-$ cells

To elucidate further the characteristics of the Ca^{2+} entry, whole-cell recordings were performed with L*tk*$^-$ cells expressing recombinant human ET_A receptors. At a holding potential of −60 mV, a brief (3–5 min) application of ET-1 (10^{-10} M) induced a slow inward current with an increase in baseline 'noise' (Figure 2a). In addition, large transient currents spontaneously occurred in some cells. In most cells, the responses continued for over 10 min after washout of ET-1 and even persisted up to 60 min or longer (Figure 2a). The amplitude of the sustained inward current depended on the cells employed, ranging from 20 pA to 200 pA. The current-voltage relationship of the ET-1-induced current was obtained by applying voltage-step command pulses (100 ms, 20 mV increment) before and during the ET-1-induced response (Figure 2b). The ET-1-induced current was linear against the membrane potential between −100 mV and +80 mV with the reversal potential close to 0 mV (1.9 ± 1.4 mV, mean ± s.e., $n = 12$). In a low Cl^- (9 mM)-containing bath solution ($E_{Cl} = +70.3$ mV), the reversal potential of the ET-1-induced current was essentially similar (0.8 ± 1.7 mV, $n = 6$). These results indicate that the current reflects opening of a cation channel, which is equally permeable to both extracellular Na^+ and intracellular Cs^+.

The ET-1-induced current was reversibly and completely inhibited by 300 μM mefenamic acid (Figure 2c), and the current persisted even when 10 mM EGTA was added to the pipette solution to prevent an increase in $[Ca^{2+}]_i$ (Figure 2d).

Even after all cations in the bath solution were replaced by Ca^{2+} and nonpermeant cation N-methyl-D-glucamine (NMDG), ET-1 evoked an inward current (Figure 3a), indicating that the cation current is carried by Ca^{2+}. As shown in Figure 3b, the reversal potential of the ET-1-induced current in the 5 mM Ca^{2+}/140 mM NMDG solution was −14.4 ± 1.8 mV ($n = 7$). $P_{Ca^{2+}}/P_{Cs^+}$ was calculated according to a modified Goldman-Hodgkin-Katz equation after Lewis (1979) and it was estimated to be 2.5. Also, the Ca^{2+} current was reversibly blocked by mefenamic acid (Figure 3c).

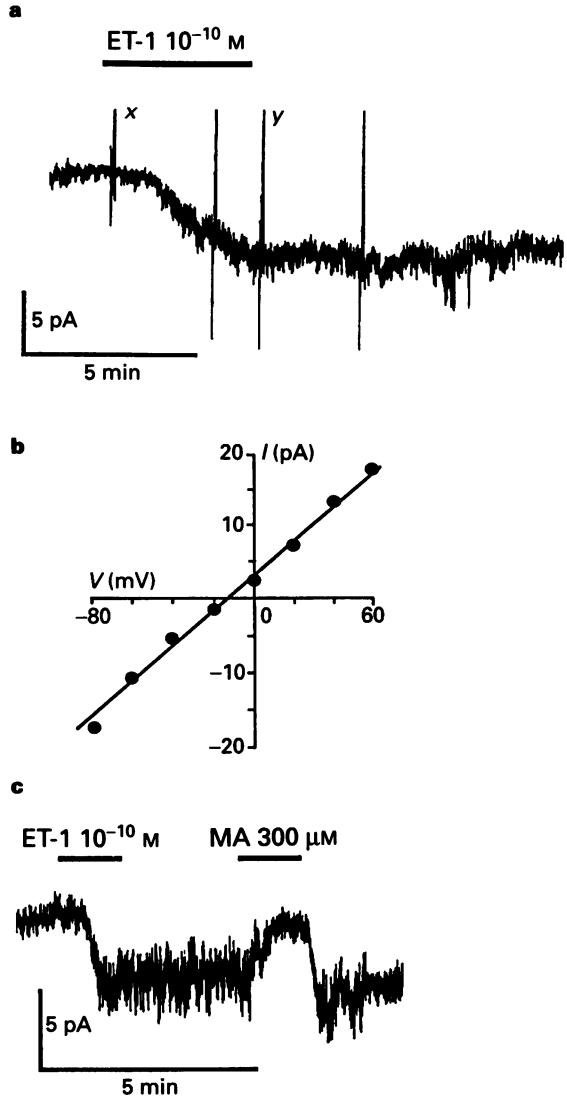

Figure 3 Whole-cell recordings of endothelin-1 (ET-1)-induced current in L*tk*$^-$ cells expressing human recombinant ET_A receptors in the Ca^{2+}/N-methyl-D-glucamine (NMDG) solution. In this experiment, the bath solution was used in which cations such as Na^+, K^+ and Mg^{2+} were replaced with 5 mM Ca^{2+} and 140 mM NMDG, a nonpermeant cation. For the pipette solution, the CsCl solution containing 10 mM EGTA was used. (a) Induction by ET-1 (10^{-10} M) of a sustained inward current in the Ca^{2+}/N-methyl-D-glucamine (NMDG) solution. (b) Current-voltage relationships for ET-1-induced current. Voltage steps ranging from −80 to +60 mV in 20-mV increments were applied before and after application of ET-1 (x and y in a) and the ET-1-induced currents at each membrane potential were determined as described in the legend to Figure 2. (c) Reversible inhibition by mefenamic acid (MA) of the ET-1-induced inward current in 30 mM Ca^{2+}/100 mM NMDG bath solution.

Whole-cell current in VSMCs

To examine whether a cation current is activated in VSMCs in response to stimulation by a low concentration of ET-1, whole-cell recordings were performed with freshly dispersed VSMCs of rabbit thoracic aortae. To block currents through VOC, 10 μM nifedipine was added to bath solution throughout the experiments. As in L*tk*$^-$ cells, 10^{-10} M ET-1 induced an inward current at a holding potential of −60 mV (Figure 4a). Characteristically, the current was sustained even after washout of ET-1 (Figure 4a). The amplitude of the ET-1-induced current was smaller than that in L*tk*$^-$ cells, ranging from 4 pA to 30 pA. Large transient currents observed in L*tk*$^-$ cells were not evoked in VSMCs. The reversal potential

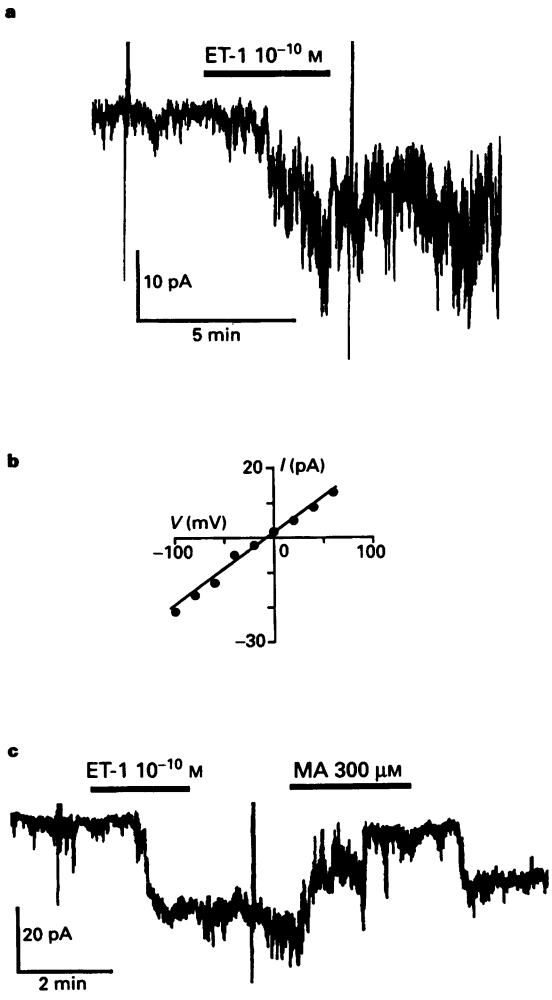

Figure 4 Whole-cell inward current induced by endothelin-1 (ET-1) in vascular smooth muscle cells freshly dispersed from rabbit thoracic aortae. The holding potential was −60 mV and the bath solution was Kreb-HEPES. For the pipette solution, the CsCl solution (a, b) or Cs-aspartate (c) was used. (a) A trace showing the ET-1-induced inward current. (b) Current-voltage relationships for ET-1 (10^{-10} M)-induced current. Voltage steps ranging from −100 to +60 mV in 20-mV increments were applied before and after the application of the ET-1 and the ET-1-induced currents at each membrane potential were determined as described in the legend to Figure 2. (c) Reversible inhibition by mefenamic acid (MA) of the ET-1-induced inward current.

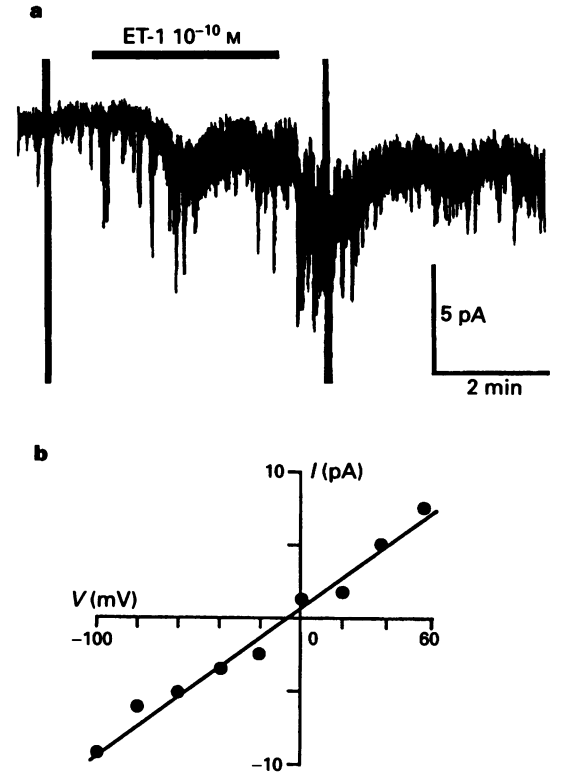

Figure 5 Whole-cell inward current induced by endothelin-1 (ET-1) in vascular smooth muscle cells freshly dispersed from rabbit thoracic aortae in the 30 mM Ca^{2+}/100 mM N-methyl-D-glucamine (NMDG) solution. In this experiment, the 30 mM Ca^{2+}/100 mM NMDG solution as described in the legend for Figure 3 was used for the bath solution, and the CsCl solution was used for the pipette solution. (a) A trace showing the ET-1-induced inward current. (b) Current-voltage relationships for ET-1-induced current. Voltage steps ranging from −100 to +60 mV in 20-mV increments were applied before and after application of ET-1, and the ET-1-induced currents at each membrane potential were determined as described in the legend for Figure 2.

of the current was unaffected by changing the Cl^- concentration in the pipette solution; −12.1 ± 2.0 mV (mean ± s.e., $n = 12$) in 139 mM Cl^- (Figure 4b) and −13.6 ± 3.6 mV ($n = 6$) in 24 mM Cl^- where the calculated E_{Cl} was −46.9 mV. This result suggests that the current is carried not through Cl^- channel but through cation channel, while the slightly negative reversal potential indicates that the channel is slightly more permeable to Cs^+ in the pipette solution than to Na^+ or K^+ in the bath solution. The sustained current was reversibly blocked by 300 μM mefenamic acid (Figure 4c).

As in L*tk*$^-$ cells, addition of 10 mM EGTA to the pipette solution did not affect the cation current activated by ET-1 (data not shown) and the inward current was induced even in 30 mM Ca^{2+}/100 mM NMDG solution (Figure 5a). Again, the current was sensitive to mefenamic acid (data not shown). As shown in Figure 5b, the reversal potential of the current was 0.3 ± 3.8 mV ($n = 4$), and P_{Ca2+}/P_{Cs+} was calculated to be 1.1.

Discussion

*Functional coupling of ET_A receptors with nonselective cation channel in L*tk$^-$ *cells and its electrophysiological properties*

In L*tk*$^-$ cells expressing human recombinant ET_A receptors, activation of the receptors by low concentrations of ET-1 was found to evoke an inward current, which persisted even after washout of ET-1 (Figure 2a). The current was considered to be carried by cations but not by anions such as Cl^-, because essentially similar reversal potentials were obtained regardless of the concentrations of Cl^- in the bath solution. Furthermore, the channel was considered to be equally permeable to Na^+ and Cs^+, judging from the reversal potential close to 0 mV (Figure 2b). In this sense, the channel activated by ET-1 is regarded as a nonselective cation channel.

Also it seemed that the inward current could be carried by Ca^{2+}, because ET-1 evoked an inward current even after Na^+ was replaced by the nonpermeant cation NMDG and the increased concentration of Ca^{2+} (Figure 3a). The P_{Ca2+}/P_{Cs+} was estimated from reversal potential values to be 2.5, indicating that the permeability of the channel to Ca^{2+} is higher than that to Cs^+. Thus these data indicate that recombinant ET_A receptors, when expressed in L*tk*$^-$ cells, can functionally couple with nonselective cation channel permeable to Ca^{2+}.

Activation of the channel was not voltage-dependent, as shown by a linear current-voltage relationship (Figure 2b). More importantly, activation of the channel was independent of elevation of $[Ca^{2+}]_i$ for the following two reasons. First, the inward current was evoked by a low concentration of ET-1 which did not induce a transient peak of $[Ca^{2+}]_i$ resulting from increased formation of IP_3 (Figure 1). Secondly the inward current was evoked by ET-1 even under the conditions where an elevation of $[Ca^{2+}]_i$ in the cell was prevented by the presence of excess amount of Ca^{2+} chelator, EGTA, in the patch pipette (Figure 2d).

The inward current activated by ET-1 persisted even after washout of the agonist (Figure 2a) and this property is consistent with the long-lasting nature of ET-1 action in vascular contraction (Kasuya *et al.*, 1989a).

The ET-1-induced current was sensitive to mefenamic acid (Figure 2c). Mefenamic acid is known as an inhibitor of cyclo-oxygenase (Flower & Vane, 1974) as well as an inhibitor of the nonselective cation channel (Gögelein *et al.*, 1990; Jung *et al.*, 1992). However inhibition of the ET-1-evoked inward current is not considered to be due to inhibition of cyclo-oxygenase, because the current was observed even after pretreatment with an inhibitor of cyclo-oxygenase, indomethacin (data not shown).

The increase in $[Ca^{2+}]_i$ in L*tk*$^-$ cells stimulated by low concentrations of ET-1 was totally dependent on Ca^{2+} entry (Figure 1b). The ET-1-induced Ca^{2+} entry into L*tk*$^-$ cells, which lacks VOC, was resistant to a specific blocker of L-type VOC (nifedipine) but was sensitive to mefenamic acid (Figure 1c). Combined with the electrophysiological results, these data strongly indicate that the ET-1-induced Ca^{2+} entry into the L*tk*$^-$ cells is carried through nonselective cation channel, leading to an increase in $[Ca^{2+}]_i$.

Properties of nonselective cation channel functionally coupled with ET_A receptors in VSMCs

As in L*tk*$^-$ cells, ET-1 evoked an inward current in VSMCs, which was considered to be carried through a cation channel mainly based on the observation that the reversal potential was not altered by changing the concentration of Cl^- in the pipette solution (Figure 4). There is discrepancy between these results and a previous report (Klöckner & Isenberg, 1991) in which ET-1 activates an inward current resulting from a Ca^{2+}-dependent Cl^- current. The discrepancy might be due to the high concentrations of ET-1 (10^{-8} M vs. 10^{-10} M in the present study) or the difference of the preparations (myocytes from porcine coronary artery and human mesenteric arteries vs. L*tk*$^-$ cells and VSMCs from rabbit thoracic aorta).

This channel is also regarded as a nonselective cation channel, because it was permeable to Na^+ and Cs^+ (Figure 4). However, the ion selectivity of the channel is slightly different from that in L*tk*$^-$ cells. That is, the reversal potential was slightly negative (around -10 mV), indicating that the channel is more permeable to Cs^+ than to Na^+ and K^+. Other properties of the nonselective cation channel in VSMCs are essentially similar to those in the L*tk*$^-$ cells. That is, activation of the channel was independent of both membrane potential (Figure 4b) and an elevation of $[Ca^{2+}]_i$ (data not shown). Again the inward current persisted even after washout of ET-1 (Figure 4a) and was sensitive to mefenamic acid (Figure 4c).

In some aspects, the properties of the channel activated by ET-1 are very similar to those of nonselective cation channels in VSMCs of rabbit portal vein (Bryne & Large, 1988; Wang & Large, 1991; Inoue & Kuriyama, 1993) and of rabbit ear artery (Amédée *et al.*, 1990; Wang *et al.*, 1993) which are activated by noradrenaline and acetylcholine. That is, activation of the channels is independent of an elevation of $[Ca^{2+}]_i$ (Amédée *et al.*, 1990; Inoue & Kuriyama, 1993), and the channels are permeable to divalent cations as well as monovalent cations. A distinctive feature of cation current activated by ET-1 is its persistence after washout of ET-1 (Figures 4a and 4c).

Physiological significance of nonselective cation channel

The present study clearly showed that recombinant and native ET_A receptors can functionally couple with a nonselective cation conductance, which is permeable to Ca^{2+} and that the permeability is high enough to induce an increase in $[Ca^{2+}]_i$. We also showed that the activation of the channel by ET-1 is long-lasting, a characteristic property of ET-1 action on vascular contraction. From these data, it is possible that the nonselective cation channel is a receptor-operated channel for vascular contraction evoked by a low concentration of ET-1.

We thank Dr R. Inoue for pertinent advice and valuable discussion. This work was supported by grants from the Ministry of Education, Science and Culture, Japan, and from the Ministry of Health and Welfare of Japan.

References

AMÉDÉE, T., BENHAM, C.D., BOLTON, T.B., BYRNE, N.G. & LARGE, W.A. (1990). Potassium, chloride and non-selective cation conductances opened by noradrenaline in rabbit ear artery cells. *J. Physiol.*, **423**, 551–568.

BYRNE, N.G. & LARGE, W.A. (1988). Membrane ionic mechanisms activated by noradrenaline in cells isolated from the rabbit portal vein. *J. Physiol.*, **404**, 557–573.

CHABRIER, P.E., AUGUET, M., ROUBERT, P., LONCHAMPT, M.O., GILLARD, V., GUILLON, J., DELAFLOTTE, S. & BRAQUET, P. (1989). Vascular mechanism of action of endothelin-1: effect of Ca^{2+} antagonists. *J. Cardiovasc. Pharmacol.*, **13** (Suppl. 5), S32–S35.

CHEN, C. & WAGONER, P.L. (1991). Endothelin induces a nonselective cation current in vascular smooth muscle cells. *Circ. Res.*, **69**, 447–454.

FLOWER, R.J. & VANE, J.R. (1974). Inhibition of prostaglandin biosynthesis. *Biochem. Pharmacol.*, **23**, 1439–1450.

FRACE, A.M. & GARGUS, J.J. (1989). Activation of single-channel currents in mouse fibroblasts by platelet-derived growth factor. *Proc. Natl. Acad. Sci. U.S.A.*, **86**, 2511–2515.

GÖGELEIN, H., DAHLEM, D., ENGLERT, H.C. & LANG, H.J. (1990). Flufenamic acid, mefenamic acid and niflumic acid inhibit single nonselective cation channels in the rat exocrine pancreas. *FEBS Lett.*, **268**, 79–82.

GOTO, K., KASUYA, Y., MATSUKI, N., TAKUWA, Y., KURIHARA, H., ISHIKAWA, T., KIMURA, S., YANAGISAWA, M. & MASAKI, T. (1989). Endothelin activates the dihydropyridine-sensitive, voltage-dependent Ca^{2+} channel in vascular smooth muscle. *Proc. Natl. Acad. Sci. U.S.A.*, **86**, 3915–3918.

HUANG, X., HISAYAMA, T. & TAKAYANAGI, I. (1990). Endothelin-1 induced contraction of rat aorta: contributions made by Ca^{2+} influx and activation of contractile apparatus associated with no change in cytoplasmic Ca^{2+} level. *Naunyn-Schmied. Arch. Pharmacol.*, **341**, 80–87.

INOUE, R. & KURIYAMA, H. (1993). Dual regulation of cation-selective channels by muscarinic and α_1-adrenergic receptors in the rabbit portal vein. *J. Physiol.*, **465**, 427–448.

INOUE, Y., OIKE, M., NAKAO, K., KITAMURA, K. & KURIYAMA, H. (1990). Endothelin augments unitary calcium channel currents on the smooth muscle cell membrane of guinea-pig portal vein. *J. Physiol.*, **423**, 171–191.

JUNG, F., SELVARAJ, S. & GARGUS, J.J. (1992). Blockers of platelet-derived growth factor-activated nonselective cation channel inhibit cell proliferation. *Am. J. Physiol.*, **262**, C1464–C1470.

KASUYA, Y., ISHIKAWA, T., YANAGISAWA, M., KIMURA, S., GOTO, K. & MASAKI, T. (1989a). Mechanism of contraction to endothelin in isolated porcine coronary artery. *Am. J. Physiol.*, **257**, H1828–H1835.

KASUYA, Y., TAKUWA, Y., YANAGISAWA, M., KIMURA, S., GOTO, K. & MASAKI, T. (1989b). Endothelin-1 induces vasoconstriction through two functionally distinct pathways in porcine coronary artery: contribution of phosphoinositide turnover. *Biochem. Biophys. Res. Commun.*, **161**, 1049–1055.

KLÖCKNER, U. & ISENBERG, G. (1991). Endothelin depolarizes myocytes from porcine coronary and human mesenteric arteries through a Ca-activated chloride current. *Pflügers Arch.*, **418**, 168–175.

KOBAYASHI, S. & TAKAHASHI, T. (1993). Whole-cell properties of temperature-sensitive neurones in rat hypothalamic slices. *Proc. R. Soc. B*, **251**, 89–94.

LEWIS, C. (1979). Ion-concentration dependence of the reversal potential and the single channel conductance of ion channels at the frog neuromuscular junction. *J. Physiol.*, **286**, 417–445.

MASAKI, T. (1994). Endothelin in vascular biology. *Ann. N.Y. Acad. Sci.*, **714**, 101–108.

MINTA, A., KAO, J.P.Y. & TSIEN, R.Y. (1989). Fluorescent indicators for cytosolic calcium based on rhodamine and fluorescein chromophores. *J. Biol. Chem.*, **264**, 8171–8178.

NEHER, E. (1988). The influence of intracellular calcium concentration on degranulation of dialysed mast cells from rat peritoneum. *J. Physiol.*, **395**, 193–214.

PEREZ-REYES, E., KIM, H.S., LACERDA, A.E., HORNE, W., WEI, X., RAMPE, D., CAMPBELL, K.P., BROWN, A.M. & BIRNBAUMER, L. (1989). Induction of calcium currents by the expression of the a1-subunit of the dihydropyridine receptor from skeletal muscle. *Nature*, **340**, 233–236.

RUBANYI, G.M. & POLOKOFF, M.A. (1994). Endothelins: molecular biology, biochemistry, pharmacology, physiology, and pathophysiology. *Pharmacol. Rev.*, **46**, 325–415.

SAKAMOTO, A., YANAGISAWA, M., SAWAMURA, T., ENOKI, T., OHTANI, T., SAKURAI, T., NAKAO, K., TOYOOKA, T. & MASAKI, T. (1993). Distinct subdomains of human endothelin receptors determine their selectivity to endothelin$_A$-selective antagonist and endothelin$_B$-selective agonists. *J. Biol. Chem.*, **268**, 8547–8553.

SIMPSON, A.W.M., STAMPFL, A. & ASHLEY, C.C. (1990). Evidence for receptor-mediated bivalent-cation entry in A10 vascular smooth-muscle cells. *Biochem. J.*, **267**, 277–280.

VAN HEESWIJK, M.P.E., GEERTSEN, J.A.M. & VAN OS, C.H. (1984). Kinetic properties of the ATP-dependent Ca^{2+} pump and the Na^+/Ca^{2+} exchange system in basolateral membranes from rat kidney cortex. *J. Membrane Biol.*, **79**, 19–31.

VAN RENTERGHEM, C., VIGNE, P., BARHANIN, J., SCHMIDAL-LIANA, A., FRELIN, C. & LAZDUNSKI, M. (1988). Molecular mechanism of action of the vasoconstrictor peptide endothelin. *Biochem. Biophys. Res. Commun.*, **157**, 977–985.

WANG, Q., HOGG, R.C. & LARGE, W.A. (1993). A monovalent ion-selective cation current activated by noradrenaline in smooth muscle cells of rabbit ear artery. *Pflügers Arch.*, **423**, 28–33.

WANG, Q. & LARGE, W.A. (1991). Noradrenaline-evoked cation conductance recorded with the nystatin whole-cell method in rabbit portal vein cells. *J. Physiol.*, **435**, 21–39.

YANAGISAWA, M., KURIHARA, H., KIMURA, S., TOMOBE, Y., KOBAYASHI, M., MITSUI, Y., YAZAKI, Y., GOTO, K. & MASAKI, T. (1988). A novel potent vasoconstrictor peptide produced by vascular endothelial cells. *Nature*, **332**, 411–415.

(Received January 4, 1995
Revised February 6, 1995
Accepted February 10, 1995)

British Journal of Pharmacology (1995) 115, 486-490

Central versus peripheral site of action of the tachykinin NK_1-antagonist RP 67580 in inhibiting chemonociception

Ulrike Holzer-Petsche & Tamara Rordorf-Nikolić

Department of Experimental and Clinical Pharmacology, Karl-Franzens-University, Universitätsplatz 4, A-8010 Graz, Austria

1 Many studies indicate an involvement of substance P in the transmission of nociceptive stimuli, without, however, presenting any conclusive evidence as to its exact site and mode of action. The present experiments tested the involvement of substance P in the mediation of chemical nociception using the non-peptidic specific tachykinin NK_1-receptor antagonist, RP 67580 (2-[1-imino-2-(2-methoxyphenyl-ethyl]-7,7diphenyl-4-perhydroisoindolone (3a**R**, 7a**R**)).

2 Mean arterial pressure (MAP) and intragastric pressure (IGP) were measured in anaesthetized rats. The reflex changes of these parameters in response to i.p. or s.c. injections of hydrochloric acid or capsaicin were taken to indicate nociception.

3 Intravenous administration of RP 67580 up to 5 mg kg^{-1} had little influence on the reflex changes in MAP or IGP in response to hydrochloric acid or capsaicin. In contrast, the sensitization of rats to i.p. capsaicin by preinjection of prostaglandin E_2 was significantly reduced by 1 mg kg^{-1} RP 67580.

4 Intrathecal injection of 5 μg RP 67580 inhibited the reflex changes of MAP and IGP in response to i.p. or s.c. capsaicin whereas the inactive enantiomer RP 68651 was ineffective.

5 The results indicate that spinal NK_1-receptors are involved in the acute transmission of chemically induced pain, while such receptors in the periphery take part in the sensitization by prostaglandin E_2. The rather minor ability of i.v. RP 67580 to inhibit the acute nociceptive reflex is attributed to an insufficient penetration of the blood-brain-barrier.

Keywords: Pain; chemonociception; substance P; NK_1-antagonist; sensitization

Introduction

Both anatomical and functional studies indicate an involvement of substance P in the spinal transmission of noxious stimuli (see Otsuka & Yoshioka, 1993). Up to now, however, no conclusive evidence exists as to whether substance P acts as a transmitter *per se* at the first spinal synapse or whether it only facilitates the action of glutamate (Dougherty & Willis, 1991; Mjellem-Joly *et al.*, 1992; Rusin *et al.*, 1992; 1993). Part of the evidence stems from the fact that non-peptidic antagonists of the NK_1-receptor, like CP-96,345 or RP 67580, display antinociceptive action, mainly in models of chemonociception (Garret *et al.*, 1991; 1992; Yamamoto & Yaksh, 1991; Berge & Ståhlberg, 1993; Chapman & Dickenson, 1993; Yashpal *et al.*, 1993). Regarding models of thermal nociception, however, reports on the effectiveness of these antagonists are conflicting (Lecci *et al.*, 1991; Radhakrishnan & Henry, 1991; Berge & Ståhlberg, 1993; Szolcsányi *et al.*, 1993). Contrary to the early antagonist substance P analogues, the new compounds are devoid of neurotoxic effects and are therefore suitable for administration to the spinal cord (Yamamoto & Yaksh, 1991).

The present study investigated the action of the selective NK_1-receptor antagonist, RP 67580, in a model of visceral and somatic chemonociception in anaesthetized rats. RP 67580 was chosen because of its higher affinity for the rat NK_1-receptor than CP-96,345 (Fong *et al.*, 1992; Fardin *et al.*, 1993b).

Methods

Experimental setup

Sprague-Dawley rats of either sex (200-300 g body weight; Forschungsanstalt für Versuchstierkunde, Himberg, Austria) were fasted overnight with free access to tap water. The experimental setup has been described in detail earlier (Holzer-Petsche, 1992). In brief, under phenobarbitone anaesthesia (250 mg kg^{-1}, i.p.) the trachea was cannulated and the oesophagus ligated in the neck. Blood pressure was monitored from a carotid artery, a jugular vein was cannulated for continuous i.v. infusion of a glucose-bicarbonate buffer (1.5 ml h^{-1}) and drug injections. After laparotomy, a cannula was introduced into the stomach via the pylorus for measurement of isometric gastric contractions at a constant volume of 5 ml isotonic saline. A fall in mean arterial blood pressure (MAP) and intragastric pressure (IGP) was taken to indicate nociception (Cervero & McRitchie, 1982; Holzer-Petsche, 1992).

For injection of algesic chemicals, up to five PE-10 cannulae were positioned in the peritoneal cavity between folds of the mesentery, taking care to avoid direct contact of the tips of the i.p. catheters with the stomach. In some experiments similar cannulae were also introduced into the abdominal subcutis. Body temperature was kept constant at 37-38°C by means of a heating pad.

HCl and capsaicin were used as algesic compounds and always injected in a volume of 100 μl. At the beginning of each experiment the threshold dose of each test substance at i.p. or s.c. administration was established for each rat. Then the antagonist or the control solution was administered i.v. (up to 2.5 ml kg^{-1}) and 10 and 20 min later the i.p. and s.c. injections of the previously established threshold doses of algesics were repeated.

In the experiments testing the effect of RP 67580 on sensitization, the threshold dose of i.p. capsaicin was arbitrarily set as '100'. After i.v. injection of RP 67580 or vehicle, 3 pmol PGE_2 was given i.p. immediately before, and through the same cannula as, each further administration of capsaicin at doses 3, 10, 30, and 100. This series of injections was always finished within 40 min after the i.v. administration of RP 67580, i.e. within the tested duration of action of the

[1] Author for correspondence.

antagonist. Because the magnitude of the responses did not correlate well with the doses of capsaicin, the results were evaluated as all-or-none effects.

For intrathecal injections, a PE-10 cannula was introduced at the beginning of the experiment through the cisterna magna so that its tip lay at the dorsal surface of the spinal cord at the lower thoracic/upper lumbar level. Injection volumes were 10 µl. The correct position of the cannula was verified by injecting 10 µl Evans blue at the end of the experiment and inspecting the distribution of the dye.

Statistics

Values are presented as means ± s.e.mean. Statistical comparisons were made using the Wilcoxon-Pratt test or Fisher's exact test for 2 × 2 tables, both one-sided, rejecting the null hypothesis if the treatment reduced the reflex response. In the case of testing RP 67580 against the hypotensive effect of substance P the Quade test was used (Conover, 1980). $P<0.05$ was regarded as statistically significant.

Substances

RP 67580 (2-[1-imino-2-(2-methoxyphenyl) ethyl]-7,7 diphenyl-4-perhydroisoindolone (3a**R**,7a**R**)) and the inactive 3a**S**,7a**S** enantiomer RP 68651 were generously supplied by Dr C. Garret, Rhône-Poulenc Rorer, Vitry, France. RP 67580 was dissolved in 23 mM HCl at a concentration of 5 mg ml^{-1}, RP 68651 in 9 mM HCl at 4 mg ml^{-1}. Capsaicin was obtained from Serva (Heidelberg, Germany) and dissolved in 10% ethanol, 10% Tween80 and 80% isotonic NaCl at 10 mg ml^{-1} (33 µmol l^{-1}). A stock solution of 1 mmol l^{-1} substance P (Cambridge Research Biochemicals, Northwich, United Kingdom) was made up with distilled water. All dilutions were made with isotonic saline.

Results

Effect of i.v. RP 67580

Both i.p. and s.c. injection of capsaicin or HCl caused a prompt and transient fall in MAP and IGP (Figure 1). The threshold doses varied widely between rats: for HCl i.p. they ranged from 0.03–10 mmol l^{-1}, for HCl s.c. from 0.03–100 mmol l^{-1}, for capsaicin i.p. from 0.01–10 pmol, and for capsaicin s.c. from 0.003–100 pmol.

In control experiments, vehicle (HCl) was administered i.v. at a concentration of 4.6 mmol l^{-1} (1 ml kg^{-1}) corresponding to 1 mg kg^{-1} RP 67580 or at a concentration of 11.5 mmol l^{-1} (2 ml kg^{-1}), which corresponded to 5 mg kg^{-1} of the antagonist. These injections did not significantly influence the reflex changes of MAP and IGP in response to i.p. or s.c. injection of threshold doses of HCl or capsaicin (Table 1). As to RP 67580, 5 mg kg^{-1} (11.4 µmol kg^{-1}) significantly inhibited only the changes in IGP after i.p. injection of capsaicin while having no statistically significant effect on the other parameters measured (Table 1). For reasons of solubility, higher doses of RP 67580 could not be tested.

In most control rats (vehicle i.v.), 3 pmol PGE_2 injected prior to, and through the same cannula as, capsaicin caused sensitization. This means that changes in MAP and IGP occurred in response to previously subthreshold doses of capsaicin. After RP 67580 (1 mg kg^{-1}, i.v.), the proportion of

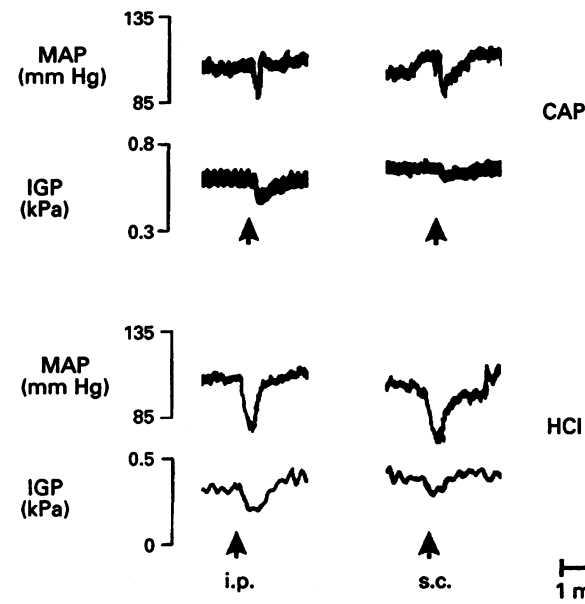

Figure 1 Typical tracings of the changes in mean arterial pressure (MAP) and intragastric pressure (IGP) caused by i.p. or s.c. injections of threshold doses of capsaicin (Cap, 10 pmol i.p. and 0.003 pmol s.c. in the experiment shown) or HCl (3 mmol l^{-1} i.p. and s.c.).

Table 1 Effect of RP 67580 (A) or vehicle (HCl; B) injected i.v. on falls in mean arterial blood pressure (MAP) and intragastric pressure (IGP) induced by threshold doses of i.p. or s.c. HCl or capsaicin (Cap)

A		*Fall in MAP* (mmHg)		*Fall in IGP* (kPa)	
Stimulus	*Dose of RP 67580*	*before*	*after* RP67580	*before*	*after* RP67580
HCl i.p.	1 mg kg^{-1}	−12 ± 2	−15 ± 6 (6)	−0.09 ± 0.05	−0.11 ± 0.04 (6)
HCl s.c.	1 mg kg^{-1}	−14 ± 3	−18 ± 3 (10)	−0.04 ± 0.02	−0.07 ± 0.03 (9)
Cap i.p.	1 mg kg^{-1}	−15 ± 2	−15 ± 4 (13)	−0.11 ± 0.03	−0.07 ± 0.02 (12)
	5 mg kg^{-1}	−14 ± 3	−7 ± 1 (6)	−0.14 ± 0.02	−0.06 ± 0.03 (5)*
Cap s.c.	1 mg kg^{-1}	−19 ± 3	−16 ± 3 (8)	−0.05 ± 0.01	−0.05 ± 0.02 (6)
	5 mg kg^{-1}	−13 ± 3	−3 ± 2 (5)	−0.04 ± 0.01	−0.03 ± 0.01 (3)
B		*Fall in MAP* (mmHg)		*Fall in IGP* (kPa)	
Stimulus	*Concentration and dose of vehicle*	*before*	*after* vehicle	*before*	*after* vehicle
HCl i.p.	4.6 mmol l^{-1}; 1 ml kg^{-1}	−13 ± 3	−12 ± 3 (7)	−0.06 ± 0.01	−0.21 ± 0.13 (7)
HCl s.c.	4.6 mmol l^{-1}; 1 ml kg^{-1}	−13 ± 4	−14 ± 5 (7)	−0.02 ± 0.01	−0.02 ± 0.01 (7)
Cap i.p.	4.6 mmol l^{-1}; 1 ml kg^{-1}	−18 ± 3	−17 ± 3 (11)	−0.11 ± 0.01	−0.13 ± 0.03 (12)
	11.5 mmol l^{-1}; 2 ml kg^{-1}	−17 ± 5	−5 ± 3 (5)	−0.13 ± 0.04	−0.04 ± 0.02 (5)
Cap s.c.	(not tested)				

Mean ± s.e.mean; *n* in parentheses; *$P<0.05$ vs. before injection, one-sided Wilcoxon test

Table 2 Effect of RP 67580 (1 mg kg^{-1}, i.v.) on sensitization to i.p. capsaicin (Cap) by i.p. prostaglandin E_2 (PGE_2) (3 pmol)

Dose of Cap after PGE_2	*Fall in MAP* (vehicle)	*Fall in Map* (RP 67580)	*Fall in IGP* (vehicle)	*Fall in IGP* (RP 67580)
3	11/14 (79%)	7/16 (44%)	11/15 (73%)	5/16 (31%)*
10	10/14 (71%)	4/16 (25%)*	9/14 (64%)	3/16 (19%)*
30	13/14 (93%)	8/16 (50%)*	13/15 (87%)	6/16 (38%)*
100	11/15 (73%)	13/16 (81%)	12/15 (80%)	13/16 (81%)

Data are the number of rats responding to capsaicin vs. total *n*, the corresponding percentage is given in parentheses. The response is defined as fall in mean arterial pressure (MAP) and fall in intragastric pressure (IGP) caused by capsaicin. The threshold dose of capsaicin was set as 100.
*$P<0.05$ vs. vehicle (Fisher's exact test for 2 × 2 tables, one-sided)

rats responding to subthreshold doses of capsaicin after PGE_2 was significantly reduced (Table 2).

Effect of i.t. RP 67580

Intrathecal administration of RP 67580 (5 μg; 11.4 nmol) to the dorsal surface of the lower thoracic/upper lumbar spinal cord significantly reduced the falls in MAP and IGP in response to threshold doses of capsaicin given i.p. or s.c. Administration of the inactive stereoisomer RP 68651 (5 μg) or of equal volumes of vehicle had no effect (Figure 2).

Antagonist action of RP 67580 against i.v. substance P

RP 67580 at 1 mg kg^{-1}, i.v., significantly antagonized the hypotensive action of substance P (0.2 nmol kg^{-1}, i.v.) up to 50 min after injection (Table 3). Intrathecally administered RP 67580 (5 μg) had no such effect: 10 min after i.t. injection, the fall in MAP caused by i.v. substance P amounted to 98 ± 18% of control ($n = 5$).

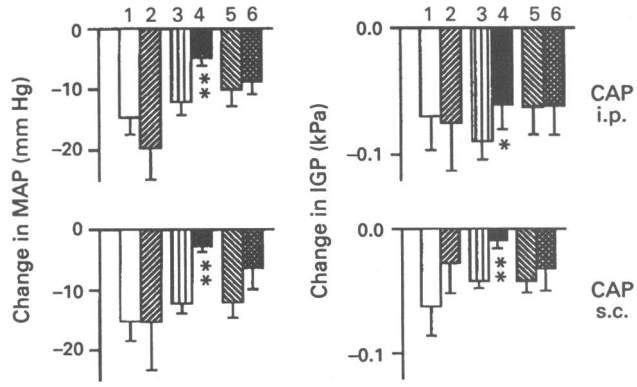

Figure 2 Effect of intrathecal injections of RP 67580 (5 μg), its inactive enantiomer RP 68651 (5 μg) or of vehicle (10 μl) on the reflex fall in mean arterial blood pressure (MAP) and intragastric pressure (IGP) in response to threshold doses of i.p. and s.c. capsaicin (Cap). (1) Before / (2) after vehicle ($n = 4$); (3) before / (4) after RP 67580 ($n = 11-13$); (5) before / (6) after RP 68651 ($n = 5-8$). Columns denote means, with s.e.mean.
*$P<0.05$; **$P<0.001$ vs. before i.t. injection (Wilcoxon-test, one-sided)

Table 3 Antagonism by RP 67580 (1 mg kg^{-1}, i.v.) of the fall in mean arterial pressure (MAP) induced by 0.2 nmol kg^{-1} substance P, i.v.

Time after injection of RP 67580	*Fall in MAP (% of control)*
10 min	6 ± 4%**
20 min	21 ± 6%**
30 min	36 ± 8%**
40 min	48 ± 7%**
50 min	62 ± 7%*
60 min	87 ± 18%

*$P<0.05$, **$P<0.001$ vs. 100% (calculated from the raw data using the Quade test).

Discussion

The present study shows that i.v. administration of the NK_1-antagonist RP 67580 up to 5 mg kg^{-1} does not substantially antagonize reflex responses to acute chemical painful stimuli. This contrasts with the marked antinociceptive effect of only 1 mg kg^{-1} of this antagonist in the phenylbenzoquinone writhing test (Garret *et al.*, 1992), where pain-related behaviour is also induced by i.p. injection of an irritant. This lack of antagonism cannot, however, be attributed to an insufficient blockade of NK_1-receptors, because in the present study 1 mg kg^{-1} RP 67580 inhibited substance P-induced hypotension.

Contrary to the lack of effect of i.v. administered RP 67580, i.t. injection reduced the reflex responses to i.p. or s.c. administered painful chemicals. Thus one has to conclude that spinal NK_1-receptors do take part in acute chemonociception, either somatic or visceral. The observed discrepancy can be explained by the limited ability of RP 67580 to cross the blood-brain barrier (Fardin *et al.*, 1993a). When tested i.t., the enantiomer RP 68651 proved ineffective, indicating that the action of RP 67580 was indeed due to the blockade of NK_1-receptors and not an unspecific effect as might be concluded from the findings of Rupniak *et al.* (1993).

However, 1 mg kg^{-1} RP 67580 administered peripherally, i.e. intravenously, was active against the sensitization of peritoneal nociceptors: the proportion of rats becoming sensitized to i.p. capsaicin by preinjected PGE_2 was lower in the RP 67580 group than in the vehicle group. Such an attenuation of sensitization phenomena by RP 67580 has also been observed by Amann & Donnerer (1993).

In assessing the above findings, one has to examine those models of nociception where NK_1-antagonists have proven active: non-peptide NK_1-antagonists display antinociceptive actions preferably in models of nociception involving inflammatory or sensitizing events. These include thermal hyperalgesia induced by heat (Yashpal *et al.*, 1993) as well as the second phase of pain-related behaviour in the formalin test (Yamamoto & Yaksh, 1991; Berge & Ståhlberg, 1993; Yashpal *et al.*, 1993; Chapman & Dickenson, 1993). This suggests that substance P plays a role in the development of the inflammation or of the hyperalgesia accompanying this inflammation rather than in the transmission of the acute noxious stimulus. Reports on acute antinociceptive actions of NK_1-antagonists are equivocal, but the tendency for the substances to block nociceptive reflexes seems to be greater when they are administered directly to the spinal cord rather than in the periphery (Radharkrishnan & Henry, 1991; Chapman & Dickenson, 1993).

While CP-96,345 has been shown to penetrate the blood-brain well enough (Lecci *et al.*, 1991), the present study indicates the opposite for RP 67580, as is also emphasized by Fardin *et al.* (1993a). This differs from the conclusion drawn by Laird *et al.* (1993) from their observation that i.v. administered RP 67580 inhibits the facilitation of a nociceptive spinal flexion reflex in anaesthetized rats. However, their results might also be interpreted as RP 67580 inhibiting facilitation at a peripheral level: the conditioning stimulus to the afferent C-fibres might release enough substance P from the peripheral nerve endings in order to lead to a short-lived sensitization of the afferent fibres.

Several studies indicate a peripheral role of substance P via NK_1-receptors in sensitizing afferent nerve endings. Kessler *et al.* (1992) have demonstrated on a rat skin-nerve preparation *in vitro* that substance P sensitizes nociceptors to a mixture of inflammatory mediators. Yamamoto *et al.* (1993) have shown that carrageenin-induced thermal hyperalgesia of the rat paw can be prevented by i.v. but not i.t. administration of the NK_1- antagonists CP-96,345 or the combined NK_1/NK_2-antagonist FK224. From differences in efficacies between i.p. and i.t. administered CP-96,345 Berge & Ståhlberg (1993) deduce a peripheral site of action of the antagonist in inhibiting the second phase of the formalin test. Analogous, though unrelated to nociception, is the ability of CP-96,345 to block hypoxia-induced afferent activity in the carotid sinus nerve of cats (Prabhakar *et al.*, 1993). According to these authors this might imply that substance P from glomus cells is involved in exciting afferent nerve endings via NK_1-receptors. Thus there is quite some evidence in favour of substance P sensitizing or even exciting peripheral afferent endings.

Even the effectiveness of RP 67580 in the writhing test (Garret *et al.*, 1992) might possibly be attributed to a peripheral action: the behaviour in the writhing test usually takes a few minutes to develop. It is conceivable that during this time lag sensitization phenomena are initiated, which might be blunted by peripherally acting NK_1-antagonists.

The mechanism of such a sensitization is, however, still far from being elucidated. It is known that substance P releases prostaglandins from a variety of cells, for example, synoviocytes (Lotz *et al.*, 1987), or spinal cord astrocytes (Marriott *et al.*, 1991). These prostaglandins, in turn, can sensitize nociceptive nerve endings to subsequent stimuli. However, there are data indicating also the opposite sequence of events, i.e. prostaglandins apparently releasing substance P: Nakamura-Craig & Smith (1989) showed that repeated subplantar injections of substance P or PGE_2 caused mechanical hyperalgesia in rats pretreated with indomethacin. A substance P antagonist blocked the sensitization by substance P as well as that by PGE_2. In fact, in cultures of chick embryo dorsal root ganglion cells PGE_2 was directly observed to release substance P (Nicol *et al.*, 1992). Such a mechanism might also apply in the present model of sensitization by PGE_2.

In conclusion, the results of the present study indicate that central NK_1-receptors contribute to the direct transmission of painful chemical stimuli, while peripheral receptors play a role in sensitization phenomena.

The authors thank Mrs B. Brodacz for excellent technical assistance and Dr C Garret, of Rhône-Poulenc Rorer, for the generous supply of RP 67580 and RP 68651. T.R.-N. held an ARGE Alpen-Adria Fellowship from the Government of Styria. The work was supported by the Austrian Research Foundation, grant no. P7858-MED.

References

AMANN, R. & DONNERER, J. (1993). Effect of RP 67580 on capsaicin-induced stimulation of afferent fibres in the rat. *Neuropeptides*, **24**, 210.

BERGE, O.G. & STÅHLBERG, M. (1993). Is the selective non-peptide NK-1 receptor antagonist CP96,345 a peripherally acting analgesic. *Regul. Pept.*, **46**, 430–432.

CERVERO, F. & MCRITCHIE, H.A. (1982). Effects of neonatal administration of capsaicin on several nociceptive systems of the rat. In *Advances in Pain Research and Therapy*. ed. Bonica, J.J. pp. 87–94. New York: Raven Press.

CHAPMAN, V. & DICKENSON, A.H. (1993). The effect of intrathecal administration of RP67580, a potent neurokinin-1 antagonist on nociceptive transmission in the rat spinal cord. *Neurosci. Lett.*, **157**, 149–152.

CONOVER, W.J. (1980). *Practical Nonparametric Statistics*. pp. 213–255. New York: John Wiley & Sons.

DOUGHERTY, P.M. & WILLIS W.D. (1991). Enhancement of spinothalamic neuron responses to chemical and mechanical stimuli following combined micro-iontophoretic application of N-methyl-D-aspartic acid and substance P. *Pain*, **47**, 85–93.

FARDIN, V., BOCK, M.D., FOUCAULT, F. & GARRET, C. (1993a). RP 67580, a non-peptide substance P antagonist with low penetration to the central nervous system. *7th World Congress on Pain*, Abstract 636.

FARDIN, V., FOUCAULT, F., BOCK, M.D., JOLLY, A., FLAMAND, O., CLERC, F. & GARRET, C. (1993b). Variations in affinities for the NK_1 receptor: differences between the non-peptide substance P antagonists RP67580 and CP-96,345 and the agonist peptide. *Regul. Pept.*, **46**, 300–303.

FONG, T.M., YU, H. & STRADER, C.D. (1992). Molecular basis for the species selectivity of the neurokinin-1 receptor antagonists CP-96,345 and RP67580. *J. Biol. Chem.*, **267**, 25668–25671.

GARRET, C., CARRUETTE, A., FARDIN, V., MOUSSAOUI, S., PEYRONEL, J.F., BLANCHARD, J.C. & LADURON, P.M. (1991). Pharmacological properties of a potent and selective nonpeptide substance P antagonist. *Proc. Natl. Acad. Sci. U.S.A.*, **88**, 10208–10212.

GARRET, C., CARRUETTE, A., FARDIN, V., MOUSSAOUI, S., PEYRONEL, J.F., BLANCHARD, J.C. & LADURON, P.M. (1992). RP 67580, un antagoniste, non peptidique, puissant et sélectif de la substance P. *C. R. Acad. Sci. Paris, Série III*, **314**, 199–204.

HOLZER-PETSCHE, U. (1992). Blood pressure and gastric motor responses to bradykinin and hydrochloric acid injected into somatic or visceral tissues. *Naunyn-Schmied. Arch. Pharmacol.*, **346**, 219–225.

KESSLER, W., KIRCHHOFF, C., REEH, P.W. & HANDWERKER, H.O. (1992). Excitation of cutaneous afferent nerve endings *in vitro* by a combination of inflammatory mediators and conditioning effect of substance P. *Exp. Brain Res.*, **91**, 467–476.

LAIRD, J.M.A., HARGREAVES, R.J. & HILL, R.G. (1993). Effect of RP 67580, a non-peptide neurokinin$_1$ receptor antagonist, on facilitation of a nociceptive spinal flexion reflex in the rat. *Br. J. Pharmacol.*, **109**, 713–718.

LECCI, A., GIULIANI, S., PATACCHINI, R., VITI, G. & MAGGI, C.A. (1991). Role of NK_1 tachykinin receptors in thermonociception: effect of (±)-CP 96,345, a non-peptide substance P antagonist, on the hot plate test in mice. *Neurosci. Lett.*, **129**, 299–302.

LOTZ, M., CARSON, D.A. & VAUGHAN, J.H. (1987). Substance P activation of rheumatoid synoviocytes: neural pathway in pathogenesis of arthritis. *Science*, **235**, 893–895.

MARRIOTT, D., WILKIN, G.P., COOTE, P.R. & WOOD, J.N. (1991). Eicosanoid synthesis by spinal cord astrocytes is evoked by substance P; possible implications for nociception and pain. *Adv. Prostaglandin Thromboxane Leukotriene Res.*, **21B**, 739–741.

MJELLEM-JOLLY, N., LUND, A., BERGE, O.G. & HOLE, K. (1992). Intrathecal co-administration of substance P and NMDA augments nociceptive responses in the formalin test. *Pain*, **51**, 195–198.

NAKAMURA-CRAIG, M. & SMITH T.W. (1989). Substance P and peripheral inflammatory hyperalgesia. *Pain*, **38**, 91–98.

NICOL, G.D., KLINGBERG, D.K. & VASKO, M.R. (1992). Prostaglandin E_2 increases calcium conductance and stimulates release of substance P in avian sensory neurons. *J. Neurosci.*, **12,** 1917–1927.

OTSUKA, M. & YOSHIOKA, K. (1993). Neurotransmitter functions of mammalian tachykinins. *Physiol. Rev.*, **73,** 229–308.

PRABHAKAR, N.R., CAO, H., LOWE III, J.A. & SNIDER, R.M. (1993). Selective inhibition of the carotid body sensory response to hypoxia by the substance P receptor antagonist CP-96,345. *Proc. Natl. Acad. Sci. U.S.A.*, **90,** 10041–10045.

RADHAKRISHNAN, V. & HENRY, J.L. (1991). Novel substance P antagonist, CP-96, 345, blocks responses of cat spinal dorsal horn neurons to noxious cutaneous stimulation and to substance P. *Neurosci. Lett.*, **132,** 39–43.

RUPNIAK, N.M.J., BOYCE, S., WILLIAMS, A.R., COOK, G., LONGMORE, J., SEABROOK, G.R., CAESER, M., IVERSEN, S.D. & HILL, R.G. (1993). Antinociceptive activity of NK_1 receptor antagonists: non-specific effects of racemic RP67580. *Br. J. Pharmacol.*, **100,** 1607–1613.

RUSIN, K.I., BLEAKMAN, D., CHARD, P.S., RANDIĆ, M. & MILLER, R.J. (1993). Tachykinins potentiate N-methyl-D-aspartate responses in acutely isolated neurons from the dorsal horn. *J. Neurochem.*, **60,** 952–960.

RUSIN, K.I., RYU, P.D. & RANDIĆ, M. (1992). Modulation of excitatory amino acid responses in rat dorsal horn neurons by tachykinins. *J. Neurophysiol.*, **68,** 265–286.

SZOLCSÁNYI, J., NAGY, J. & PETHÖ, G. (1993). Effect of CP-96,345 a non-peptide substance P antagonist, capsaicin, resiniferatoxin and ruthenium red on nociception. *Regul. Pept.*, **46,** 437–439.

YAMAMOTO, T., SHIMOYAMA, N. & MIZUGUCHI, T. (1993). Effects of FK224, a novel cyclopeptide NK_1 and NK_2 antagonist, and CP-96,345, a nonpeptide NK_1 antagonist, on development and maintenance of thermal hyperesthesia evoked by carrageenan injection in the rat paw. *Anesthesiology*, **79,** 1042–1050.

YAMAMOTO, T. & YAKSH, T.L. (1991). Stereospecific effects of a nonpeptidic NK-1 selective antagonist, CP-96345: antinociception in the absence of motor dysfunction. *Life Sci.*, **49,** 1955–1963.

YASHPAL, K., RADHAKRISHNAN, V., CODERRE, T.J. & HENRY, J.L. (1993). CP-96,345, but not its stereoisomer, CP-96,344, blocks the nociceptive responses to intrathecally administered substance P and to noxious thermal and chemical stimuli in the rat. *Neuroscience*, **52,** 1039–1047.

(Received July 18, 1994
Accepted October 25, 1994)

British Journal of Pharmacology (1995) 115, 491-497

Characterization of the effects of two new arginine/citrulline analogues on constitutive and inducible nitric oxide synthases in rat aorta

Ghislaine A. Joly, *Krish Narayanan, *Owen W. Griffith & [1]Robert G. Kilbourn

Department of Genitourinary Oncology, The University of Texas M.D. Anderson Cancer Center, Houston, Texas 77030 and *Department of Biochemistry, Medical College of Wisconsin, Milwaukee, Wisconsin 53226, U.S.A.

1 New potent inhibitors of nitric oxide synthase (NOS) may be useful in the treatment of septic shock, a disorder characterized by a vascular hyporeactivity to catecholamines caused by an overproduction of nitric oxide (NO^-). We examined the effects of L-thiocitrulline (L-TC) and S-methyl-L-thiocitrulline (L-SMTC), novel NOS inhibitors, on the constitutive and inducible NOS in rat aorta and compared those effects with inhibition due to N^G-methyl-L-arginine (L-NMA).

2 Phenylephrine evoked similar concentration-contraction curves in the control rings and in the rings treated with these different NOS inhibitors (10 μM), whereas 100 μM of L-NMA, L-TC or L-SMTC increased significantly, and to a similar extent, contractions evoked by phenylephrine in aortic rings with endothelium without significantly affecting the maximal responses.

3 Relaxations evoked by acetylcholine, adenosine triphosphate, or calcium ionophore were significantly inhibited in a dose-dependent manner by L-NMA, L-SMTC, or L-TC (10-100 μM). The potencies of these inhibitors in reducing the relaxations of these vasodilators were not significantly different.

4 In endotoxin-treated preparations with endothelium, the three L-arginine analogues (10 μM) significantly potentiated contractile responses to phenylephrine (pEC_{50}: 6.73 ± 0.12 and 7.3 ± 0.12, 7.34 ± 0.13, or 7.22 ± 0.14; in the absence and the presence of L-NMA, L-TC, or L-SMTC respectively) and increased maximal contractions from 1.53 ± 0.15 g to 1.95 ± 0.13 g, 2.08 ± 0.12 g, and 2.03 ± 0.13 g with L-NMA, L-TC, and L-SMTC respectively. A higher concentration of these NOS inhibitors (100 μM) further increased contractions evoked by this α_1-agonist without further enhancing the maximal contractions; however, contractions evoked by 10 nM phenylephrine were significantly greater in the presence of L-SMTC or L-TC than in the presence of L-NMA (100 μM) (L-NMA: 0.4 ± 0.11 g; L-TC: 0.78 ± 0.14 g and L-SMTC: 0.82 ± 0.17 g). The effects of these inhibitors on NO^- synthesis induced by endotoxin were significantly reversed by addition of L-arginine (1 mM) but not by L-citrulline (1 mM). In LPS-treated rings with endothelium, all three NOS inhibitors (100 μM) shifted the concentration-contraction curves evoked by phenylephrine significantly to the left (pEC_{50}: 7.19 ± 0.03 and 7.79 ± 0.08, 8.01 ± 0.07, or 8.02 ± 0.07, in the absence and the presence of L-NMA, L-TC, or L-SMTC, respectively) and increased significantly maximal contractions from 2.05 ± 0.05 g to 2.38 ± 0.14 g, 2.5 ± 0.12 g, and 2.4 ± 0.21 g with L-NMA, L-TC, and L-SMTC, respectively. L-TC and L-SMTC were significantly more potent than L-NMA in potentiating contractions evoked by 10 nM and 30 nM phenylephrine.

5 L-TC and L-SMTC produced dose-dependent increases in tone in LPS-treated aortic rings with and without endothelium. In LPS-treated rings with endothelium, L-NMA induced contractions but in preparations without endothelium low concentrations of L-NMA induced small contractions while high concentrations of this inhibitor evoked relaxations. In both preparations L-TC and L-SMTC were significantly more potent than L-NMA in increasing vascular tone.

6 These results suggest that L-SMTC, L-TC and L-NMA were equipotent on basal and agonist-stimulated NO^- synthesis produced by the constitutive isoform of NOS, whereas the two new L-arginine analogues were more potent than L-NMA in inhibiting the production of NO^- induced by endotoxin in rat aorta.

Keywords: Nitric oxide synthase; N^G-methyl-L-arginine; L-thiocitrulline; S-methyl-L-thiocitrulline; rat aorta

Introduction

The nitric oxide synthases (NOS) constitute a family of closely related isoenzymes (Stuehr & Griffith, 1992). In endothelial cells (Palmer *et al.*, 1988; Forsterman *et al.*, 1991) and in neurones (Bredt *et al.*, 1990; Bohme *et al.*, 1991; Snyder, 1992) they are constitutively present and activated by calcium/calmodulin. In contrast, a calcium-calmodulin independent NOS is expressed in macrophages (Marletta *et al.*, 1988) and in vascular smooth muscle (Busse & Mulsch, 1990; Fleming *et al.*, 1990; Beasley *et al.*, 1991; Schini *et al.*, 1991) and endothelial cells (Gross *et al.*, 1990; Kilbourn & Belloni, 1990) of vascular wall cells only after stimulation by endotoxin or cytokines. Constitutive production of nanomolar amounts of nitric oxide (NO^-) by endothelial cells appears vital to blood pressure homeostasis, whereas the inducible isoform of NOS (iNOS) can generate micromolar quantities of NO^- that probably contribute to both the local tissue damage and the systemic hypotension that characterize septic shock (Julou-Schaeffer *et al.*, 1990; Kilbourn *et al.*, 1990).

Structural modification of one of the two equivalent guanidino nitrogens of L-arginine results in compounds that inhibit NOS. Of these compounds, N^G-methyl-L-arginine (L-NMA), N^G-nitro-L-arginine (L-NOARG), and N^G-nitro-L-arginine methyl ester (L-NAME) have been found to be effective inhibitors (Moore *et al.*, 1990; Rees *et al.*, 1989; 1990), but have been observed to have different potencies against the various NOS isoenzymes. For example, L-NNA preferentially

[1] Author for correspondence.

blocks the calcium/calmodulin-dependent NOS found in brain (Lambert *et al.*, 1991) and endothelial cells (Gross *et al.*, 1990), whereas L-NMA is more potent against the calcium/calmodulin-independent NOS (Gross *et al.*, 1990). Since both L-NNA and L-NMA inhibit the constitutive isoform of NOS present in endothelial cells (Moore *et al.*, 1990; Rees *et al.*, 1990), these agents can have hypertensive effects even in normotensive animals (Moncada *et al.*, 1991). Newer NOS inhibitors that are isoform-specific or which show an increased potency against NO^- production by the inducible isoform of NOS may be useful in treating patients with septic shock.

In the present study we examined the effects of L-NMA, the prototypic inhibitor of NOS, on constitutive NOS (basal and agonist-stimulated production of NO^-) and on inducible NOS (endotoxin-induced production of NO^-). In addition, we have characterized the effects of two new arginine/citrulline analogues (Figure 1): L-thiocitrulline (L-TC) and S-methyl-L-thiocitrulline (L-SMTC) (Narayanan & Griffith, 1994), on both isoenzymes in rat aorta.

Methods

Male Wistar rats (300–400 g) were anaesthetized by intraperitoneal injection of sodium pentobarbitone (50 mg kg^{-1}). The thoracic aortae were excised and stored in cold modified Krebs-Ringer solution containing (composition in mM): NaCl 118.3, KCl 4.7, $MgSO_4$ 1.2, KH_2PO_4 1.2, $CaCl_2$ 2.5, $NaHCO_3$ 25.0; CaEDTA 0.016 and glucose 11.1 (control solution). Arteries were cleaned of fat and connective tissue and cut into rings. In some rings the endothelium was removed mechanically by inserting a small metal wire into the lumen and rolling the tissue back and forth several times on a paper towel wetted with control solution. The preparations were suspended in organ chambers containing 10 ml of control solution at 37°C and aerated with 95% O_2 and 5% CO_2. The aortic rings were stretched progressively to an optimal tension of 2.5 g–3 g. Changes in isometric tension were recorded with an isometric force transducer connected to an analog-to-digital input board in an IBM 386/30 mHz personal computer. The presence or absence of the endothelium was verified by addition of acetylcholine (1 μM) to arteries contracted with phenylephrine (1 μM). The preparations were then rinsed three times with warm control solution, rested for 30 min, and incubated with either solvent, L-NMA, L-TC, or L-SMTC (10 or 100 μM for 30 min, with or without 1 mM L-arginine or L-citrulline) before a concentration-contraction curve to phenylephrine (1 nM–10 μM) was obtained. In another set of experiments, after incubation with solvent or one of the NOS inhibitors, the preparations were contracted with phenylephrine (0.3 μM–1 μM) and a cumulative dose-response curve was obtained for acetylcholine (ACh), adenosine triphosphate (ATP), or calcium ionophore (A23187). In a separate series of experiments cumulative contraction curves to these NOS inhibitors were obtained in LPS-treated rings with and without endothelium. The preparations were contracted submaximally by addition of phenylephrine (10–50 nM) before the dose-response curves of these NOS inhibitors were obtained. After the maximal response was evoked by these compounds, L-arginine or L-citrulline (1 mM) was added to rings with endothelium.

To induce NOS activity, aortic rings were placed in 24-well multiwell plates with Dulbecco's modified Eagle's medium and Ham's F12 medium (DMEM/F12) (1 ml) containing 100 iu ml^{-1} streptomycin and 100 iu ml^{-1} penicillin. The preparations were incubated in culture medium containing 200 ng ml^{-1} endotoxin (LPS) for 5 h at 37°C in a cell culture incubator before being suspended in the organ chambers.

Drugs

Phenylephrine hydrochloride, acetylcholine chloride, adenosine triphosphate, calcium ionophore (A23187), endotoxin (lipopolysaccharide, Escherichia coli, 0128:B12), L-citrulline and L-arginine were purchased from Sigma Chemical Co. (St. Louis, MO, U.S.A.); Dulbecco's Modified Eagle's/Ham's F12 medium (DMEM/F12) was purchased from GIBCO BRL (Grand Island, NY, U.S.A.). N^G-methyl-L-arginine monoacetate was synthesized by the general procedure of Corbin & Reporter (1974). L-Thiocitrulline hydrochloride and S-methyl-L-thiocitrulline hydrochloride were prepared as previously described (Narayanan & Griffith, 1994). All drugs were prepared in distilled water.

Statistical analysis

Results are expressed as the mean ± s.e.mean. Statistical evaluation of the data was performed by Student's *t* test for paired or unpaired observations. When data of more than two groups were compared, an analysis of variance (ANOVA) was used, and individual means were compared with Scheffe's *F* test. *P* values less than 0.05 were considered significant.

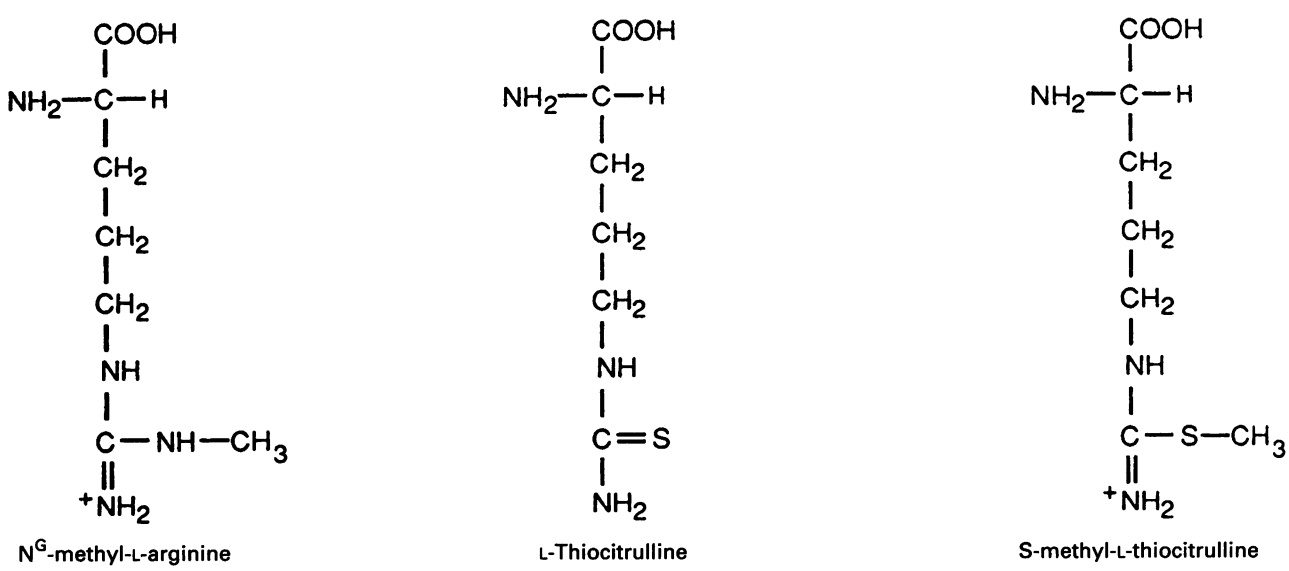

Figure 1 Structure of N^G-methyl-L-arginine, L-thiocitrulline and S-methyl-L-thiocitrulline.

Results

Basal release of NO⁻

The addition of L-NMA, L-TC, or L-SMTC (10 μM or 100 μM) to the preparations for 30 min had no effect on the basal tension. Phenylephrine (1 nM–1 μM) evoked concentration-dependent contractions in aortic rings with endothelium. The contractile responses to phenylephrine were not affected in the presence of a 10 μM concentration of any of these inhibitors and the pEC_{50} and E_{max} were similar in control and treated rings with endothelium (Table 1), whereas 100 μM of L-NMA, L-TC, or L-SMTC shifted the dose-response curves to this α_1-agonist significantly to the left without significantly affecting the maximal responses (E_{max}: 1.95±0.08 g to 2.13±0.1, 2.12±0.19, or 2.2±0.14 g, respectively) (Table 1). Enhancement of the contractions to phenylephrine was similar for all three inhibitors studied (pEC_{50}: 7.5±0.14 to 7.84±0.08, 7.82±0.12, or 7.78±0.08, with L-NMA, L-TC, or L-SMTC respectively) (Table 1).

Agonist-induced NO⁻ synthase activity

Following induction of a submaximal contraction with phenylephrine (0.3 μM–1 μM), acetylcholine (ACh) (1 nM–10 μM), adenosine triphosphate (ATP) (0.1 μM–100 μM), or calcium ionophore (A23187) (10 nM–1 μM) induced concentration-dependent relaxations in aortic rings with endothelium. The maximal responses to phenylephrine were not significantly different for the three vasodilators in the presence or the absence of inhibitors (data not shown).

Treatment of aortic rings with endothelium with either L-NMA, L-TC, or L-SMTC (10 μM) for 30 min resulted in a small but significant inhibition of the relaxations seen at higher concentrations of acetylcholine (Figure 2a), whereas treatment with 100 μM of these inhibitors produced a significant inhibition of relaxations induced by either low or high concentrations of this vasodilator (Figure 2b). In addition, relaxations evoked by ATP or A23187 were significantly reduced in the presence of 100 μM L-NMA, L-TC, or L-SMTC (Figure 3a and b). The potency of these three NOS inhibitors in inhibiting relaxations evoked by ACh, ATP, and A23187 were similar.

LPS-induced NOS activity

L-NMA, L-TC, or L-SMTC did not significantly affect the basal tension in LPS-treated rings with and without endothelium (data not shown). The incubation of aortic rings with and without endothelium for 5 h in culture medium containing LPS 200 ng ml^{-1}, shifted the concentration-contraction curves to phenylephrine significantly to the right (pEC_{50}: 7.5±0.14 to 6.73±0.12 and 7.95±0.16 to 7.19±0.03, with and without endothelium respectively) and significantly decreased the maximal contractions from 1.95±0.08 g to 1.53±0.15 g and from 2.34±0.12 g to 2.05±0.12 g, with and without endothelium respectively. Treatment of LPS-treated rings with endothelium with NOS inhibitors (10 μM) for 30 min shifted the concentration-contraction curves to phenylephrine significantly to the left and significantly increased the maximal response from 1.53±0.15 g to 1.95±0.13,

Table 1 Effects of N^G-methyl-L-arginine (L-NMA), L-thiocitrulline (L-TC) and S-methyl-L-thiocitrulline (L-SMTC) 10 μM and 100 μM (30 min) on concentration-contraction curves evoked by phenylephrine in aortic rings with endothelium

	pEC_{50}	E_{max} (g)
Untreated	7.34±0.16	2.08±0.05
L-NMA (10)	7.49±0.21	2.07±0.1
L-TC (10)	7.54±0.1	2.12±0.12
L-SMTC (10)	7.47±0.14	2.03±0.05
Untreated	7.5±0.14	1.95±0.08
L-NMA (100)	7.84±0.08*	2.13±0.1
L-TC (100)	7.82±0.12*	2.12±0.19
L-SMTC (100)	7.78±0.08*	2.2±0.14

pEC_{50}: negative logarithm of the effective molar concentration of phenylpharine causing 50% of the maximal contraction. E_{max}: maximal contraction evoked by phenylephrine. Statistically significant differences between the untreated and NOS inhibitors-treated rings *$P<0.05$.

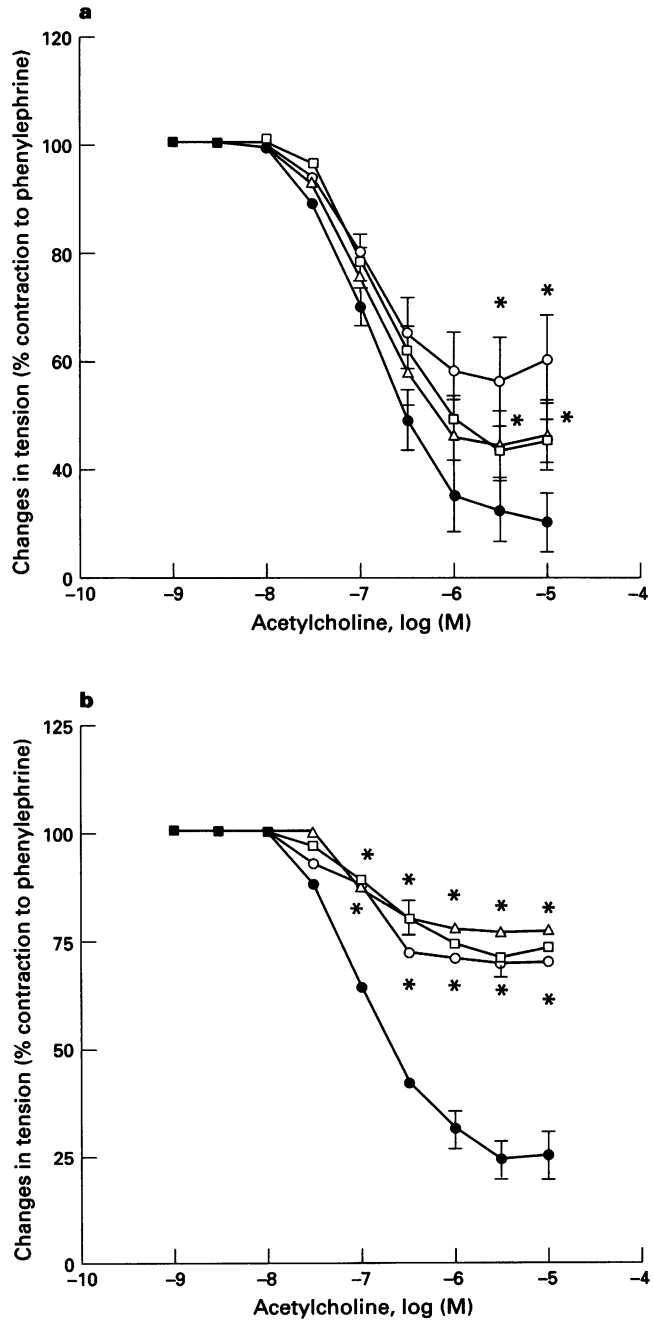

Figure 2 Effects of N^G-methyl-L-arginine (L-NMA, □), L-thiocitrulline (L-TC, △), or S-methyl-L-thiocitrulline (L-SMTC, ○) (a: 10 μM and b: 100 μM; 30 min) on the concentration-relaxation curves evoked by acetylcholine in rat aortic rings with endothelium (●). Results are presented as means ±s.e. of 5–6 different experiments and are expressed as the percentage of the contraction evoked by phenylephrine (0.3 μM–1 μM). Statistically significant differences between the control and NOS inhibitors-treated rings, *$P<0.05$.

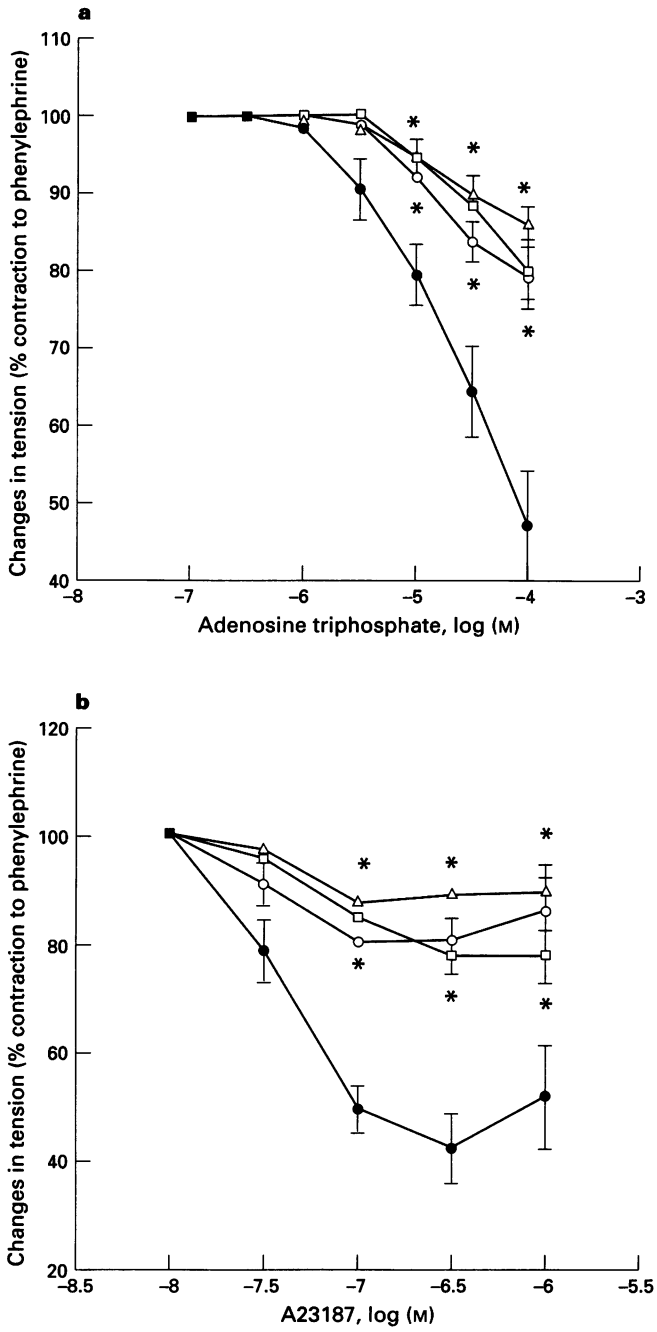

Figure 3 Effects of L-NMA (□), L-TC (△), or L-SMTC (○) (100 μM; 30 min) on the concentration-relaxation curves evoked by adenosine triphosphate (a) and calcium ionophore (b) in rat aortic rings with endothelium (●). Results are presented as means ± s.e. mean of 4 different experiments and are expressed as the percentage of the contraction evoked by phenylephrine (0.3 μM – 1 μM). Statistically significant differences between the control and NOS inhibitors-treated rings, $*P<0.05$.

2.08 ± 0.12, and 2.03 ± 0.13 g with L-NMA, L-TC, and L-SMTC, respectively (Figure 4a) (pEC_{50}: 6.73 ± 0.12 and 7.3 ± 0.12, 7.34 ± 0.13, or 7.22 ± 0.14; in the absence and the presence of L-NMA, L-TC, or L-SMTC). Contractions to this α_1-agonist obtained in the presence of NOS inhibitors (10 μM) were not significantly different in LPS-treated rings. The hyporeactivity induced by LPS in aortic rings was reversed in a concentration-dependent manner by L-NMA, L-TC, and L-SMTC, since a higher concentration of these compounds (100 μM) further potentiated contractions evoked by phenylephrine (Figure 4b) without further increasing maximal responses (pEC_{50}: 6.78 ± 0.08 and 7.63 ± 0.09, 7.80 ± 0.12, or 7.82 ± 0.11 in the absence and the presence of L-NMA, L-TC, or L-SMTC). In addition, at 10 nM phenylephrine, contractile responses were significantly greater in the presence of L-SMTC or L-TC than in the presence of L-NMA (100 μM) (L-NMA: 0.4 ± 0.11 g; L-TC: 0.78 ± 0.14 g and L-SMTC: 0.81 ± 0.17 g). The coincubation of L-arginine (1 mM) with L-NMA (100 μM) for 30 min abolished the effect of this inhibitor on the vascular hyporeactivity to phenylephrine induced by LPS (Figure 5), but only partially inhibited the increased contractions to the α_1-agonist induced by L-TC or L-SMTC (100 μM) in LPS-treated rings with endothelium (Figure 5). In contrast the co-incubation of L-citrulline (1 mM) for 30 or 60 min did not alter the effects of the three inhibitors on the production of NO^- induced by LPS in rat aortic rings (data not shown). In a similar manner, in LPS-treated rings without endothelium, NOS inhibitors (100 μM) shifted the concentration-contraction curves evoked by phenylephrine significantly to the left (pEC_{50}: 7.19 ± 0.03 to 7.79 ± 0.08, 8.01 ± 0.07, and 8.02 ± 0.07 with L-NMA, L-TC, and L-SMTC respectively) and increased significantly the maximal responses from 2.05 ± 0.05 g to 2.38 ± 0.14 g, 2.5 ± 0.12 g, and 2.4 ± 0.21 g with L-NMA, L-TC, and L-SMTC, respectively (Figure 4c). In addition, at 10 nM and 30 nM phenylephrine contractions were significantly greater in the presence of L-TC or L-SMTC than in the presence of L-NMA (Figure 4c).

Following the induction of a submaximal contraction with phenylephrine (10 nM to 50 nM), L-NMA, L-TC, and L-SMTC (1 μM – 100 μM) induced concentration-dependent contractions in aortic rings with endothelium incubated for 5 h with LPS (200 ng ml^{-1}) (Figure 6a). Contractions induced by L-SMTC were significantly greater than those induced by L-TC or L-NMA (L-SMTC > L-TC > L-NMA) (Figure 6a). In LPS-treated aortic rings without endothelium, L-TC and L-SMTC evoked concentration-dependent contractions while L-NMA exhibited small contractions at low concentrations (1 μM – 30 μM) and relaxations at high concentrations (100 μM – 300 μM). The submaximal contractions induced by phenylephrine were similar for the three compounds in LPS-treated rings with (L-NMA: 0.67 ± 0.1 g; L-TC: 0.62 ± 0.07 g; L-SMTC: 0.62 ± 0.07 g) and without endothelium (L-NMA: 0.86 ± 0.02 g; L-TC: 0.92 ± 0.04 g; 0.88 ± 0.03 g). The ability of these NOS inhibitors to increase phenylephrine-induced tone in LPS-treated rings with endothelium was significantly reversed by L-arginine (1 mM) but not by L-citrulline added at the maximum contractile response to L-NMA, L-TC, or L-SMTC (100 μM) (data not shown).

Discussion

The present results demonstrate that L-NMA, L-TC, and L-SMTC exhibit similar potencies as inhibitors of the basal and agonist-stimulated NO^- production in control rat aortic rings with and without endothelium. In contrast, the two new arginine/citrulline analogues L-TC and L-SMTC, are more potent than L-NMA in reversing the vascular hyporeactivity to phenylephrine and increasing tone in LPS-treated rings with endothelium. This suggests that L-SMTC and L-TC have greater potency than L-NMA against the inducible isoform of NOS. Recent studies with isolated constitutive brain and inducible smooth muscle cells NOS support this finding (Narayanan & Griffith, 1994).

Endothelium containing rings of rat aorta are less sensitive to a wide range of vasoconstrictor stimuli than endothelium-denuded rings (Allan *et al.*, 1983; Frew *et al.*, 1993; Martin *et al.*, 1986). This difference is explained by the high basal production of NO^- by endothelial cells in this tissue. In our study, L-NMA, L-TC, and L-SMTC increased, to a similar extent, contractions evoked by phenylephrine in a dose-dependent manner in rat aortic rings with endothelium, suggesting that the three compounds are equipotent in inhibiting the basal release of NO^- in rat aorta. In vascular endothelial cells, the production of NO^- is subject to complex control and is sti-

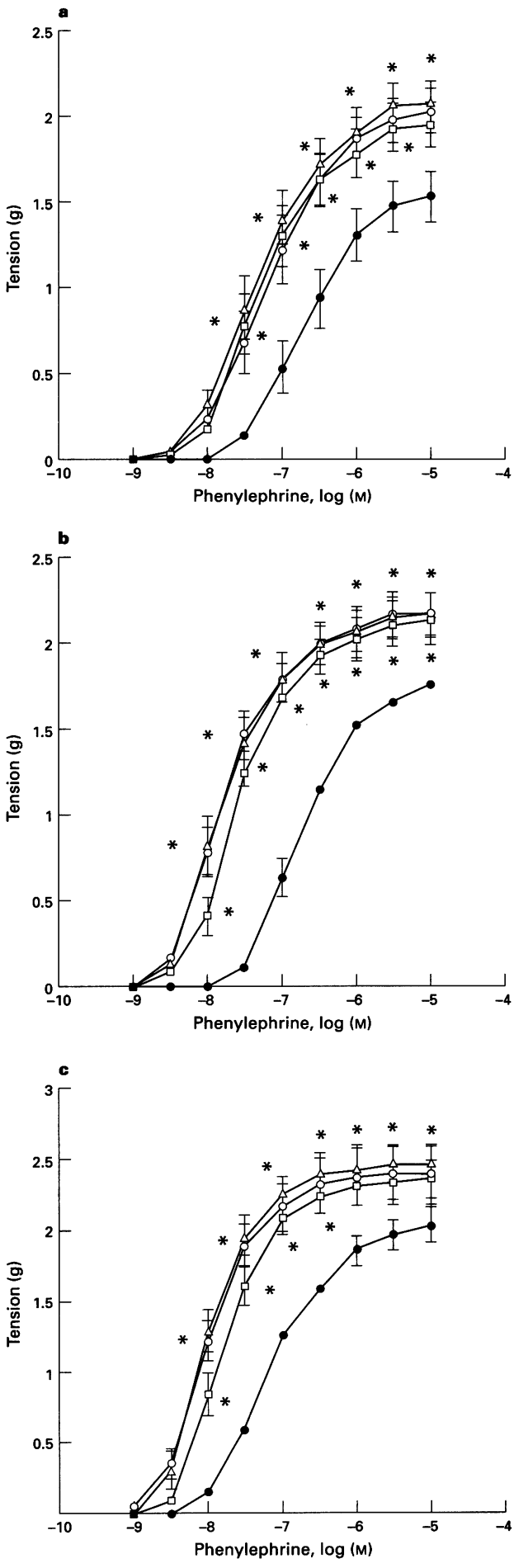

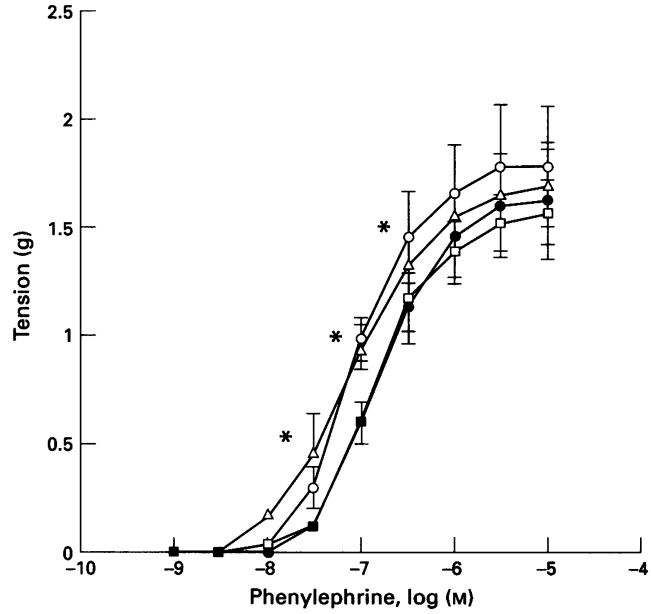

Figure 5 Effects of L-NMA (□), L-TC (△), or L-SMTC (○) (100 μM; 30 min), in the presence of L-arginine (1 mM; 30 min) on the concentration-contraction curves evoked by phenylephrine in rat aortic rings with endothelium (■) which were preincubated for 5 h in culture medium containing lipopolysaccharide (200 ng ml^{-1}). Results are presented as means ± s.e.mean of 4 different experiments and are shown in absolute values. Statistically significant differences between the untreated and NOS inhibitors-treated rings, $^*P<0.05$.

mulated by a large number of biological mediators such as acetylcholine, peptides, and purine nucleotides (Furchgott, 1984; Furchgott & Zawadzki, 1984). The effects of L-NMA differ according to the species studied or the source of the isolated vessels used. For example, while L-NMA inhibits basal as well as acetylcholine-stimulated production of NO^- in a wide range of tissues (Amezcua *et al.*, 1989; Moore *et al.*, 1990; Rees *et al.*, 1989; 1990; Joly *et al.*, 1994), it inhibits the basal production of NO^- in female rat aorta but not that stimulated by vasorelaxant agents (Frew *et al.*, 1990). In our experiments in aortic rings with endothelium, L-NMA induced a dose-dependent inhibition of relaxations evoked by acetylcholine. These inhibitory effects are not specific to acetylcholine, since L-NMA also blocked relaxations evoked by adenosine triphosphate, a receptor-dependent vasodilator, as well as those evoked by a receptor-independent vasodilator, A23187 calcium ionophore. Furthermore, L-TC and L-SMTC produced equipotent effects on relaxations evoked by these three vasodilators. Taken together, these results indicate that the three compounds are comparable in their abilities to inhibit the basal and the agonist-stimulated production of NO^-.

Treatment of aortic rings with and without endothelium with endotoxin results in a decreased reactivity to phenylephrine. That L-NMA restores contractions to this α_1-agonist which are impaired by LPS suggests that NO^- production via the L-arginine pathway is involved in the alteration of vascular hyporeactivity to phenylephrine. These data confirm previous

Figure 4 Effects of L-NMA (□), L-TC (△), or L-SMTC (○) on the concentration-contraction curves evoked by phenylephrine in rat aortic rings (●) with (a: 10 μM and b: 100 μM NOS inhibitors; 30 min) and without (c: 100 μM NOS inhibitors; 30 min) endothelium which were preincubated for 5 h in culture medium containing lipopolysaccharide , (200 ng ml^{-1}). Results are presented as means ± s.e.mean of 6 different experiments and are shown in absolute values. Statistically significant differences between the untreated and NOS inhibitors-treated rings, $^*P<0.05$.

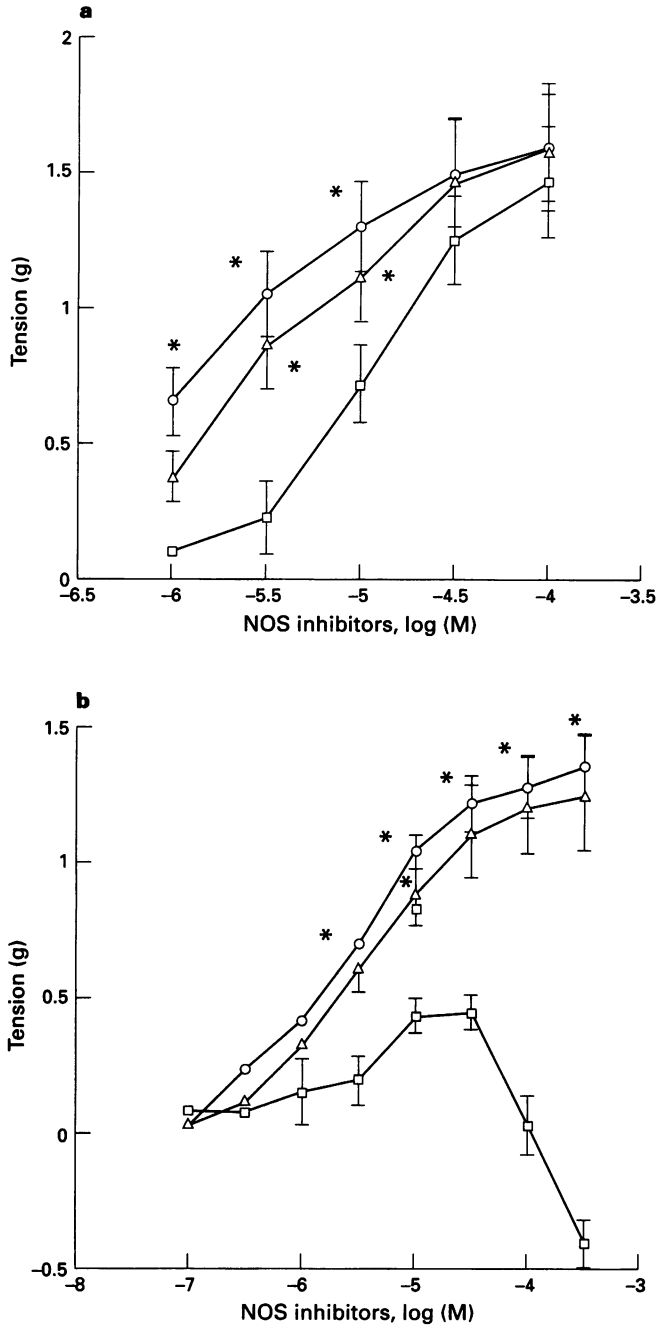

Figure 6 Contractions induced by L-NMA (□), L-TC (△), or L-SMTC (○) following a submaximal contraction evoked by phenylephrine (10–50 nM) in aortic rings with (a) and without (b) endothelium which were preincubated for 5 h in culture medium containing lipopolysaccharide (200 ng ml^{-1}). Results are presented as means ± s.e.mean of 4 different experiments and shown in absolute values. Statistically significant differences between the contractions evoked by L-NMA and those evoked by L-TC or L-SMTC, $*P<0.05$.

results showing that endotoxin and cytokines induce the production of NO^- in cell culture (Gross *et al.*, 1991; Schini *et al.*, 1991) and in isolated blood vessels (Julou-Schaeffer *et al.*, 1990; Joly *et al.*, 1994). The fact that L-SMTC and L-TC as well as L-NMA potentiate the contractions to phenylephrine suggests that these two new L-arginine analogues inhibit the production of NO^- induced by LPS in rat aorta. Comparison of the vascular effects of the three compounds in this study demonstrates that L-NMA is less potent than the other two analogues, which are relatively equipotent in augmenting the contractions to phenylephrine in LPS-treated preparations. The observation that L-SMTC and L-TC produce greater dose-dependent increases in tone in LPS-treated rings with and without endothelium than L-NMA, confirms the enhanced potency of these two new compounds in inhibiting the production of NO^- induced by the inducible isoform of NOS, and these results are consistent with studies using isolated inducible NOS enzyme (Narayanan & Griffith, 1994). In addition, the fact that L-TC and L-SMTC have demonstrated similar potency in inducing contractions in LPS-treated rings with and without endothelium suggests that these compounds exert potent inhibitory effects on iNOS in both endothelial and smooth muscle cells of vascular wall. The observations that high concentrations of L-NMA induced relaxations in LPS-treated preparations without endothelium are consistent with previous results obtained in rat aorta (Thomas & Ramwell, 1991) or in canine coronary arteries (Winn *et al.*, 1993). Different hypotheses have been put forward to explain the relaxant effects of L-NMA: one interesting explanation is that L-NMA may have undergone metabolism to L-arginine (Hecker *et al.*, 1990); this could, in turn, lead to increased substrate availability (Hecker *et al.*, 1990).

L-Arginine is a substrate for NOS, and its availability can be rate limiting for induced NO^- synthesis (Julou-Schaeffer *et al.*, 1990; Schini & Vanhoutte, 1991). The fact that in LPS-treated rings the increased contractions to phenylephrine induced by L-NMA was fully abolished and those evoked by L-SMTC and L-TC were partially inhibited by L-arginine is consistent with a mechanism involving substrate-inhibitor competition. Furthermore, the observation that L-arginine reverses the increases in tone induced by these inhibitors indicates that these L-arginine analogues exert their actions by a competitive and reversible mechanism of inhibition. A difference in affinity for the inducible NOS among these inhibitors may explain the limited effect of L-arginine against L-SMTC and L-TC. However, since L-SMTC and L-TC are more potent than L-NMA in restoring the contractile response to phenylephrine in LPS-treated rings, a greater molar excess of L-arginine may be required to reverse their effects fully.

This study demonstrates that the two new arginine/citrulline analogues are as potent as L-NMA in inhibiting the NO^- synthesis produced by the constitutive isoform of NOS, but L-SMTC and L-TC have greater potency than L-NMA for restoring the contractile response to phenylephrine and producing increases in tone in endotoxin-treated preparations. Further experiments are required to determine whether these new compounds act only through direct inhibition of NOS or also affect L-arginine transport or utilization, resulting in changes in the intracellular L-arginine concentration.

References

ALLAN, G., BROOK., C.D., CAMBRIDGE, D. & HLADKIWSKYJ, J. (1983). Enhanced responsiveness of vascular smooth muscle to vasoactive agents after removal of endothelial cells. *Br. J. Pharmacol.*, **79**, 334P.

AMEZCUA, J.L., PALMER, R.M.J., DE SOUZA, B.M. & MONCADA, S. (1989). Nitric oxide synthesized from L-arginine regulates vascular tone in the coronary circulation of the rabbit. *Br. J. Pharmacol.*, **97**, 1119–1124.

BEASLEY, D., SCHWARTZ, J.H. & BRENNER, B.M. (1991). Interleukin 1 induces prolonged L-arginine-dependent cyclic guanosine monophasphate and nitrite production in rat vascular smooth muscle cells. *J. Clin. Invest.*, **87**, 602–608.

BOHME, G.A., BON, C., STUTZMANN, J.M., DOBLE, A. & BLANCHARD, J.C. (1991). Possible involvement of nitric oxide in long-term potentiation. *Eur. J. Pharmacol.*, **199**, 379–381.

BREDT, D.S., HWANG, P.M. & SNYDER, S.H. (1990). Localisation of nitric oxide synthase indicating a neural role for nitric oxide. *Nature*, **347**, 768–770.

BUSSE, R. & MULSCH, A. (1990). Induction of nitric oxide synthase by cytokines in vascular smooth muscle cells. *FEBS Lett.*, **275**, 87–90.

CORBIN, J.A., & REPORTER, M. (1974). A convenient method for the preparation of N^G-monomethyl-L-arginine. *Anal. Biochem.*, **57**, 310–315.

FLEMING, I., GRAY, G.A., JULOU-SCHAEFFER, G., PARRAT, J.R. & STOCLET, J.C. (1990). Incubation with endotoxin activates the L-arginine pathway in vascular tissue. *Biochem. Biophys. Res. Commun.*, **171**, 562–568.

FOSTERMAN, U., POLLOCK, J.S., SCHMIDT, H.H.H.W., HELLER, M. & MURAD, F. (1991). Calmodulin-dependent endothelium-derived relaxing factor-nitric oxide synthase activity is present in the particule and cytosolic fractions of bovine aortic endothelial cells. *Proc. Natl. Acad. Sci. U.S.A.*, **88**, 1788–1792.

FREW, J.D., PAISLEY, K. & MARTIN, W. (1993). Selective inhibition of basal but not agonist-stimulated activity of nitric oxide in rat aorta by N^G-monomethyl-L-arginine. *Br. J. Pharmacol.*, **110**, 1003–1008.

FURCHGOTT, R.F. (1984). The role of the endothelium in the responses of vascular smooth muscle to drugs. *Annu. Rev. Pharmacol. Toxicol.*, **24**, 175–197.

FURCHGOTT, R.F. & ZAWADZKI, J.V. (1980). The obligatory role of endothelial cells in the relaxation of arterial smooth muscle by acetylcholine. *Nature*, **288**, 373–376.

GROSS, S.S., JAFFE, E.A., LEVI, R. & KILBOURN, G.R. (1991). Cytokine-activated endothelial cells express an isotype of nitric oxide synthase which is tetrahydrobiopterin-dependent, calmodulin-independent and inhibited by L-arginine analogues with a rank-order of potency characteristic of activated macrophages. *Biochem. Biophys. Res. Commun.*, **178**, 823–829.

GROSS, S.S., STUEHR, D.J., AISAKA, K., JAFFE, E., LEVI, R. & GRIFFITH, O.W. (1990). Macrophage and endothelial cell nitric oxide synthesis: Cell-type selective inhibition by N^G-aminoarginine, N^G-nitro-L-arginine and N^G-methyl-L-arginine. *Biochem. Biophys. Res. Commun.*, **170**, 96–103.

HECKER, M., MITCHELL, J.A., HARRIS, H.J., KATSURA, M., THIEMERMANN, C. & VANE, J.R. (1990). Endothelial cells metabolize N^G-monomethyl-L-arginine to L-citrulline and subsequently to L-arginine. *Biochem. Biophys. Res. Commun.*, **167**, 1037–1043.

JOLY, G.A., AYRES, M., CHELLY, F. & KILBOURN, R.G. (1994). Effects of N^G-methyl-L-arginine, N^G-nitro-L-arginine, and aminoguanidine on constitutive and inducible nitric oxide synthase in rat aorta. *Biochem. Biophys. Res. Commun.*, **199**, 155–162.

JULUO-SCHAEFFER, G., GRAY, G., FLEMING, I., PARRAT, J.R. & STOCLET, J.C. (1990). Loss of vascular responsiveness induced by endotoxin involves L-arginine pathway. *Am. J. Physiol.*, **259**, H1038–H1043.

KILBOURN, G.R. & BELLONI, P. (1990). Endothelial cell production of nitrogen oxides in response to interferon-gamma in combination with tumor necrosis factor, interleukin-1, or endotoxin. *J. Natl. Cancer Inst.*, **82**, 772–776.

KILBOURN, G.R., JUBRAN, A., GROSS, S.S., GRIFFITH, O.W., LEVI, R., ADAMS, J. & LODATO, R.F. (1990). Reversal of endotoxin-mediated shock by N^G-methyl-L-arginine, an inhibitor of nitric oxide synthesis. *Biochem. Biophys. Res. Commun.*, **172**, 1132–1138.

LAMBERT, L.E., WHITTEN, J.P., BARON, B.M., CHENG, H.C., DOHERTY, N.S. & MCDONALD, I.A. (1991). Nitric oxide synthesis in the CNS, endothelium and macrophages differs in its sensitivity to inhibition by arginine analogues. *Life Sci.*, **48**, 69–75.

MARLETTA, M.A., YOON, P.S., LYENGAR, R., LEAF, C.D. & WISHNOK, J.S. (1988). Macrophage oxidation of L-arginine to nitrite and nitrate; nitric oxide is an intermediate. *Biochemistry*, **27**, 8706–8711.

MARTIN, W., FURCHGOTT, R.F., VILLANI, G.M. & JOTHIANANDAN, D. (1986). Depression of contractile responses in rat aorta by spontaneously released endothelium-derived relaxing factor (EDRF). *J. Pharmacol. Exp. Ther.*, **237**, 529–538.

MONCADA, S., PALMER, R.M.J. & HIGGS, E.A. (1991). Nitric oxide: Physiology, pathophysiology, and pharmacology. *Pharmacol. Res.*, **43**, 109–141.

MOORE, P.K., AL-SWAYEH, O.A., CHONG, N.W.S., EVANS, R. & GIBSON, A. (1990). N^G-nitro-L-arginine (L-NOARG) a novel, L-arginine reversible inhibitor of endothelium-dependent vasodilatation *in vitro*. *Br. J. Pharmacol.*, **99**, 408–412.

NARAYANAN, K. & GRIFFITH, O.W. (1994). Synthesis of L-thiocitrulline, L-homothiocitrulline and S-methyl-L-thiocitrulline: a new class of potent nitric oxide synthase inhibitors. *J. Medic. Chem.*, **37**, 885–887.

PALMER, R.M., ASHTON, D.S. & MONCADA, S. (1988). Vascular endothelial cells synthesize nitric oxide from L-arginine. *Nature*, **333**, 664–666.

REES, D.D., PALMER, R.M.J., HODSON, H.F. & MONCADA, S. (1989). A specific inhibitor of nitric oxide formation from L-arginine attenuates endothelium-dependent relaxations. *Br. J. Pharmacol.*, **96**, 418–424.

REES, D.D., PALMER, R.M.J., SCHULZ, R., HODSON, H.F. & MONCADA, S. (1990). Characterization of three inhibitors of nitric oxide synthase *in vitro* and *in vivo*. *Br. J. Pharmacol.*, **101**, 746–752.

SCHINI, V.B., JUNQUERO, D.C., SCOTT-BURDEN, T. & VANHOUTTE, P.M. (1991). Interleukin-1 β induces the production of an L-arginine-derived relaxing factor from cultured smooth cells from rat aorta. *Biochem. Biophys. Res. Commun.*, **176**, 114–121.

SCHINI, V.B. & VANHOUTTE, P.M. (1991). L-arginine evokes both endothelium-dependent and -independent relaxations in L-arginine-depleted aortas of the rat. *Circ. Res.*, **68**, 209–216.

SNYDERS, S.H. (1992). Nitric oxide: first in a new class of neurotransmitters? *Science*, **257**, 494–496.

STUEHR, D.J. & GRIFFITH, O.W. (1992). Mammalian nitric oxide synthases. *Adv. Enzymol.*, **65**, 287–346.

THOMAS, G. & RAMWELL, P.W. (1991). Effects of guanidino compounds on the endothelium-derived relaxing factor inhibitor N^G-monomethyl-L-arginine. *J. Pharmacol. Exp. Ther.*, **259**, 490–494.

WINN, M.J., ASANTE, N.K. & KU, D.D. (1993). Vasomotor responses of canine coronary arterial rings to N^G-monomethyl-L-arginine and N^ω nitro-L-arginine methyl ester. *J. Pharmacol. Exp. Ther.*, **264**, 265–270.

(Received October 31, 1994
Revised February 10, 1995
Accepted February 16, 1995)

British Journal of Pharmacology (1995) 115, 498–502

Attenuation by nitrosothiol NO donors of acute intestinal microvascular dysfunction in the rat

F. László, [1]B.J.R. Whittle & S. Moncada

Wellcome Foundation Ltd, Langley Court, Beckenham, Kent BR3 3BS

1 The effects of the nitric oxide (NO) donors, S-nitroso-glutathione (SNOG) and S-nitroso-N-acetyl-penicillamine (SNAP), on the acute intestinal microvascular dysfunction induced by N^G-nitro-L-arginine methyl ester (L-NAME) in combination with low doses of endotoxin were investigated in the anaesthetized rat.

2 Administration of L-NAME (5 mg kg^{-1}, s.c.) concurrently with *E. coli* lipopolysaccharide (LPS, 3 mg kg^{-1}, i.v.) provoked the leakage of radiolabelled albumin in the ileum and colon, as a measure of microvascular damage, determined 1 h after challenge.

3 Intravenous infusion of SNOG or SNAP (1–10 μg kg^{-1} min^{-1}) dose-dependently attenuated the microvascular leakage induced by L-NAME and LPS.

4 Infusion of the lowest doses of SNOG or SNAP (1 μg kg^{-1} min^{-1}, i.v.) that significantly reduced the albumin leakage, did not affect the increase in blood pressure in response to L-NAME in LPS-treated rats. Higher doses of SNOG or SNAP (5–10 μg kg^{-1} min^{-1}, i.v.) dose-dependently reduced this increase in blood pressure.

5 In control studies, intravenous infusion of glutathione (10 μg kg^{-1} min^{-1}) or N-acetyl-penicillamine (10 μg kg^{-1} min^{-1}) had no effect on microvascular leakage in the ileum and colon induced by LPS and L-NAME.

6 Pretreatment with rabbit anti-rat neutrophil serum (0.4 ml kg^{-1}, i.p., 4 h before challenge), which reduced the neutrophil count in peripheral arterial blood, also inhibited the microvascular leakage in the ileum and colon.

7 The protective effects of the nitrosothiol NO donors in this model may reflect, in part, modulation of neutrophil interactions within the microcirculation or actions on endothelial cell integrity, in addition to any local vasodilator action.

Keywords: Nitric oxide; NO synthase inhibitors; N^G-nitro-L-arginine methyl ester; NO donors; S-nitroso-glutathione; S-nitroso-N-acetyl-penicillamine; neutrophils; rat intestinal vasculature; intestinal inflammation; endothelial injury; nitrosothiols

Introduction

The NO synthase inhibitor, N^G-nitro-L-arginine methyl ester (L-NAME) provokes a substantial acute increase of vascular permeability in the rat small and large intestine following the concurrent administration of low doses of endotoxin, under conditions where neither L-NAME nor endotoxin alone caused such permeability changes (Laszlo *et al.*, 1994a). These changes in vascular permeability involve the acute release of platelet activating factor (PAF) and thromboxanes, mediators that can be released from neutrophils (Laszlo *et al.*, 1994b).

The nitrosothiol, S-nitroso-*N*-acetyl-penicillamine (SNAP) attenuates the acute gastrointestinal injury induced by PAF or high doses of endotoxin (Boughton-Smith *et al.*, 1990b; 1992). In the cat small intestine, NO donors reduce the microvascular injury caused by NO synthase inhibitors (Kubes & Granger, 1992) and attenuate the changes in epithelial cell permeability caused by such inhibitors administered alone or during ischaemia reperfusion (Kubes, 1992; Payne & Kubes, 1993). Infusion of acidified sodium nitrate also has beneficial effects in a shock syndrome induced by splanchnic artery occlusion in the rat (Aoki *et al.*, 1990). Low doses of SNAP have also been shown to exert protective actions against vascular injury induced by endothelin-1 in the rat gastric mucosa (Lopez-Belmonte *et al.*, 1993).

The aim of the present study was to evaluate the effects of the nitrosothiol NO donors, S-nitroso-glutathione (SNOG; Kowaluk & Fung, 1990; Radomski *et al.*, 1992) or SNAP (Ignarro *et al.*, 1981) on the acute microvascular leakage induced by L-NAME in combination with LPS in the intestine of the anaesthetized rat and to determine their concurrent actions on systemic arterial blood pressure. In addition, the effects of an anti-neutrophil antibody on such microvascular injury have been investigated.

Some of this work has been presented to the British Pharmacological Society (Laszlo *et al.*, 1994c).

Methods

Experimental protocol

Male Wistar rats (225–275 g) were deprived of food overnight, but received water *ad libitum*. The rats were anaesthetized with pentobarbitone sodium (60 mg kg^{-1}, i.p.) and *E. coli* lipopolysaccharide (LPS, 3 mg kg^{-1}, i.v.), ^{125}I-labelled human serum albumin ([^{125}I]-HSA, 2 μCi kg^{-1}, i.v.) and L-NAME (5 mg kg^{-1}, s.c.) were administered through a tail vein (Laszlo *et al.*, 1994a). Plasma leakage in the ileum and colon was determined 1 h after endotoxin injection. The dose of L-NAME was selected as producing near-maximal effects from previous studies in this model (Laszlo *et al.*, 1994b).

[1] Author for correspondence.

Plasma leakage

Plasma leakage of [^{125}I]-HSA was determined in the ileum and colon, as an index of vascular endothelial damage. Blood was collected from the abdominal aorta into syringes containing trisodium citrate (final concentration 0.318%) and centrifuged (10,000 *g*, 10 min, 4°C). The [^{125}I]-HSA content of the plasma and segments of ileal and colonic tissue was determined in a gamma-spectrometer (Nuclear Enterprises NE 1600) and the albumin content in the intestine was calculated, taking into account any changes in intestinal blood volume as described previously (Boughton-Smith *et al.*, 1993). Values from control tissue were subtracted from the values of treated tissue and the data were expressed as plasma leakage, μl plasma g^{-1} tissue.

Effect of SNOG or SNAP infusion on blood pressure and intestinal plasma leakage response induced by LPS and L-NAME

The effect of L-NAME (5 mg kg^{-1}, s.c.) administered concurrently with LPS (3 mg kg^{-1}, i.v.) on rat intestinal plasma leakage was determined after 1 h. Intravenous infusion of SNOG (1–10 μg kg^{-1} min^{-1}) or SNAP (1–10 μg kg^{-1} min^{-1}) was initiated concurrently with LPS and L-NAME administration and plasma leakage in the ileum and colon were determined 1 h later.

Systemic arterial blood pressure (BP) was measured from the right carotid artery of a separate group of rats with a blood pressure transducer (Elcomatic) connected to a Grass Polygraph. LPS and L-NAME were administered concurrently with the initiation of intravenous infusion of SNOG (1–10 μg kg^{-1} min^{-1}) or SNAP (1–10 μg kg^{-1} min^{-1}) and the blood pressure was monitored over 1 h. The effects on BP of LPS or L-NAME administration alone or in combination, and of the NO donors alone, was also measured during the 1 h investigation period.

Effect of glutathione or N-acetyl-penicillamine infusion on intestinal plasma leakage induced by LPS and L-NAME

In control studies, infusion of glutathione (10 μg kg^{-1} min^{-1}, i.v.) or N-acetyl-penicillamine (10 μg kg^{-1} min^{-1}, i.v.) was initiated concurrently with the administration of LPS and L-NAME and plasma leakage in the ileum and colon was determined after 1 h.

Effect of anti-neutrophil antiserum on intestinal plasma leakage induced by LPS and L-NAME

Rabbit anti-rat neutrophil antiserum (0.4 ml kg^{-1}, i.p.) was administered 4 h before the concurrent injection of LPS (3 mg kg^{-1}, i.v.) and L-NAME (5 mg kg^{-1}, s.c.). Plasma leakage in the ileum and colon was determined 1 h after this challenge. Neutrophil count in peripheral arterial blood (collected from the abdominal aorta) was determined by the staining of blood smears (Diff-Quick, Camlab Ltd., Cambridge, U.K.).

Materials

E. coli lipopolysaccharide (0111:B4), L-NAME and glutathione were obtained from Sigma Chemical Co. (Poole, Dorset). SNOG and SNAP were synthesized in the Department of Medicinal Chemistry, Wellcome Research Laboratories. ^{125}I-labelled human serum albumin was from Amersham International (U.K.). Rabbit anti-rat neutrophil antiserum was obtained from Accurate Chemical and Scientific Corporation (Westbury, New York, U.S.A.). N-acetyl-penicillamine was generated by the incubation of SNAP solution in ambient light for 48 h at 37°C to deplete its NO content. The compounds were dissolved freshly in isotonic saline immediately prior to use.

Statistical evaluation

Data are shown as the mean ± s.e.mean of (*n*) studies. For statistical comparisons, analysis of variance with the Bonferroni test was utilised, where $P<0.05$ was taken as significant.

Results

Effect of SNOG or SNAP infusion on intestinal plasma leakage

Neither LPS (3 mg kg^{-1}, i.v.) nor L-NAME (5 mg kg^{-1}, s.c.) alone affected plasma leakage in the ileal (Δ0 ± 5 and Δ6 ± 11 μl g^{-1} tissue, respectively; $n=4-5$) or colonic tissue (Δ0 ± 4 and Δ8 ± 14 μl g^{-1} tissue, respectively; $n=4-5$) over 1 h. In contrast, the administration of L-NAME concurrently with LPS significantly provoked plasma leakage in the ileum and colon after 1 h (Figure 1).

Concurrent infusion of SNOG (1–10 μg kg^{-1} min^{-1}, i.v.) dose-dependently reduced plasma leakage in the ileum and colon induced by LPS and L-NAME. The lower dose of SNOG (1 μg kg^{-1} min^{-1}, i.v.) produced a 36 ± 8% and 45 ± 9% reduction in albumin leakage provoked by LPS and L-NAME in the ileum and colon, respectively ($P<0.01$; $n=5$), whereas the highest dose of SNOG (10 μg kg^{-1} min^{-1}, i.v.) abolished such leakage in both tissues (Figure 1).

Similarly, concurrent infusion of SNAP (1–10 μg kg^{-1} min^{-1}, i.v.) dose-dependently reduced such plasma leakage in the ileum and colon. The lower dose of SNAP (1 μg kg^{-1} min^{-1}, i.v.) produced a 73 ± 3% and 74 ± 4% reduction in albumin leakage provoked by LPS and L-NAME in the ileum and colon, respectively ($P<0.001$; $n=4$), while the highest dose of SNAP (10 μg kg^{-1} min^{-1}, i.v.) abolished such leakage in both tissues (Figure 2).

Effect of SNOG or SNAP infusion on blood pressure

Intravenous administration of LPS (3 mg kg^{-1}) did not significantly affect BP over the 1 h investigation period; the changes in BP (compared to the 0 min value) were 8 ± 2, 2 ± 4, −11 ± 7 and −11 ± 8 mmHg 15, 30, 45 and 60 min following LPS administration ($n=5$). Concurrent injection of L-NAME (5 mg kg^{-1}, s.c.) in endotoxin-treated rats elevated arterial BP, with a maximum increase of 44 ± 8 mmHg at 30 min ($P<0.001$; $n=6$) as shown in Figure 3.

Infusion of SNOG (1–10 μg kg^{-1} min^{-1}, i.v.) caused a dose-dependent decrease of L-NAME-induced BP elevation over the 1 h period in endotoxin-treated rats. The lower dose of SNOG (1 μg kg^{-1} min^{-1}, i.v.) had no effect on the increase in BP by L-NAME, whereas the highest dose of SNOG (10 μg kg^{-1} min^{-1}) abolished this BP response ($P<0.01$, $n=4$) as shown in Figure 3.

Likewise, infusion of SNAP (1–10 μg kg^{-1} min^{-1}, i.v.) caused a dose-dependent decrease of L-NAME-induced BP elevation over the 1 h period in endotoxin-treated rats. The lower dose of SNAP (1 μg kg^{-1} min^{-1}, i.v.) had no effect on this increase in BP, while the highest dose of SNAP (10 μg kg^{-1} min^{-1}, i.v.) significantly attenuated the BP elevation ($P<0.01$, $n=4$) as shown in Figure 4.

Infusion of SNOG (5 and 10 μg kg^{-1} min^{-1}, i.v., for 1 h) in control rats not receiving LPS or endotoxin affected the resting BP by a maximal value −4 ± 7 (NS; $n=4$) and by −17 ± 4 mmHg ($P<0.05$; $n=4$), respectively. Likewise, infusion of SNAP (5 and 10 μg kg^{-1} min^{-1} i.v. for 1 h) in control rats affected resting BP by a maximal value of −10 ± 5 and by −23 ± 7 mmHg ($P<0.05$; $n=4$) respectively.

Effect of glutathione or N-acetyl-penicillamine infusion on intestinal plasma leakage

In these control studies, the concurrent infusion of glutathione (10 μg kg^{-1} min^{-1}, i.v.) or N-acetyl-penicillamine (10 μg kg^{-1} min^{-1}, i.v.) did not affect ileal and colonic plasma leakage induced by LPS and L-NAME after 1 h ($n = 4$; Figures 1 and 2).

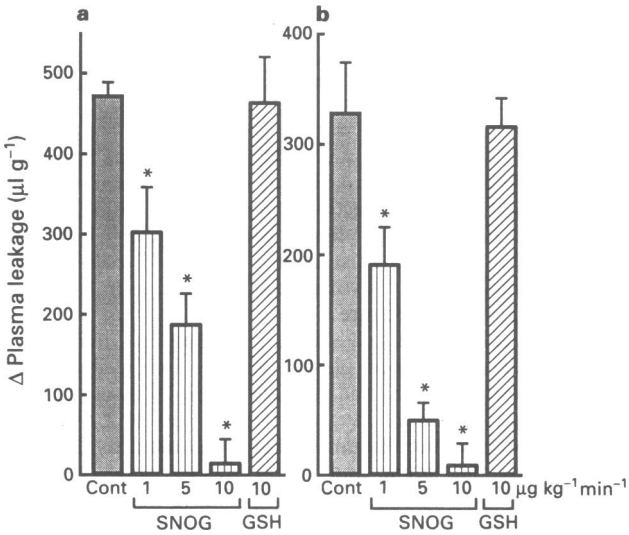

Figure 1 Effects of a 1 h infusion of S-nitroso-glutathione (SNOG, 1–10 μg kg^{-1} min^{-1}, i.v.) or glutathione (GSH, 10 μg kg^{-1} min^{-1}, i.v.) on vascular leakage of radiolabelled albumin provoked by the concurrent administration of N^G-nitro-L-arginine methyl ester (L-NAME, 5 mg kg^{-1}, s.c.) and lipopolysaccharide (LPS, 3 mg kg^{-1}, i.v.) in the rat (a) ileum and (b) colon. Albumin leakage (expressed as plasma leakage, Δμl g^{-1} tissue) was determined 1 h after challenge. Data are given as the mean ± s.e.mean of 4–5 rats per group; statistical significance is shown as $^*P<0.05$ compared to the control LPS + L-NAME (Cont).

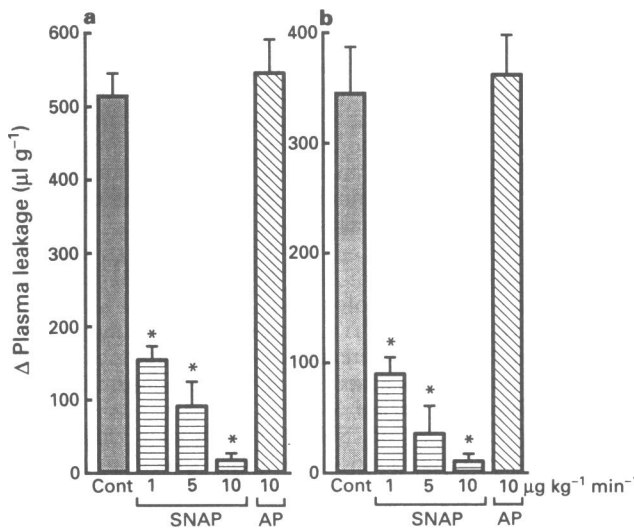

Figure 2 Effects of a 1 h infusion of S-nitroso-*N*-acetyl-penicillamine (SNAP, 1–10 μg kg^{-1}, min^{-1} i.v.) or N-acetyl-penicillamine (AP, 10 μg kg^{-1} min^{-1}, i.v.) on vascular leakage of radiolabelled albumin provoked by the concurrent administration of N^G-nitro-L-arginine methyl ester (L-NAME 5 mg kg^{-1}, s.c.) and lipopolysaccharide (LPS, 3 mg kg^{-1}, i.v.) in the rat (a) ileum and (b) colon. Albumin leakage (expressed as plasma leakage, Δμl g^{-1} tissue) was determined 1 h after challenge. Data are given as the mean ± s.e.mean of 4–5 rats per group; statistical significance is shown as $^*P<0.05$ compared to the control LPS + L-NAME group (Cont).

Effect of anti-neutrophil antiserum on intestinal plasma leakage

The intraperitoneal administration of an anti-neutrophil serum (0.4 ml kg^{-1}), 4 h before challenge, significantly attenuated LPS and L-NAME-induced plasma leakage in the ileum and colon (by 49 ± 6% and by 43 ± 9%, respectively; $P<0.01$; $n = 5$) as shown in Figure 5. The anti-neutrophil serum reduced the neutrophil count in the peripheral arterial blood by 85 ± 5% after 4 h following its administration ($n = 5$). Higher doses of the antiserum were not investigated since in preliminary studies, its specificity was reduced, with significant reductions in other blood cell types. Pre-immune rabbit serum (0.4 ml kg^{-1}) had no significant effect on neutrophil count or the increase in plasma leakage ($n = 4$).

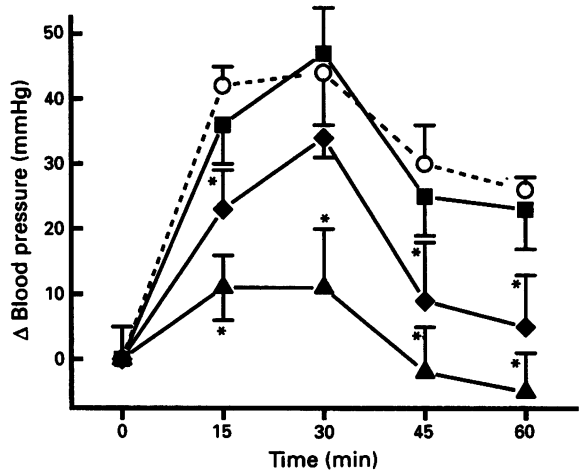

Figure 3 Reduction by S-nitroso-glutathione infusion (1 [■], 5 [◆] and 10 [▲] μg kg^{-1}, min^{-1} i.v., from 0 min) of blood pressure elevation induced by N^G-nitro-L-arginine methyl ester (L-NAME, 5 mg kg^{-1}, s.c., at 0 min) (○, broken line) following the administration of lipopolysaccharide (3 mg kg^{-1}, i.v., at 0 min). Arterial blood pressure (expressed as ΔmmHg) was measured over a 1 h period. Data are shown as the mean ± s.e.mean of 4–6 rats per group; statistical significance is given as $^*P<0.05$ compared to the control L-NAME group.

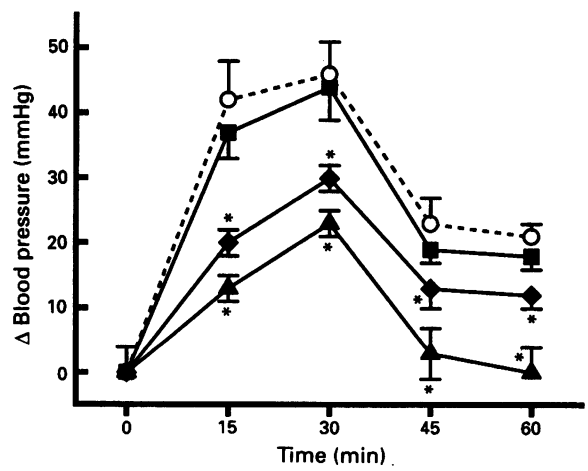

Figure 4 Reduction by S-nitroso-*N*-acetyl-penicillamine infusion (1 [■], 5 [◆] and 10 [▲] μg kg^{-1} min^{-1}, i.v., from 0 min) of blood pressure elevation induced by N^G-nitro-L-arginine methyl ester (L-NAME, 5 mg kg^{-1}, s.c., at 0 min) (○, broken line) following the administration of lipopolysaccharide (3 mg kg^{-1}, i.v., at 0 min). Arterial blood pressure (expressed as ΔmmHg) was measured over a 1 h period. Data are shown as the mean ± s.e.mean of 4–6 rats per group; statistical significance is given as $^*P<0.05$ compared to the control L-NAME group.

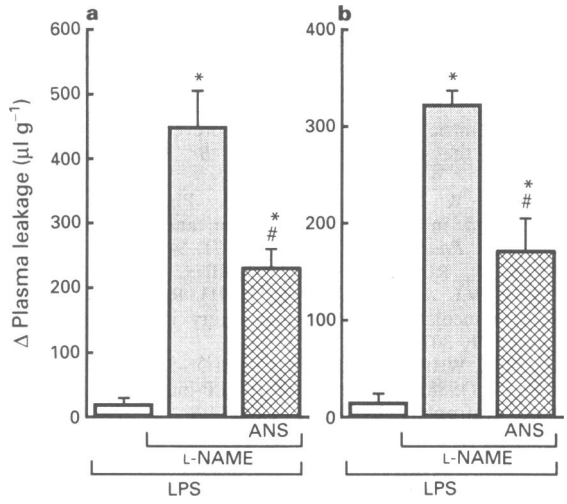

Figure 5 Inhibition of (a) ileal and (b) colonic leakage of radiolabelled albumin provoked by the concurrent administration of N^G-nitro-L-arginine methyl ester (L-NAME, 5 mg kg^{-1}, s.c.) and lipopolysaccharide (LPS, 3 mg kg^{-1}, i.v.) by the pretreatment of anti-neutrophil antiserum (ANS, 0.4 ml kg^{-1}, i.p., 4 h before challenge). Albumin leakage (expressed as plasma leakage, $\Delta\mu l\ g^{-1}$ tissue) was determined 1 h after challenge. Data are given as the mean ± s.e.mean of 4–5 rats per group; statistical significance is shown as $*P<0.05$ compared to the LPS-alone group and $\#P<0.05$ compared to the LPS + L-NAME group.

Discussion

This study confirms the previous observation (Laszlo *et al.*, 1994a,b) that following the administration of NO synthase inhibitors, challenge with low doses of endotoxin causes acute increases in intestinal microvascular permeability to albumin. Such microvascular leakage is indicative of local injury and is associated with the macroscopic appearance of intestinal mucosal injury (Laszlo *et al.*, 1994b). Concurrent infusion of NO donors, SNOG or SNAP dose-dependently reduced ileal and colonic microvascular leakage induced by a combination of LPS and L-NAME over the 1 h investigation period. In control studies, the concurrent infusion of the corresponding carrier molecules devoid of NO, glutathione or N-acetyl-penicillamine did not affect the microvascular plasma leakage following endotoxin challenge. The doses of SNAP found to be effective in this model were 50 fold lower than those previously demonstrated to attenuate acute microvascular injury following challenge with high doses of endotoxin (Boughton-Smith *et al.*, 1990b).

NO may prevent microvascular leakage and injury in the ileum and colon by counteracting the vasoactive or tissue damaging actions of pro-inflammatory mediators, such as PAF and thromboxanes. The early release of these mediators into intestinal tissue has been shown previously in experimental models of intestinal inflammation (Whittle *et al.*, 1987; Boughton-Smith *et al.*, 1989; 1990a). Furthermore, the inhibition of thromboxane synthesis or the administration of PAF-receptor antagonists prevents the development of the acute intestinal microvascular plasma leakage and mucosal damage induced by the concurrent administration of LPS and L-NAME (Laszlo *et al.*, 1994b). In the present study, the lowest dose of SNOG or SNAP significantly inhibited microvascular leakage without affecting the increase in BP induced by L-NAME in endotoxin-treated rats. Although changes in intestinal blood flow by these low doses of the NO donors cannot yet be excluded, these present findings could suggest that mechanisms are involved other than local vasodilatation in the protection of the microcirculation. One such mechanism could involve inhibition of neutrophil-dependent vascular endothelial damage, since in addition to being a vasodilator (Moncada *et al.*, 1991), NO can attenuate the aggregation of neutrophils and their adhesion to the microvasculature (McCall *et al.*, 1988; Kubes & Granger, 1992) as can SNAP (Xin-Liang *et al.*, 1993).

Exposure to PAF or endotoxin enhances the adherence of neutrophils to the endothelium (Matsuda *et al.*, 1991; Koltai *et al.*, 1991; Worthen *et al.*, 1992) and such leukocytes play a key role in the elevation of vascular permeability during inflammation (Wedmore & Williams, 1981). Moreover, neutrophils are considered to be involved in the evolution of microvascular injury of the gut under acute pathological conditions (Hernandez *et al.*, 1987; Kvietys *et al.*, 1990; Chmaisse *et al.*, 1994). During the development of such acute microvascular damage, neutrophils adhere to the vascular endothelium, releasing cytotoxic agents such as oxygen radicals and pro-inflammatory mediators including PAF (Sacks *et al.*, 1978; Pabst & Johnston, 1980; Tauber & Babior, 1985; Hernandez *et al.*, 1987; Kubes *et al.*, 1990; 1991; Lefer & Lefer, 1993). In addition to inhibiting neutrophil adhesion, NO donors can also inhibit the release of superoxide anions and PAF from neutrophils (Moilanen *et al.*, 1993). Endogenous NO appears to play a similar modulatory role since the increased neutrophil adherence and migration in mesenteric venules of the anaesthetized rat that follows NO synthase inhibition is significantly reduced by PAF and leukotriene receptor antagonists (Arndt *et al.*, 1993).

Administration of an anti-neutrophil serum protects the intestinal mucosa against ischaemia-reperfusion and indomethacin-induced damage (Hernandez *et al.*, 1987; Chmaisse *et al.*, 1994) and reduces the susceptibility of the gastric mucosa to injury by ethanol (Kvietys *et al.*, 1990; Tepperman *et al.*, 1993), indomethacin (Wallace *et al.*, 1990) or PAF (Etienne *et al.*, 1988). The involvement of neutrophils in at least part of the intestinal vascular injury in the current acute model is suggested by the findings that the administration of an anti-neutrophil serum significantly inhibited the microvascular leakage.

Our findings thus demonstrate that the NO donors, SNOG or SNAP can attenuate microvascular permeability changes in the ileum and colon. This could reflect protective effects of NO on the microvascular bed, in addition to any local vasodilator action, which may involve modulation of neutrophil activity, as well as a possible more-direct action on endothelial barrier integrity through elevation of cyclic GMP levels (Buchan & Martin, 1992). While studies on intestinal microvascular blood flow and cellular adhesion will help to clarify the mechanisms involved, the present observations suggest that parenteral administration of these nitrosothiol NO donors can prevent local microvascular injury independently of any change in systemic haemodynamics.

F.L. was supported by the Royal Society and by the European Commission.

References

AOKI, N., JOHNSON, III G. & LEFER, A.M. (1990). Beneficial effects of two forms of NO administration in feline splanchnic artery occlusion shock. *Am. J. Physiol.*, **258**, G275–G281.

ARNDT, H., RUSSEL, J.B., KUROSE, I., KUBES, P. & GRANGER, D.N. (1993). Mediators of leukocyte adhesion in rat mesenteric venules elicted by inhibition of nitric oxide synthesis. *Gastroenterology*, **105**, 675–680.

BOUGHTON-SMITH, N.K., DEAKIN, A.M. & WHITTLE, B.J.R. (1992). Actions of nitric oxide on the acute gastrointestinal damage induced by PAF in the rat. *Agents Actions, Special Conference Issue*, C3–C9.

BOUGHTON-SMITH, N.K., EVANS, S.M., LASZLO, F., WHITTLE, B.J.R. & MONCADA, S. (1993). The induction of nitric oxide synthase and intestinal vascular permeability by endotoxin in the rat. *Br. J. Pharmacol.*, **110**, 1189–1195.

BOUGHTON-SMITH, N.K., HUTCHESON, I.R., DEAKIN, A.M. & WHITTLE, B.J.R. (1990a). Inflammatory and protective mediators in experimental intestinal inflammation. In *Proc. Of the 60th Falk Symposium*, ed. Goebell, H., Ewe, K., Malchow, H. & Koelbel, Ch. pp. 137–152. Dordrecht/Boston/London: Kluwer Academic Publisher.

BOUGHTON-SMITH, N.K., HUTCHESON, I.R., DEAKIN, A.M., WHITTLE, B.J.R. & MONCADA, S. (1990b). Protective effect of S-nitroso-N-acetyl-penicillamine in endotoxin-induced acute intestinal damage in the rat. *Eur. J. Pharmacol.*, **191**, 485–488.

BOUGHTON-SMITH, N.K., HUTCHESON, I. & WHITTLE, B.J.R. (1989). Relationship between PAF-acether and thromboxane A_2 biosynthesis in endotoxin-induced intestinal damage in the rat. *Prostaglandins*, **38**, 319–333.

BUCHAN, K.W. & MARTIN, W. (1992). Modulation of barrier function of bovine aortic and pulmonary artery endothelial cells: dissociation from cytosolic calcium content. *Br. J. Pharmacol.*, **107**, 932–938.

CHMAISSE, H.M., ANTOON, J.S., KVIETYS, P.R., GRISHAM, M.B. & PERRY, M.A. (1994). Role of leukocytes in indomethacin-induced small bowel injury in the rat. *Am. J. Physiol.*, **266**, G239–G246.

ETIENNE, A., THONIER, F., HECQUET, F. & BRAQUET, P. (1988). Role of neutrophils in gastric damage induced by platelet activating factor. *Naunyn-Schmied. Arch. Pharmacol.*, **338**, 422–425.

HERNANDEZ, L.A., GRISHAM, M.B., TWOHIG, B., ARFORS, K.E., HARLAN, J.M. & GRANGER, D.N. (1987). Role of neutrophils in ischaemia-reperfusion-induced microvascular injury. *Am. J. Physiol.*, **253**, H699–H703.

IGNARRO, L.J., LIPPTON, H., EDWARDS, J.C., BARICOS, W.H., HYMAN, A.L., KADOWITZ, P.J. & GRUETTER, C.A. (1981). Mechanism of vascular smooth muscle relaxation by organic nitrates, nitrites, nitroprusside and nitric oxide: evidence for the involvement of S-nitrosothiols as active intermediates. *J. Pharmacol. Exp. Ther.*, **218**, 739–749.

KOLTAI, M., HOSFORD, D., GUINOT, P., ESANU, A. & BRAQET, P. (1991). Platelet activating factor (PAF). A review of its effects, antagonists and possible future clinical implications (Part I). *Drugs*, **42**, 9–29.

KOWALUK, E.A. & FUNG, H-L. (1990). Spontaneous liberation of nitric oxide cannot account for *in vitro* vascular relaxation by S-nitrosothiols. *J. Pharmacol. Exp. Ther.*, **255**, 1256–1264.

KUBES, P. (1992). Nitric oxide modulates epithelial permeability in the feline small intestine. *Am. J. Physiol.*, **262**, G1138–G1142.

KUBES, P. & GRANGER, D.N. (1992). Nitric oxide modulates microvascular permeability. *Am. J. Physiol.*, **262**, H611–H615.

KUBES, P., SUZUKI, M. & GRANGER, D.N. (1990). Platelet-activating factor-induced microvascular dysfunction: role of adherent leukocytes. *Am. J. Physiol.*, **258**, G158–G163.

KUBES, P., SUZUKI, M. & GRANGER, D.N. (1991). Nitric oxide: an endogenous modulator of leukocyte adhesion. *Proc. Natl. Acad. Sci. U.S.A.*, **88**, 4651–4655.

KVIETYS, P.R., TWOHIG, B., DANZELL, J. & SPECIAN, R.D. (1990). Ethanol-induced injury to the gastric mucosa: Role of neutrophils and xanthine oxidase-derived radicals. *Gastroenterology*, **98**, 909–920.

LASZLO, F., WHITTLE, B.J.R. & MONCADA, S. (1994a). Time-dependent enhancement or inhibition of endotoxin-induced vascular injury in rat intestine by nitric oxide synthase inhibitors. *Br. J. Pharmacol.*, **111**, 1309–1315.

LASZLO, F., WHITTLE, B.J.R. & MONCADA, S. (1994b). Interactions of constitutive nitric oxide with PAF and thromboxane on rat intestinal vascular integrity in acute endotoxaemia. *Br. J. Pharmacol.*, **113**, 1131–1136.

LASZLO, F., WHITTLE, B.J.R. & MONCADA, S. (1994c). Protective actions of the nitric oxide donor S-nitroso-glutathione or an anti-neutrophil antibody in acute microvascular injury in rat intestine. *Br. J. Pharmacol.*, **112**, 68P.

LOPEZ-BELMONTE, J., WHITTLE, B.J.R. & MONCADA, S. (1993). The actions of nitric oxide donors in the prevention or induction of injury to the rat gastric mucosa. *Br. J. Pharmacol.*, **108**, 73–78.

LEFER, A.M. & LEFER, D.J. (1993). Pharmacology of the endothelium in ischaemia-reperfusion and circulatory shock. *Annu. Rev. Pharmacol. Toxicol.*, **33**, 71–90.

MATSUDA, T., RUBINSTEIN, I., ROBBINS, R.A., KOYAMA, S., JOYNER, W.L. & RENNARD, S.I. (1991). Role of neutrophils in endotoxin-mediated microvascular injury in hamsters. *J. Appl. Physiol.*, **71**, 307–313.

MCCALL, T.B., WHITTLE, B.J.R., BOUGHTON-SMITH, N.K. & MONCADA, S. (1988). Inhibition of FMLP-induced aggregation of rabbit neutrophils by nitric oxide. *Br. J. Pharmacol.*, **95**, 571P.

MOILANEN, E., VUORINEN, P., KANKAANRANTA, H., METSÄ-KETELÄ, T. & VAPAATALO, H. (1993). Inhibition by nitric oxide-donors of human polymorphonuclear leucocyte functions. *Br. J. Pharmacol.*, **109**, 852–858.

MONCADA, S., PALMER, R.M.J. & HIGGS, E.A. (1991). Nitric oxide: physiology, pathophysiology, and pharmacology. *Pharmacol. Rev.*, **43**, 109–142.

PABST, M.J. & JOHNSTON, JR R.B. (1980). Increased production of superoxide anion by macrophages exposed *in vitro* to muramyl dipeptide or lipopolysaccharide. *J. Exp. Med.*, **151**, 101–114.

PAYNE, D. & KUBES, P. (1993). Nitric oxide donors reduce the rise in reperfusion-induced intestinal mucosal permeability. *Am. J. Physiol.*, **265**, G189–G195.

RADOMSKI, M.W., REES, D.D., DUTRA, A. & MONCADA, S. (1992). S-nitroso-glutathione inhibits platelet activation *in vitro* and *in vivo*. *Br. J. Pharmacol.*, **107**, 745–749.

SACKS, T., MOLDOW, C.F., CRUDDOCK, P.R., BOWERS, T.K. & JACOBS, H.S. (1978). Oxygen radicals mediate endothelial cell damage by complement-stimulated granulocytes. An *in vitro* model of immune vascular damage. *J. Clin. Invest.*, **61**, 1161–1167.

TAUBER, A.I. & BABIOR, B.M. (1985). Neutrophil oxygen reduction: The enzymes and the products. *Adv. Free Radical Biol. Med.*, **1**, 265–307.

TEPPERMAN, B.L., VOZZOLO, B.L. & SOPER, B.D. (1993). Effect of neutropenia on gastric mucosal integrity and mucosal nitric oxide synthesis in the rat. *Dig. Dis. Sci.*, **38**, 2056–2061.

WALLACE, J.L., KEENAN, C.M. & GRANGER, D.N. (1990). Gastric ulceration induced by nonsteroidal antiinflammatory drugs is a neutrophil-dependent process. *Am. J. Physiol.*, **259**, G462–G467.

WEDMORE, C.V. & WILLIAMS, T.J. (1981). Control of vascular permeability by polymorphonuclear leukocytes in inflammation. *Nature*, **289**, 646–650.

WHITTLE, B.J.R., BOUGHTON-SMITH, N.K., HUTCHESON, I.R., ESPLUGUES, J.V. & WALLACE, J.L. (1987). Increased intestinal formation of Paf in endotoxin-induced damage in the rat. *Br. J. Pharmacol.*, **92**, 3–4.

WORTHEN, G.S., AVDI, N., VUKAJLOVICH, S. & TOBIAS, P.S. (1992). Neutrophil adherence induced by lipopolysaccharide in vitro. *J. Clin. Invest.*, **90**, 2526–2535.

XIN-LIANG, M.A., LEFER, A.M. & ZIPKIN, R.E. (1993). S-nitroso-N-penicillamine is a potent inhibitor of neutrophil-endothelial interaction. *Endothelium*, **1**, 31–39.

(Received November 14, 1994
Accepted February 8, 1995)

British Journal of Pharmacology (1995) 115, 503-509

The use of microdialysis for the study of drug kinetics: some methodological considerations illustrated with antipyrine in rat frontal cortex

[1]P.N. Patsalos, [2]W.T. Abed, M.S. Alavijeh & M.T. O'Connell

Pharmacology and Therapeutics Unit, Epilepsy Research Group, University Department of Clinical Neurology, Institute of Neurology, Queen Square, London, WC1N 3BG

1 The neuropharmacokinetics of antipyrine, a readily dialysable drug, in rat frontal cortex were studied and the effect of sampling time and contribution of period sampling and dialysate dead volume investigated in relation to t_{max}, C_{max}, AUC and $t_{1/2}$ values.

2 After i.p. administration, antipyrine (35 mg kg^{-1}, $n=5$) concentrations rose rapidly in rat frontal cortex (t_{max}, 12 min) and then declined exponentially. t_{max}, C_{max}, AUC and $t_{1/2}$ values were determined after 2 min dialysate sampling and compared to values obtained from simulated sampling times of 4, 6, 8, 10 and 20 min.

3 Antipyrine t_{max} and C_{max} values were directly dependent on sampling frequency. Thus, mean 2 min sampling t_{max} and C_{max} values were 63% lower and 27% higher, respectively, compared to 20 min sampling values. AUC and $t_{1/2}$ values were unaffected.

4 Adjustment for dialysate dead volume (the volume of dialysate within the dialysis probe and sampling tube) reduced t_{max} values significantly but did not affect the other neuropharmacokinetic parameters.

5 Contribution of period sampling on neuropharmacokinetic parameters were investigated by comparing plots of antipyrine concentration data at midpoint and at endpoint of sampling time interval. Only t_{max} values were affected with values decreasing with increasing sampling time interval.

6 In conclusion, although microdialysis is a useful method for monitoring events at the extracellular level and for kinetic studies, it is important to understand its inherent characteristics so that data can be interpreted appropriately. Sampling frequency, particularly during monitoring of periods of rapid change, is very important since C_{max} and t_{max} values will be significantly underestimated and overestimated respectively, if sampling time is longer rather than shorter. These considerations are particularly important in relation to microdialysis studies of pharmacokinetic-pharmacodynamic interrelationships and modelling.

Keywords: Microdialysis; antipyrine; neuropharmacokinetics; period analysis; pharmacodynamic modelling

Introduction

During the last 10-15 years the technique of intracerebral microdialysis has contributed significantly to our understanding of brain neurochemistry (Lehmann *et al.*, 1983; Abercombie *et al.*, 1988; Benveniste *et al.*, 1989; Yamamoto & Davy, 1992; Millan *et al.*, 1993; Yadid *et al.*, 1993). By use of intracerebral microdialysis it has been possible to monitor the release of various neurotransmitters into the extracellular fluid of specific brain sites and, at the same time, to manipulate pharmacologically the dialysed areas under physiological conditions (Hernandez *et al.*, 1991; Mizuno *et al.*, 1991; Bustos *et al.*, 1992).

As the extracellular fluid is the liquid compartment where the traffic of compounds and the exchange of chemical information between cells takes place, monitoring of the fluid by microdialysis has been considered to reflect synaptic events and of events at the site of action or biophase of drugs. Consequently, neurochemical changes in the extracellular fluid have been correlated with various pharmacodynamic paradigms including behaviour (Abercombie *et al.*, 1988; Hutson & Curzon, 1989; Stahle *et al.*, 1990; Mizuno *et al.*, 1991) and electrical activity (Delgado *et al.*, 1984; Vezzani *et al.*, 1985; Ludvig *et al.*, 1992). Also numerous studies of the effects of a variety of drugs on neurochemical changes have been undertaken (Hurd *et al.*, 1988; O'Connell *et al.*, 1991; Semba *et al.*, 1992). These studies have now been extended to man (Meyerson *et al.*, 1990; Carlson *et al.*, 1992; Persson & Hillered, 1992; During & Spencer, 1993).

The use of the microdialysis technique to study peripheral pharmacokinetics and CNS neuropharmacokinetics of drugs has recently been advocated and numerous reports relating to studies in animals (Hurd *et al.*, 1988; Sabol & Freed, 1988; Stahle *et al.*, 1991b; Steele *et al.*, 1991; Telting-Diaz *et al.*, 1992; Alavijeh *et al.*, 1993; Deleu *et al.*, 1993; Dykstra *et al.*, 1993; Golden *et al.*, 1993; Kurata *et al.*, 1993; O'Connell *et al.*, 1993; Patsalos *et al.*, 1993) and man (O'Connell *et al.*, 1994; Scheyer *et al.*, 1994a,b; Stahle *et al.*, 1991a) have been published. Also published are a number of studies on methodological considerations, particularly the mathematical handling of microdialysis drug concentration data and the correlation between pharmacokinetic data derived from microdialysis and that derived from direct blood sampling (Scott *et al.*, 1990; Morrison *et al.*, 1991; Stahle, 1992; Dykstra *et al.*, 1993; Stenken *et al.*, 1993). Of additional concern has been the recovery characteristics of microdialysis probes and methodologies have been described to enable absolute concentrations to be determined. However, although methods are straightforward in relation to the blood compartment, they are rather tedious and cumbersome in relation to the brain (Scheller & Kolb, 1991; Menacherry *et al.*, 1992; Sjoberg *et al.*, 1992; Yokel *et al.*, 1992; Justice, 1993; Stenken *et al.*, 1993).

A fundamental omission of all kinetic studies (both pharmacokinetic and neuropharmacokinetic) to date has been consideration of the effect of sampling rate and sample

[1] Author for correspondence.
[2] Present address: Jordan University for Women Faculty of Pharmacy & Medical Technology, PO Box 961343 Amman, Jordan.

batching on kinetic profiles. Indeed the effect of sampling rate on neurotransmitter and other analytical profiles in general, using the microdialysis technique, has not been studied. This is particularly relevant since microdialysis sampling involves period sampling and not point sampling.

In the present study we have investigated the effect of sampling time on the neuropharmacokinetics of antipyrine in rat frontal cortex. Also investigated was the contribution of the sampling methodology to the calculated neuropharmacokinetic constants of antipyrine. Antipyrine was selected because it distributes rapidly throughout body water, cerebrospinal fluid and cerebral cortex (Johanson & Woodbury, 1977), is unionised at physiological pH (Rall *et al.*, 1959), is minimally bound to plasma proteins (Gumbleton & Benet, 1991) and has a low hepatic extraction ratio (Rane *et al.*, 1977), suggesting that extracellular fluid antipyrine concentrations should not differ significantly between different organs. In addition, antipyrine is readily dialysable (Yokel *et al.*, 1992; Kurata *et al.*, 1993).

Methods

Five male Sprague-Dawley rats (B&K Universal Ltd, Hull) weighing 250–300 g with free access to a normal laboratory diet (SDS R and M number 1 expanded. Scientific Dietary Services, Witham, Essex) and water were used. Rats were individually housed in contiguous cages at constant temperature (22°C) under a 12 h light-dark cycle (lights on 06 h 00 min).

Intracerebral microdialysis

All animal procedures were in strict accordance with the Home Office guidelines and specifically licenced under the Animals (Scientific Procedures) Act of 1986. Anaesthesia was induced by sodium pentobarbitone (60 mg kg^{-1}, i.p.) and dialysis probes stereotactically implanted in the frontal cortex (3.2 mm anterior and 5.5 mm ventral to bregna, 2.5 mm lateral to midline) according to the atlas of Paxinos & Watson (1986). The dialysis probes were concentric in design and were the same as those previously described (Semba *et al.*, 1992). The following day, the inflow line of each probe was connected to a syringe pump (model 22, Harvard Apparatus Ltd, Edenbridge) and artificial cerebrospinal fluid (composition mM: NaCl 125, KCl 2.5, $MgCl_2$ 1.18 and $CaCl_2$ 1.26) was perfused through the probes at a flow rate of 2 $\mu l\ min^{-1}$. The outlet line of each probe was connected to a refrigerated fraction collector (CMA/170, Biotech Instruments Ltd, Luton) so as to enable automated dialysate collection. After an initial 30 min perfusion interval, animals were injected intraperitoneally with antipyrine (35 mg kg^{-1}; BDH Ltd, Poole) and sampling continued at 2 min intervals for 5.93 h. Dialysates were stored at −70°C until analysis of antipyrine content.

Antipyrine relative recovery *in vitro*, for each microdialysis probe, was determined by a traditional *in vitro* recovery study at 37°C. The five microdialysis probes used for implantation were first tested by immersing in a beaker of constantly stirred dialysate containing 80 $\mu mol\ l^{-1}$ antypirine. After perfusing with dialysate at 2 $\mu l\ min^{-1}$ for 10 min, three 20 min dialysate samples were collected from each probe. These were analysed for antipyrine content and compared to known dialysate antipyrine concentration (80 $\mu mol\ l^{-1}$ in beaker dialysate) so as to quantitate recovery.

Antipyrine analysis

Antipyrine concentrations in the dialysis samples (4 μl) were determined by high performance liquid chromatography (h.p.l.c.) essentially as previously described (Patsalos *et al.*, 1988). Briefly, 4 μl of dialysate were injected directly into a Spectra Physics liquid chromatogram with data processing capability (Spectra Physics, Maidenhead). The chromatogram comprised a P4500 pump, an A53000 autosampler, a UV2000 detector and a Chromjet integrator. A Lichrosorb RP8 10 μm column (Hichrom, Reading) and an acetonitrile: water: acetic acid (40 : 48 : 12) mobile phase (1.3 ml min^{-1}) were used. The column eluent was monitored at 270 nm and the retention time for antipyrine was 6.7 min. The lower limit of detection of antipyrine was 0.5 $\mu mol\ l^{-1}$ and the inter-assay coefficient of variation was <2.5%.

Neuropharmacokinetic analysis

Using the non-linear least-square regression programme PCNONLIN 3.0, dialysate antipyrine concentration versus time data were analysed with a one compartment model and a weighting factor of 1/concentration (Metzler & Weiner, 1988). However, as the programme (and indeed most such programmes) requires initial parameter estimates, and the success of the least-square analysis often depends on how good the initial parameter estimates are, initial parameter estimates were obtained using JANA (Dunn, 1985). Both programmes were implemented on a Hewlett Packard Vectra 486 computer. The parameters computed were: area under the concentration versus time curve ($AUC_{0\rightarrow 356\ min}$) and elimination half-life ($t_{1/2}$). As antipyrine was administered i.p. and not as a bolus (e.g. i.v.), the $t_{1/2}$ values computed can be considered as apparent $t_{1/2}$ values since they encompass both absorption and elimination processes. Time to maximum concentration (t_{max}) and maximum concentration (C_{max}) were obtained by visual inspection of the antipyrine versus time profiles.

Data and statistical analysis

In order to simulate dialysate sampling at 4, 6, 8, 10 and 20 min intervals, the antipyrine concentration data were summated accordingly. Thus, in order to simulate 4 min sampling, the first two 2 min antipyrine concentrations were averaged and also all subsequent two 2 min data sets were averaged. Similarly, in order to simulate 20 min sampling, the first ten 2 min antipyrine concentrations were averaged and all subsequent ten 2 min data sets were averaged.

Since microdialysis sampling represents period sampling (e.g. 2 min or 10 min sampling) and consequently measured dialysate concentrations represent mean values during the sampling time period, the effect of plotting the antipyrine concentration versus time data at midpoint of sampling time (e.g. during 2 min sampling data are plotted at 1 min) as compared to plotting at endpoint of sampling period, on kinetic constants was investigated. These data are referred to as time-adjusted data. Finally, the contribution of a non-synchronized sampling protocol in relation to antipyrine administration on kinetic constants was investigated by adjusting antipyrine concentration versus time data to compensate for dialysate dead volume. The dialysate dead volume being the volume of dialysate within the dialysis probe and the tubing leading to the sampling tubes. These data are referred to as dead-volume adjusted data.

Statistical analysis of the neuropharmacokinetic parameters were made by *t* test and paired *t* test.

Results

Mean ± s.e.mean antipyrine relative recovery *in vitro* of the five microdialysis probes was 23.3 ± 1.5% at a dialysate flow rate of 2 $\mu l\ min^{-1}$. Because of debate as to the justification of translating *in vitro* recovery determinations into those expected *in vivo*, the concentration data shown in this study are those measured *in vivo* and are not adjusted to take into consideration *in vitro* relative recovery. This does not affect data interpretation in any way.

Figure 1 shows the mean frontal cortex dialysate concentration versus time profile of antipyrine after the intraperitoneal administration of antipyrine (35 mg kg^{-1}, $n=5$).

After a time lag of 16 min, antipyrine concentrations rapidly increased to peak 12 min later. Concentrations then fell exponentially.

Figure 2a shows a comparison of frontal cortex antipyrine concentration versus time profiles for 2 min sampling and simulated 20 min sampling intervals in a typical rat and Figure 2b shows that of rat 5. The profiles are only shown up to 122 min since the terminal concentration versus time points are essentially superimposable and not dependent on sampling time interval. For clarity the simulated concentration versus time profiles for 4, 6, 8 and 10 min sampling are not included but are intermediate of the profiles for 2 and 20 min sampling.

Figures 3–5 show the same profiles as for Figure 2a except that the data have been plotted at midpoint of sampling time interval to compensate for period sampling (Figure 3), adjusted to compensate for dialysate dead volume (Figure 4) and finally a combination of dead volume adjusted and plotted at midpoint of sampling time interval (Figure 5).

Table 1 shows the apparent neuropharmacokinetic constants for individual rats together with the mean values as calculated from log concentration versus time plots. The microdialysate concentration data have not been adjusted to take into consideration microdialysate dead volume or period sampling analysis. The neuropharmacokinetic constants for individual rats showed moderate variability within each sampling time interval. Although sampling time interval did not affect AUC and $t_{1/2}$ values, t_{max} and C_{max} values were significantly affected. Thus, compared to 2 min sampling, t_{max} and C_{max} values increased and decreased respectively with increase in sampling time interval. These differences were sig-

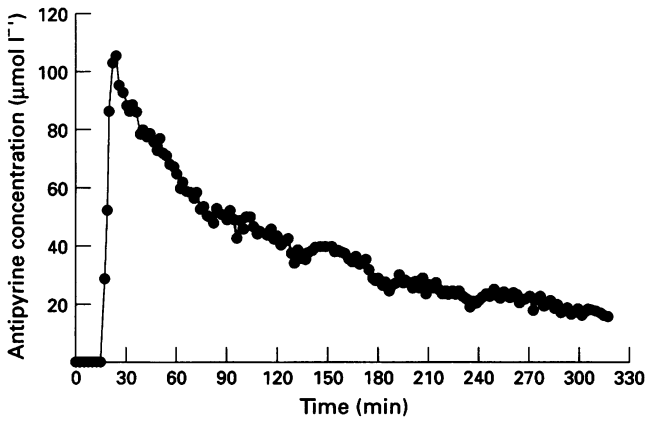

Figure 1 Antipyrine frontal cortex dialysate concentration versus time profile after i.p administration of 35 mg kg^{-1} antipyrine. Values are mean of 5 rats. For clarity, s.e.bars are not shown but do not exceed 5%.

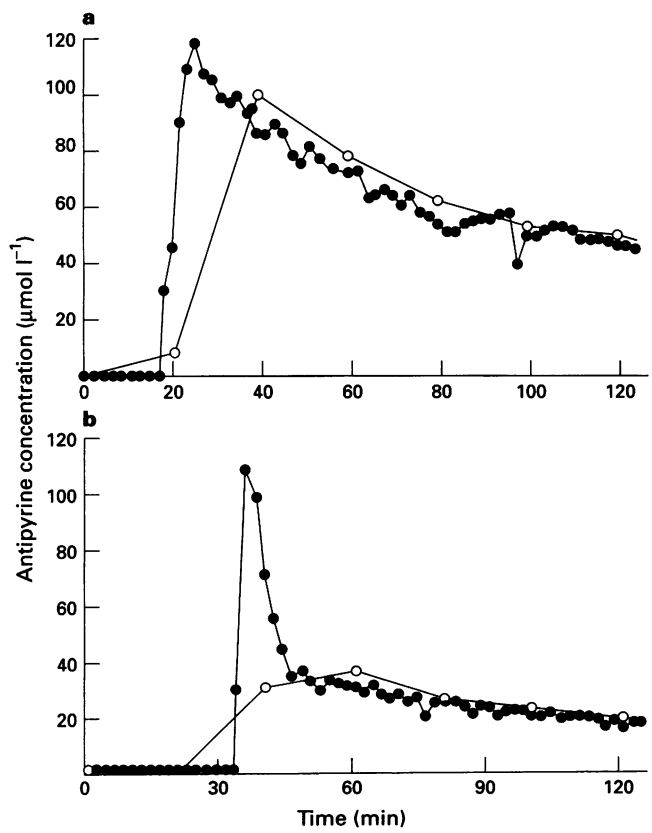

Figure 2 (a) A comparison of frontal cortex antipyrine concentration versus time profiles for 2 min sampling (●) and simulated 20 min sampling (○) time intervals. Values are mean of 5 rats. For clarity, s.e.bars are not shown but do not exceed 5%. (b) A comparison of frontal cortex antipyrine concentration versus time profiles for 2 min sampling (●) and simulated 20 min sampling (○) time intervals for rat 5. The figure illustrates the largest difference in C_{max} values seen in the study. For clarity, s.e.bars are not shown but do not exceed 5%.

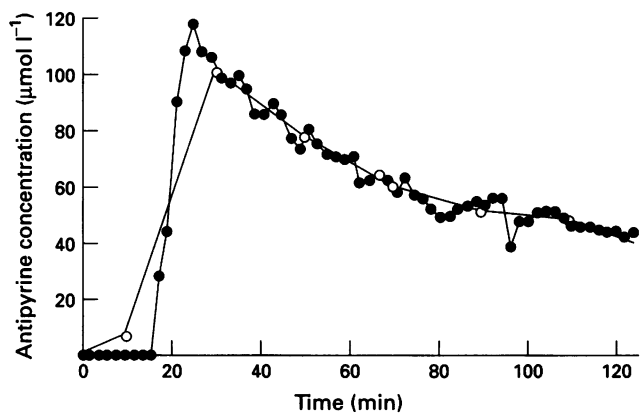

Figure 3 A comparison of frontal cortex antipyrine concentration versus time profiles for 2 min sampling (●) and simulated 20 min sampling (○) time intervals where concentration values are plotted at midpoint of sampling time interval. Values are mean of 5 rats. For clarity, s.e.bars are not shown but do not exceed 5%.

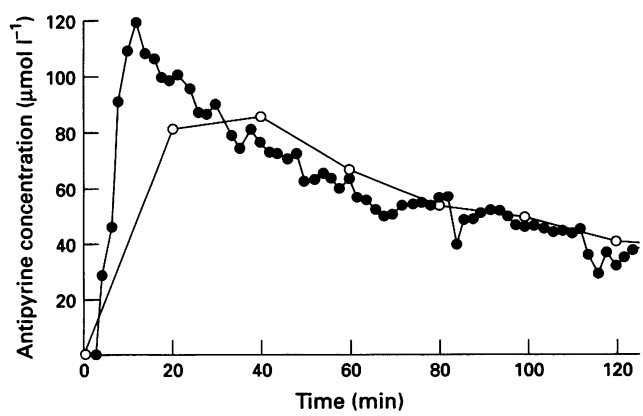

Figure 4 A comparison of frontal cortex antipyrine concentration versus time profiles for 2 min sampling (●) and simulated 20 min sampling (○) time intervals where concentration values are plotted so as to compensate for dialysate dead volume. Values are mean of 5 rats. For clarity, s.e.bars are not shown but do not exceed 5%.

nificantly different at all sampling time intervals for C_{max} values and from 6 min for t_{max} values. Twenty minute sampling was therefore associated with a mean 63% increase in t_{max} values and a mean 27% reduction in C_{max} values compared to the corresponding 2 min values. However, for rat 5, C_{max} values were 67% lower during 20 min sampling compared to 2 min sampling (Figure 2a).

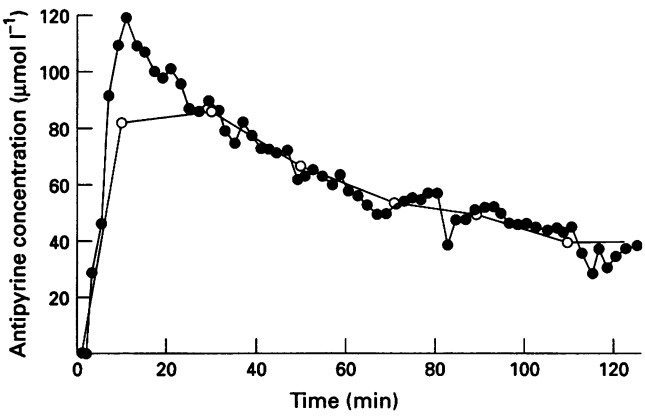

Figure 5 A comparison of frontal cortex antipyrine concentration versus time profiles for 2 min sampling (●) and simulated 20 min sampling (○) time intervals where concentration values are plotted at midpoint of sampling time interval and also compensated for dialysate dead volume. Values are mean of 5 rats. For clarity, s.e.bars are not shown but do not exceed 5%.

Table 2 shows a comparison of mean microdialysate neuropharmacokinetic constants for frontal cortex antipyrine before and after adjustment for microdialysis sampling methodology at 2, 4, 6, 8, 10 and 20 min sampling intervals. Within the 2 min sampling time interval, it can be seen that compared to unadjusted data, time adjusted data (i.e. plotting individual concentrations at midpoint of sampling time interval to compensate for period sampling) had no significant effect on any neuropharmacokinetic parameter studied. However, t_{max} values decreased, compared to unadjusted data, with increasing sampling time interval so that the reduction was 23% for 20 min sampling. However, this did not attain statistical significance.

In contrast, adjustment for dialysate dead volume was associated with significant decreases in t_{max} values (Table 2). The decreases were particularly significant for the shorter sampling times with a decrease of approximately 50% observed for 2, 4, 6 and 8 min sampling and 31% and 18% for 10 and 20 min sampling respectively. However, adjustment for dialysate dead volume had no significant effect on C_{max}, AUC and $t_{1/2}$ values. Furthermore, although the combination of time adjustment and dead volume adjustment had no additional significant effect on the neuropharmacokinetic constants compared to dead volume adjustment only, t_{max} values showed a tendency towards reduction with increasing sampling time.

Discussion

With the increasing use of the microdialysis technique in *in vivo* monitoring of a wide range of analytes including neurotransmitters and drugs, it is important to characterize the

Table 1 Antipyrine neuropharmacokinetic constants derived from 2 min microdialysate sampling and from projected sampling times up to 20 min

	Microdialysate sampling time (min)					
	2	*4*	*6*	*8*	*10*	*20*
Rat	t_{max} (min)					
1	26	28	30	32	30	40
2	24	28	30	32	30	40
3	24	28	30	32	30	40
4	24	24	30	32	30	40
5	36	40	42	40	40	60
Mean	27[b]	30	32[a]	34[a]	32[a]	44[a]
± s.e.mean	2	2	2	1	2	4
	C_{max} (μmol l⁻¹)					
1	118.9	114.1	111.5	108.8	107.3	101.9
2	96.6	89.6	87.1	85.5	88.1	82.3
3	101.4	91.9	90.8	87.6	82.8	78.0
4	91.9	88.7	82.8	82.3	85.0	79.6
5	108.8	85.0	74.9	77.0	61.6	36.1
Mean	103.5[b]	93.9[c]	89.4[c]	88.1[c]	85.0[c]	75.6[c]
± s.e.mean	4.7	5.2	6.1	5.3	7.3	10.8
	AUC (μmol l⁻¹ min)					
1	175.2	174.7	174.2	174.2	173.6	172.0
2	167.3	166.7	166.2	165.7	165.1	163.0
3	152.9	152.4	151.9	151.3	151.3	149.2
4	149.2	148.7	148.1	148.1	147.6	146.5
5	68.0	68.0	67.4	67.4	67.4	66.9
Mean	142.5	142.1	141.6	141.3	141.0	139.5
± s.e.mean	19.2	19.1	19.1	19.1	19.0	18.7
	$t_{1/2}$ (min)					
1	86.7	86.8	86.8	86.8	86.6	86.9
2	129.2	130.9	131.1	130.9	128.8	129.0
3	103.9	105.0	105.0	105.0	105.3	105.0
4	97.1	97.0	97.9	98.0	96.9	96.8
5	79.8	82.3	82.4	79.4	80.6	87.8
Mean	99.4	100.4	100.6	100.0	99.6	101.1
± s.e.mean	7.6	7.7	7.7	7.9	7.5	6.9

t_{max} = time to maximum concentration; C_{max} = maximum concentration
AUC = area under the dialysate concentration versus time curve; $t_{1/2}$ = apparent elimination half-life
[a] Significantly different from [b], $P < 0.001$; [c] Significantly different from [b], $P < 0.05$

Table 2 A comparison of mean (±s.e.mean) neuropharmacokinetic constants for antipyrine before and after adjustments for microdialysis sampling methodology

	t_{max} (min)					C_{max} (μmol l^{-1})					AUC (μmol l^{-1} min)					$t_{1/2}$ (min)				
	2	4	6	8	10	20	2	4	6	8	10	20	2	4	6	8	10	20	2	4	6	8	10	20
Unadjusted data	27[b]	30[b]	32[b]	34[b]	32[b]	44[b]	103.5	93.9	89.4	88.1	85.0	75.6	142.5	142.1	141.6	141.3	141.0	139.5	99.4	100.4	100.6	100.0	99.6	101.1
	2	2	2	1	2	4	4.7	5.2	6.1	5.3	7.3	10.8	19.2	19.1	19.1	19.1	19.0	18.7	7.6	7.7	7.7	7.9	7.5	6.9
Dead volume adjusted	13[a]	14[a]	16[a]	18[a]	22[a]	36[a]	103.5	100.9	89.7	87.6	86.5	69.0	146.5	146.0	146.0	145.5	145.5	145.5	101.2	101.1	102.1	101.3	101.8	104.9
	2	2	2	1	2	4	4.2	3.7	4.2	7.4	4.8	4.2	17.5	17.5	17.5	17.5	17.5	17.5	6.9	6.9	7.6	6.9	7.2	8.0
Time adjusted	26	28	29	30	27	34	103.5	94.0	89.2	88.1	85.0	75.4	142.3	141.8	141.8	141.2	141.2	139.1	99.4	100.4	100.6	100.0	99.6	101.1
	2	2	2	1	2	4	4.2	4.8	5.3	4.8	6.4	9.5	17.0	17.0	17.0	17.0	17.0	17.0	7.6	7.7	7.7	7.9	7.5	6.9
Dead volume plus	12[a]	13[a]	13[a]	14[a]	18[a]	28[a]	103.5	100.9	89.7	87.6	86.5	69.0	146.5	156.5	118.4	144.4	143.4	139.1	101.2	101.1	102.1	101.3	101.8	104.9
time adjusted	2	2	2	2	2	4	4.2	3.7	4.2	7.4	4.8	4.2	17.5	17.5	17.5	17.5	17.0	16.5	6.9	6.9	7.6	6.9	7.2	8.0

Values are mean ± s.e.mean of 5 rats
t_{max} = time to maximum concentration; C_{max} = maximum concentration
AUC = area under the dialysate concentration versus time curve; $t_{1/2}$ = apparent elimination half-life
[a]Significantly different from [b], $P < 0.001$

methodology and to take into consideration its inherent properties which may impact significantly on data interpretation. The primary purpose of the present study was to investigate the effect of sampling time on the neuropharmacokinetics of antipyrine in rat frontal cortex. The second purpose was to ascertain the contribution of period sampling and of dialysate dead volume. The study design justifies some comment. Firstly, 2 min sampling intervals were chosen because preliminary experiments indicated that such sampling was within our quantitation range for h.p.l.c. antipyrine concentration measurement in dialysate sample volumes of 4 μl. Secondly, antipyrine dialysate concentration data were simulated for 4, 6, 8, 10 and 20 min from the 2 min data, as opposed to generating the data from different experiments, in order to overcome potential variability in data sets consequent to factors such as variability in antipyrine administration, inter-rat handling of antipyrine, dialysate collection and analytical variability. Thus, the study design was optimumly focused to answer the questions posed.

The major findings of this study are that t_{max} and C_{max} are directly dependent on dialysate sampling frequency. Thus, mean 2 min sampling t_{max} and C_{max} values were 63% lower and 27% higher, respectively, compared with that of 20 min sampling values. However, in one rat (rat 5, Figure 2b) where apparently a 2 min sample exactly coinsided with the 'true' C_{max} (i.e. dilution of antipyrine concentration due to period sampling was minimal), the C_{max} value was 67% higher during 2 min sampling compared to 20 min sampling. Scanning the microdialysis literature, the range of dialysate sampling frequency reported as being used varies from 5 min (e.g. Stahle, 1993; Golden *et al.*, 1993) to 60 min (e.g. Chen & Steger, 1993; Kurata *et al.*, 1993), with most authors using 20 or 30 min sampling time protocols (e.g. Anderson & DiMicco, 1992; Menacherry *et al.*, 1992; Semba *et al.*, 1992). All microdialysis studies report concentration changes of the substance analysed e.g. neurotransmitters or drugs relative to baseline as a percentage or as an absolute concentration. Clearly, from the present study, it can be concluded that during periods of rapid change e.g. neurotransmitter release and uptake or drug absorption, the concentration changes reported are underestimated if sampling time is longer rather than shorter. Furthermore, the present data suggest that studies should not be directly and quantitatively compared if the same sampling time protocol is not used. Perhaps the best approach to monitoring analyte by microdialysis, is to sample as frequently as possible during periods of rapid concentration changes and less frequently during slower concentration changes. With the continuing development of capillary liquid chromatography and the emergence of capillary electrophoresis as practical analytical techniques for quantitating (fmol) substances in very small volumes (nl), frequent sampling during microdialysis studies will be more widely undertaken.

An extrapolation of the same arguments indicated above would apply for the time course of events (t_{max}) monitored by microdialysis. Data reported in this respect would be overestimated if sampling time is longer rather than shorter. As $t_{1/2}$ and AUC are not discrete variables, they should not depend on sampling time and indeed microdialysate sampling time had no significant effect on these values.

Because brain microdialysis monitors events at the extracellular level and is therefore considered to reflect events at the synaptic site of action, studies of drug pharmacokinetic-pharmacodynamic inter-relationships and modelling are feasible and indeed desirable. However, appreciation of the effects of sampling time on C_{max} and t_{max} values is imperative in such studies.

As one might expect, adjustment of data to take into consideration dialysate dead volume, resulted in significant reductions in t_{max} values but had no significant effect on the other neuropharmacokinetic parameters. Although conceptually

dead volume adjustment should be a fundamental consideration in microdialysis studies, in fact publications rarely indicate its consideration.

As microdialysis sampling represents period sampling and therefore concentrations of the substance under analysis in any particular sample represent a mean of the time sampled, there has been some debate as to whether microdialysis data in general should be represented on the time-axis by the endpoint, the starting point or the midpoint of the sampling interval since the concentration versus time curves will be different depending on representation chosen (Morrison *et al.*, 1991; Stahle, 1993). In the present study, plotting antipyrine concentration data at the midpoint of the sampling interval compared to endpoint, resulted in some difference in the concentration versus time plots (Figures 3 and 5). However, only t_{max} values were affected with values decreasing with increasing sampling time. In contrast, C_{max}, AUC and $t_{1/2}$ values were unaffected. Thus, in most situations endpoint or midpoint representation of concentration data will not have a significant effect on kinetic values, except that for long sampling times t_{max} values will be lower when plotted at the midpoint of the sampling time interval. In order to avoid this potential problem, a midpoint sampling interval should be routinely used in plots of concentration versus time.

The neuropharmacokinetic properties of antipyrine in rat frontal cortex, as characterized in the present study using microdialysis, in comparison to its pharmacokinetic and neuropharmacokinetic properties using traditional sampling methodologies (i.e. serial blood or cerebrospinal fluid sampling), need some comment. The pharmacokinetics of antipyrine in blood, as ascertained by blood sampling, has been extensively investigated with reported mean $t_{1/2}$ values ranging from 71.0 ± 7.5 min to 148.0 ± 9.6 min (Pei *et al.*, 1986; Shaw *et al.*, 1986; Svensson & Liu, 1987; Tanaka *et al.*, 1989; Van Bezooijen *et al.*, 1989; Van Bree *et al.*, 1989; Ben Zvi *et al.*, 1991; Kurata *et al.*, 1993). Also there appears to be no significant difference in blood antipyrine $t_{1/2}$ values when traditional blood sampling and microdialysis blood sampling are directly compared (Kurata *et al.*, 1993). As antipyrine readily and rapidly distributes throughout body water, cerebrospinal fluid and cerebral cortex, one might expect its central neuropharmacokinetics not to differ significantly from that of its peripheral pharmacokinetics. Indeed, in studies comparing antipyrine $t_{1/2}$ values obtained by direct sampling of blood and cerebrospinal fluid, the two compartments were indistinguishable (85 ± 8 min versus 90 ± 4 min respectively; Johnson & Woodbury, 1977; Van Bree *et al.*, 1989). Furthermore, mean frontal cortex $t_{1/2}$ values obtained in the present study (99.4 ± 7.6 min) are very comparable to values previously reported and confirm the suitability of microdialysis in studies of drug neuropharmacokinetics.

Finally, although the present study involved antipyrine neuropharmacokinetics in rat frontal cortex, clearly the conclusions would be valid for drug blood pharmacokinetics and indeed should be a major consideration in such studies. This is particularly important as blood and tissue drug pharmacokinetic studies, using the microdialysis technique in man, are still in their infancy (Stahle *et al.*, 1991a; Bolinder *et al.*, 1993; O'Connell *et al.*, 1994).

We wish to thank The Great Britain Sasakawa Foundation for financial support and Nathalie Vomsheid for secretarial assistance.

References

ABERCOMBIE, E.D., KELLER, R.W. & ZIGMOND, M.J. (1988). Characterisation of hippocampal norepinephrine release as measured by microdialysis perfusion: pharmacological and behavioural studies. *Neuroscience*, **27**, 897–904.

ALAVIJEH, M.S., ABED, W.T., O'CONNELL, M.T. & PATSALOS, P.N. (1993). A comparison of classical and microdialysis sampling techniques: a study of carbamazepine (CBZ) pharmacokinetics. *Epilepsia*, **34**, (Suppl. 2), 76.

ANDERSON, J.J. & DIMICCO, J.A. (1992). The use of microdialysis for studying the regional effects of pharmacological manipulation on extracellular levels of amino acids - some methodological considerations. *Life Sci.*, **51**, 623–630.

BENVENNISTE, H., HANSEN, H.J. & OTTEOSEN, N.S. (1989). Determination of brain interstitial concentrations by microdialysis. *J. Neurochem.*, **52**, 1741–1750.

BEN-ZVI, Z., HREASH, F. & KAPLANSKI, J. (1991). Disposition of hexobarbitone and antipyrine in DOCA-hypertensive rats. *J. Pharm. Pharmacol.*, **43**, 349–352.

BOLINDER, J., UNGERSTEDT, U. & ARNER, P. (1993). Long-term continuous glucose monitoring with microdialysis in ambulatory insulin-dependent diabetic patients. *Lancet.*, **342**, 1080–1085.

BUSTOS, G., ABARCA, J., FORRAY, M.I., GYSLING, K., BRADBERRY, C.W. & ROTH, R.H. (1992). Regulation of excitatory amino acid release by N-methyl-D-aspartate receptors in rat striatum: in vivo microdialysis studies. *Brain Res.*, **585**, 105–115.

CARLSON, H., RONNE-ENGSTROM, E., UNGERSTEDT, U. & HILLERID, L. (1992). Seizure related elevations of extracellular amino acids in human focal epilepsy. *Neurosci. Lett.*, **140**, 30–32.

CHEN, Z. & STEGER, R.W. (1993). Plasma microdialysis. A technique for continuous plasma sampling in freely moving rats. *J. Pharmacol. Toxicol. Methods*, **29**, 111–118.

DELEU, D., SARRE, S., MICHOTTE, Y. & EBINGER, G. (1994). Simultaneous in vivo microdialysis in plasma and skeletal muscle: a study of the pharmacokinetic properties of levodopa by non compartmental analysis. *J. Pharmaceut. Sci.*, **83**, 25–28.

DELGADO, J.M.R., LERMA, J., MARTIN DEL RIO, R. & SOLIS, S.M. (1984). Dialytrode technology and local profiles of amino acids in the awake rat brain. *J. Neurochem.*, **42**, 1218–1228.

DUNN, A. (1985). A new iterative polyexponential curve fitting program. *Comput. Methods Biomed.*, **20**, 601–608.

DURING, M.J. & SPENCER, D.D. (1993). Extracellular hippocampal glutamate and spontaneous seizure in the conscious human brain. *Lancet.*, **341**, 1607–1610.

DYKSTRA, K.H., ARYA, A., ARRIOLA, D.M., BUNGAY, P.M., MORRISON, P.F. & DEDRICK, R.L. (1993). Microdialysis study of zidovudine (AZT) transport in rat brain. *J. Pharmacol. Exp. Ther.*, **267**, 1227–1236.

GOLDEN, P.L., BROUWER, K.R. & POLLACK, G.M. (1993). Assessment of valproic acid serum-cerebrospinal fluid transport by microdialysis. *Pharmac. Res.*, **10**, 1765–1771.

GUMBLETON, M. & BENET, L.Z. (1991). Metabolism and laboratory anesthetic protocols in the rat: examination of antipyrine pharmacokinetics. *Pharmacol. Res.*, **8**, 544–546.

HERNANDEZ, L., GUZMAN, N.A. & HOEBEL, B.G. (1991). Bidirectional microdialysis in vivo shows differential dopaminergic potency of cocaine, procaine and lidocaine for calibration of drug outward diffusion. *Psychopharmacol.*, **105**, 264–268.

HURD, J.L., KEHR, J. & UNGERSTEDT, U. (1988). In vivo microdialysis as a technique to monitor drug transport: correlation of extracellular cocaine levels and dopamine overflow in the rat brain. *J. Neurochem.*, **51**, 1314–1316.

HUTSON, P.H. & CURZON, G. (1989). Concurrent determination of effects of p-chloramphetamine on central extracellular 5-hydroxytryptamine concentration and behaviour. *Br. J. Pharmacol.*, **96**, 801–806.

JOHANSON, C.E. & WOODBURY, D.M. (1977). Penetration of ^{14}C-antipyrine and ^{14}C- barbital into the choroid plexus and cerebrospinal fluid of the rat in vivo. *Exp. Brain Res.*, **30**, 65–74.

JUSTICE, J.B. (1993). Quantitative microdialysis of neurotransmitters. *J. Neurosci. Methods*, **48**, 263–276.

KURATA, N., INAGAKI, M., KOBAYASHI, S., NISHIMURA, Y., OGUCHI, K. & YASUHARA, H. (1993). Antipyrine concentrations in liver and blood monitored by microdialysis of unrestrained conscious rats. *Res. Commun. Chem. Pathol. Pharmacol.*, **79**, 363–369.

LEHMANN, A., ISACSSON, H. & HAMBER, A. (1983). Effect of in vivo administration of kainic acid on extracellular amino acid pool in the rabbit hippocampus. *J. Neurochem.*, **40,** 1314–1320.

LUDVIG, N., MISHRA, P.K., YAN, Q.S., LASLEY, S.M., BURGER, R.L. & JOBE, P.C. (1992). The combined EEG-intracerebral microdialysis technique: a new tool for neuropharmacological studies on freely behaving animals. *J. Neurosci. Methods*, **43,** 129–137.

MENACHERRY, S., HUBERT, W. & JUSTICE, J.B. (1992). In vivo calibration of microdialysis probes for exogenous compounds. *Anal. Chem.*, **64,** 577–583.

METZLER, C.M. & WEINER, D.L. (1988). *A User's Manual for PCNONLIN*. Lexington, KY, USA: Statistical Consultants.

MEYERSON, B.A., LINDEROTH, B., KARLSSON, H. & UNGERSTEDT, U. (1990). Microdialysis in the human brain: extracellular measurements in the thalamus of Parkinsonian patients. *Life Sci.*, **46,** 301–308.

MILLAN, H., CHAPMAN, A.G. & MELDRUM, B.S. (1993). Extracellular amino acid levels in hippocampus during pilocarpine-induced seizures. *Epilepsy Res.*, **14,** 139–148.

MIZUNO, T., ENDO, Y., ARITA, J. & KIMURA, F. (1991). Acetylcholine release in the rat hippocampus as measured by the microdialysis method correlates with motor activity and exhibits a diurnal variation. *Neuroscience*, **44,** 607–612.

MORRISON, P.F., BUNGAY, P.M., HSIAO, J.K., BALL, B.A., MEFFORD, I.N. & DEDRICK, R.L. (1991). Quantitative microdialysis: analysis of transients and application to pharmacokinetics in brain. *J. Neurochem.*, **57,** 103–119.

O'CONNELL, M.T., ABED, W.T., ALAVIJEH, M.S. & PATSALOS, P.N. (1993). A chronic neuropharmacokinetic study of carbamazepine (CBZ) in rat frontal cortex using microdialysis. *Epilepsia*, **34,** (Suppl. 2), 88–89.

O'CONNELL, M.T., PORTAS, C.M., SARNA, G.S. & CURZON, G. (1991). Effect of *p*-chlorophenylalanine on release of 5-hydroxytryptamine from the rat frontal cortex *in vivo*. *Br. J. Pharmacol.*, **102,** 831–836.

O'CONNELL, M.T., TISON, F., QUINN, N. & PATSALOS, P.N. (1994). A newly developed microdialysis probe for monitoring substances in blood of man: pharmacokinetics of levodopa and its primary metabolite, 3-O-methyldopa in patients with Parkinson's disease, preliminary findings. In *Monitoring Molecules in Neuroscience*. ed. Louilot, A., Durkin, T., Spampinato, U. & Cador, M. pp. 53–54. Gradignan: Publi Typ.

PATSALOS, P.N., ALAVIJEH, M.S., ABED, W.T., ELYAS, A.A. & O'CONNELL, M.T. (1993). Use of microdialysis to study brain kinetics: valproate and carbamazepine in rat frontal cortex. *Epilepsia*, **34,** (Suppl. 6), 87.

PATSALOS, P.N., DUNCAN, J.S. & SHORVON, S.D. (1988). Effect of the removal of individual antiepiletic drugs on antipyrine kinetics in patients taking polytherapy. *Br. J. Clin. Pharmacol.*, **26,** 253–259.

PAXINOS, G. & WATSON, C. (1986). *The Rat Brain in Stereotactic Coodinates*. (second edition). San Diego: Academic Press.

PEI, Y.Y., BIALER, M. & LEVY, R.H. (1986). Effects of phenobarbital steady state levels on antipyrine clearance and distribution in the rat. *Biopharm. Drug Dispos.*, **7,** 11–19.

PERSSON, L. & HILLERID, L. (1992). Chemical monitoring of neurosurgical intensive care patients using intracerebral microdialysis. *J. Neurosurg.*, **76,** 72–80.

RALL, D.P., STABENAU, J.R. & ZUBROD, C.G. (1959). Distribution of drugs between blood and cerebrospinal fluid: general methodology and effect of pH gradients. *J. Pharmacol. Exp. Ther.*, **125,** 185–193.

RANE, A., WILKINSON, G.R. & SHAND, D.G. (1977). Prediction of hepatic extraction ratio from in vitro measurement of intrinsic clearance. *J. Pharmacol. Exp. Ther.*, **200,** 420–424.

SABOL, K.E. & FREED, C.R. (1988). Brain acetaminophen measurement by in vivo dialysis, in vivo electrochemistry and tissue assay: a study of the dialysis technique in the rat. *J. Neurosci. Methods*, **24,** 163–168.

SCHELLER, D. & KOLB, J. (1991). The internal reference technique in microdialysis: a practical approach to monitoring dialysis efficiency and to calculating tissue concentrations from dialysate samples. *J. Neurosci. Methods*, **40,** 31–38.

SCHEYER, R.D., DURING, M.J., HOCHHOLZER, J.M., SPENCER, D.D., CRAMER, J.A. & MATTSON, R.H. (1994a). Phenytoin concentrations in the human brain: an in vivo microdialysis study. *Epilepsy Res.*, **18,** 227–232.

SCHEYER, R.D., DURING, M.J., SPENCER, D.D., TOFTNESS, B.R. & MATTSON, R.H. (1994b). Measurement of carbamazepine and carbamazepine epoxide in the human brain using in vivo microdialysis. *Neurology*, **44,** 1469–1472.

SCOTT, D.O., STEELE, K.L. & LUNTE, C.E. (1990). Microdialysis sampling for pharmacokinetic studies. *Curr. Separations*, **10,** 11–15.

SEMBA, J., DOHENY, M., PATSALOS, P.N., SARNA, G. & CURZON, G. (1992). Effect of milacemide on extracellular and tissue concentrations of dopamine and 5-hydroxytryptamine in rat frontal cortex. *Br. J. Pharmacol.*, **105,** 59–62.

SHAW, P.N., TSETI, J., WARBURTON, S., ADEDOYIN, A. & HOUSTON, J.B. (1986). Inhibition of antipyrine metabolite formation. Steady state studies with cimetidine and metyrapone in rats. *Drug Metab. Dispos.*, **14,** 217–276.

SJOBERG, P., OLOFSSON, I.M. & LUNDQUIST, T. (1992). Validation of different microdialysis methods for the determination of unbound steady-state concentrations of theophylline in blood and brain tissue. *Pharmac. Res.*, **9,** 1592–1598.

STAHLE, L. (1993). Microdialysis in pharmacokinetics. *Eur. J. Drug Metab. Pharmacokin.*, **18,** 89–96.

STAHLE, L., ARNER, P. & UNGERSTEDT, U. (1991a). Drug distribution studies with microdialysis. III. Extracellular concentration of caffeine in adipose tissue in man. *Life Sci.*, **49,** 1853–1858.

STAHLE, L., SEGERSVARD, S. & UNGERSTEDT, U. (1990). Theophylline concentration in the extracellular space of the rat brain: measurement by microdialysis and relation to behaviour. *Eur. J. Pharmacol.*, **185,** 187–193.

STAHLE, L., SEGERSVARD, S. & UNGERSTEDT, U. (1991b). Drug distribution studies with microdialysis. II. Caffeine and theophylline in blood, brain and other tissues in rats. *Life. Sci.*, **49,** 1843–1852.

STEELE, K.L., SCOTT, D.O. & LUNTE, C.E. (1991). Pharmacokinetic studies of aspirin in rats using in vivo microdialysis sampling. *Anal. Chim. Acta*, **246,** 181–186.

STENKEN, J.A., TOPP, E.M., SOUTHARD, M.Z. & LUNTE, C.E. (1993). Examination of microdialysis sampling in a well-characterized hydrodynamic system. *Anal. Chem.*, **65,** 2324–2328.

SVENSSON, C.K. & LIU, L.L. (1987). Dose- and time-dependent effect of levamisole on the elimination of antipyrine in the rat. *Drug Metab. Dispos.*, **15,** 432–433.

TANAKA, E., KOBAYASHI, S., UCHIDA, E., OGUCHI, K. & YASUHARA, H. (1989). Antipyrine metabolism in female Lewis and dark Agousti strains of rats, which are extensive and poor metabolizers, respectively. *Jpn. J. Pharmacol.*, **49,** 433–435.

TELTING-DIAZ, M., SCOTT, D.O. & LUNTE, C.E. (1992). Intravenous microdialysis sampling in awake, freely-moving rats. *Anal. Chem.*, **64,** 806–810.

VAN BENZOOIJEN, C.F.A. & VAN OORSCHOT, R.M. (1989). The effect of age on antipyrine pharmacokinetics and metabolite formation in rats. *J. Pharmacol. Exp. Ther.*, **251,** 683–686.

VAN BREE, J.B.M.M., BALJET, A.V., VAN GEYT, A., DE BOER, A.G., DANHOF, M. & BREIMER, D.D. (1989). The unit impulse response procedure for the pharmacokinetic evaluation of drug entry into the central nervous system. *J. Pharmacokin. Biopharmaceut.*, **17,** 441–462.

VEZZANI, A., UNGERSTEDT, U., FRENCH, E.D. & SCWARCZ, R. (1985). In vivo brain dialysis of amino acids and simultaneous EEG measurement following intra-hippocampal quinolinic acid injection: evidence for dissociation between neurochemical changes and seizures. *J. Neurochem.*, **45,** 335–344.

YADID, Y., PACAK, K., GOLOMB, E., HARVEY-WHITE, J.D., LIEBERMANN, D.M., KOPIN, I.J. & GOLDSTEIN, D.S. (1993). Glycine stimulates striatal dopamine release in conscious rats. *Br. J. Pharmacol.*, **110,** 50–53.

YAMAMOTO, B.K. & DAVY, S. (1992). Dopaminergic modulation of glutamate release in striatum as measured by microdialysis. *J. Neurochem.*, **58,** 1736–1742.

YOKEL, R.A., ALLEN, D.D., BURGIO, D.E. & MCNAMARA, P.J. (1992). Antipyrine as a dialyzable reference to correct differences in efficiency among and within sampling devices during in vivo microdialysis. *J. Pharmacol. Toxicol. Methods*, **27,** 135–142.

(Received October 20, 1994
Revised February 14, 1995
Accepted February 17, 1995)

British Journal of Pharmacology (1995) 115, 510-514

Effect of methylguanidine on rat blood pressure: role of endothelial nitric oxide synthase

Raffaella Sorrentino & [1]Aldo Pinto

Department of Experimental Pharmacology, Via Domenico Montesano, 49. 80131 Naples, Italy

1 The effect of acute i.v. administration of methylguanidine (MG) on mean arterial blood pressure (MABP) was investigated in anaesthetized male Wistar rats.

2 MG (1-30 mg kg^{-1} i.v.) produced an increase in MABP in a dose-dependent manner both in normal and in hexamethonium (5 mg kg^{-1}, i.v)-treated rats.

3 L-Arginine (30 or 150 mg kg^{-1}, i.v.), but not its enantiomer D-arginine (30 or 150 mg kg^{-1}, i.v.), reversed the effect of MG on MABP in both normal and hexamethonium-treated rats.

4 L-Arginine (150 mg kg^{-1}, i.v.) administered 2 min before MG (30 mg kg^{-1}, i.v.) prevented the increase in MABP caused by MG in either normal or hexamethonium-treated rats. This effect was not observed with D-arginine (150 mg kg^{-1}, i.v.).

5 Thus, the rise in MABP caused by MG in the anaesthetized rat is due to inhibition of endothelial NO-synthase activity. We speculate that the rise in the plasma concentration of endogenous MG associated with uraemia may contribute to the hypertension seen in patients with chronic renal failure.

Keywords: Methylguanidine; nitric oxide; L-arginine; hexamethonium; rat blood pressure; hypertension; uraemia

Introduction

Nitric oxide (NO) produced by endothelial cells is a mediator involved in the regulation of vascular tone (Rees *et al.*, 1989; Amezcua *et al.*, 1989). NO is synthesized from the guanidino group of the amino acid L-arginine, and an impairment in its synthesis has been implicated in several diseases (Moncada *et al.*, 1991). In fact, hypertension of different aetiologies is associated with a decrease in either synthesis or release of NO (Linder *et al.*, 1990; Panza *et al.*, 1990; Pinto *et al.*, 1992). The reasons of these alterations are as yet unclear. In principle, a reduced formation of NO can be caused either by direct endothelial cell damage (Forstermann *et al.*, 1986; Jacobs *et al.*, 1990) or by accumulation of endogenous NO-synthase inhibitors in the plasma (Iyengar *et al.*, 1987; Vallance *et al.*, 1992; Sorrentino *et al.*, 1993).

Studies regarding the physiological and pathological role of NO have been conducted with specific inhibitors of NO-synthase, such as N^G-methyl-L-arginine (Palmer *et al.*, 1988) or N^G-nitro-L-arginine methyl ester (Rees *et al.*, 1990). These and several other inhibitors of NO-synthase have modifications of the guanidino group of L-arginine (Moncada *et al.*, 1991). Vallance and coworkers (1992) have shown that asymmetrical dimethylarginine, an analogue of L-arginine, is an endogenous inhibitor of NO synthesis which accumulates in the plasma of patients with end-stage chronic renal failure and might contribute to the hypertension and immune dysfunction associated with this pathology.

Patients with chronic renal failure show a retention of several nitrogen-containing products derived from protein catabolism. It has been hypothesized that the high blood concentration of these products may cause uraemic symptoms, i.e. hypertension, immune dysfunction and neurological disorders (Jones & Burnett, 1975). In fact, a dietary protein restriction or haemodialysis reduces these symptoms (Lowrie *et al.*, 1981). Methylguanidine (MG) is a product of protein catabolism that increases and accumulates within cells in chronic renal failure (Matsumoto *et al.*, 1976; Orita *et al.*, 1981; Yokozawa *et al.*, 1989). MG is structurally related to the functional group of L-arginine, the natural substrate for NO-synthase. In a previous paper, we have shown that MG reduced endothelium-dependent, but not endothelium-independent relaxations of the rabbit aorta *in vitro* (Sorrentino *et al.*, 1993).

In this study we describe the effect of acute intravenous administration of MG on systemic blood pressure in urethane-anaesthetized rats.

Methods

Male Wistar rats were obtained from Charles River Italia. Upon arrival the rats were housed in an environment with controlled temperature (21-24°C) and lighting (12:12 h light-darkness cycle). Standard laboratory chow and drinking water were provided *ad libitum*. A period of seven days was allowed for acclimatization of the rats before any experimental manipulation was undertaken. At the time of the experiments, the body weight ranged from 200 to 300 g.

A tracheotomy was performed after urethane anaesthesia (1 g kg^{-1}, i.p.). A polyethylene cannula (PE-50) was placed in the internal jugular vein for administration of drugs. A PE-50 catheter was inserted into the left carotid artery and connected to a Bentley 800 Trantec (Basile, Comerio, Italy) for blood pressure monitoring. The lines were filled with heparinized saline (10 units ml^{-1}) to maintain patency. Blood pressure was recorded by a Thermal Arraycorder WR 7400 (Graphtec, Tokyo). After surgery, animals were divided into two groups: normal saline-treated rats and hexamethonium (5 mg kg^{-1}, i.v.)-treated rats. After 30 min of stabilization, MG was administered i.v. at cumulative doses (1, 3, 10 and 30 mg kg^{-1}) with 2 min intervals. At 5 min after the last MG injection, cumulative doses of L-arginine or D-arginine were administered (30 and 150 mg kg^{-1}, i.v.) with an interval of 2 min between injections. To evaluate the preventive and stereospecific effect of L-arginine on the increase in blood pressure induced by MG, the aminoacid or its enantiomer (D) was administered 2 min before MG injection.

[1] Author for correspondence.

Drugs

L-Arginine and D-arginine methylguanidine, hexamethonium, urethane were purchased from Sigma Chemical Co. Italy. All drugs were dissolved in normal saline (NaCl 0.9% w v^{-1}) and prepared daily.

Statistics

Results are expressed as mean ± s.e.mean of mean arterial blood pressure (MABP) of number (n) of experiments. Statistical comparisons were carried out by using analysis of variance (ANOVA, two-way) and Bonferroni multiple comparisons test. Results were considered significant at a P value <0.05.

Results

The MABP of anaesthetized rats was 102 ± 1 mmHg ($n = 50$) with an heart rate (HR) of 385 ± 13 beats min^{-1}. In animals treated with the ganglionic blocking agent, hexamethonium, blood pressure was (within 2 min) reduced to 71 ± 2 mmHg ($n = 36$) and HR to 373 ± 20 beats min^{-1} reaching a plateau of 87 ± 3 mmHg and an HR 401 ± 16 beats min^{-1} within 25 min.

Effect of MG on MABP

Cumulative bolus injections of MG (1, 3, 10 and 30 mg kg^{-1}, i.v.) induced a dose-related increase in MABP ($P<0.01$, $n = 12$; Figures 1 and 2). The increase in MABP induced by MG was rapid in onset, reaching a plateau within 2 min without any significant change in heart rate (406 ± 31 beats min^{-1}). The hypertensive effect of MG (30 mg kg^{-1}, i.v.), lasted for about 1 h (53 ± 10 min). Administration of cumulative doses of L-arginine (30 and 150 mg kg^{-1}, i.v.), which had no direct effect on blood pressure, significantly ($P<0.05$ and $P<0.01$ respectively; $n = 6$) reversed the increase in MABP induced by MG in a dose-dependent manner (Figure 3a). In contrast, D-arginine did not reverse the pressor effect elicited by MG ($P>0.05$; $n = 6$; Figure 3a).

Pretreatment of rats with L-arginine (150 mg kg^{-1}, i.v.) or vehicle (control) 2 min before MG, did not significantly modify MABP and HR (L-arginine: 97 ± 3 mmHg and 399 ± 23 beats min^{-1}, $n = 4$; D-arginine: 98 ± 4 mmHg and 389 ± 38 beats min^{-1}, $n = 4$; vehicle 102 ± 2 mmHg and 385 ± 42 beats min^{-1}, $n = 4$). In these experiments, the time-course of the MG-induced increase of MABP was monitored for 30 min. Pretreatment of rats with L-arginine significantly ($P<0.001$, versus normal saline; $n = 4$) prevented the pressor effect of MG (30 mg kg^{-1}, i.v.; Figure 4a). In contrast, pretreatment of rats with D-arginine did not affect the degree of the pressor response caused by the subsequent injection of MG ($P>0.05$, $n = 4$). Thus, the rise in MABP caused by MG in rats pretreated with D-arginine was significantly greater than the one caused by MG in rats pretreated with L-arginine ($P<0.001$, $n = 4$; Figure 4a).

Effect of MG on MABP in hexamethonium-treated rats

Hexamethonium (5 mg kg^{-1}, i.v.) pretreatment did not modify the changes in MABP caused by MG, although a reduction of basal MABP after hexamethonium treatment was observed. Indeed, in these animals cumulative bolus injections of MG (1, 3, 10 and 30 mg kg^{-1}, i.v.) induced a dose-related increase in MABP ($P<0.01$, $n = 12$; Figure 2). As in rats, not treated with hexamethonium, L-arginine (30 and 150 mg kg^{-1}, i.v.) significantly reversed the pressor effect of MG ($P<0.05$ and $P<0.01$ respectively, $n = 6$; Figure 3b), while D-arginine was ineffective ($P>0.05$, $n = 6$; Figure 3b). The duration of the increase in MABP elicited by MG (30 mg kg^{-1}, i.v.) in hexamethonium-treated rats was significantly longer (183 ± 19 min; $P<0.01$; $n = 4$) than in normal rats.

Also in hexamethonium-treated rats, L-arginine, D-arginine (150 mg kg^{-1}, i.v.) or vehicle administration did not significantly modify MABP and HR (L-arginine: 90 ± 5 mmHg and 391 ± 15 beats min^{-1}, $n = 6$; D-arginine: 89 ± 4 mmHg and 380 ± 24 beats min^{-1}, $n = 6$; vehicle 88 ± 7 mmHg and 387 ± 13 beats min^{-1}, $n = 6$). The subsequent (2 min) injection of MG (30 mg kg^{-1}, i.v.) caused a pressor effect which was similar to the one seen in rats not

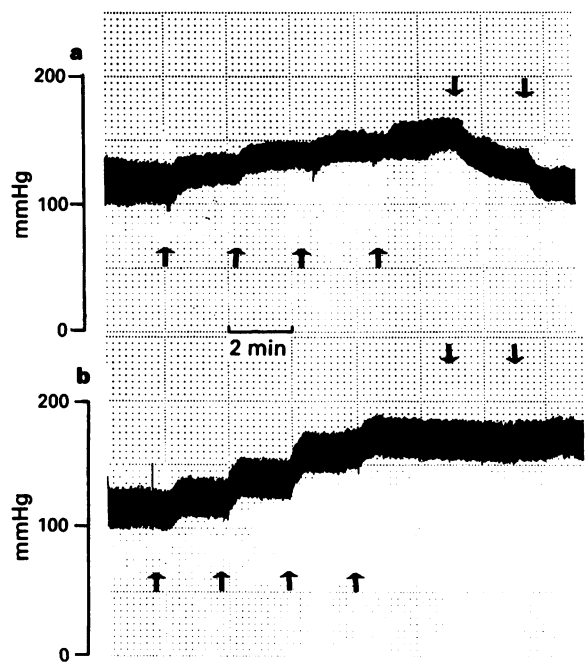

Figure 1 Experimental records illustrating the dose-dependent increase in blood pressure to methylguanidine (MG) and its reversal by L-arginine but not D-arginine. Cumulative administration of MG (1, 3, 10, 30 mg kg^{-1}, i.v.; arrows pointing upwards) in anaesthetized rats followed by L-arginine (30, 150 mg kg^{-1}, i.v. (a), arrows pointing downwards) or D-arginine (30, 150 mg kg^{-1}, i.v.; (b), arrows pointing downwards).

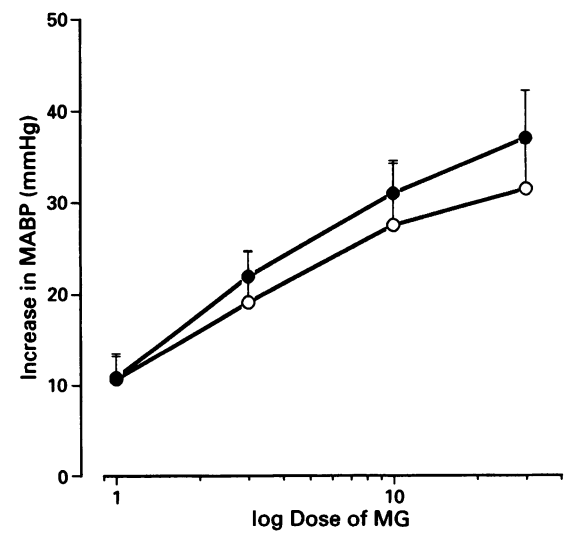

Figure 2 Dose-dependent increase of mean arterial blood pressure (MABP) induced by methylguanidine (MG, 1, 3, 10, 30 mg kg^{-1}, i.v.) in normal rats (○) and in rats treated with hexamethonium (5 mg kg^{-1}, i.v.; ●). Results are expressed as mean ± s.e.mean of 12 rats for both normal and hexamethonium-treated animals. There is no significant difference between normal saline and hexamethonium-treated rats ($P>0.05$).

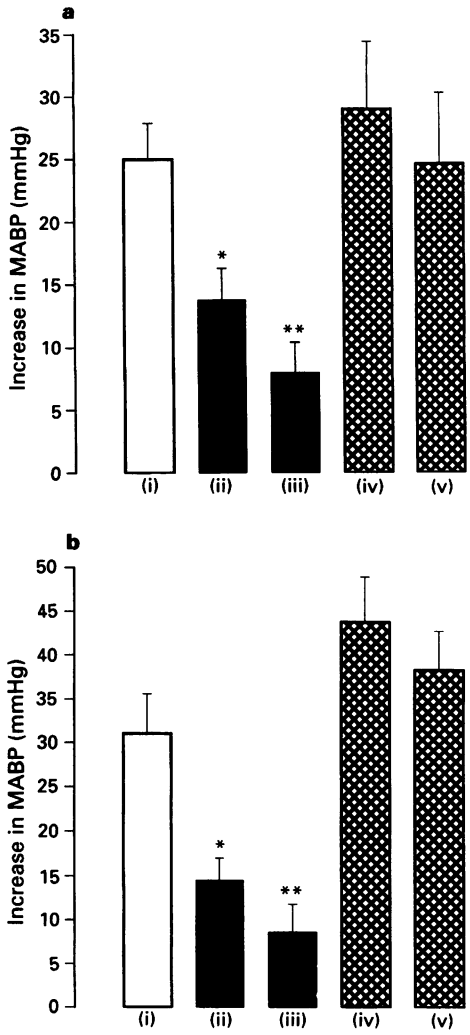

Figure 3 L-Arginine 30 (ii) and 150 (iii) mg kg^{-1}, i.v., but not D-arginine 30 (iv) and 150 (v) mg kg^{-1}, i.v., reduced the increase in mean arterial blood pressure (MABP) induced by methylguanidine (i) 30 mg kg^{-1}, i.v., in normal rats (a) and in rats treated with hexamethonium (5 mg kg^{-1}) (b). *$P<0.05$, $n=6$; **$P<0.001$, $n=6$.

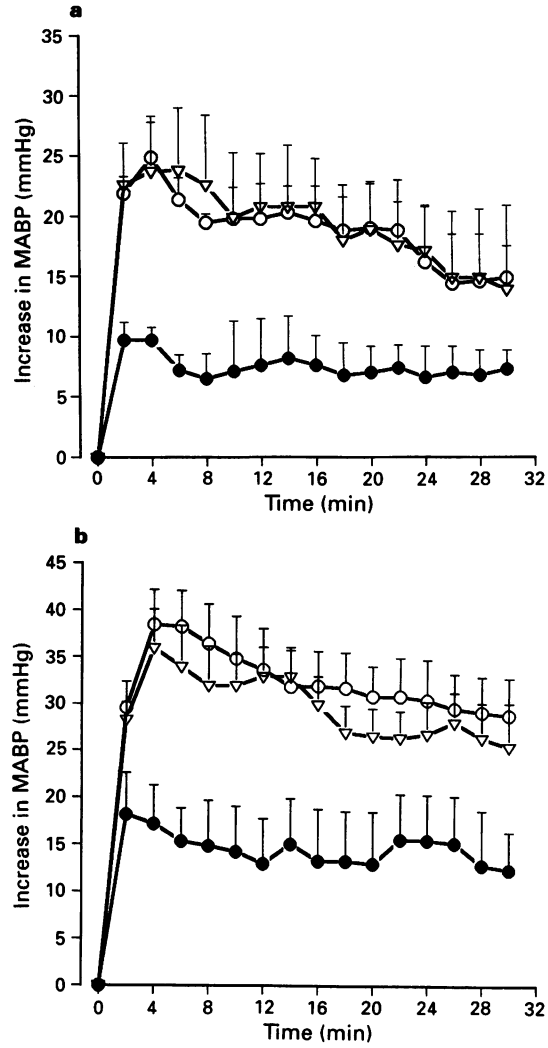

Figure 4 In (a) is shown the effect of L-arginine (150 mg kg^{-1}; $n=4$; ●), D-arginine (150 mg kg^{-1}; $n=4$; Δ) and vehicle ($n=4$; ○) administered i.v. 2 min before methylguanidine (MG) injection (30 mg kg^{-1}, i.v.) in rats. L-Arginine, but not D-arginine, significantly ($P<0.05$) prevents the increase in mean arterial blood pressure (MABP) induced by MG. In (b) the effect of L-arginine (150 mg kg^{-1}; $n=6$; ●), of D-arginine (150 mg kg^{-1}; $n=6$; Δ) and of vehicle ($n=6$; ○) administered i.v. 2 min before MG injection (30 mg kg^{-1} i.v.) in hexamethonium-treated rats is shown. L-Arginine, but not D-arginine, significantly ($P<0.05$) prevents the increase in MABP induced by MG. Results are expressed as mean ± s.e.mean.

treated with hexamethonium. The pretreatment of rats with L-arginine significantly ($P<0.001$, versus normal saline; $n=6$) prevented this pressor effect of MG (Figure 4b). In contrast, pretreatment of rats with D-arginine did not affect the degree of the pressor response caused by the subsequent injection of MG ($P>0.05$, $n=6$; Figure 4b). Thus, the rise in MABP caused by MG in rats pretreated with D-arginine was significantly greater than the one caused by MG in rats pretreated with L-arginine ($P<0.001$, $n=6$; Figure 4b).

Discussion

In this study we analyzed the effect of MG, a product of protein catabolism structurally related to the guanidino group of L-arginine, on MABP and HR in the rat.

We demonstrated that MG caused dose-dependent increases in MABP in the anaesthetized rat. Similar increases in MABP induced by MG were shown in rats treated with hexamethonium.

L-Arginine, the substrate of the enzyme for the NO synthesis, reversed the increases in MABP caused by MG, whereas D-arginine was ineffective. These results suggest that the pressor effect produced by MG is due to inhibition of endothelial NO-synthase activity, confirming our previous *in vitro* study (Sorrentino *et al.*, 1993).

We can exclude the possibility that the increase in MABP induced by MG is due to a direct or indirect action on the peripheral nervous system, as the treatment of rats with hexamethonium, a classical ganglionic blocker, neither modified the effect of MG nor the actions of L-arginine or D-arginine. The response to MG in hexamethonium-treated rats differed only in the duration of the hypertensive response. This last finding could imply that there is a neuronal adjustment of blood pressure following the MG-induced increase in MABP, ruling out rapid metabolism or excretion of MG.

Endogenous MG is normally excreted in the urine. In patients with chronic renal failure, who have a reduced, if any, urine production, plasma MG concentration increases (Giovannetti *et al.*, 1973; Matsumoto *et al.*, 1976; Orita *et al.*, 1981; Yokozawa *et al.*, 1989). This increase is either due to reduced excretion or due to increased production. Indeed, it

has been proposed that in patients with chronic renal failure, an increase in MG production may arise from the conversion of creatinine to MG (Orita *et al.*, 1978; Yokozawa *et al.*, 1990; Yokozawa *et al.*, 1991). Furthermore, Natelson & Sherwin (1979) suggested that urea could be converted to creatine, via canavanine in a supposed 'guanidinic cycle', and subsequently converted in creatinine to be included in the formation of MG.

The plasma concentration of MG in patients with chronic renal failure is still in dispute (Pfiffner & Myers 1926; Giovannetti *et al.*, 1968; Stein *et al.*, 1971; Baker & Marshall 1971; Menichini *et al.*, 1971). Some investigators questioned the different levels of MG that have been found citing methodological difficulties, including the production of MG during assay procedure (Orita *et al.*, 1981). Furthermore, it is noteworthy that MG can accumulate intracellularly, resulting in intracellular concentrations which are 5 to 7 times higher than the ones reported in the plasma (Matsumoto *et al.*, 1976; Orita *et al.*, 1981; Yokozawa *et al.*, 1989). Indeed, MG easily accumulates in cells and in tissues, such as erythrocytes, liver, kidney and muscle, either because of the basic characteristic of molecule and/or the systemic acidosis which occurs in this disease (Kikuchi *et al.*, 1981; Yokozawa *et al.*, 1990). At the moment, it is uncertain to what extent MG accumulates in endothelial cells, but here we have shown that MG, acting as an inhibitor of NO-synthase, could be considered as an uraemic toxin. The doses of MG used in our study may well lead to theoretical plasma concentrations (16–468 $\mu g\ ml^{-1}$) which are higher than the ones reported for rats with chronic renal failure (3 $\mu g\ ml^{-1}$, Orita *et al.*, 1981; Yokozawa *et al.*, 1989), but they are not so high if we consider the accumulation as μg per g of tissue in rats with chronic renal failure estimated by the report of Orita and coworkers (1981) (our dosage: 1–30 $\mu g\ g^{-1}$; rats with chronic renal failure: red blood cells, 24 $\mu g\ g^{-1}$, liver, 28 $\mu g\ g^{-1}$; muscle, 20 $\mu g\ g^{-1}$; colon, 21 $\mu g\ g^{-1}$). Furthermore, our range of doses was similar to the ones used by other investigators. In fact, chronic administration of MG (30 $mg\ kg^{-1}$) in dogs causes a uraemia-like syndrome (Giovannetti *et al.*, 1969), and chronic MG administration in rats (5-50 $mg\ kg^{-1}$) produces a dose-dependent decrease in survival rate (Yokozawa *et al.*, 1989).

In patients with chronic renal failure, other endogenous molecules have been found, such as canavanine, N^G-methy-L-arginine, N^G,N^G-dimethylarginine (asymmetrical) and guanidine, all of which are inhibitors of NO-synthase (Schmidt *et al.*, 1988; Vallance *et al.*, 1992; Sorrentino *et al.*, 1993). We cannot exclude a synergism between MG and these endogenous inhibitors.

These endogenous inhibitors of NO-synthase could be part of the aetiological mechanism which predisposes patients with chronic renal failure to hypertension and impaired host defence. Furthermore our results may lead to an improved understanding of the role of NO-synthase in this pathology, and possibly suggest a novel therapeutic approach.

The authors are grateful to Professor Ludovico Sorrentino for surgical assistance and helpful discussions.

References

AMEZCUA, J.L., PALMER, R.M.J., DE SOUZA, B.M. & MONCADA, S. (1989). Nitric oxide synthesized from L-arginine regulates vascular tone in the conorary circulation of the rabbit. *Br. J. Pharmacol.*, **97**, 1119–1124.

BAKER, L.R.I. & MARSHALL, R.D. (1971). A reinvestigation of methylguanidine concentration in sera from normal and uremic subjects. *Clin. Sci.*, **41**, 563–568.

FÖRSTERMANN, U. (1986). Properties and mechanisms of production and action of endothelium-derived relaxing factor. *J. Cardiovasc. Pharmacol.*, **8**, S45–S51.

GIOVANNETTI, S., BALESTRI, P.L. & BARSOTTI, G. (1973). Methylguanidine in uremia. *Arch. Intern. Med.*, **131**, 709–713.

GIOVANNETTI, S., BIAGINI, M., BALESTRI, P.L., NAVALESI, R., GIAGNONI, P., DE MATTEIS, A., FERRO-MILONE, P. & PERFETTI, C. (1969). Uraemia-like syndrome in dogs chronically intoxicated with methylguanidine and creatinine. *Clin. Sci.*, **36**, 445–452.

GIOVANNETTI, S., CIONI, L., BALESTRI, P.L. & BIAGINI, M. (1968). Evidence that guanidine and some related compounds cause hemolysis in chronic uremia. *Clin. Sci.*, **34**, 141–148.

IYENGAR, R., STUEHR, D.J. & MARLETTA, M.A. (1987). Macrophage synthesis of nitrite, nitrate and N-nitrosamines: precursors and role of the respiratory burst. *Proc. Natl. Acad. Sci. U.S.A.*, **84**, 6369–6373.

JACOBS, M., PLANE, F. & BRUCKDORFER, R. (1990). Inhibition of endothelium-derived nitric oxide and atherosclerosis. In *Nitric Oxide from L-arginine: A Bioregulatory System*. ed. Moncada, S. & Higgs, E.A., pp. 107–114. Amsterdam: Elsevier.

JONES, J.D. & BURNETT, P.C. (1975). Creatinine metabolism and toxicity. *Kidney Int.*, **7**, S294–S298.

KIKUCHI, T., ORITA, Y., ANDO, A., MIKAMI, H., FUJII, M., OKADA, A. & ABE, H. (1981). Liquid-chromatographic determinations of guanido compounds in plasma and erythrocytes of normal person and uraemic patients. *Clin. Chem.*, **27**, 1899–1902.

LINDER, L., KIOWSKI, W., BUHLER, F.R. & LUSCHER, T.F. (1990). Indirect evidence for release of endothelium-derived relaxing factor in human forearm circulation *in vivo*. Blunted response in essential hypertension. *Circulation*, **81**, 1762–1767.

LOWRIE, E.G., LAID, N.M., PARKER, T.F. & SARGENT, S.A. (1981). The effect of emodialysis prescriptions on patients morbidity: Report from the National Cooperative Dialysis Study. *N. Engl. J. Med.*, **305**, 1176–1181.

MATSUMOTO, M., KISHIKAWA, H. & MORI, A. (1976). Guanido compounds in the sera of uraemic patients and in the sera and brain of experimental uraemic rabbit. *Biochem. Med.*, **16**, 1–8.

MENICHINI, G.C., GONELLA, M., BARSOTTI, G. & GIOVANNETTI, S. (1971). Determination of methylguanidine in serum and urine from normal and uremic subjects. *Experientia*, **27**, 1157–1158.

MONCADA, S., PALMER, R.M.J. & HIGGS, E.A. (1991). Nitric oxide: physiology, pathophysiology and pharmacology. *Pharmacol. Rev.*, **43**, 109–142.

NATELSON, D. & SHERWIN, J.W. (1979). Proposed mechanism for urea nitrogen re-utilization: relationship between urea and proposed guanidine cycles. *Clin. Chem.*, **25**, 1343–1344.

ORITA, Y., ANDO, A., TSUBAKIHARA, Y., MIKAMI, H., KIKUCHI, T. & NAKATA, K. (1981). Tissue and blood cell concentration of methylguanidine in rats and patients with chronic renal failure. *Nephron*, **27**, 35–39.

ORITA, Y., TSUBAKIHARA, Y. & ANDO, A. (1978). The effect of arginine or creatinine administration on the urinary excretion of methylguanidine. *Nephron*, **22**, 328–336.

PALMER, R.M.J., REES, D.D., ASHTON, D.S. & MONCADA, S. (1988). L-Arginine is the physiological precursor for the formation of nitric oxide in endothelium-dependent relaxation. *Biochem. Biophys. Res. Commun.*, **153**, 1251–1256.

PANZA, J.A., QUYYUMI, A.A., BRUSH, J.E. Jr & EPSTEIN, S.E. (1990). Abnormal endothelium-dependent relaxation in patients with essential hypertension. *N. Engl. J. Med.*, **323**, 22–27.

PFIFFNER, J.J. & MYERS, V.C. (1926). Colorimetric estimation of methylguanidine in biological fluids. *Proc. Soc. Exp. Biol. Med.*, **23**, 830–832.

PINTO, A., SORRENTINO, R., SAUTEBIN, L., MIRANDA, L. & SORRENTINO, L. (1992). Identification and partial purification of an endothelium-derived relaxing factor-inhibitor factor(s) in serum of hypertensive pre-eclamptic parturients. In *The Biology of Nitric Oxide: Physiological and Clinical Aspects*. ed. Moncada, S., Marletta, M.A., Hibbs, J.B. Jr & Higgs, E.A. pp. 373–376. London and Chapel Hill: Portland Press.

REES, D.D., PALMER, R.M.J. & MONCADA, S. (1989). Role of endothelium-derived nitric oxide in the regulation of blood pressure. *Proc. Natl. Acad. Sci.*, **86**, 3375–3378.

REES, D.D., PALMER, R.M.J., SCHULZ, R., HODSON, H.F. & MONCADA, S. (1990). Characterization of three inhibitors of endothelial nitric oxide synthase *in vitro* and *in vivo*. *Br. J. Pharmacol.*, **101**, 746–752.

SCHMIDT, H.H.H.W., KLEIN, M.M., NIROOMAND, F. & BÖHME, E. (1988). Is arginine a physiological precursor of endothelium-derived nitric oxide? *Eur. J. Pharmacol.*, **148**, 293–295.

SORRENTINO, R., SORRENTINO, L. & PINTO, A. (1993). Effect of some products of protein catabolism on the endothelium-dependent and -independent relaxation of rabbit thoracic aorta rings. *J. Pharmacol. Exp. Ther.*, **266**, 626–633.

STEIN, I.M., PEREZ, G., JOHNSON, R. & CUMMINGS, N.B. (1971). Serum levels and urinary excretion of methylguanidine in chronic renal failure. *J. Lab. Clin. Med.*, **77**, 1020–1024.

VALLANCE, P., LEONE, A., CALVER, A., COLLIER, J. & MONCADA, S. (1992). Accumulation of an endogenous inhibitor of nitric oxide synthesis in chronic renal failure. *Lancet*, **339**, 572–575.

YOKOZAWA, T., FUJITSUKA, N. & OURA, H. (1989). Variation in the distribution of methylguanidine with the progression of renal failure after methylguanidine loading. *Nephron*, **52**, 347–351.

YOKOZAWA, T., FUJITSUKA, N. & OURA, H. (1990). Production of methylguanidine from creatinine in normal rats and rats with renal failure. *Nephron*, **56**, 249–254.

YOKOZAWA, T., FUJITSUKA, N. & OURA, H. (1991). Studies on the precursor of methylguanidine in rats with renal failure. *Nephron*, **58**, 90–94.

(Received December 6, 1994
Revised February 7, 1995
Accepted February 8, 1995)

British Journal of Pharmacology (1995) 115, 515-521

Potentiation of P1075-induced K^+ channel opening by stimulation of adenylate cyclase in rat isolated aorta

Claudia Linde & [1]Ulrich Quast

Department of Pharmacology, Medical Faculty, University of Tübingen, Wilhelmstr. 56, D-72074 Tübingen, Germany

1 The effects of analogues and stimulators of cyclic AMP on the $^{86}Rb^+$efflux-stimulating and binding properties of P1075, an opener of ATP-dependent potassium channels, were studied in rat aortic rings. The increase in $^{86}Rb^+$efflux stimulated by P1075 was taken as a qualitative measure of K^+channel opening.

2 Forskolin, a direct activator of adenylate cyclase, isobutylmethylxanthine (IBMX), a phosphodiesterase inhibitor, and dibutyryl-cyclic AMP (db-cyclic AMP), a membrane permeant cyclic AMP-analogue, relaxed rat aortic rings contracted by noradrenaline with EC_{50} values of 0.06, 2 and 10 μM, respectively.

3 Forskolin, IBMX and db-cyclic AMP produced concentration-dependent increases of the $^{86}Rb^+$efflux induced by P1075 (50 nM) by up to twofold with EC_{50} values of about 0.1, 1.7 and 81 μM. At these concentrations the agents had little effect on the basal rate of $^{86}Rb^+$efflux.

4 The $^{86}Rb^+$efflux produced by P1075 in the presence of the cyclic AMP stimulators was inhibited by glibenclamide, a blocker of ATP-sensitive potassium channels.

5 IBMX (100 μM) induced a leftward shift of the concentration - $^{86}Rb^+$efflux curve of P1075 without increasing the maximum. The enhancements of P1075-stimulated $^{86}Rb^+$efflux produced by combinations of forskolin and IBMX were either additive or less than additive.

6 The protein kinase A inhibitor, H-89, inhibited P1075-stimulated $^{86}Rb^+$efflux in the presence of IBMX significantly more than in the absence of IBMX, suggesting that the effect of increased cyclic AMP levels is mediated by protein kinase A.

7 At high concentrations, forskolin and IBMX slightly increased basal $^{86}Rb^+$efflux and inhibited the tracer efflux induced by P1075.

8 Binding of [^{3}H]-P1075 to rat aortic rings was either unaffected or inhibited by forskolin, IBMX and db-cyclic AMP.

9 This study shows that moderate stimulation of the cyclic AMP system potentiates the K^+channel opening effect of P1075 by activation of protein kinase A. The fact that binding of [^{3}H]-P1075 remains unchanged or is diminished favours the hypothesis that the K^+channel openers activate ATP-dependent K^+channels by an indirect mechanism.

Keywords: Cyclic AMP; potassium channel openers; P1075; dibutyryl-cyclic AMP; isobutylmethylxanthine; forskolin; H-89; glibenclamide; $^{86}Rb^+$efflux; P1075 binding

Introduction

The activity of many ion channels is modulated by phosphorylation (Rosenthal & Schultz, 1987; Levitan, 1994). This holds true also for the ATP-sensitive potassium channel (K_{ATP} channel), a voltage-independent K^+channel which is gated by the ratio of ATP to nucleoside diphosphates like ADP and which couples the metabolic state of the cell to excitability (Ashcroft & Ashcroft, 1990; Edwards & Weston, 1993a). First discovered in the heart (Noma, 1983), K_{ATP} channels form a heterogeneous group; they are found in excitable cells like pancreatic β-cells and the various muscle types (Ashcroft & Ashcroft, 1990; Edwards & Weston, 1993a) and in non-excitable cells like kidney epithelial cells (Wang *et al.*, 1990a,b; Tsuchiya *et al.*, 1992) and follicular cells of the *Xenopus* oocyte (Honoré & Lazdunski, 1991; 1993). In various tissues, particularly in smooth muscle, K_{ATP} channels are opened by a heterogeneous group of organic molecules, the K^+channel openers which induce smooth muscle relaxation (for reviews see Quast, 1993; Edwards & Weston, 1994a). Both the K^+channel opening and the vasorelaxant effects of these compounds are inhibited by the sulphonylurea, glibenclamide, with IC_{50} values ranging from 20 to 200 nM according to the concentration of the agonist used (Quast & Cook 1989; Quast, 1995).

It is generally agreed that adenosine 3':5'-cyclic monophosphate (cyclic AMP)-dependent phosphorylation is necessary to keep K_{ATP} channels in a functional state and to prevent 'run-down' of the channel in various tissues (for review see Ashcroft & Ashcroft, 1990; Nichols & Lederer, 1991; Terzic & Kurachi, 1995; but see de Weille (1992) for the opposite view). There is some controversy whether increased cyclic AMP levels and subsequent phosphorylation by protein kinase A are sufficient to open K_{ATP} channels. In follicular cells of *Xenopus* oocytes where the K_{ATP} channel has a pharmacological profile broadly similar to that in vascular smooth muscle cells, cyclic AMP-dependent phosphorylation is sufficient to open the channel (Honoré & Lazdunski, 1991; 1993). Similarly, in rabbit mesenteric artery cells, protein kinase A activation induced an outward K^+current which was abolished by 10 μM glibenclamide, suggesting that this intervention activated K_{ATP} channels (Quayle *et al.*, 1994). On the other hand, Edwards and colleagues have shown that dephosphorylating conditions like the intracellular application of the specific protein kinase A inhibitor, PKI(6-22)amide, led to the opening of K_{ATP} channels in rat isolated portal vein cells (Edwards *et al.*, 1993) and in insulinoma cells (Edwards & Weston, 1993b).

In an earlier investigation in rat portal vein we had found that the membrane permeant cyclic AMP analogue, dibutyryl-cyclic AMP (db-cyclic AMP) enhanced the $^{86}Rb^+$efflux stimulating effect of the K_{ATP} channel opener, cromakalim, at some agonist concentrations; this effect was considered to be

[1] Author for correspondence.

only of minor importance (Quast, 1987). In the present study in rat isolated aorta the potent pinacidil analogue, P1075, was used as the K^+channel opener (Steinberg *et al.*, 1988; Quast *et al.*, 1993) and the cyclic AMP system was stimulated by db-cyclic AMP, forskolin (a direct stimulator of adenylyl cyclase), and isobutylmethylxanthine (IBMX, a phosphodiesterase inhibitor). Opening of K_{ATP} channels was assessed by measuring the increase in the rate constant of $^{86}Rb^+$efflux from the preparation, a method which is a reliable qualitative measure of the increase in membrane K^+permeability produced by the openers (Quast & Baumlin, 1988; for review see Quast, 1995). A preliminary account of some of the results has been presented to the German Pharmacological Society (Linde *et al.*, 1994).

Methods

Preparation of rat aortic strips

Male Sprague-Dawley rats (350–500g) were decapitated and exsanguinated. The aorta was carefully removed and washed in HEPES-buffered PSS (in mM): NaCl 139, KCl 5, $CaCl_2$ 2.5, $MgCl_2$ 1.2, glucose 11 and HEPES 5, continuously gassed with 95% O_2/5% CO_2 and titrated to pH 7.4 with NaOH at 37°C; for the $^{86}Rb^+$efflux studies the buffer was changed to (in mM): NaCl 120, KCl 5, $CaCl_2$ 2.5, $MgCl_2$ 1.2, glucose 11 and HEPES 20. Adherent fat and the adventitia were removed and the aorta was cut into rings.

Tension studies

The endothelium of aortic rings (4 mm in length) was removed by carefully rubbing with a rough steel pin. The rings were mounted in a thermostatic organ bath for isometric tension recordings at 37°C under continuous gassing and a resting tension of 1 g. After a 60 min equilibration period, tissues were exposed to 1 μM noradrenaline for 5 to 10 min to reach maximum tension and then allowed to relax again. After 1 h, the rings were contracted by 0.1 μM noradrenaline. A maintained contraction was allowed to develop (15 ± 0.2 mN; $n = 36$). Tissues were then exposed to substances of interest using a cumulative (IBMX, forskolin) or non-cumulative (db-cyclic AMP) protocol (cumulative application of db-cyclic AMP resulted in an unusually steep relaxation curve). Complete relaxation was induced by addition of Na-nitroprusside (10 μM). Drug-induced relaxation was corrected for spontaneous decrease in tension by comparison with time-matched solvent controls using dimethylsulphoxide or ethanol (< 0.1%) as the solvent.

$^{86}Rb^+$efflux studies

Aortic rings (15–20 mm in length) with intact endothelium were incubated for 120 min at 37°C in PSS containing $^{86}Rb^+$(5 μCi ml^{-1}). The rings were transferred to thermostatic perfusion chambers and superfused with continuously gassed PSS at a rate of 2.5 ml min^{-1} at 37°C. The perfusate was collected at 2 min intervals and counted for radioactivity as previously described in detail (Quast, 1987). The data were expressed as the efflux rate coefficient (k, in 10^{-2} min^{-1}), which represents the radioactivity released per minute expressed as a percentage of the radioactivity remaining in the tissue. Effects of the openers were assessed by the area under the curve (AUC) of the k *versus* time plot. AUCs were cut out and their weights compared to that of a unit square ($\Delta k = 1 \times 10^{-2}$ min^{-1} × 100 min). At concentrations ≤150 nM, P1075 was applied for 20 min, at concentrations >150 nM for 10 min. Modulation of P1075-stimulated efflux was assessed in a double-pulse protocol by comparison of the AUCs in the presence and absence of modulator (e.g. glibenclamide or cyclic AMP-increasing substances).

Modulation of [^{3}H]-P1075 binding in rat aortic strips

[^{3}H]-P1075 binding was performed in endothelium-denuded rat aortic strips (2–4 mg of wet weight) as described (Bray & Quast, 1992). The tissues were incubated in quadruplet at 37°C for 90 min under light gassing with 95% O_2/5% CO_2 in PSS containing [^{3}H]-P1075 (0.3 nM) and the unlabelled test substance. They were then washed in ice-cold PSS for 1 min, blotted, weighed and assigned to individual vials containing 0.3 ml of Soluence-350. After 2 h at 37°C, the samples were supplemented with 50 μl 1 M HCl and 3 ml Ultima Gold and counted for ^{3}H. Nonspecific binding (≈160 d.p.m. mg^{-1} of tissue wet weight) was determined in the presence of unlabelled P1075 (1 μM) and ranged between 27 and 35% of total binding.

Drugs and solutions

[^{3}H]-P1075 (specific activity, 105 Ci mmol^{-1}) and ^{86}RbCl were obtained from Amersham (Amersham, UK). Dibutyryl-cyclic AMP (db-cyclic AMP) and 3-isobutyl-1-methylxanthine (IBMX) were purchased from Sigma (Deisenhofen, Germany) and were dissolved in dimethylsulphoxide and further diluted into ethanol. Forskolin, a generous gift of Hoechst (Frankfurt, Germany), was dissolved in ethanol; the protein kinase A inhibitor H-89 (N-[(2-(*p*-bromocinnamylamino)ethyl)]-5-isoquinoline sulphonamide) was from Biomol (Hamburg, Germany) and was dissolved in ethanol/dimethylsulphoxide (1 : 1). In all cases, the final concentration of solvents never exceeded 0.5% and was without any pharmacodynamic effect. P1075 was kindly donated by Leo Pharmaceuticals (Ballerup, Denmark) and was dissolved in distilled water. Soluene-350 and Ultima Gold were from Packard (Groningen, The Netherlands).

Calculations and statistics

Results are expressed as mean ± s.e.mean. Concentration-dependencies were fitted to the Hill equation according to the method of linear least squares using the programmes Fig. P (Biosoft, Cambridge, U.K) or the RS/1 (BBN Inc, Cambridge, MA, U.S.A.). Errors in the fitting parameters were estimated using the univariate approximation (Draper & Smith 1981). Differences in tissue responses were assessed using Student's two-tailed unpaired t test. In calculations involving two mean values with standard errors, propagation of errors was taken into account according to Bevington (1969).

Results

Vasorelaxant effects of forskolin, IBMX and db-cyclic AMP

In order to assess the relevant concentration range of the cyclic AMP stimulants and analogues used in this study, concentration-relaxation curves were measured in rat aortic rings precontracted with noradrenaline (0.1 μM). As shown in Figure 1, forskolin was the most potent agent (EC_{50} ≈0.06 μM) followed by IBMX (EC_{50} ≈2 μM) and db-cyclic AMP (EC_{50} ≈10 μM). Relaxation curves were regular in shape with Hill coefficients near unity.

Modulation of P1075-stimulated $^{86}Rb^+$efflux by analogues and stimulators of cyclic AMP

Figure 2a shows traces where stimulation of the tissue by P1075 (50 nM, for 20 min) was followed by a recovery period and a second stimulus; in these control experiments, the second response was similar in magnitude to the first. The other traces in Figure 2 show the effect of forskolin (1 μM), IBMX (100 μM) and db-cyclic AMP (100 μM) superfused prior to the second stimulation with P1075 until to the end of the experiment. All agents increased P1075-stimulated $^{86}Rb^+$efflux.

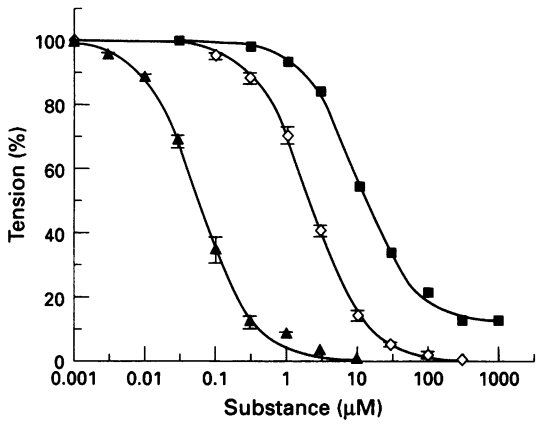

Figure 1 Relaxation of endothelium-denuded rat aortic rings precontracted by noradrenaline (100 nM) by (▲) forskolin, (◇) IBMX and (■) db-cyclic AMP. Hill analysis of the data yielded the following parameter values (forskolin/IBMX/db-cyclic AMP): Midpoints (EC_{50}, μM), 0.057 ± 0.003/1.9 ± 0.1/10 ± 1; maximum relaxations (% inhibition of initial tension), 97 ± 1/98 ± 1/88 ± 3; Hill coefficients, 1.11 ± 0.06/1.13 ± 0.07/1.09 ± 0.09. Data are means ± s.e.mean from 6–10 (forskolin and IBMX) and 4–5 experiments (db-cyclic AMP).

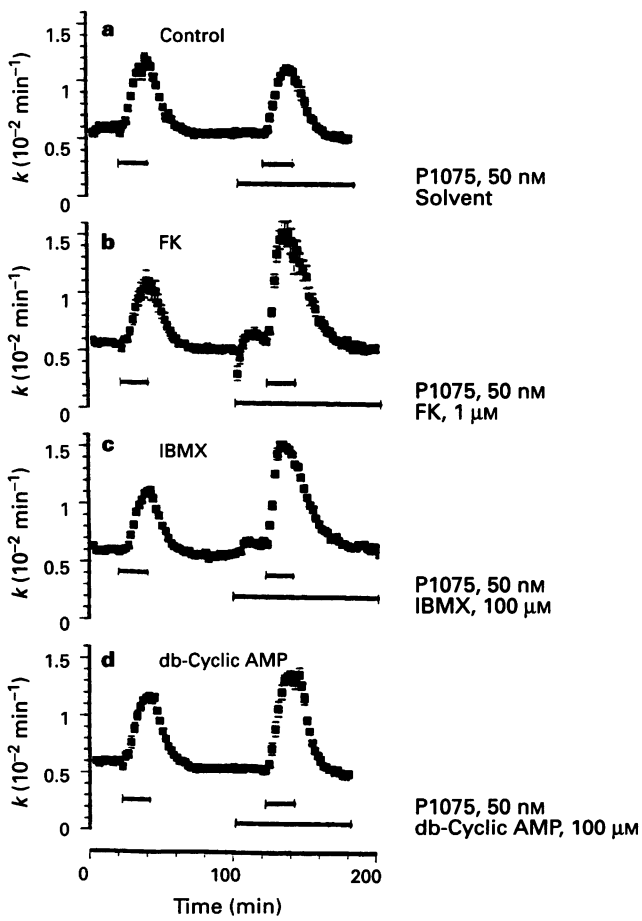

Figure 2 Mean traces showing modulation of P1075-stimulated $^{86}Rb^+$efflux in rat aorta by analogues and stimulators of cyclic AMP. (a) Control: 50 nM P1075 was superfused for 20 min at the times indicated and gave a ratio of the areas under the curve $AUC_2/AUC_1 = 1.03 \pm 0.05$ (9 experiments). (b-d) Effects of (b) forskolin (FK, 1 μM, 6 experiments), (c) IBMX (100 μM, 4 experiments) and (d) db-cyclic AMP (100 μM, 12 experiments) on the rate constant, k, of P1075-stimulated $^{86}Rb^+$efflux. The agents increased the AUC ratio by 101 ± 8% (b), 96 ± 13% (c) and 56 ± 7% (d), respectively. Substances were superfused 20 min before the second application of P1075 until the end of the experiment.

Forskolin and IBMX alone induced a small increase in the rate of basal $^{86}Rb^+$efflux which was well maintained during the application of the compound (Figure 2b and c); in the case of forskolin this was preceded by a transient inhibition. The small increase in basal $^{86}Rb^+$efflux shown here with high concentrations of IBMX and forskolin is also produced by other interventions which massively increase cyclic AMP (Quast *et al.*, unpublished).

The concentration-dependent modulation of P1075-stimulated tracer efflux by forskolin, IBMX and db-cyclic AMP is presented in Figure 3. The maximum effect of the three agents was an approximate doubling of the $^{86}Rb^+$efflux produced by P1075 alone; the midpoints of the concentration-response curves were near 0.1 μM (forskolin), 1.7 μM (IBMX) and 80 μM (db-cyclic AMP). At concentrations at least 20 times higher than the respective EC_{50} values, the stimulatory effects of forskolin and IBMX on P1075-induced tracer efflux were converted into inhibition; with db-cyclic AMP, such concentrations (>2 mM) could not be reached, due to limited solubility of the compound.

Figures 4 and 5 present the glibenclamide-sensitivity of the $^{86}Rb^+$efflux produced by P1075 (50 nM) in the presence of stimulators of the cyclic AMP system. Figure 4a shows control traces of double stimulation experiments with P1075 in the presence of 100 μM db-cyclic AMP. In this case, the response to the second stimulus was slightly smaller than that to the first ($AUC_2/AUC_1 = 95 \pm 3\%$); therefore, the following results were corrected for this difference. Superfusion with glibenclamide (1 μM) 20 min prior to and during the second stimulation by P1075 completely abolished the response (Figure 4b). The concentration-dependence of this effect is shown in Figure 4, inset and yielded an IC_{50} value of 79 ± 5 nM for glibenclamide. Figure 5 shows that glibenclamide (1 μM) essentially abolished the $^{86}Rb^+$efflux response to P1075 (50 nM) also in the presence of maximally effective concentrations of forskolin (1 μM) and IBMX (100 μM). Inspection of the traces also shows that increases in basal flux induced by forskolin and IBMX were little, if at all, affected by glibenclamide.

Combination of forskolin and IBMX and dependence on P1075 concentration

The effects of the combined stimulation of synthesis and inhibition of degradation of cyclic AMP were studied by su-

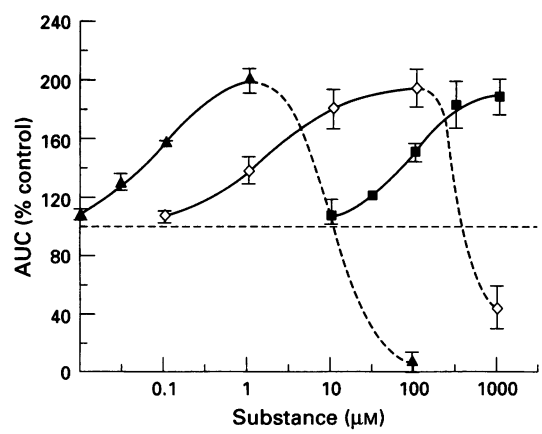

Figure 3 Concentration-dependent modulation of P1075-induced $^{86}Rb^+$efflux by forskolin (▲), IBMX (◇) and db-cyclic AMP (■). The Hill fit of the ascending limbs of the curves yielded the following parameter values (forskolin/IBMX/db-cyclic AMP): Midpoints (EC_{50}, μM): 0.09 ± 0.02/1.67 ± 0.09/81.2 ± 14.2; maximum stimulation (% control): 201 ± 9/197 ± 13.0/191 ± 12; Hill coefficients: 1.10 ± 0.08/0.88 ± 0.03/1.21 ± 0.19. At higher concentrations of forskolin and IBMX, P1075-stimulated tracer efflux was inhibited. Experiments were performed as shown in Figure 2; the data are means ± s.e.mean from 4–6 (forskolin, IBMX) and 4–9 experiments (db-cyclic AMP).

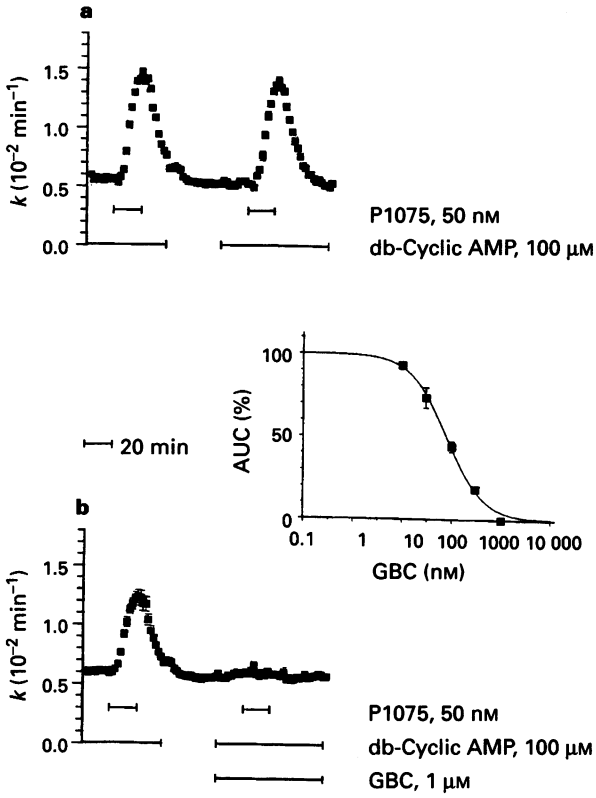

Figure 4 Inhibition by glibenclamide of P1075-stimulated $^{86}Rb^+$ efflux in the presence of 100 μM db-cyclic AMP. (a) Control traces: double stimulation of the preparation by P1075 (50 nM for 20 min) in the presence of db-cyclic AMP. db-cyclic AMP was superfused 20 min prior to, during and after the application of P1075 as indicated; the ratio of the AUCs was 95±3% (4 experiments). (b) Glibenclamide (GBC), 1 μM superfused together with the second application of db-cyclic AMP until to the end of the experiment, completely inhibited the reponse to P1075 in the presence of db-cyclic AMP (6 experiments). Inset: concentration dependence of the inhibition by glibenclamide. The fit of the data to the Hill equation gave a midpoint (IC_{50}) of 79±5 nM and a Hill coefficient of 1.18±0.08 (4 to 6 experiments per point). The data are corrected for the difference of control values ($AUC_2/AUC_1 = 0.95$).

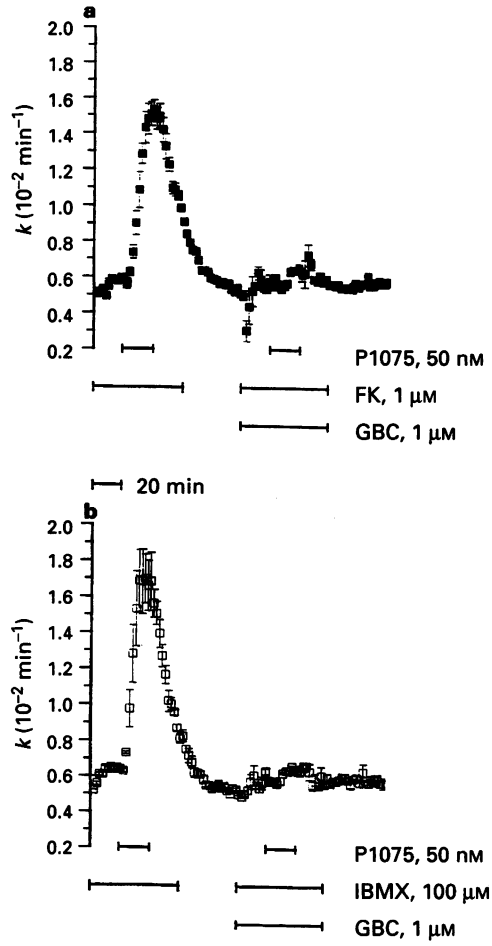

Figure 5 Effects of glibenclamide (GBC, 1 μM) on P1075-stimulated $^{86}Rb^+$efflux in the presence of forskolin (FK, 1 μM, a) and IBMX (100 μM, b). The inhibition amounted to 90±2 and 93±1% of the first stimulus ($n = 4$). Control experiments analogous to those shown in Figure 7, upper trace, indicated that in the absence of glibenclamide, AUC_2 was less than 5% smaller than AUC_1. Note the small increase in $^{86}Rb^+$efflux due to the application of forskolin and IBMX prior to stimulation with P1075.

perfusion of forskolin (1 μM) in the presence of various concentrations of IBMX. The results, expressed as Δ % values, are listed in Table 1. At 0.1 and 1 μM IBMX, the effects of the combination with forskolin (1 μM) were additive, i.e. equal to the sum of the individual contributions. At 1 μM IBMX + 1 μM forskolin, a maximum enhancement was reached which amounted to ≈150 Δ %, i.e. AUC was 2.5 times that of control. At higher concentrations of IBMX (10 and 100 μM), the effects of the combination were smaller than the sum of the individual contributions; they were also smaller than that of

Table 1 Effects of the combination of forskolin (1 μM) and isobutylmethylxanthine (IBMX) on P1075-induced $^{86}Rb^+$ efflux (AUC_2) and on specific binding (SB) of [^{3}H]-P1075[1] in rat aortic rings

Forskolin (μM)	*IBMX (μM)*	*AUC_2 (Δ%)[2]*	*SB (%)*	n
1	–	101±9	107±9	6
–	0.1	7±3	–	6
1	0.1	112±4	–	4
–	1	39±9	94±6	6
1	1	146±14	93±5	6
–	10	72±14	90±3	6
1	10	94±12**	98±5	6
–	100	97±13	98±3	4
1	100	51±4**	96±2	4
–	1000	−53±15	37±1	4

[1] $^{86}Rb^+$ efflux experiments were performed as shown in Figure 2. Binding assays were conducted at 0.3 nM [^{3}H]-P1075 (see Methods section); specific binding under control conditions was 1.52 fmol mg^{-1} tissue wet weight.
[2] AUC_2 values are given as Δ%, i.e. 100 × (AUC_2/AUC_1)−100, where AUC_1 and AUC_2 are the areas under the curve of the k versus time plot produced by P1075 in the absence and presence of the cyclic AMP stimulators, respectively.
**Effect of the combination is significantly smaller than the sum of the individual contributions, $P < 0.01$.

the maximally effective combination of 1 μM IBMX + 1 μM forskolin. At 1 mM IBMX alone, P1075-induced tracer efflux was strongly reduced, probably due to interference of IBMX at this concentration with the binding of P1075 to its drug receptor (Table 1).

So far, all experiments were performed at a P1075 concentration of 50 nM. Hence it was of interest to determine whether the degree of modulation of P1075-induced $^{86}Rb^+$ efflux by cyclic AMP stimulation depended on the concentration of the opener. Figure 6 shows the concentration-dependent stimulation of $^{86}Rb^+$efflux by P1075 in the absence and the presence of 100 μM IBMX. IBMX induced a leftward shift of the concentration-response relationship to P1075 by a factor of two without affecting the maximum response; also the Hill slopes of the curves were not significantly different.

Effect of H-89

In order to investigate whether the effects of increased cyclic AMP levels were mediated by protein kinase A, experiments were conducted with the protein kinase A inhibitor, H-89 (Chijiwa *et al.*, 1990). Up to 1 μM, H-89 had no effect on increased $^{86}Rb^+$efflux induced by P1075 in the presence of 100 μM IBMX (data not shown); at 3 and 10 μM, a substantial inhibition was seen (Figure 7). H-89 also inhibited the P1075-stimulated tracer efflux in the absence of IBMX (Figure 7) and the specific binding of [^{3}H]-P1075 to rat aortic rings (data not shown). However, the inhibition of P1075-induced $^{86}Rb^+$efflux by H-89 was significantly greater in the presence of IBMX than in its absence (Figure 7c).

Specific binding of [^{3}H]-P1075

Specific binding of [^{3}H]-P1075 to rat aortic rings was not affected by forskolin and IBMX at concentrations which enhanced the $^{86}Rb^+$efflux response to P1075 (Table 2); similarly, the combination of both compounds did not affect specific [^{3}H]-P1075 binding at concentrations which potentiated P1075-stimulated tracer efflux (Table 1). At high concentrations, however, both agents inhibited [^{3}H]-P1075 binding (Tables 1 and 2). db-cyclic AMP inhibited [^{3}H]-P1075 binding to 63% of control with a bell-shaped concentration dependence in the concentration-range where P1075-stimulated tracer efflux was potentiated (see Table 2).

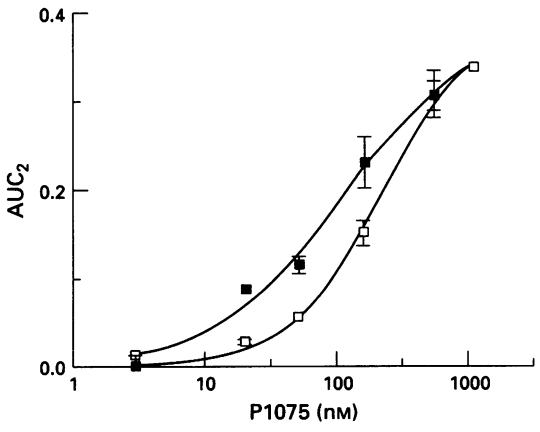

Figure 6 Effect of IBMX (100 μM) on the concentration-dependent $^{86}Rb^+$efflux stimulated by P1075. The efflux response is represented by the AUC values normalized to 10 min application of P1075 (see Methods); values are means ± s.e.mean from 4 to 9 experiments. Hill analysis of the concentration-response curves in the absence (□) and presence (■) of IBMX, respectively, yielded EC_{50} values of 200 ± 40/99 ± 62 nM, maximum values of 0.39 ± 0.03/0.38 ± 0.08 and Hill slopes of 1.26 ± 0.18/0.92 ± 0.29. The EC_{50} values of the two curves are significantly different.

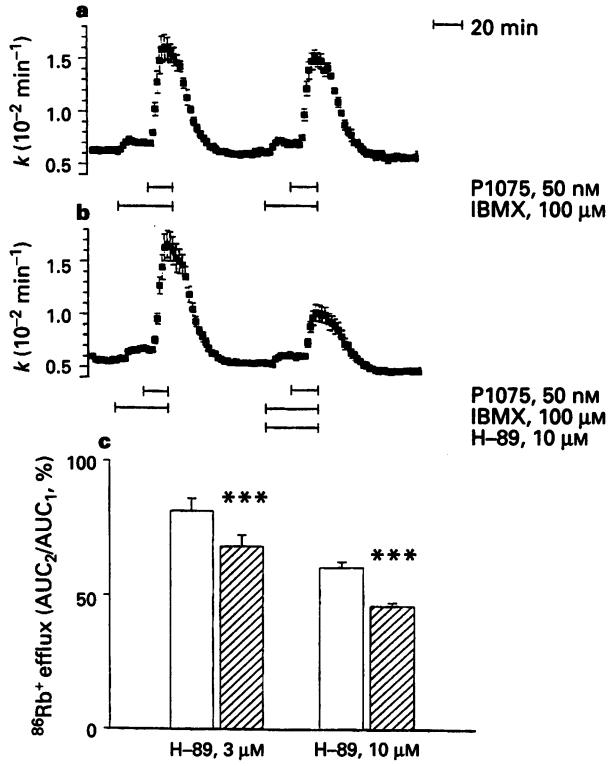

Figure 7 Inhibition of P1075-stimulated $^{86}Rb^+$efflux by H-89 in the presence of IBMX. (a) Double stimulation protocol with P1075 in the presence of IBMX; the ratio AUC_2/AUC_1 was 0.97 ± 0.05 (n = 4). (b) Application of H-89 (10 μM) before the second stimulus reduced this ratio to 0.46 ± 0.01 (n = 5). Note that the small effect of IBMX on the basal rate of $^{86}Rb^+$efflux persisted in the presence of H-89. (c) Comparison of the effects of H-89 on P1075-induced $^{86}Rb^+$efflux in the absence (open columns) and presence (hatched columns) of IBMX (100 μM); the difference is significant (P < 0.005; n = 5–6).

Table 2 Specific binding (% of control) of [^{3}H]-P1075 in presence of analogues and stimulators of cyclic AMP

[μM]	*Forskolin*	*IBMX*	*db-cyclic AMP*
0.1	93 ± 12	–	–
0.3	89 ± 1	–	–
1.0	107 ± 9	94 ± 6	94 ± 6
3.0	97 ± 4	–	79 ± 3
10.0	100 ± 8	90 ± 3	63 ± 3
30.0	81 ± 7	–	88 ± 5
100.0	53 ± 3	98 ± 3	84 ± 4
300.0	–	–	101 ± 6
1000.0	–	37 ± 1	85 ± 6

Values are means ± s.e.mean of 4 to 21 experiments.
Binding assays were conducted at 0.3 nM [^{3}H]-P1075 as described in the Methods section; specific binding under control conditions was 1.52 fmol mg^{-1} tissue wet weight.

Discussion

This study shows that moderate stimulation of the cyclic AMP signalling chain potentiates the $^{86}Rb^+$efflux generating effect of the K_{ATP} channel opener, P1075, whereas excessive stimulation leads to an inhibition. Under conditions which cause potentiation of the P1075-induced tracer efflux, specific binding of [^{3}H]-P1075 to its drug receptor is either not affected or reduced.

Facilitation of P1075-induced K^+ channel opening

The potentiation of P1075-induced tracer efflux by cyclic AMP stimulants was observed at concentrations which are similar to (or at most 10 times higher than) those which induce vasorelaxation. This finding may be of pharmacotherapeutical interest if combinations of cyclic AMP increasing drugs with K^+ channel openers are to be used. The $^{86}Rb^+$ efflux stimulated by P1075 in the presence of increased intracellular levels of cyclic AMP and db-cyclic AMP has two remarkable properties. First, it is inhibited by glibenclamide at relatively low concentrations similar to those which inhibit P1075-induced $^{86}Rb^+$ efflux in the absence of cyclic AMP stimulation (Quast & Cook, 1989; Quast, 1995). This suggests that the P1075-induced $^{86}Rb^+$ efflux also in the presence of cyclic AMP stimulation is passing entirely through K_{ATP} channels. Second, the facilitatory effect of increased cyclic AMP levels on P1075-induced $^{86}Rb^+$ efflux is more pronounced at lower concentrations of the opener, the effect disappears at saturating levels of the opener such that the maximum P1075-induced $^{86}Rb^+$ efflux is not increased (Figure 6). Hence, in rat aorta, increased cyclic AMP levels seemingly sensitize the system for the K_{ATP} channel opener. These results also suggest that this sensitization does not involve an increase in the number of channels that can be activated by P1075 at maximally effective concentrations nor does it involve modifications of the channel that lead to the permeation of more Rb^+ ions per channel per unit time. Since we have observed that low concentrations of forskolin also augment the $^{86}Rb^+$ efflux induced by the K_{ATP} channel opener, cromakalim (Quast *et al.*, unpublished), it appears that increased cyclic AMP levels sensitize the pathway by which the chemically different classes of openers activate the K_{ATP} channel in rat aorta.

Reversal of stimulation by high concentrations of forskolin and IBMX

The enhancement of P1075-induced $^{86}Rb^+$ efflux by the combination of forskolin and IBMX was additive at low concentrations; at higher concentrations it was less than additive and lower than the maximum effect, thus showing a bell-shaped concentration-dependence. This result requires further investigation.

At very high concentrations, forskolin and IBMX inhibited P1075-stimulated $^{86}Rb^+$ efflux. In the case of IBMX, this inhibition (to $\approx$50% of control at 1000 μM) is quantitatively explained by the inhibition of binding of P1075 to its drug receptor. The almost complete inhibition of P1075-induced tracer efflux observed at 100 μM forskolin is in agreement with earlier observations where cromakalim was used as the agonist (Quast, 1988; Quast *et al.*, 1994). The binding data show that this inhibition cannot be attributed solely to interference with P1075 binding; in addition one has to take into consideration that forskolin inhibits several ion channels, including voltage-dependent K^+ channels, by an action unrelated to stimulation of adenylyl cyclase (Laurenza *et al.*, 1989).

Involvement of protein kinase A

There are several ion channels which are activated directly by cyclic nucleotides (Latorre *et al.*, 1991; Matthews, 1991); in most cases, however, the effects of cyclic nucleotides on ion channels are mediated by protein phosphorylation (see Introduction). In order to distinguish between these possibilities we have used the potent (K_i = 48 nM), relatively selective and membrane permeant, protein kinase A inhibitor H-89 (Chijiwa *et al.*, 1990). This inhibitor is competitive with ATP (Chijiwa *et al.*, 1990); thus, for inhibition of protein kinase A to occur, the ratio of inhibitor concentration over K_i must exceed the ratio of ATP concentration over K_m(ATP), the Michaelis constant of the kinase for ATP. Since the ATP concentration in vascular smooth muscle is approximately 2 mM (Butler & Davies, 1980) and K_m (ATP) = 8 μM (Whitehouse *et al.*, 1983), the concentration of H-89 in the cell should exceed the μM range in order to obtain inhibition of protein kinase A. Indeed, we found that H-89 was inactive up to 1 μM and only at 3 and 10 μM, was substantial inhibition of P1075-stimulated $^{86}Rb^+$ efflux in presence of 100 μM IBMX observed. At these concentrations, however, H-89 loses its selectivity for protein kinase A (Chijiwa *et al.*, 1990); in agreement with this point we observed that H-89 also inhibited binding of [^{3}H]-P1075 and, consequently, P1075-induced efflux in the absence of IBMX. However, these effects of H-89 were significantly smaller than the reduction of P1075-induced efflux in the presence of IBMX. This strongly suggests that the potentiating effect of increased cyclic AMP levels on P1075-induced $^{86}Rb^+$ efflux is mediated by protein kinase A.

Obviously, this study does not give any indication of the target which is phosphorylated. At present it is not known whether the K_{ATP} channel openers activate the channel by directly binding to it or indirectly by initiating a complex chain of events (see below); hence the results presented here should be interpreted with caution. Indirect mechanisms like a phosphorylation-induced decrease in intracellular Ca^{2+} concentration which is known to favour K_{ATP} channel opener-induced $^{86}Rb^+$ efflux (Coldwell & Howlett, 1988) might also be envisaged. However, the finding that moderate stimulation of cyclic AMP in rat aorta sensitizes the preparation for the K_{ATP} channel opening action of P1075 is in agreement with electrophysiological studies in rabbit mesenteric artery (Quayle *et al.*, 1994) and in follicle-enclosed *Xenopus* oocytes (Honoré & Lazdunski, 1991; 1993); these studies also show that activation of protein kinase A by increased cyclic AMP facilitates K_{ATP} channel opening. However, in rat portal vein it has been found that dephosphorylating conditions open the K_{ATP} channel and that the openers may activate the channel activation by inducing dephosphorylating conditions (Edwards *et al.*, 1993, Edwards & Weston, 1994b). At present there is no convincing explanation for this apparent discrepancy.

Modulation of [^{3}H]-P1075 binding

A surprising finding of this study was the observation that moderate stimulation of cyclic AMP levels, which enhanced P1075-induced K_{ATP} channel opening, left specific [^{3}H]-P1075 binding unchanged (forskolin, IBMX) or reduced binding with a biphasic concentration dependence (db-cyclic AMP). This was quite unexpected since previous experiments had shown an excellent correlation between the potencies of major K_{ATP} channel openers in binding and $^{86}Rb^+$ efflux assays (Bray & Quast, 1992; Quast *et al.*, 1993).

In the case of voltage-dependent Na^+ and dihydropyridine-sensitive Ca^{2+} channels, ligands which induce a certain state of the channel (e.g. open or desensitized) have the highest affinity for the channel in this particular state (Catterall, 1984; Glossmann *et al.*, 1984). Obviously, this is not the case here, where stimulation of cyclic AMP promotes K_{ATP} channel opening but not the binding of the opener. We feel that this tends to support an indirect mechanism of action of the K_{ATP} channel openers where channel opening is some steps further downstream from binding, resembling the hypothesis of Edwards & Weston (1993b) in this aspect. Such a mechanism could also explain apparent discrepancies between the K^+ channel opening and the vasorelaxant properties of these compounds (Quast, 1993). On the other hand, it has recently been shown that the rat cardiac K_{ATP} channel expressed in a kidney epithelial cell line, can be activated by the opener, pinacidil, in isolated inside-out patches (Ashford *et al.*, 1994). This may be considered evidence for a direct mode of action of this compound although it cannot be ruled out that the observed sensitivity to pinacidil may have been conferred to the cloned channel by another protein present in the patch. Undoubtedly, the ongoing effort in channel cloning and expression in combination with the use of electrophysiological and biochemical techniques will soon elucidate the mechanism of action of the K_{ATP} channel openers.

We gratefully acknowledge the expert help of Ms C. Löffler and Mr F. Metzger (Tübingen) with some of the experiments and the preparation of the Figures; fruitful discussions with Drs G. Edwards and A.H. Weston (University of Manchester) are also acknowledged. We thank Amersham for the gift of [3H]-P1075, Hoechst for forskolin and Leo Pharmaceuticals for P1075. This study was supported by Deutsche Forschungsgemeinschaft (grant QU 100/1-1).

References

ASHCROFT, S.J.H. & ASHCROFT, F.M. (1990). Properties and functions of ATP-sensitive K-channels. *Cell. Signal.*, **2**, 197–214.

ASHFORD, M.L.J., BOND, C.T., BLAIR, T.A. & ADELMAN, J.P. (1994). Cloning and functional expression of a rat heart K_{ATP} channel. *Nature*, **370**, 456–459.

BEVINGTON, P.R. (1969). *Data Reduction and Error Analysis for the Physical Sciences*. pp. 55–65 and 92–118. New York: McGraw-Hill.

BRAY, K.M. & QUAST, U. (1992). A specific binding site for K^+channel openers in rat aorta. *J. Biol. Chem.*, **267**, 11689–11692.

BUTLER, T.M. & DAVIES, R.W. (1980). High-energy phosphates in smooth muscle. In *Handbook of Physiology, Section 2: Cardiovascular System, Vascular Smooth Muscle*. ed. Bohr, D.F., Somlyo, A.P. & Sparks, H.V. Vol. 2, pp. 237–252. Bethesda, MD: Am. Physiol. Soc.

CATTERALL, W.A. (1984). The molecular basis of neuronal excitability. *Science*, **223**, 653–661.

CHIJIWA, T., MISHIMA, A., HAGIWARA, M., SANO, M., HAYASHI, K., INOUE, T., NAITO, K., TOSHIOKA, T. & HIDAKA, H. (1990). Inhibition of forskolin-induced neurite outgrowth and protein phosphorylation by a newly synthesized selective inhibitor of cyclic AMP-dependent protein kinase, *N*-[2-(p-bromocinnamylamino)ethyl]-5-isoquinolinesulfonamide (H-89), of PC12D pheochromocytoma cells. *J. Biol. Chem.*, **265**, 5267–5272.

COLDWELL, M.C. & HOWLETT, D.R. (1988). Potassium efflux enhancement by cromakalim (BRL 34915) in rabbit mesenteric artery: an indirect effect independent of calcium? *Biochem. Pharmacol.*, **37**, 4105–4110.

DE WEILLE, J.R. (1992). Modulation of ATP sensitive potassium channels. *Cardiovasc. Res.*, **26**, 1017–1020.

DRAPER, N.B. & SMITH, H. (1981). *Applied Regression Analysis*. pp. 85–96, 458–517. New York: Wiley.

EDWARDS, G., IBBOTSON, T. & WESTON, A.H. (1993). Levcromakalim may induce a voltage-independent K^+-current in rat portal veins by modifying the gating properties of the delayed rectifier. *Br. J. Pharmacol.*, **110**, 1037–1048.

EDWARDS, G. & WESTON, A.H. (1993a). The pharmacology of ATP-sensitive K^+channels. *Annu. Rev. Pharmacol. Toxicol.*, **33**, 597–637.

EDWARDS, G. & WESTON, A.H. (1993b). Induction of a glibenclamide-sensitive K-current by modification of a delayed rectifier channel in rat portal vein. *Br. J. Pharmacol.*, **110**, 1280–1281.

EDWARDS, G. & WESTON, A.H. (1994a). Effect of potassium channel modulating drugs on isolated smooth muscle. In *Handbook of Experimental Pharmacology Volume 111*. ed. Szerkeres, L. & Gy Papp, J. pp. 469–531. Heidelberg: Springer.

EDWARDS, G. & WESTON, A.H. (1994b). K_{ATP} - fact or artefact? New thoughts on the mode of action of the potassium channel openers. *Cardiovasc. Res.*, **28**, 735–737.

GLOSSMANN, H., FERRY, D.R., GOLL, A. & ROMBUSCH, M. (1984). Molecular pharmacology of the calcium channel: Evidence for subtypes, multiple drug-receptor sites, channel subunits, and the development of a radioiodinated, 1,4-dihydropyridine calcium channel label, [^{125}I]iodipine. *J. Cardiovasc. Pharmacol.*, **6**, Suppl. 6, S608–S621.

HONORÉ, E. & LAZDUNSKI, M. (1991). Hormone-regulated K^+channels in follicle enclosed oocytes are activated by vasorelaxing K^+channel openers and blocked by antidiabetic sulfonylureas. *Proc. Natl. Acad. Sci. U.S.A.*, **88**, 5438–5442.

HONORÉ, E. & LAZDUNSKI, M. (1993). Single-channel properties and regulation of pinacidil/glibenclamide-sensitive K^+channels in follicular cells from Xenopus oocytes. *Pflügers Arch.*, **424**, 113–121.

LATORRE, R., BACIGALUPO, J., DELGADO, R. & LABARCA, P. (1991). Four cases of direct ion channel gating by cyclic nucleotides. *J. Bioenerg. Biomembr.*, **23**, 577–597.

LAURENZA, A., MCHUGH SUTKOWSKI, E. & SEAMON, K.B. (1989). Forskolin: a specific stimulator of adenylyl cyclase or a diterpene with multiple sites of action? *Trends Pharmacol. Sci.*, **10**, 442–447.

LEVITAN, I.B. (1994). Modulation of ion channels by protein phosphorylation and dephosphorylation. *Annu. Rev. Physiol.*, **56**, 193–212.

LINDE, C., LÖFFLER, C. & QUAST, U. (1994). Phosphorylation: Effects on K^+channel opening and K^+channel openers in rat isolated aorta. *Naunyn Schmied. Arch. Pharmacol.*, **349**, R47.

MATTHEWS, G. (1991). Ion channels that are directly activated by cyclic nucleotides. *Trends Pharmacol. Sci.*, **12**, 245–247.

NICHOLS, C.G. & LEDERER, W.K. (1991). Adenosine triphosphate-sensitive potassium channels in the cardiovascular system. *Am. J. Physiol.*, **261**, H1675–H1686.

NOMA, A. (1983). ATP-regulated K^+channels in cardiac muscle. *Nature*, **305**, 147–148.

QUAST, U. (1987). Effect of the K^+efflux stimulating vasodilator BRL34915 on $^{86}Rb^+$efflux and spontaneous activity in guinea-pig portal vein. *Br. J. Pharmacol.*, **91**, 569–578.

QUAST, U. (1988). Inhibition of the effects of the K^+channel stimulator cromakalim (BRL 34915) in vascular smooth muscle by glibenclaminde and forskolin. *Naunyn-Schmied. Arch. Pharmacol.*, **337**, R72.

QUAST, U. (1993). Do the K^+channel openers relax smooth muscle by opening K^+channels? *Trends Pharmacol. Sci.*, **14**, 332–336.

QUAST, U. (1995). Effects of potassium channel activators in isolated blood vessels. In *Potassium Channels and their Modulators*. ed. Evans, J.M., Hamilton, T.C., Longman, S.D. & Stamp, G. Prentice Hall: Ellis Horwood, (in press).

QUAST, U. & BAUMLIN, Y. (1988). Comparison of the effluxes of $^{42}K^+$and $^{86}Rb^+$elicited by cromakalim (BRL34915) in tonic and phasic vascular tissue. *Naunyn-Schmied. Arch. Pharmacol.*, **338**, 319–326.

QUAST, U., BAUMLIN, Y. & DOSOGNE, J. (1994). Forskolin blocks and opens K^+channels in rat isolated aorta. *Can. J. Physiol. Pharmacol.*, **72**, Suppl. 1, 518.

QUAST, U., BRAY, K.M., ANDRES, H., MANLEY, P.W., BAUMLIN, Y. & DOSOGNE, J. (1993). Binding of the K^+channel opener [3H]-P1075 in rat isolated aorta: relationship to functional effects of openers and blockers. *Mol. Pharmacol.*, **43**, 474–481.

QUAST, U. & COOK, N.S. (1989). *In vitro* and *in vivo* comparison of two K^+channel openers, diazoxide and cromakalim, and their inhibition by glibenclamide. *J. Pharmacol. Exp. Ther.*, **250**, 261–270.

QUAYLE, J.M., BONEV, A.D., BRAYDEN, J.E. & NELSON, M.T. (1994). Calcitonin gene-related peptide activated ATP-sensitive K^+currents in rabbit arterial smooth muscle via protein kinase. *Am. J. Physiol.*, **475**, 9–13.

ROSENTHAL, W. & SCHULTZ, G. (1987). Modulations of voltage-dependent ion channels by extracellular signals. *Trends Pharmacol. Sci.*, **8**, 351–354.

STEINBERG, M.I., ERTEL, P., SMALLWOOD, J.K., WYSS, V. & ZIMMERMAN, K. (1988). The relation between vascular relaxant and cardiac electrophysiological effects of pinacidil. *J. Cardiovasc. Pharmacol.*, **12**, Suppl. 2, S30–S40.

TERZIC, A. & KURACHI, Y. (1995). Potassium channel opening drugs activate cardiac ATP-sensitive K^+channels through distinct molecular mechanisms: A novel basis for a functional classification. *Trends Pharmacol. Sci.*, (in press).

TSUCHIYA, K., WANG, W., GIEBISCH, G. & WELLING, P.A. (1992). ATP is a coupling modulator of parallel Na, K-ATPase-K-channel activity in the renal proximal tubule. *Proc. Natl. Acad. Sci. U.S.A.*, **89**, 6418–6422.

WANG, W., SCHWAB, A. & GIEBISCH, G. (1990a). Regulation of small-conductance K^+channel in apical membrane of rat cortical collecting tubule. *Am. J. Physiol.*, **259**, F494–F502.

WANG, W., WHITE, S., GEIBEL, J. & GIEBISCH, G. (1990b). A potassium channel in the apical membrane of rabbit thick ascending limb of Henle's loop. *Am. J. Physiol.*, **258**, F244–F253.

WHITEHOUSE, S., FERAMISCO, J.R., CASNELLIE, J.E., KREBS, E.G. & WALSH, D.A. (1983). Studies on the kinetic mechanism of the catalytic subunit of the cAMP-dependent protein kinase. *J. Biol. Chem.*, **258**, 3693–3701.

(Received December 5, 1994
Revised February 10, 1995
Accepted February 16, 1995)

British Journal of Pharmacology (1995) 115, 522–526

All-or-none augmentation of Ca^{2+} sensitivity in α-toxin-permeabilized single smooth muscle cells from guinea-pig taenia caecum

[1]Mitsuo Mita & Takao Hashimoto

Department of Pharmacology, Meiji College of Pharmacy, 1-35-23 Nozawa, Setagaya-Ku, Tokyo 154, Japan

1 Isolated smooth muscle cells from guinea-pig taenia caecum were permeabilized by use of *Staphylococcus aureus* α-toxin, and the sarcoplasmic reticulum Ca^{2+} store was depleted by exposure to 0.1 μM A23187.

2 Shortening of α-toxin-permeabilized single smooth muscle cells was induced by increasing free Ca^{2+} but was not induced by 0.2 μM free Ca^{2+}.

3 Shortening of the permeabilized cells was caused by application of acetylcholine (ACh) with free Ca^{2+} concentration held at 0.2 μM. Permeabilized smooth muscle cells responded to 0.3 μM or 1 μM ACh with 0.2 μM Ca^{2+} with maximal shortening. The concentration-response relationship to ACh had a very steep slope and the cell shortening appeared to be an all-or-none response rather than a graded response, as was the shortening of intact cells to ACh.

4 The shortening of permeabilized cells was also induced by application of guanosine 5'-triphosphate (GTP) with 0.2 μM free Ca^{2+}, showing an all-or-none response. The threshold concentration of GTP that induced an all-or-none response was between 10 μM and 30 μM.

5 These results suggest that Ca^{2+} sensitivity is augmented by stimulation of the muscarinic receptor or GTP-binding protein(s) in an all-or-none manner. It seems probable that this contributes to the all-or-none response to ACh in intact smooth muscle cells.

Keywords: Ca^{2+} sensitivity; smooth muscle cells; all-or-none response; permeabilization; α-toxin; acetylcholine; muscarinic receptor; GTP-binding protein; taenia caecum

Introduction

We reported previously that isolated single smooth muscle cells from guinea-pig taenia caecum showed an all-or-none response to acetylcholine (ACh) (Mita & Uchida, 1987; 1988; 1991; Mita *et al.*, 1988; 1993). These are the first smooth muscle cells to demonstrate a large and prompt all-or-none response repeatedly and with the same dose-response relationship. Moreover, we found that isolated single smooth muscle cells from a different organ, the fundus of guinea-pig stomach, also showed an all-or-none response to ACh (Mita *et al.*, 1993).

Ca^{2+} plays a central role in the contraction of smooth muscle induced by neurotransmitters and hormones. The rise in cytoplasmic free Ca^{2+} triggers smooth muscle contraction by activating myosin light chain kinase. However, the relationship between cytosolic Ca^{2+} concentration and the contraction level is not always constant (Bradley & Morgan, 1987; Karaki *et al.*, 1988; Karaki, 1989), suggesting the existence of additional mechanisms through which agonists can modulate the sensitivity of the contractile apparatus to Ca^{2+}. Augmentation of Ca^{2+} sensitivity in receptor-operated contraction has been studied in α-toxin-permeabilized whole smooth muscles (Nishimura *et al.*, 1988; Kitazawa *et al.*, 1989; 1991). This mechanism was shown to be mediated by GTP-binding protein(s) on the basis of the observation that GTP or GTPγS lowers the Ca^{2+} concentration necessary for the contraction. We demonstrated previously that the shortening of α-toxin-permeabilized single smooth muscle cells from two different organs, the fundus of the guinea-pig stomach and the guinea-pig taenia caecum, was induced by increasing the concentration of free Ca^{2+} and the cells responded to either 0.3 μM or 0.6 μM Ca^{2+} with maximal shortening, showing an all-or-none response, but did not respond to 0.2 μM Ca^{2+} or lower (Ono *et al.*, 1992; Oishi *et al.*, 1992; Mita *et al.*, 1994). This result suggested that the threshold concentration of Ca^{2+} for developing cell shortening lies between 0.3 μM and 0.6 μM Ca^{2+}, and α-toxin-permeabilized cells show an all-or-none response as a result of a slight increase in the intracellular free Ca^{2+} level over the threshold concentration. Moreover, the addition of ACh (10 μM) or GTP (100 μM) resulted in a decrease in the concentration of Ca^{2+} required to trigger a threshold response from 0.6 μM to 0.2 μM and from 0.3 μM to 0.1 μM, but the concentration of Ca^{2+} required to trigger the maximal shortening was not changed (Ono *et al.*, 1992; Oishi *et al.*, 1992; Mita *et al.*, 1994). Therefore, the cell shortening showed a graded response. These results suggested that these permeabilized cells retained their receptor function, and that augmentation of Ca^{2+} sensitivity was induced by the stimulation of muscarinic receptors with ACh and GTP-binding proteins with GTP. In this paper, in order to elucidate further the mechanisms determining the threshold for the shortening of intact single smooth muscle cells in response to ACh, we studied the relationship between an all-or-none response to ACh and the augmentation of Ca^{2+} sensitivity using the shortening of α-toxin-permeabilized single smooth muscle cells from guinea-pig taenia caecum.

Methods

Cell isolation

Isolated smooth muscle cells from guinea-pig taenia caecum were prepared by the method described previously (Mita & Uchida, 1987). Strips of taenia caecum were minced and incubated with 0.1% collagenase (about 250 u ml^{-1}) in Ca^{2+}-free solution containing 0.2% trypsin inhibitor and 1.0% bovine serum albumin at 37°C for 80 min with gentle stirring.

[1] Author for correspondence.

The suspension of cells was centrifuged at 120 *g* and the precipitate was suspended in Ca^{2+}-free solution. The cells were dispersed by pipetting the suspension several times with a wide-bore pipette. The medium was HEPES-Tyrode solution composed of (mM): NaCl 137, KCl 2.7, $CaCl_2$ 1.8, $MgCl_2$ 1.0, glucose 5.6 and HEPES 4.2, pH 7.4 at 37°C (normal solution). The Ca^{2+}-free solution had the same composition except that $CaCl_2$ was omitted.

Measurement of the shortening of single cells

Shortening of individual isolated smooth muscle cells was measured by the method of Mita & Uchida (1987). The cell suspension was placed on a silicon-coated glass slide with a cover slip, and the cells were perfused continuously with Ca^{2+}-free solution at 30°C. The perfusion fluid was introduced from one side and was blotted off by filter paper from the other side of the slide. The silicon-coated glass slide was placed on a temperature-controlled stage (30°C) of a phase contrast microscope. The shortening of individual cells observed by phase contrast microscopy was recorded on video tape, and the cell length was measured with an ARUGUS-10 Image Analyzer (Hamamatsu Photonics K.K., Japan).

Cell permeabilization

In order to ensure that intact isolated cells did not respond to extracellular Ca^{2+}, individual cells were perfused before permeabilization with the cytosolic substitution solution containing an ascending concentration of free Ca^{2+} buffered at 10 nM to 30 μM. The cytosolic substitution solution was composed of (mM): potassium propionate 114, $MgCl_2$ 4, ATP 4, creatine phosphate 10, EGTA 1, and piperazine-N,N'-*bis*(2-ethanesulphonic acid) (PIPES) 20, (pH 7.1 at 30°C). Free Ca^{2+} concentrations were determined according to the method of Harafuji & Ogawa (1980). The free Ca^{2+} concentration of cytosolic substitution solution with no added Ca^{2+} (Ca^{2+}-free) was estimated to be 2.5 nM. After washing the cells with the Ca^{2+}-free cytosolic substitution solution, the cells were permeabilized by perfusing with the solution containing α-toxin, 10 $\mu g\ ml^{-1}$, and Ca^{2+}, 0.1 μM, for 5 min. After washing the cells with Ca^{2+}-free cytosolic substitution solution for 3 min, permeabilized cells were perfused continuously with Ca^{2+}-free cytosolic substitution solution containing 0.1 μM of the Ca^{2+}-translocator A23187 for 10 min. The permeabilized cells were then perfused with cytosolic substitution solution containing Ca^{2+}, 0.2 μM, and A23187 for 5 min to eliminate the function of sarcoplasmic reticulum Ca^{2+} stores. Itoh *et al.* (1985) previously reported that 0.1 μM A23187 had no effect on the Ca^{2+}-tension relation in saponin-treated skinned muscle tissues of the rabbit mesenteric artery and did not change the resting tension, but inhibited caffeine-induced contractions, suggesting that these effects of A23187 (0.1 μM) may be due to an ability to act selectively on the Ca^{2+} store site and increase the Ca^{2+} leakage from the store. Therefore, with A23187 (0.1 μM) treatment the Ca^{2+} stores will be depleted. The first shortening was evoked by perfusion with cytosolic substitution solution containing increasing concentrations of ACh or GTP with 0.2 μM Ca^{2+} and A23187. After washing with Ca^{2+}-free cytosolic substitution solution plus A23187 for 15 min and cytosolic substitution solution containing 0.2 μM Ca^{2+} and A23187 for 5 min, the second cell shortening in response to ACh or GTP in the presence of 0.2 μM Ca^{2+} and A23187 was determined. After washing with Ca^{2+}-free cytosolic substitution solution plus A23187 for 20 min, the effectiveness of permeabilization was determined by exposing the cells to the cytosolic substitution solution containing free Ca^{2+} buffered at 1 μM.

Chemicals

Staphylococcus aureus α-toxin (Ono *et al.*, 1992) was kindly provided by Drs M.K. Uchida and K. Oishi (Department of Molecular Pharmacology, Meiji College of Pharmacy). Collagenase (Type I), soybean trypsin inhibitor (Type II-S), creatine phosphate and adenosine 5'-triphosphate dipotassium (ATP) were purchased from Sigma Chemical Co. (St. Louis, MO, U.S.A.). Guanosine 5'-triphosphate disodium salt (GTP) was from Boehringer Mannheim. Bovine serum albumin (Fraction V) and potassium propionate were from Nakarai Tesque (Kyoto, Japan). Acetylcholine (Ovisot) was from Daiichi Pharmaceutical Co., Ltd. (Tokyo, Japan). N-2-hydroxyethylpiperazine-N'-2-ethanesulphonic acid (HEPES), piperazine-N,N'-*bis*(2-ethanesulphonic acid) (PIPES), O,O'-*bis*(2-aminoethyl)ethyleneglycol-N,N,N',N'-tetraacetic acid (EGTA) and inositol 1,4,5-trisphosphate (IP_3) were from Dojindo Laboratories (Kumamoto, Japan). All other chemicals were of reagent grade.

Results

Figure 1 shows the effect of A23187 on inositol 1,4,5-trisphosphate (IP_3)-induced shortening of α-toxin-permeabilized smooth muscle cells. The decrease in the length of the cells induced by 10 μM IP_3 with free Ca^{2+} concentration held at 0.2 μM was 15.5±1.5% (n=3). However, the shortening of permeabilized cells was not induced by 0.2 μM Ca^{2+} alone (Mita *et al.*, 1994). The cell shortening in response to IP_3 with

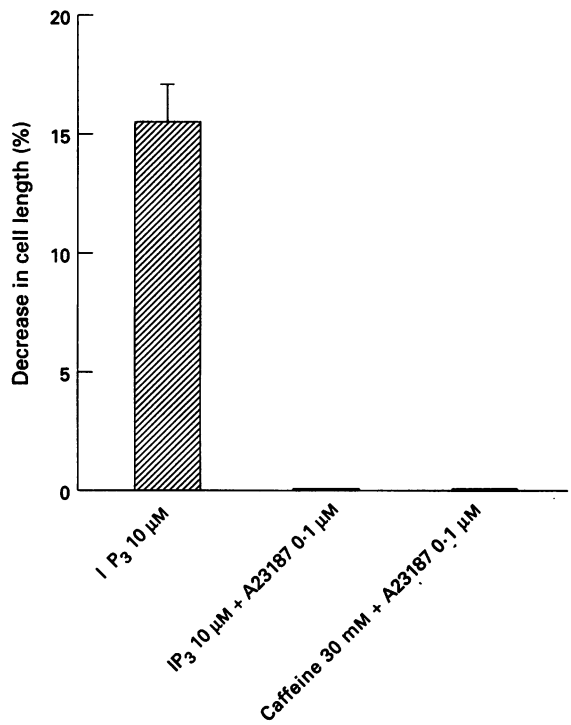

Figure 1 Effect of A23187 on inositol 1,4,5-trisphosphate (IP_3)-induced shortening of α-toxin-permeabilized single smooth muscle cells. Permeabilized cells were perfused with cytosolic substitution solution containing 0.2 μM free Ca^{2+} for 5 min. None of the cells responded to 0.2 μM Ca^{2+}. The first cell shortening was then evoked by perfusion with 10 μM IP_3 in the presence of 0.2 μM Ca^{2+}. After washing with Ca^{2+}-free cytosolic substitution solution for 10 min, permeabilized cells were treated with Ca^{2+}-free cytosolic substitution solution containing 0.1 μM A23187 for 10 min and were perfused with cytosolic substitution solution containing Ca^{2+} (0.2 μM) in the presence of A23187 (0.1 μM) for 5 min. The cells were then exposed to 10 μM IP_3 in the presence of Ca^{2+} (0.2 μM) and A23187. After washing with cytosolic substitution solution containing Ca^{2+} (0.2 μM) and A23187 for 5 min, cells were further exposed to 30 mM caffeine in the presence of Ca^{2+} (0.2 μM) and A23187. Values are means±s.e. (n=3). The ordinate scale represents the decrease in cell length as a percentage of original length. After exposure to A23187, shortening in response to IP_3 or caffeine was abolished.

0.2 μM Ca^{2+} was completely inhibited by 0.1 μM A23187. Moreover, permeabilized cells did not show caffeine (30 mM) induced cell shortening on treatment with A23187. Therefore, to maintain cytoplasmic Ca^{2+} constant in permeabilized cells, subsequent experiments were carried out in cytosolic substitution solutions containing A23187 (0.1 μM), which depleted the sarcoplasmic reticulum of Ca^{2+}.

The shortening of permeabilized cells was evoked by increasing the concentration of ACh, when the concentration of free Ca^{2+} was held at 0.2 μM Ca^{2+} in the presence of A23187. Permeabilized smooth muscle cells responded to 0.3 μM or 1 μM ACh in an all-or-none manner (Figure 2a). These threshold concentrations of ACh were identical with those in intact cells showing an all-or-none response (Mita & Uchida, 1987; 1988; Mita *et al.*, 1988). Permeabilized cells were almost completely relaxed again by washing with the Ca^{2+}-free cytosolic substitution solution. Moreover, the cells responded repeatedly to the same threshold concentration of ACh in the same manner (Figure 2). Thus, although individual permeabilized cells showed an all-or-none response to ACh with 0.2 μM Ca^{2+}, the average contractile response of all the cells was graded because of the difference in the threshold concentration of ACh (Figure 2b). The maximal decreases in the length of the cells induced by ACh with 0.2 μM Ca^{2+} in the first and second cell shortening were 17.3±0.1% and 15.8±1.4%, respectively. The difference between these values was not significant. The shortening of α-toxin-permeabilized single cells was also induced by application of GTP with 0.2 μM free Ca^{2+} in the presence of A23187, showing an all-or-none response (Figure 3a). The threshold concentration of GTP that induced an all-or-none response was either 10 μM or 30 μM. However, the average contractile response of all the cells was graded because of the difference in the threshold concentration of GTP (Figure 3b). The maximal decrease in the length of the cells induced by GTP with 0.2 μM Ca^{2+} was 17.3±3.1%. This value was not significantly different from that induced by ACh.

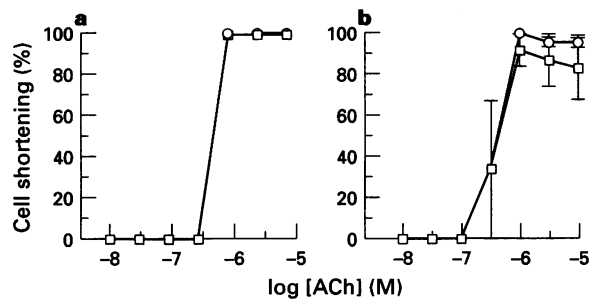

Figure 2 Contractile response to acetylcholine (ACh) of α-toxin-permeabilized single smooth muscle cells in cytosolic substitution solution with the free Ca^{2+} concentration held at 0.2 μM in the presence of A23187. Permeabilized cells were treated with Ca^{2+}-free cytosolic substitution solution containing 0.1 μM A23187 for 10 min and were perfused with cytosolic substitution solution containing 0.2 μM Ca^{2+} and 0.1 μM A23187 for 5 min. The first shortening was evoked by successive perfusion with cytosolic substitution solution containing increasing concentrations of ACh with Ca^{2+} (0.2 μM) in the presence of A23187 (○). After washing with Ca^{2+}-free cytosolic substitution solution in the presence of A23187 for 15 min and perfusing cytosolic substitution solution containing Ca^{2+} (0.2 μM) and A23187 for 5 min, the second cell shortening in response to ACh in the presence of Ca^{2+} (0.2 μM) and A23187 was observed (□). (a) A typical shortening of an α-toxin-permeabilized smooth muscle cell in response to increasing concentrations of ACh. (b) Mean contractile responses of all the cells. Results were obtained with cells from different preparations made on different days. Points and bars are means±s.e. ($n=3$). This plot shows that the dose-response relationship in the first and second cell shortening were the same. The ordinate scale represents the maximal shortening of the first dose-response curve to ACh as 100%.

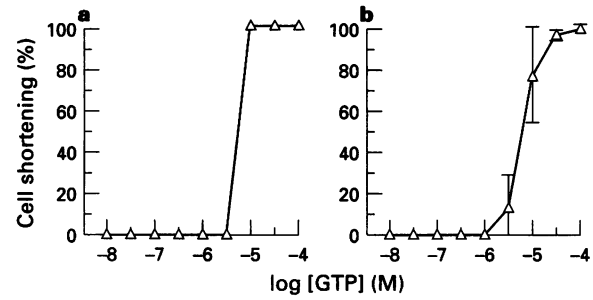

Figure 3 Contractile response to guanosine 5'-triphosphate (GTP) of α-toxin-permeabilized single smooth muscle cells in cytosolic substitution solution with the free Ca^{2+} concentration held at 0.2 μM in the presence of A23187. Permeabilized cells were treated with Ca^{2+}-free cytosolic substitution solution containing 0.1 μM A23187 for 10 min and were perfused with cytosolic substitution solution containing 0.2 μM Ca^{2+} and 0.1 μM A23187 for 5 min. Shortening was evoked by successive perfusion with cytosolic substitution solution containing increasing concentrations of GTP with Ca^{2+} (0.2 μM) in the presence of A23187 (Δ). (a) A typical shortening of an α-toxin-permeabilized smooth muscle cell in response to increasing concentrations of GTP. (b) Mean contractile responses of all the cells. Results were obtained with cells from different preparations made on different days. Points and bars are means±s.e. ($n=4$). The ordinate scale represents the maximal shortening to GTP as 100%.

Discussion

The addition of IP_3 (10 μM) with Ca^{2+} (0.2 μM) in α-toxin permeabilized smooth muscle cells caused cell shortening (Figure 1). This result suggests that the function of intracellular Ca^{2+} store in permeabilized cells remains intact. In fact, because the pores formed in the membrane by α-toxin are too small to allow an α-toxin molecule itself to pass, α-toxin attaches only to the plasma membrane and does not reach intracellular organelles (Ahnert-Hilger & Gratzl, 1988; Bhakdi & Tranum-Jensen, 1991). However, the cell shortening in response to IP_3 with Ca^{2+} (0.2 μM) was abolished by treatment with A23187 (0.1 μM). Furthermore, permeabilized smooth muscle cells also did not respond to caffeine (30 mM) on treatment with A23187. Kitazawa *et al.* (1989) showed that the sarcoplasmic reticulum was depleted of Ca^{2+} by A23187 in α-toxin-permeabilized guinea-pig portal vein and A23187 abolished IP_3-induced Ca^{2+} release. It is well known that two mechanisms of Ca^{2+} release from the Ca^{2+} store exist in smooth muscle. They are Ca^{2+}-induced Ca^{2+} release (CICR), which is sensitive to caffeine, and IP_3-induced Ca^{2+} release (IICR). It has been shown that the Ca^{2+} store in taenia caecum consists of two compartments, one with both CICR and IICR mechanisms, and the other with only an IICR mechanism (Iino, 1987; Yamazawa *et al.*, 1992). Our results suggest that neither mechanism of Ca^{2+} release function on treatment with A23187 in α-toxin-permeabilized smooth muscle cells, and cytoplasmic Ca^{2+} is maintained constant under these conditions. Therefore, we can determine the real Ca^{2+} sensitization stimulated by ACh or GTP without Ca^{2+} mobilization.

α-Toxin-permeabilized single smooth muscle cells showed repeatedly an all-or-none response to 0.3 μM or 1 μM ACh in the presence of Ca^{2+} (0.2 μM) (Figure 2). A similar all-or-none response was also induced by GTP in the presence of Ca^{2+} (0.2 μM) (Figure 3). These results suggest that the Ca^{2+} sensitivity is augmented in an all-or-none manner by stimulation of muscarinic receptors or GTP-binding proteins under a constant Ca^{2+} concentration. This is the first observation that Ca^{2+} sensitization of smooth muscle contraction is induced by the stimulation of receptors in an all-or-none manner. The augmentation of Ca^{2+} sensitivity stimulated by an α-adrenoceptor agonist, phenylephrine, in the contraction of α-toxin-permeabilized whole tissues (guinea-pig portal vein) was in-

duced concentration-dependently in the presence of 0.5 μM free Ca^{2+} (Kitazawa *et al.*, 1991). The difference in these results may be explained by the distinction between whole tissues and isolated cells used in experiments. In general, intact whole muscle tissues including taenia caecum respond concentration-dependently to ACh. On the other hand, as we found previously, isolated intact individual smooth muscle cells from guinea-pig taenia caecum and the fundus of the stomach respond to ACh in an all-or-none manner. However, in these cells the average response of all the cells is graded because of the difference in the threshold concentration of ACh (Mita & Uchida, 1987; Mita *et al.*, 1988; 1993).

The threshold concentrations of ACh causing an all-or-none response in the intact cells were identical with those showing all-or-none augmentation of Ca^{2+} sensitivity in α-toxin-permeabilized cells. This result suggests that the all-or-none response of intact cells to ACh may be connected with the all-or-none augmentation of Ca^{2+} sensitivity to ACh. However, the shortening was greater to ACh in these permeabilized cells when Ca^{2+} concentration was raised beyond 0.2 μM (Mita *et al.*, 1994). It is suggested that the Ca^{2+} sensitivity is augmented to ACh in an all-or-none manner, but the magnitude of the maximal shortening induced by ACh depends on the Ca^{2+} concentration. The maximal decrease in the length of the permeabilized cells induced by increasing the concentration of free Ca^{2+} in the absence and presence of 10 μM ACh was 38.6 ± 2.9% and 44.0 ± 2.4%, respectively; the difference between these values was significant at $P = 0.01$ on a paired basis ($n = 6$; Mita *et al.*, 1994). On the other hand, the maximal shortening of the all-or-none response to ACh in intact single cells was 54.9 ± 1.0% ($n = 85$; Mita & Uchida, 1988). The intact cells shorten significantly more than the permeabilized cells in response to muscarinic receptor activation. Furthermore, the shortening of the permeabilized cells in response to Ca^{2+} only reached a maximum after 3–4 min, but the intact cells shortened within 30 s. It seems that the difference in these rates of shortening may result from different rates of Ca^{2+} mobilization. Ca^{2+} release from the sarcoplasmic reticulum, and influx from the extracellular space may raise $[Ca^{2+}]_i$ more rapidly in the normal cells than Ca^{2+} diffusion into the permeabilized cells (Mita & Uchida, 1988). Intact cells may also have a positive feedback mechanism of Ca^{2+} entry, as shown in ileal smooth muscle by Inoue & Isenberg (1990), who reported that the inward current through muscarinic receptor-activated non-selective cation channels was enhanced by a rise in intracellular Ca^{2+}, thus maintaining Ca^{2+} influx by sustaining depolarization. In sum, it seems that the intact cells may shorten more, and more rapidly than the permeabilized cells due to the rapid Ca^{2+} mobilization with these mechanisms when muscarinic receptor stimulation augments the Ca^{2+} sensitivity.

We do not think that all the cells which constitute the whole tissue show an all-or-none Ca^{2+} sensitization to ACh. Only about 50% of the intact cells responded to ACh (Mita & Uchida, 1987). This phenomenon may be due to the pattern of innervation of smooth muscle cells. Burnstock & Iwayama (1971) reported that there are three types of cells in smooth muscle: directly innervated cells (key cell), coupled cells and indirectly coupled cells. Therefore, only the key cell may contain the receptors and signal transduction pathways to respond to ACh. The all-or-none response to individual cells may be masked by the tissue behaving as a functional syncytium with the cells being affected by their neighbours. Moreover, we cannot observe an all-or-none Ca^{2+} sensitization in intact cells, because muscarinic receptor activation involves a rapid, large increase of intracellular Ca^{2+} concentration above threshold through Ca^{2+} release from sarcoplasmic reticulum and Ca^{2+} influx from the extracellular space. Only the key cell, when isolated alone and permeabilized, shows the augmentation of Ca^{2+} sensitivity to ACh in an all-or-none manner.

At present, we cannot explain the molecular mechanisms of development of Ca^{2+} sensitization in an all-or-none manner. However, the addition of GTP also induced an all-or-none augmentation of Ca^{2+} sensitivity (Figure 3). This result suggests that the augmentation of Ca^{2+} sensitivity is evoked as a result of activation of GTP-binding proteins, and that an all-or-none Ca^{2+} sensitization to ACh is induced downstream from the GTP-binding proteins. Others have suggested that Ca^{2+} sensitization results from imbalance between the activities of myosin light chain kinase and myosin light chain phosphatase (Stull *et al.*, 1990), which may involve inhibition of myosin phosphatase via arachidonic acid (Somlyo *et al.*, 1989; Kitazawa *et al.*, 1991; Kubota *et al.*, 1992; Gong *et al.*, 1992), a GTP-binding protein coupled mechanism possibly involving small GTP-binding proteins such as rhoA p21 (Hirata *et al.*, 1992) and ras p21 (Satoh *et al.*, 1993), or phosphorylation of myosin light chain kinase by Ca^{2+}/calmodulin-dependent protein kinase II (Tang *et al.*, 1992; Tansey *et al.*, 1992). Nishimura *et al.* (1988) reported that protein kinase C is involved in the increase of Ca^{2+} sensitivity in α-toxin-permeabilized smooth muscle tissues. However, protein kinase C is not involved in the muscarinic receptor-operated augmentation of Ca^{2+} sensitivity in permeabilized single smooth muscle cells (Oishi *et al.*, 1992). A regulatory mechanism that is independent of myosin light chain phosphorylation has also been reported (Oishi *et al.*, 1991) and this mechanism may possibly be involved in the Ca^{2+} sensitization. In addition, it has been suggested that thin filament-associated proteins such as caldesmon and calponin may regulate smooth muscle contraction on the side of the actin filament (Winder & Walsh, 1993). Further study is clearly needed to identify fully the mechanisms of development of Ca^{2+} sensitization to ACh in α-toxin-permeabilized single smooth muscle cells.

In conclusion, it is suggested that intact smooth muscle cells show an all-or-none shortening to ACh as a result of a slight increase in the intracellular Ca^{2+} level over the threshold concentration and an all-or-none augmentation of Ca^{2+} sensitivity via the activation of GTP-binding protein(s) when muscarinic receptor stimulation reaches the threshold to evoke Ca^{2+} influx and IP_3-induced Ca^{2+} release. It should be pointed out, however, that the single cells are shortening under unloaded conditions, and the affect of load has not been assessed.

We thank Drs M.K. Uchida and K. Oishi, Department of Molecular Pharmacology, Meiji College of Pharmacy, for providing *Staphylococcus aureus* α-toxin, and for helpful discussions and comments on the manuscript.

This work was supported by a Grant-in-Aid for Encouragement of Young Scientists (No. 04857292 and 05857261) from the Ministry of Education, Science and Culture of Japan, and by a Special Grant from Meiji College of Pharmacy.

References

AHNERT-HILGER, G. & GRATZL, M. (1988). Controlled manipulation of the cell interior by pore-forming proteins. *Trends Pharmacol. Sci.*, **9**, 195–197.

BHAKDI, S. & TRANUM-JENSEN, J. (1991). Alpha-toxin of *Staphylococcus aureus*. *Microbiol. Rev.*, **55**, 733–751.

BRADLEY, A.B. & MORGAN, K.G. (1987). Alterations in cytoplasmic calcium sensitivity during porcine coronary artery contractions as detected by aequorin. *J. Physiol.*, **385**, 437–448.

BURNSTOCK, G. & IWAYAMA, T. (1971). Fine-structural identification of autonomic nerves and their relation to smooth muscle. *Prog. Brain Res.*, **34**, 389–404.

GONG, M.C., FUGLSANG, A., ALESSI, D., KOBAYASHI, S., COHEN, P., SOMLYO, A.V. & SOMLYO, A.P. (1992). Arachidonic acid inhibits myosin light chain phosphatase and sensitizes smooth muscle to calcium. *J. Biol. Chem.*, **267**, 21492–21498.

HARAFUJI, H. & OGAWA, Y. (1980). Re-examination of the apparent binding constant of ethylene glycol bis(β-aminoethyl ether)-N,N,N',N'-tetraacetic acid with calcium around neutral pH. *J. Biochem.*, **87**, 1305–1312.

HIRATA, K., KIKUCHI, A., SASAKI, T., KURODA, S., KAIBUCHI, K., MATSUURA, Y., SEKI, H., SAIDA, K. & TAKAI, Y. (1992). Involvement of rho p21 in the GTP-enhanced calcium ion sensitivity of smooth muscle contraction. *J. Biol. Chem.*, **267**, 8719–8722.

IINO, M. (1987). Calcium dependent inositol trisphosphate-induced calcium release in the guinea-pig taenia caeci. *Biochem. Biophys. Res. Commun.*, **142**, 47–52.

INOUE, R. & ISENBERG, G. (1990). Intracellular calcium ions modulate acetylcholine-induced inward current in guinea-pig ileum. *J. Physiol.*, **424**, 73–92.

ITOH, T., KANMURA, Y. & KURIYAMA, H. (1985). A23187 increases calcium permeability of store sites more than of surface membranes in the rabbit mesenteric artery. *J. Physiol.*, **359**, 467–484.

KARAKI, H. (1989). Ca^{2+} localization and sensitivity in vascular smooth muscle. *Trends Pharmacol. Sci.*, **10**, 320–325.

KARAKI, H., SATO, K. & OZAKI, H. (1988). Different effects of norepinephrine and KCl on the cytosolic Ca^{2+}-tension relationship in vascular smooth muscle of rat aorta. *Eur. J. Pharmacol.*, **151**, 325–328.

KITAZAWA, T., GAYLINN, B.D., DENNEY, G.H. & SOMLYO, A.P. (1991). G-protein-mediated Ca^{2+} sensitization of smooth muscle contraction through myosin light chain phosphorylation. *J. Biol. Chem.*, **266**, 1708–1715.

KITAZAWA, T., KOBAYASHI, S., HORIUTI, K., SOMLYO, A.V. & SOMLYO, A.P. (1989). Receptor-coupled, permeabilized smooth muscle: role of the phosphatidylinositol cascade, G-proteins, and modulation of the contractile response to Ca^{2+}. *J. Biol. Chem.*, **264**, 5339–5342.

KUBOTA, Y., NOMURA, M., KAMM, K.E., MUMBY, M.C. & STULL, J.T. (1992). GTPγS-dependent regulation of smooth muscle contractile elements. *Am. J. Physiol.*, **262**, C405–C410.

MITA, M., MATSUO, N. & UCHIDA, M.K. (1988) Effect of Ca^{2+} deprivation on short-term desensitization of isolated smooth muscle cells showing an all-or-none response to acetylcholine. *Gen. Pharmacol.*, **19**, 441–445.

MITA, M., OISHI, K., UCHIDA, M.K. & HASHIMOTO, T. (1994). All-or-none shortening of α-toxin-permeabilized single smooth muscle cells from guinea-pig taenia caecum and acetylcholine-induced Ca^{2+} sensitization. *Comp. Biochem. Physiol.*, **107C**, 41–49.

MITA, M., ONO, T., HASHIMOTO, T. & UCHIDA, M.K. (1993). All-or-none shortening of isolated single smooth muscle cells from different organs to acetylcholine. *Gen. Pharmacol.*, **24**, 1085–1090.

MITA, M. & UCHIDA, M.K. (1987). Desensitization of isolated smooth muscle cells from guinea-pig taenia caecum to acetylcholine. *Can. J. Physiol. Pharmacol.*, **65**, 293–297.

MITA, M. & UCHIDA, M.K. (1988). Muscarinic receptor binding and Ca^{2+} influx in the all-or-none response to acetylcholine of isolated smooth muscle cells. *Eur. J. Pharmacol.*, **151**, 9–17.

MITA, M. & UCHIDA, M.K. (1991). The change in the threshold for short-term desensitization in isolated smooth muscle cells showing an all-or-none response to acetylcholine. *Br. J. Pharmacol.*, **104**, 603–608.

NISHIMURA, J., KOBLER, M. & VAN BREEMEN, C. (1988). Norepinephrine and GTP-γ-S increase myofilament Ca^{2+} sensitivity in α-toxin permeabilized arterial smooth muscle. *Biochem. Biophys. Res. Commun.*, **157**, 677–683.

OISHI, K., MITA, M., ONO, T., HASHIMOTO, T. & UCHIDA, M.K. (1992). Protein kinase C-independent sensitization of contractile proteins to Ca^{2+} in α-toxin-permeabilized smooth muscle cells from the guinea-pig stomach. *Br. J. Pharmacol.*, **107**, 908–909.

OISHI, K., TAKANO-OHMURO, H., MINAGAWA-MATSUO, N., SUGA, O., KARIBE, H., KOHAMA, K. & UCHIDA, M.K. (1991). Oxytocin contracts rat uterine smooth muscle in Ca^{2+}-free medium without any phosphorylation of myosin light chain. *Biochem. Biophys. Res. Commun.*, **176**, 122–128.

ONO, T., MITA, M., SUGA, O., HASHIMOTO, T., OISHI, K. & UCHIDA, M.K. (1992). Receptor-coupled shortening of α-toxin-permeabilized single smooth muscle cells from the guinea-pig stomach. *Br. J. Pharmacol.*, **106**, 539–543.

SATOH, S., RENSLAND, H. & PFITZER, G. (1993). Ras proteins increase Ca^{2+}-responsiveness of smooth muscle contraction. *FEBS Lett.*, **324**, 211–215.

SOMLYO, A.P., KITAZAWA, T., HIMPENS, B., MATTHIJS, G., HORIUTI, K., KOBAYASHI, S., GOLDMAN, Y.E. & SOMLYO, A.V. (1989). Modulation of Ca^{2+}-sensitivity and of the time course of contraction in smooth muscle: A major role of protein phosphatases? *Adv. Protein Phosphatases*, **5**, 181–195.

STULL, J.T., HSU, L.-C., TANSEY, M.G. & KAMM, K.E. (1990). Myosin light chain kinase phosphorylation in tracheal smooth muscle. *J. Biol. Chem.*, **265**, 16683–16690.

TANG, D.-C., STULL, J.T., KUBOTA, Y. & KAMM, K.E. (1992). Regulation of the Ca^{2+} dependence of smooth muscle contraction. *J. Biol. Chem.*, **267**, 11839–11845.

TANSEY, M.G., WORD, R.A., HIDAKA, H., SINGER, H.A., SCHWORER, C.M., KAMM, K.E. & STULL, J.T. (1992). Phosphorylation of myosin light chain kinase by the multifunctional calmodulin-dependent protein kinase II in smooth muscle cells. *J. Biol. Chem.*, **267**, 12511–12516.

WINDER, S.J. & WALSH, M.P. (1993). Calponin: thin filament-linked regulation of smooth muscle contraction. *Cell. Signal.*, **5**, 677–686.

YAMAZAWA, T., IINO, M. & ENDO, M. (1992). Presence of functionally different compartments of Ca^{2+} store in single intestinal smooth muscle cells. *FEBS Lett.*, **301**, 181–184.

(Received September 30, 1994
Revised February 13, 1995
Accepted February 16, 1995).

British Journal of Pharmacology (1995) 115, 527-533

Induction of a novel form of hippocampal long-term depression by muscimol: involvement of $GABA_A$ but not glutamate receptors

S. Akhondzadeh & [1]T.W. Stone

Pharmacology Laboratories, Institute of Biomedical and Life Sciences, West Medical Bldg, University of Glasgow, Glasgow G12 8QQ

1 Unlike long-term potentiation, long-term depression (LTD) in the central nervous system remains poorly understood. The present study was undertaken to investigate the role of $GABA_A$ receptors in LTD and synaptic plasticity.

2 Extracellular recordings were made in the CA1 pyramidal cell layer of rat hippocampal slices following orthodromic stimulation of Schaffer collateral fibres in stratum radiatum (0.01 Hz).

3 Muscimol induced a time- and concentration-dependent LTD of the amplitude of orthodromic potentials. Increasing the stimulation frequency from 0.01 Hz to 1 Hz for 10 s reversed the LTD induced by muscimol. Muscimol also induced LTD in the absence of electrical stimulation.

4 Adenosine decreased the spike size in a concentration-dependent manner, but failed to induce LTD.

5 Alphaxalone and 5α-pregnan-3α-ol-20-one at concentrations that did not have any effect themselves on the population spike (0.5 and 1 μM), potentiated the inhibitory effect of muscimol on the population spike size, including concentrations which were not effective by themselves. Both steroids were able to potentiate the ability of muscimol to induce LTD.

6 Bicuculline, 5 μM, reversed the LTD induced by muscimol, 10 μM.

7 The NMDA receptor antagonist (±)-2-amino-5-phosphonopentanoic acid (2-AP5), the NMDA/metabotropic antagonist 2-AP3 and selective metabotropic antagonist L-(+)-2-amino-3-phosphonopropionic acid (L(+)-AP3) failed to modify the LTD. Similarly, quisqualic acid and (1S, 3R)-aminocyclopentane dicarboxylic acid (ACPD) a selective agonist at metabotropic receptors did not induce LTD or short-term depression, whereas kynurenic acid prevented the reversal of the LTD obtained at 1 Hz.

8 It is concluded that LTD can be induced by the selective activation of $GABA_A$ receptors. The lack of involvement of glutamate receptors in our protocol confirms the unique nature of the LTD described here. The phenomenon of GABA-induced LTD and its reversal by 1 Hz stimulation may represent a novel type of long-lasting depression by which inhibitory interneurones can modulate pyramidal cell excitability in a frequency-dependent manner.

Keywords: GABA receptors; muscimol; adenosine; glutamate receptors; long-term depression; LTD; hippocampus; metabotropic receptors

Introduction

Although both excitation and inhibition are important in controlling neuronal activity, long-term depression (LTD) remains less extensively studied compared to long-term potentiation (LTP) (Stanton & Sejnowski, 1989; Yang & Faber, 1991). The importance of both phenomena is suggested by their demonstration in many regions of the central nervous system, including hippocampus, cerebellar cortex, striatum, nucleus accumbens and neocortex (Levy & Steward, 1979; Ekerot & Kano, 1985; Ito, 1989; Kimura *et al.*, 1989; Stanton & Sejnowski, 1989; Calabresi *et al.*, 1992; Pennartz *et al.*, 1993).

A variety of different protocols can be used to induce LTD including those which involve homosynaptic or heterosynaptic pathways. When LTD occurs at inputs whose activation contributes to the induction of modification, it is known as homosynaptic LTD and when it shows itself at inputs that had been inactive during induction it is referred to as heterosynaptic LTD. There are two ways to induce homosynaptic LTD: (a) With high frequency stimulation in the neocortex, striatum and nucleus accumbens (Lovinger *et al.*, 1993; Walsh, 1993); (b) With low frequency stimulation in the CA1 region of the hippocampus (Bramham & Srebro, 1987; Artola & Singer, 1993; Linden, 1994). Long-term changes of transmission induced in this way seem to involve the ionotropic and/or metabotropic receptors for glutamate. Several groups studying the pharmacology of LTD and LTP, for example, have reported that the ionotropic sites sensitive to N-methyl-D-aspartate (NMDA) and some forms of metabotropic receptor may play critical roles in these long-lasting changes of neuronal activity (Kano & Kato, 1987; Aroniadou & Teyler, 1991; Yang & Faber, 1991; Bashir & Collingridge, 1992; Dudek & Bear, 1992; Mulkey & Malenka, 1992; Yang *et al.*, 1994).

There has been relatively little interest in the role of the inhibitory transmitter GABA in LTP or LTD and the main purpose of the present study was to improve our understanding of the role of $GABA_A$ receptors in LTD and synaptic plasticity in the hippocampus. We have observed the induction of a novel form of LTD which does not involve glutamate receptors and which cannot be reproduced by activation of receptors for adenosine, another well studied inhibitory neuromodulator in the CNS (Stone, 1991).

Finally, we have examined the pharmacology of the GABA receptors involved, in comparison with classical $GABA_A$ receptors, by studying the effects of neurosteroids. Certain synthetic and endogenous steroids like alphaxalone and 5α-pregnan-3α-ol-20-one have been reported to act as positive modulators of the $GABA_A$ receptor (Harrison & Simmonds, 1984; Turner & Simmonds, 1989). At low concentrations, they

[1] Author for correspondence.

potentiate $GABA_A$ action, while at higher concentrations they can directly open the chloride channel associated with the $GABA_A$ receptor (Majewska *et al.*, 1988; Puia *et al.*, 1991).

Methods

Male Wistar rats (170–200g) were anaesthetized with urethane (1.3 g kg^{-1}, i.p.) and decapitated. The brains were rapidly taken out and put in ice-cold artificial cerebrospinal fluid (ACSF) with the following composition (mM): NaCl 115, KH_2PO_4 2.2, KCl 2.0, $MgCl_2$ 1.2, $CaCl_2$ 2.5, $NaHCO_3$ 25 and glucose 10. The hippocampi were cut transversely into 450 μm thick slices with a McIlwain tissue chopper. The slices were kept in an incubation chamber containing an ACSF-saturated atmosphere of 95% O_2 and 5% CO_2 at room temperature for at least 1 h before use. Individual slices were then transferred to a 1 ml capacity recording chamber and superfused with ACSF at 30°C ± 0.5, gassed with O_2/CO_2 mixture to yield a pH of 7.4. The slices were completely submerged in the medium which was perfused continuously at a rate of 4 ml min^{-1}. The slices were maintained in the perfusion chamber for 15 min before proceeding with any further experimentation.

Recordings of orthodromic extracellular field potentials were made from the CA1 pyramidal cell layer following stimulation of the Schaffer collateral fibres in Stratum radiatum near the border of the CA2-CA3. Recording was achieved via glass microelectrodes (Clark Electromedical) of tip diameter approx. 2 μm and filled with 2 M NaCl solution. Stimulation was effected by concentric bipolar electrodes (Clark) at a frequency of 0.01 Hz (0.25 ms duration pulses, 100–400 μA amplitude). Only slices exhibiting maximal orthodromic potentials of between 9 and 12 mV were used for drug applications. Other slices were discarded. Stimulus strength was reduced to submaximal levels during experimentation so as to yield spike size of approximately 75% of maximum.

The size of the population spike was measured as the peak to peak amplitude after perfusion for at least 15 min to allow the attainment of stable responses. Results are presented as mean ± s.e.mean for n experiments and statistical significance was assessed by Student's t test. Differences were considered significant with $P \leqslant 0.05$.

All agents were purchased from Sigma Chemical Ltd Co. except bicuculline methobromide, L-(+)-2-amino-3-phosphonopropionic acid [L-(+)-AP3], (±)-2-amino-5-phosphonopentanoic acid (2-AP5), (1S, 3R)-aminocyclopentane dicarboxylic acid ((1S, 3R)-ACPD) and quisqualic acid which were purchased from Research Biochemicals Inc. All agents were dissolved in ACSF except alphaxalone and 5α-pregnan-3α-ol-20-one which were dissolved in ethanol. The concentration of ethanol in all experiments was less than 0.01% v/v; ethanol at this dilution did not show any effect by itself.

Results

Under normal experimental conditions, when the Schaffer collateral/commissural fibres were stimulated at a frequency of 0.01 Hz, muscimol induced a concentration-dependent inhibition of the amplitude of the evoked population potential. The maximum effect of muscimol was obtained at 10 μM. When used at concentrations of 0.1 to 5 μM, perfused for 10 min, this inhibition was readily reversible and upon washing the slices, potential size was restored to control levels within 10 min. When tested at the higher concentration of 10 μM, however, a stable, long-lasting depression of the population potential was obtained. The potential remained depressed, with no sign of recovery, for at least 20 min after washing, the minimum period of washout investigated. This is illustrated in Figure 1a. Whenever tested, the depression was found to persist for at least 60 min after washout.

It was later realised that a similar long-lasting depression could be induced by using a lower concentration of muscimol applied for longer periods. Thus, a concentration of 5 μM could reliably induce long-lasting depression if applied for 20 min (Figure 1b). However, this relationship did not seem to apply at lower concentrations. Superfusion of muscimol at 2 μM for 30 min, for instance, was able to produce a depression of population spike amplitude which attained equilibrium within 10 min but which was readily reversible on washing (Figure 2b). Conversely, reducing the time of application of muscimol at 10 μM prevented the establishment of LTD (Figure 2a), even though the potential had been diminished by about 90% at the commencement of washing (Figure 2a). This finding indicates that the establishment of LTD is not simply dependent on the extent of spike depression, a view which is

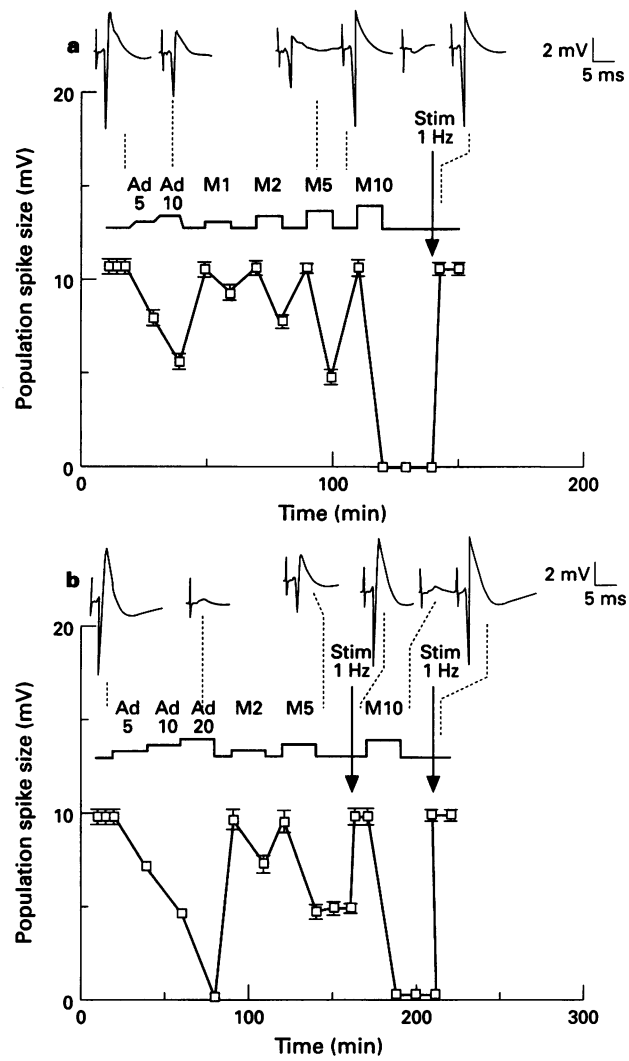

Figure 1 The effects of adenosine (Ad) and muscimol (M) on the amplitude of population spikes. The concentrations (μM) and time of application of the agonists are indicated above the data points. Slices were superfused with drug-free artificial CSF between agonist applications. (a) When applied for 10 min, muscimol was able to induce long-term depression (LTD) at a concentration of 10 μM. At the time indicated, the frequency of orthodromic stimulation was raised to 1 Hz, which reversed LTD and restored the potentials to control size. (b) When applied for 20 min, the lower concentration of 5 μM muscimol was able to induce LTD, even though the potential size was reduced by only 50%. At the times indicated, the frequency of orthodromic stimulation was raised to 1 Hz, which reversed LTD and restored the potentials to control size. Adenosine, even at 20 μM for 20 min, which abolished the evoked potential, did not induce LTD. Data points are shown as mean ± s.e.mean (n = 4). Sample records of orthodromic potentials are illustrated above the graphs; calibrations 2 mV and 5 ms.

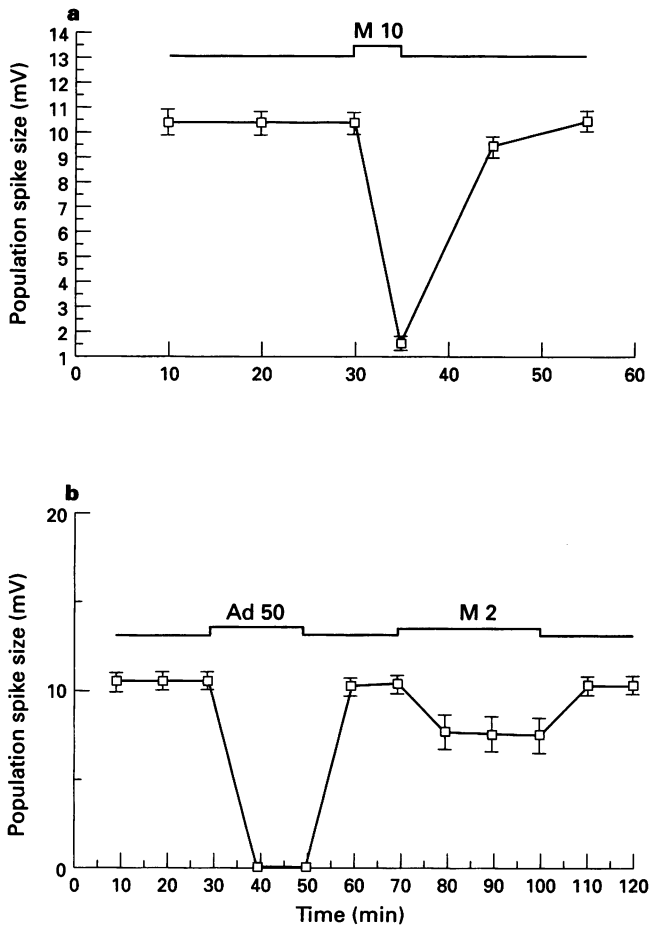

Figure 2 The effects of adenosine (Ad) and muscimol (M) on the amplitude of population spikes. The concentrations (μM) and time of application of the agonists are indicated above the data points. Slices were superfused with drug-free artificial CSF between agonist applications. (a) Illustrates the finding that a concentration of 10 μM muscimol, which induced LTD after 10 min application (Figure 1a) did not induce LTD after a shorter application of 5 min, even though potential size was reduced more than by 5 μM muscimol (Figure 1b). (b) The abolition of response size by adenosine even at 50 μM for 20 min was still unable to induce LTD. The need for a threshold concentration of muscimol is suggested by the failure of 2 μM to induce LTD, even after a partial suppression of response size for 30 min. Data points are shown as mean ± s.e.mean ($n=4$).

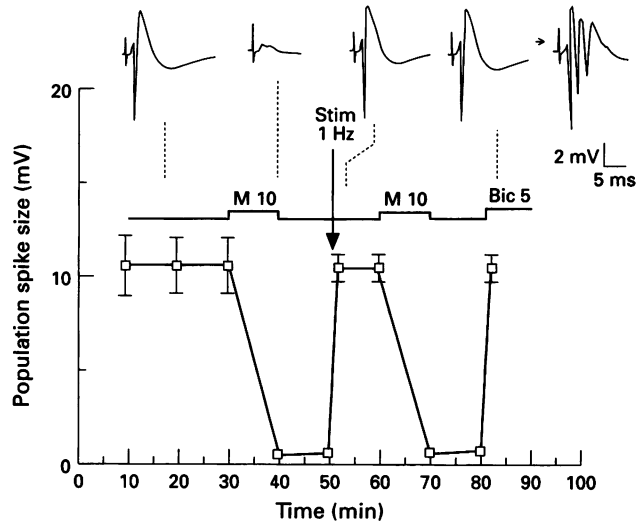

Figure 3 The effects of muscimol (M) on the amplitude of population spikes. The concentrations (μM) and time of application of the agonists are indicated above the data points. Slices were superfused with drug-free artificial CSF between agonist applications. When applied for 10 min, muscimol was able to induce long-term depression (LTD) at a concentration of 10 μM. At the time indicated, the frequency of orthodromic stimulation was raised to 1 Hz, which reversed LTD and restored the potentials to control size. A similar reversal was achieved by the addition of bicuculline, 5 μM, which restored potential size almost immediately. The development of increased neuronal excitability, with multiple population spikes did not occur until several minutes later. The sample records above the graph illustrate this. Data points are shown as mean ± s.e.mean ($n=4$).

supported by the fact that at 5 μM, muscimol could induce LTD when the population spike was reduced by only about 50% (Figure 1b).

Reversal of LTD

Electrical stimulation Once long-term depression had been established and the inability of washing to reverse it confirmed, the potentials could be restored to control size by delivering stimuli at a rate of 1 Hz for 10 s (Figure 1a, b and others).

Bicuculline In order to confirm the involvement of $GABA_A$ receptors in the effect of muscimol, bicuculline methobromide was used as a receptor antagonist. When added to hippocampal slices, however, bicuculline can induce multiple epileptiform bursts of spikes which can complicate interpretation. In these experiments, therefore, LTD was induced by muscimol and bicuculline was then added to the perfusing medium. In each of 4 slices, bicuculline reversed the LTD within 2 min, and before the appearance of multiple population spikes (Figure 3).

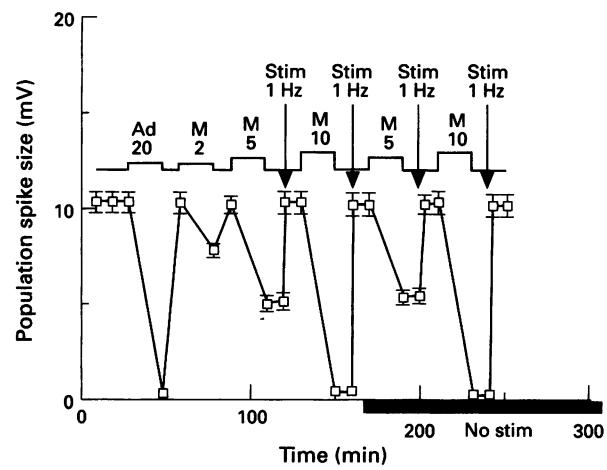

Figure 4 The effects of adenosine (Ad) and muscimol (M) on the amplitude of population spikes. The concentrations (μM) and time of application of the agonists are indicated above the data points. Slices were superfused with drug-free artificial CSF between agonist applications. A sequence is illustrated in which the applications of 5 μM or 10 μM muscimol for 10 min were able to induce long-term depression (LTD). At the times indicated, the frequency of orthodromic stimulation was raised to 1 Hz, which reversed LTD and restored the potentials to control size. A similar pattern was observed even in the absence of the normal background stimulation at 0.01 Hz, indicated by the solid bar on the X-axis. Data points are shown as mean ± s.e.mean ($n=4$).

Adenosine

In order to draw a comparison with muscimol, a similar series of experiments was carried out using adenosine. At concentrations of 5, 10 and 20 μM, adenosine depressed the size of the population spikes, as reported on many previous occasions

(by 24.88% ± 1.33, 48.75% ± 1.4 and 99.25% ± 0.48 respectively; mean ± s.e.mean, $n=4$, $P<0.001$). However, adenosine failed to induce any sign of long-term depression; potentials always recovered to control levels within 5 min of washout (Figure 1a, b). This was so even when adenosine was applied at the highest concentration of 50 μM for 20 min, applications which led to abolition of the population spike for periods of well over 10 min (Figure 2a).

Absence of stimulation

In view of the efficacy of 1 Hz stimulation in terminating LTD and restoring potential size to control levels, experiments were also conducted to assess the importance of maintained stimulation for the induction of LTD by muscimol. In these experiments, the normal stimulation was turned off during the application of muscimol. This absence of synaptic activity did not modify the induction of LTD, as illustrated in Figure 4.

Neurosteroids

In order to assess the role of conventional $GABA_A$ receptors in the induction of LTD, without the need for inducing the neuronal hyperexcitability and spontaneous epileptiform bursting which results from the use of bicuculline or picrotoxin, two neurosteroids were used in an attempt to enhance the effect of activating $GABA_A$ receptors.

The natural steroid, 5α-pregnan-3α-ol-20-one and the steroidal anaesthetic agent, alphaxalone, were superfused over the slices at concentrations of 0.5 to 10 μM. Neither compound had any effect itself on population potentials at the lower concentrations (0.5–1 μM) but at 5 μM or above both were able to depress potential size. This activity is illustrated in Figure 5 for alphaxalone, but similar results were obtained for 5α-pregnan-3α-ol-20-one.

However, even at the lower concentrations both steroids proved able to potentiate the inhibitory activity of muscimol on population spikes; at 5 μM the effect of muscimol was increased almost 4 fold (Figure 5).

Both agents similarly potentiated the ability of muscimol to induce LTD. A normally ineffective concentration of 1 μM of the GABA agonist, applied for 10 min, for example, was able to induce LTD in the presence of only 1 μM 5α-pregnan-3α-ol-20-one or alphaxalone (Figure 5a, b). As for muscimol alone, increasing stimulation frequency to 1 Hz for 10 s was sufficient to reverse the LTD and restore potentials to their control size.

Antagonist and agonist of glutamate receptors

To examine the possible involvement of glutamate receptors in the effect of muscimol, experiments were performed using the N-methyl-D-aspartate (NMDA) antagonist (±)-2-amino-5-phosphonopentanonic acid (2-AP5; 300 μM), the mixed metabotropic and NMDA receptor antagonist (±)-2-amino-3-phosphonopropionic acid (2-AP3; 200 μM) and the selective antagonist of metabotropic receptors L-(+)-2-amino-3-phosphonopropionic acid [L(+)-AP3; 150 μM].

At 300 μM, 2-AP5 perfused for 10 min produced a depression of the population spike size from 10.59 ± 0.70 mV to 4.61 ± 0.47 mV, but this was readily reversible on washing out

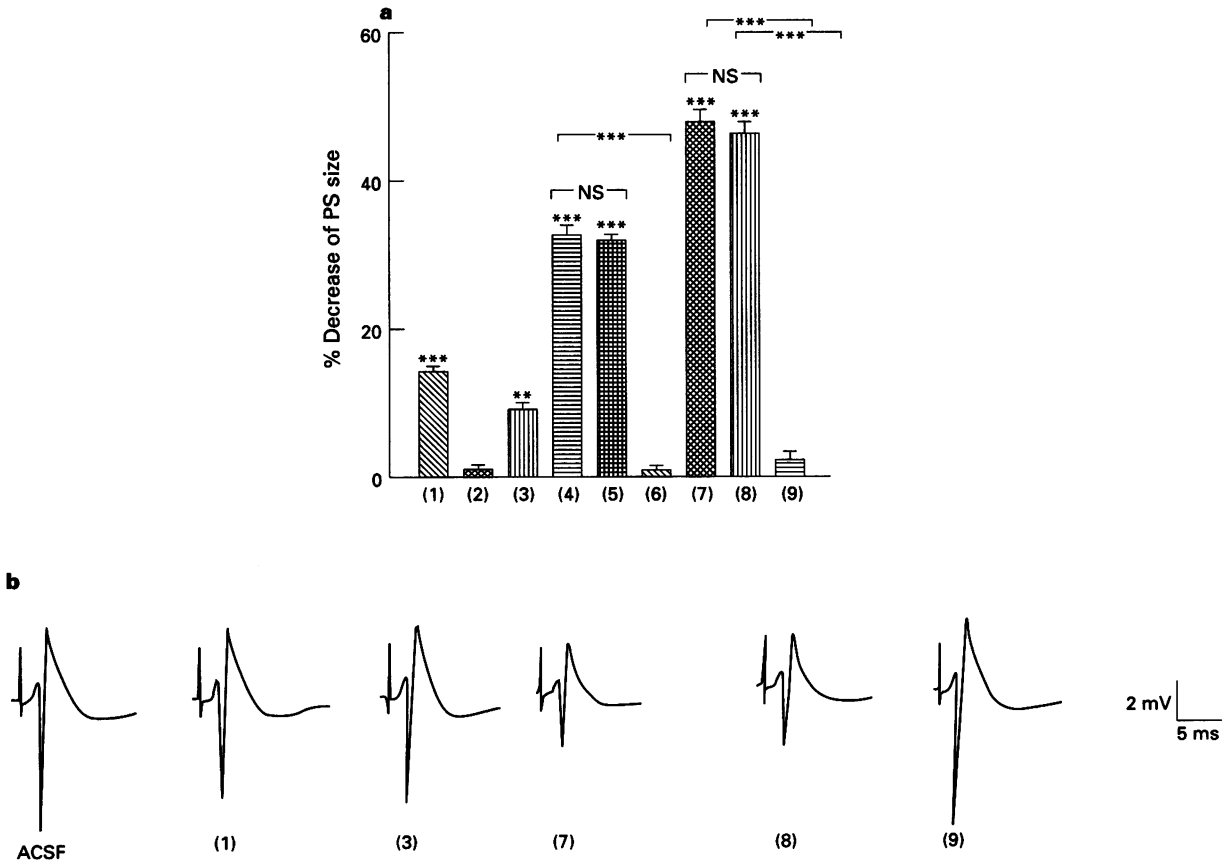

Figure 5 (a) Histogram summarising the effects of muscimol, alphaxalone, and combinations of muscimol with alphaxalone on the amplitude of orthodromic spikes. Alphaxalone alone has little effect on spike size, but potentiates the effect of muscimol. (1) Muscimol 1 μM; (2) alphaxalone 1 μM; (3) alphaxalone 5 μM; (4) muscimol 1 μM plus alphaxalone 1 μM; (5) wash; (6) wash plus increase of frequency; (7) muscimol 1 μM plus alphaxalone 5 μM; (8) wash; (9) wash plus increase of frequency. The columns indicate the mean ± s.e.mean ($n=4$). $^{**}P<0.01$; $^{***}P<0.001$. (b) Sample records of orthodromic potentials; calibrations 2 mV, 5 ms. Key as in (a).

the compound. When perfused simultaneously with muscimol 10 μM for 10 min, 2-AP5 did not prevent the induction of LTD, which was typically reversed by stimulation at 1 Hz.

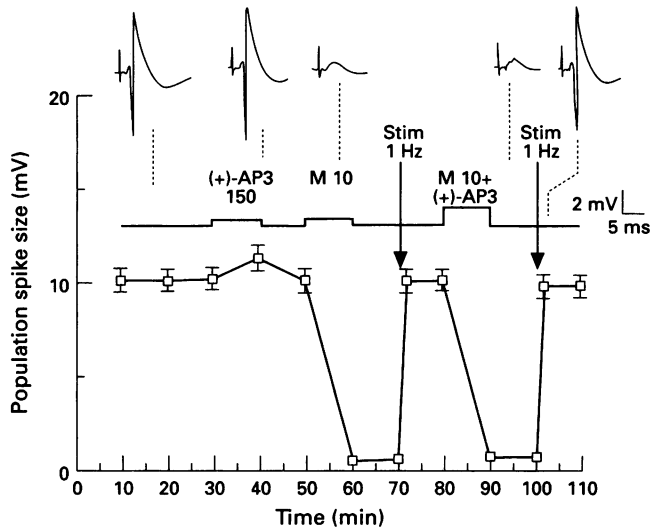

Figure 6 The effects of L-(+)-2-amino-3-phosphonopropionic acid [(+)-AP3], muscimol (M) and a combination of these on the amplitude of population spikes. The concentrations (μM) and time of application of the compounds are indicated above the data points. Slices were superfused with drug-free artificial CSF between agonist applications. When applied for 10 min at a concentration of 10 μM, muscimol was able to induce long-term depression (LTD). At the time indicated, the frequency of orthodromic stimulation was raised to 1 Hz, which reversed LTD and restored the potentials to control size. (+)-AP3 alone induced a small enhancement of spike size, but did not prevent the induction of LTD by muscimol, or its reversal by stimulation at 1 Hz. Data points are shown as mean ± s.e.mean (n=4). Sample records of orthodromic potentials are illustrated above the graphs; calibrations 2 mV and 5 ms.

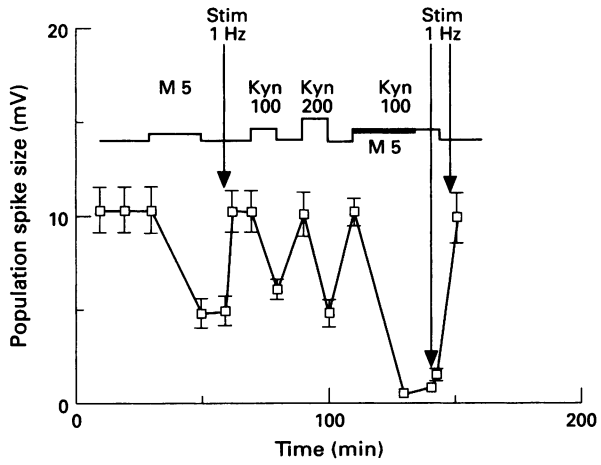

Figure 7 The effects of muscimol (M), kynurenic acid (Kyn) and a combination of these on the amplitude of population spikes. The concentrations (μM) and time of application of the compounds are indicated above the data points. Slices were superfused with drug-free artificial CSF between agonist applications. When applied for 20 min at a concentration of 5 μM, muscimol was able to induce long-term depression (LTD). At the time indicated, the frequency of orthodromic stimulation was raised to 1 Hz, which reversed LTD and restored the potentials to control size. Kynurenic acid alone reduced spike size. When applied together with muscimol, kynurenate prevented the reversal of LTD normally produced by 1 Hz stimulation. On washing out the kynurenate, reversal could rapidly be demonstrated as normal. Data points are shown as mean ± s.e.mean (n=4).

At 200 μM, 2-AP3, perfused for 10 min, produced a depression of population spike size from 10.01 ± 0.64 mV to 4.99 ± 0.1 mV, which was readily reversible on washing. When perfused simultaneously with muscimol 10 μM for 10 min, 2-AP3 did not prevent the induction of LTD.

At 150 μM, L-(+)-AP3 produced a small increase in the size of the population spike from 10.03 ± 0.66 mV to 11.17 ± 0.65 mV after 10 min perfusion. This increase was readily reversible on washing, and muscimol 10 μM was subsequently able to induce LTD. When L-(+)-AP3 was perfused simultaneously with muscimol, it did not prevent the induction of LTD or its reversal by stimulation at 1 Hz (Figure 6).

Treatment of the slices with the non-selective metabotropic receptor agonist, quisqualic acid at 10 and 50 μM and the selective metabotropic receptor agonist (1S, 3R)-ACPD 100 μM did not induce LTD whereas, both agents showed inhibitory effects on the population spike size. In addition to this, kynurenic acid, a broad spectrum antagonist of NMDA and non-NMDA receptors (100 and 200 μM) did not induce LTD but prevented termination of LTD by stimulation at 1 Hz (Figure 7).

Discussion

Long-term depression is an activity-dependent form of synaptic plasticity that may be important in learning and memory. The hippocampus is probably involved in processes such as learning and memory and hippocampal slices are a convenient model for investigating synaptic plasticity.

The present results demonstrate that the application of a selective $GABA_A$ agonist to hippocampal slices can induce a long-term depression of synaptically-evoked population potentials when stimulation was effected at a low frequency of 0.01 Hz. Increasing stimulation frequency to 1 Hz abolished the LTD. This stands in contrast to the work of Yang *et al.* (1994) who observed that LTD could be induced while stimulating at 1 Hz, but is in agreement with the work of other groups which have indicated that low frequency stimulation is more effective in inducing LTD in the hippocampus than in neocortex, striatum or nucleus accumbens (Bramham & Srebro, 1987; Staubli & Lynch, 1990; Artola & Singer, 1993; Lovinger *et al.*, 1993; Walsh, 1993; Linden, 1994). Indeed, in the present work we have found that muscimol alone is effective in inducing LTD even in the absence of afferent stimulation. This would seem to rule out a possible mechanism for LTD which involves an interaction between $GABA_A$ receptors and a synaptically released agent or a second messenger molecule released from postsynaptic sites in response to a neurotransmitter.

It has also been found that the ability of muscimol to produce LTD is not dependent on the extent of its inhibition of evoked potential size, since 5 μM for 20 min was able to induce LTD even though the potential was reduced by only 50%, whereas a relatively brief application of 10 μM muscimol did not induce LTD despite the profound reduction of spike size. Rather, the ability to induce LTD appears to be a function of the concentration of muscimol used and the duration of application: lower concentrations can be effective if in contact with the slices for a longer period. These various results would be consistent with the need for accumulation of a secondary compound which must attain a critical level in order to establish LTD, or the involvement of a time- and concentration-dependent modification of cell membrane properties.

It is of particular interest that activation of adenosine receptors which, like $GABA_A$ receptors, are capable of depressing neuronal excitability partly via the opening of chloride channels (Mager *et al.*, 1990; Akhondzadeh & Stone, 1994), was not able to induce LTD. Adenosine proved ineffective at concentrations which were able to abolish orthodromic potentials. This suggests that $GABA_A$ receptor activation involves some form of transduction system which is not activated indiscriminately by all neuronal inhibitory agents.

Pharmacology of the GABA receptors

Although muscimol is recognised as a selective agonist at $GABA_A$ receptors, its ability to induce this previously undescribed form of LTD demanded confirmation that it was not acting on a novel neuronal receptor, possibly unrelated to GABA. However, bicuculline reversed the LTD induced by muscimol at a time before excitability had increased sufficiently for the appearance of multiple population spikes.

The steroidal anaesthetic, alphaxalone and the related compound, 5-α-pregnan-3α-ol-20-one, had no effect themselves upon population spike amplitude at low micromolar concentrations, whereas they were both able, at these same concentrations, to potentiate significantly the depressant activity of muscimol on evoked spikes. At the higher concentrations tested here, 5 and 10 μM, both steroids had a direct depressant effect on evoked potentials, consistent with evidence that at these levels they can directly open chloride channels (Harrison & Simmonds, 1984; Turner & Simmonds, 1989; Puia *et al.*, 1991). When examined on LTD, both the steroids were able to potentiate the effects of muscimol to the extent that concentrations which had been insufficient to induce LTD did so in the presence of the steroids. As with the LTD observed normally in response to muscimol alone, the LTD produced by 1 μM muscimol plus steroids was also reversed by increasing the stimulation frequency to 1 Hz.

Role of glutamate receptors

Previously described forms of LTD appear to involve NMDA receptors and glutamate metabotropic receptors (or both) (Kano & Kato, 1987; Aroniadou & Teyler, 1991; Yang & Faber, 1991; Yang *et al.*, 1994). However, the failure of the NMDA receptor antagonist, 2-AP5, the mixed NMDA/metabotropic antagonist, 2-AP3 and the selective metabotropic antagonist L-(+)-AP3 to modify muscimol-induced LTD excludes a role of these glutamate receptors in the present paradigm. On the other hand, kynurenic acid, a glutamate receptor antagonist (Perkins & Stone, 1982; Stone, 1993), could prevent the reversal of the LTD that is induced by increasing stimulation to 1 Hz. This would suggest that the increase of stimulation frequency reverses muscimol-induced LTD as a result of the release of excitatory amino acids.

Physiological significance

While several previous reports of LTD have been concerned with heterosynaptic interactions (e.g. Zhuo *et al.*, 1994), the present data indicate that LTD can be established in a homosynaptic pathway, since it is evoked by perfusing slices with muscimol even during the absence of neuronal stimulation.

More importantly, the ability of $GABA_A$ receptor-activation to induce LTD raises the possibility that this is a major mechanism by which interneurones in the hippocampus may exert a long-term control over pyramidal cell excitability, in a frequency-dependent manner. Thus, in the presence of low frequency activation of the pyramidal neurones, interneuronal firing would be able to induce a long-lasting depression of excitability. However, this would be readily reversed as soon as a higher frequency input is delivered to the cells. Indeed, it may be that the reversal of pyramidal cell inhibition, readily established by interneuronal firing during periods of low hippocampal activity, is as critical to an understanding of learning and forgetting, as is the phenomenon of LTP.

In summary, the present work has presented a new protocol for inducing LTD through activation of $GABA_A$ receptors in the hippocampal slice. This activity is not shared by adenosine, but is reversed by 1 Hz stimulation or by bicuculline, and is potentiated by neurosteroids known to enhance the binding and postsynaptic hyperpolarization induced by classical $GABA_A$ receptors. Moreover, the lack of involvement of glutamate receptors in producing LTD, suggests that activation of $GABA_A$ receptors alone is sufficient to induce LTD. This indicates that the phenomenon described in the present report represents a novel type of long-term synaptic inhibition.

S.A. is sponsored by the Secretary of the Health and Medical Education of I.R. Iran, and wishes to thank Dr M.T. Jogatai for the support.

References

AKHONDZADEH, S. & STONE, T.W. (1994). Interactions between adenosine and $GABA_A$ receptors on hippocampal neurones. *Brain Res.*, **665**, 229–236.

ARONIADOU, V.A. & TEYLER, T.J. (1991). The role of NMDA receptors in long-term potentiation (LTP) and depression (LTD) in rat visual cortex. *Brain Res.*, **562**, 136–143.

ARTOLA, A. & SINGER, W. (1993). Long-term depression of excitatory synaptic transmission and its relationship to long-term potentiation. *Trends Neurosci.*, **16**, 480–487.

BASHIR, Z.I. & COLLINGRIDGE, G.L. (1992). NMDA receptors-dependent transient homo- and heterosynaptic depression in picrotoxin-treated hippocampal slices. *J. Neurosci.*, **4**, 485–490.

BRAMHAM, C.R. & SREBRO, B. (1987). Induction of long-term depression and potentiation by low and high frequency stimulation in the dentate areas of the anaesthetised rat. *Brain Res.*, **405**, 100–107.

CALABRESI, P., MAJ, R., MERCURI, N.B. & BERNARDI, G. (1992). Coactivation of D_1 and D_2 dopamine receptors is required for long-term synaptic depression in the striatum. *Neurosci. Lett.*, **142**, 95–99.

DUDEK, S.M. & BEAR, M.F. (1992). Homosynaptic long-term depression in area CA1 of hippocampus and the effects of NMDA receptor blockade. *Proc. Natl. Acad. Sci. U.S.A.*, **89**, 288–293.

EKEROT, C.F. & KANO, M. (1985). Long-term depression of parallel fibres synapses following stimulation of climbing fibres. *Brain Res.*, **342**, 357–360.

HARRISON, N.L. & SIMMONDS, M.A. (1984). Modulation of GABA receptor complex by a steroid anaesthetic. *Brain Res.*, **323**, 287–292.

ITO, M. (1989). Long-term depression. *Annu. Rev. Neurosci.*, **12**, 85–102.

KANO, M. & KATO, M. (1987). Quisqualic receptors are specifically involved in cerebellar synaptic plasticity. *Nature*, **325**, 276–279.

KIMURA, F., NISHIGORI, A., SHIROKAWA, T. & TSUMOTO, T. (1989). Long-term potentiation and N-methyl-D-aspartate receptor in the visual cortex of young rats. *J. Physiol.*, **414**, 125–144.

LEVY, W.B. & STEWARD, O. (1979). Synapses as associative memory elements in the hippocampal formation. *Brain Res.*, **175**, 233–245.

LINDEN, D.J. (1994). Long-term synaptic depression in the mammalian brain. *Neuron.*, **12**, 457–472.

LOVINGER, D.M., TYLER, E.C. & MERRITT, A.J. (1993). Short and long-term synaptic depression in rat neostriatum. *J. Neurophysiol.*, **70**, 1937–1949.

MAGER, R., FERRONI, S. & SCHUBERT, P. (1990). Adenosine modulate a voltage-dependent chloride conductance in cultured hippocampal neurons. *Brain Res.*, **532**, 58–62.

MAJEWSKA, M.D., HARRISON, N.L., SCHWARTZ, R.D., BARKER, J.L. & PAUL, S.M. (1988). Steroid hormone metabolites are barbiturate-like modulators of the GABA receptor. *Science N.Y.*, **232**, 1004–1007.

MULKEY, R.M. & MALENKA, R.C. (1992). Mechanisms underlying indication of homosynaptic long-term depression in area CA1 of the hippocampus. *Nature*, **9**, 967–975.

PENNARTZ, C.M.A., AMEERUN, R.F., GROENEWEGEN, H.J. & LOPES DE SILVA, F.H. (1993). Synaptic plasticity in an in vitro slice preparation of the rat nucleus accumbens. *Eur. J. Neurosci.*, **5**, 107–117.

PERKINS, M.N. & STONE, T.W. (1982). An iontophoretic investigation of the action of convulsant kynurenines and their interaction with the endogenous excitant quinolinic acid. *Brain Res.*, **247**, 184–187.

PUIA, G., VICINI, S., SEEBURG, P.H. & COSTA, E. (1991). Influence of recombinant γ-aminobutyric acid A-receptor subunit composition on the action of allosteric modulators of γ-aminobutyric acid gated Cl^- currents. *Mol. Pharmacol.*, **39**, 691–696.

STANTON, P.K. & SEJNOWSKI, T.J. (1989). Associative long-term depression in the hippocampus induced by Hebbian covariance. *Nature*, **339**, 215–218.

STAUBLI, U. & LYNCH, G. (1990). Stable depression of potentiated synaptic responses in the hippocampus with 1-5 Hz stimulation. *Brain Res.*, **513**, 113–118.

STONE, T.W. (ed.) (1991). *Adenosine in the Nervous System*. London: Academic Press.

STONE, T.W. (1993). The neuropharmacology of quinolinic and kynurenic acids. *Pharmacol. Rev.*, **45**, 309–379.

TURNER, J.P. & SIMMONDS, M.A. (1989). Modulation of the $GABA_A$ receptor complex by steroids in slices of rat cuneate nucleus. *Br. J. Pharmacol.*, **96**, 409–417.

WALSH, J.P. (1993). Depression of excitatory synaptic input in rat striatal neurons. *Brain Res.*, **680**, 123–128.

YANG, X.D. & FABER, D.S. (1991). Initial synaptic efficacy influences induction and expression of long-term changes in transmission. *Proc. Natl. Acad. Sci. U.S.A.*, **88**, 4299–4303.

YANG, X.D., CONNOR, J.A. & FABER, D.S. (1994). Weak excitation and stimultaneous inhibition induce long-term depression in hippocampal CAl neurons. *J. Neurophysiol.*, **71**, 1586–1590.

ZHUO, M., KANDEL, E.R. & HAWKINS, R.D. (1994). Nitric oxide and cGMP can produce synaptic depression or potentiation depending on the frequency of presynaptic stimulation in the hippocampus. *Neuroreport*, **5**, 1033–1036.

(Received October 27, 1994
Revised February 6, 1995
Accepted February 22, 1995)

British Journal of Pharmacology (1995) 115, 534-538

Effect of platelet-derived growth factor on voltage-operated calcium channels in rabbit isolated ear artery cells

[1]S. Wijetunge & A.D. Hughes

Department of Clinical Pharmacology, St. Mary's Hospital Medical School, Imperial College of Science Technology & Medicine, London W2 1NY

1 Platelet derived growth factor (PDGF), AB and BB isoforms (100 pM) increased calcium channel currents measured by whole cell voltage clamp technique in single vascular smooth muscle cells isolated from rabbit ear arteries.

2 Tyrphostin-23 (100 μM) a selective inhibitor of protein tyrosine kinases, reduced calcium channel currents. Pre-incubation with tyrphostin-23 prevented PDGF-AB induced increase in calcium channel currents. However, in these same cells 10 nM (+)-202791, a dihydropyridine calcium channel agonist, did increase calcium channel currents.

3 Bistyrphostin (10 μM), a selective inhibitor of epidermal growth factor (EGF)-kinase also reduced calcium channel currents and inhibited PDGF-AB-induced increases in calcium channel currents.

4 Genistein (100 μM) a selective inhibitor of tyrosine kinases, structurally unrelated to the tryphostins, also inhibited calcium channel currents and pre-incubation with genistein prevented the PDGF-AB-induced rise in calcium channel currents.

5 These results indicate that PDGF increases calcium channel currents in vascular smooth muscle. This action of PDGF probably involves a tyrosine kinase.

Keywords: Platelet-derived growth factor; calcium channels; vascular smooth muscle; tyrosine kinase; tyrphostin; bistyrphostin; genistein

Introduction

Platelet derived growth factor (PDGF) is a 28-32 kDa peptide which acts as a potent mitogen and chemotactic factor for many cells of mesenchymal origin including vascular smooth muscle cells (Ross, 1989; Bobik & Campbell, 1993). It is a dimeric glycoprotein formed of two distinct but related peptide chains; peptide A of molecular weight 14-18 kDa and peptide B (16 kDa). The two chains are linked by disulphide bonds to form two homologous (PDGF-AA and PDGF-BB) isoforms and a heterologous (PDGF-AB) isoform, all of which have been isolated from natural sources (Johnsson *et al.*, 1982; Stroobant & Waterfield, 1984; Heldin *et al.*, 1986). In the vasculature, PDGF is produced by several types of cells including platelets, endothelial cells, macrophages and vascular smooth muscle cells although each cell may produce different amounts of each isoform (Bobik & Campbell, 1993).

Membrane receptors for PDGF are 170-180 kDa, transmembrane spanning glycoproteins formed of two subunits, α and β (Hart *et al.*, 1988). Binding of the PDGF isoforms to the extracellular domain of the receptors promotes formation of dimers; αα, ββ and αβ, the dimer formed being dependent on the isomer of PDGF (Seifert *et al.*, 1989). The consequence of binding and dimerization of receptors is to activate a tyrosine kinase which is intrinsic to the receptor (Heldin *et al.*, 1989), leading to autophosphorylation of the receptor at multiple tyrosine residues of the intracellular domain (Pazin & Williams, 1992). The autophosphorylated receptors act as specific binding sites for a variety of cytoplasmic proteins containing src homologous (SH2) domains, which link the receptor to a variety of cytoplasmic and nuclear events (Pazin & Williams, 1992). The tyrosine kinase activity of PDGF receptors is known to be critical for the signal transduction pathway required for PDGF-induced mitogenesis (Ullrich & Schlessinger, 1990).

It has been found that PDGF elicits vascular smooth muscle contraction (Berk *et al.*, 1986; Berk & Alexander, 1989; Hughes, 1995). However, the mechanism by which PDGF causes contraction of vascular smooth muscle or whether there is a link between contraction and cell proliferation is not known. PDGF-induced vasoconstriction is reported to be unaffected by inhibition of 5-hydroxytryptamine (5-HT) receptors, α-adrenoceptors or cyclo-oxygenase (Berk *et al.*, 1986) and therefore probably involves a direct action of the PDGF receptor. The role of protein tyrosine kinase (PTK) in regulating calcium channels is also not clear, although we have previously shown that selective inhibitors of PTK such as tryphostin-23 and genistein, which inhibit tyrosine kinase by different mechanisms, inhibit voltage-operated calcium channels in rabbit ear artery cells (Wijetunge *et al.*, 1992).

The objective of this study was to investigate the effect of PDGF on the regulation of voltage-operated calcium channels in vascular smooth muscle cells and to study the role of tyrosine phosphorylation in the action of PDGF by use of selective PTK inhibitors, tryphostin-23, bistyrphostin and genistein.

Methods

Single smooth muscle cells were freshly dispersed from rabbit ear arteries by a method previously described (Benham & Bolton, 1986). Short (2-3 mm) segments of artery were incubated for 50 min in a modified physiological salt solution (PSS) containing (mM): NaCl 130, KCl 6, $CaCl_2$ 0.01, $MgCl_2$ 1.2, glucose 14, and HEPES 10.7 buffered to pH 7.2 with NaOH, 2 mg ml^{-1} bovine serum albumin, 1 mg ml^{-1} collagenase (130 u mg^{-1}), 0.5 mg ml^{-1} papain (15 u mg^{-1}) and 5 mM dithiothreitol. Cells were dispersed by mild agitation and resuspended after centrifugation in normal PSS containing 1.7 mM $CaCl_2$. Cells were stored on cover slips at 4°C and used within 4-6 h. Internal pipette solution contained (mM): NaCl 126, $MgCl_2$ 1.2, EGTA 2, MgATP 2, TEA 10, and HEPES 11 buffered to pH 7.2 with NaOH. Patch pipettes were made from borosilicate glass and had resistances of 3-5 MΩ.

Calcium channel currents were measured by the whole cell configuration of the patch clamp technique (Hamill *et al.*,

[1] Author for correspondence.

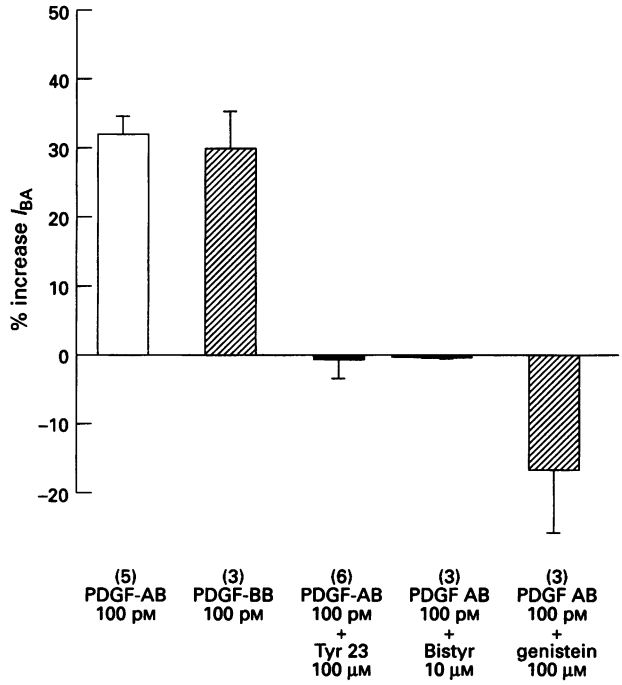

Figure 1 The effects of platelet-derived growth factor (PDGF) and inhibitors of tyrosine kinase on calcium channel currents in rabbit ear artery cells. Figure shows % increase in peak calcium current induced by PDGF, evoked by 200 ms depolarization to +10 mV from a holding potential of −60 mV. Columns represent means ± s.e.means of (*n*) observations. Bistyr, bistyrphostin; Tyr, tyrphostin.

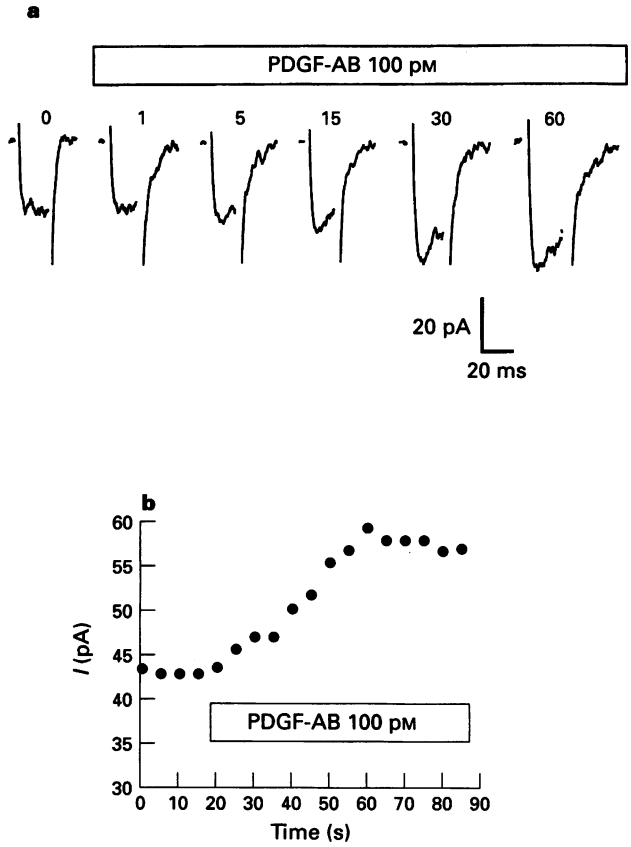

Figure 2 Onset of platelet-derived growth factor (PDGF)-AB induced increase of calcium currents. Currents were evoked every 1s using a 20 ms pulse to +10 mV from a holding potential of −60 mV. (a) Currents recorded in a single cell at 1 s, 5 s, 15 s, 30 s and 60s following addition of PDGF-AB are shown. (b) Each dot represents the average current recorded over a 5 s period from a single cell before and after addition of PDGF-AB. Period of exposure to PDGF-AB (100 pM) is indicated by the bar. Similar results were observed in four other cells.

1981) using a List EPC-7 amplifier and a Labmaster A/D interface board with commercially available software (Pclamp 5.5, Axon Instruments CA, U.S.A.) on an IBM compatible PC. The experiments were carried out in a 'high barium' solution ($BaCl_2$ 110 mM, HEPES 10 mM and buffered to pH 7.2 with TEA-OH) to increase the size of the inward current and to minimize calcium-dependent inactivation of currents (Aaronson *et al.*, 1988). Data were recorded on-line, or on digital audio tape with a DAT recorder (Biologic, France), and analysed off-line after analogue-to-digital conversion. The currents were digitally filtered at 2 kHz and leak currents were subtracted digitally, using average values of steady leakage currents elicited by a 10 mV hyperpolarizing pulse (Aaronson *et al.*, 1988). Drugs were applied by bath perfusion and exchange of bath perfusate was complete in approximately 1 s. All recordings were made at room temperature (22–25°C). A standard concentration of PDGF (100 pM) which was found to be a near maximal effective dose in previous studies (Hughes, 1995) was used. For the inhibitors, concentrations in excess of the IC_{50} from previous studies (Levitzki & Gilon, 1991; Wijetunge *et al.*, 1992) were used.

Drugs and chemicals

The following (source in parentheses) were used: (+)-202791 (isopropyl-4-(2,1,3-benzoxadiazol-4-yl)-1,4-dihydro-2,6-dimethyl-5-nitro-3-pyridine-carboxylate) (gift from Sandoz Switzerland), bistyrphostin (Calbiochem, Nottingham), bovine serum albumin (essentially fatty acid free) (Sigma, Dorset), collagenase (Worthington, Reading), genistein (Gibco BRL, Scotland), PDGF-AB and PDGF-BB (Calbiochem, Nottingham), papain (Sigma, Dorset), tyrphostin-23 (Calbiochem, Nottingham).

Statistics and data analysis

Data are presented as means ± s.e.means of (*n*) observations. Comparisons of data were made with a Wilcoxon signed ranks test for single paired comparisons. Multiple comparisons were made using non-parametric two-way analysis of variance by the Friedman test followed by the multiple comparison method described by Conover (1980). $P < 0.05$ was considered statistically significant.

Results

In cells voltage-clamped at a holding potential of −60 mV, 100 pM PDGF-AB increased the peak calcium channel currents evoked every 1s by a 200 ms step to +10 mV from 37.2 ± 3 to 49.6 ± 4 pA which corresponds to a 31.6 ± 2% ($P < 0.05$, $n = 5$) increase in current (Figure 1). To examine the onset of the effect of PDGF-AB, currents were evoked every 1 s by a 20 ms depolarizing step to + mV from a holding potential of −60 mV. The onset of this effect was rapid and observed within a minute of application of PDGF (Figure 2). Following washout of PDGF-AB, currents slowly recovered to levels similar to those seen prior to application of PDGF ($n = 2$). PDGF increased currents across the range of depolarizing test potentials from −50 mV to +60 mV (Figure 3 and Figure 4a). PDGF-BB (100 pM increased the peak calcium channel currents evoked every 1 s by a 200 ms step to +10 mV from 45.1 ± 2.0 to 58.0 ± 6.4 pA which corresponds to a 28.5 ± 6.0% increase in currents ($P < 0.05$, $n = 3$), (Figure 1).

Addition of 100 μM tyrphostin-23, a selective inhibitor of PTK, decreased peak calcium current evoked by a 200 ms

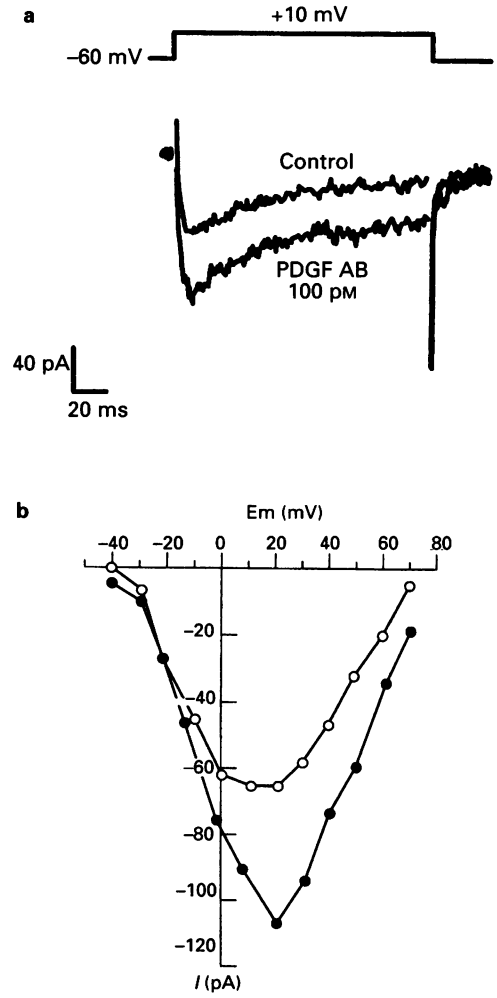

Figure 3 The effect of platelet-derived growth factor (PDGF)-AB on calcium channel currents in a rabbit ear artery cell. (a) Traces of control and PDGF-AB-induced currents evoked by a 200 ms depolarizing step to +10 mV from a holding potential of −60 mV. Control = current prior to application of PDGF-AB; PDGF-AB = current in the presence of PDGF-AB (100 pM). (b) The effect of 100 pM PDGF-AB on the peak current-voltage relationship. Currents were evoked by 200 ms depolarizing steps from −50 mV to +70 mV from the holding potential, −60 mV. (○) Control; (●) PDGF-AB 100 pM. Similar results were observed in four other cells.

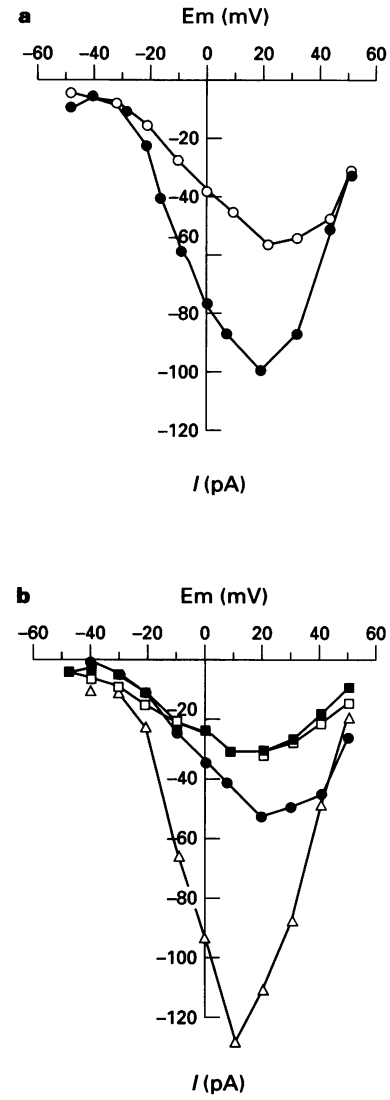

Figure 4 The effect of tyrphostin-23 on responses to platelet-derived growth factor (PDGF)-AB and (+)-202791. Plots show current-voltage relationships in a single rabbit ear artery cell. Current was evoked by a 200 ms depolarization steps from a holding potential of −60 mV. (a) (○) Control; (●) following PDGF-AB 100 pM. Similar results were shown in four other cells. (b) (●) Control; (□) tyrphostin-23 100 μM; (■) 100 pM PDGF-AB in the presence of 100 μM tyrphostin-23; (Δ) (+)-202791 10 nM in the presence of 100 μM tyrphostin-23. Similar results were observed in two more cells.

depolarization to +10 mV from a holding potential of −60 mV from 44.1 ± 2 to 29.6 ± 2 pA ($P < 0.05$, $n = 6$). Application of PDGF-AB (100 pM) in the presence of tyrphostin-23 had no statistically significant effect on calcium channel currents (Figure 1 and Figure 4b). However, addition of 10 nM (+)-202791 a dihydropyridine calcium channel agonist (Williams *et al.*, 1985) which acts independently of tyrosine kinase did increase calcium currents significantly in the same cells, despite the presence of tyrphostin-23 ($P < 0.01$, $n = 3$), (Figure 4b).

Bistyrphostin (10 μM), a selective inhibitor of epidermal growth factor (EGF)-kinase, reduced calcium current evoked by a 200 ms depolarization to +10 mV from a holding potential of −60 mV from 52.3 ± 2 to 41.5 ± 4 pA ($P < 0.05$, $n = 3$). Pre-incubation with bistyrphostin (10 μM) abolished the PDGF-AB induced increase in calcium current (Figure 1).

Genistein (100 μM) a selective tyrosine kinase inhibitor reduced calcium currents evoked by a 200 ms depolarization to +10 mV from a holding potential of −60 mV from 38.0 ± 5.0 to 16.5 ± 0.8 pA ($P < 0.05$, $n = 3$). PDGF-AB (100 pM) in the presence of genistein did not cause a significant rise in calcium channel currents (Figure 1).

Effects of PDGF-AB in the presence of tryphostin-23, bistyrphostin and genistein were tested in batches of cells that responded to PDGF-AB in the absence of these inhibitors.

Discussion

Voltage-operated calcium channels are a major route of calcium entry into vascular smooth muscle cells (Van Breeman & Saida, 1989) and play an important role in excitation-contraction coupling in response to most contractile agonists (Bolton, 1979). PDGF is known to contract vascular smooth muscle and increase intracellular Ca^{2+} by a mechanism involving voltage-operated calcium channels in rabbit isolated ear artery (Hughes, 1995). A rise in intracellular Ca^{2+} is also believed to be an important, though not an essential, mitogenic

signal evoked by several growth factors including PDGF (Magni *et al.*, 1991; Kobayashi *et al.*, 1994). The role of voltage-operated calcium channels in mediating this rise in intracellular Ca^{2+} in dividing cells is unclear, although calcium channel antagonists such as nifedipine and verapamil have been reported to inhibit smooth muscle proliferation (Nilsson *et al.*, 1985; Stein *et al.*, 1987). Protein phosphorylation on tyrosine residues is known to occur during both normal and malignant cell growth and in particular tyrosine phosphorylation has been shown to be critical in the mitogenic response of vascular smooth muscle cells (Tsuda *et al.*, 1991). Several other growth factors such as EGF, fibroblast growth factor (FGF) and insulin like growth factor-1 (IGF-1) also appear to act by binding to receptors which are themselves tyrosine kinases (Ullrich & Schlessinger, 1990). The possibility that tyrosine phosphorylation plays a critical role in other processes such as calcium entry and force development by smooth muscle is now also receiving attention (Hollenberg, 1994a). A recent report by Hollenberg showed that EGF causes contraction of gastric smooth muscle and that this was inhibited by selective PTK inhibitors tyrphostin and genistein (Hollenberg, 1994b). Intracellular Ca^{2+} ($[Ca^{2+}]_i$) was not measured in these studies, but $[Ca^{2+}]_i$ is known to regulate the tone of smooth muscle and EGF has been reported to cause Ca^{2+} influx into fibroblasts (Magni *et al.*, 1991). Recently it was reported by Selinfreund & Blair (1994) that IGF-1, which is also linked to a PTK caused a rapid increase in voltage-operated calcium channel currents in clonal pituitary cells. This action of IGF-1 was inhibited by genistein a selective inhibitor of tyrosine kinases. Similarly we found that two tyrphostins, tyrphostin-23 and bistyrphostin, also inhibited the stimulatory effect of PDGF on voltage-operated calcium channel currents in vascular smooth muscle cells.

Tyrphostins are selective inhibitors of tyrosine kinase which bind to the substrate binding site of the PTK (Gazit *et al.*, 1989). They are low molecular weight compounds which have been shown to inhibit the effects of PTK in a number of systems (Gazit *et al.*, 1989). Tryphostins have been shown to possess no significant effects on several serine or threonine protein kinases such as protein kinase C (PKC), cyclic AMP-dependent kinase or cyclic GMP-dependent kinase (Levitzki & Gilon, 1991). However some tyrphostins have been reported to interfere with other cellular processes and enzymes such as fatty acid synthesis, pyruvate oxidation and aldehyde dehydrogenase (Young *et al.*, 1993), therefore some caution with regard to their specificity towards PTK is needed. Nevertheless, tyrphostins have been shown to inhibit tyrosine autophosphorylation of the PDGF-receptor accompanying PDGF-induced proliferation in vascular smooth muscle cells (Bilder *et al.*, 1991). Tyrphostins have also been reported to inhibit rises in $[Ca^{2+}]_i$ and contraction in vascular smooth muscle at concentrations consistent with a selective action on tyrosine kinases (Sauro & Thomas, 1993; Hughes, 1995). In this study tyrphostin-23, reduced calcium currents as we have previously reported (Wijetunge *et al.*, 1992) at a concentration which inhibits PTKs (Gazit *et al.*, 1989). At present it is unclear whether the effect of tyrphostin-23 on calcium currents involves a tyrosine kinase but it is unlikely to represent a non-specific block of calcium channels because the dihydropyridine calcium channel agonist (+)-202791 (Williams *et al.*, 1985; Hughes *et al.*, 1990), which activates calcium channels by a mechanism independent of PTK increased currents in the presence of tyrphostin-23.

Bistyrphostin is a more selective and potent inhibitor of EGF and PDGF receptor-linked tyrosine kinases. Bistyrphostin alone, at a concentration in excess of that necessary to inhibit EGF-kinase had reduced calcium currents, although less potently than tyrphostin-23, and also blocked PDGF-AB-induced increases in calcium currents.

Genistein is an inhibitor of PTK which competitively binds to the ATP binding site on the PTK. It is an isoflavanoid compound and has been shown to inhibit specifically tyrosine kinases in a variety of systems without inhibiting the activities of serine and threonine-specific protein kinases (Akiyama *et al.*, 1987). Like the tyrphostins, genistein also prevented the PDGF-induced increase in calcium channel currents.

Together these results are consistent with tyrosine phosphorylation being an obligate signal in PDGF-induced increase in calcium channel currents.

The mechanism by which tyrosine phosphorylation may modulate calcium channel activity is not clear. It is possible that the tyrosine kinases may phosphorylate the voltage-operated calcium channel itself. At present, there is no evidence of tyrosine phosphorylation of the L-type calcium channel, though tyrosine phosphorylation of the nicotinic acetylcholine receptor channel and of a delayed rectifier potassium channel has been reported (Siegelbaum, 1994). Alternatively PDGF acting through a tyrosine kinase may modulate channel activity by activation of a second messenger system such as stimulation of PKC via phospholipase C-γ (PLCγ). Dimerization and autophosphorylation of growth factor receptors leads to activation of several cytoplasmic and nuclear events including activation of ras p21 (Schlessinger, 1993), mitogen-activated protein kinases (Cadena & Gill, 1992), PLCγ (Rhee, 1991), GTPase activating protein (GAP) for ras (Cadena & Gill, 1992) and phosphotidylinositol-3-kinase (Schlessinger & Ullrich, 1992). Each of these is believed to possess important second messenger roles, though in many cases their precise functions remain to be defined.

In conclusion PDGF, a potent mitogen for vascular smooth muscle, increases voltage-operated calcium channel currents. This effect is probably mediated by a process involving tyrosine phosphorylation. This action of PDGF may be important for Ca^{2+} entry into vascular smooth muscle cells in response to PDGF and therefore play an important role in the contractile and mitogenic action of this growth factor.

This work was supported by a grant from the Medical Research Council.

References

AARONSON, P.I., BOLTON, T.B., LANG, R.J. & MACKENZIE, I. (1988). Calcium currents in single isolated smooth muscle cells from the rabbit ear artery in normal calcium and high barium solutions. *J. Physiol.*, **405**, 57–75.

AKIYAMA, T., ISHIDA, J., NAKAGAWA, S., OGAWARA, H., WATANABE, S., ITOH, N., SHIBUYA, M. & FUKAMI, Y. (1987). Genistein, a specific inhibitor of tyrosine-specific protein kinases. *J. Biol. Chem.*, **262**, 5592–5595.

BENHAM, C.D. & BOLTON, T.B. (1986). Spontaneous transient outward currents in single visceral and vascular smooth muscle cells of the rabbit. *J. Physiol.*, **381**, 385–406.

BERK, B.C. & ALEXANDER, R.W. (1989). Vasoactive effects of growth factors. *Biochem. Pharmacol.*, **38**, 219–225.

BERK, B.C., ALEXANDER, R.W., BROCK, T.A., GIMBRONE, M.A. Jr., & WEBB, R.C. (1986). Vasoconstriction: a new activity for PDGF. *Science*, **232**, 87–90.

BILDER, G.E., KRAWIEC, J.A., MCVETY, K., GAZIT, A., GILON, C., LYALL, R., ZILBERSTEIN, A., LEVITZKY, A., PERRONE, M.H. & SCHREIBER, A.B. (1991). Tyrphostins inhibit PDGF-induced DNA synthesis and associated early events in smooth muscle cells. *Am. J. Physiol.*, **260**, C721–C730.

BOBIK, A. & CAMPBELL, J.H. (1993). Vascular derived growth factors: Cell biology, pathophysiology and pharmacology. *Pharmacol. Rev.*, **45**, 1–42.

BOLTON, T.B. (1979). Mechanisms of action of transmitters and other substances on smooth muscle. *Physiol. Rev.*, **59**, 606–718.

CADENA, D.L. & GILL, G.N. (1992). Receptor tyrosine kinases. *FASEB J.*, **6**, 2332–2337.

CONOVER, C.W. (1980). *Practical Non-Parametric Statistics*, 2nd Edition, New York: John Wiley.

GAZIT, A., YAISH, P., GILON, C. & LEVITZKI, A. (1989). Tyrphostins 1: synthesis and biological activity of protein tyrosine kinase inhibitors. *J. Med. Chem.*, **32**, 2344–2352.

HAMILL, O.P., MARTY, A., NEHER, E., SAKMANN, B. & SIGWORTH, F.J. (1981). Improved patch clamp techniques for high resolution current recording from cells and cell-free membrane patches. *Pflügers Arch.*, **391**, 85–100.

HART, C.E., FORSTROM, J.W., KELLY, J.D., SEIFERT, R.A., SMITH, R.A., ROSS, R., MURRAY, M.J. & BOWEN-POPE, D.F. (1988). Two classes of PDGF receptor recognize different isoforms of PDGF. *Science*, **240**, 1529–1531.

HELDIN, C.H., ERNLUND, A., ROSSMAN, C. & RONNSTRAND, L. (1989). Dimerization of B-type platelet derived growth factor receptors occurs after ligand binding and is closely associated with the receptor tyrosine kinase activation. *J. Biol. Chem.*, **264**, 8905–8912.

HELDIN, C.H., JOHNSSON, A., WENNERGREEN, S., WERNSTEDT, C., BETSHOLTZ, C. & WESTERMARK, B. (1986). A human osteosarcoma cell line secretes a growth factor structurally related to a homodimer of PDGF-A chains. *Nature*, **319**, 511–514.

HOLLENBERG, M.D. (1994a). The acute actions of growth factors in smooth muscle systems. *Life Sci.*, **54**, 223–235.

HOLLENBERG, M.D. (1994b). Tyrosine kinase pathways and the regulation of smooth muscle contractility. *Trends Pharmacol. Sci.*, **15**, 108–114.

HUGHES, A.D., HERING, S. & BOLTON, T.B. (1990). Evidence that agonist and antagonist enantiomers of the dihydropyridine PN 202791 act at different sites on the voltage-dependent calcium channel of vascular muscle. *Br. J. Pharmacol.*, **101**, 3–5.

HUGHES, A.D. (1995). Increase in tone and intracellular Ca^{2+} in rabbit isolated ear artery by platelet derived growth factor. *Br. J. Pharmacol.*, **114**, 138–142.

JOHNSSON, A., HELDIN, C.H., WESTERMARK, B. & WASTESON, A. (1982). Platelet-derived growth factor: identification of constituent polypeptide chains. *Biochem. Biophys. Res. Commun.*, **104**, 66–74.

KOBAYASHI, S., NISHIMURA, J. & KANAIDE, H. (1994). Cytosolic Ca^{2+} transients are not required for platelet derived growth factor to induce cell cycle progression of vascular smooth muscle cells in primary culture. *J. Biol. Chem.*, **269**, 9011–9018.

LEVITZKI, A. & GILON, C. (1991). Tyrphostins as molecular tools and potential antiproliferative drugs. *Trends Pharmacol. Sci.*, **12**, 171–174.

MAGNI, M., MELDOLESI, J. & PANDIELLA, A. (1991). Ionic events induced by epidermal growth factor. *J. Biol. Chem.*, **246**, 6329–6335.

NILSSON, J., SJOLUND, M., PALMBERG, L., VON EULER, A.M., JONZON, B. & THYBERG, J. (1985). The calcium antagonist nifedipine inhibits arterial smooth muscle proliferation. *Atherosclerosis*, **58**, 109–122.

PAZIN, M.J. & WILLIAMS, L.T. (1992). Triggering signalling cascades by receptor tyrosine kinases. *Trends Biochem. Sci.*, **17**, 374–378.

RHEE, S.G. (1991). Inositol phospholipid specific phospholipase C: interaction of the γ_1 isoform with tyrosine kinase. *Trends Biochem. Sci.*, **16**, 297–300.

ROSS, R. (1989). Platelet derived growth factor. *Lancet*, **i**, 1179–1182.

SAURO, M.D. & THOMAS, B. (1993). Tyrphostin attenuates platelet derived growth factor induced contraction in aortic smooth muscle through inhibition of protein tyrosine kinases. *J. Pharmacol. Exp. Ther.*, **267**, 1119–1125.

SCHLESSINGER, J. (1993). How receptor tyrosine kinases activate Ras. *Trends Biochem. Sci.*, **18**, 273–275.

SCHLESSINGER, J. & ULLRICH, A. (1992). Growth factor signalling by tyrosine kinases. *Neuron*, **9**, 383–391.

SEIFERT, R.A., HART, C.E., PHILLIPS, P.E., FORSTROM, J.W., ROSS, R., MURRAY, M.J. & BOWEN-POPE, D.F. (1989). Two different subunits associate to create isoform-specific platelet derived growth factor receptors. *J. Biol. Chem.*, **264**, 8771–8778.

SELINFREUND, R.H. & BLAIR, L.A.C. (1994). Insulin-like growth factor-1 induces a rapid increase in calcium currents and spontaneous membrane activity in clonal pituitary cells. *Mol. Pharmacol.*, **45**, 1215–1220.

SIEGELBAUM, S.A. (1994). Ion channel control by tyrosine phosphorylation. *Current Biol.*, **4**, 242–245.

STEIN, O., HALPERIN, G. & STEIN, Y. (1987). Long term effects of verapamil on aortic smooth muscle cells cultured in the presence of hypercholesterolaemic serum. *Arteriosclerosis*, **7**, 585–592.

STROOBANT, P. & WATERFIELD, M.D. (1984). Purification and properties of porcine platelet derived growth factor. *EMBO J.*, **3**, 2963–2967.

TSUDA, T., KAHAWARA, Y., SHII, K., KOIDE, M., ISHIDA, Y. & YOKOYAMA, M. (1991). Vasoconstrictor induced protein-tyrosine phosphorylation in cultured vascular smooth muscle cells. *FEBS. Lett.*, **285**, 44–48.

ULLRICH, A. & SCHLESSINGER, J. (1990). Signal transduction by receptor tyrosine kinase activity. *Cell*, **61**, 203–212.

VAN BREEMAN, C. & SAIDA, K. (1989). Cellular mechanisms regulating Ca^{2+} in smooth muscle. *Annu. Rev. Physiol.*, **51**, 315–329.

WIJETUNGE, S., AALKJAER, C., SCHACTER, M. & HUGHES, A.D. (1992). Tyrosine kinase inhibitors block calcium channel currents in vascular smooth muscle cells. *Biochem. Biophys. Res. Commun.*, **189**, 1620–1623.

WILLIAMS, J.S., GRUPP, I.L., DUMONT, L., SCHWARTZ, A., YATANI, A., HAMILTON, S. & BROWN, A.M. (1985). Profile of the oppositely acting enantiomers of the dihydropyridine 202791 in cardiac preparations: receptor binding, electrophysiological and pharmacological studies. *Biochem. Biophys. Res. Commun.*, **131**, 13–21.

YOUNG, S.W., POOLE, R.C., HUDSON, A.T., HALESTRAP, A.P., DENTON, R.M. & TAVARE, J.M. (1993). Effects of tyrosine kinase inhibitors on protein-kinase independent systems. *FEBS Lett.*, **316**, 278–282.

(Received November 30, 1994
Revised February 10, 1995
Accepted February 17, 1995)

British Journal of Pharmacology (1995) 115, 539-545

Enhancement by GABA of the association rate of picrotoxin and *tert*-butylbicyclophosphorothionate to the rat cloned $\alpha1\beta2\gamma2$ $GABA_A$ receptor subtype

Glenn H. Dillon, [1]Wha Bin Im, Don B. Carter & Denise D. McKinley

CNS Diseases Research, The Upjohn Company, Kalamazoo, MI 49001, U.S.A.

1 We examined how γ-aminobutyric acid (GABA) influences interaction of picrotoxin and *tert*-butylbicyclophosphorothionate (TBPS) with recombinant rat $\alpha1\beta2\gamma2$ $GABA_A$ receptors stably expressed in human embryonic kidney cells (HEK293), as monitored with changes in Cl^- currents measured by the whole-cell patch clamp technique.

2 During application of GABA (5 μM) for 15 s, picrotoxin and TBPS dose-dependently accelerated the decay of inward GABA-induced currents (a holding potential of −60 mV under a symmetrical Cl^- gradient). The drugs, upon preincubation with the receptors, also reduced the initial current amplitude in a preincubation time and concentration-dependent manner. This indicates their interaction with both GABA-bound and resting receptors.

3 The half maximal inhibitory concentration for picrotoxin and TBPS at the beginning of a 15 s GABA (5 μM) pulse was several times greater than that obtained at the end of the pulse. GABA thus appears to enhance picrotoxin and TBPS potency, but only at concentrations leading to occupancy of both high and low affinity GABA sites, i.e., 5 μM. Preincubation of the receptors with the drugs in the presence of GABA at 200 nM, which leads to occupancy of only high affinity GABA sites in the $\alpha1\beta2\gamma2$ subtype, produced no appreciable change in potency of picrotoxin or TBPS. This indicates that they preferentially interact with multiliganded, but not monoliganded receptors, unlike U-93631, a novel ligand to the picrotoxin site, which has higher affinity to both mono- and multiliganded receptors than resting receptors.

4 The time-dependent decay and preincubation time-dependent reduction of initial amplitude of GABA-induced Cl^- currents followed monoexponential time courses, and time constants thus obtained displayed a linear relationship with drug concentration. Analysis of the data using a kinetic model with a single drug site showed that GABA (5 μM) enhanced the association rate for picrotoxin and TBPS nearly 100 fold, but their dissociation rate only 10 fold. The dissociation rate obtained from current recovery from picrotoxin or TBPS block yielded nearly identical values to the above analysis.

5 We conclude that picrotoxin and TBPS interact with both resting and GABA-bound receptors, but their affinity for the latter is about 10 times greater than that for the former, largely due to a markedly increased association rate to the multiliganded receptors (but not monoliganded ones). This and our earlier study with U-93631 improves our understanding of functional coupling between GABA and picrotoxin sites, which appears to be useful in characterizing the mode of interaction for various picrotoxin site ligands.

Keywords: $GABA_A$ receptor; recombinant receptor; picrotoxin; *tert*-butylbicyclophosphorothionate; patch clamp; desensitization; Cl^- channel

Introduction

Picrotoxin and *tert*-butylbicyclophosphorothionate (TBPS) share the same binding site on the $GABA_A$ receptor/channel complex, presumably near the mouth of the Cl^- channel (Squires *et al.*, 1983), and inhibit neuronal GABA-activated Cl^- currents (Bowery *et al.*, 1976; Squires *et al.*, 1983; Ramanjaneyulu & Ticku, 1984; Smart & Constanti, 1986). Recent electrophysiological studies have shown an acceleration of Cl^- current decay (time-dependent block) by the drugs in whole cell patches and a reduction in the channel open probability without altering mean open times in single channel recordings (Hamann *et al.*, 1990; Newland & Cull-Candy, 1992). This supports the hypothesis that picrotoxin and TBPS stabilize the $GABA_A$ receptor in a non-conducting state rather than acting as direct open channel blockers (Takeuchi & Takeuchi, 1969; Barker *et al.*, 1983; Segal & Barker, 1984; Akaike *et al.*, 1985; Smart & Constanti, 1986; Newland & Cull-Candy, 1992). Also, their time-dependent block of the Cl^- channel implies that they interact favourably with GABA-bound receptors in the open state(s), although not as open channel blockers. However, the question of how GABA influences interactions of picrotoxin and TBPS with $GABA_A$ receptors, has not been well understood, partly because most previous studies have been carried out with $GABA_A$ receptors consisting of multiple and functionally diverse subtypes, such as those $GABA_A$ receptors in cultured primary neurones (Barker *et al.*, 1983; Segal & Barker, 1984; Akaike *et al.*, 1985; Yakushiji *et al.*, 1987; Newland & Cull-Candy, 1992), those expressed in *Xenopus* oocytes with injection of isolated brain mRNA (Van Renterghem *et al.*, 1987; Woodward *et al.*, 1992), or those receptors at the invertebrate neuromuscular junction (Takeuchi & Takeuchi, 1969; Constanti, 1978; Smart & Constanti, 1986). In this study, we investigated the effect of GABA on interaction of picrotoxin and TBPS with cloned rat $\alpha1\beta2\gamma2$ $GABA_A$ receptors. This study was also prompted by our recent finding that U-93631 [4-dimethyl-3-t-butylcarboxyl-4,5-dihydro(1,5-a)imidazoquinoxaline], a novel ligand to the picrotoxin site (Dillon *et al.*, 1994), preferentially interacts with mono- or multi-liganded $GABA_A$ receptors over resting ones (Dillon *et al.*, 1993). Our present results demonstrate that picrotoxin and TBPS interact with both resting and GABA-bound receptors,

[1] Author for correspondence.

but their affinity for the latter is about 10 times greater than that for the former, largely due to a markedly increased association rate to the multiliganded receptors (but not monoliganded ones, unlike U-93631).

Methods

Cloned GABA$_A$ receptors

Rat $\alpha 1$, $\beta 2$, and $\gamma 2$ subunits of the GABA$_A$ receptor were expressed in human embryonic kidney cell lines (HEK293) as described previously (Hamilton *et al.*, 1993). Briefly, the cells were transfected with plasmids containing cDNA and a plasmid encoding G418 resistance. After 2 weeks of selection in 1 mg ml^{-1} G418, resistant cells were assayed by Northern blotting for the ability to synthesize GABA$_A$ receptor mRNAs. Positive cells for appropriate subunits were used for electrophysiology. All studies were conducted on cells expressing the $\alpha 1\beta 2\gamma 2$ receptor configuration.

Electrophysiology

The whole-cell configuration of the patch clamp technique (Hamill *et al.*, 1981) was used to study GABA-induced Cl$^-$ currents. Patch pipettes were constructed from borosilicate glass (Kimax-51, Kimble Products, Toledo) pulled (Flaming/Brown, P-80/PC, Sutter Instrument Co., Novato, CA, U.S.A.) and fire-polished to a tip impedence of 0.5 to 2 MΩ when filled with the following pipette solution (in mM): CsCl 140, EGTA 4, HEPES 10, $MgCl_2$ 0.4, pH 7.2. Coverslips containing the cultured cells were transferred to a small chamber (1 ml) on the stage of an inverted light microscope (Nikon), and superfused continuously (2 ml min^{-1}) with the following external solution (in mM): NaCl 125, KCl 5.5, $CaCl_2$ 3.0, $MgCl_2$ 0.8, HEPES-Na 20, dextrose 25, pH 7.3.

Whole-cell currents were recorded with an Axopatch-1D amplifier (Axon Instruments, Foster City, CA, U.S.A.) equipped with a CV-4 headstage. A bath headstage (BH-1) was used to compensate for bath potentials. GABA-induced Cl$^-$ currents were monitored on an oscilloscope and stored on a computer using commercially available software (PCLAMP, Axon Instruments). All studies were conducted at room temperature, with the cells voltage-clamped at −60 mV.

Chemicals

GABA and picrotoxin were purchased from Sigma Chemical Co. (St. Louis, MO, U.S.A.); TBPS was purchased from Research Biochemicals International (Natick, MA, U.S.A.).

Experimental protocol

GABA was dissolved in the external solution (above) and applied to the target cell through a U-tube positioned within 100 μm of the cell. In experiments where preincubation with drugs was required, the cells were bathed in the external solution containing the drugs (picrotoxin or TBPS) at indicated concentrations for 2–20 min (5 min unless noted otherwise). Typically, to monitor GABA response, a GABA pulse (5 μM) was applied before, during and after drug incubation. In experiments examining the kinetic parameters for picrotoxin (PX) and TBPS in the presence of GABA, the GABA pulse applied during incubation was carried out with a mixture of GABA and the incubated drug, so the concentration of the drug was not altered during the pulse.

Data analysis

We examined the effect of picrotoxin and TBPS on peak current and rate of current decay. The time constant for current decay (tau) was obtained by fitting a one-exponential function to time course-current profiles with the aid of a computer software programme (Origin, Microcal Software).

Results

Effect of picrotoxin and TBPS on GABA-induced Cl$^-$ currents

We examined the effects of picrotoxin at various concentrations on GABA (5 μM)-induced Cl$^-$ current in recombinant rat GABA$_A$ receptors of the $\alpha 1\beta 2\gamma 2$ subtype (Figure 1a), using

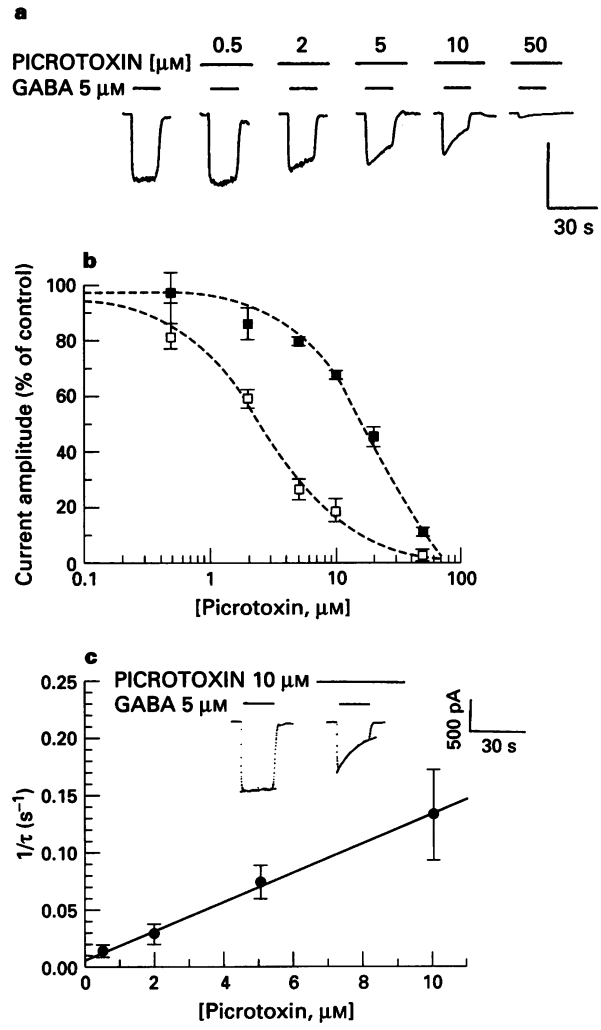

Figure 1 Effect of picrotoxin at various concentrations on GABA-induced Cl$^-$ currents. (a) Picrotoxin decreased the peak amplitude and increased the decay rate of 5 μM GABA-induced Cl$^-$ currents in the $\alpha 1\beta 2\gamma 2$ subtype of GABA$_A$ receptors. Because of the slow current recovery from picrotoxin block at the drug concentrations above 0.5 μM, data were collected from multiple cells, and the differences between cells were adjusted by normalizing to the 5 μM GABA response in each cell. The vertical calibration bar represents 500 pA in the standard cell. (b) Relative changes in the current amplitude at the beginning and end of GABA application were plotted as a function of picrotoxin concentration, then analyzed using a logistic equation (see text). (■) Without GABA; (□) with GABA. Application of GABA for 15 s shifted the IC_{50} for picrotoxin from 17 to 2.4 μM with no effect on the slope. (c) The decay phase of Cl$^-$ currents was fitted with a monoexponential function and the reciprocal of the time constants ($1/\tau$) was plotted as a function of picrotoxin concentration. The solid line represents the best fit to the equation $1/\tau = k_{+1}[PX] + k_{-1}$ with the k_{+1} (the association rate) and the k_{-1} (dissociation rate) values as follows: $k_{-1} = 5.78 \times 10^{-3}\,s^{-1}$; $k_{+1} = 1.31 \times 10^{4}\,M^{-1}s^{-1}$; $K_d = 443$ nM. The inset shows examples of monoexponential fits of the decaying GABA current with and without picrotoxin.

the whole-cell patch clamp technique. The receptors were preincubated with picrotoxin for 5 min and then activated with a 15 s pulse of 5 μM GABA. In the dose-response profiles (Figure 1a), application of picrotoxin was not cumulative; at low picrotoxin concentrations, the cell was washed until the full GABA response was recovered, but at high picrotoxin concentrations a new cell was used because of extremely slow current recovery (see below). Differences in current amplitude between cells were normalized to the 5 μM GABA response. Picrotoxin reduced both the initial peak amplitude of GABA-induced Cl^- currents, and accelerated the current decay (Figure 1a). Changes in the current amplitude at the beginning and the end of GABA application were measured in the presence of picrotoxin at various concentrations, and the data were analyzed with a logistic equation, $I/I_{max} = [\text{picrotoxin}]^n/([\text{picrotoxin}]^n + IC_{50}^n)$, where I is Cl^- current amplitude and n is the slope factor (Figure 1b). Note that the values for the initial current amplitude were obtained upon extrapolation of the decay phase to zero time point using a monoexponential function (see below). From the analysis, we obtained a half maximal inhibitory concentration for picrotoxin of 17 and 2.4 μM at the beginning and the end of GABA pulse, respectively, with a slope factor (n) of 1.1 ± 0.2 and 0.9 ± 0.2, respectively. The increased potency of picrotoxin in the presence of GABA certainly indicates enhancement of picrotoxin interaction with GABA-bound receptors. Furthermore, the reduction of the initial current amplitude appears to reflect its interaction with unliganded resting receptors, because the magnitude of the current reduction was dependent on the duration of incubation time with picrotoxin and its concentration (see below). Similar GABA-dependent changes were observed with TBPS (Figure 2). The half maximal concentration for TBPS was 2.3 μM and 0.8 μM at the beginning and end, respectively, of a 15 s GABA application (Figure 2b). The slope factor 1.2 ± 0.2, was not changed.

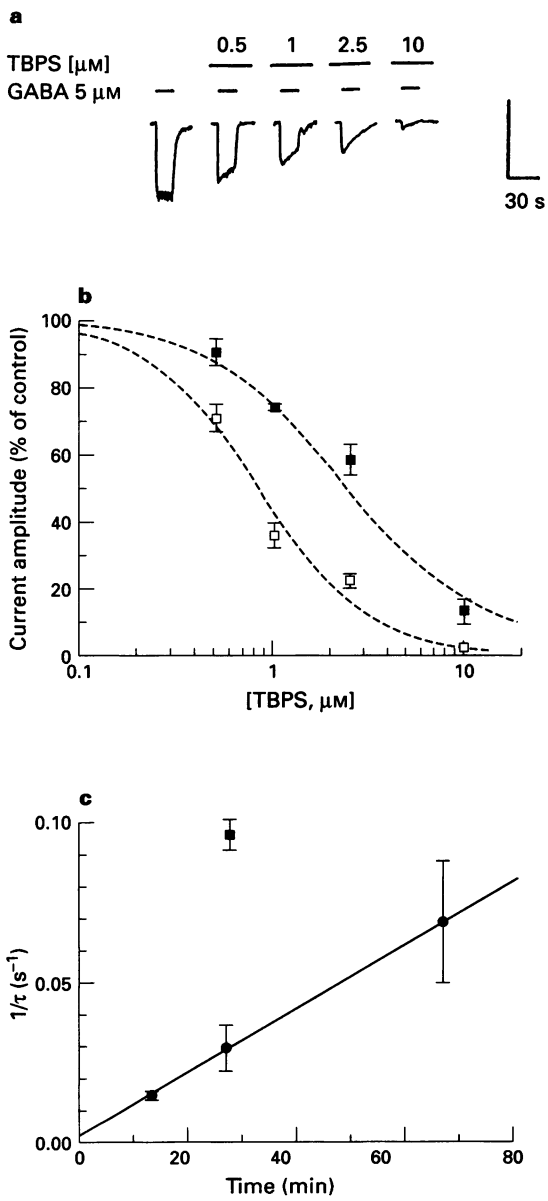

Figure 2 Effects of TBPS at various concentrations on GABA-induced Cl^- currents. The figures represent similar studies to Figure 1, but with TBPS instead of picrotoxin. (a) Current traces with TBPS at various concentrations. (b) Dose-response curves at the beginning (■) and the end (□) of the GABA pulse. Application of GABA for 15 s shifted the IC_{50} for TBPS from 2.4 to 0.8 μM, with no significant change in the slope factor. (c) The decay phase of Cl^- currents was fitted with a monoexponential function and the values of 1/tau were plotted as a function of picrotoxin concentration. The solid line represents the best fit to the equation $1/\text{tau} = k_{+1}[\text{TBPS}] + k_{-1}$, yielding the association and dissociation rates as follows: $k_{-1} = 1.81 \times 10^{-3}\,s^{-1}$; $k_{+1} = 2.71 \times 10^{4}\,M^{-1}s^{-1}$; $K_d = 67$ nM.

GABA at 5 μM, as in the above experiments, occupied both high and low affinity GABA sites of the α1β2γ2 subtype (K_d of 83 and 7100 nM, respectively, Pregenzer *et al.*, 1993), albeit partial. We tested whether occupation of only high affinity GABA sites is sufficient for enhancing picrotoxin potency. To test this hypothesis, the receptors were preincubated with 5 μM picrotoxin or 2.5 μM TBPS in the presence or absence of 200 nM GABA, a concentration at which approximately 70% of high affinity GABA sites were occupied during a 5 min-preincubation period at room temperature. Preincubation with 200 nM GABA did not alter the potency of picrotoxin or TBPS on current induced by subsequent 5 μM GABA. For example, in picrotoxin-treated cells, the initial peak amplitude (after normalization to the control) was reduced to 77 ± 5 and 69 ± 8% with and without 200 nM GABA, respectively, and in TBPS-treated cells, 59 ± 3 and 58 ± 5%, respectively. Likewise, the rate of current decay (time-dependent block) was not altered by preincubation with 200 nM GABA. GABA (5 μM)-induced currents from picrotoxin-treated cells decayed at rates of 12.3 ± 0.7 and 14.7 ± 2.1 s, respectively, with and without 200 nM GABA. Currents from TBPS-treated cells also decayed at comparable rates with and without 200 nM GABA present (10.5 ± 1.4 and 14.4 ± 3.4 s, respectively). Under the same conditions, GABA (200 nM) enhanced the potency of U-93631 (a novel ligand to picrotoxin site) on blocking whole cell Cl^- currents, but did not induce single channel events in cell-attached patches (Dillon *et al.*, 1993). This property differentiates picrotoxin and TBPS from U-93631, another time-dependent blocker of GABA-induced Cl^- currents (Dillon *et al.*, 1993), which preferably interacts with both mono- and multiliganded receptors over unliganded receptors. Overall, our present data suggest that picrotoxin and TBPS preferably interact with multiliganded (probably open channels) over monoliganded or resting receptors.

Effects of GABA on kinetic parameters for picrotoxin and TBPS binding

The decay of GABA-induced Cl^- current accelerated as a function of picrotoxin concentration (Figure 1a) and followed an exponential time course (Figure 1c). A minimal model for picrotoxin interaction with GABA-bound receptors is

$$R^* + D \underset{k_{-1}}{\overset{k_{+1}}{\rightleftharpoons}} R^*D$$

where R* is the GABA-bound receptor, D is picrotoxin, R*D is the drug-bound, non-conducting receptor, and k_{+1} and k_{-1} are the drug association and dissociation rates, respectively.

This model is justified because the current decay in the presence of 5 μM GABA alone was minimal (see traces in Figure 1a, 1c, $\tau > 200$ s) (Dillon *et al.*, 1993), and the picrotoxin-bound receptors which were produced during resting states display a very slow dissociation rate for picrotoxin (see below) and are not likely to be activated with 5 μM GABA pulses. According to this model, the time constant for current decay (τ) is equal to $1/(k_{+1}[D]+k_{-1})$. The plot of $1/\tau$ vs the concentration of picrotoxin (Figure 1c) was fitted with a linear regression. We obtained a value of 5.78×10^{-3} s^{-1} for k_{-1} (from the y-intercept), 1.31×10^4 M^{-1} s^{-1} for k_{+1} (from the slope), and the dissociation constant ($K_d = k_{-1}/k_{+1}$) of 0.44 μM for picrotoxin in the presence of GABA (5 μM). Similar plots for TBPS yielded k_{-1} of 1.81×10^{-3} s^{-1}, k_{+1} of

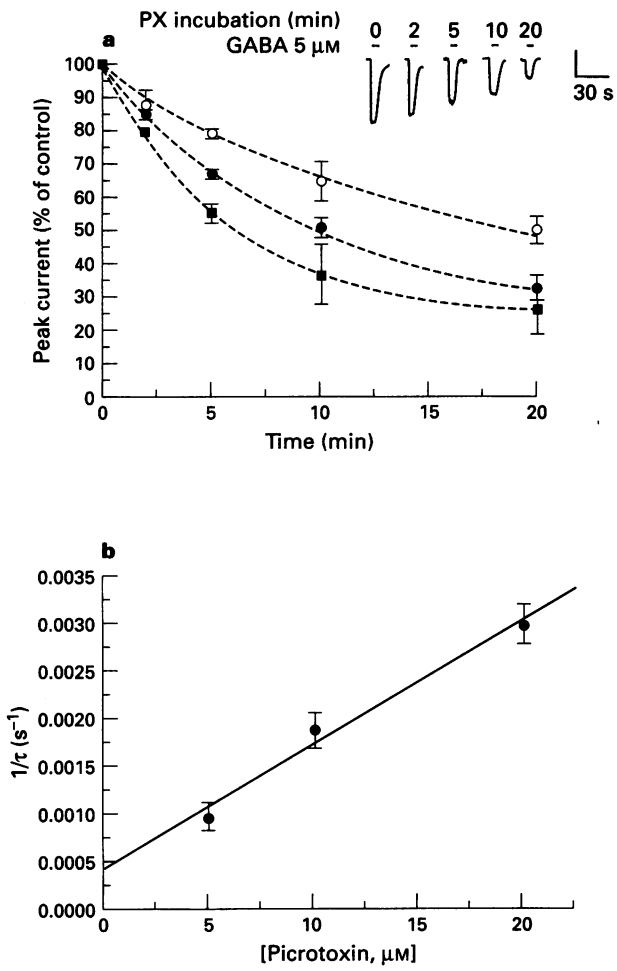

Figure 3 Reduction of the initial amplitude of GABA-induced Cl^- currents by picrotoxin in a preincubation time- and drug concentration-dependent manner. (a) Receptors were incubated for 2, 5, 10 or 20 min with picrotoxin at 5 (○), 10 (●) and 20 μM (■). A 5 μM GABA pulse for 5 s was applied at the end of each incubation period to monitor the change in the initial amplitude of the currents. No picrotoxin was included in the GABA pulse solution and no time-dependent decay was observed. Between the pulses, the cells was washed free of picrotoxin or a new cell was employed. The differences between the cells were normalized as described in Figure 1 legend. The relative changes in the initial current amplitude were plotted as a function of preincubation time at a given picrotoxin concentration, and the plots were fitted with a single exponential function. (b) The reciprocal of the time constants from the monoexponential fitting was plotted as a function of picrotoxin concentrations. The solid line represents $1/\tau = k_1$ [Drug] $+ k_{-1}$ with the association and the dissociation rate for picrotoxin in the absence of GABA: $k_{-1} = 4.2 \times 10^{-4}$ s^{-1}; $k_{+1} = 1.3 \times 10^2$ M^{-1} s^{-1}; $K_d = 3.2$ μM.

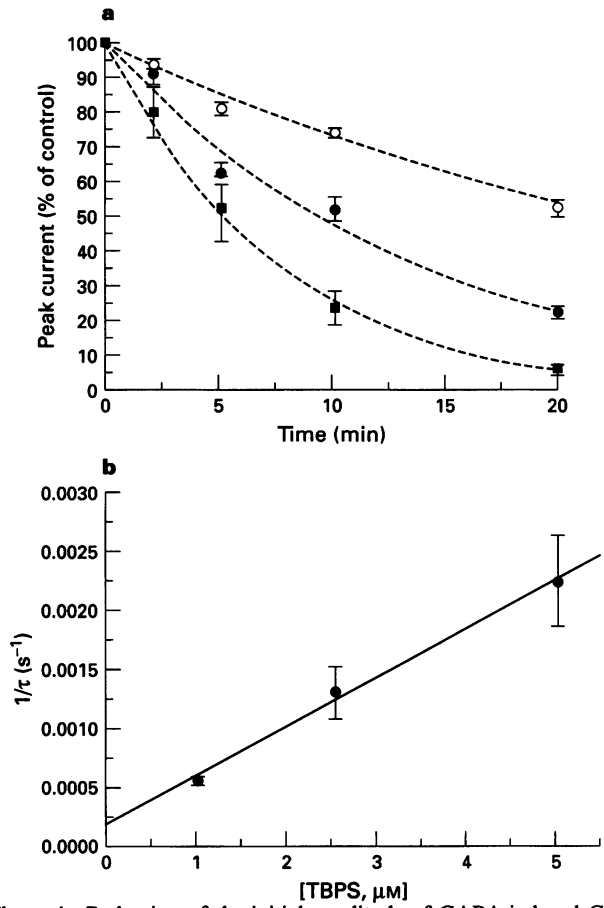

Figure 4 Reduction of the initial amplitude of GABA-induced Cl^- currents by TBPS in a preincubation time- and concentration-dependent manner. The same studies as shown in Figure 3, but with TBPS instead of picrotoxin. (a) Receptors were incubated for 2, 5, 10 or 20 min with TBPS at 1 (○), 2.5 (●) and 5 μM (■). Relative changes in the initial amplitude of GABA-induced Cl^- currents were plotted as a function of preincubation time. The dotted lines represent monoexponential fitting of the data. (b) The reciprocal of the time constants from the monoexponential fitting was plotted as a function of TBPS concentrations. The solid line represents $1/\tau = k_1$ [Drug] $+ k_{-1}$ with the association and the dissociation rate for TBPS in the absence of GABA: $k_{-1} = 1.8 \times 10^{-4}$ s^{-1}; $k_{+1} = 4.2 \times 10^2$ M^{-1} s^{-1}; $K_d = 429$ nM.

Table 1 Effect of GABA on kinetic interactions of picrotoxin and *tert*-butylbicyclophosphorothionate (TBPS) with cloned rat $GABA_A$ receptors of the α1β2γ subtype (see text for details describing how rate constants were determined.)

	Assoc. rate (k_{+1})	*Dissoc. rate* (k_{-1})	K_d (k_{-1}/k_{+1})
Picrotoxin			
No GABA	1.3×10^2 M^{-1} s^{-1}	4.2×10^{-4} s^{-1}	3.2 μM
GABA 5 μM	1.3×10^4 M^{-1} s^{-1}	5.8×10^{-3} s^{-1}	443 nM
TBPS			
No GABA	4.2×10^2 M^{-1} s^{-1}	1.8×10^{-4} s^{-1}	429 nM
GABA 5 μM	2.7×10^4 M^{-1} s^{-1}	1.8×10^{-3} s^{-1}	67 nM

2.71×10^4 M^{-1} s^{-1} and a K_d of 67 nM for TBPS in the presence of 5 μM GABA (Figure 2b and c).

Interaction of picrotoxin and TBPS with $GABA_A$ receptors in the absence of GABA

As noted above, preincubation of the receptors with both picrotoxin and TBPS led to concentration-dependent decreases in the initial current amplitude of GABA-induced currents. The reduction was also dependent on the duration of preincubation period (Figure 3a, inset). For example, picrotoxin at 20 μM reduced the amplitude of the Cl^- currents by 20, 50, 75 and 95% with the preincubation period of 2, 5, 10 and 20 min, respectively. The IC_{50} value, therefore, decreased from much greater than 20 μM with the 2 min preincubation period to approximately 20, 10 and 5 μM as the preincubation period was prolonged to 5, 10 and 20 min, respectively. In order to obtain the reaction rates and the dissociation constant, the relative changes (as normalized to 5 μM GABA response) in the initial current amplitude were plotted as a function of preincubation time of 2, 5, 10 and 20 min (Figure 3a), and the plots were fitted with one exponential function (dotted lines). The time constant decreased linearly as a function of picrotoxin concentration during the preincubation period (Figure 3b). For instance, the τ values were 17 ± 2, 9 ± 0.9, and 6 ± 0.4 min in the presence of picrotoxin at 5, 10 and 20 μM, respectively. This indicates interaction of picrotoxin (and TBPS, see below) with resting receptors in a monophasic manner. Again, one can analyze the data using the same model with a single drug site by simply replacing the term for GABA-bound with resting receptors. Thus, the plot of $1/\tau$ vs picrotoxin concentrations yielded a k_{+1} of 1.3×10^2 M^{-1} s^{-1}, a k_{-1} of 4.2×10^{-4} s^{-1} and a K_d of 3.2 μM for picrotoxin interaction with resting receptors. These results show that GABA markedly enhanced the association rate of picrotoxin to the receptors by 100 fold, and at the same time increased the dissociation rate 14 fold, leading to a 7 fold decrease in the K_d. Similar analysis of TBPS interaction with resting receptors demonstrated comparable effects; i.e., the association rate of TBPS was 64 fold slower with resting receptors than with multiliganded receptors, while the dissociation rate was decreased 10 fold. A summary of the effects of GABA on the kinetic parameters for picrotoxin and TBPS is given in Table 1.

GABA current recovery from picrotoxin and TBPS block

Dissociation rates for picrotoxin and TBPS were also measured from GABA current recovery from picrotoxin and TBPS block (Figure 5). Picrotoxin at 5 μM reduced GABA-induced Cl^- currents by approximately 75% at the end of GABA pulse, including both the initial peak reduction from preincubation and the time-dependent block (Figure 5a). Upon removal of picrotoxin from the superfusing medium, current recovery was monitored with a GABA (5 μM) pulse every 5 min. The amplitude of Cl^- currents progressively increased as a function of time. The plot of fractional recovery vs time (Figure 5b) followed a monoexponential time course (dotted line in Figure 5b) with a time constant of 36.6 min in this cell. The average τ from several cells was 33 ± 4 min. This monoexponential recovery suggests the existence of one population of picrotoxin-bound receptors with a dissociation rate ($1/\tau$) of 5×10^{-4} s^{-1}, which was nearly identical to that observed in the absence of GABA (4×10^{-4} s^{-1}). Current recovery time TBPS (1 μM) also followed a monoexponential time course with a time constant of 38 ± 2 min, which corresponds to a dissociation rate of 4.4×10^{-4} s^{-1}. Again, this value was similar to the value derived using the model (see Figure 4), further strengthening the one-site model.

Previous studies using other $GABA_A$ receptor populations have reported that frequent applications of GABA at high concentrations (0.5 to 2.5 Hz and [GABA] $\geq$ 40 μM, Van Renterghem *et al.*, 1987; Newland & Cull-Candy, 1992)

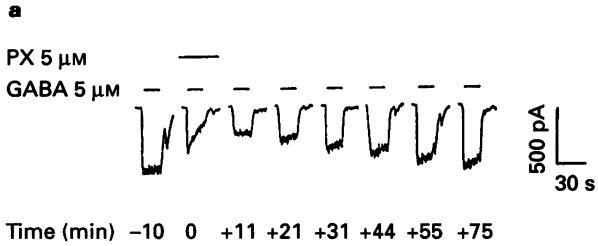

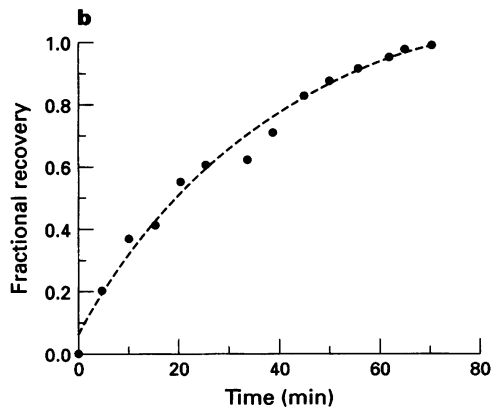

Figure 5 Time course profile for the recovery of GABA-induced Cl^- currents from picrotoxin block. (a) Treatment of the receptors with 5 μM picrotoxin for 5 min reduced Cl^- currents by nearly 70%. Following the treatment, a 5 μM GABA pulse (10 s) was applied every 5 min to monitor the current recovery. (b) Fractional recovery of the current was plotted as a function of time, and the dotted line represents monoexponential fitting of the data. The time constant from this experiment was 36.6 min, and its reciprocal is nearly identical to the dissociation rate obtained from the kinetic analysis of picrotoxin-induced reduction of the initial amplitude of Cl^- currents using the one-site model as described in the legend for Figure 3 and in the text.

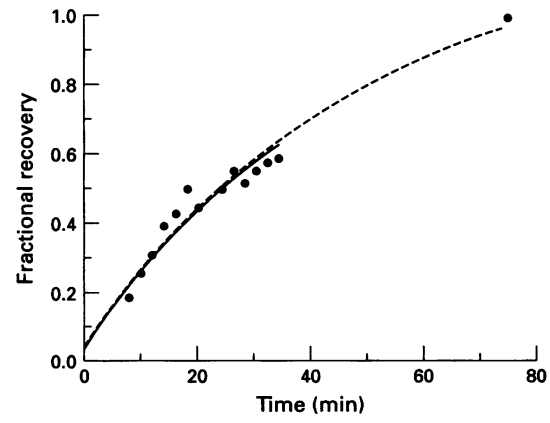

Figure 6 A plot illustrating no use-dependent recovery of GABA-induced Cl^- currents from TBPS block under our experimental conditions. Following treatment with 2 μM TBPS for 5 min, a 5 μM GABA pulse (10 s) was applied every 2 min during the first 36 min period of recovery, and then followed with a final pulse 40 min later. The recovery time course followed an exponential time course during the first 36 min with frequent GABA pulses (solid line), and during the last 40 min without a GABA pulse (dotted line). No appreciable difference was detected in the recovery time constant with ($\tau = 31 \pm 6$ min) or without ($\tau = 38 \pm 2$ min) GABA pulses.

accelerate the recovery of channel activity from picrotoxin or TBPS inhibition (use-dependent recovery). Although the frequency (every 5 min) and the concentration (5 μM) we employed in the current study were well below those used for analysis of use-dependent recovery, we tested whether GABA application at a higher frequency (i.e. every 2 min) affects the dissociation rate for TBPS (Figure 6). This is to ensure not to overestimate the dissociation rate. The fractional increase in Cl^- current with GABA pulses applied every 2 min (as opposed to every 5 min) during the first 30 min was fitted with an exponential function with a time constant of 31 ± 6 min, which was not significantly different from that obtained with GABA pulses applied every 5 min ($\tau = 38 \pm 2$ min, see above). Furthermore, the recovery for the next 40 min without GABA pulses appeared to continue at the same rate, because the final recovery point (70 min from the beginning) reached the level predicted with the same exponential function for the first 30 min (dotted line in Figure 6). It appears that GABA (5 μM) applications at the frequency we used here did not appreciably facilitate the dissociation of TBPS from the $\alpha 1\beta 2\gamma 2$ receptor, which was probably in an inactivated state.

Discussion

In this study, we examined interactions of picrotoxin and TBPS with cloned $\alpha 1\beta 2\gamma 2$ $GABA_A$ receptors by investigating their action on GABA-induced Cl^- currents. The drugs, upon preincubation with the receptors, reduced the initial current amplitude, and also produced a time-dependent block of the currents during GABA application. The time (or preincubation time)- and concentration-dependency for the two modes of drug action indicate that picrotoxin and TBPS interact with both resting and GABA-bound receptors. Analysis of the data using a model with a single drug site (see the Results section) revealed that their association rate for GABA-bound receptors was about 100 times (100 fold for PX, 64 fold for TBPS) greater than that for resting receptors, while the dissociation rate, on the other hand, was increased only about 10 fold in GABA-bound receptors. The dissociation rates were also obtained from current recovery from picrotoxin or TBPS block, and were close to the values obtained with the kinetic model in the absence of GABA. Thus, the net effect of the rate changes was to increase the affinity of picrotoxin or TBPS to GABA-bound receptors by approximately 10 fold. Also, it is apparent from our analysis that the time-dependent block of Cl^- currents by picrotoxin or TBPS could be primarily explained by the large increase in their association rate to the site on GABA-bound receptors. According to the model, the time constant for decay is equal to $1/(k_{+1}[D]+k_{-1})$, and at micromolar concentration of the drugs, the term $k_{+1}[D]$ becomes predominant because of relatively small dissociation rates, even in GABA-bound receptors.

Furthermore, the increase in picrotoxin potency (largely due to the association rate) was observed in the presence of 5 μM GABA, but not 200 nM GABA, a concentration at which only high affinity GABA sites are occupied (by approximately 70%). This indicates a preferable interaction of picrotoxin (and TBPS) with multiple-liganded, but not with monoliganded $GABA_A$ receptors (those with only high affinity sites occupied), and is consistent with the view that picrotoxin and TBPS gain much better access to their binding site, probably when the channel enters the open configuration. Although the drugs displayed greater affinity for GABA-bound open channels, they may not act as open channel blockers, but rather as allosteric modulators. This proposal is supported by the work of others (Barker *et al.*, 1983; Segal & Barker, 1984; Smart & Constanti, 1986; Van Renterghem *et al.*, 1987; Woodward *et al.*, 1992; Newland & Cull-Candy, 1992). In these studies, however, changes in kinetic parameters for picrotoxin or TBPS were not quantitatively evaluated, although enhanced association of picrotoxin or TBPS with $GABA_A$ receptors, cloned or native, has been suggested. Further evaluation of previous results is difficult because the subtype composition of $GABA_A$ receptor preparations has not been defined in these studies; i.e., *Xenopus* oocytes injected with either chick brain mRNA (Van Renterghem *et al.*, 1987) or bovine poly(A)$^+$ RNA (Woodward *et al.*, 1992), mouse cultured spinal neurones (Barker *et al.*, 1983), rat cultured hippocampal neurones (Segal & Barker, 1984), or lobster neuromuscular junction (Smart & Constanti, 1986). Overall, the results appear to be in agreement with the view that picrotoxin and TBPS preferentially interact with multiliganded open $GABA_A$ receptors and stabilize the receptors in a desensitized or closed (inactivated) state.

Recently, we discovered a new ligand for the picrotoxin site, U-93631 ([4-dimethyl-3-*t*-butylcarboxl-4,5-dihydro(1,5-a)imidazoquinoxaline]), which also induced a time-dependent block of GABA-activated Cl^- currents in the $\alpha 1\beta 2\gamma 2$ subtype and competitively displaced [^{35}S]-TBPS binding (Dillon *et al.*, 1993; 1994). However, U-93631 is different from picrotoxin and TBPS in that the drug displayed an enhanced interaction with receptors which were preincubated with 200 nM GABA, and thus largely monoliganded. This suggests that although U-93631 shares overlapping binding domains with picrotoxin and TBPS, it also has a unique domain(s) which seems to be coupled to the high affinity GABA sites.

In summary, picrotoxin and TBPS interact with both resting and GABA-bound receptors (multiliganded ones), but their affinity for the latter is about 10 times greater than that for the former, largely due to a markedly increased association rate to the multiliganded receptors. In particular, their enhanced interaction with only multiliganded, but not with monoliganded $GABA_A$ receptors, differentiates them from a new picrotoxin site ligand, U-93631, which showed a higher affinity for monoliganded and multiliganded receptors as compared to nonliganded receptors. It appears that conformational coupling between the GABA and picrotoxin sites is useful in characterizing various picrotoxin site ligands.

References

AKAIKE, N., HATTORI, K., OOMURA, Y. & CARPENTER, D.O. (1985). Bicuculline and picrotoxin block γ-aminobutyric acid-gated Cl^- conductance by different mechanisms. *Experientia.*, **41**, 70–71.

BARKER, J.L., MCBURNEY, R.N. & MATHERS, D.A (1983). Convulsant-induced depression of amino acid responses in cultured mouse spinal neurones studied under voltage clamp. *Br. J. Pharmacol.*, **80**, 619–629.

BOWERY, N.G., COLLINS, J.F. & HILL, R.G. (1976). Bicyclic phosphorous esters that are potent convulsants and GABA antagonists. *Nature*, **261**, 601–603.

CONSTANTI, A. (1978). The 'mixed' effect of picrotoxin on the GABA dose/conductance relation recorded from lobster muscle. *Neuropharmacol.*, **17**, 159–167.

DILLON, G.H., IM, H.K., HAMILTON, B.J., CARTER, D.B., GAMMILL, R.B., JUDGE, T.M. & IM, W.B. (1993). U-93631 causes rapid decay of GABA-induced Cl^- current in recombinant rat $GABA_A$ receptors. *Mol. Pharmacol.*, **44**, 860–865.

DILLON, G.H., IM, W.B., PREGENZER, J.F., CARTER, D.B. & HAMILTON, B.J. (1995). U-93631 is a novel ligand to the picrotoxin site on $GABA_A$ receptors, and decreases single-channel open probability. *J. Pharmacol. Exp. Ther.*, **272**, 597–603.

HAMANN, M., DESARMENIEN, M., VANDERHEYDEN, P., PIGUET, P. & FELTZ, P. (1990). Electrophysiological study of *tert*-butylbicyclophosphorothionate-induced block of spontaneous chloride channels. *Mol. Pharmacol.*, **37**, 578–582.

HAMILL, O.P., MARTY, A., SAKMANN, E. & SIGWORTH, F.J. (1981). Improved patch-clamp techniques for high-resolution current recording from cells and cell-free membrane patches. *Pflügers Arch.*, **391**, 85–100.

HAMILTON, B.J., LENNON, D.L., IM, H.K., SEEBURG, P.H. & CARTER, D.B. (1993). Stable expression of cloned rat $GABA_A$ receptor subunits in a human kidney cell line. *Neurosci. Lett.*, **153**, 206–209.

NEWLAND, C.F. & CULL-CANDY, S.G. (1992). On the mechanism of action of picrotoxin on GABA receptor channels in dissociated sympathetic neurones of the rat. *J. Physiol.*, **447**, 191–213.

PREGENZER, J.F., IM, W.B., CARTER, D.B. & THOMSEN, D.R. (1993). Comparison of interactions of [^{3}H]muscimol, *t*-butylbicyclophosphoro[^{35}S]thionate, and flunitrazepam with cloned γ-aminobutyric $acid_A$ receptor subtypes of the α1β2 and the α1β2γ2. *Mol. Pharmacol.*, **43**, 801–806.

RAMANJANEYULU, R. & TICKU, M.K. (1984). Binding characteristics and interactions of depressant drugs with [^{35}S]*t*-butylbicyclophosphorothionate, a ligand that binds to the picrotoxinin site. *J. Neurochem.*, **42**, 221–229.

SEGAL, M. & BARKER, J.L. (1984). Rat hippocampal neuron in culture: voltage-clamp analysis of inhibitory synaptic connections. *J. Neurophysiol.*, **52**, 469–487.

SMART, T.G. & CONSTANTI, A. (1986). Studies on the mechanism of action of picrotoxinin and other convulsants at the crustacean muscle GABA receptor. *Proc. R. Soc, B.*, **227**, 191–216.

SQUIRES, R.F., CASIDA, J.E., RICHARDSON, M. & SAEDURUP, E. (1983). [^{35}S]t-butylbicyclo-phosphorothionate binds with high affinity to brain specific sites coupled to gamma-aminobutyric acid-A and ion recognition sites. *Mol. Pharmacol.*, **23**, 326–336.

TAKEUCHI, A. & TAKEUCHI, N. (1969). A study of the action of picrotoxin on the inhibitory neuromuscular junction of the crayfish. *J. Physiol.*, **205**, 377–391.

VAN RENTERGHEM, C., BILBE, G., MOSS, S., SMART, T.G., CONSTANTI, A., BROWN, D.A. & BARNARD, E.A. (1987). GABA receptors induced in *Xenopus* oocytes by chick brain mRNA: evaluation of TBPS as a use-dependent channel-blocker. *Mol. Brain Res.*, **2**, 21–31.

WOODWARD, R.M., POLENZANI, L. & MILEDI, R. (1992). Characterization of bicuculline/baclofen-insensitive γ-aminobutyric acid receptors expressed in *Xenopus* oocytes I. Effects of Cl^{-1} channel inhibitors. *Mol. Pharmacol.*, **42**, 165–173.

YAKUSHIJI, T., TOKUTOMI, N., AKAIKE, N. & CARPENTER, D.O. (1987). Antagonists of GABA responses, studied using internally perfused frog dorsal root ganglion neurons. *Neurosci.*, **22**, 1123–1133.

(Received September 20, 1994
Revised February 16, 1995
Accepted February 23, 1995)

British Journal of Pharmacology (1995) 115, 547

Erratum

Br. J. Pharmacol. (1994) **113,** 1147-1152.

F.L.M. Ricciardolo, J.A. Nadel, S. Yoshihara & P. Geppetti. Evidence for reduction of bradykinin-induced bronchoconstriction in guinea-pigs by release of nitric oxide

In the above paper the author Shigemi Yoshihara's name was spelt incorrectly. The publishers would like to apologise for any inconvenience caused. The correct spelling appears above.

British Journal of Pharmacology

VOLUME 115 (3) JUNE 1995

STOCKTON

BRITISH JOURNAL OF PHARMACOLOGY

The *British Journal of Pharmacology* welcomes contributions in all fields of experimental pharmacology including neuroscience, biochemical, cellular and molecular pharmacology. The Board of Editors represents a wide range of expertise and ensures that well-presented work is published as promptly as possible, consistent with maintaining the overall quality of the journal.

Edited for the British Pharmacological Society by

A.T. Birmingham
(Chairman)

R.W. Horton **W.A. Large**
(Secretaries)

Submission of manuscripts: Manuscripts (two copies) should be sent to The Editorial Office, British Journal of Pharmacology, St. George's Hospital Medical School, Cranmer Terrace, London SW17 0RE.

Authors should consult the Instructions to Authors and the Nomenclature Guidelines for Authors in Vol. **114,** 245–255. These Instructions and Guidelines also appear with the journal Index for Volumes **111–113,** 1994. A checklist of the essential requirements is summarised in each issue of the journal, or as the last page of the issue.

The *British Journal of Pharmacology* is published by Stockton Press, a division of Macmillan Press Ltd. It is the official publication of the British Pharmacological Society.

Scope The *British Journal of Pharmacology* is published twice a month. It welcomes contribution in all field of experimental pharmacology including neuroscience, biochemical, cellular and molecular pharmacology. The Board of Editors represents a wide range of expertise and ensures that well-presented work is published as promptly as possible, consistent with maintaining the overall quality of the journal

This journal is covered by Current Contents, Excerpta Medica, BIOSIS, CABS and Index Medicus.

Editorial Manuscripts (plus two copies) and all editorial correspondence should be sent to: The Editorial Office, British Journal of Pharmacology, St George's Hospital Medical School, Cranmer Terrace, London SW17 0RE, UK. Tel: +44 (0)181 767 6765; Fax: +44 (0)181 767 5645.

Advertisements Enquiries concerning advertisements should be addressed to: Michael Rowley, Hasler House, High Street, Great Dunmow, Essex CM6 1AP, UK. Tel: +44 (0)1371 874613; Fax: +44 (0)1371 872273.

Publisher All business correspondence, supplement enquiries and reprint requests should be addressed to British Journal of Pharmacology, Stockton Press, Houndmills, Basingstoke, Hampshire RG21 2XS, UK. Tel: +44 (0)1256 29242; Fax: +44 (0)1256 810526. Publisher: Marija Vukovojac. Editorial Assistant: Alice Ellingham. Production Controller: Karen Stuart.

Subscriptions – EU/Rest of World Subscription price per annum (3 volumes, 24 issues) £620, rest of world £820 (Airmail), £685 (Surface mail) or equivalent in any other currency. Orders must be accompanied by remittance. Cheques should be made payable to Macmillan Magazines and sent to: The Subscription Department, Macmillan Press Ltd, Houndmills, Basingstoke, Hampshire RG21 2XS, UK. Where appropriate, subscribers may make payments into UK Post Office Giro Account No. 519 2455. Full details must accompany the payment. Subscribers from EU territories should add sales tax at the local rate.

Subscriptions – USA USA subscribers call toll free 1-800-221-2123 or send check/money order/credit card details to: Stockton Press, 49, West 24th Street, New York, NY 10010; Tel: 212 627 5757, Fax: 212 627 9256. USA annual subscription rates: $1230 Airmail; $1030 Surface (Institutional/Corporate); $225 (Individual making personal payment).

British Journal of Pharmacology (ISSN 0007–1188) is published twice a month by Macmillan Press Ltd, c/o Mercury Airfreight International Ltd, 2323 Randolph Avenue, Avenel, NJ 07001, USA. Subscription price for institutions is $1030 per annum (surface). 2nd class postage is paid at Rahway NJ. Postmaster: send address corrections to Macmillan Press Ltd, c/o Mercury Airfreight International Ltd, 2323 Randolph Avenue, Avenel NJ 07001.

Reprints of any article in this journal are available from Stockton Press, Houndmills, Basingstoke, Hampshire RG21 2XS, UK. Tel: +44 (0)1256 29242; Fax: +44 (0)1256 810526.

ISSN 0007–1188

PREPARATION OF MANUSCRIPTS

Authors are strongly recommended to read the full *Instructions to Authors* and *Nomenclature Guidelines for Authors* (*Br. J. Pharmacol.* 1995, **114,** 245–255) before submitting a manuscript for publication in the *British Journal of Pharmacology*. The manuscript and cover letter should be checked against the following list before mailing.

The original and one copy of the manuscript must be supplied. Manuscripts must be typed in double-line spacing on one side of A4 paper, in type not smaller than 12 characters per inch or 10 point. Both copies to include Tables and a set of labelled Figures. One set of Figures without numbers or letters is also to be included. The text to be arranged in the following subsections:

1. **Title**—To have no more than 150 characters on a separate page, which should also include a Short Title (50 characters maximum) and the name and address of the author for correspondence.
2. **Summary**—To be arranged in numbered paragraphs (Full Papers) or a single paragraph (Special Reports).
   —to include aims, principal results and conclusions.
   —to include Key words (10 maximum) at end of summary.
3. **Introduction**—To contain concise statements of the problem and the aims of the investigation.
4. **Methods**—To have brief but adequate account of the procedures; *full names of drugs (including those referred to by manufacturer's code)*, sources of drugs and statistical tests to be stated.
5. **Results**—To have no repetition of data in Figures, Tables and text.
6. **Discussion**—Findings and conclusions to be placed in context of other relevant work.
   NB Simple repetition of results and unwarranted speculation are not acceptable.
7. **Acknowledgements**—Sources of support. Sources of drugs not widely available commercially.
8. **References**—All references in the text to be included in the Reference List and *vice versa*. References in alphabetical order with complete citations; Journals publishing 'in press' papers identified.
   References to manuscripts submitted to other journals but not yet accepted are not allowed.
9. **Tables**—Each on a separate page and prepared in accordance with current requirements of the Journal.
10. **Figures**—Both labelled and non-labelled Figures to be prepared in accordance with current requirements of the Journal (see *Instructions to Authors*, 1995, **114,** 245–251) and provided with Figure Number and Authors' names on back (*in pencil*).
    —each legend to be typed on a separate page and carrying keys to symbols.
    —keys to symbols and histograms must not appear on the figures themselves, but in the respective legends.
    —'box style' figures are not in keeping with the Journal style; line drawings etc must have only left-hand and bottom axes.
11. **Manuscripts**—To be accompanied by a declaration signed by each author that
    (a) results are original
    (b) approval of all persons concerned has been given to submit manuscripts for consideration (see also 12b)
    (c) the same material is neither 'in press' (i.e. is in proof or has definitely been accepted for publication) nor under consideration elsewhere. Furthermore it will not be submitted or published elsewhere before a decision has been reached by the Editorial Board of the *British Journal of Pharmacology* and will not be submitted elsewhere if accepted by the *British Journal of Pharmacology*.
    (d) Copyright assignment is included.
12. **Cover letter**—To state clearly
    (a) Corresponding author's full postal address, telephone, telex or Fax number
    (b) where appropriate, that *either* ethical approval has been given for investigation *or* Company or Institutional permission to publish work has been received.
13. **Reminder**—Packaging to be sufficiently robust to protect Figures and to withstand mailing.

Failure to comply with *Instructions to Authors* may lead to substantial delays in processing, review and publication and may even jeopardize acceptance of the manuscript.

NOMENCLATURE

Authors are reminded that accepted receptor and associated terminology is laid out in *Nomenclature Guidelines for Authors*, as published in the *British Journal of Pharmacology, Br. J. Pharmacol.*, 1995, **114,** 253–255.

SPECIAL REPORTS

The purpose of *Special Reports* is to provide rapid publication for **new** and **important** results which the Editorial Board considers are likely to be of special pharmacological significance. *Special Reports* will have publication priority over all other material and so authors are asked to consider carefully the status of their work before submission.

In order to speed publication there is normally no revision allowed beyond very minor typographical or grammatical corrections. If significant revision is required, the Board may either invite rapid re-submission or, more probably, propose that it be re-written as a Full Paper and be re-submitted for consideration. In order to reduce delays, proofs of *Special Reports* will be sent to authors but **essential corrections must reach the Production Office within 48 hours of receipt.** Authors should ensure that their submitted material conforms exactly to the following requirements.

Special Reports should normally occupy no more than two printed pages of the Journal; two illustrations (Figures or Tables, with legends) are permitted. As a guideline, with type face of 12 pitch and double-line spacing, a page of A4 paper could contain about 400 words. The absolute maximum length of the *Special Report* is 1700 words. For each Figure or Table, please deduct 200 words. The manuscript should comprise a Title page with key words (maximum of 10), a Summary consisting of a single short paragraph, followed by Introduction, Methods, Results, Discussion and References (maximum of 10). In all other respects, the requirements are the same as for Full Papers (see current 'Instructions to Authors').

BRITISH JOURNAL OF PHARMACOLOGY VOLUME 115 (3) 1995

SPECIAL REPORTS

PAPERS

STOCKTON

Typeset by Elite Typesetting Techniques, Eastleigh, Hants
and printed in Great Britain by Unwin Brothers Ltd., The Gresham Press, Old Woking, Surrey